Probabilistic Analysis and Prediction of Bend Migration in Meandering Alluvial Streams

by

Mohammad Abdus Salam Sikder

Thesis submitted to
The University of Nottingham for the degree of Doctor of Philosophy

June 2012

Dedication

To my two fathers. One is, *Abdul Karim Sikder*, for whom I came into being in this world. The other is, *Bangabandhu Sheikh Mujibur Rahman*, from whom my national identity was returned and I could rise to the challenges posed by the world.

Abstract

A meandering river is one which exhibits a serpentine course, formed by a series of alternating bends connected by short, relatively straight reaches. Meandering behaviour has been found to be ubiquitous in alluvial streams and rivers. The tendency of the bends in meandering rivers to evolve and shift is a natural outcome of interactions between the flowing water, sediment in transport and the resistance to erosion of the boundary sediments. The resulting formation, evolution and shifting of bends is intrinsic to the morphological behaviour of meandering, alluvial streams. The need to understand and predict this behaviour stems not only from the desire to explain the morphodynamics of meandering rivers, but is also required to manage down the risks to property and infrastructure located along the course of meandering rivers, as well as the people who live, work or travel in the vicinity of alluvial streams with meandering planforms. In this context, the aim of this research is to develop an original, scientifically-based, and practical approach to the risk-based prediction of the hazard associated with bend migration that accounts for the uncertainty inherent to the morphological behaviour of rivers. A database compiled for the National Cooperative Highway Research Program (NCHRP) was used as the primary source of data. This includes data for 1,505 bends taken from 125 locations on 89 rivers spread across 24 States.in the USA The rivers were classified into nine categories of meandering, based on a modified Brice Typology. Bend geometry data in the database were measured from aerial photographs and maps representing the bends in the 1930/40s, 1950/60s and 1990s. It has long been recognised that the dimensionless rate of bend migration (M/W) is related to the stage of bend evolution (initiation, growth, translation, termination) and that this can be represented by the ratio of the bend radius of curvature to the channel width (R/W). It was decided to analyse bend migration based on these parameters and use the dimensionless form of the bend radius as the independent variable in the probabilistic analysis. Using normal conditional density functions fitted to the data, rates of meander migration were estimated corresponding to: 50%, 60%, 75%, 80%, 90%, 95%, 97%, 98%, and 99% probabilities of not being exceeded. The risk associated with a hazard depends not only on the probability that it will occur but also the consequences should it do so. In selecting the acceptable level of probability that the predicted rate of migration will not be exceeded, care should therefore be exercised by the user in considering all the possible consequences should this occur.

Table of Contents

Acknowledgement

This research work was carried out at the University of Nottingham in partial fulfilment of the requirements for the degree of Doctor of Philosophy under the *New Route PhD* programme. New Route PhD is a 4-year programme introduced in the UK during 2001-02 with a view to giving a broader knowledge base, wider understanding and clearer vision than a conventional PhD, and designed to make the holders of New Route PhDs more useful to the potential employers. It involves taking at least 180 credits of taught modules to provide intensive training in relevant areas of science and engineering, in additional to conventional thesis-oriented research. Modules may be selected from any School of study in the University. My PhD was based in the School of Geography, under the supervision of Prof. Colin R. Thorne.

First of all, I would like to express my heartiest thanks and profound gratefulness to Prof. Colin R. Thorne for his guidance and supervision of this research. Without his continued support completion of this thesis would not have been possible.

I express my thanks and gratitude to the University of Nottingham for granting me a full tuition fee *International Office Scholarship*, which enabled me to pursue my PhD study.

This thesis is, at the same time, the outcome of a morphological study performed under a collaborative agreement between HR Wallingford, University of Nottingham and myself. The funding contributed by HR Wallingford provided maintenance support during my study period at Nottingham. I express my sincere thanks and gratitude to HR Wallingford. In this regard, today I duly acknowledge the role of Mr. James P. Dent, who recommended me to HR Wallingford.

I express my sincere thanks to Prof. Ian Dryden for his advice and support concerning probabilistic and statistical methods. He convened the modules on Statistics and Probability Techniques that I took as part of my New Route PhD studies. However, he was not a co-supervisor and had no formal obligation to assist me with this research work. He did so as an act of kindness to me. I can only thank him and wish him well.

I would like to express my sincere thanks to the Ministry of Water Resources, People's Republic of Bangladesh for granting me the deputation to carry out this doctoral study.

Undoubtedly, the research work presented in this thesis could only be achieved with the aid and support of many people. At the outset of the study, thanks to Dr. Dilip Kumar Barua, who introduced me to Colin Thorne. I also express my thanks to Prof. Ainun Nishat and Prof. M. Monwar Hossain for recommending me for the PhD programme in the School of Geography,

University of Nottingham. I would like to express my warm thanks to Mr. James Dent, Dr. Roger Bettes and Mr. Darren Lumbroso at HR Wallingford for monitoring the progress of my research and giving valuable advice and feedback. A special thanks is due to Dr. Bettes for giving his time and effort in reading my draft thesis and passing his comments. Very definitely, I would like to express my sincere thanks to Dr. Paul Samuel at HR Wallingford for his continued support and interest in my research work.

I duly acknowledge the financial support of School of Geography in providing part of my house rent for living with family members. Specially, I express my heart-felt thanks to Rosemary Hoole and Mr. John Love for their cordial, warm support and care throughout my long period of study. I have no language to express my due thanks to John Love, how a man can be so good!!

I express my sincere thanks and gratitude to Mrs. Eileen Thorne who kindly extended her help, support and care in various ways to me and my family throughout our time in Nottingham. We are indebted to her indeed.

I recall the help and support from my neighbours at Florence Boot Close Mr. Ian Tarrant and Dr. Sally Burton. Their kindness and cooperation are unforgettable memories. Thanks also to Macdonald Dally for his friendly cooperation.

Over my period of study my relatives have in various ways helped and supported my family, particularly after during my illness in 2005. Among many, I particularly wish to mention: Shahadat Hossain Sikder, Selim Ahmad, Emdadul Haq, and Hemayet Uddin Sikder. I express my indebtedness to them. I especially recall the help and support received from my father-in-law: Mohammad Abdul Mannan Sikder and mother-in-law: Setara Begum Sikder. I also recall the passionate support of my uncles Mohammad Shamsul Huq Sikder and Abdul Manech Howlader.

Finally, I express my thanks, gratitude and respect to my close family. First, my mother, Saleha Begum Sikder for making the life-long sacrifices necessary to make it possible for me to study for a PhD. Next, my wife Rashida Begum Sikder for her relentless support, endless patience, sacrifice and care. Lastly, many thanks to my children Rahmat, Barkat, Tawfeeqa and Hiba for their patience and sacrifice.

Mohammad Abdus Salam Sikder

List of Tables

List of Figures

Abbreviations, Symbols and Notations

Abbreviations

NCHRP	National Cooperative Highway Resarch Programme
TRB	Transportation Research Board (in USA)

Symbols

M	meander **mi**gration (bend erosion magnitude), in general
MMA	**m**agnitude of meander **mi**gration for bend **a**pex
MOA	**mi**gration **o**rientation for bend **a**pex
MMA/WbCr	**m**eander **mi**gration at bend **a**pex/river channel **w**idth at **cr**ossing at **b**eginning of a time period (note MMA/WbCr and MMA_WbCr are used interchangeably)
MMA/WbCr/Y	**m**eander **mi**gration at bend **a**pex/river channel **w**idth at **cr**ossing per **y**ear (note MMA/WbCr/Y and MMA_WbCr_Y are used interchangeably)
MMA12	meander migration through movement of the bend **apex** from time point 1 to time point 2
MMC12	meander migration through movement of the bend **centre** from time point 1 to time point 2

R	meander bend **r**adius of curvature, in general
R1	**r**adius of curvature of outer bank at **time point 1**
R2	radius of curvature of outer bank at time point 2
ΔR12	change in bend radius between time point 1 and time point 2
R3	radius of curvature of outer bank at time point 3
Rb	radius of curvature of outer bank at the beginning of a time period

T	time point in general, say Year 1960
T1	**Time Point 1** (first survey date: for example, 1935)
T2	Time Point 2 (second survey date: for example, 1965)
T3	Time Point 3 (third survey date: for example, 1996)
TP	time period, in general, say from Year 1930 to 1960
TP1	**Time Period 1** (interval between first survey at T1 and second survey at T2)
TP2	Time Period 2 (interval between second survey at T2 and third survey at T3)

W	river channel **w**idth, in general
W1Cr	river channel **w**idth at **cr**ossing at **T1**
W2Cr	river channel width at crossing at T2
W3Cr	river channel width at crossing at T3
W1A	river channel **w**idth at bend **a**pex at **T1**
W2A	river channel width at bend apex at T2
W3A	river channel width at bend apex at T3
WbCr	river channel **w**idth at **cr**ossing at the **b**eginning of a time period
WbA	river channel width at bend **a**pex at the beginning of a time period

R/W	ratio of radius of curvature to river channel width, in general
M/W	magnitude of migration per river channel width, in general
Bend 1	position of a bend at **time point 1** (or bend number, say bend number 1)
BC	**b**end **c**entre, in general
BA	**b**end **a**pex, in general
BC1	**b**end **c**entre at **time point 1**
BA1	position of **b**end **a**pex at **time point 1**
BO1	bend **o**rientation at time point 1

Notations used in figure headings

Example:

Figure 5.2: Scatter plot of MMA_WbCr_Y 2257 vs Rb_WbCr 2415
data: AB1B2CDEFG1G2 v11 1512 3024

MMA_WbCr_Y	y-variable = meander migration at bend apex per unit river channel width at crossing at the beginning of a time period per annum
2257	number of data points available for the variableMMA_WbCr_Y
Rb_WbCr	x-variable = radius of curvature of outer bank per unit river channel width at crossing
2415	number of data points available for the variable Rb_WbCr
AB1B2CDEFG1G2	pooled data from all modified Brice Types from A1 to G2
v11	data in the analysis are from Version 11 of the corrected database
1512	total number of bends for which measurements are available in each period
3024	total number of data points for all two periods

Key Words

Alluvial, meandering rivers, Bank erosion risk assessment, Bend migration, Bend migration analysis, Bend migration prediction, Modes of movement Magnitude of bend migration, Orientaition of bend migration, Types of meander change

It is easy to understand all truths once they are discovered. But the point is to discover them

--- Galileo

Chapter 1
Introduction

1.1 Meandering Streams: Definition and Classification

In nature, alluvial rivers predominantly display one of three patterns when viewed from above: *straight*, *meandering*, or *braided* (multi-threaded) and these categories are still commonly used to define the planforms of alluvial rivers. An alluvial river is one whose bed and banks are composed of materials transported and deposited by the river itself. That means the channel is *self formed*. As the river can re-entrain materials that it has itself deposited, the channel is also free to adjust. That is, it is neither constrained by artificial materials, nor confined by bedrock or non-erodible materials in terraces; rather it is flanked by its own floodplain. Within this context, this study concerns the lateral shifting of the bends of meandering, alluvial rivers.

A meandering river is one which exhibits a serpentine course, formed by a series of alternating bends connected by short, relatively straight reaches. More specifically, meandering rivers have been defined as streams that posses loop-like bends characterised by a river cliff at the outside of the curve and a gently shelving point bar at the inside of the bend (Whittlow, 1984). Meandering has been found to be ubiquitous in alluvial streams and rivers. The presence of morphological complexity, such as that provided by alternating bends and the serpentine nature of the course of a meandering stream, is not only fundamental to the hydraulic and geomorphological functioning of a natural watercourse, it is also vital to supporting a healthy ecosystem that achieves maximum biodiversity and it also adds immeasurably to the aesthetics of the riverscape.

The term meandering is actually derived from the name of a river in southwestern Turkey, which debouches into the Mediterranean Sea 426 km southeast of Istanbul after following a serpentine course that is 195 km long (Lane, 1957). In the past the name of this river was variously spelt Meanderes, Maender, Maiandros and Menderez. It is now called the Buyuk Menderes. In English the word has evolved to 'meander'.

Meanders are usually described in terms of their planform attributes. Early investigators defined the path of a meandering river in terms of *circular*, *parabolic* and *sine* curves. Later, researchers concluded that a *sine-generated curve* could best fit the shape of a natural meander bend (Leopold and Langbein, 1966). However, in practice meanders seldom follow such idealised curves. Subsequent investigations have failed to establish a mathematical function which can describe the shape of meanders satisfactorily (Ferguson, 1973; Carson and Lapointe, 1983). In fact, in nature no two meander bends are identical in shape or symmetry, even in the case of consecutive bends along the same watercourse (Weihaupt, 1989).

Local variability in meander shape may be attributed to non-uniformity of the bank materials, variation in bank vegetation and/or subtle but important changes in entrance flow conditions from one bend to the next. For example, in a study on the Lower Mississippi River, Fisk (1944) found that clay plugs (generated by in-filling of cut-off bends by fine-grained sediment) encountered by migrating bends had a profound effect upon the planform geometry of a bend. As none of the idealised curves proposed in the literature can represent the variable planforms of real meander bends precisely, for practical use it is sensible to use the simplest schematisation and to approximate bends as circular arcs defined by their minimum radius of curvature. For example, in bend measurements made as part of an NCHRP study of meander migration (Lagasse et al., 2003) the geometry of the bends was approximated by a best-fit circular arc (see Section 3.1).

The scope of the study presented here is limited to meandering rivers and consequently it is necessary at the outset of any application of the method developed in this thesis to establish whether or not the watercourse in question is, in fact, a meandering river. However, river patterns

represent a continuum – in nature the boundaries of the three categories described above are fuzzy. Hence, categorising a river planform correctly is not a simple task. It is further complicated in that, in addition to the three major categories of planform, there are three sub-classes to be considered: *wandering* (a pattern that switches between meandering and braiding), *anabranching* (a braided channel that exhibits long distances between the junctions between sub-channels while remaining one river), and *anastomosing* (a braided channel made up of multiple channels each of which behaves as if it were a separate alluvial stream). Therefore, some form of screening is essential to identify whether a river is meandering and to exclude the possibility of inadvertently applying the analysis to rivers with other types of planform.

James Brice, of the United States Geological Survey, developed a planform classification method by assembling a large collection of aerial photographs depicting alluvial reaches of over 350 rivers in the continental United States (Brice, 1975). Brice screened streams through comparison of three attributes of the planform, simultaneously – the degree of *sinuosity*, the degree of *braiding*, and the degree of *anabranching*. Using this approach, it is possible to determine whether a stream has a significant degree of meandering in its pattern, for the purpose of finding solutions to the river engineering problems and river management.

Brice further sub-classified meandering rivers, on the basis of the character of the *sinuosity*, into seven different meander types. He used typical morphological features to distinguish the different types. These features are: phase (single or multiple), variability in width, presence of bars, depth and degree of incision, existence of chutes, modality, and change in planform depending on stage. The resulting Brice Types for meandering rivers are:

- Type A : single phase, equiwidth, incised or deep channel
- Type B : single phase, equiwidth channel
- Type C : single phase, wider at bends, chutes rare
- Type D : single phase, wider at bends, chutes common
- Type E : single phase, irregular width variation
- Type F : two phases, underfit low water sinuosity
- Type G : two phases, bimodal bankfull sinuosity

This classification system is useful as it offers a practical approach to using aerial photographs to classify meandering rivers. It provides the basis for using current and historical aerial photographs to assess their stability, migration rate (by hind-casting) and, on the basis of their past behaviour, make predictions of future migration. Brice's own historical analyses revealed that, in actively meandering rivers, the width varies gradually and in a regular fashion as a function of the position in the planform, with bends generally being wider than crossings. In contrast, equiwidth channels with little width variation were found to exhibit greater stability. This has subsequently been supported in many practical applications of Brice's approach **(**Brice 1977, 1984**)**.

Brice's classification correctly identifies that sinuous and braiding behaviours are not mutually exclusive and that rivers close to the meandering-braiding threshold may display features of both planforms (Carson, 1986). However, caution must be exercised in its application. For example, one possible source of error might arise due to the possibility that channels in multi-thread rivers may seem similar to meanders, although they behave differently (Carson, 1986). For instance, the Brahmaputra River in Bangladesh is one of the greatest braided rivers in the world, but if viewed from above at bankfull stage during the summer monsoon peak flow (July-August) the planform appears to be that of a meandering river with low sinuosity (Thorne et al., 1993). Another issue arises when attempting to apply the classification on a basin-scale or regional basis because few rivers have the same pattern (or type of meandering) throughout their course (Alabyan and Chalor, 1998). This raises the difficulty of deciding the appropriate reach length and the limits of the reaches over which planform classification is either meaningful or useful.

While classifying a watercourse can indicate the presence and type of meandering present, it does not shed any light on the causes, processes or hazards associated with meandering behaviour.

1.2 Aims and Objectives

The tendency of the bends in meandering rivers to evolve and shift is a natural outcome of interactions between the flowing water, sediment in transport and the resistance to erosion of the boundary sediments. The resulting formation, evolution and shifting of bends is intrinsic to the morphological behaviour of meandering, alluvial streams.

The need to understand and predict this behaviour stems not only from the desire to explain the morphodynamics of meandering rivers. It is also required to manage down the risks to property and infrastructure located along the course of meandering rivers, as well as the people who live, work or travel in the vicinity of alluvial streams with meandering planforms. For example, bend shifting poses significant hazards not only to agricultural land, homes, businesses, factories, but also key infrastructure including bridges, flood embankments and hydraulic structures. In this context:

*The **aim** of this research is to develop an original, scientifically-based, and practical approach to the risk-based prediction of the hazard associated with bend migration that accounts for the uncertainty inherent to the morphological behaviour of rivers.*

Attaining this broad aim depends on the achievement of a series of specific objectives. These are outlined in the remainder this section and expanded upon in the remainder of this chapter. They will be returned to in Chapter 9, where the conclusions of the thesis are summarised and recommendations are made for further research.

Objective 1: To study and define modes of bend migration in meandering streams with different types of morphology

The research reported in this thesis focuses on entirely bend migration in meandering rivers and there is an obvious need to review previous work on the modes by which bend movement takes place and the way bend movement varies between rivers with different morphological classifications. Four modes of bend movement are generally recognised: *extension*, *translation*, *expansion* and *rotation*. However, they are defined in a general sense, which lacks precision. For example, extension is described as being in the 'lateral' direction and yet it is unclear exactly what the 'lateral' direction is and so the term does not provide the basis for quantitative prediction of the direction (compass heading) in which a bend is likely to migrate. Also, these four modes are treated as if they are independent of one another, which manifestly is not the case. In light of these initial observations, the first objective is to explore and establish how each of the four modes acts and they interact to drive bend migration. This objective is addressed later in Chapter 1.

Objective 2: To select an analysis approach suited to development of practical tools for predicting the rate of future bend migration

A functional relationship between the curvature of a bend (R) and its migration rate (M) has long been recognised in the literature. While there is no process-based, quantitative explanation for this relationship, its general form is well established based on long-term monitoring of bend evolution and its validity is generally accepted in the relevant scientific and engineering communities. The concept that the migration rate can be expressed as a function of the ratio of bend radius to channel width can, therefore, serve as a general principle in the assessment of problems related to bend movement and it provides the starting point for the research reported here. However, while upper envelope curves may be fitted to scatter plots of migration rate versus R/W, these cannot be used predictively because the range of migration rates associated with a given value of R/W is huge. Also, there is no guarantee that the migration rate indicated by an envelope curve based on the past behaviour of a river could not be exceeded in future. In light of the limitations of existing analyses, the third objective is to identify a better approach to migration analysis and develop practical tools for predicting future bend migration rate that are new and original. This objective is addressed in Chapter 2.

Objective 3: To determine how best to represent bend curvature for the purpose of predicting migration rate in practice

The success of a predictive tool depends on selection of elements of the bend's planform capable of representing the geometry and migration rate of a bend. Past researchers have used a number of different planform features to represent bend curvature and migration rate. Most often, the curvature of the channel centre line and its movement between two successive points in time have been used in this context. However, the line of the outer, concave bank, and scroll bars left in the floodplain behind the convex bank have also been used for these purposes. It is therefore necessary to investigate which features of a bend are, in practice, best suited to supporting prediction of its future migration rate. This objective is addressed in Chapters 4 to 7.

Objective 4: To select a bend feature suitable for characterising bend migration and the hazard posed by this migration

It is also necessary to select a feature of the bend the movement of which can represent bend migration. In the literature, movement of the centre of curvature of the bend has been widely adopted to represent meander bend migration. However, the erosion hazard that is the main topic of this research derives from movement of the outer bankline rather than the bend centre. Consequently, it is necessary to check whether movement of the bend centre can represent bend migration in such a risk-based approach, or whether the bend apex could be a viable candidate. This objective is addressed in Chapters 3 and 4.

Objective 5: To obtain, quality check and analyse a suitable database of historical bend geometries and movements

Given the lack of a comprehensive theory of meandering, prediction of future bend migration rate depends on compilation of a large, comprehensive database coupled with statistical and probabilistic analyses of historical bend geometries and movements. A suitable database was published by Lagasse et al. in 2003 and this was obtained from the authors. Achieving this objective then required that the database be quality checked and corrected, that the required data be extracted, that migration rates be computed and that the relationship between bend curvature and migration be analysed. This objective is addressed in Chapter 4.

Objective 6: To develop a probabilistic, predictive tool for bend migration rate

Having compiled and analysed the relationship between bend curvature and migration, the next objective is to use the results to develop a probabilistic tool with which to make quantitative predictions of future migration rates. This objective is addressed in Chapters 5 and 6.

Objective 7: To demonstrate how the risk to an asset on the floodplain posed by a problem bend can be assessed by reviewing and discussing the prediction tool on a step by step basis

Given that the aim is to produce a predictive tool that is practical as well as being scientifically-based, it is important that the steps necessary to apply the method are clearly set out, that issues likely to arise when it is used in practice are identified and that advice is made available on how the tool may be applied correctly in order to support reliable risk assessments. This objective is addressed in Chapters 7 and 8.

1.3 Bend Formation and Development: Causes and Processes

The natural tendency for fluid shear flows to meander explains why this behaviour is an inherent characteristic of natural rivers. Even in straight channels, the filament of maximum velocity is found to follow a sinuous course, while in braided rivers individual anabranches display many of the characteristics of a meandering stream. As meandering is inherent to fluid shear flow, it is unnecessary to attribute the initiation of meandering to some local non-uniformity in fluvial processes or bank characteristics. In fact, the formation of a meander bend may be initiated by any one of a range of possible triggers in streams that are predisposed to meander. The outcome is that meanders can effectively form spontaneously if the flow field combines with the characteristics of the channel's deformable boundaries in the appropriate manner, as observed in the case of water escaping from a ruptured dam (Davis, 1908).

While the precise mechanism of meander initiation remains unknown, it appears that it stems from the existence of coherent flow structures within the flow field, that have dimensions scaled on those of the channel width (Ashworth et al., 1996). These 'large eddies' (termed Prandtl's secondary flow of the second kind) interact with the distribution of time-averaged velocities to induce cells of secondary circulation that generate a sinuous path in the filament of maximum primary velocity. The resulting flow field generates a persistent pattern of boundary shear stresses

that, in turn, produces spatially organised areas of scour and fill at the bed. This results in the formation of pools and riffles that are skewed towards alternate sides of the channel. The curvature introduced by curvature of the filament of maximum velocity as it follows the sinuous thalweg reinforces the secondary flow cells and introduces skew-induced secondary velocities, termed secondary flow of Prandtl's first kind (Bathurst, 1979). If the channel banks are nonerodible, the filament of maximum velocity will meander within a straight reach (Einstein and Shen, 1964) as bank erosion is a necessary condition for the initiation of channel meandering. However, in alluvial channels, meandering of the flow quickly results in the channel becoming sinuous, as the banks retreat in areas of flow convergence and deep, near-bank scour, while the banks accrete in areas of divergence and bed siltation. As the sinuosity increases, at some point the channel can no longer be considered to be straight and can be classed as meandering, although the threshold for this condition is not universally agreed. For example, Leopold and Wolman (1957) set a sinuosity of 1.5 as the lower boundary for meandering, but this seems quite high and channels with sinuosities as low as 1.06 have been classed as meandering (Brice, 1983).

Migration processes at the bends of meandering, alluvial rivers are complex, being governed by interactions between fluvial processes of sediment erosion, transport and deposition, and geotechnical mechanisms of bank stability and collapse. In terms of fluvial processes, the key drivers are the distributions of velocity (primary and secondary) and boundary shear stress at bends. Early researchers found the dominant flow structure at a bend to be helical flow generated by the combination of primary flow vectors and secondary currents. As early as the 19th century it was recognised that a skew-induced, secondary flow cell drives fast, near-surface water outwards and slow, near-bed water inwards at a bend.

For most of the 20th century, it was believed that helical flow occupied the whole cross section at the bend apex (Leopold et al., 1964; Henderson, 1966). However, during the 1970s and 80s, direct measurements in rivers revealed that a counter-rotating cell might exist near the outer bank (Bathurst et al., 1977). This cell interacts with the main, skew-induced circulation to generate elevated velocities and high local boundary shear stresses on the lower bank and bed adjacent to

the outer bank (Bathurst et al., 1979; Lapointe and Carson, 1986). The resulting, high intensity near-bank flow may undercut the bank, erode the bed at the toe of the bank and, thereby, accelerate bank retreat (Thorne and Lewin, 1979; Thorne, 1982).

It was also believed for many years that helical flow extended to the inner bank (Richards, 1982; Knighton, 1998). However, in the 1980s it was suggested by new theoretical analyses and proven by direct measurements that over the shallow part of the point bar at the inner bank, topographic steering of the flow may lead to secondary currents that are directed radially outwards through whole flow depth (Thorne et al., 1985). It is this outward flow which encourages the filament of maximum velocity to cross to the outer bank earlier in the bend than is predicted in analytical models that ignore the effects of these convective accelerations when solving the equations of motion for curved flows (Smith and McLean, 1984).

Taken together, the results obtained from theoretical and empirical studies performed during the 1970s and 80s present a picture of bend flow morphology interactions that is more complex than initially realised, but which is consistent with the observed bedforms, channel features and the morphological behaviour of bends (Figure 1.1).

As bends evolve, they tend to increase in amplitude and decrease in radius of curvature. Bagnold (1960) opined that flow in meandering channels might display similar resistance processes to those in the bends of closed pipes. Through laboratory experiments, he noted that, as bends tighten, a zone of flow separation develops at the inner bank downstream of the convex bank, reducing the effective flow width and concentrating flow near the outer bank at the bend exit. Bagnold further noted that this situation became pronounced when the ratio of radius of curvature to channel width (R/W) of the bend was reduced to a value between 2 and 3. The result is that, for bends with this geometry, the tendency for further growth in amplitude is decreased, while the tendency for downstream migration is enhanced. As a result, such bends migrate rapidly, while retaining their characteristic geometry. In this configuration, Bagnold found that energy losses due to bend effects are minimised. In this way, from the geomorphological point of view, Bagnold

successfully synthesised theory with observation. His finding was later supported by the work of Chang (1984), who found that a river does least work in turning when the R/W of a bend is approximately 3.

However, if migration of the outer bank at the bend exit is impeded, so that the bend becomes very tight (that is the R/W value drops below about 2), another zone of separation develops at the outer bank (Bagnold, 1960). Bagnold showed that this separation zone had the effect of disrupting the spatially-organised pattern of helical flow, intensifying turbulence and increasing energy losses. A common outcome was rapid local bank retreat upstream of the bend apex, leading to the bend stalling, being cut-off or becoming 'double-headed'. The existence of multiple possible patterns of bend development made it difficult to characterise or predict the behaviour of very tight bends with R/W values less than 2. The existence of complex patterns of bend growth at the outer bank of migrating bends helps explain why measurements of scroll-bars created at the inner margin of bends were used by Hickin (1974) to estimate historical migration rates. An example is illustrated in Figure 1.2 (Hickin, 1978).

The factors governing the processes of meander initiation, growth and migration have been identified in several hallmark studies (Nanson and Hickin, 1986; Thorne and Osman, 1988a; Hooke and Redmond, 1992). They may be summarised as: discharge, mobility of bed material, supply of sediment from upstream, bank erodibility, bank geotechnics, bank vegetation, fluvial processes in the basal area of the retreating bank, and engineering interventions in the fluvial system.

In summary, in slightly curved bends, curvature effects are weak and bends evolve slowly – mostly through growth in amplitude, but with a tendency for increased curvature. As bend curvature increases, helical flow strengthens and bend migration accelerates. The onset of inner bank separation switches the thrust of meander evolution from lateral growth to downstream migration. When outer bank separation occurs, the bend may either stall, be divided into a double headed bend or cut-off. These characteristic behaviours may be related to threshold values of R/W. R/W values from about 12 down to 4 characterise the bend growth stage, from 4 down to 2

they represent the phase of downstream migration at approximately constant geometry, while values less than about 2 are associated with stalling, double heading or cut-off.

1.4 Bend Migration and its Relation to Bend Radius of Curvature

The tendencies for bank erosion along the outer bank and sediment deposition at the inner bank of a meander bend can be explained, qualitatively, in terms of the pattern of flow and distribution of velocity, as explained in the previous section. However, our ability to quantify the processes responsible for these morphological changes and, hence, understand bend evolution completely, is still imperfect. Consequently, prediction of bend migration may be approached by another route, based on historical records of the evolutionary trends and sequences of bend morphology actually displayed by meandering rivers, and relating migration analytically to the geometric parameters of the bend that presage those changes.

This is possible because long term records of bend evolution exist, based on monitoring and measurement of meander changes that have contributed a great deal of knowledge and understanding of meander morphology, morphological change and resulting bend migration. For example, Edward Hickin and Gerald Nanson conducted a series of studies based on historical evolution and migration of bends in the Beaton River in north western Canada (Hickin, 1974; Hickin and Nanson, 1975; Hickin, 1978; Nanson and Hickin, 1983; Hickin, 1983; Nanson, 1980).

Initially, the history of meander evolution was reconstructed from scroll bar features left on the floodplain at the inner margin of migrating bends. Hickin (1974) reported that, morphologically, the river was in a state of a dynamic equilibrium and that, over prolonged periods, the migrating bends maintained a ratio of bend (i.e. scroll bar) radius to width (R/W) of about 2 (where R = bend radius of curvature, as inferred from meander scrolls; W = channel width ignoring the width of the point bar). In a further analysis, Hickin and Nanson (1975) concluded that the maximum rate of bend migration occurred when the bend had an R/W value of around 3, with the migration rate rapidly declining for values above or below 3. Later, Hickin (1978) observed that, for many bends, migration was characterised by discontinuous and distinct phases of migration. He noted

that the evolution of an individual bend featured phases of initiation, growth and termination. These stages were differentiated within a continuous scale of R/W such that the *initiation stage* was associated with R/W values around 4.6, the *growth stage* was associated with $2.8 < R/W < 4.6$, and the *termination stage*, $R/W < 2.8$. It was further noted that the termination stage occurs very rapidly compared to the other two stages.

In other published work, Nanson and Hickin (1983), and Hickin and Nanson (1984) built on their findings from the Beaton River by adding data from other rivers, with the aim of producing generalised descriptions of bend migration, suitable for engineering applications. The tool they developed relates the maximum amount of non-dimensional migration at a bend (M/W = migration divided by channel width) to the non-dimensional radius of curvature of the bend (R/W = radius divided by channel width). Expressed mathematically this is:

$$M/W = f\,(R/W) \tag{1.1}$$

Within this function, Hickin and Nanson (1983; 1984) noted that, in general:

- Newly evolving bends have a long radius and develop slowly. This is the *initiation stage* (characteristically, $R/W > 10$)
- As bends grow, the radius reduces and the rate of migration increases. This is the *growth stage* ($3 < R/W < 10$)
- Later, bends migrate rapidly, while maintaining a constant radius. This is the *migration stage* ($2 < R/W < 3$).
- Finally, bends become overly tight and the erosion rate decreases abruptly. The bend then approaches a *cut-off*. This is the termination stage ($R/W < 2$).

Many subsequent studies have supported these basic principles regarding the different stages of bend evolution. However, they have also demonstrated a wide variation in the dimensionless rates of migration associated with different evolutionary stages and particular values of relative

curvature (Lewis and Lewin, 1983; Martinson and Meade, 1983; Begin, 1986; Petts et al., 1989; Harvey, 1989; Biedenharn, 1989; Hooke, 1991; Thorne, 1991; Sidorchuk and Matveev, 1997).

At least some of this variability might be explained by geological controls on bend migration. For example, when clay plug, backswamp, or Pleistocene materials are encountered by an eroding bank, this can hinder or even prevent further meander development. Consequently, while Hickin and Nanson's work provides a useful, empirical template for characterising the pattern of bend evolution, it also illustrates the futility of trying to make deterministic predictions of bend migration in channels flowing through heterogeneous floodplain materials. Other options for predicting bend migration are examined in Chapter 2.

1.5 River Channel Patterns

1.5.1 Classification Systems

In their widely quoted paper, Leopold and Wolman (1957) classified channel patterns into three categories: braided, meandering and straight. In the paper they defined a channel reach as meandering only when it displayed relatively mature, smooth, regular alternating bends with a sinuosity of 1.5 or greater. Setting the critical value for meandering at a sinuosity of 1.5 prevented many non-straight reaches from being classed as meandering. Effectively, these channels represented a fourth planform category that might have been classed as 'sinuous'.

In defining sinuosity Leopold and Wolman (1957) used the ratio of the length of the thalweg to the straight line, valley distance (rather than that of the centreline) as this parameter appeared to be better related to the flow processes and morphological mechanisms responsible for the initiation of meandering (as described earlier). Schumm (1963) expressed sinuosity as the ratio of stream length to valley distance. He may be criticised in that he did not explicitly mention whether the stream length referred to the channel or thalweg length. In his work Schumm studied the sinuosity using aerial photographs. Hence, it can reasonably be assumed that he used the

centreline, outer bankline or inner bankline of a river to define the stream length, although again this is not explicitly stated. He defined a river as sinuous provided that it has sinuosity greater than 1. This is reasonable, since, in principle, any departure from 1 can be attributed to the river displaying some degree of meandering. However, it would in practice be unfeasible to define whether a natural river is or is not sinuous based on this definition, since it is too strict. This is the case because a sinuosity of 1 can only be achieved by a completely straight channel, and such channels rarely occur in nature. In practice one can expect to find straight alluvial channels only in the laboratory. Hence Schumm's definition, though theoretically valid, seriously lacks practicality. It follows that a higher threshold value is required for practical classification purposes. Conversely, the value of 1.5 that was selected by Leopold and Wolman (1957) is to a degree arbitrary and the same can be said of the alternative values of 1.3 (chosen by Moody-Stuart (1966)) and 1.7 (preferred by Leeder (1973)).

In selecting the criteria used to differentiate between different channel patterns, Leopold and Wolman (1957) relied on sinuosity and the occurrence of bars and islands as exclusive indicators of planform type. They consequently generated what may be considered to be three sharply defined patterns. A sinuosity of 1 indicated a straight channel, a sinuosity greater than 1.5 indicated meandering, while the occurrence of exposed bars and islands defined a braided condition. The outcome was for many natural rivers that displayed combinations of these attributes to be effectively excluded from a defined category and relegated to one of several 'transitional' patterns. This notable disadvantage was discussed by Rust (1978).

Chitale (1970) took multiplicity of channels as a criterion for classifying river channel patterns. Using this criterion he initially recognised two main groups – single channel streams and multichannel streams. Single channel streams were further categorised as straight, meandering or in transition between these patterns. Meandering channels were then sub-categorised into six classes using three criteria - acuteness (as opposed to flatness), regularity (meaning a train of bends with similar curvatures and frequencies) and simplicity (meaning bends with a single dominant amplitude and frequency). These are:

i) regular and flat meanders,
ii) irregular and flat meanders,
iii) regular and acute meanders,
iv) irregular and acute meanders,
v) simple meanders, and
vi) compound meanders.

In characterising the planform of the bends formed by meanders, Chitale (1970) used four geometric curves: parabolic, sine, circular and sine-generated. He illustrated these by providing definition sketches and substantiated their presence in nature by providing sketches of bends observed on several Indian rivers. Multichannel streams were divided into two categories: braided (meaning interlaced, multichannel rivers), and anastomosed (a river with numerous separate channels branching out from the parent streams, such as the Kosi River in Bihar, India). Chitale (1970) did not explicitly mention whether particular bend geometries (parabolic, sine, circular or sine-generated) were associated with a specific one of the six types of meandering. Hence, the question arises as to whether, for example, parabolic bends might be found in channels with either simple or regular meanders.

Brice (1984) used four channel properties as the criteria for classifying channels. These were: sinuosity, point bars, braiding and anabranching. He identified four major types of river: sinuous canaliform, sinuous point bar, sinuous braided and non-sinuous braided. Rather than using 'braiding' as a causative property, it might have been better for Brice to have used the presence or absence of mid-channel bars and islands, as this would have been consistent with the causative properties used to characterise meandering, which were sinuosity and presence of point bars. If this had been done then the term 'braiding' could have been used as a parallel class to meandering. By this classification Brice could have explicitly accounted for more rivers within his four classes. For example, a 'sinuous-braided' form could be recognised, which could not be the case using the classification of Leopold and Wolman (1957). Interestingly, while Brice attempted to classify all types of planform, he did not actually assign the name 'meandering' to any class of river (see Figures 1 and 2 in Brice (1984)).

1.5.2 Sinuosity and Other Operating Variables

Schumm (1963) developed a relationship linking the sinuosity to morphological, boundary material, and hydrological variables, based on a study of 43 reaches of alluvial rivers crossing the Great Plains in USA. He found that sinuosity increases with decreasing values of the width-depth ratio. A similar inverse relationship had earlier been suggested by Mackin (1956). A positive correlation was found between the percentage of silt-clay in the channel perimeter sediments and sinuosity. In contrast to the finding of Leopold and Wolman (1957), who demonstrated an inverse relationship between stream discharge and gradient, Schumm showed that, for a particular discharge, less sinuous streams had a steeper gradient. However, there seems to be an anomaly in Table 1 of Schumm's 1963 paper, where a channel with a sinuosity of 1.1 is classed as straight, even though the definition of a straight channel is given on page 1090 as being a stream with a sinuosity of unity.

Schumm (1963) also mentioned that there might be an inverse function linking mean annual discharge and sinuosity, though he could not find a significant relationship in his data. He explained the absence of a relationship by observing that, for a particular value of sinuosity, the variation in observed discharges is large. In this context, he stated,

"That discharge only affects the dimensions of the meanders can be demonstrated by noting that the sinuosity of the Mississippi River between Mellwood, Arkansas and Lake Providence, Louisiana, is 2.1. Average discharge between these two points is on the order of 500 000 cfs. Table 2 shows that Red Willow Creek, with a sinuosity also of 2.1, has an average discharge of only 42 cfs. Discharge therefore seems to have little effect on the sinuosity of rivers".

However, while it seems unlikely that a generalised relationship between discharge and sinuosity exists, further analysis of the data presented by Schumm suggests that a relationship may exist for Great Plain Rivers. This is illustrated in Figure 1.3. The form of the relationship is:

$$Q_{ma} = 711 + (-301.1)p \qquad (1.2)$$

where, Q_{ma} = mean annual discharge in cfs and p = sinuosity. This relationship is based on a line fitted to the data by the method of Tukey (1977). Residual analysis did not show any non-constant variance (Figure 1.4**)**.

The problem of huge variation in discharges for a particular value of sinuosity that Schumm mentioned may be avoided if a relationship is sought for rivers of similar types in similar environmental settings. Hence, the mean annual discharge of rivers in a particular physiographic region could be predicted from the sinuosity observed in an aerial photograph using empirical relationships like Equation 1.2. Another approach might be to categorise rivers into discharge classes, and then attempt to find a relationship between sinuosity and discharge. The possibility could and should be explored through further research to resolve the paradox apparent in Schumm's analyses and pronouncements.

1.5.3 Slope and Discharge

The article by Leopold and Wolman (1957) is perhaps mostly remembered for the slope – discharge relationship that it proposes. In their analysis, the threshold line between meandering and braiding was drawn by eye. This approach has been criticised on the basis that it could have led to inaccurate fitting of the line separating data points for braided and meandering watercourses (Chitale, 1970; Ferguson, 1984).

In establishing their relationship, Leopold and Wolman (1957) used channel gradient and bankfull discharge. However, the paper does not describe the method used to determine the channel gradient. There are a number of potential problems in defining channel gradient, including specification of the length of the river reach over which the gradient is calculated, how the channel length is measured in meandering or braided streams and the number of elevations that were used to determine the change in elevation. It is an undeniable fact that the channel gradient is a very difficult parameter to define and it is sensitive to differences in the way it is calculated. In any case, it is the water surface slope that is of most significance to the processes responsible for meander initiation and growth and, as shown in Figure 1.5 (Leopold and Wolman, 1957) there may be large variations between channel gradient and water surface slope.

Sikder (1997) investigated variability in water surface slope using hydrological data from a reach of the braided Brahmaputra River between Kamarjani and Bahadurabad in Bangladesh. The data covered two years and came from 14 water level stations located along both banks and showed huge seasonal variations in water surface slope (Figure 1.6). Even within a season there was notable spatial variation in water surface slope, both along the same bank and between the opposite banks. Another feature to note in Sikder's data is that the water surface slope may vary widely with stage (Figure 1.7). These findings illustrate just how variable water surface slope may be spatially and temporally and they suggest that channel gradient may be a poor proxy variable for water surface slope when attempting to identify a threshold between different river types.

A further limitation on Leopold and Wolman's (1957) threshold diagram is that the data do not display constant variance in channel gradient across the range of discharge values - which is an important requirement for a single threshold relationship to cover the full range of discharges. In fact, the variance in gradient values is smaller for lower discharges than it is for larger discharges. This suggests that fitting of a single threshold line may be inappropriate and that two threshold relationships may exist, one for smaller discharges and another one for larger discharges. This issue could be investigated through further research.

A final point concerning the threshold behaviour observed by Leopold and Wolman (1957) may be illustrated by comparing their experiment with that of Ackers and Charlton (1970). In both experiments the initial planform pattern was a single, straight channel. In Leopold and Wolman's experiment evolution of the straight channel into a braided form was initiated by the formation of a mid-channel bar that caused bank retreat after just 3 hours, leading to a braided planform after only 22 hours. In Ackers and Charlton's experiment, the ultimate channel pattern was meandering, but this only developed after 559 hours.

A possible explanation of why Leopold and Wolman's channel transformed so rapidly and adopted a braided rather than meandering, could lie in the sediment feeding rate (which was sufficiently high (833 mgl^{-1}) to overwhelm the transport capacity of the flow), rather than the gradient of the flume. In this regard Ackers and Charlton (1970) concluded that,

"When the valley slope is insufficient for the development of the hydraulic gradient necessary to transport the discharge and sediment as a straight and meandering channel, depending on the sediment discharge, then a braided channel pattern develops".

The point here is that Leopold and Wolman's experiment may actually be taken to suggest that it is the ratio of sediment supply to transport capacity that is causative in triggering planform change, rather than channel gradient *per se*.

1.6 Meander Geometry and Bend Evolution

Early investigators believed that meander bends follow some kind of regular mathematical curve. Leopold and Langbein (1966) concluded that a typical meander describes a sine-generated curve, which is the most probable path of a meandering river according to a random-walk model. They further maintained that a meandering river follows such a path because in doing so it does the least work possible in transporting water and sediment along the valley. The notion that a sine-generated curve can adequately describe meander geometry was later investigated further by Chitale (1970) and Ferguson (1973).

Chitale (1970) put forward an alternative approach to describing the meander form using circular arcs as the elementary form. Through this method he found that a theoretical upper limit to the sinuosity of meandering streams of 5.5. Sinuosity cannot exceed this due the development of bend cut-offs. Brice (1973) attempted to represent meandering streams using consecutive circles of different radii and tried to justify his approach on the basis that a good match with the actual curves can be obtained. Ferguson (1975) tried using five different, regular geometric curves to fit meander bends and found that three of them - sine-generated, Van Schelling and Fargue's spiral, fitted bends quite well. Based, on this research, it may be concluded that a variety of curves may approximate to the geometries displayed by meander bends.

The word 'development' is used here in a general sense that covers the all stages of bend growth and changes. Brice (1974) proposed an evolution model for meander growth and development. In

this model for bend development through time and space, he recognised 16 different forms/shapes of meander loops (Figure 1.8). He divided these 16 forms into 4 categories depending on two criteria – *simplicity* and *symmetry* of a bend. These 4 categories are: i) simple symmetrical (7 forms out of 16), ii) simple asymmetrical (2 forms out of 16), compound symmetrical (3 forms) and iv) compound asymmetrical (4 forms). Here the term *simple* indicates that the bend desribes a single loop. A *compound* meander is defined as with more than one, non-opposing loop.

Brice (1984) put forward a mathematical definition for a loop based on the proposal that,

"The minimum curvature required for an arc to be considered an individual meander loop is that its length just exceeds its radius and the central angle is about 1 radian".

In this definition, the term 'minimum curvature' strictly refers to the 'minimum arc length', since the definition of curvature in geometry is the inverse of the radius of curvature and thus the units of curvature would be length^{-1}. This definition of a 'loop' appears to be robust in the sense that, since a radian is a constant angle, the minimum subtended angle at the centre of the loop is 1 radian whatever the absolute size of the loop. However, the definition is to an extent arbitrarily, since no morphological implications were mentioned in support of choosing a minimum arc angle of 1 radian.

Brice (1984) stated that,

"A simple symmetrical loop becomes asymmetrical by the growth on its perimeter of a second arc of constant curvature".

and went on to say that,

"A simple loop becomes compound when the second arc on its perimeter has developed into a loop"

as illustrated in Figure 1.9.

Brice's definitions suggest that the early evolution of a bend involves growth of a simple loop until the bend arc angle approaches a value of around 56° (that is it less than 1 radian which equals approximately 57°) at which point the driving processes start to produce a more complex,

compound meander bend. While the setting of an arbitrary threshold for the onset of complexity in bend evolution may be criticised, the general observation that bends begin their lives as simple, single loops and become increasingly complex as they develop through time and space is widely observed in nature. In this respect, Brice's definitions and descriptions have some value at least as qualitative predictors of bend behaviour.

1.7 Describing and Modelling Different Modes of Meander Change

1.7.1 Overview

Describing and modelling different modes of bend change and movement refers to attempts to characterise and simulate the direction, spatial distribution and time rates of bankline shifting that occur in meandering rivers between consecutive points in time, due to different mechanisms (modes) of bend change.

Daniel (1971) recognised five types of movement of river bends represented by sine-generated curves. Hooke (1977) identified six simple modes of bend change and, by applying these in combination, she identified numerous types of change (Figure 1.10). Hooke and Harvey (1983) later rationised this to ten types of change (including a 'no change' scenario) based on a study of the River Dane in Cheshire, UK (Figure 1.11).

Comparing these and other schemes for describing bend changes through time, it is clear that there is no standardised terminology: different authors use the same term for different modes of change and/or different terms to describe the same mode of change. For example, in Figure 1.10, *translation* is used by Hooke (1977) to describe absolute down-valley or longitudinal movement of a bend. However, in Figure 1.11, Hooke and Harvey use the term *migration* for this kind of movement. Indeed, Hooke (1991) later used the term *migration* for a mode of bend change that does not involve down valley movement at all (Figure 1.12). Similarly, the term *growth* is used in different senses in Figures 1.10 and 1.11. It follows that the terminology concerning different modes of bend change is neither consistently applied nor universally agreed.

Knighton (1998) defined four types of meander growth and shifting (Figure 1.13). In his classification, bend rotation is placed on an equal footing with extension and translation. However, when a bend exhibits translation, rotation occurs as a consequence of this change. Hence, it can be argued that rotation is actually a secondary or consequential outcome of primary modes of bend change involving, for example, extension or translation. This issue is considered further in Sections 1.7.2 to 1.7.4. When more than one mode of change occurs simultaneously at a bend, it can be said to have undergone a compound change.

1.7.2 Representing the Outer Bank Line Using a Circular Arc

In Section 1.4 it was explained that, for a channel of given width, there is a well known relationship between the radius of curvature of a bend and its migration rate. However, a question arises as to how to represent bend radius, practically. The outer bank line usually presents the most distinct geometry in an aerial photograph of a bend and it certainly follows a curved path. However, the outer bank may consist of more than one curve, and each may have a different radius of curvature. In many studies, a single, semi-circle is fitted to the curve of the outer bank, approximating the radius of the bend as a whole. For example, the bend geometry database used in this research was built by the NCHRP (for details see Chapter 3 and Chapter 4) using best fit semi-circles based on measurements made using aerial photographs and maps.

In nature, although truly semi-circular bends are rare, some portion of the outer bank line around the bend apex can usually be approximated closely by fitting a circular arc. Experience shows that planform changes are often concentrated around the bend apex, an area where the radius of curvature of the outer bank is often a minimum for the bend as a whole. For these reasons, it is widely accepted that characterising bend radius using the minimum radius of curvature of the outer bank of a bend around its apex is acceptable.

1.7.3 Modes of Bend Movement

Based on the discussion above, it may be concluded that there are two broad categories of bend change: *simple* and *compound*. Within the category of simple changes, bends may change through *extension, translation or expansion*. Compound changes take place through combinations of these three simple modes. Bend *rotation* occurs as a consequence of the operation of one or more of the three simple modes and, hence, is not regarded as a primary mode of change itself. Each of the primary modes of bend change is now described in detail.

Extension

Knighton (1998) defined *extension* as retreat of the outer bank of a bend orthogonal to the long-stream direction, leading to lateral shifting of the bend and an increase in meander amplitude (Figure 1.13). Hooke (1977) used the terms *extension* and *growth* interchangeably to describe bank retreat leading to an increase in bend amplitude perpendicular to the valley axis. However, to unambiguously define *extension* a clear definition of the lateral direction or the valley axis is required as this is to a degree dependent on the reach length over which these directions are measured. However, generally, *extension* is the mode of bend change through which the outer bank line retreats in the cross-stream direction, so that the bend shifts laterally and grows in amplitude (Figure 1.14). This mode of movement is associated with only one zone of erosion (Figure 1.15).

Translation

Knighton (1998) defined *translation* as the downstream movement of a bend due to retreat of the outer bank along the channel orientation (Figure 1.13), although definition of the downstream direction is also somewhat scale dependent and open to interpretation (Figure 1.15). Here in this research, *translation* is defined as being the mode of bend change that occurs when the outer bank line migrates perpendicular to the axis of the bend at the previous time point i.e., perpendicular to the bend orientation of the previous time point (Figure 1.17). This mode of bend movement is associated with 3 zones of erosion/deposition: a zone of deposition, a zone which is first eroded then deposited, and a zone of erosion Figure 1.15.

Expansion

Hooke (1977) defined *expansion* as occurring through radial shifting of the upstream and/or downstream limbs of a bend such that the bend becomes broader (Figure 1.10). Here *Expansion* is taken to be the mode of bend change where the outer bank line migrates radially with respect to the bend centre. In this mode the bend radius increases in comparison with the previous time point (Figure 1.18). In this mode of change, the bend does not migrate in either the lateral or downstream directions. This type of change can also result in a reduction in the radius, a form of bend *contraction*. In this mode of movement, there is only a single zone of either erosion (*expansion*) or deposition (*contraction*) (Figure 1.15**)**.

Complex Modes of Change

Combinations of the three primary modes of change may produce complex modes of change where the outer bank line migrates neither in the direction of the bend nor perpendicular to it, nor even radially (though there may be an increase or decrease in the radius) (Figure 1.19). However, it may still be possible to identify components of complex migration representative of the simple modes of movement**.** In Figure 1.19, Bend 1 is the initial position of the bend, at time 1. Later (time 2) the bend has migrated to position Bend 2. This mode of movement is associated with multiple zones of erosion and deposition (Figure 1.15).

1.7.4 Resolving Bend Migration into Components

It is argued later in this thesis that bend migration may be represented by movement of the bend apex (see Chapters 3 and 4 for details). Accepting this, in Figure 1.19 it can be seen that the bend apex migrates from position P to Q (through a distance PQ) in the direction defined by MOA12. If PQ is resolved into lateral and longstream components PD and PC, PD constitutes bend extension and PC constitutes bend translation.

In this hypothetical example, each and every point on the bend moves in the same direction as the movement of the apex. Hence, a point, A, on the Bend 1 moves to point B on Bend 2 along the

same heading as the movement of the apex (that is, MOA12). Migration of point A to point B can also be resolved into two lateral and longstream components AE and AF but, interestingly, these no longer correspond to extension and translation, respectively. In fact they would better be defined as two new modes of bank movement with AF constituting *normal migration* and AE *tangential migration*.

The question then arises as to whether extension (Figure 1.14), translation (Figure 1.17) and expansion (Figure 1.18) can be defined in terms of normal and tangential migration. Taking apex migration as representative of migration of the entire bend:

- In Figure 1.14, apex migration PQ (extension of the apex) is purely normal migration.
- In Figure 1.17, apex migration PQ (translation of the apex) is purely tangential migration.
- In Figure 1.18, not only apex migration but also that of all other points is purely normal migration.
- Finally in Figure 1.19, apex migration (PQ) can be described in terms of its normal (PD) and tangential (PC) components.

Hence, it can be concluded that the two new modes of movement proposed here (normal and tangential) could be very useful in describing and defining bend migration based on its representation by movement of the bend apex. Further research is needed to explore this possibility.

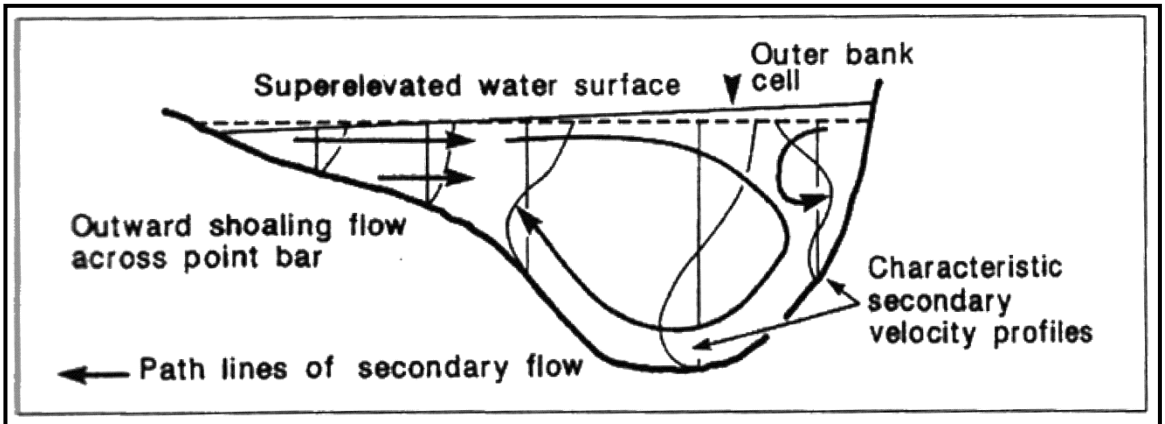

Figure 1.1: Secondary flow pattern at the bend apex in a meandering stream (from arkham and Thorne, 1992).

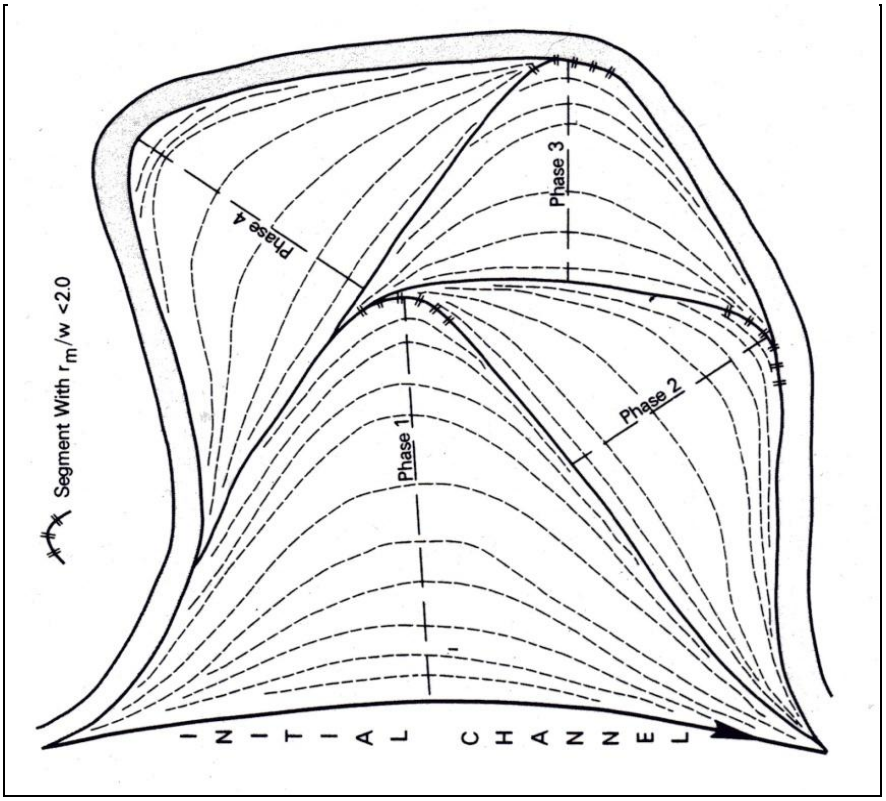

Figure 1.2: Evolution of a complex loop inferred to occur through four distinct phases of migration from examination of meander scroll bars (from, Hickin 1978).

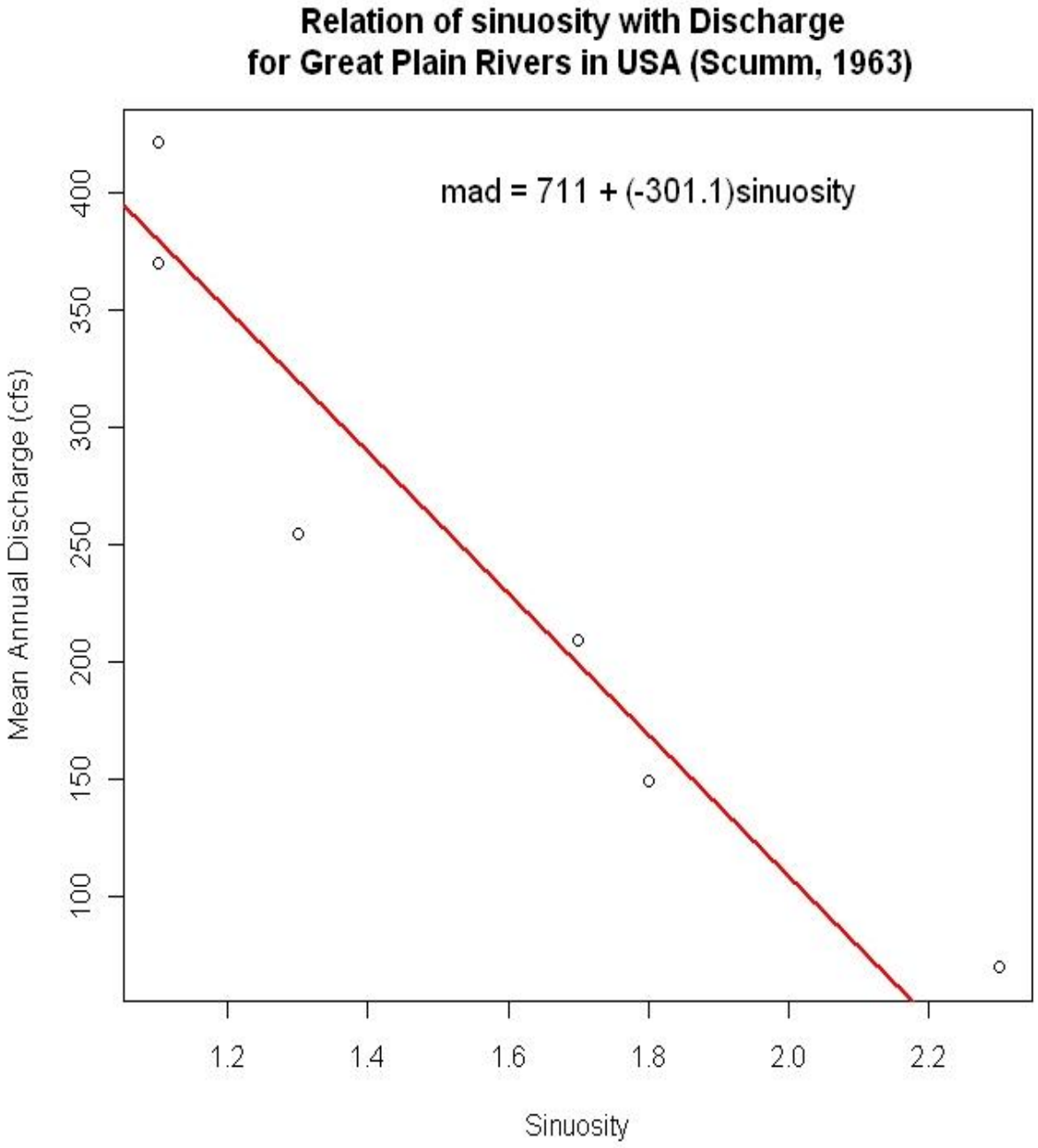

Figure 1.3: Relation between mean annual discharge and sinuosity for alluvial rivers in the Great Plains, USA (based on re-analysis of data from Schumm (1963)).

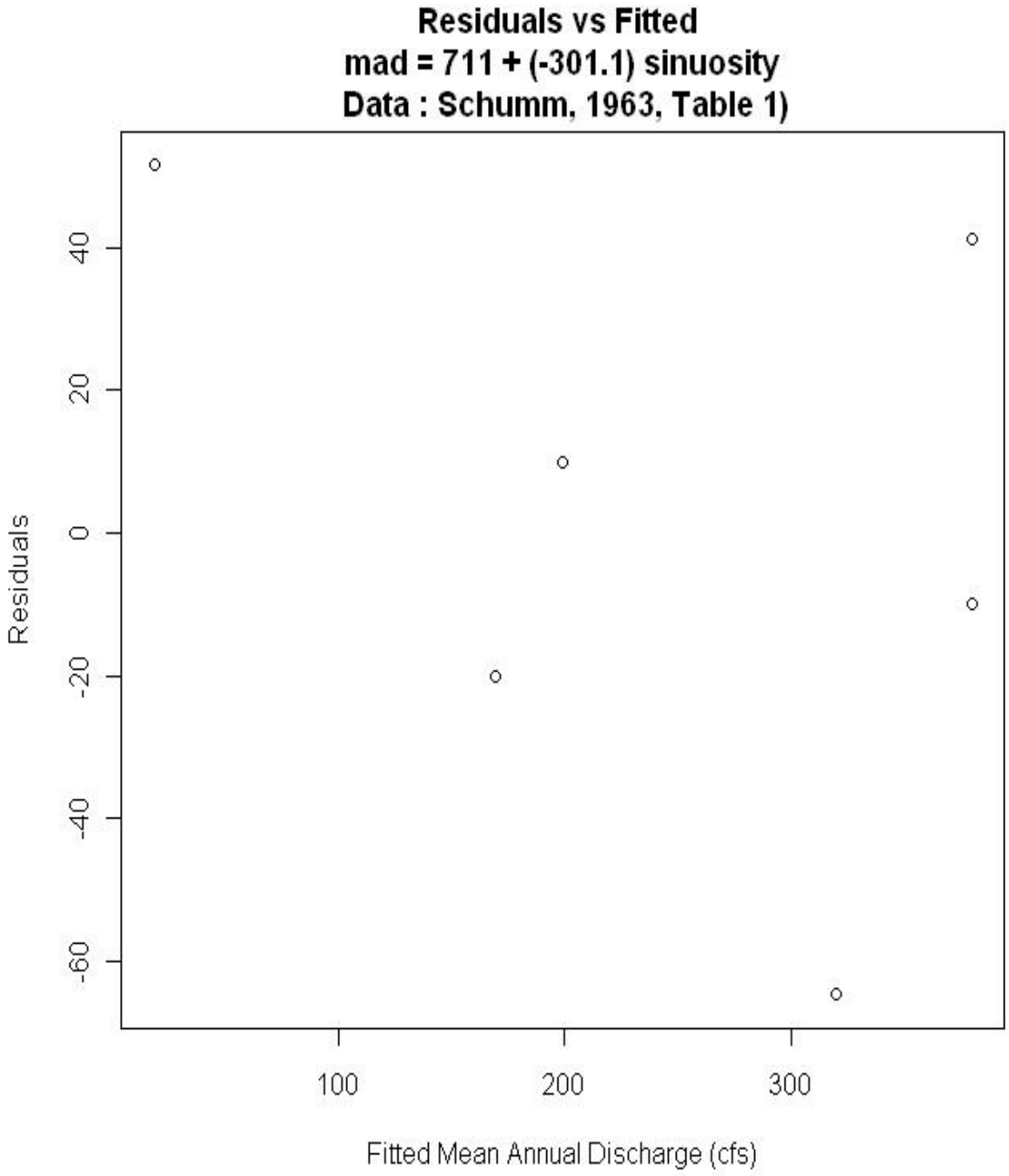

Figure 1.4: Residuals versus fitted values for the regression relation between mean annual discharge and sinuosity for alluvial rivers in the Great Plains, USA.

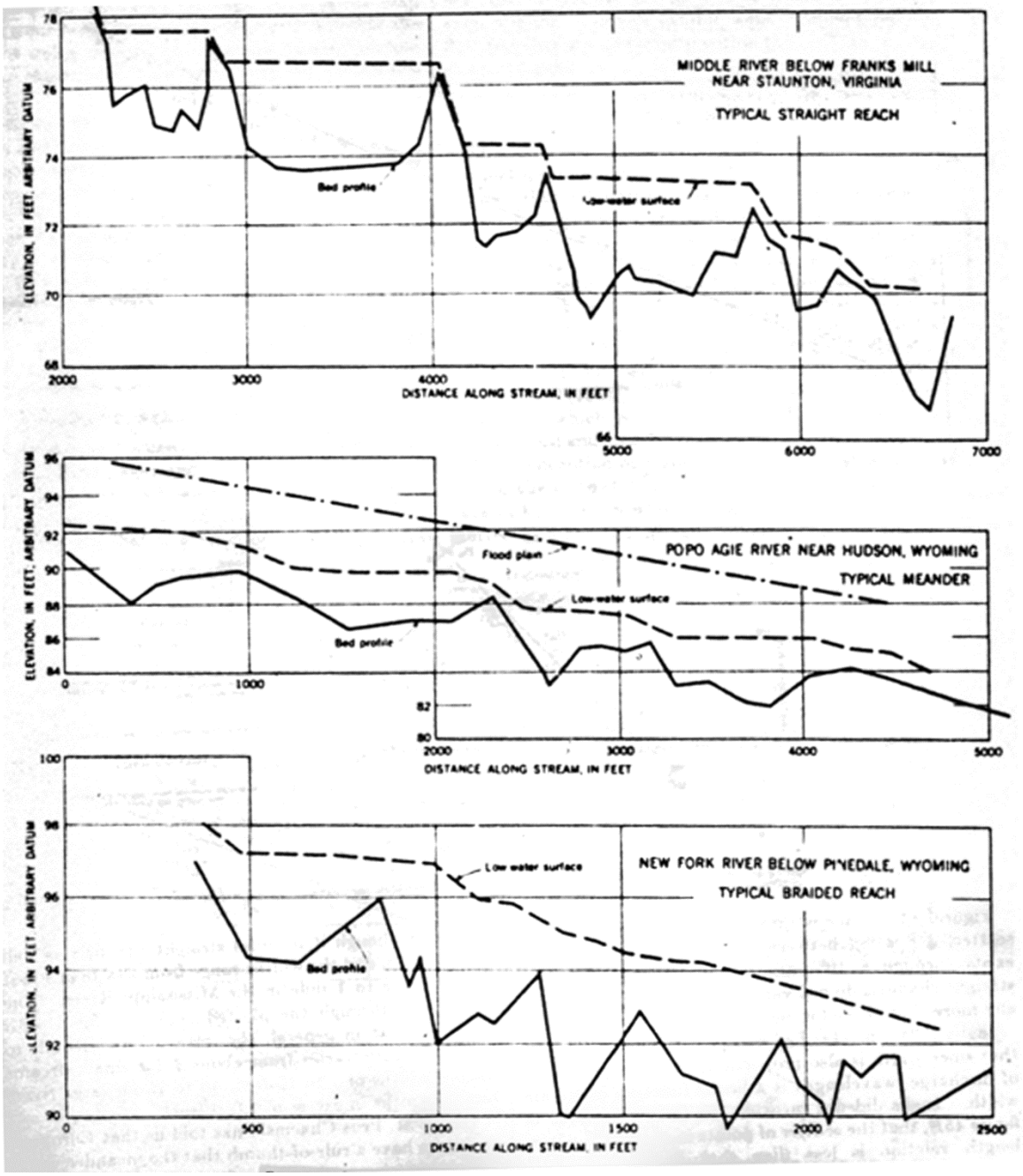

Figure 1.5: Bed and water surface long profiles for the rivers with straight, meandering and braided planforms (from, Leopold and Wolman (1957)).

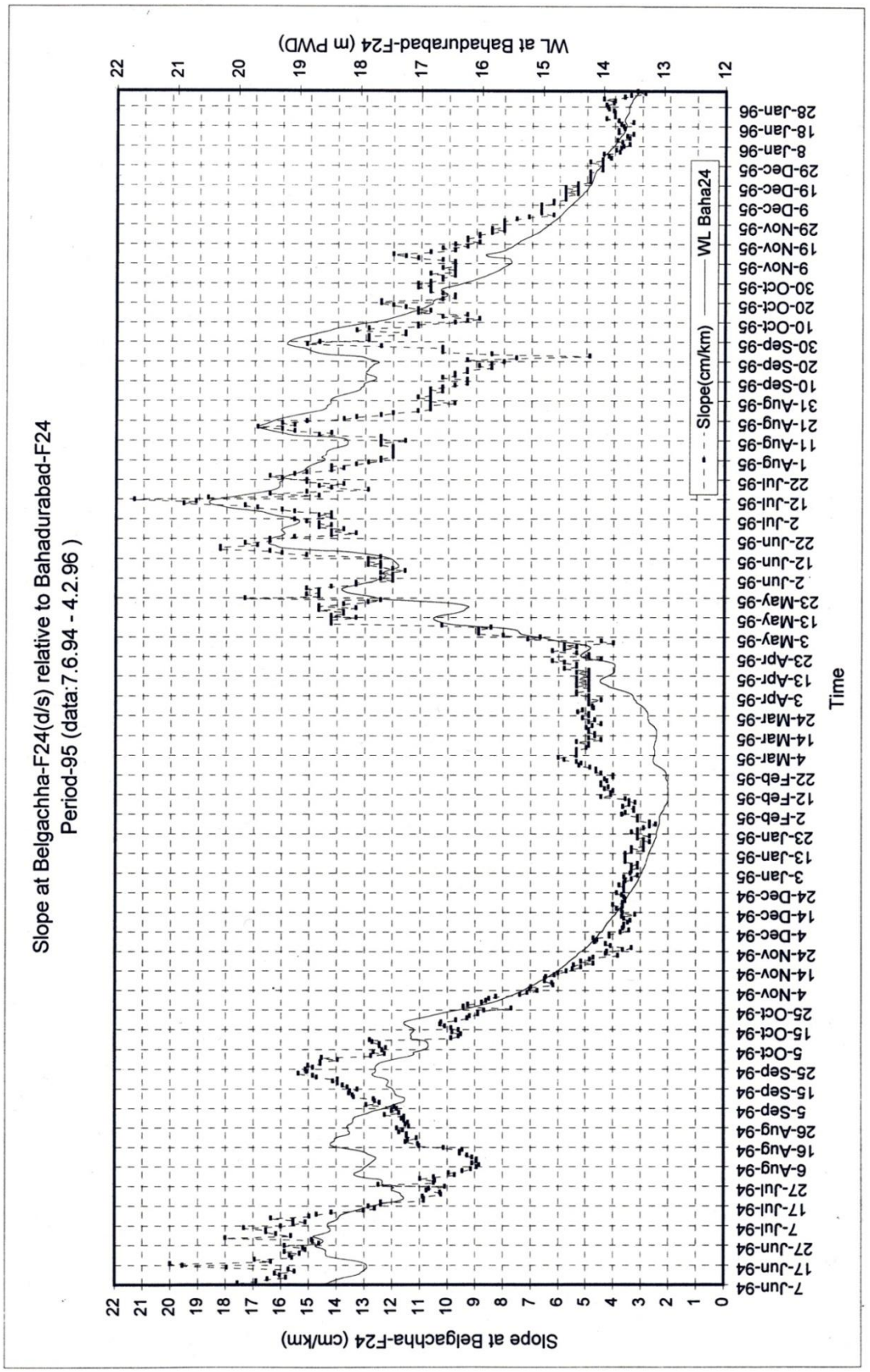

Figure 1.6: Seasonal variation in hydraulic gradient between two gauging stations in a reach of the braided Brahmaputra River near Bahadurabad, Bangladesh (from Sikder (1997)).

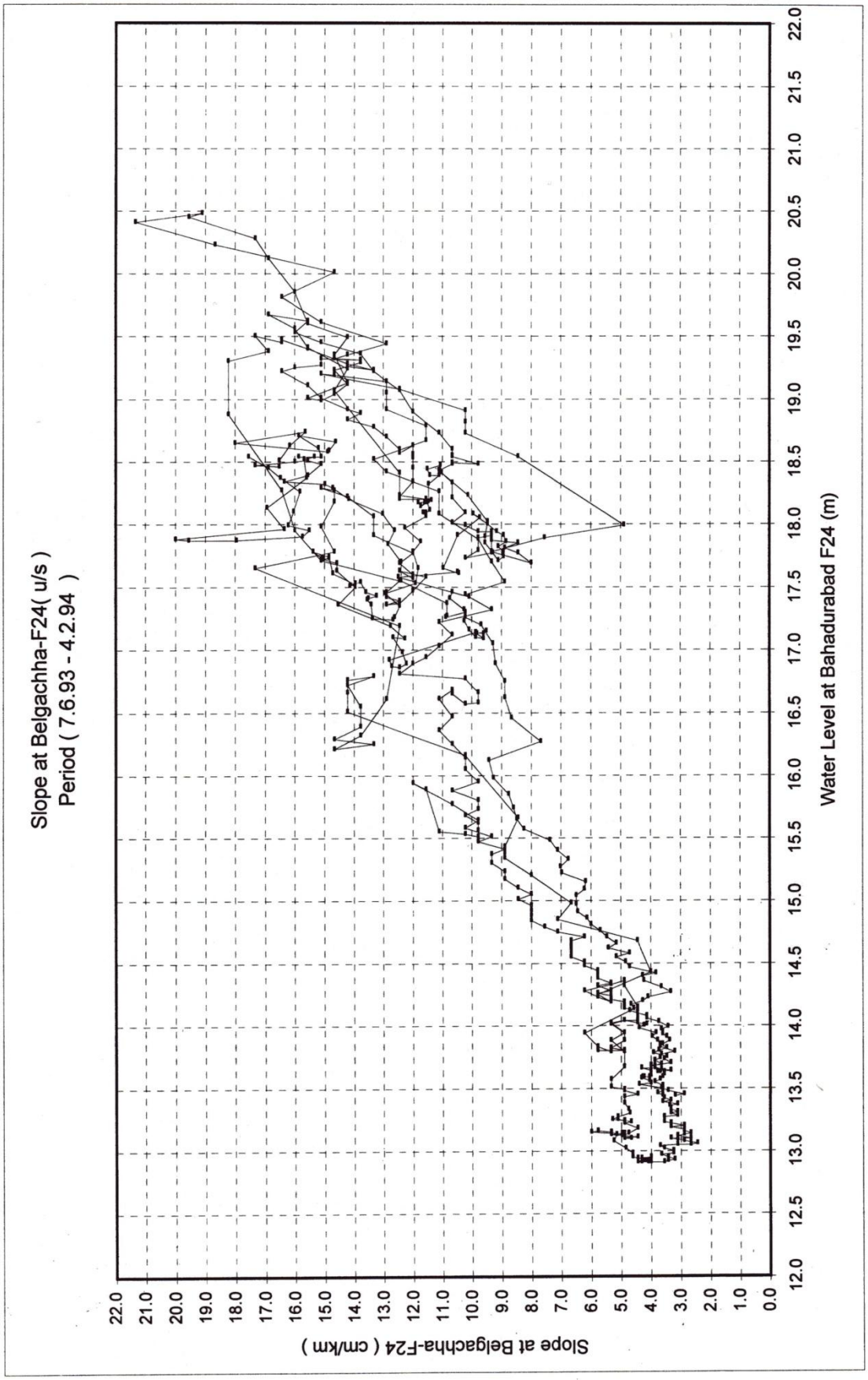

Figure 1.7: Change in hydraulic gradient with stage in a reach of the braided Brahmaputra River near Bahadurabad, Bangladesh (from Sikder (1997)).

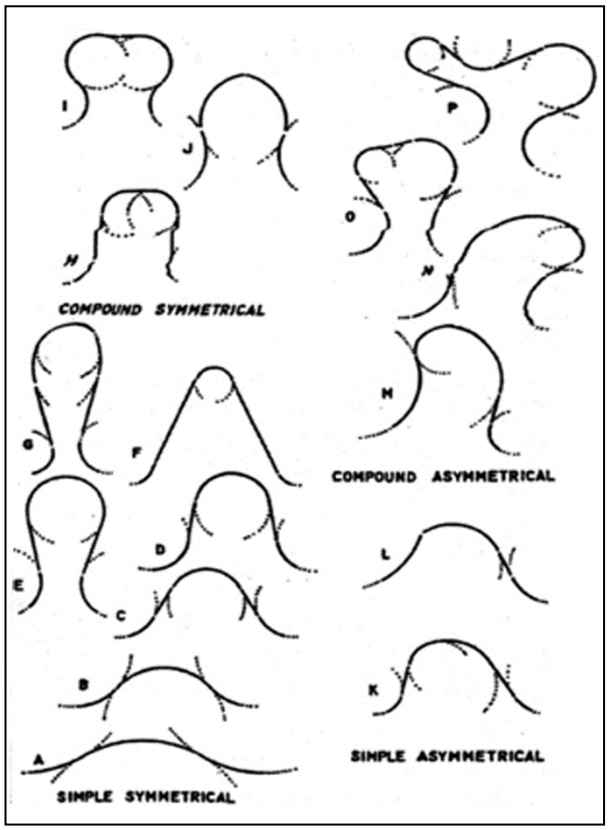

Figure 1.8: Evolution of meander loops (from Brice (1974)).

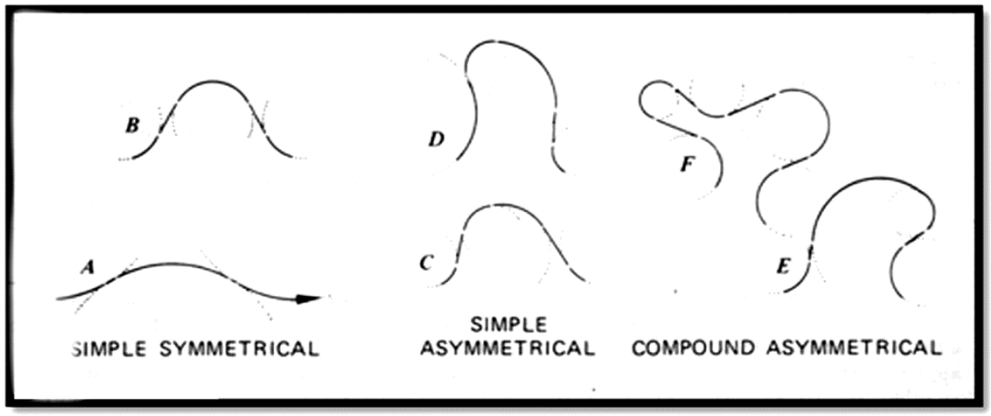

Figure 1.9: Common types of meander loop (from Brice, 1983).

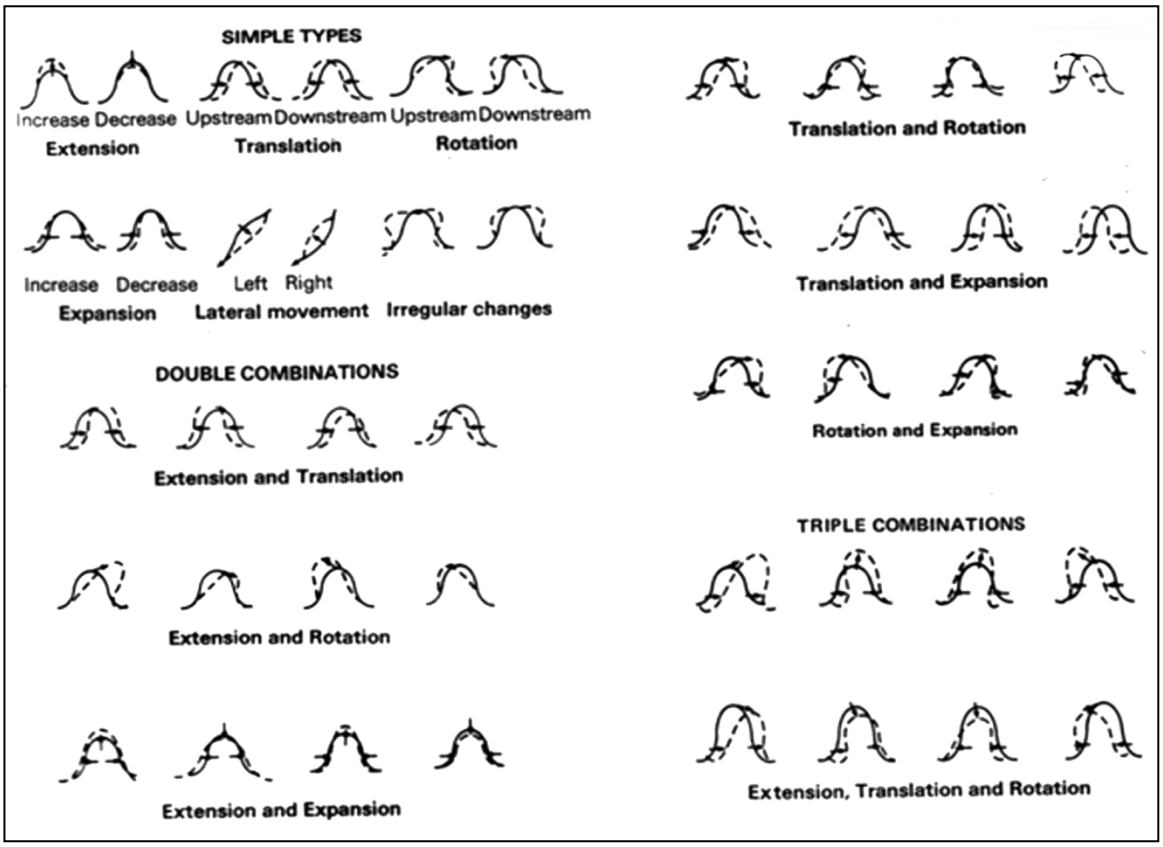

Figure 1.10: Modes of meander change (from Hooke, 1977).

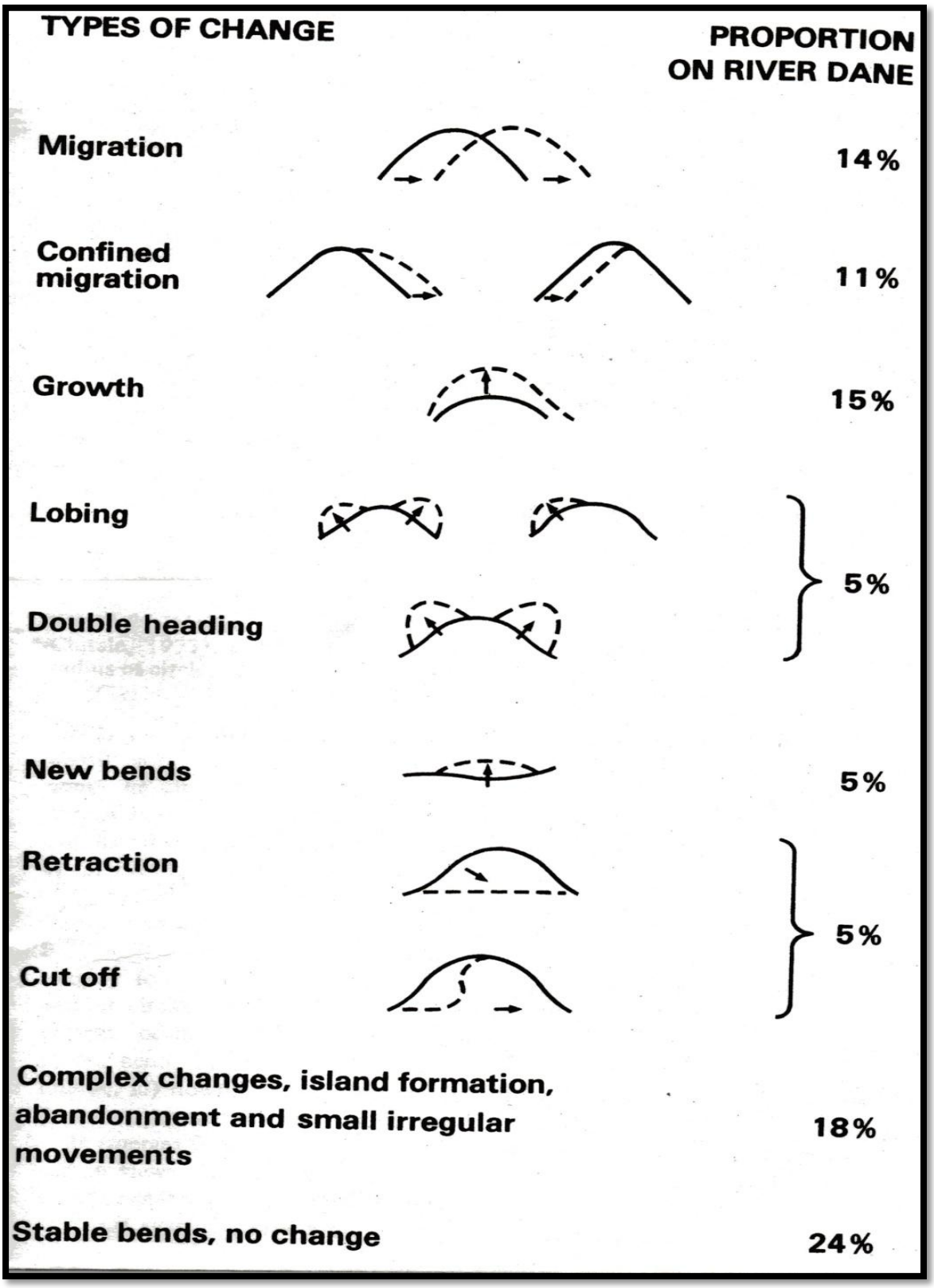

Figure 1.11: Types of meander change (from Hooke and Harvey, 1983).

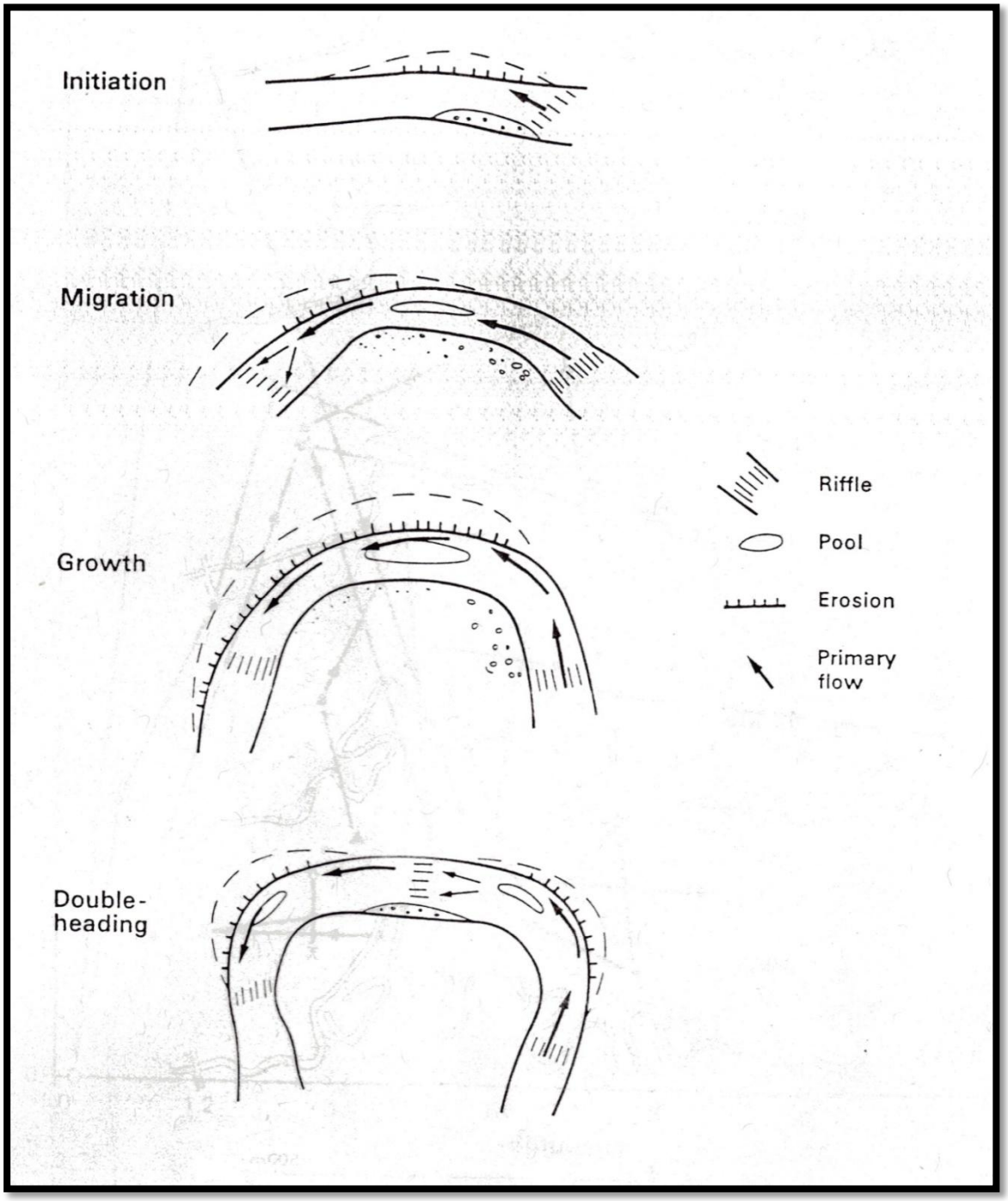

Figure 1.12: Sequence of meander development (from Hooke, 1991).

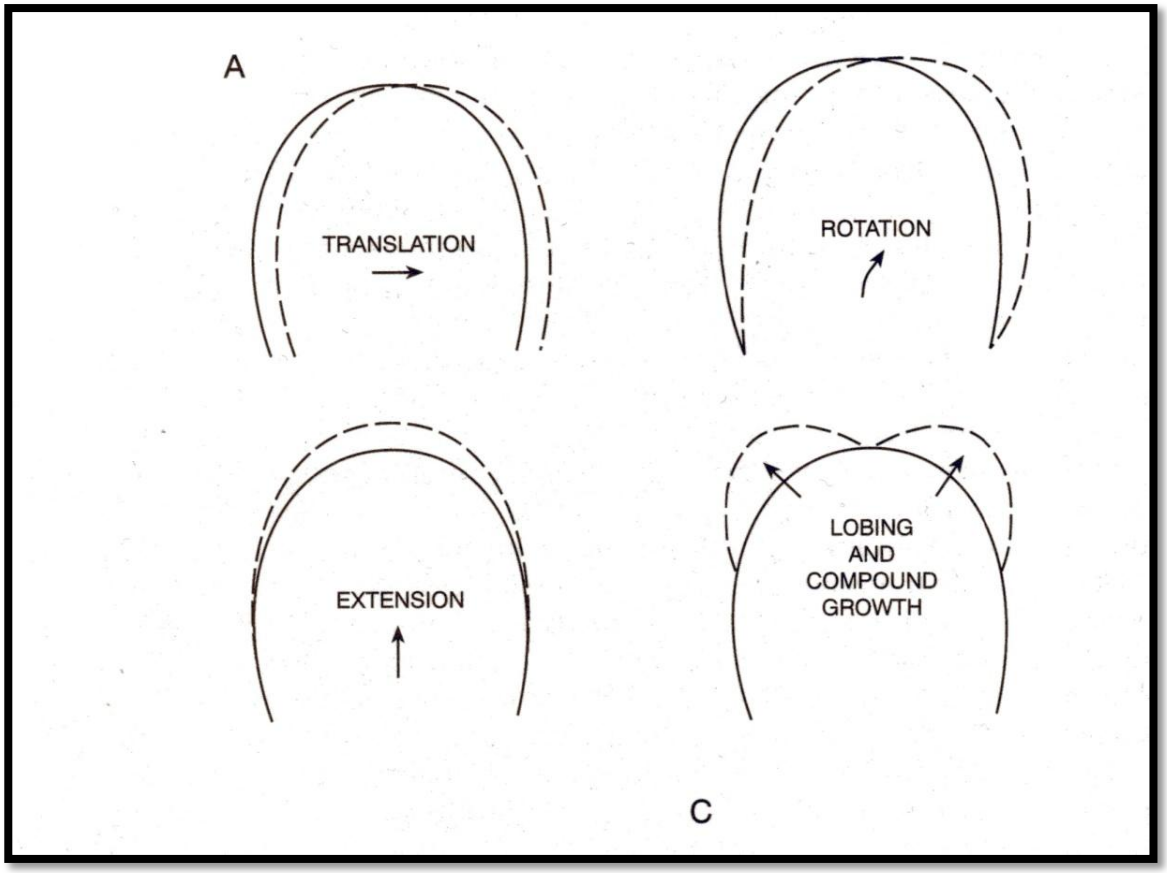

Figure 1.13: Types of meander movement (from Knighton, 1998).

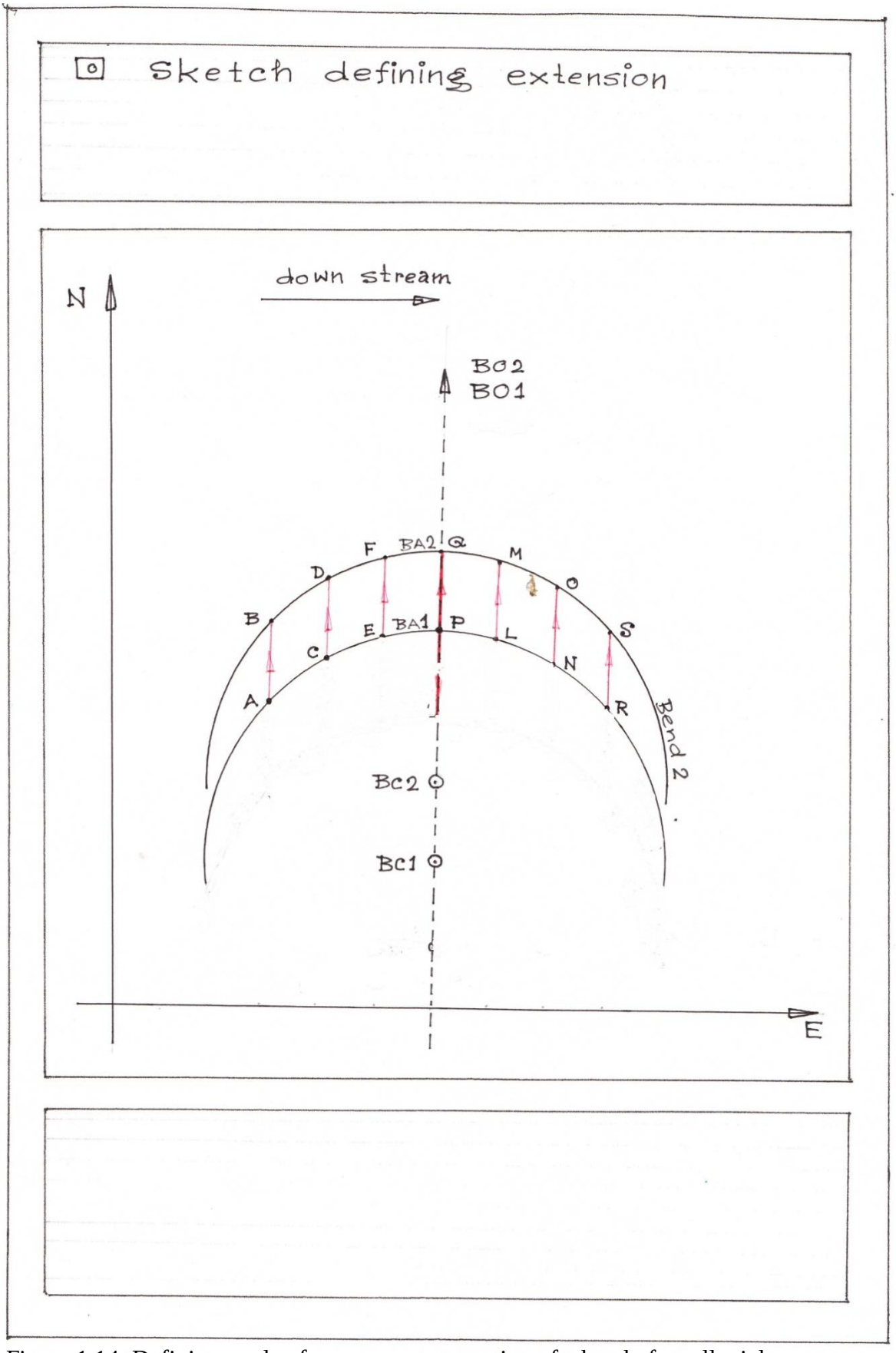

Figure 1.14: Defining mode of movement - extension of a bend of an alluvial stream

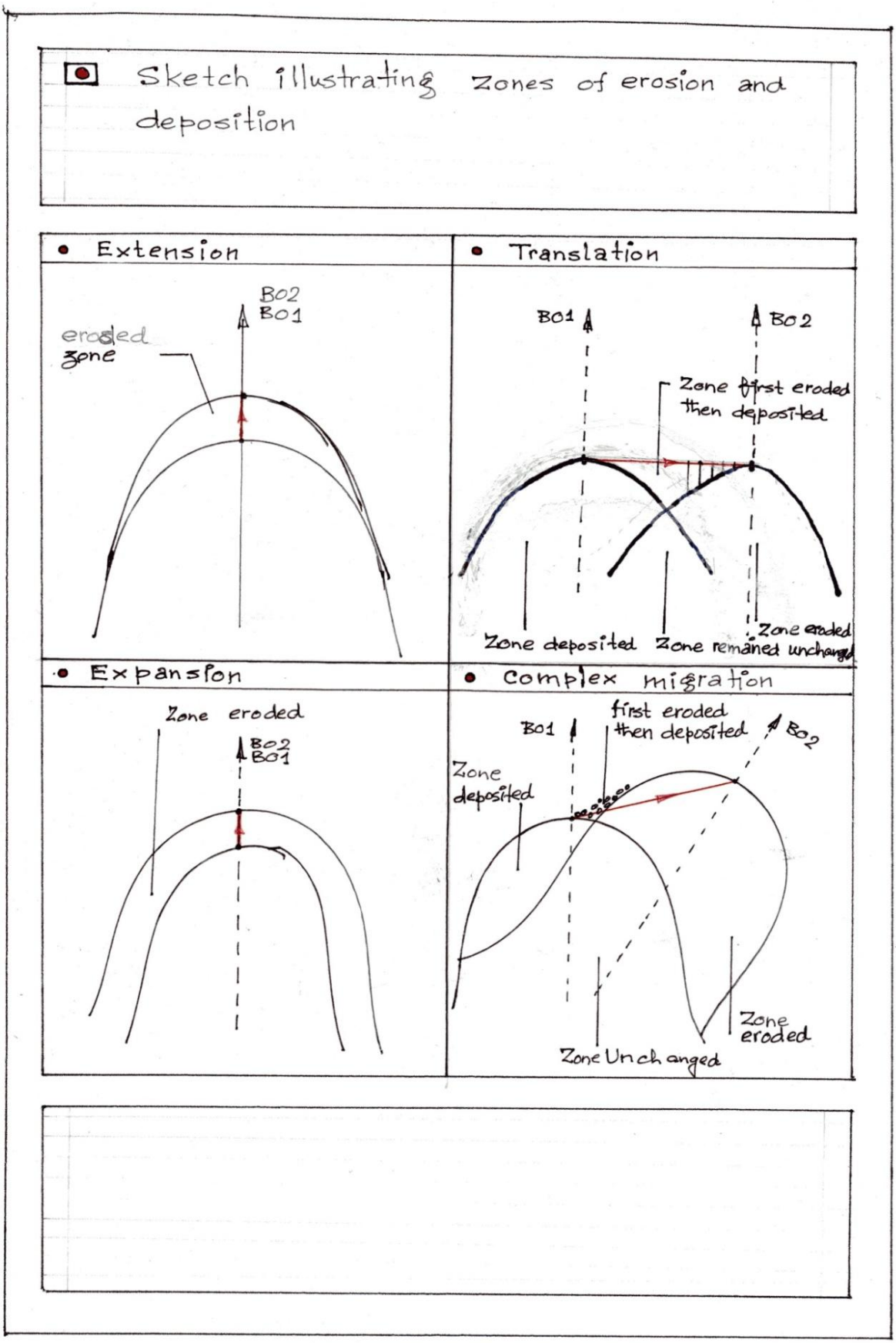

Figure 1.15: Illustrating zones of erosion and deposition during migration of an outer bank of a bend of an alluvial stream.

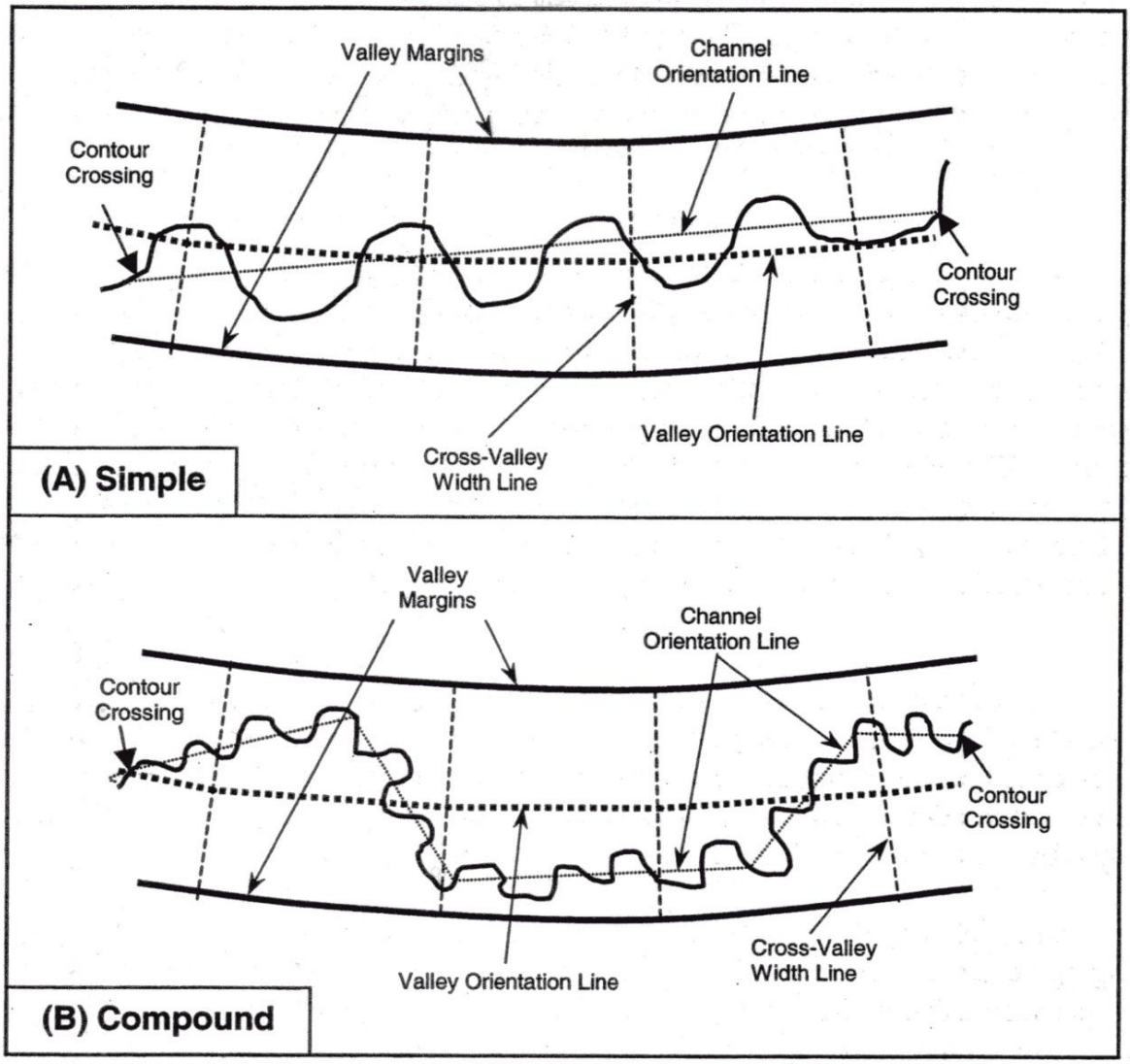

Figure 1.16: Bend with respect to valley (from Lagasse et al 2003, p83).

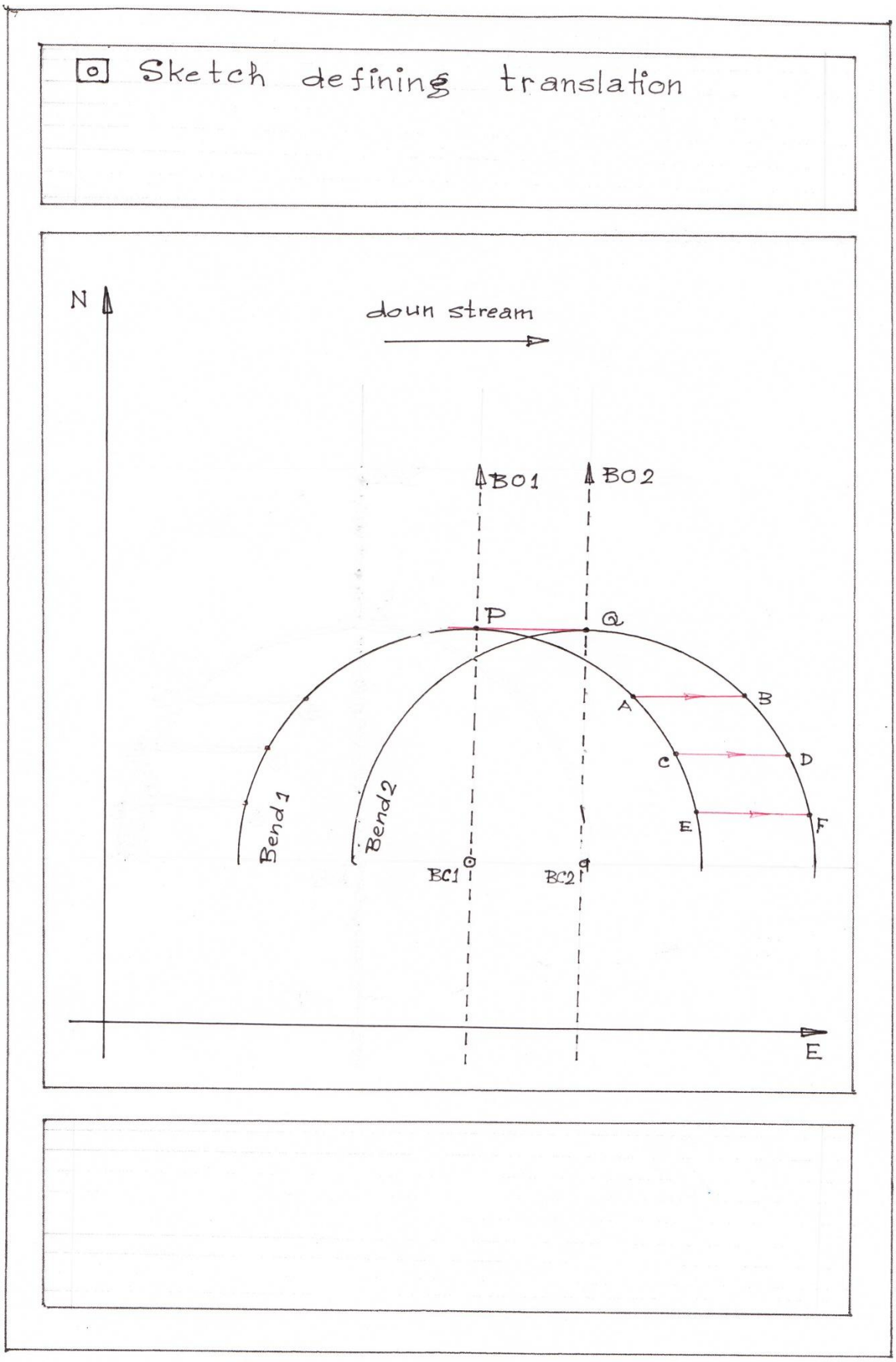

Figure 1.17: Defining mode of movement - extension of a bend of an alluvial stream.

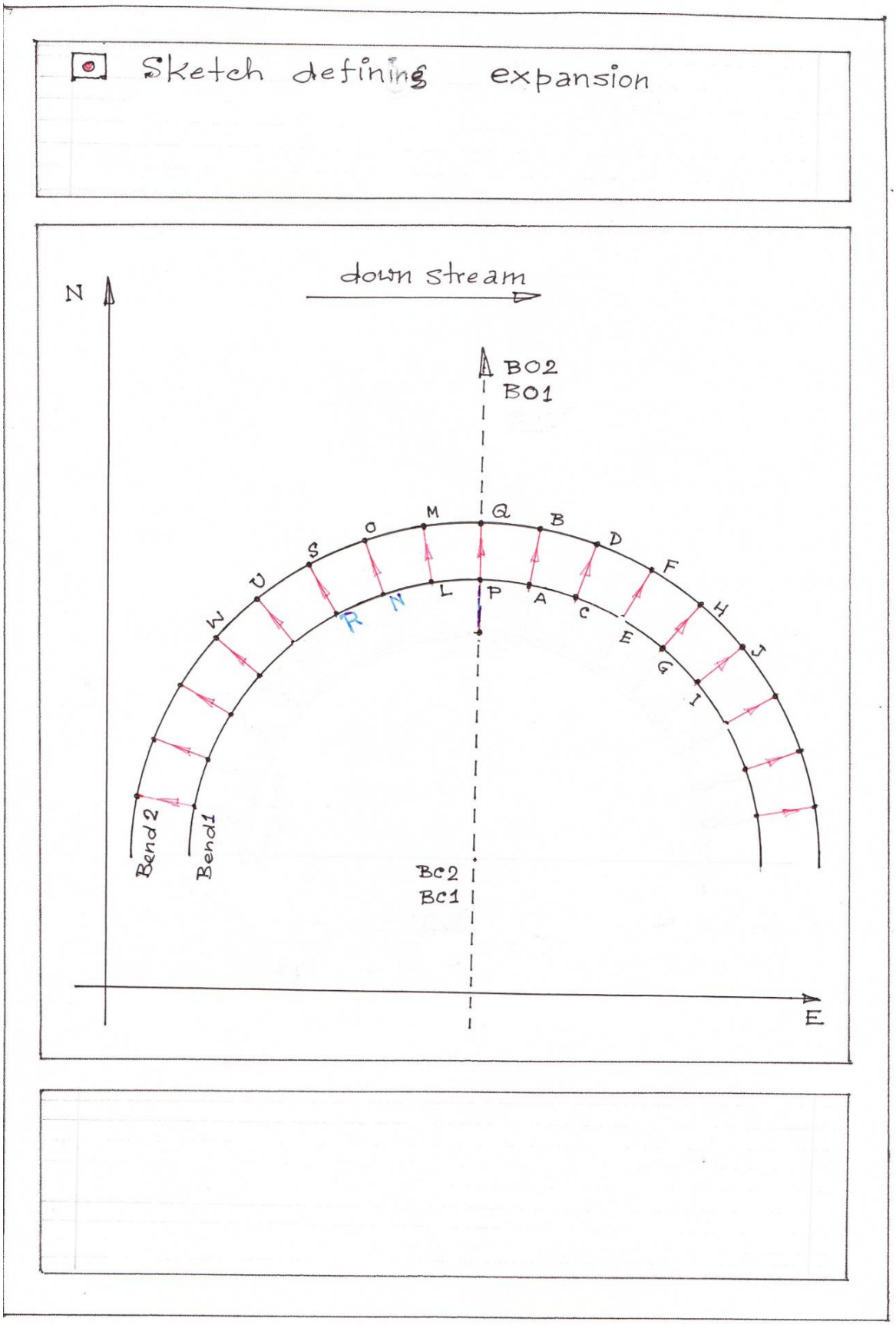

Figure 1.18: Defining mode of movement - expansion of a bend of an alluvial stream.

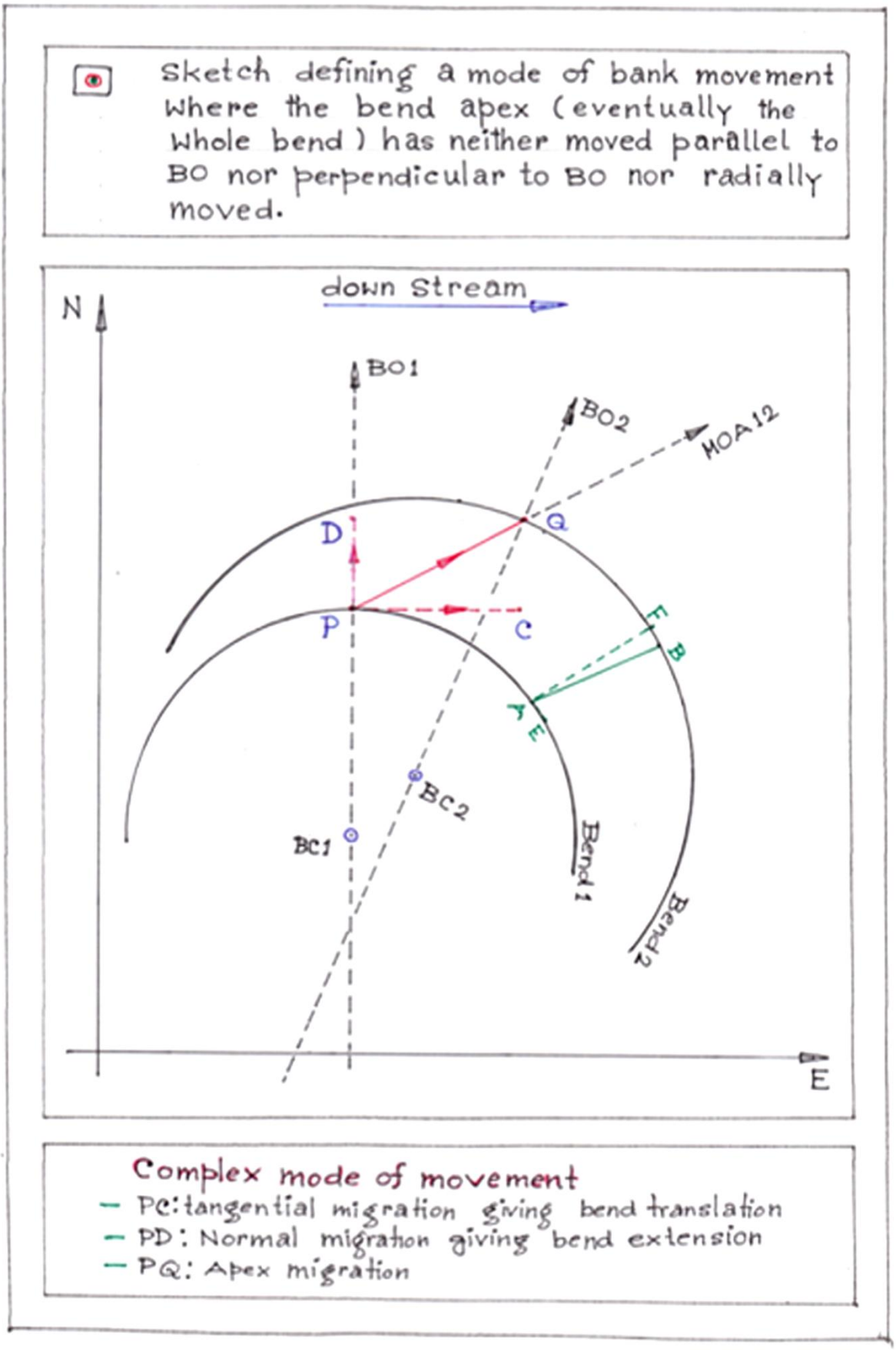

Figure 1.19: Defining complex mode of movement of a bend of an alluvial stream

It is impossible to trap modern physics into predicting with perfect determinism because it deals with probabilities with the outset.

--- Sir Arthur Stanley Eddington

Chapter 2
Options for Simulating and Predicting Bend Migration

2.1 Physically-based Approach

Deterministic methods for the analysis of bend migration can be developed based on analysis of the physical processes responsible for bend migration. Adopting a physically-based, analytical approach means that the fluvial processes and soil mechanics responsible for driving morphological changes at bends through time and space, and more specifically those associated with bend migration, must be described using explicit, analytical formulations. A practical, deterministic model can then be built by employing numerical techniques to solve those formulations without losing the virtues inherent to them. In this way a deterministic model should be capable of simulating the actual migration of a meander bend. However, it may be questioned whether such formulations are known for all of the processes and mechanics relevant to bend migration. Also, many of the variables required to solve existing formulations are either unknown or the data needed to define them are unobtainable in terms outside of controlled, laboratory conditions so that it is doubtful that they properly represent *natural* processes. Finally, the specialised equipment, technical skills and prohibitive costs of gathering high quality data on those variables that can be measured in the field severly limit applications of physically-based models.

Putting these problems aside, it can be conceived that a process-based model capable of simulating bend migration deterministically should include not only algorithms describing hydrological, hydraulic, sediment transport and geotechnical factors, but also numerical analyses

representing bank and floodplain vegetation types and densities. Such a model would also need to account for spatial and temporal variations in soil and vegetation properties. Representing all these processes and the variability that is a fundamental attribute of natural systems, in mathematical formulations appears, on the face of it, to be a major challenge. In this context, it seems likely that physically-based simulations are likely to be partial representations of nature at best though they may still be sufficient for useful purposes. These issues can be amplified by examining some attempts at using numerical modelling to simulate meander migration.

Nagabhushanaiah (1967) developed an early equation for meander expansion which related the origin and development of meanders in an alluvial channel to the erosion of bed material and its subsequent deposition downstream. This treatment falls short of the requirements outlined above as it does not account for the properties of the bank material and their affects on bend mechanics, which have been demonstrated to influence the geometric properties and migration rates of bends (see for example, Thorne (1992)). Conversely, Chang (1984) developed a water and sediment routing model (Fluvial-11) that accounts for bank properties using a proxy variable: bank geometry. However, the bank profile is assumed to be simple and planar, which is a geometry associated with banks formed in homogenous, non-cohesive materials. Therefore, this model has limited applications, since very few natural rivers have outer banks at bends featuring planar profiles formed in functionally non-cohesive sediments. In this context, Cunge (1984) concluded that the then existing analytical models should not be taken as representing reality, since complexity in bank characteristics were not properly simulated. Sun et al. (1996) developed a deterministic model in which bend geometry and shifting depends mostly on the discharge and valley slope, and does not depend on the erodibility of the sedimentary deposits making up the banks. They concluded that numerical simulations were capable of realistically reproducing the configuration of bends observed in nature through hindcasting, but were unable to use the model to predict meander change or migration rate.

Odgaard (1989) developed a meander model in which he used the ratio of near-bank, depth-averaged velocity to the section-averaged velocity to predict bank retreat. The relationship between these variables was represented by linearization of the flow equations, which renders it inapplicable to bends with large curvatures because the distribution of velocity at a bend becomes

non-linear as the bend radius shortens. In spite of having many good attributes, Odgaard's modelling approach is weak theoretically, in that it does not account for convective accelerations that are now generally regarded as being crucial in affecting the pattern of flow at bends with prominent point bars (Dietrich et al, 1983).

In an extensive review on mathematical models of planform changes, Mosselman (1995) found some utility in several 2-dimensional, depth-averaged models in that they helped provide an understanding of how meandering planforms evolve. However, none of the models reviewed can be regarded as generally applicable due to various limiting assumptions, and none is available in the form of easy-to-apply software suitable for routine practical applications. For example, Garcia et al. (1994) used two-dimensional, depth-averaged velocity distributions in bends to devise a tool for stream management and engineering, but the assumption that the channel width is constant seriously limits its applicability. Even more fundamentally, there is a theoretical limitation in that sediment continuity is neglected.

The applicability of more recent, numerical modelling approaches is also limited, since they do not account for all the degrees of freedom involved in channel adjustments. Rivers respond to input/controlling variables through natural adjustment in channel roughness, channel geometry, planform geometry, gradient, boundary materials characteristics (Simon and Darby, 1997). However, most meander models neglect adjustment of channel width through time (Darby and Thorne, 1993). In fact, neglecting width adjustment in models of channel morphology seriously biases predictions of bed-level change in rivers with erodible banks, as shown, for example, by Thorne and Osman (1988a, 1988b) and Darby et al. (1996).

2.2 Empirical Approach

2.2.1 Meader Wavelength and Channel Width

Studies investigating relationships between planform variables in meandering channels date from the 1950s, 1960s and thereafter. In an early study, Leopold and Wolman (1957) developed a regression relationship between meander wavelength and channel width with the form:

$$L = 6.5W^{1.1} \quad (2.1)$$

where, L = meander wave length (in ft) and W = bankfull stream width (in ft), for channel widths ranging from less than one foot for a flume channel, to a mile, in the case of the Mississippi River, and based on data derived from straight as well as meandering rivers.

Later, Leopold and Wolman (1960) developed the following relationship:

$$L = 10.9W^{1.01} \quad (2.2)$$

where, L = meander wave length (in ft) and W = bankfull stream width (in ft).

Williams (1986), using a wide range of data (191 observations), later found the relationship:

$$L = 7.5W^{1.12} \quad (2.3)$$

where, L = meander wavelength (m), W = bankfull width of the river (m).

Comparison of these equations reveals considerable differences between them. For Equation 2.1, the width range is huge and L/W values vary from around 7 to around 15. However, Equations 2.1 and 2.3 yield L/W values that are more consistent and, in fact, quite similar. Taking Equations 2.1, 2.2 and 2.3 together, it becomes difficult to conclude that there is a unique relationship between meander wavelength and width. It must, therefore, be accepted that there is real variation in the relationship between meander wavelength and width as a function of the range of channel widths in the database from which the relationship was derived. This is, perhaps, inevitable given that the relations are empirical and derived from data that represent situations particular to the rivers from which they were derived. Hence, we find such variations in all empirical equations. In principle such relationships cannot be applied to rivers or situations other than those for which they were derived without calibrating and or validating them by analysing adequate amounts of data derived from those new rivers and situations. In practice, this means fitting a new relationship again and again, every time the empirical approach is adopted. In conclusion, though these empirical relationships should not be applied directly to other situations without being recalibrated, they can still provide a general understanding of meander geometry and information of the relationship between morphological parameters describing the channel planform.

2.2.2 Meander Wavelength and Bend Radius of Curvature

Leopold and Wolman (1960) derived the following relationship between meander wave length and radius of curvature:

$$L = 4.7R^{0.98} \quad (2.4)$$

where, L = meander wave length (ft), R = radius of curvature of the centre line of the stream channel (ft).

Williams (1986) computed on 79 available data values and found geometric mean value of

$$R/W = 2.43 \quad (2.5)$$

where, R = centreline radius of curvature (m), and W = bankfull width of the river (m). The range of R/W values was from 1.02 to 6.97.

If the exponents in Equations 2.2 and 2.4 are approximated by unity, then this suggests that the characteristic value of R/W for a mature meander bend is 2.3. Taken together with Equation 2.5, there is considerable empirical evidence that dynamically stable bends have R/W values of the order of 2.3 to 2.4. These values are also in the range suggested by the theoretical work of Bagnold (1960).

Bagnold (1960) worked on the physics of flow in bendways and the associated energy losses. His work indicated that energy loss was a minimum when the flow was guided by bends with an R/W (ratio of the centre line radius to width) between 2 and 3. For a given channel width, as R decreases the bend gets tighter. When the value of the ratio R/W falls below the range 2 to 3 flow separation occurs both at the outer bank at the bend entrance and at the inner bank at the bend exit. These separation zones constrict the flow width, produce large-scale reverse eddies and distort the free surface; hence there is an increase in energy losses in comparison with bends with values of R/W in the range 2 to 3. The empirical equations above indicate that, in nature, many bends do indeed develop to the point that their R/W value falls between 2 and 3, coinciding with

the minimum energy loss condition. It may be the case that this allows flow in the bend to drive more migration and it could explain why many of the empirical plots of migration rate versus R/W show the highest migration rates for bends with R/W values in the range ≈ 2 – 3.

2.2.3 Meander Bend Migration Rate

Hickin and Nanson (1975) derived regression models to relate the amount of migration to the ratio of the radius of curvature of the bend to the channel width (Figure 2.1). The form of the relationships is:

$$M = 0.1(r_m/w_m)^{2.05} \qquad (1.3 < r_m/w_m < 2.9) \qquad (2.6)$$

$$M = 5.5/(r_m/w_m)^{1.73} \qquad (2.9 < r_m/w_m < 7) \qquad (2.7)$$

where, M = average rate of migration (my^{-1}) and r_m/w_m = ratio of mean radius of curvature to mean channel width.

These relationships were developed using data from only 10 sites on the Beaton River in north western Canada. The usefulness of these models appears to be very limited for two reasons. Firstly, Equation 2.6 was derived from only four data points and Equation 2.7 was derived from just 6 data points. Secondly, the data distribution is dissimilar to the distributions that have been obtained later with many more data points. For example, Nanson and Hickin (1986) obtained a different relationship based on 118 data points, while Biedenharn et al. (1989) used 160 data points. Generally, it is found that, when there are a large number of data points for a specific value of R/W, there is wide variation in the observed values of migration rate (M). Under these circumstances, attempting to fit regression relationships like Equations 2.6 and 2.7 does not appear meaningful.

In the literature we also find attempts to apply multiple regression models. Nanson and Hickin (1986), with a view to predicting bend migration, developed several regression relations using more than one explanatory variable. In this approach, data were obtained from 118 bends from 18 rivers in provinces of British Columbia and Alberta in Canada. The resulting multiple regression relationships were:

$$M_{bar}^* = 1.663Q^{0.482} \quad S^{0.368} \tag{2.8}$$

$$M_{bar}^* = 0.301W_{bar}^{0.895} \quad S^{0.271} \tag{2.9}$$

where, M_{bar}^* = river-averaged lateral migration rate (my^{-1}) of the channel along the erosional axis of bends falling into the range $2 < R/W < 4$, Q = discharge for the 5-yr flood (m^3s^{-1}), S = water surface slope, and W_{bar} = reach-averaged width (where the width is measured at and around the inflection point between bends)

The authors found that in Equation 2.8 the model could explain about 52% of the variability while Equation 2.9 explained 54%. Hence, though the fit of the relationships is not really good enough to support reliable predictions, it still appears promising.

The authors suggested that the total amount of erosive work performed during bend migration could be expressed by the volumetric erosion rate at the point of maximum migration. Hence, they obtained:

$$M_{bar}*hbar = 25.06 \quad Q^{0.788} \quad S^{0.74} \quad D_{50}^{-0.209} \tag{2.10}$$

$$M_{bar}*hbar = 62.6 \quad Wbar^{1.369} \quad D_{50}^{-0.021} \quad S^{0.568} \tag{2.11}$$

where, D_{50} = median size of the basal sediment in the outer bank (mm).

The authors found that in the case of Equation 2.10 the model could explain 69% of the variability, with the equivalent figure being 63% for Equation 2.11. Although the fit of these two equations is better than for Equations 2.8 and 2.9, there is still, however, a considerable amount of unexplained variance. While these equations could help in predicting the sediment yield due to bend migration, they cannot help with predicting the likely distance of migration during a specified period or the probability of bank erosion threatening a particular asset or structure near the river. Also, it must be remembered that their use should be limited to those rivers, situations and data ranges from which they were developed.

In addition to the models discussed above, the authors also developed multiple-regression models based on combinations of other variables such as stream power and slope, and stream power and median size of the basal sediment in the outer bank. Unfortunately, these models did not produce any better fits to the data than those discussed above.

2.3 An Evaluation of Empirical and Analytical Approaches

Johns Hopkins University conducted a study on behalf of the US Army Corps of Engineers, Waterways Experiment Station (Cherry et al., 1996) to evaluate the usefulness of empirical and analytical approaches to predicting planform changes and bankline migration in meandering rivers. They evaluated the use of empirical approaches using statistical relationships between planform variables and controlling variables such as water discharge, sediment load, and stream gradient. To evaluate deterministic approaches, they used a flow-based computational model.

In this evaluation the Hopkins team used data first collected and analysed by Brice (1982). Within the Brice dataset, there were 133 sites on meandering rivers. The data recorded for the meandering sites included width, sinuosity, gradient, wavelength and some hydrological data. Among these 133 sites there was a small group of 26 sites at which the radius of curvature and erosion rate for each bend were also reported. Data from these 26 sites were used to evaluate the predictive capability of the numerical models.

The Hopkins study developed a simple, linear regression in order to establish a predictive relationship between the independent and dependent variables. However, the results were not promising and commenting on this outcome, the report concluded that, “clearly, this multidimensional variability cannot be captured in a simple regression equation”.

The Hopkins evaluation tested bend flow meander migration models developed by Ikeda et al. (1981) and Garcia et al. (1994). They evaluated the predictions made using the numerical models against observed values for the 26 sites as discussed earlier. In evaluating the models the team

noted that some of the over simplifying assumptions they included (e.g. a single, steady discharge and a uniform channel width) were the main factors contributing to errors in predicting planform changes and bend migration.

Another flaw apparent in the numerical models was that they treated the migration process as smooth and continuous. But in nature, bend migration is a discontinuous process (as noted by Hickin (1974); Nanson and Hickin (1983) and many other researchers). This is the case because bank erosion takes place, not only through the detachment, entrainment and removal of bank material as individual grains or aggregates under the action of fluvial and sub-aerial processes, but also when all or part of the bank collapses *en masse*, in response to geotechnical instability. This explains why bank erosion and, hence, meander migration rates vary both temporally and spatially from bend to bend (Lawler et al, 1997).

The outcomes of the Hopkins study show that the validity and applicability of the numerical models they tested are limited. They also highlighted the importance of further investigation of how local factors influence the rate of erosion. In closing, the Hopkins team concluded that, "Further refinements in bendflow modelling will not improve our predictive capability until we find a more rational way to wed the flow model to a bank erosion model."

2.4 Probabilistic Approach

The arguments put forward in Sections 1 to 3 of this chapter highlight limitations to the utility of numerical and empirical approaches to meander migration analysis and prediction. The approaches discussed so far have all been deterministic in that they attempt to express and predict the future migration rate using a mathematical function involving the controlling variables. In this section, it is argued that a probabilistic approach could be useful as an alternative means of analysing and predicting meander bend migration.

The approach described here is empirical in that it is entirely based on historical records of river behaviour. It may appear initially that an empirical approach does not describe or represent the

physical processes and the mechanics that drive bank erosion, bank failure and, hence, bend migration. However, empirical data on bend migration reflect the morphological outcomes of those causative processes as they have operated in the past. Hence, historical data do represent the combined outcome of all the operating processes, at the bend in question.

For this approach to be useful, the main issues are the authenticity and sufficiency of the historical data. In this context, authenticity rests on:

1. choosing appropriate variables to represent the causative processes, which reflect the effects of those processes in driving bend evolution, and,
2. employing valid methods of measuring and averaging the data correctly.

Sufficiency rests on the volume and range of measured data being adequate to support the required probabilistic and statistical methods so that they can reliably be employed.

In order to predict future bend migration using this approach, it is necessary to build a model in which the selected parameters can be incorporated as explanatory variables. In doing this the researcher has to understand the degree of importance of the pertaining variables and choose as many as possible depending on the data, resources, time, and budget available. Then, through analysis and experimentation, the researcher has to produce an optimised approach (i.e., one that has the least number of variables required to support acceptable prediction of bend migration rate). It follows that the success of an empirical model depends on selection of appropriate variables, the availability of an adequate amount of accurate data and the expertise of the researcher. Therefore, in th first instance, this type of approach hinges on obtaining access to a large volume of data representing historical bend migration.

In considering the variables to be selected and the form of the function used to predict bend migration, the R/W approach developed by Hickin and Nanson (as described in Section 1.4) provides a useful starting point. In this approach there is a functional relationship between the rate of migration and the bend radius - both expressed in non-dimensional form. Since this is a tool

that is well established and which has been verified by many researchers working independently, the general form of the relationship between bend radius and migration rate has now been established and generally accepted. However, past investigations have also shown that, while the form of the relationship between bend radius and migration rate is well known and the stages of evolution characteristically displayed by bends are repeatable, *absolute* rates of bend migration vary widely for bends of a given radius. Therefore, in terms of practical river engineering problems one cannot use a tool of the type developed by Hickin and Nanson unless site specific data on observed rates of bend shifting are available for calibration purposes. Unfortunately, the opportunity to use data to calibrate Hickin and Nanson's tool for application to a particular river is limited by the availability of the necessary data and the fact that it is time and resource consuming to develop the calibration equations.

A further problem arises if it is proposed to use a Hickin and Nanson type of analysis to predict (rather than explain) bend shifting. In predicting a future condition, uncertainty exists because future values of the variables governing bend evolution are not only unknown – in fact they cannot be known. For example, velocities and shear stresses on the outer bank depend on discharge and the future magnitudes and sequences of bank eroding flows – which are indeterminate. Similarly, the erosion resistance of the bank depends on bank properties such as height and slope angle (which are spatially heterogeneous and unknown) and local conditions of bank strength (which is both spatially and temporarily highly variable, in unpredictable ways).

The only way to deal with these uncertainties practically is to adopt a probabilistic approach. In such an approach, historical data on bend geometry and migration rate are analysed to develop relationships representing the *distributions* of observed migration rates as well as their central tendencies. The approach recognises that not one but many possible future records of migration are possible for any bend, depending on the magnitudes and frequencies of forcing events and the conditions of bank resistance to erosion that actually operate when a driving event occurs. It then provides the person making the prediction with the option to be as conservative as he or she wishes in making a prediction of bend shifting, based on selecting a probability that the predicted

rate not being exceeded. This type of approach is not only more realistic than a deterministic prediction, it is also consistent with applications based on assessing the risks posed by bend migration in terms of the probability of erosion-related hazards occurring through land loss or damage to infrastructure.

The empirical, probabilistic method requires a large amount of reliable data in the form of historical records of bend migration in meandering rivers, obtained from aerial photographs and/or historical surveys and maps. The functional relation proposed by Hickin and Nanson contains just three parameters:

1. maximum magnitude of migration by a bend between two successive observations (M),
2. minimum bend radius of curvature (R) and,
3. channel width (W).

The variables can be arranged into dimensionless form by taking the ratio of radius of curvature to channel width (R/W) as the independent variable (x) and ratio of annual meander migration rate to channel width ((M/W)/Y) as the dependent variable (y). Statistical analysis of the Hickin and Nanson type of expression can then be performed using a bi-variate probability distribution. The great advantage of this approach is that the probabilistic tool produced requires only simple measurements of bend radius and channel width to support prediction of the future rate of bend migration, together with a user-selected probability that the predicted rate will not be exceeded.

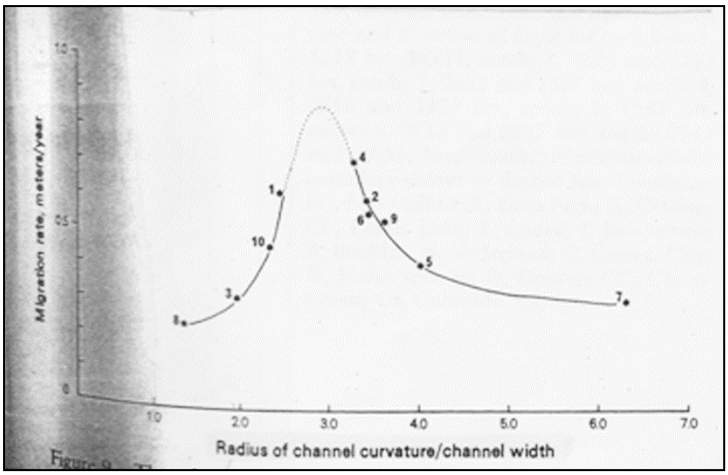

Figure 2.1: The relation of migration rate to the ratio of radius of curvature to channel width based on the data at 10 survey sites on the Beaton River in Canada (from Hickin and Nanson, 1975).

If a man will begin with certainties, he shall end in doubts; but if he will be content to begin with doubts, he shall end in certainties.

--- Francis Bacon

Chapter 3
NCHRP Bend Migration Study (2003)

3.1 Study Approach, Measurements and Database

In the USA, the National Cooperative Highway Research Program (NCHRP) commissioned a project (Project No. 24-16) with the objective of developing a practical methodology to predict the rate and extent of channel migration in proximity to road bridges. The project was sponsored by the American State Highway and Transportation Officials (ASHTO), in cooperation with the Federal Highway Administration (FHA).

In the study, an empirical approach was selected, with bend migration data being obtained from aerial photographs and maps that were already available for rivers in 24 states of the USA, in the 1930/40s, 1950/60s and 1990s. A map showing the states that contain the rivers in the NCHRP database is shown in Figure 3.1 and the names of the rivers are listed in Table A4.3. The chief source of data was the Brice data set held by the US Army Corps of Engineers, although supplementary data were obtained from other researchers. The NCRHP study team also obtained hydrologic, hydraulic and sediment data for those study sites where such data was already available.

In the NCHRP study, only meandering rivers were selected from among all river patterns represented in the available data sets. Meandering channels were classified according to the Brice Typology from A to G, as described in Section 1.1. Individual bends were identified and numbered at each site. For each bend, planform and position changes were detected by comparing

time sequential, aerial photographs and/or maps. Since relatively stable rivers require less attention from highway bridge inspectors, another objective of the project was to identify stable meandering reaches.

Based on the original work of Brice, the NCHRP study investigated the data base and found that equi-width channels (where the channel width is uniform and steady through time and space) are more stable than those in which the channel is wider at bends or in which the width varies in an irregular fashion. On this basis, they reclassified Brice Type B meandering into B1 and B2, and Brice Type G meandering into G1 and G2, depending on the degree and spatial distribution of width variability. The definitions of B1, B2, G1 and G2 type meandering are illustrated in in Chapter 5 of this thesis (Figure 5.1). In this way, the NCHRP database used a Modified Brice Typology in which there are 9 channel types (rather than 7, as in the original Brice Typology).

The variables listed for each bend in the data base include, among others:

- radius of curvature of outer bank
- northing of the centre point of the bend
- easting of the centre point of the bend
- valley orientation
- bend orientation
- meander sinuosity
- meander wavelength
- meander amplitude
- channel width at crossing,
- channel width at bend apex
- channel hydraulic depth at crossing
- maximum channel depth at bend apex
- crossing width/depth ratio
- channel slope
- valley slope

Measurements

This research uses secondary data that were measured and compiled in the NCHRP study performed by Ayres and Associates (Lagasse et al. 2003, 2004). A brief description of the means used to measure the main parameters that are used in the present research study is provided here.

In compiling the data, historical maps and aerial photographs were scanned and geo-referenced. In determining changes in banklines and measurements of other parameters, wherever possible, both

manual overlay techniques and automated procedures were applied, to improve accuracy. The automated procedures used for delineation of the banklines and measuring bend geometry were CAD software (Bentleys Microstation) and an ArcView Extension (Data Logger).

The procedures required to use Data Logger to take measurements at a bend were:

1. Locating registration points along the outer bank of a bend in question;
2. Inscribing the arc of a circle fitted to those registration points;
3. Measuring the desired parameters defining bend geometry, for example radius, channel width etc.

Bankline Delineation

On an aerial photograph accurate delineation of a bankline mostly depends on the distribution and density of riparian vegetation. Where vegetation was intermittently dense along a bank, the bankline could be approximated by connecting the visible portions between less densely vegetated sections of the river. But where the bank was completely obscured by vegetation, the bankline had to be approximated by assuming that it connects the centres of each of the trees growing at the edge of the stream. Hence, in these cases, a line was drawn connecting the crowns of trees growing along the edge of the channel.

Radius of Curvature

A best-fitted circular arc was inscribed by setting 5 to 7 registration points along the outer bankline, between the beginning and the end of the bend. The centre of that fitted circular arc was considered to be the centre of curvature of the outer bank. Hence, the length of the line connecting the centre to a point on the arc was taken to represent the radius of curvature of the outer bank of the bend.

Channel Width at Crossing

Top bank widths were measured at the upstream and downstream crossings as defined by the upstream and downstream ends of the best-inscribed arcs. The channel width at the crossing listed in the database is the average of these two measurements.

Channel Width at Bend Apex

This was measured at the widest point in a bend from the top of one bank to the other.

Bend Apex

The bend apex was defined as the mid-point of the best-fitted circular arc, as described above.

Bend Orientation

Bend orientation was defined by the angle that a line connecting the bend centre to the bend apex made with the Easting axis, with the convention that counter clockwise with reference to due east is positive.

Detailed discussion on defining, identifying and characterising bends for the purpose of migration analysis is provided in Chapter 7.

Database

A sample of the database for Bend 5 on the Brazos River at Thompson, Texas (Brice Type C) can be seen in Figure 3.2. In total, the NCHRP database contains such data for 1,505 bends from 140 sites in 125 reaches along 89 meandering rivers, spread across 24 States in the contiguous states of the USA. A type-wise summary of the bend data is listed Table 3.1.

Table 3.1: Summary of bend classification in the NCHRP database

Brice Types	Number of Locations	Number of Sites	Number of Bends	Cumulative Number of Bends
A	7	7	61	61
B1	17	20	232	293
B2	18	20	207	500
C	53	63	634	1134
D	5	5	48	1182
E	13	13	137	1319
F	4	4	19	1338
G1	6	6	125	1463
G2	2	2	42	1505
	125	**140**	**1505**	

3.2 Evaluation of the NCHRP Study

The main objective of the NCHRP study was, as stated in their final report**,** *"to develop a practical methodology to predict the rate and extent of channel migration (i.e., lateral channel shift and down valley migration) in proximity to transportation facilities."*

(Lagasse et al., 2003, page 4).

The principal product of this research is a stand-alone *Handbook* for predicting stream meander migration using aerial photographs and maps. The study team claim that,

"The methodology should enable practicing engineers to evaluate and determine bridge and other highway facility locations and sizes and ascertain the need for countermeasures considering the potential impacts of channel meander migration over the life of a bridge or highway river crossing".

(Lagasse et al., 2003, page 4).

The NCHRP study not only supplied the database used in the research reported in this thesis, but also provided the possibility for a detailed consideration of bend migration analysis and prediction that informed development of the probabilistic model developed herein. It is in this context, that the subsequent sections of this chapter present a detailed evaluation and commentary on the NCHRP methodology and the lessons that can be learned from considering whether the research achieved the objective recounted above.

3.2.1 Can Movement of the Bend Centre Adequately Represent Bend migration?

The aim of the NCHRP study was to quantify historical meander bend migration and use the results in predicting the potential for future migration. Hence, it was necessary for the researchers to choose an element/variable pertaining to the bends capable of adequately representing the

historical migration of the bend in question. The NCHRP study used movement of the centre of curvature of the bend for this purpose. The adequacy of this decision is examined in Box 3.1.

Box 3.1

In the Final Report (Lagasse et al., 2003, page 55) it is stated that, "Each of the three modes of bend movement are vectors, i.e., they each have a magnitude and direction. Figure 12 (which is reproduced here as Figure 3.3) depicts the modes of meander movement (positive rates are shown for each mode). The direction for extension is in the bend orientation direction and the direction for translation is perpendicular to the bend orientation. The bend radius does not have a specific direction. In order to assess the amount of bank movement, the three vectors representing migration were combined into a resultant magnitude, termed "apex movement". Apex movement is the movement of the outer bank at the bend apex and is computed as the vector sum of the three components of movement at the apex location."

A paragraph of the Final Report (Lagasse et al., 2003, page 84) says, "Bend migration can be reasonably described by four modes of movement. Extension is across valley migration and is easily measured at the bend centroid. Similarly, translation is down-valley migration and is also measured at the bend centroid. Expansion (or contraction) increases (decreases) bend radius. Rotation is a change in the orientation of the meander bend with respect to the valley alignment." This was illustrated in Figure 27 of the Final Report, which is reproduced here in Figure 3.4.

In the Handbook (Lagasse et al., 2004), in describing the methodology and setting illustrative examples, the study used movement of the bend centre to represent meander migration. This is illustrated here in Figure 3.5, which is a reproduction of Figure 7.6 in Lagasse et al. (2004). The original caption is: "Depiction of the bends from the 1937 and 1966 outer bank lines as defined by best-fit circles. The movement of the bend centroids (arrows) defines migration of the bends". The related text on this figure describes how, "Figure 7.6 compares the best-fit circles and bend centroids for each bend traced from the aerial photographs from 1937 and 1996. The vector arrow at each bend shows the direction and magnitude of movement of the bend centroid between 1937 and 1996. For each bend, this vector may be resolved into cross and down valley components to determine the rates of meander migration. The change in radius of curvature of each bend is defined by the difference between the magnitudes of the vectors for 1937 and 1966."

Based on the material summarised in Box 3.1, it can be concluded that the NCHRP study considered bend centre (i.e. "centroid") movement as being representative of the bend migration and clearly used this both in quantifying the magnitude and direction of migration, and in predicting potential future migration. However, two criticisms that can be levelled concerning the way that bend movement was represented and resolved into vectors in the NCHRP study are that:

(a) the report is unclear on how this was actually achieved, and;

(b) the treatment of orientation is unsatisfactory.

To justify and examine these two issues, three aspects of the NCHRP methodology were considered, to investigate whether the NCHRP methods are meaningful in principle:

1. using scaled drawing to examine bend movement.
2. using practical examples (i.e. observing the movement of bends as depicted in aerial photographs and maps taken from NCHRP database).
3. computing meander movement using the NCHRP database.

3.2.2 Analytical Investigation

In the NCHRP Study Report it is claimed that the movement of the bend apex can be found by computing the movement of the bend centre and adding to this the change in radius. It follows that:

$$MMA12 = (MMC12 + \Delta R12) \quad (3.1)$$

where, MMA12 = movement of the bend apex between time 1 and time 2; MMC12 = movement of the bend centre between time 1 and time 2; ΔR12 = change in radius between time 1 and time 2.

MMC12 can be computed using the coordinates of the bend centre using:

$$MMC = SQRT[(EBC2 - EBC1)^2 + (NBC2 - NBC1)^2] \quad (3.2)$$

where, EBC1 = Easting of the bend centre at time 1; EBC2 = Easting of the bend centre at time 2; NBC1 = Northing of the bend centre at time 1; NBC2 = Northing of the bend centre at time 2.

ΔR12 can be found from:

$$\Delta R12 = R2 - R1 \tag{3.3}$$

where, R1 = radius of curvature of the bend at time 1; R2 = radius of curvature of the bend at time 2.

To check whether the claim made in the NCHRP Report is valid, migration distances measured at 15 representative bend apices were compared to those computed based on bend centre movement plus change in radius of curvature. The results are listed in Table 3.2 and illustrated in Figure 3.6.

Table 3.2: Comparison of migration distances based on measured apex movement and centre movement plus change in radius for 15 representative bends selected from the UoN/HRW database (all values in metres)

River	Location No.	Location	State	River Type	Bend No.	BIN	T1	T2	T3	MMA12	MMA13	MMC12+R12	MMC23+R23
Savanah River		Augusta	GA	B2	1	2B298	1938	1969	1993	93.43	102.70	80.21	33.19
					2	2B299	1938	1969	1993	78.45	111.26	70.90	37.08
					3	2B300	1938	1969	1993	45.48	63.13	39.24	34.63
					4	2B301	1938	1969	1993	81.71	144.92	73.67	132.41
					5	2B302	1938	1969	1993	111.13	101.58	93.54	91.12
Big Black River	Location 1	near Big Black	MS	C	1	C9	1938	1966	1996	55.85	118.36	33.96	50.19
					2	C10	1938	1966	1996	139.42	207.94	167.51	86.90
					3	C11	1938	1966	1996	116.94	86.47	54.04	129.58
					4	C12	1938	1966	1996	40.83	69.12	41.89	37.18
					5	C13	1938	1966	1996	68.78	42.94	51.36	116.60
English River		Kalona	IA	C	1	C138	1957	1969	1994	45.93	113.04	41.07	58.28
					2	C139	1957	1969	1994	38.92	33.09	53.56	5.31
					3	C140	1957	1969	1994	19.50	40.18	19.14	22.42
					4	C141	1957	1969	1994	20.25	40.70	30.31	20.44
					5	C142	1957	1969	1994	34.00	87.00	21.41	34.86

Examination of these results reveals that not in a single case does the measured distance correspond to the sum of the movement of the centre and the change of radius. Indeed, this is also true for the entire database. Therefore, it can be concluded that movement of the apex of a bend cannot be found based on the movement of the centre plus the change in radius. It appears that the claim made in the NCHRP study was a misconception.

3.2.3 Investigations Based On Scaled Drawing

Further to the analytical investigations as given in Section 3.2.2 above, the issue of whether the movement of the apex of a bend can be found based on the movent of the bend centre plus the

amount of change in radius was also investigated graphically, and details are provided in Section A3.1 of the Appendix to Chapter 3. This graphical investigation also shows that movement of the apex of a bend cannot be represented by the movement of the bend centre plus the change in radius. In support to this, explanations are given in Column 4 in Table A3.1 under the heading 'Comment' in Appendix to Chapter 3. For example, in Case 1 the bend centre has not moved at all but there is an apex movement. Therefore, the fact is that apex can register movement even when the bend centre does not move at all. To provide another example, in Case 2, the bend centre has moved and bend radius has changed, but magnitude and direction of apex movement is entirely different.

The concluding explanation is that the bend apex can register movement even when the centre does not move at all. Even when the centre undergoes a movement involving a change in radius, the movement of the apex may have no concordance with the movement of the centre, in terms of magnitude and orientation. This is why the claim by NCHRP that apex movement can be predicted from movement of the centre was a misconception.

3.3 Conclusions

- The NCHRP Study did not investigate which element of the bend can best represent migration of the bend as a whole.
- The NCHRP Study does not resolve whether the bend centre or bend apex can better represent bend migration.
- The movement of the bend centre cannot fully represent migration of the bend as a whole.
- Despite what is stated in the NCHRP Report, movement of the bend apex cannot be found by computing migration of the bend centre and adding the change in radius.
- Although reference is made in the NCHRP Report and Handbook to computed rates of migration, the archived database only contains the measured data on bend geometry.
- Commendable points concerning the NCHRP Study are its extensive literature review and conclusion that an empirical, probabilistic analysis based on historical records provided a more practically useful approach to bend migration prediction than any existing, deterministic approach.

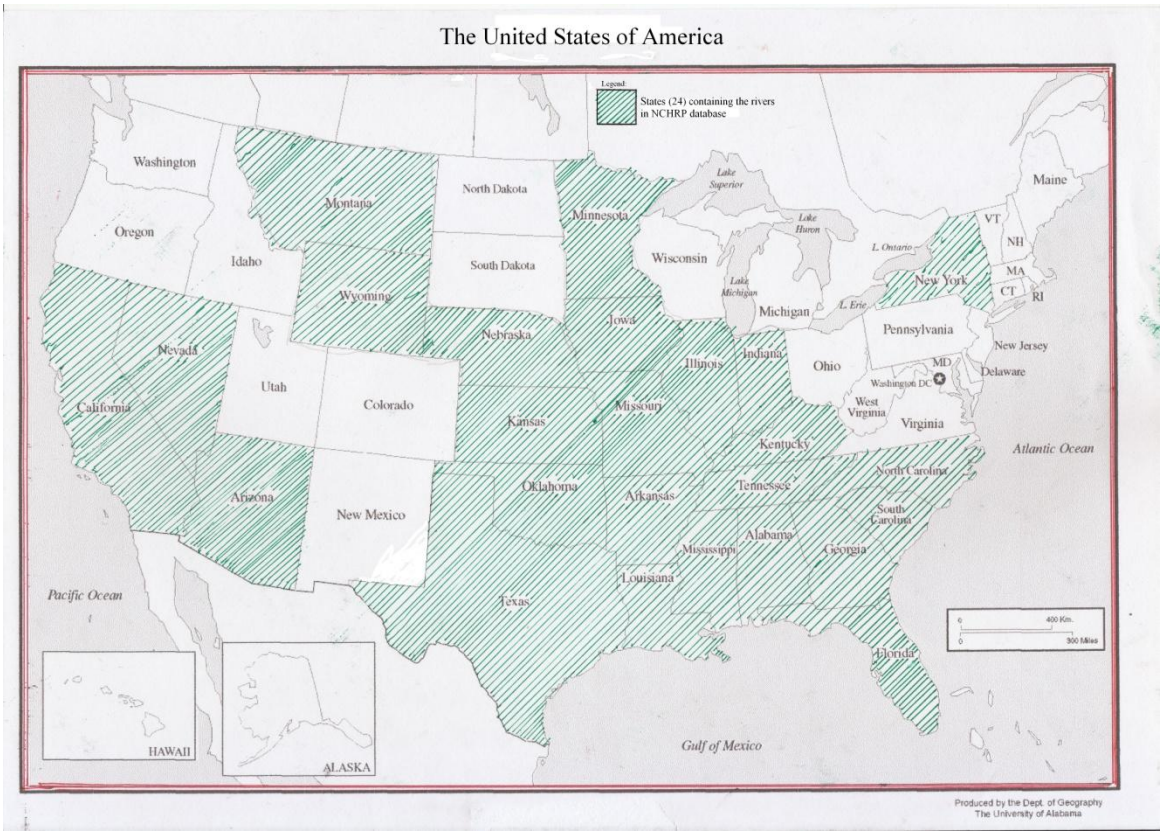

Figure 3.1: Distribution of States that contain the rivers represented in the NCHRP database.

Brazos River

BEND #5

(Each bend has a separate worksheet in this workbook.)

Location:	at Thompsons, TX
USGS 7.5' Quad Name:	Missouri City, TX
Nearest Gage Name and Number:	at Richmond, TX 08114000

SITE CLASSIFICATION

Flow Habit:	PERENNIAL
River Classification:	C
Sediment Load Type:	Mixed Load
Brice Bend Type:	Simple Symmetrical

Group	Variable	English Value			Units	Metric Value			Units
		1941	1964	1995		1941	1964	1995	
Planform	Outside Bank Avg. Radius of Curvature	1063	1192	1277	feet	324.0	363.4	389.4	meter
	Right or Left Hand Bend	L	L	L	---	L	L	L	---
	Center Point of Bend - Northing	10723107	10722996	10722950	feet	3268410	3268376	3268362	meter
	Center Point of Bend - Easting	818133	818039	817937	feet	249367	249339	249308	meter
	Valley Orientation	309.3	309.3	309.3	deg.	309.3	309.3	309.3	deg.
	Bend Orientation	307.6	292.9	289.4	deg.	307.6	292.9	289.4	deg.
	Channel Sinuosity	1.60	1.69	1.80	ft/ft	1.60	1.69	1.80	m/m
	Meander Wavelength	5176	6491	5475	feet	1577.8	1978.6	1668.9	meter
	Meander Amplitude	1240	1507	1197	feet	377.9	459.3	364.9	meter
Geometry	Channel Width at Crossing	452	446	417	feet	137.7	136.0	127.1	meter
	Channel Width at Bend Apex	512	751	436	feet	156.0	228.9	132.8	meter
	Channel Hydraulic Depth at Crossing	27	27	27	feet	8.2	8.2	8.2	meter
	Maximum Channel Depth at Bend Apex	NM	NM	NM	feet	NM	NM	NM	meter
	Crossing Width/Depth Ratio	16.8	16.5	15.5	ft/ft	16.8	16.5	15.5	m/m
	Maximum Point Bar Width in Bend	0.0	0.0	107.3	feet	0.0	0.0	32.7	meter
	Average Floodplain Width	1967	1967	1967	feet	599.5	599.5	599.5	meter
Slope	Channel Slope	0.00030	0.00029	0.00027	ft/ft	0.00030	0.00029	0.00027	m/m
	Valley Slope	0.00049	0.00049	0.00049	ft/ft	0.00049	0.00049	0.00049	m/m
Rough-ness	Estimated Channel Manning's n	0.03	0.03	0.03	---	0.03	0.03	0.03	---
	Estimated Floodplain Manning's n	0.09	0.09	0.09	---	0.09	0.09	0.09	---
Sediment	Bed Material D50	0.009	0.009	0.009	in	0.2	0.2	0.2	mm
	Bed Material % Si/Cl	4.33	4.33	4.33	%	4.33	4.33	4.33	%
	Bank Toe Material D50	NM	NM	NM	in	NM	NM	NM	mm
	Bank Toe Material % Si/Cl	59.47	59.47	59.47	%	59.47	59.47	59.47	%
Riparian Veg	Percent Vegetation Cover	NM	NM	>50% T	%	NM	NM	>50% T	%
	Root Depth as Percent of Bank Height	19	19	19	%	19	19	19	%
Discharge Data	Mean Annual Discharge	7882	6624	7854	cfs	223.2	187.6	222.4	cms
	Average Peak Discharge	66057	51268	54265	cfs	1870.7	1451.9	1536.8	cms
	Bankfull Discharge	---	---	51267	cfs	---	---	1451.9	cms
	Effective Discharge	---	---	16350	cfs	---	---	463.0	cms

REACH LIST

Vegetation Types:

Dense trees, swampland, and farming

***Activity Indicators:**

Old oxbows in floodplain; farming to edge of channel (vertical eroding banks) along most of right bank

Upstream Controls:

Flows regulated since 1941 by upstream reservoirs, floodwater-retarding structures, and irrigation diversions.

Downstream Controls:

0

*Activity Indicators (e.g. ridges and swales, neck cutoffs, chute cutoffs, recently abandoned meander bends, farming to edge of channel, crevasse splays, etc.)
NM = Not Measured or No Data

Figure 3.2: A typical database entry in the NCHRP Study for Bend 5 of the Brazos River at Thompson, Texas (from Lagasse et al. 2003, Figure 25).

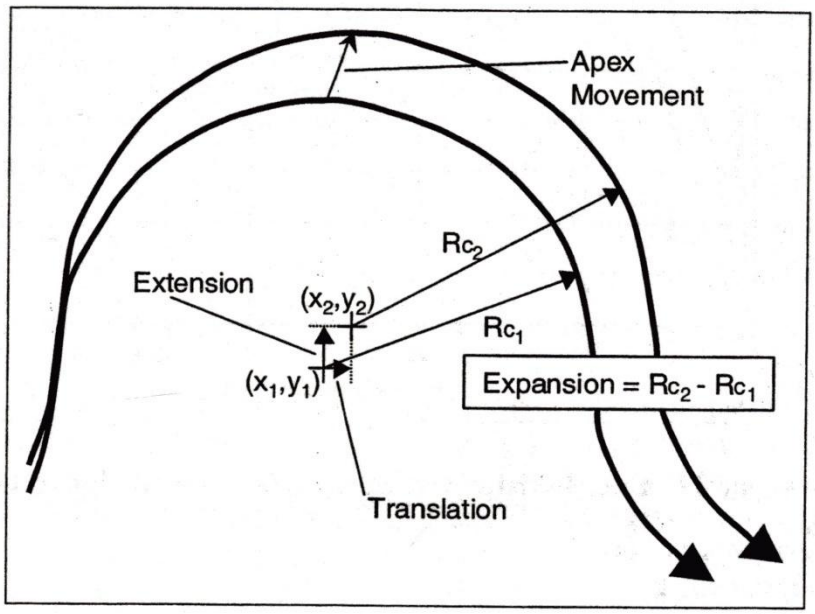

Figure 3.3: Modes of meander bend movement (from Lagasse et al., 2003, Figure 12).

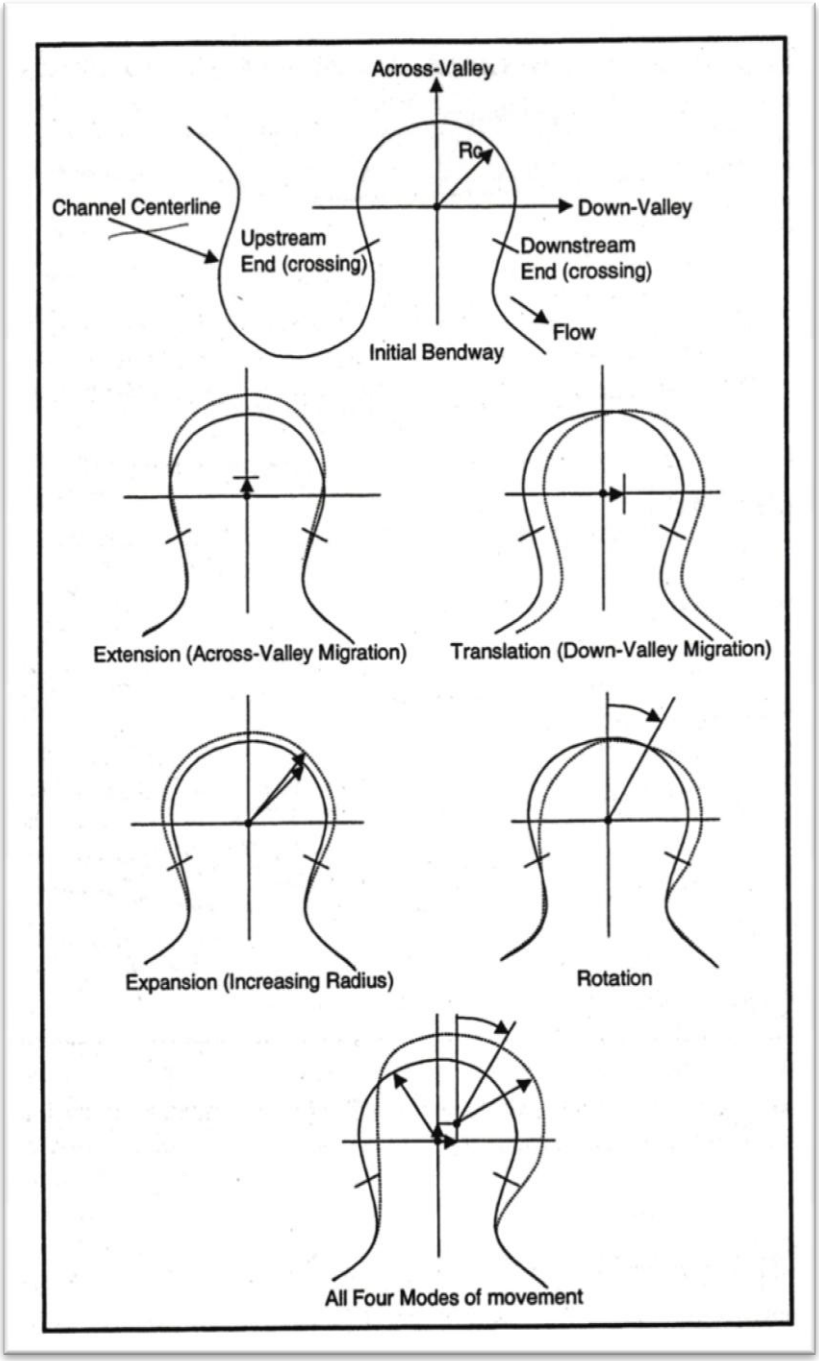

Figure 3.4: Measuring meander migration (from Lagasse et al., 2003, Figure 27).

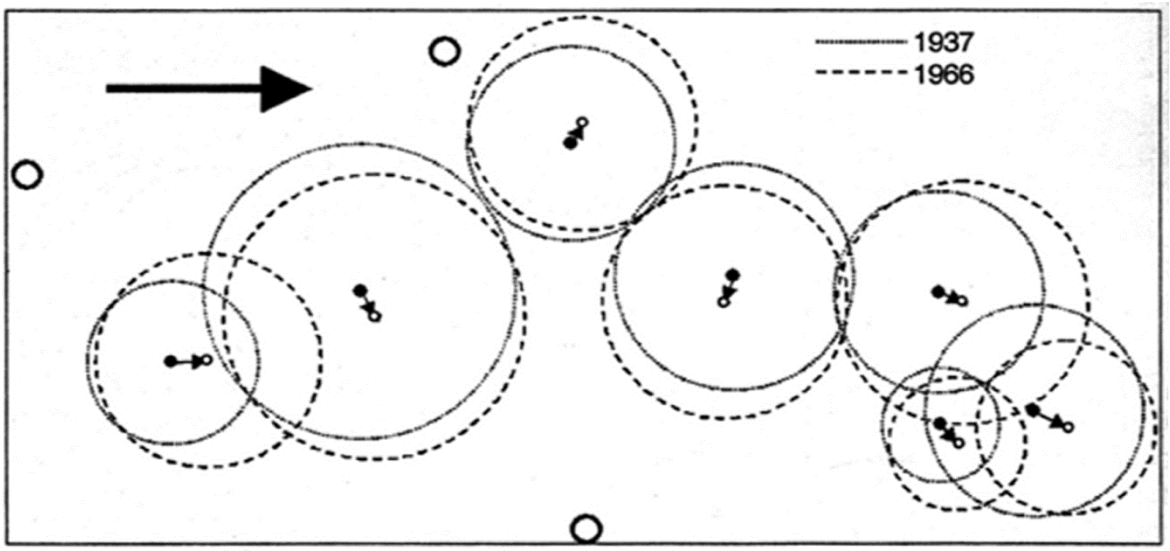

Figure 3.5: Depiction of bends based on the 1937 and 1966 outer banklines, as defined by best-fit circles. The movement of the bend centroids (arrows) is taken to define migration of the bends as a whole (from, Lagasse et al., 2004, Figure 7.6).

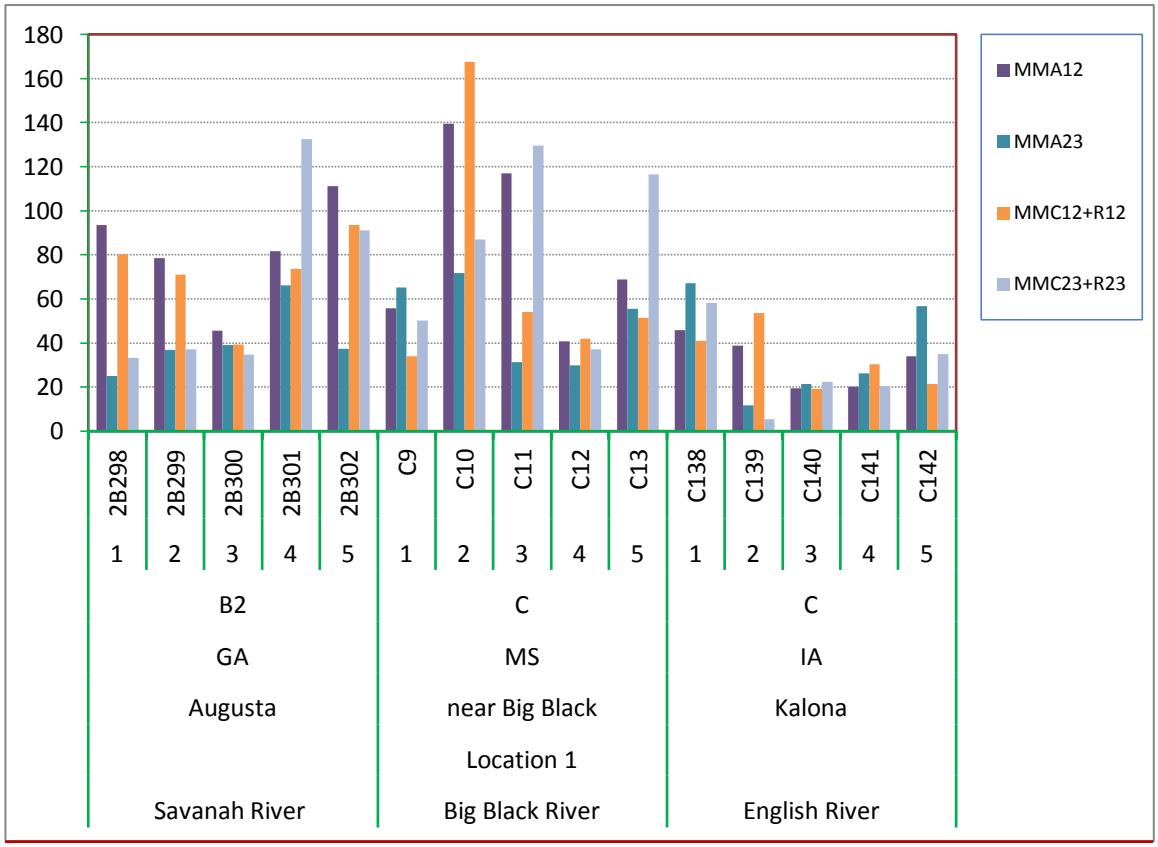

Figure 3.6: Comparison of measured bend apex migration with migration of the bend centre plus change in bend radius for selected bends of the Savannah, Big Black and English Rivers. Note that centre migration plus change in radius is not the same as the apex migration measured at any of the bends.

What I tell you three times is true.

---Lewis Caroll

Chapter 4

Refining the NCHRP Database and Developing a Method for Computing Meander Migration

4.1 University of Nottingham/HR Wallingford Database

The NCHRP database contains a huge amount of measured data, however due to the issues identified in Chapter 3, it was necessary to build a new database by extracting the relevant variables from the raw data in the NCHRP database, refining them and creating the University of Nottingham/HR Wallingford database. In building the new database due attention was given to the generation of metadata. This involved arranging bend information in a disciplined fashion that followed a progressive hierarchy (refer to the database file in Section A4.4 of Appendix to Chapter 4).

In the database, each bend is located at a site (or a river reach by the terms used in the NCHRP database). There may be one or several bends at a site. Each site is at a specified location, which may have one more site. Each location is on a river and a river may have more than one location. Where this is the case, the locations along a river are numbered and named. For example, the Apalachicola River has multiple locations – Location 1: Bristol, Location 2: Orange, etc. If a location has data for more than one site, the sites have been numbered. For example, the Choctawhatchee River at Caryville has data from two sites. Therefore, to identify a particular bend requires a sequence such as: Choctawhatchee River, Caryville, Site 1, Bend 1.

As this study uses an empirical, probabilistic approach, the quality and quantity of data are of paramount importance. In fact, compiling a reliable and accurate dataset is a vital prerequisite for

successful analysis. In terms of quantity, the NCHRP dataset includes data for 89 rivers at 125 locations and 140 sites, with data for 1505 bends (Table 3.1). Further, the sites selected by the team that compiled the NCHRP data base were chosen to constitute a representative sample of the population of meandering rivers in the 24 States of the USA. However, detailed inspection of the NCHRP database revealed multiple inconsistencies, errors and omissions. In light of these data quality issues, emphasis and attention was given to checking and correcting all the entries in the NCHRP database.

4.1.1 Production of the University of Nottingham/HR Wallingford Database

Given that the research reported here relies on, as stated above, secondary data, considerable effort was expended in scrutinising all entries listed in the NCHRP database. Based on that scrutiny, questionable entries were either accepted, rejected, reclassified (that is, the Brice type was altered from that indicated in the database), or split and reclassified (that is, the bend was divided into two bends, each of which was reclassified separately). The work was performed in three stages: first, through inspection while compiling the raw data; second, through performing exploratory statistical analysis of the data for the various river types and for the dataset as a whole; and third by reclassification of bends according to their modified Brice classification, based on exploratory data analysis and inspection of the aerial photographs.

Examples are provided in Boxes 4.1 to 4.4, respectively.

Box 4.1: Examples of questionable entries in the NCHRP database that were accepted after being closely scrutinised

Site 29. Leaf River, Location 2, near Hattiesburg, Site 1, MS, Brice-type C, 8 bends

The very high migration distance recorded in the entry for Bend 6 during time period 2, cast doubt about its validity. Close examination of the relevant aerial photographs demonstrated that the bend did erode rapidly as it was migrating into highly erodible, sand deposits. Therefore, the data point appears to be ok, and hence it was accepted.

Site 3. Rock River, near Rock Valley, IA, Brice-type D, 17 bends

In a scatter plot (data: D v8 44 88), the points for Bends 8, 9, and 12 during time period 1 form a cluster located far away from the rest of the points for bends of this river, casting doubt on their validity. Further examination established that the bends of this river do act erratically, being prone to abrupt changes due to large, chute cutoffs and rapid bankline shifting under some, poorly defined, circumstances. The data for Bends 8, 9 and 12 during TP1 reflect this behaviour and, recognising this, it was decided to accept them.

Site 1. Cimmaron River, Location 1, near Fairview, OK, Brice-type F, 4 bends

The entry for Bend 1 during time period 1 suggested an unusual rate and direction of migration when compared to the other bends at this location. Inspection of the relevant aerial photographs revealed that migration occurred due to development of a bend in the low flow channel that was $\pi/2$ out of phase with a bend in the high flow channel. Hence, the rate and direction of migration was the result of a complex form of planform evolution characteristic of 2-phase meandering in Brice-Type F channels. Hence, the entry in the data set was accepted as being a valid representation of bankline migration exhibited by Bend 1.

Note: further examples of situations where questionable entries were accepted after scrutiny can be found in Section A4.2 of the Appendix to Chapter 4.

Box 4.2: Examples of bends in the NCHRP database that were rejected

Site 4: Sacramento River, Compton Landing, CA, Brice-type D, 4 bends

Bend data were entered in the NCHRP database based on aerial photographs taken in1935, 1964 and 1998. However, the Northing coordinates for 1935 were 8-digit numbers. This was flagged as being questionable because northing coordinates are given as 7-digit numbers throughout the NCHRP database. Enquiries were made at Ayres Associates, but it proved impossible to resolve the problem with the coordinates and so data for these bends were rejected.

Site 50. Sacramento River, Location 2, Colusa, CA, Brice-type C, 5 bends

Inspection of the aerial photographs revealed signs of engineering interventions throughout this reach. Bends were identified as being impacted by the presence of revetments and flood bypass structures installed at various dates within the period of record, between 1935 and 1998. Bends whose natural shifting and evolution were heavily modified by engineering interventions were excluded from analysis as their behaviour is certainly 'non-alluvial'.

Following careful inspection, data from Bends 2 and 3 were excluded while data related to TP3 were excluded for Bend 1. However, Bends 4 and 5 were unaffected by river engineering and those data were accepted.

Site 4. Washita River, Location 2, Jollyville, OK, Brice-type F, 2 bends

This river reach was classified in the NCHRP Report as Brice Type F. However, inspection of aerial photographs revealed that the low flow channel and meander wavelengths were the same, which is inconsistent with the morphological characteristics of Type F channels. Also, river widths were found to increase by factors of between 2.4 and 5 during the 55 year period of record (1940 to 1995). This represents a non-stationary condition, indicating progressive change in river morphology with time. Hence, it was decided to reject the entries from this reach as the method is designed to represent the migration of bends in rivers that are in a state dynamic, meta-stable, equilibrium.

Note: further examples of situations where scrutiny of the entry led to data rejection can be found in Section A4.2 of the Appendix to Chapter 4.

Box 4.3: Examples of entries in the NCHRP database that were reclassified

Site 2: Buffalo Creek, near Glencoe, MN, Brice-type B1, 20 bends

The river in this reach was classified as B1 in the NCHRP Report. However, inspection of the relevant aerial photographs revealed the presence of point bars in 1967 that were not visible in either 1950 or 1994. Also, it was evident that the channel width was variable. Based on careful consideration of the aerial photographs it was concluded that the reach should be reclassified as either C or E. After discussion, it was reclassified as Brice-type C.

Site 26. Kansas River, Location 1, Ogden, KS, Brice-type C, 10 bends

Bends 2 to 4 of this reach were found to be of Type C. However, when the entire length of the reach, including Bend 1 and Bends 5 to 7 was considered, it emerged that the channel had the characteristics of Type F. After discussion, it was agreed that it would be better to reclassify the entire reach as Brice Type F.

Site 38. Powder River, near Broadus, Site 1, MT, Brice-type C, 9 bends

Inspection of the aerial photographs showed the point bars to be well vegetated. This was inconsistent with the situation which is required for a reach to be classified as Type C (meandering with point bars). Therefore, it was decided to reclassify this reach as Brice-type B2.

Note: further examples of situations where scrutiny led to reclassification according to the Brice-type may be found in Section A4.2 of the Appendix to Chapter 4.

Box 4.4: Examples of bends in the NCHRP database that were split (and reclassified into two Brice-types)

Site 48. Root River, near Houston, MN, Brice-type C, 10 bends

For this reach, aerial photographs are available for 1947, 1968 and 1994. A valley wall is evident around bends 9 and 10 on the photograph taken in 1994 and sedimentary features/point bars are much less pronounced during TP2 than they were in TP1. Possibly, river regulation/flood control structures reduced the sediment load and, thus, point bar formation between the 1960s and 1990s. Based on these observations, reach classification was left as Type C for TP1 (because point bars are evident), while for TP2 it was reclassified as Type B2 (because point bars are absent).

Note: further examples where reaches were split and reclassified may be found in Section A4.2 of the Appendix to Chapter 4.

A detailed account of the data correction effort is given in Sections A4.1 and A4.2 of Appendix to Chapter 4 (here the word 'correction' covers all types of correction including numerical correction of errors, exclusion of bends with incomplete or inconsistent data, and reclassification of bends mis-classified under the modified Brice method). A comparative account of the site types before and after reclassification can be found in Table A4.1 in Appendix to Chapter 4. A description of how Table A4.1 works (movement of sites) is provided below the table in the appendix. A list of reclassified river sites according to the modified Brice Method is provided in Section A4.3 of the Appendix to Chapter 4. The refined database generated by the correction effort is provided in Section A4.4 of the Appendix to Chapter 4. As mentioned in Chapter 3, and earlier in this chapter, the rivers on which this research study are based are located in 24 states in the USA. A state-wise account of the names of the rivers in the UoN/HRW database is given in Table A4.2 in Section A4.4 of the Appendix to Chapter 4.

Summary of Problems Encountered in the NCHRP Database

- *Data ambiguities*. For example, at the Black Warrior River, Tuscaloosa, AL, all 10 bends were classed as Brice-type B1 in the final report (Lagasse et al. 2003, page B-1, Appendix B), yet they were listed as Brice-type B2 in the electronic database. There were many incidences of this sort.

- *Data misplaced in a different folder*. For example, the Ouchita River, Arkadelphia, AR was classified as Brice-type B1, but it was placed in the NCHRP Data-Disk 1 within the B2 folder.
- *Impractical values such as 8-digit coordinates*. For example, at time point 1, data for all bends for the Sacramento River at Compton Landing, CA, have 8-digit Northings.
- *Implausible data values* – zero values. In many instances, 0 was entered as a data value when this appeared to be implausible. For example, at Bend 8 of the Pearl River, near Columbia, MS where, at time point 3, a value of zero was entered, including channel width at crossing. It might be thought that a value of zero indicates that measurements were not taken. However, for some other variables 'NM' was entered to inicate 'not measured'.
- *Inconsistent measurements*. For example, for the Canoochee River, near Claxton, GA, no migration was indicated for all bends during the first period (duration = 28 years). However, during time period 2 (25 years) all bends are recorded as having considerable migration. The fact is that all measurements for time 1 and 2 are identical, indicating duplicate entries in the database.
- *Possible data entry errors*. For example, for the Republican River, Location 3, Orleans, NE, Brice-type C, all bends have the same northing value at time point 3.
- *Misclassification of river types*. For example, the Tombigbee River, near Amory, MS was classified as Brice-type C. However, following careful inspection of the relevant aerial photographs, it was reclassified as B2. More examples may be found in Box 4.3.
- For some reaches, measurements indicate different river types between the two periods of observation. For example, the Wild Rice River, Twin Valley, MN was classified in the NCHRP Report as being Brice-type C. However, as a result of close scrutiny, the reach was reclassified as B2 during TP 2.
- *Non-stationarity*. For example, the Washita River, Location 2, Jollyville, OK, showed progressive widening throughout the period of observation, which indicates a non-stationary condition and progressive morphological change. Hence, bend migration cannot be represented based on observed rates of bank retreat.

Summary of Characteristics of the Resulting UoN/HRW Database

- Metadata are now properly and neatly structured in a hierarchy. Bends are under a Site, a Site is under a Location, a Location is under a River name. If a river has more than one location, locations are now numbered (Location 1, Location 2 and so on). If data were measured at a location that possesses more than one site, sites are now numbered (Site 1, Site 2 and so on).

- Data are properly placed within a corresponding folder, according to Brice Types. This work was done at data compilation stage from NCHRP data disk.
- As a result of corrections to Brice-types, data are now properly classified.
- Through corrections to numerical values, the database is now believed to be largely error free.
- All missing data are labelled as 'NA' - as appropriate for treatment in a statistical package.

Statistics on the distribution of bends and sites in the refined database are given in Table 4.1.

Table 4.1: Summary of bends classification according to the modified Brice Method in revised, University of Nottingham/HR Wallingford Database

Modified Brice Type	Number of river sites	Number of bends
A	7	61
B1	19	199
B2	37	365
C	41	423
D	6	46
E	18	217
F	5	34
G1	6	125
G2	2	42
Total	141	1512

4.2 Developing a Method for Computing the Magnitude and Orientation of Bend Apex Migration

Chapter 3 investigated whether measurements of the centre of a bend can represent movement of the bend apex or migration of the bend more generally. The results showed that, in practice, movement of the bend centre cannot represent either aspect of bend migration. Hence, it was clear that, in characterising and predicting channel migration, it would be unwise to consider bend centre movement as being representative of channel migration. It is evident from the literature review in Chapter 1, that in a meandering stream bends grow and migrate primarily through erosion and retreat of the outer bank matched to a greater or lesser degree by deposition at the inner bank. Consequently, an erosion hazard threatens land, buildings, infrastructure and engineering structures located on the floodplain adjacent to the outer margins of active meander

bends. In this context, the bend apex is the point furthest from the bend centre and lies at the heart of the zone of active erosion along the outer bank. On this basis, it was decided that the apex of the bend should be taken to represent bend migration when characterising and predicting the hazard posed to floodplain land and the assets placed on it.

The next task was to develop a method to compute migration of the bend apex from the data available in the revised University of Nottingham /HR Wallingford database.

Two parameters are required to define bend migration based on movement of the bend apex; the magnitude and orientation of movement of the bend apex. The following sections of this chapter report how methods were developed for computing these two parameters. Section 4.2.1 deals with the procedure for computing the coordinates of the bend apex. Section 4.2.2 reports development of the procedure for finding the magnitude of migration of bend apex between two points in time. Section 4.2.3 reports how the method was developed to find the orientation of bend apex migration. Section 4.2.4 addresses verification of the correctness of the methods developed to compute the magnitude and orientation of bend apex between consecutive aerial photographs or maps.

4.2.1 Computing the Coordinates of the Bend Apex

The steps necessary to find the coordinates of a bend apex (BA) are described in this section. In describing the method developed to compute the coordinates of the bend apex, sample calculations for each step are provided in Box 4.5 at the end of this sub-section. Data for Bend 1 of the Altamaha River, Doctortown, GA, are used to support the sample calculations. The notations used in the method at a given point in time are:

EBC Easting of the Bend Centre
NBC Northing of the Bend Centre
R Radius of curvature of the bend
BO Bend Orientation
EBA Easting of the Bend Apex
NBA Northing of the Bend Apex
αBCBA angle between the line connecting BC to BA and the Easting axis
αBCBA angle between the line connecting BC to BA and the Easting axis

Step 1: Extracting the coordinates of the bend centre, radius of curvature and bend orientation

To determine the coordinates of the apex of a bend it is necessary to extract from the database the coordinates of its centre, its radius of curvature and its orientation. The University of Nottingham /HR Wallingford database provides these parameters for each bend. The coordinates of the centre of each bend are specified in terms of transverse Mercator coordinates for the Easting (EBC) and Northing (NBC), expressed in SI units (metres).

The radius of a bend (R) is defined by the radius of a circular arc fitted to the curve of the outer bank.

Bend orientation (BO) defines the heading of the bend as a whole in plane of the Easting and Northing axes. In the database it is the angle (measured counter-clockwise and expressed in degrees) between due east and the heading of a line drawn from the centre to the apex of a bend. Hence, bend orientation depends on the planform position of the bend apex with respect to the bend centre, as illustrated in Figure 4.1.

In the sample case of Bend 1 on the Altamaha River at Doctortown, GA, the parameters for 1941 define the location of the bend at Time 1. These are: EBC1 = 425064 m, NBC1 = 3500642 m, R1 = 496.8 m, and BO1 = 341°.

Step 2: Computing the coordinates of the bend apex

The following two equations are used in order to compute the easting and northing co-ordinates of a bend apex, respectively:

$$EBA = EBC + R\cos(BO) \quad (4.1)$$

$$NBA = NBC + R\sin(BO) \quad (4.2)$$

Note that the second part of Equation 4.1 is the easterly component of the radius of curvature. Depending on the value of the bend orientation, this term produces either a positive or negative value. By computing this term it is possible to define the position of the bend apex with respect to the bend centre. When positive value is found, the bend apex lies to the east of the bend centre. When a negative value is found, it lies to the west of the bend centre. In the same way the position of the bend apex with respect to the bend centre can also be found by computing the second term

of Equation 4.2. The side the bend apex falls on depends on the value of bend orientation, being in one of the four quadrants in the Easting-Northing coordinate plane. Hence, there can be four different scenarios. A scenario-based computation of coordinate of bend apex can be found in Section A4.5 in Appendix to Chapter 4.

Box 4.5: Sample calculations to find the coordinates of a bend apex

The data used in this example come from Bend 1 (BIN: 2B18), the Altamaha River, Doctortown, GA, (modified Brice Type B2) at Times 1 (1941) and 2 (1968) within the NU/HRW database.

Step 1: *Extract the coordinates of the bend centre, the radius of curvature and the bend orientation at Time 1:*

EBC1 = 425064 m, NBC1 = 3500642 m, R1 = 496.8, BO1 = 341°

Step 2: *Compute the coordinates of the bend apex:*

The easting coordinate of the bend apex,

EBA1 = EBC1 + R1cos(BO1) (following Eq. 4.1)

= 425064 + 496.8cos(341°)

= 425064 + (+469.73)

= 425534 m

The northing coordinate of bend apex,

NBA1 = NBC1 + R1sin(BO) (following Eq. 4.2)

= 3500642 + 496.8sin(341°)

= 3500642 + (-161.74)

= 3500480 m

4.2.2 Computing the Magnitude of Migration of the Bend Apex

The distance that a bend has migrated between any two observations is represented by the movement of the bend apex. Hence, the magnitude of bend migration may be found by comparing the coordinates of the bend apices at the times of the earlier (T1) and later (T2) observations. The following additional notation is used:

EBA2 Easting of the bend apex at Time 2

NBA2 Northing of the bend apex at Time 2

MMA12 Migration magnitude for the bend apex between Times 1 and 2

Hence, the migration distance may be found using simple trigonometry.

$$MMA12 = SQRT\ [(EBA2 - EBA1)^2 + (NBA2 - NBA1)^2\ ] \quad (4.3)$$

Box 4.6 below illustrates this for the sample bend.

Box 4.6: Sample calculation to compute magnitude of migration for bend apex movement

In this sample calculation, the data come from Bend 1, the Altamaha River, Doctortown, GA, Brice Type B2 at Time 1 (1941) and time 2 (1968).

Step 1: *Extract the coordinates of the bend centre, the radius of curvature and the bend orientation at Time 2 (1968):*

EBC2 = 425042 m, NBC2 = 3500611 m, R2 = 529.7, BO2 = 337.9°

Step 2: *Computing the angle between the line joining the bend centre to the bend apex and due east:*

αBC2BA2 = (360° - BO2) = 360° - 337.9° = 22.1°

Step 3: *Computing the coordinates of the bend apex at T2:*

Easting of bend apex, EBA2 = EBC2 + R2 cos(αBC2BA2)
= 425042 + 529.7cos(22.1°)
= 425532.78 m

Northing of bend apex, NBA2 = NBC2 – R2sin(αBC2BA2)
= 3500611 – 529.7sin(22.1°)
= 3500411.71 m

Step 4: *Computing the magnitude of bend apex migration between T1 and T2:*

Given that:

EBA1 = 425533.74 m (computed in Box 4.5)
NBA1 = 3500480.26 m (computed in Box 4.5)
The migration magnitude can be found using Equation 4.3

$MMA12 = SQRT\ [(EBA2 - EBA1)^2 + (NBA2 - NBA1)^2\ ]$
$= SQRT\ [(425532 - 425533.74)^2 + (3500411 - 3500480.26)^2]$
= **68.6 m**

4.2.3 Computing the Orientation of Bend Apex Migration

This section presents the method developed to compute the orientation of bend apex migration between any two points in time as illustrated in Figure 4.2. The approach developed here focuses on analysis and prediction of rate of migration. It does not deal with prediction of the orientation of migration. However, the capacity to predict the direction in which a bend is likely to migrate as well as the rate at which is likely to shift would be useful to river and risk managers and this might be a suitable topic for future research based on the University of Nottingham /HR Wallingford database. Hence, data defining the orientation of migration was extracted from the raw data and included in the database.

For this purpose, the orientation of migration is represented by the angle between due east and the heading of a line connection the positions of the bend apex at times T1 and T2, expressed in degrees and taking the anti-clockwise sense as positive. This convention concurs with that used in the database to measure bend orientation. The following notation is used:

MOA	Migration orientation (Heading) of bend apex movement
αMMA12	angle between the heading of bend apex migration and due East
NE	North-East
NW	North-West
SW	South-West
SE	South-East

Computation of the migration orientation angle is accomplished in three steps:

Step 1: Computing meander orientation for apex movement in terms of natural direction and hence formulating migration orientation

When considering migration orientation it is helpful to visualise the movement of the bend apex. Visualisation is possible because the coordinates of the bend apices at the beginning and end of the period being studied are already known (see Section 4.2.1), In visualising the direction of apex movement, there are broadly speaking 4 possibilities for apex movement (as illustrated in Figure 4.2) and set out below.

Scenario 1: North-Eastward Migration

EBA2 – EBA1 = + indicates Eastward movement
NBA2 – NBA1 = + indicates Northward movement | North-eastward
So MOA12 $\Longrightarrow$ NE

and, in general MOA12 = 0 + αMMA12 (4.4)

Scenario 2: North-westward Migration

EBA2 – EBA1 = - indicates Westward movement
NBA2 – NBA1 = + indicates Northward movement | North-westward
So MOA12 $\Longrightarrow$ NW

and, in general MOA12 = 180 - αMMA12 (4.5)

Scenario 3: South-Westward Migration

EBA2 – EBA1 = - indicates Westward movement
NBA2 – NBA1 = - indicates Southward movement | South-westward
So MOA12 $\Longrightarrow$ SW

and, in general MOA12 = 180 + αMMA12 (4.6)

Scenario 4: South-eastward Migration

EBA2 – EBA1 = + indicates Eastward movement
NBA2 – NBA1 = - indicates Southward movement | South-eastward
So MOA12 $\Longrightarrow$ SE

and, in general MOA12 = 360 - αMMA12 (4.7)

Note: There may be situations where a bend undergoes only eastward or westward migration with no northward or southward component. In the same way a bend may move only in northward or southward movement with no eastward or westward movement. However, in practice during a finite period of migration, a bend will have some movement in two directions. Therefore, four scenarios have been provided here.

Step 2: Computing the angle between the MOA and due East

Based on the coordinates of the bend apex at T1 and T2, it is straightforward to calculate the angle between a line defining the direction of bend apex migration (MOA) and due East (αMMA12) using trigonometry:

$$\alpha MMA12 = \tan^{-1} [(NBA2 - NBA1) / (EBA2 - EBA) \quad (4.8)$$

Step 3: Computing the migration orientation, MO

We have already computed the natural direction of meander orientation (from Step 1) and the angle that the line of migration makes with the easting axis (from Step 2), we can now compute the orientation of migration for bend apex movement from one time point to another by using the appropriate formula from Formula 4.4 to Formula 4.7.

Box 4.7 provides a sample calculation to illustrate the method used to find the orientation of bend apex migration.

Box 4.7: Sample calculation to find the migration orientation for bend apex movement between two points in time

In this sample calculation, the data come from Bend 1, the Altamaha River, Doctortown, GA, Brice Type B2 at Times 1 (1941) and time 2 (1968).

***Step 1**: Computing Migration Orientation for apex movement in terms of its broad direction:*

EBA2 – EBA1 = 425532.78 – 425533.74 = - 0.96 m → southward

NBA2 – NBA1 = 3500411.71 – 3500480.26 = - 68.55 m → westward

So MOA12 ⟹ SW

***Step 2**: Computing αMMA12, the angle between the line of migration of bend apex and due East*

$\alpha MMA12 = \tan^{-1} [abs(NBA2 - NBA1)/abs(EBA2 - EBA)]$

$= \tan^{-1} [abs(- 68.55) /abs(- 0.96)]$

$= 89.2°$

***Step 3:** Computing the migration orientation, MO in numerical terms*

MOA12 $= 180° + \alpha MMA12$ (following Equation 4.6)

$= 180° + 89.2°$

$= \mathbf{269.2°}$

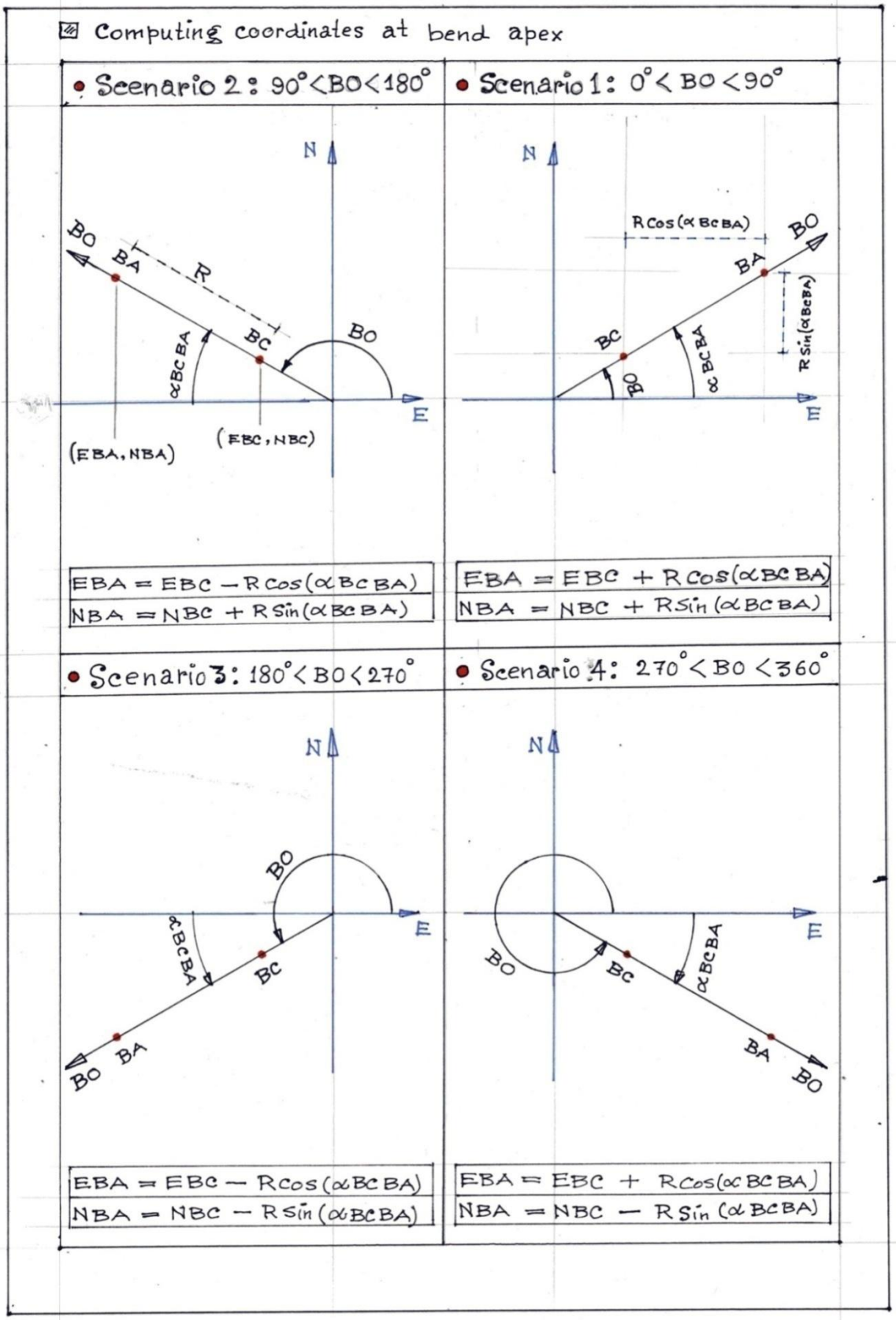

Figure 4.1: Diagrams illustrating bend orientation, the angle between the line connecting the bend centre to its apex and the east axis, and equations used to compute the coordinates of the bend apex

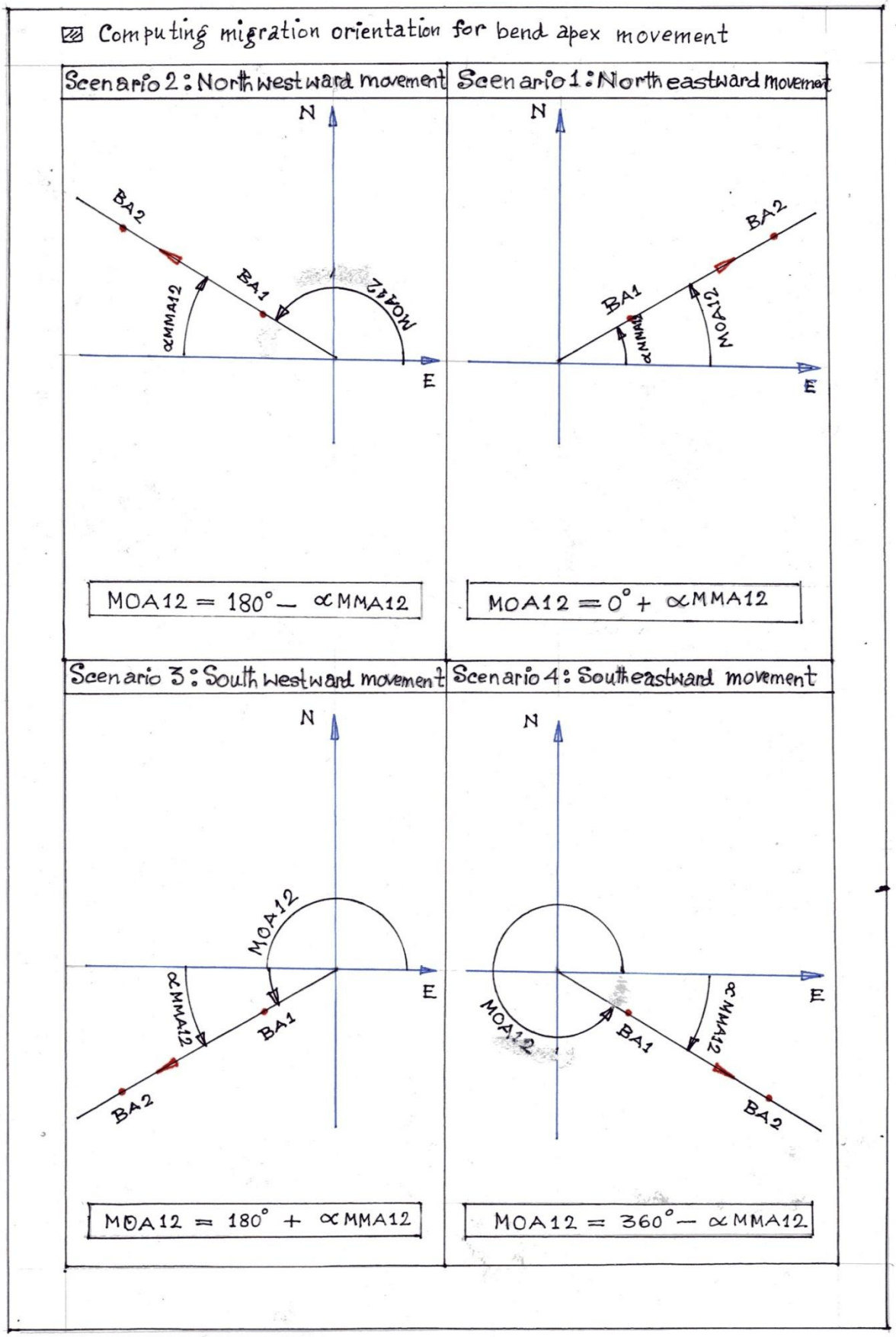

Figure 4.2: Diagrams illustrating the angle between line defining migration of the bend apex and the east axis, and the equations used to calculate the orientation of bend apex migration.

Happy the man, who, studying nature's laws, through known effects can trace the secret cause.

---Virgil

Chapter 5
Probabilistic Analysis of Bend Migration

5.1 Modified Brice Classification

In the NCHRP study, bends were classified using a modified version of the Brice Typology, as described in Section 1.1 and justified in Section 4.1. For ease of reference, the modified Brice Typology is illustrated here in Figure 5.1.

5.2 Data and Variables

Bends of all modified Brice Types in the University of Nottingham /HR Wallingford database described in Section 4.1 were used in developing the probabilistic analysis. The refined database contains data for a total of 1,512 bends. The variable used to represent the geometry of the bend is the ratio of the bend radius (R) to the channel width at the crossing (WCr) at the time when the relevant aerial photograph was taken or the map was made. For each bend in the database, there are three aerial photographs or maps, referring to three points in time and, thus, there are two periods over which the rate of bend migration can be assessed. Hence, there are 1,512 values of R1/W1Cr for the first period and a further 1,512 values of R2/W2Cr for the second period.

In selecting values to act as the independent variable in the probabilistic analysis of bend migration (the dependent variable) it was decided to use only parameters for the *beginning* of each time period. This is essential if, as intended, the results of the analysis are to be used *predictively*. Clearly, when predicting the future possible behaviour of a bend, only the current geometry of the meandering channel is known or even knowable and, consequently, it is on the basis of these

known parameters that a prediction must be based. The accuracy of the analysis could have been improved by adding into it values of bend geometry at the end of a period of change, but this advantage would be gained at the cost of negating the possibility of the method to be used as a predictive tool in assessing and managing future risks related to bend migration. To make it clear in the subsequent analysis when a parameter refers solely to the bend geometry at beginning of a time period, it will always be given the subscript 'b'.

5.2.1 Selection of the Appropriate Radius of Curvature

Many researchers have investigated the relation between the rate of migration of a meander bend and its radius of curvature. However, they have used different definitions of the radius of curvature. For example, Leopold and Wolman (1960) used the radius of curvature of the centre line of the channel, as did Hickin (1974). However, Hickin and Nanson (1975) actually used the temporal average of the radius of curvature of scroll bars left in the floodplain inside a meander that is extending or migrating laterally. The radii of these features probably approximates to that of the inner bank of the meander that formed them. Hickin (1978) reverted to using the radius of the centre line of a stream channel. Biedenharn et al. (1989) report using the radius of curvature about the bend axis, but they do not make it clear whether this relates to the curve of the inner bank, centre line or outer bank. In the literature, the most frequently used radius seems to have been that of the channel centre line. However, as mentioned earlier, the NCHRP study (Lagasse et al., 2003) preferred the curve of the outer bank as the basis for the radius of curvature used in their predictions of bend migration rate.

In this study, it was decided to continue using the outer bank radius of curvature in deriving a relationship with the bend migration rate and, eventually, making predictions of the rate of migration. This decision was made for two main reasons. Firstly, defining and delineating the centre line of an actively meandering channel with well-developed bars featuring successional vegetation growth can be difficult. This is especially true when the edge of the bank at the inside of a bend is obscured or difficult to identify unequivocally in the aerial photograph. Secondly, the cross-section of an alluvial channel changes through time in response to erosion

and sedimentation processes unrelated to bend curvature. Consequently, the mean radius of the channel centre line may not accurately reflect the effects of active migration of the outer bank. Conversely, the radius of the outer bank reflects the geometry of that part of the bend with which the analysis is most directly concerned within the migration analysis and prediction developed herein.

5.2.2 Selection of the Appropriate Channel Width

As set out in Chapter 1, the aim of the research described in this thesis is to analyse and predict meander bend migration. Given the limitations of deterministic methods in supporting prediction of future bend migration, the analysis developed here will employ a probabilistic approach that calculates the probability of a given rate of migration being equalled or but not exceeded as a function of the radius of the outer bank of the bend.

However, in developing the necessary relation, it must be noted that the absolute quantity of migration at a bend scales with both the size of the river of which the bend is a part and the length of time over which migration takes place, as well as the radius of the bend. Consequently, it is not possible to derive a single, dimensioned function that can apply to the huge range of river sizes and the different lengths of the periods between observations due to scale effects. For example, in the sample calculations presented in Chapter 4, data came from two bends: Bend 1, Altamaha River, Doctortown GA and Bend 1, Zumbro River, Kellogg, MN (Table 5.1**)**.

Table 5.1: Measured planform geometry data and computed migration parameters for the bend apex at Bend 1, Altamaha River, Doctortown, GA (second row) and Bend 1, Zumbro River, Kellogg, MN (third row).

Bend	T1T2	T2T3	T1T3	R1	R2	R3	W1Cr	W2Cr	W3Cr	W1A	W2A	W3A	MMA12	MMA23	MMA13
BIN 2B18	27	25	52	496.82	529.69	661.87	184.78	161.99	247.04	231.66	221.21	278.28	68.18	108.50	174.39
BIN C404	20	23	43	132.58	138.47	153.68	47.06	53.13	55.47	70.8	43.41	74.14	75.47	16.07	64.90

Comparison of the data reveals a huge variation in the sizes of the rivers. Specifically, the Altamaha River is about 4 times wider than the Zumbro River. Similarly, the period between T1 and T2 observations on the Altamaha River (27 years) is 35% longer than that on the Zumbro River (20 years). Hence, there are both spatial and temporal scale effects in the parameters controlling the amount of meander migration displayed by these two bends.

It is, therefore, necessary to transform the data to remove spatial and temporal scale effects. This is very straightforward for the bend radius data and, in fact, it has long been customary when considering bend curvature to remove the dimensions from the bend radius by dividing it by the channel width. Hence, R/W is the dimensionless bend radius.

Bend migration data involve units of both length and time, and it is necessary to remove both of these to eliminate scale effects. This can be achieved by dividing migration distance, first, by the width of the river channel and, second, the number of years in the time period over which the migration occurred. Hence, the migration rate is the average annual migration distance expressed as a proportion of the channel width.

However, a question remains concerning the appropriate channel width to use: for example, the width at the crossing or the width at the bend apex. This issue is an important issue as these two widths differ considerably in all meandering rivers except those that fall into Brice Type A (canaliform). Selection of the appropriate width may be considered from both morphological and statistical perspectives.

With regard to morphology, there are a number of arguments that favour selection of crossing width to nondimensionalise bend radius and migration distance. Specifically:

1. On aerial photographs, it is usually a lot easier to make out the banklines at the crossing than at the bends;
2. Channel top width (i.e. bankfull stage and width) is more uniform around the point of inflection than it is at the bends;

3. The banks are generally more stable around the crossing than at the bend apex so that the channel top width is also more steady;
4. At the bend apex, the inner bank is usually formed in a low, unconsolidated point bar, while the outer bank is formed in older formations, with a higher elevation. This makes it difficult to select a representative 'top bank' channel width. Conversely, the banks around the meander crossing are usually of approximately similar age, properties and elevations;
5. At bends (especially at and downstream of the apex) only a portion of a channel width actually conveys water and sediment downstream. This is the case because flow at the inner and (in very tight bends) outer banks is separated from the channel boundary. Conversely, downstream flow usually occupies the full width of the channel around the meander crossing.

Of these arguments, the first is particularly important to measuring width accurately and consistently using aerial photographs. This is directly relevant to the reliability of the raw NCHRP data, which were measured from maps and, mostly, aerial photographs or satellite imageries. For example, outer banklines with mature trees, shrubs, bushes that obscure the bank edge or cast shadows into the channel can hide the bank edge and this generally proves more problematic at the bend apex than at the meander crossing. Considering this, and the other morphological arguments listed above, it may be concluded that width measurements can be made relatively more accurately, consistently and reliably at the meander crossing than at the bend apex.

From a statistical perspective, the utility of the width parameter used to nondimensionalise the radius and average annual migration distance can be explored by examining the variability in widths measured at the bend apex and the meander crossing that are reported in the database (Table 5.2). Considering the whole data set and putting measurements for the two time periods together yields 3,024 pairs of bend and crossing width measurements (1,512 bends x 2 periods = 3024). The results in Table 5.2 show that each and every statistic indicating the spread (dispersion) of the variable is considerably higher for the width at the bend apex (WbA) than it is for the width at the crossing (WbCr).

Table 5.2: Tukey's five number summary and other measures of spread for measured channel widths at crossings (WbCr) and the bend apices (WbA).

Variable	Minimum	Q1	Median	Q3	Maximum	Range	IQR	Max/Min	Q3/Q1	Mean	sd	cv
WbCr	8.50	30.49	50.57	89.05	641.20	632.68	58.57	75.44	2.92	71.06	62.20	0.875
WbA	10.08	36.48	60.75	109.17	905.11	895.03	72.69	89.79	2.99	87.68	83.92	0.955

It follows that, for bendways and crossings on the same sample of rivers, measured values of channel width at the bend apices are a great deal more dispersed than those for channel width at the meander crossings. Hence, from a statistical perspective, crossing width provides a more consistent parameter with which to scale the river than does bend apex width.

Taking the morphological and statistical arguments together, it is clearly reasonable to use the channel width measured at the meander crossing as the scaling parameter with which to nondimensionalise the bend radius and average annual migration rate.

Following transformation to remove scale effects, the two variables to be treated in the probabilistic analysis are:

1. Independent variable - radius of outer bank curvature per unit channel crossing width (Rb/WbCr) and,
2. Dependent variable – average annual migration distance for the bend apex per unit channel crossing width MMA/WbCr/Y.

5.2.3 Combining Data for the Two Time Periods into a Single Set

In this research, just like any approach that employs an empirical approach and probabilistic methods the quantity of data, as well as its quality, is an important consideration. The UoN/HRW database has data for 1,512 meander bends, over 2 time periods. In principle, in any empirical analysis and study, the more the data points the better and the more reliable the result of the analysis can be expected.

Hence, it would be advantageous to double the number of cases by combining the bend radius and migration data for the two periods. However, before doing so it is first necessary to check that the data for the two time periods can be considered to be two samples drawn independently from the same population. It is reasonable to hypothesise that they do constitute independent samples from the same population because the raw data measured in the NCHRP study come from freely migrating bends that are known to have shifted incrementally over the period of record. It is, therefore, reasonable to assume that the behaviour of each bend took place through fluvial process-response mechanisms that were unchanged throughout the two periods, and which were driven by flow events that were essentially similar during the two time periods. This means that bend growth and development was governed by the same mechanisms and similar driving variables operating within river systems and environments that did not change radically over the 60 year period of record. There is, therefore, *a priori* case to suggest that the measurements are time independent. Moreover, the accounts in the NCHRP Report (Lagassee et al., 2003, 2004) indicate that data collection and measurement actions for each of the 3 different time points were performed consistently, but independently. It follows, therefore, that there is a strong *prima facie* evidence that it is permissible to combine the data from the two periods.

While there is no reason to suppose that the data should *not* be combined, it is prudent before doing so to look for statistical evidence that the act of combining the data from the two periods into a single set is justifiable.

This was approached initially by plotting the sample quantiles to examine whether they were drawn from the same distribution. An example is shown in Figure 5.2, where the radius per unit channel crossing width at time T2 (R2/W2Cr) is plotted against the value for T1 (R1/W1Cr) with the pair wise missing data removed.

Figure 5.2 shows that the data fall on or near to the line of perfect agreement (the red line). It may, therefore, be concluded that values of the dimensionless radius measured at T1 and T2 do, in fact, follow the same distribution. Removal of all data (the radius data) for all 3 time points where any

one time point is missing has the same outcome. Likewise, quantile plotting of dimensionless migration data produced the same conclusion.

The validity of combining measured data for the two periods can further be assessed by applying an appropriate statistical test to the data. The Kolmogorov-Smirnov two sample test has the capability of testing two data sets to assess whether or not they are from the same population. This test was performed on the dimensionless versions of both bend radius and average annual migration rate. The results provided in Table 5.3.

In the table it can be seen that both variables successfully passed the test, with high p-values. Therefore, based on this test result, it may be concluded that the data from Time Period 1 and that from Time Period 2 have been derived from the same population.

Table 5.3: Results of Kolmogorov-Smirnov tests to check whether radius of curvature (Row 1) and migration (Row 2) for time periods 1 and 2 come from the same population.

Variables	Test statistic	p-value	Test type
X=R1/W1Cr, Y=R2/W2Cr	0.0419	0.268	Two tailed
X=MMA12/W1Cr/Y, Y=MMA23/W2Cr/Y	0.0369	0.458	Two tailed

Therefore, the statistical evidence derived from descriptive (quantile plotting) and inferential approaches (hypothesis testing) both suggest that data from the two time periods can be combined.

In conclusion, the logical arguments and statistical evidence presented in this section provide solid reasoning and the justification for combining the data from the two time periods into a single data set to provide the largest available data set from which to develop a probabilistic bend migration analysis and prediction tool.

5.2.4 Selection of Radius and Width at the Beginning of a Time Period

In analysing bend migration, one could use the data from the beginning or end of a time period, or use an average value based on both measurements. In this context, the average value for a period,

would be most acceptable since it represents the bend geometry over the period and also because time-average values show less dispersion in their distribution. However, as the purpose of the analysis is to support a predictive tool for bend migration, values of dimensionless bend radius and crossing width at the start of each time period have been selected for use in the analysis. Hence, Rb/WbCr and MMA/WbCr/Y are the variables representing bend geometry and migration rate during a time period, where the subscript "b" indicates that they refer to the beginning of the time period. There are then, potentially 3,024 values in the pooled data set for time periods 1 and 2. However, in practice the number is actually somewhat lower due to there being missing values for some bends during one or other of the time periods (Table 5.4**).**

Table 5.4: Data actually available for the variables used in the probabilistic analysis

Variables	Time Period 1			Time Period 2			2 Periods together		
	n total	n missing	n avail	n total	n missing	n avail	n total	n missing	n avail
R1/W1Cr	1512	580	932	-	-	-	-	-	-
MMA12/W1Cr/Y	1512	637	875	-	-	-	-	-	-
R2/W2Cr	-	-	-	1512	29	1483	-	-	-
MMA23/W2Cr/Y	-	-	-	1512	130	1382	-	-	-
Rb/WbCr	-	-	-	-	-	-	3024	609	2415
MMA/WbCr/Y	-	-	-	-	-	-	3024	767	2257

The distribution of the combined data set is shown in a scatter plot in Figure 5.3, with Rb/WbCr plotted on the abscissa and MMA/WbCr/Y on the ordinate axis. In the heading, the numbers 2,415 and 2,257 refer to the number of available data points for the x and y variables, respectively. The data point symbol "1" indicates that the point is derived from the first time period (TP1). Likewise, the data point symbol "2" indicates data measurement from the second time period (TP2). Hence, inspection of this plot allows a further visual check to detect any dependence of migration on which time period the data derive from. Inspection reveals no systematic differences in the spread of data from TP1 compared to TP2.

Before using the data in a bivariate, probabilistic analysis, it is advisable to investigate their individual distributions. Hence, univariate investigations of the distributions of the dimensionless versions of bend radius and average annual migration rate are reported in the next two sections of this chapter.

5.3 Univariate Distribution and Normal Transformation of Rb/WbCr

A number of numerical descriptors have been calculated to describe the distribution of the variable Rb/WbCr, and these have been investigated using a number of well established, exploratory, graphical techniques. A detailed description of the statistical methods used in the univariate analysis is given in Section A5.1 in the Appendix to Chapter 5 and their use is only summarised here in the main text. Initially, and in order to generate an overview of the nature and spread of distribution of the data, the range and inter-quartile features of the distribution were considered. These attributes can be obtained from Tukey's five number summary, which is given in Table 5.5.

Table 5.5: Tukey's five number summaries for bend variables

Variable	Minimum	Lower Quartile	Median	Upper Quartile	Maximum
Rb/WbCr	0.55	1.9925	2.688	3.784	12.263
$\log_{10}$(Rb/WbCr)	-0.25964	0.2993983	0.4294	0.5779511	1.088597
MMA/WbCr/Y	0.00036	0.017475	0.0319	0.056996	0.366787
$(MMA/WbCr/Y)^{0.16}$	0.28095	0.5233434	0.5763	0.6323174	0.851738

The minimum and maximum values of the dimensionless radius are 0.55 and 12.26, respectively. The maximum value is 22.3 times greater than the minimum, indicating a very wide variety of bend curvatures that range from a short-radius elbow to a long, gentle bend. However, the median value is only 2.69 and the 3rd quartile is 3.78, indicating a strongly right skewed distribution. This indicates that data points are concentrated in the lower half of the distribution and there is a relative scarcity of data for bends of low curvature.

The five-number summary is illustrated using a box and whisker plot in Figure 5.4, which makes clear the strong asymmetry in the density of the data that results from the concentration of points in the lower part of the plot. The fact that around half the data points in the UoN/HR database are derived from bends with radius to width ratios in the range from 2 to 3. This is not surprising given that many of the researchers quoted in Chapters 1 and 2 noted that most migrating bends quickly evolve to an R/W value between 2 and 3 but then maintain that geometry for quite some time, until they eventually enter their terminal stage.

In addition to the box and whisker plots, a number of other graphical statistical techniques were employed to explore the univariate distribution. These included a *strip chart, stem-and-leaf plot, and histogram*. A strip chart is a plot (termed a *dotplot* in the statistical package MINITAB) of data frequency against data values. A stem-and-leaf plot is a graphical representation of data frequency together with exact numerical values. These plots also showed data density to be higher in the lower range of Rb/WbCr values, with a right-skewed distribution, in a manner similar to that in Figure 5.4. This was also the case for the histogram (Figure 5.5)**,** as well being reflected in the estimated kernel density curve that is superimposed on the histogram in this figure.

The next step in examining the univariate distribution of this variable was to explore whether this variable follows any formal statistical distribution. Many statistical methods are applicable only to variables that follow the Gaussian (or normal) distribution. Thus, it was important to determine whether the variable Rb/WbCr follows a normal distribution.

A number of descriptors were computed and gathered with the aim of investigating normality numerically and these are listed in Table 5.6**,** along with other, basic statistics. All the descriptors that judge the normality of a distribution lie well away from the values that indicate a normal distribution. For example, in a normal distribution, the mean and median should be approximately the same. However, the mean is 3.11 (to 3 sig. figs.) and the median is 2.69, so that the mean is 16% higher than the median. The situation is more pronounced in the tails of the distribution; for example, the coefficient of skewness is 1.56.

Several exploratory graphical methods were employed to investigate the normality of this variable. The methods applied were: *normal probability plot, empirical cumulative distribution function plot, histogram plot and box plot*. The box and whisker plot (Figure 5.4) and histogram (Figure 5.5) were also examined. Niether Figure 5.4 nor Figure 5.5 show any symmetry or support for normality in the distribution. In Figure 5.6 sample quantiles do not form a straight line. In Figure 5.7 the empirical, cumulative distribution function (ecdf) deviates markedly from the shape expected for a normal cumulative distribution function.

Therefore, taking the results of the numerical and graphical explorations together it must be concluded that the variable Rb/WbCr does not follow a normal distribution.

Consideration was next given to whether the variable could be normalised by mathematical means. In this initiative both power and logarithmic transformations were investigated. Over a huge range of powers and bases, and with due care and attention, a trial-and-error approach was used with the aim of obtaining a satisfactory fit between a Gaussian model and the transformed data.

For the variable (Rb/WbCr), a common logarithmic transformation (Table 5.6) produced the best result. In fact, the transformed variable does satisfactorily follow the normal distribution, as illustrated in Figures 5.8 to Figure 5.11. Specifically, Figure 5.8 shows that, after transformation, the distribution of data points is symmetric with respect to the median. In Figure 5.9, the histogram is now symmetrical, as expected for a normal distribution. In Figure 5.10 the data points for the transformed variable closely follow the line of perfect agreement (i.e. a straight line with a gradient of one). This suggests that there is no shift in location. Figure 5.11 also shows very good agreement between the empirical cumulative distribution function and the expected normal cumulative distribution function.

Considering these graphs together, therefore, they all suggest that the transformed variable $\log_{10}$(Rb/WbCr) follows a normal distribution.

Table 5.6: Basic numerical description of bend variables – non-transformed and transformed (data: for Modified Brice Types AB1B2CDEFG1G2_v11_1512_3024).

Statistics	Rb/WbCr	Log_{10}(Rb/WbCr)	MMA/WbCr	$(MMA/WbCr/Y)^{0.16}$
N total	3024	3024	3024	3024
N missing	609	609	767	767
N available	2415	2415	2257	2257
Minimum	0.55	-0.259637	0.000358	0.280945
Maximum	12.263	1.088597	0.366787	0.851738
First Quartile	1.9925	0.299398	0.017475	0.523343
Median	2.688	0.429429	0.031904	0.576256
Third quartile	3.784	0.577951	0.056996	0.632317
SE mean	0.032707	0.004238	0.000854	0.001747
Mean	3.110839	0.44221	.044105	0.577589
LCL mean	3.046707	0.4339	0.042431	0.574163
UCL mean	3.174976	0.450519	0.045779	0.581016
Variance	2.583421	0.043367	0.001645	0.006891
Standard Deviation	1.607302	0.208247	0.040564	0.083013
Coefficient of Variation	0.51667797	0.470923	20.852835	0.143723
Skewness	1.556212	0.10661	2.439515	-0.013101
Kurtosis	3.369963	-0.033775	9.534374	0.053884

In addition to the graphical techniques, an inferential method was also employed in verifying normality. A *Shapiro-Wilk normality test* provides a p-value for the untransformed variable of $2.2x10^{-16}$, whereas this value is 0.002726 for the transformed variable (Table 5.7).

The low probability may cast some doubt on the assumption of normality based on this result. However, it should be recalled that this test has been performed on a relatively large sample (n = 2,415). Hence, even very small departures from normality would lead to rejection of the null hypothesis. In fact, the results indicate that the null hypothesis must be accepted and that the data probably follows a Gaussian distribution.

Table 5.7: Results of the Shapiro-Wilk normality test

Variable	Test statistic	p-value
Rb/WbCr	0.8828	2.20E-16
$\log_{10}$(Rb/WbCr)	0.9979	0.002726
MMA/WbCr/Y	0.7867	2.20E-16
$(MMA/WbCr/Y)^{0.16}$	0.9994	0.7232

Taking the outcomes of the numerical descriptions, graphical representations and inferential techniques (hypothesis testing) together, it can safely and satisfactorily be concluded that the transformed variable $\log_{10}$(Rb/WbCr) follows a normal distribution.

5.4 Univariate Distribution and Normal Transformation of MMA/WbCr/Y

Precisely the same statistical methods, techniques (both exploratory and inferential) and sequence of procedures were employed in investigating the univariate distribution of the variable MMA/WbCr/Y and its transformation to obtain a normal distribution (as employed in case of the variable Rb/WbCr and described above in Section 5.3). *Tukey's five number summary* (Table 5.5), other statistics (Table 5.6) and all the previously described graphical methods (Figures 5.12 to Figure 5.15) revealed that MMA/WbCr/Y also has a right-skewed distribution. In addition, it does not follow a normal distribution, the results of hypothesis testing (Table 5.7) demonstrated that it

is not normally distributed. However, although the univariate distribution of this variable could not be normalised using a logarithmic transformation, a power-transformation of the form $(MMA/WbCr/Y)^{0.16}$ does follow a normal distribution, as evidenced in Figures 5.16, Figure 5.17, Figure 5.18, Figure 5.19 and Table 5.7.

Having dealt with the univariate distributions of the two key variables, the next step in the analysis is to address their joint variation, which is illustrated in Figure 5.3 with the aim of developing a means of predicting the probability of a certain average annual migration rate being equalled but not exceeded for a bend with a specified radius of a bend. Therefore, the next section deals with joint analysis of the transformed variables.

5.5 Bivariate Analysis of Bend Migration $(MMA/WbCr/Y)^{0.16}$ as a Function of Bend Radius $\log_{10}(Rb/WbCr)$

5.5.1 Overview

Due to the dynamic morphological characteristics of meandering rivers, the bends in sinuous, alluvial channels undergo changes through time and space. The literature reviewed in Chapters 1 and 2 report how bends grow, evolve, migrate and terminate through erosion at the outer bank and deposition at the inner bank. The literature further indicates that the dimensionless, average rate of bend migration varies during the life span of a bend, and that this can be related to the dimensionless radius of curvature of the bend. The distribution of the data assembled in the UoN/HRW database and plotted in the scatter plot in Figure 5.3 is broadly similar to that in several earlier graphs of this nature, differing mainly in that Figure 5.3 includes many more points, from a wider range of river types, than usually appear in such graphs. It is clear from Figure 5.3 that the dependency of migration on radius of curvature includes wide scatter for any particular value of the radius.

Given the high variability in the migration rates associated with particular values of the bend radius and bearing in mind the aim of the research reported in this thesis, analysis of the dependency of bend migration rate on variability in bend radius using a bivariate probability

analysis is the logical next step. This analysis is based on the transformed versions of the variables, as obtained and discussed in Sections 5.3 and 5.4, due to the advantages inherent to the analysis of data that are normally distributed. The joint distribution of the transformed variables is shown in a scatter plot in Figure 5.20.

It should be noted that, in the following mathematical formulations, the symbols X and Y refer to the x-random variable and the y-random variable, respectively. In this context, the X variable is $\log_{10}$(Rb/WbCr) and the Y variable is $(MMA/Wb/Y)^{0.16}$. For economy of description Y will be used in place of $(MMA/Wb/Y)^{0.16}$ and X in place of $\log_{10}$(Rb/WbCr).

5.5.2 Mathematical Description of Bivariate, Continuous, Random Variables

If X and Y are joint random variables whose outcomes resulted from a composite random experiment, mathematical description of their *joint probability density function* is defined by:

$$f_{X,Y}(x, y) = \delta^2 F_{X,Y}(x, y) / \delta_x \delta_y \qquad (5.1)$$

where, $\delta^2 F_{X,Y}(x, y)$ = the joint cumulative probability distribution function, and the function is valid over the possible range of values of X and the possible range of values of Y.

The graphical presentation of this bivariate density function is shown in Figure 5.21. However, in the case in point, neither bivariate probability density function $f_{X,Y}(x, y)$ nor a bivariate cumulative distribution function $F_{X,Y}(x, y)$ are known *a priori* for the variables as there is no complete theory linking them. Therefore, it is necessary to obtain estimated probability densities for the distribution of X and Y empirically from the data, through the use of an appropriate statistical treatment within a suitable statistical software package. Both the variables are continuous so, theoretically, the probability densities should be described by a continuous surface. However, when estimating probability densities empirically (with the help of a statistical method), densities are computed at grid points and the resulting probability densities are treated as though

they resulted from bivariate analysis of discrete, random variables. Hence, in practice, the estimated densities at grid points appear as shown in Figure 5.22. The graph of the estimated density is given in Figure 5.23.

5.5.3 Kernel Density Function and Estimator, and Estimation of Bivariate Densities

Kernel Density Function and Estimator

Conventionally, when a data set follows a specified parametric distribution the unknown population parameter(s) are estimated by using the sample data set. Similarly, when the sample distribution is known, the probability of an event is conventionally calculated using that known distribution. Conversely, in situations where a sample distribution is not known, or is known but is not mathematically tractable, nonparametric approaches can be used. Recent increases computing power have introduced the possibility of estimating probability density functions from data directly using techniques developed in the area of computational statistics. For example, kernel density estimation is a specific, nonparametric technique that can reliably estimate the underlying densities of a data set.

In this approach, a kernel function, K, is defined as the function that satisfies the following conditions (Wilkinson, 2011):

-- $\int_{-\infty}^{\infty} K(x)dx = 1$

-- $K(x) \geq 0$

-- has sufficient derivatives (meaning it is sufficiently smooth)

The kernel function has the same properties as the formal (definite mathematical formulation) probability density function, and hence it is capable of generating probability densities by way of a computational algorithm.

Given a sample of data $\{x_i\}$, where i=1,2,3, ..., n, with unknown density function $f(x)$ the kernel density estimator (KDE) is given by:

$$\hat{f}(x) = \frac{1}{nh}\sum_{i=1}^{n} K(\frac{(x-x_i)}{h})$$

where, K is the kernel and h is a smoothing parameter, called the band width. The properties relating to KDE are (Wilkinson, 2011):

- The estimator $\hat{f}(x)$ is also a probability density;
- As h approaches zero the estimator $\hat{f}(x)$ shows spikes at the observations;
- As h approaches infinity, the estimator $\hat{f}(x)$ becomes flat and changes very slowly with x;
- The estimator $\hat{f}(x)$ will definitely inherit the continuity and differentiability properties of K (meaning when K smooth, then obviously the estimator is smooth);
- There is a huge flexibility in choosing K and h. But the degree of smoothing is determined by h and is the same at each point of x;
- Kernel density estimators converge asymptotically to any density function, which imparts to the function a general capability to estimate densities of any kind, theoretically.

There are different forms of kernel function, but the Gaussian (normal) kernel is mostly widely used due to its advantages in providing estimates and local properties that vary smoothly (meaning they possess continuity and differentiability: commonly used kernels should have many derivatives) (Wilkinson, 2011; Elgamel et al., 2002). Band width can be selected either subjectively or automatically. In the analysis used here, the default normal reference bandwidth was set in R, which worked well (as claimed in R help, in version 2.13.0).

Estimation of Bivariate Densities

In the bivariate, probabilistic analysis the normalised variables: $\log_{10}$(Rb/WbCr) and (MMA/WbCr/Y)$^{0.16}$ have been used, as shown in Figure 5.20. This plot illustrates the concentration, extent and distribution of the data. To find the estimated densities, the statistical method employed is termed *two dimensional kernel density estimation*. This method computes densities at grid points formed by lines in the (x,y) plane: that is parallel to the x and y-axes. An equal number of grid lines divides the range of data on each axis, producing square grids in the

(x,y) plane. It follows that, the greater the number of grid lines that divide the data range on each axis, the smoother the density surface that is obtained. In this analysis, the number of grid lines was selected so as to obtain a suitable estimation of density and a sufficiently smooth density surface. The resulting concentration of data and contours of joint density is shown in Figure 5.24. The estimated density surface in the (x, y) plane defined by the graph of the function $f_{X,Y}$ (x, y) is illustrated as a 3-D plot in Figure 5.25. As a metaphor, it can be visualised as a mountain rising from the (x,y) plane.

5.6 Conditional Probability Distribution for Migration Rate for a Given Value of Bend Radius

5.6.1 Overview

When attempting to predict the future migration rate for a meander bend, the value of the bend radius (X) is known but the probabilities of the various, possible values of average annual migration rate (Y) are unknown. Hence, it is necessary to calculate the conditional probabilities when assessing and predicting bend migration. In this context, this section examines mathematical and graphical aspects of the conditional probabilities before estimating them from the data.

5.6.2 Mathematical and Graphical Descriptions of the Marginal Probability Density Function for X

X and Y are continuous, random variables having a joint distribution that is determined by the bivariate probability density function $f_{X,Y}(x,y)$ as defined in Equation 5.1. Since X is a continuous, random variable, within the context of joint distribution of X and Y, the probability density function fx of X is called the *marginal probability density function* when the distribution of X is considered without taking account of any information concerning the value of Y. The *marginal probability density function* of X can be obtained from:

$$f_X(x) = \int_y f_{X,Y}(x, y)\, dy \qquad (5.2)$$

where, $f_{X,Y}$ (x, y) is the joint probability density function of X and Y, as defined in Equation 5.1.

The mathematical definition in the formula above shows that the joint probability density function $f_{X,Y}(x, y)$ not only contains the information about X and Y simultaneously, but also contains relevant information on X and Y, *individually*. In this analysis, $\log_{10}(Rb/WbCr)$ is taken as the X-variable throughout and when applying the analysis in practice, it is necessary to write the formula for marginal probability density function for the X variable.

The marginal probability density function $f_X(x)$ and the marginal probability can be visualised through representing it graphically. To achieve this, the marginal probability density function at X=x* (a particular numerical value of X within the range of possible values of X), can be visualised as a plane that is perpendicular to the (x,y) plane and lies along the line x=x*. This plane will intersect the density surface $f_{X,Y}$ (x, y), to produce an intersecting curve called $f_{X,Y}$ (x*, y). Thus, $f_{X,Y}$ (x*, y) is a particular case of $f_{X,Y}$ (x, y) when X=x*. Therefore, $f_{X,Y}$ (x*, y) is now the joint probability density function of X at X=x*. The area of the plane described above is the marginal probability of X at X=x*. The joint probability density function at X=x* and the marginal probability density function at X=x* are both shown in Figure 5.26.

5.6.3 Mathematical and Graphical Description of the Conditional Probability Density Function for Y, Given X

As X and Y are continuous, random variables with a joint distribution, the conditional probability density function for Y given that X=x is given by:

$$f_{Y|X=x}(y|x) = f_{X,Y}(x, y) / f_{X=x}(x) \quad \text{when } f_{X=x}(x) > 0 \qquad (5.3)$$

where, $f_{X,Y}(x,y)$ is the bivariate probability density function of X and Y, as defined in Equation 5.1, and $f_{X=x}(x)$ is the marginal probability density function of X at X=x.

Having determined the conditional probability density function of Y given that X=x, the conditional probability distribution function for Y given that X=x is found from:

$$\begin{aligned} F_{Y|X=x}(y) &= P(Y <= y \mid X=x) \\ &= \int^{y}_{\text{minimum of y}} f_{Y|X=x}(y)\, dy \end{aligned} \qquad (5.4)$$

where, $f_{Y|X=x}$ (y) is the bivariate conditional probability density function of Y, while X=x, as defined in Equation 5.3.

A particular point on the density surface may be defined by the coordinates X=x and Y=y. For this point the function $f_{X,Y}$ (x, y) in the Equation 5.3 has a value greater than zero. At the particular value of X=x, the value of the function $f_{X=x}(x)$ in Equation 5.3 is also a fraction. But the value of the marginal function $f_{X=x}(x)$ is greater than that of the function $f_{X,Y}$ (x, y), since at X=x every individual value of $f_{X,Y}$ (x, y) constitutes the value of $f_{X=x}(x)$. Consequently, the quotient on the right side of Equation 5.3 results in fraction that is bigger than the numerator.

As a result, the area under the conditional density graph defined by the function $f_{Y|X=x}(y)$ is greater than areas under the bivariate density function $f_{X,Y}(x,y)$ and $f_{X=x}(x)$. Therefore, as expected, at a particular value of X such that X=x and up to a value of Y=y, the conditional cumulative probability determined by Equation 5.4 is larger than the cumulative probability obtained from $f_{X,Y}(x,y)$.

Figure 5.26 was used to visualise the bivariate probability density function of the joint random variables X and Y and the marginal probability density function of X at X=x. It would also be possible to visualise the conditional probability density function of Y given that X=x and the conditional probability distribution function of Y given that X=x. This can be pictured as a plane that is perpendicular to the (x,y) plane and runs along the line X=x. This plane will intersect the conditional density graph defined by $f_{Y|X=x}(y|x)$ as indicated in Equation 5.3. The area under this plane up to a Y= y defines the conditional cumulative probability, as defined by Equation 5.4. The conditional probability density function $f_{Y|X=x}(y|x)$ of Y=y given X=x and conditional cumulative probability of y of Y given X=x ($F_{Y|X=x}$ (y)) are both shown in Figure 5.27.

5.6.4 Estimating Conditional Probability from the Estimated Bivariate Density

The purpose of the probabilistic analysis is to support prediction of average annual bend migration rate (MMA/WbCr/Y) for a bend with a known ratio of bend radius to crossing width (Rb/WbCr). To do this it is necessary to find the conditional probability distribution for

MMA/WbCr/Y at a known value of Rb/WbCr. Ideally, this could be achieved using Equation 5.4. However, as noted in Section 5.5**,** there is no theory to support development of a bivariate density model that can be used to calculate the conditional probability distribution. Consequently, the densities estimated at the grid points (using the approach described in Section 5.5**)** must be used instead.

The approach is as follows. At a particular grid line, with a known value of $\log_{10}$(Rb/WbCr), the marginal probability densities at each grid point were estimated by using Equation 5.2 to represent the joint estimated densities for all values of $(MMA/WbCr/Y)^{0.16}$ within the dataset. Then conditional densities were computed from the estimated joint densities and marginal densities using Equation 5.3. Next, cumulative probability distributions were calculated from these conditional densities, using Equation 5.4. Here the advantage of using normalised data becomes apparent. Because the data can be safely described by a normal distribution, a normal model can be fitted to $(MMA/WbCr/Y)^{0.16}$ and the probability distribution from this fitted, normal conditional probability distribution may be used for predictive purposes.

Hence, the conditional density function of $(MMA/WbCr/Y)^{0.16}$ has been computed from the bivariate density function for 76, selected values of $\log_{10}$(Rb/WbCr) across the entire range of values of $\log_{10}$(Rb/WbCr) (for example, see the red line in Figure 5.30). Consequently, for each selected value of $\log_{10}$(Rb/WbCr), a mean and standard deviation has been generated for the distribution of $(MMA/WbCr/Y)^{0.16}$. An explanation on how why and how 76 grids were selected is given in Appendix A5.3 of the Appendix to Chapter 5.

Using the resulting data set of 76 means and standard deviations, a fitted mean and standard deviation has been obtained using the regression model LOESS (see Figures 5.28 and 5.29 for the means and standard deviations, respectively).

Next, for each selected value of $\log_{10}$(Rb/WbCr), a fitted normal density function has been computed (for example, see the green line in Figure 5.30). There is reasonable agreement between the conditional density function and the fitted normal conditional density function from values of Rb/WbCr between 1 and 8.5 in Figures 5.30 to Figure 5.55 (upper graph).

However, inspection of the graphs for values of Rb/WbCr less than about 1 and greater than around 8.5, reveals that differences between the actual and normal distributions in these ranges are noticeably more marked (see Figures A5.1 to A5.6 (upper graph), and Figures A5.6 (lower graph) to Figure A5.13 in Section A5.2 of the Appendix to Chapter 5). These differences result from the scarcity of data in these ranges (which reflect the rare occurrence of such bends in the field). The outcome is to limit the aplicability of the bivariate probability analysis developed here to values of Rb/WbCr that greater than about 1 and less than around 8.5.

5.7 Probabilistic Tool for Predicting Future Migration Rates

Using the fitted normal conditional density function described in Section 5.6, rates of meander migration have been estimated corresponding to: 50%, 60%, 75%, 80%, 90%, 95%, 97%, 98%, and 99% probabilities of not being exceeded. The resulting curves are presented in Figure 5.56 (for the transformed variables) and Figure 5.57 (for the untransformed variables). In addition to these graphical representations, migration quantiles at 76 values of dimensionless bend radius for a number of selected probability levels are listed in Table 5.8.

Three zones can be identified by visual inspection of the distributions of data points and the shapes of the probabilistic migration prediction curves. These zones are indicated by the dotted lines in Figure 5.56 and Figure 5.57 and the use of different background colours in Table 5.8.

The left zone, where the curves are shown as dotted lines, covers bends with values of dimensionless radius (R_b/W_bCr) less than 1. This zone corresponds to bend behaviour during the *meander termination stage* in Hickin and Nanson's analysis (Hickin, 1978). The middle zone, where the curves are shown as solid lines, covers the range $1 < (Rb/WbCr) < 8.5$. This zone includes the *meander growth and migration stages* of Hickin and Nanson's characterisation of bend evolution. The right zone, where the curves are again represented by dotted lines, covers values of $(Rb/WbCr) > 8.5$. This corresponds to the *meander initiation stage* described by Hickin and Nanson.

The shape of the probability curves and data listed in the tables suggest that, in the left zone, average annual migration rates are highly variable and that extreme values could be higher than those for less tightly curved bends in the central zone. These observations are consistent with the descriptive accounts of bend behaviour during the termination stages provided by Hickin and Nanson and corroborated by subsequent researchers. It is well established that very tight bends, where the bend radius is close to or less than the channel width, may behave erratically. Some bends remain almost unchanging for considerable periods, while others are cut off by the movement of a migrating bend from upstream or exhibit rapid erosion and retreat at their inner banks, and still others migrate very rapidly through erosion of their outer banks. This makes very short-radius bends unpredictable and dangerous in terms of potential for floodplain erosion and property damage, so that the erosion hazard associated with them may be very high. In the right zone, average annual migration rates are generally lower than in the central zone, which is consistent with the descriptive accounts provided by Hickin and Nanson and corroborated by subsequent researchers, of the relatively slow rates of bend evolution being exhibited by bends during the *initiation stage*.

However, the conditional densities of the bend migration variable in both the left and right zones deviated from the fitted normal conditional densities, as described in Section 5.6 and, P-values in these zones primarily reflect the relatively low numbers of points, rather than variability in migration rates. Accordingly, drawing any conclusions concerning extreme migration rates being higher or lower for short or long radius bends would be an over-interpretation. That said, the shapes of the dotted probability curves in Figures 5.56 and 5.57 are consistent with pre-existing conceptualisations of bend behaviour, so perhaps they should not be rejected out of hand. This underpins the decision to leave the curves on the graphs, but represent them by dotted rather than solid lines. It follows that in predicting future erosion rates associated with a selected probability level, users of the predictive method should exercise additional caution when dealing with bends that have values dimensionless radius less than one or greater than 8.5. In highly sensitive cases, where the consequences of under-estimating the average annual migration rate are particularly serious, it would wise to use extreme caution and employ additional, site specific, analyses when making predictions bends that plot in either of these zones.

Table 5.8: Average annual bend migration rates (in terms of average channel width at the crossings up and downstream) at selected probability levels for 76 values of dimensionless bend radius.

Rb/WbCr	50%	60%	75%	80%	90%	95%	97%	98%	99%
0.61	0.035	0.048	0.078	0.093	0.147	0.209	0.260	0.304	0.385
0.64	0.035	0.047	0.075	0.090	0.140	0.198	0.245	0.286	0.361
0.68	0.034	0.046	0.072	0.086	0.134	0.188	0.232	0.270	0.339
0.71	0.033	0.044	0.070	0.083	0.128	0.179	0.220	0.255	0.320
0.75	0.033	0.043	0.068	0.080	0.122	0.170	0.209	0.242	0.302
0.79	0.032	0.042	0.066	0.077	0.117	0.162	0.199	0.230	0.286
0.83	0.031	0.041	0.064	0.075	0.113	0.155	0.190	0.219	0.272
0.88	0.031	0.041	0.062	0.073	0.109	0.149	0.181	0.209	0.259
0.92	0.031	0.040	0.060	0.071	0.105	0.143	0.174	0.200	0.247
0.97	0.030	0.039	0.059	0.069	0.102	0.138	0.167	0.192	0.236
1.02	0.030	0.039	0.058	0.067	0.099	0.134	0.161	0.185	0.227
1.08	0.030	0.038	0.057	0.066	0.096	0.130	0.156	0.178	0.219
1.13	0.029	0.038	0.056	0.064	0.094	0.126	0.151	0.173	0.211
1.20	0.029	0.037	0.055	0.063	0.092	0.123	0.147	0.168	0.205
1.26	0.029	0.037	0.054	0.062	0.090	0.120	0.143	0.163	0.199
1.33	0.029	0.037	0.053	0.061	0.088	0.117	0.140	0.159	0.194
1.40	0.029	0.036	0.053	0.061	0.087	0.115	0.137	0.156	0.189
1.47	0.029	0.036	0.052	0.060	0.086	0.113	0.135	0.153	0.185
1.55	0.029	0.036	0.052	0.060	0.085	0.112	0.133	0.151	0.182
1.63	0.029	0.036	0.052	0.059	0.084	0.111	0.131	0.149	0.180
1.72	0.029	0.036	0.052	0.059	0.084	0.110	0.131	0.148	0.178
1.81	0.029	0.036	0.052	0.059	0.084	0.110	0.130	0.147	0.177
1.90	0.029	0.037	0.052	0.060	0.084	0.110	0.130	0.147	0.177
2.01	0.030	0.037	0.053	0.060	0.085	0.111	0.131	0.148	0.178
2.11	0.030	0.037	0.053	0.061	0.085	0.111	0.132	0.149	0.179
2.22	0.030	0.038	0.054	0.061	0.086	0.112	0.133	0.150	0.181
2.34	0.031	0.038	0.054	0.062	0.087	0.114	0.134	0.151	0.182
2.47	0.031	0.039	0.055	0.063	0.088	0.115	0.136	0.153	0.184
2.60	0.031	0.039	0.055	0.063	0.089	0.116	0.137	0.155	0.186
2.74	0.032	0.040	0.056	0.064	0.090	0.118	0.139	0.157	0.188
2.88	0.032	0.040	0.057	0.065	0.092	0.120	0.142	0.160	0.192
3.03	0.033	0.041	0.058	0.067	0.094	0.123	0.145	0.163	0.197
3.19	0.034	0.042	0.060	0.068	0.096	0.126	0.149	0.168	0.202
3.36	0.034	0.043	0.061	0.070	0.099	0.129	0.153	0.172	0.208
3.54	0.035	0.044	0.062	0.072	0.101	0.132	0.157	0.177	0.214
3.73	0.036	0.045	0.064	0.073	0.103	0.136	0.161	0.182	0.219
3.93	0.036	0.045	0.065	0.074	0.105	0.138	0.164	0.186	0.224
4.14	0.037	0.046	0.066	0.076	0.107	0.141	0.167	0.189	0.228
4.36	0.037	0.047	0.067	0.077	0.109	0.143	0.170	0.192	0.232
4.59	0.037	0.047	0.068	0.078	0.111	0.146	0.173	0.196	0.237
4.83	0.038	0.048	0.069	0.079	0.112	0.148	0.177	0.200	0.242
5.09	0.038	0.048	0.070	0.080	0.114	0.151	0.180	0.204	0.247
5.22	0.038	0.048	0.070	0.081	0.115	0.152	0.181	0.205	0.249
5.36	0.038	0.049	0.070	0.081	0.116	0.153	0.182	0.207	0.251
5.50	0.039	0.049	0.071	0.081	0.116	0.154	0.183	0.208	0.252
5.64	0.039	0.049	0.071	0.082	0.116	0.154	0.184	0.208	0.253
5.79	0.039	0.049	0.071	0.082	0.117	0.154	0.184	0.208	0.252
5.94	0.039	0.049	0.071	0.082	0.116	0.154	0.183	0.208	0.252

Rb/WbCr	50%	60%	75%	80%	90%	95%	97%	98%	99%
6.10	0.039	0.049	0.071	0.082	0.116	0.153	0.182	0.207	0.250
6.26	0.039	0.049	0.071	0.081	0.116	0.153	0.182	0.206	0.249
6.42	0.039	0.049	0.071	0.081	0.115	0.152	0.181	0.204	0.247
6.59	0.039	0.049	0.071	0.081	0.115	0.151	0.179	0.203	0.245
6.76	0.039	0.049	0.071	0.081	0.114	0.150	0.178	0.201	0.243
6.94	0.039	0.049	0.070	0.081	0.114	0.149	0.177	0.199	0.240
7.12	0.040	0.049	0.070	0.080	0.113	0.148	0.175	0.197	0.237
7.31	0.040	0.049	0.070	0.080	0.112	0.146	0.173	0.195	0.234
7.50	0.040	0.049	0.070	0.079	0.111	0.145	0.171	0.192	0.231
7.70	0.040	0.049	0.069	0.079	0.110	0.143	0.168	0.189	0.227
7.90	0.040	0.049	0.069	0.078	0.109	0.141	0.166	0.186	0.223
8.11	0.040	0.049	0.068	0.078	0.108	0.139	0.163	0.183	0.218
8.32	0.040	0.049	0.068	0.077	0.106	0.137	0.160	0.180	0.214
8.54	0.040	0.049	0.067	0.076	0.105	0.134	0.157	0.176	0.209
8.76	0.040	0.049	0.067	0.076	0.103	0.132	0.154	0.172	0.204
8.99	0.040	0.048	0.066	0.075	0.102	0.130	0.151	0.168	0.199
9.23	0.040	0.048	0.066	0.074	0.100	0.127	0.148	0.164	0.194
9.47	0.040	0.048	0.065	0.073	0.098	0.124	0.144	0.160	0.189
9.72	0.040	0.048	0.064	0.072	0.097	0.122	0.141	0.156	0.183
9.97	0.040	0.048	0.064	0.071	0.095	0.119	0.137	0.152	0.178
10.23	0.040	0.047	0.063	0.070	0.093	0.116	0.133	0.147	0.172
10.50	0.040	0.047	0.062	0.069	0.091	0.113	0.129	0.142	0.166
10.78	0.039	0.047	0.061	0.068	0.089	0.109	0.125	0.138	0.160
11.06	0.039	0.046	0.060	0.067	0.087	0.106	0.121	0.133	0.154
11.35	0.039	0.046	0.059	0.066	0.084	0.103	0.117	0.128	0.148
11.64	0.039	0.046	0.059	0.064	0.082	0.100	0.113	0.123	0.142
11.95	0.039	0.045	0.058	0.063	0.080	0.097	0.109	0.119	0.135
12.26	0.039	0.045	0.057	0.062	0.078	0.093	0.105	0.114	0.129

Table 5.8 presents average annual migration rates at very closely spaced values of R_b/W_bCr so that a user can easily find migration values corresponding to the relevant dimensionless bend radius. Table 5.9 below provides an abbreviated version of Table 5.8 in which migration rates are provided for 24 values of R_b/W_bCr, corresponding to integer and half values of dimensionless radius.

Table 5.9: Average annual bend migration rates (MMA/WbCr/Y) at selected probability levels for 24 values of dimensionless bend radius.

R_bW_bCr	50%	60%	75%	80%	90%	95%	97%	98%	99%
0.75	0.030	0.041	0.067	0.080	0.126	0.180	0.224	0.262	0.332
1	0.034	0.043	0.063	0.073	0.105	0.139	0.167	0.189	0.230
1.5	0.027	0.034	0.050	0.057	0.082	0.109	0.130	0.147	0.178
2	0.028	0.035	0.050	0.057	0.081	0.105	0.125	0.141	0.169
2.5	0.031	0.038	0.054	0.063	0.088	0.115	0.136	0.154	0.185
3	0.033	0.041	0.059	0.068	0.095	0.124	0.146	0.165	0.198
3.5	0.035	0.043	0.061	0.070	0.098	0.129	0.152	0.171	0.206
4	0.037	0.046	0.066	0.075	0.106	0.138	0.163	0.184	0.222

R_bW_bCr	50%	60%	75%	80%	90%	95%	97%	98%	99%
4.5	0.037	0.047	0.067	0.076	0.107	0.140	0.166	0.187	0.225
5	0.038	0.047	0.068	0.078	0.110	0.144	0.171	0.193	0.233
5.5	0.039	0.049	0.071	0.081	0.116	0.153	0.182	0.206	0.249
6	0.039	0.050	0.072	0.083	0.120	0.158	0.189	0.214	0.260
6.5	0.039	0.049	0.071	0.082	0.119	0.158	0.1883	0.214	0.260
7	0.038	0.048	0.070	0.080	0.115	0.152	0.181	0.205	0.2478
7.5	0.039	0.049	0.070	0.080	0.112	0.147	0.174	0.197	0.2367
8	0.040	0.050	0.071	0.080	0.112	0.145	0.171	0.192	0.231
8.5	0.041	0.050	0.071	0.081	0.112	0.145	0.170	0.192	0.229
9	0.040	0.050	0.070	0.079	0.110	0.142	0.167	0.188	0.225
9.5	0.039	0.048	0.067	0.076	0.105	0.135	0.158	0.178	0.212
10	0.038	0.046	0.063	0.072	0.097	0.124	0.144	0.162	0.191
10.5	0.038	0.046	0.061	0.068	0.090	0.113	0.130	0.143	0.167
11	0.039	0.046	0.060	0.066	0.085	0.103	0.117	0.128	0.148
11.5	0.040	0.046	0.057	0.062	0.078	0.093	0.104	0.112	0.127
12	0.040	0.045	0.055	0.060	0.073	0.086	0.095	0.102	0.115

5.8 Predicting Migration Rate

In order to estimate the possible migration rate for a bend using the tool developed and presented here, it is first necessary for the user to measure the minimum radius of curvature for the bend in question and the width of the channel at the meander crossings immediately up and downstream of that bend. This may be done in the field by stream reconnaissance or from a contemporary aerial photograph, satellite image or map.

The user then calculates the ratio of bend radius to channel width (R/W) and locates this value on the x-axis in Figure 5.57. The user then draws a line straight up the graph until it intersects the curve for the selected level of probability, where probability in this case corresponds to the likelihood that the actual rate of bend migration will be equal to or less than the predicted value. The user selects the level of probability based on a judgment of the acceptable risk, where risk is defined as the probability that the bend migration rate will exceed the predicted rate multiplied by the consequences should it do so.

For example, if an important piece of infrastructure, such as a high tension electricity pylon, is located in an area of the floodplain that is exposed to bank erosion due to bend migration, the consequences of the bend encountering the pylon would be very serious and a high level of

probability that the predicted rate of migration will not be exceeded (say, 95%) would be appropriate. Conversely, if the asset at risk was an agricultural flood embankment, for which the consequences of failure would be less serious, a lower probability could be selected (say, 75%). Having intersected the selected probability curve, a horizontal line is drawn to the y-axis, and the predicted migration rate is read from the scale there.

The probability levels expressed on the graph are the non-exceedence probability. That is the probability, p, that the migration that the actual, future average annual migration rate will be equal to or less than the predicted value, y, for the current ratio of bend radius to width, x. In mathematical terms this can be expressed as:

$$P\{MMA/WbCr/Y <= y \mid Rb/WbCr = x\} = p \quad (5.5)$$

Usually, p is expressed in decimal form. However, in the graph, probabilities are given as percentages.

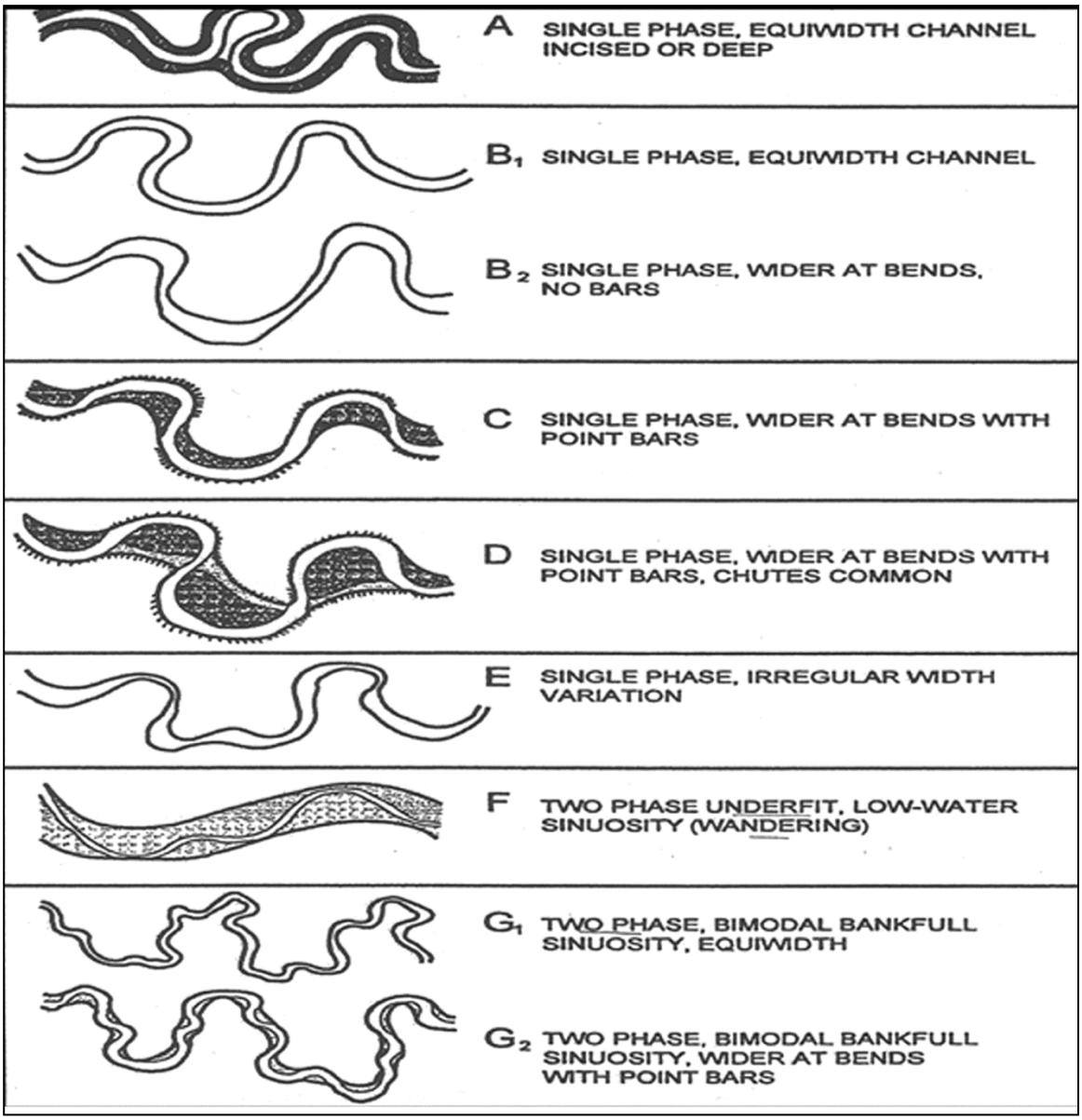

Figure 5.1: Schematic diagram illustrating the modified Brice Types from A to G2 (from Lagasse et al, 2003).

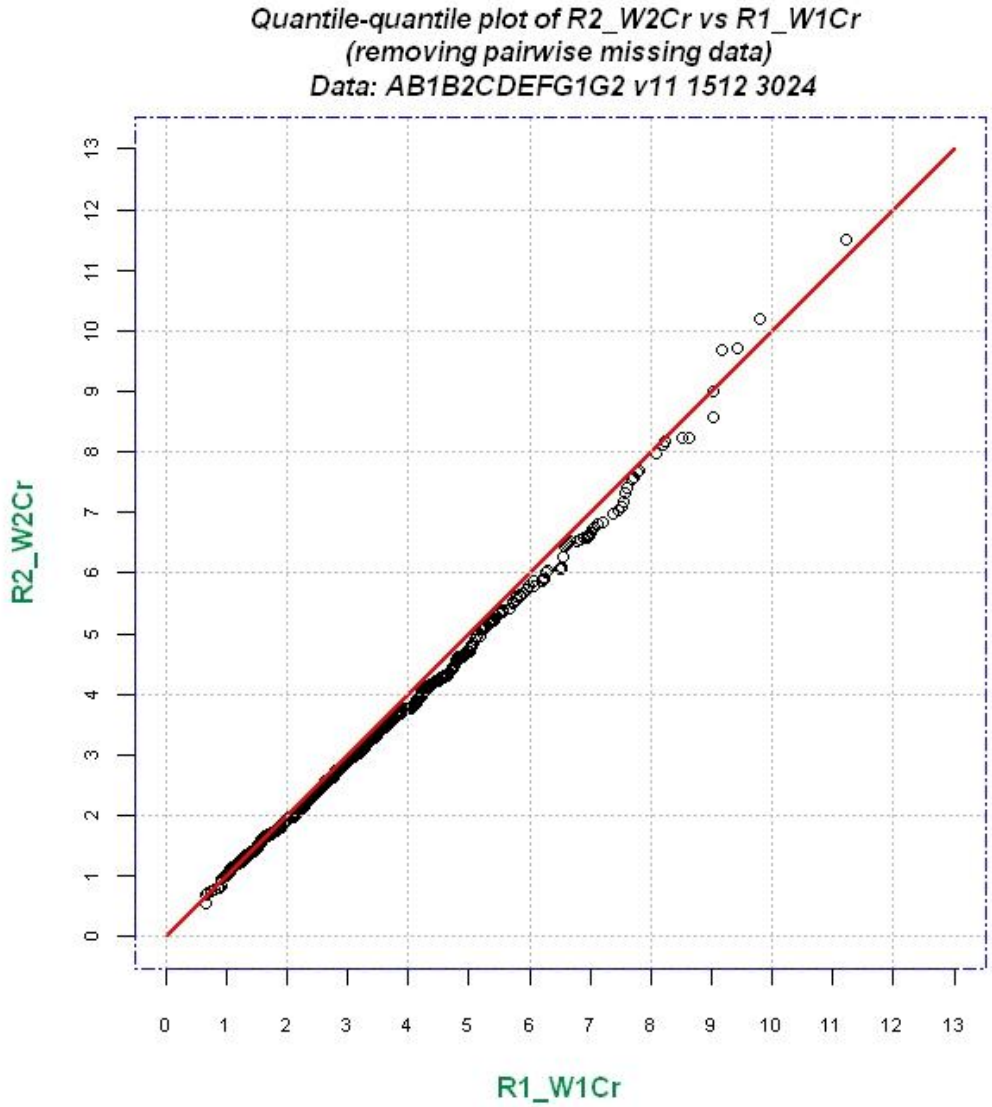

Figure 5.2: Sample quantiles for dimensionless bend radius of curvature data at times T1 and T2 plotted against each other. The fact that the data closely follow the line of perfect agreement suggests that they were drawn from the same population.

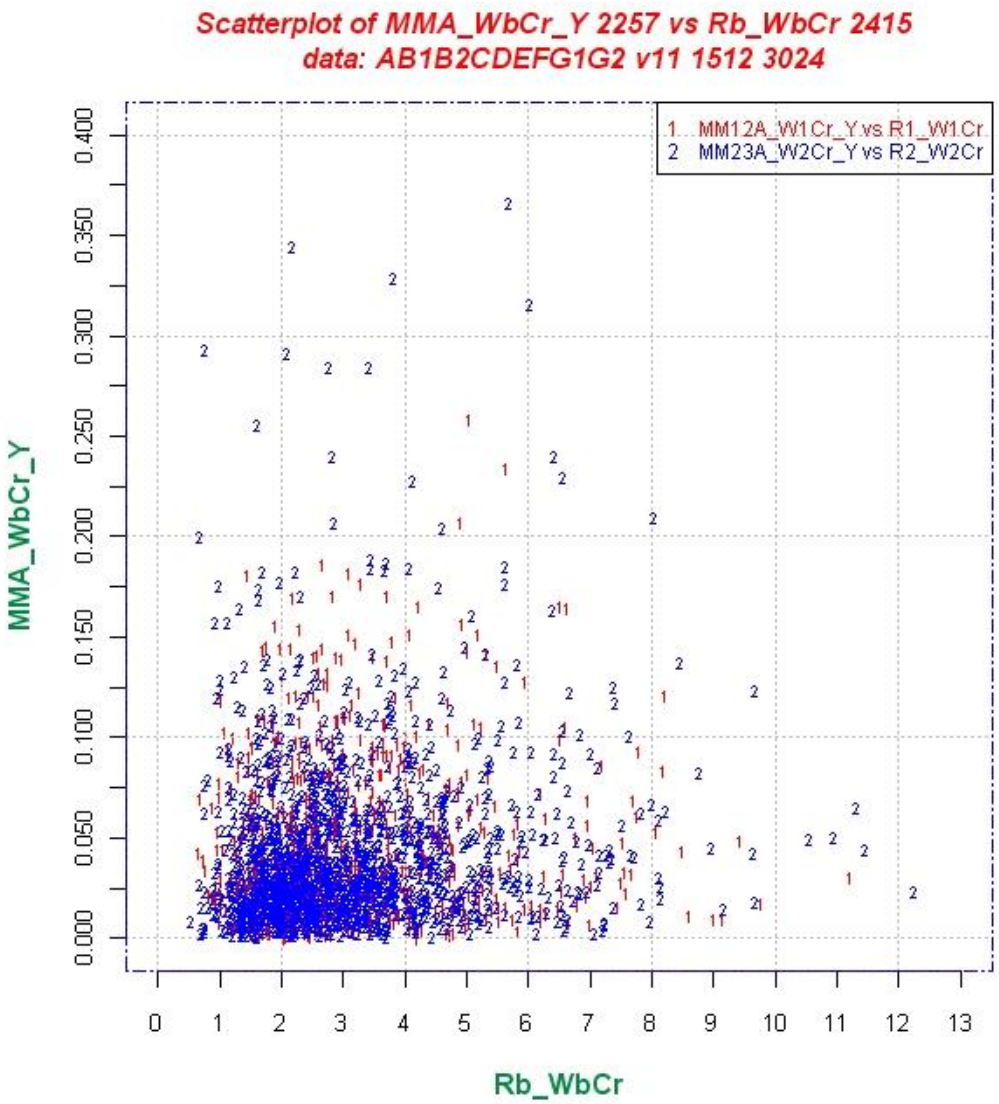

Figure 5.3: Scatter plot of dimensionless average annual migration rate measured at the bend apex (MMA/WbCr/Y) as a function of the ratio of outer bank radius of curvature to river channel width at the crossing (Rb/WbCr).

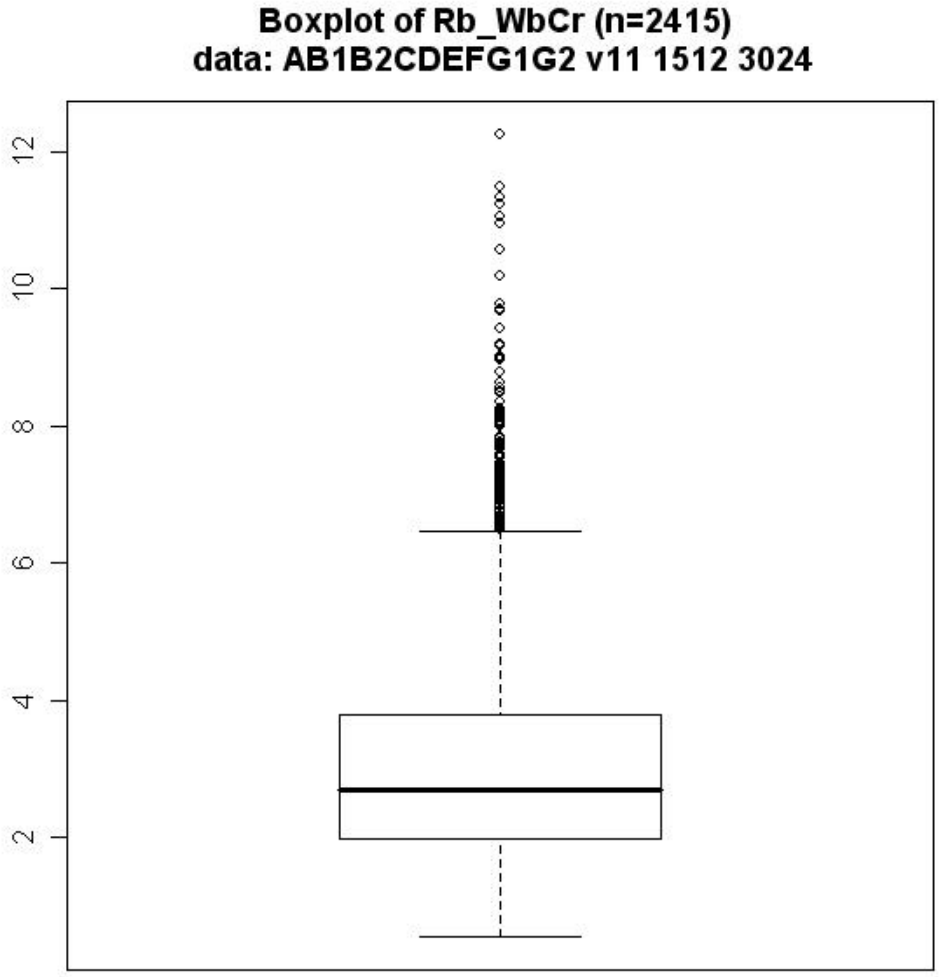

Figure 5.4: Box and whisker plot of the variable ratio of outer bank radius of curvature to river channel width at the crossing (Rb/WbCr).

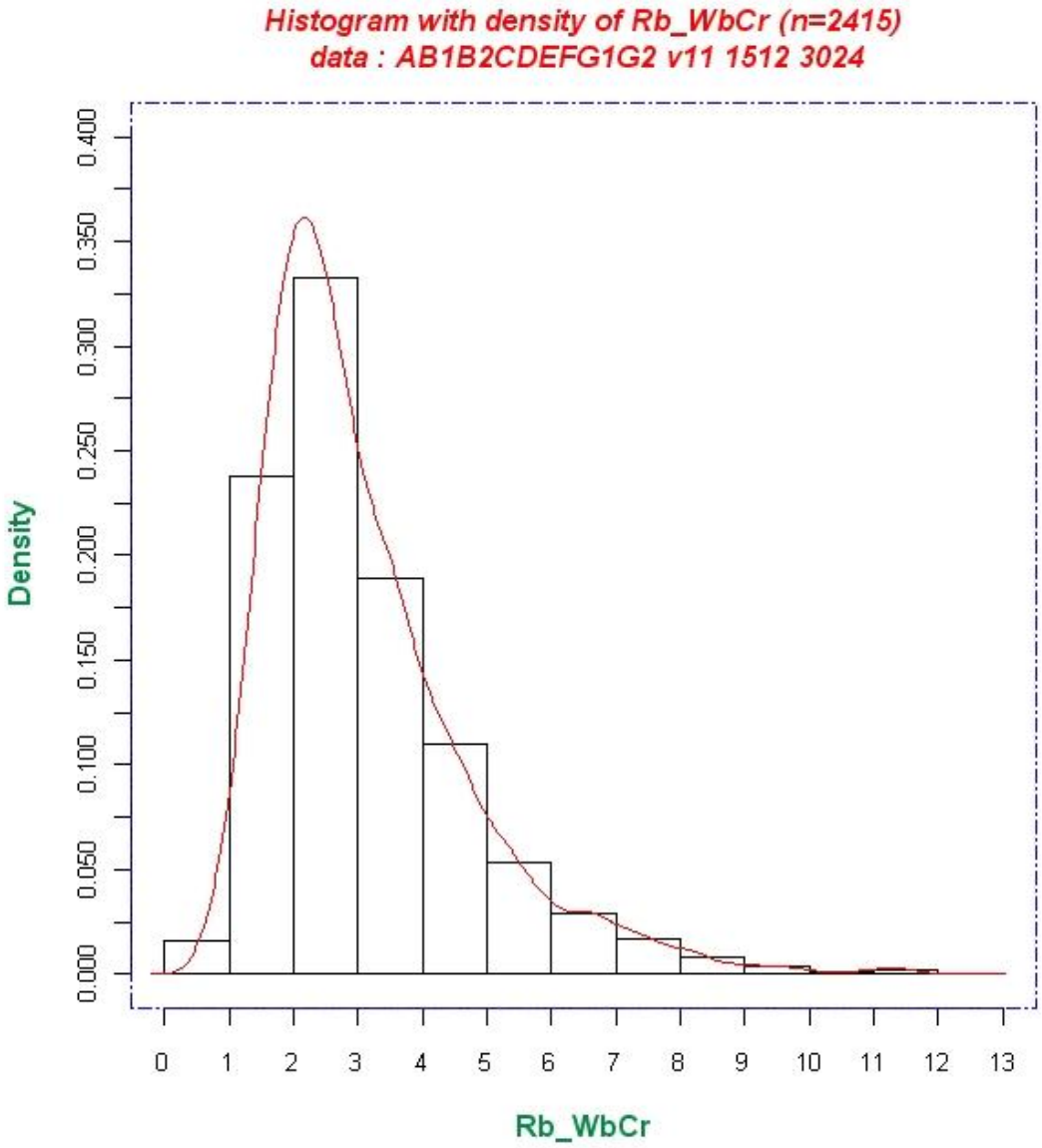

Figure 5.5: Histogram and estimated density distribution for the variable – ratio of outer bank radius of curvature to river channel width at the crossing (Rb/WbCr).

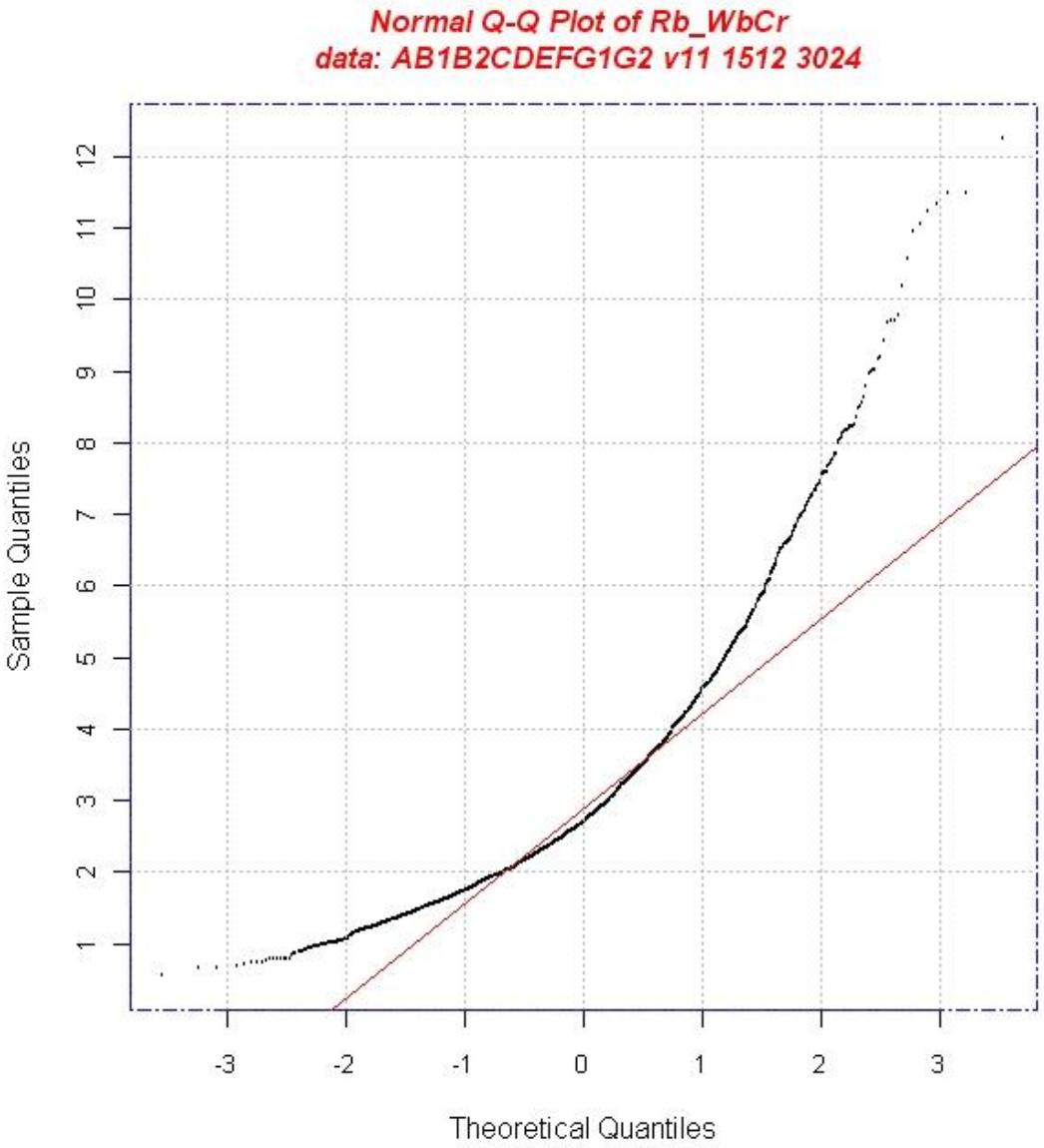

Figure 5.6: Normal probability plot for the variable - ratio of outer bank radius of curvature to river channel width at the crossing (Rb/WbCr).

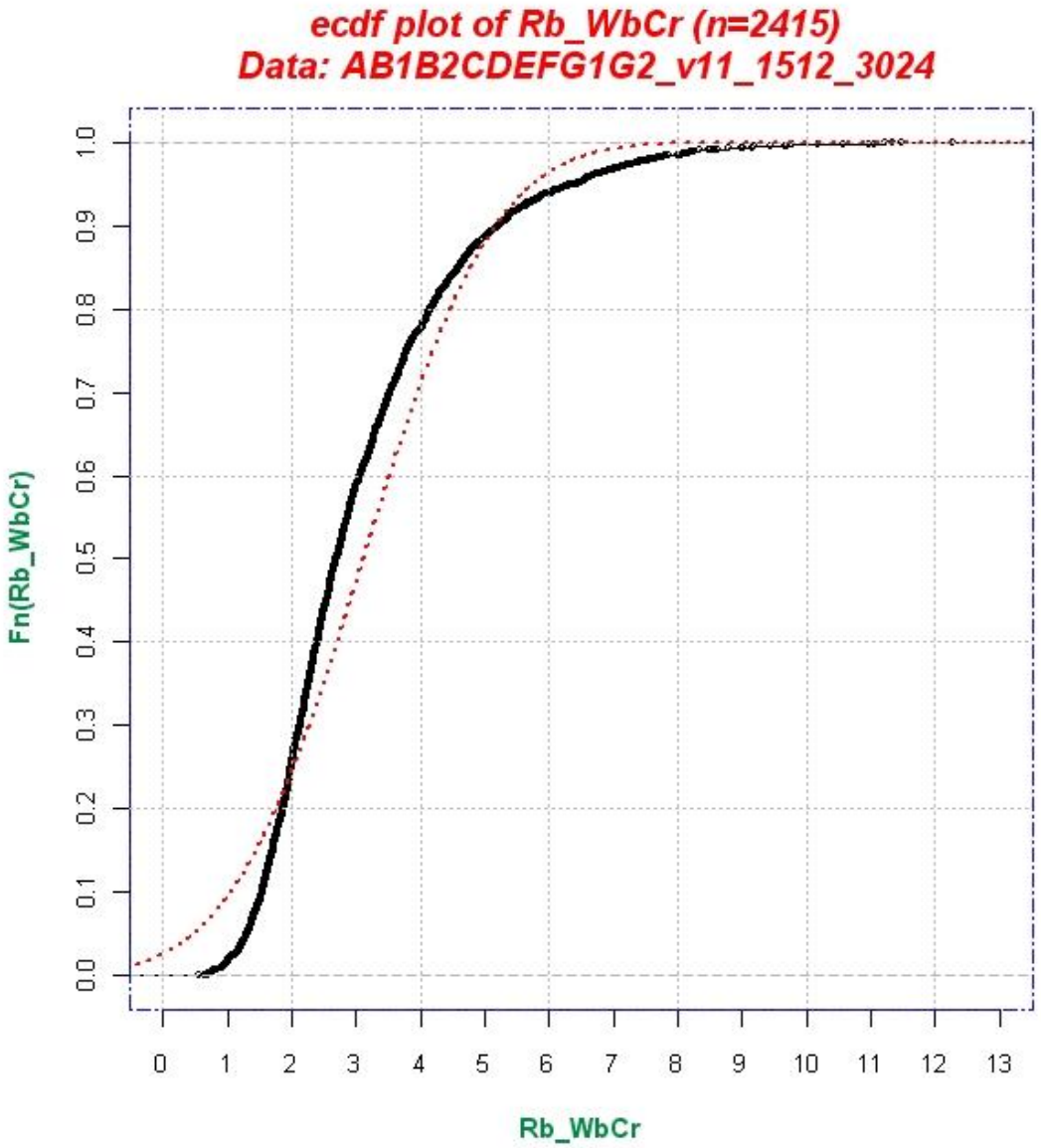

Figure 5.7: Empirical cumulative probability and the fitted normal probability distributions for the variable - ratio of outer bank radius of curvature to river channel width at the crossing (Rb/WbCr).

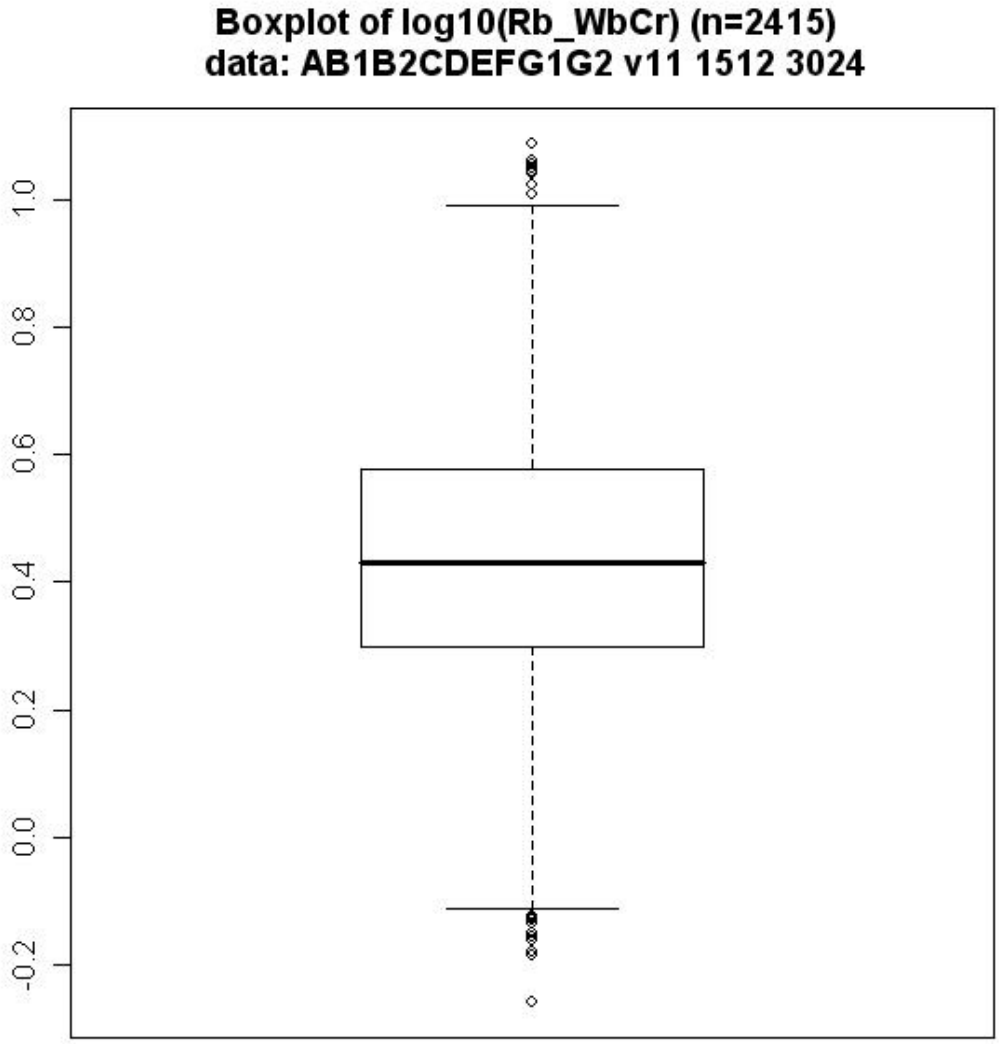

Figure 5.8: Box and whisker plot of the logarithmically transformed variable - ratio of outer bank radius of curvature to river channel width at the crossing (Rb/WbCr).

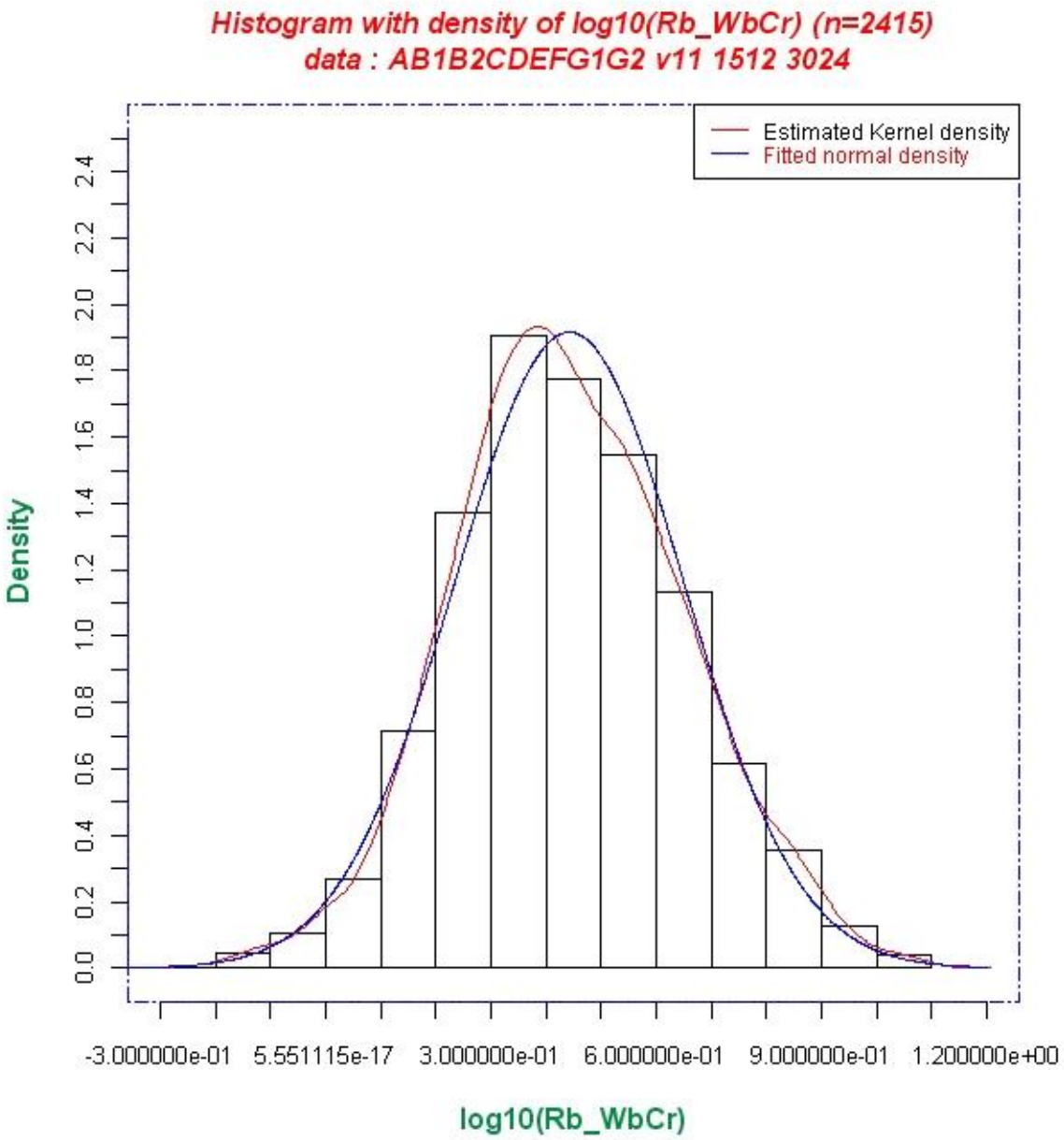

Figure 5.9: Histogram, estimated density and fitted normal density distributions for the logarithmically transformed variable - ratio of outer bank radius of curvature to river channel width at the crossing ($\log_{10}$(Rb/WbCr)).

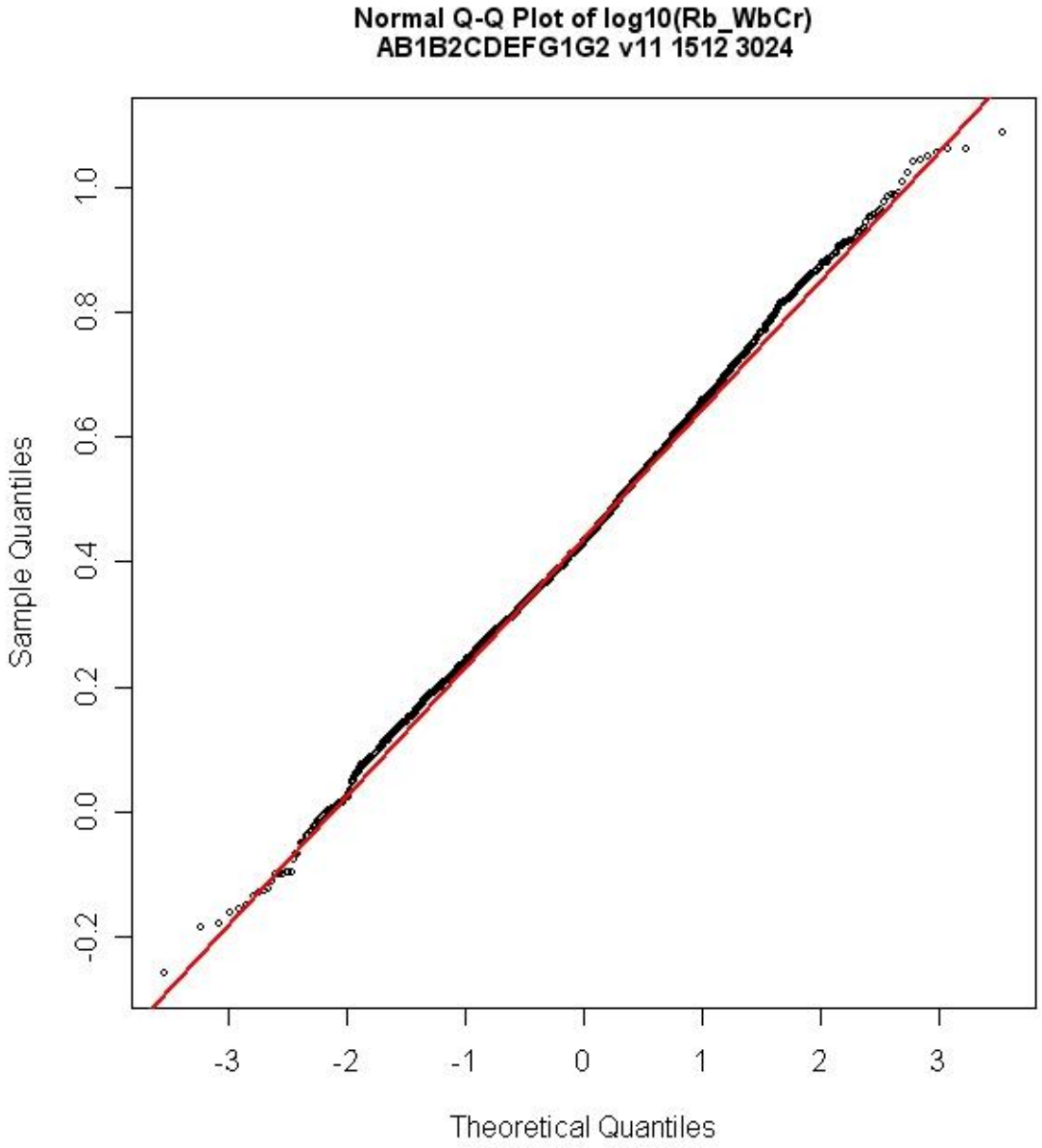

Figure 5.10: Normal probability plot for the logarithmically transformed variable - ratio of outer bank radius of curvature to river channel width at the crossing (Rb/WbCr).

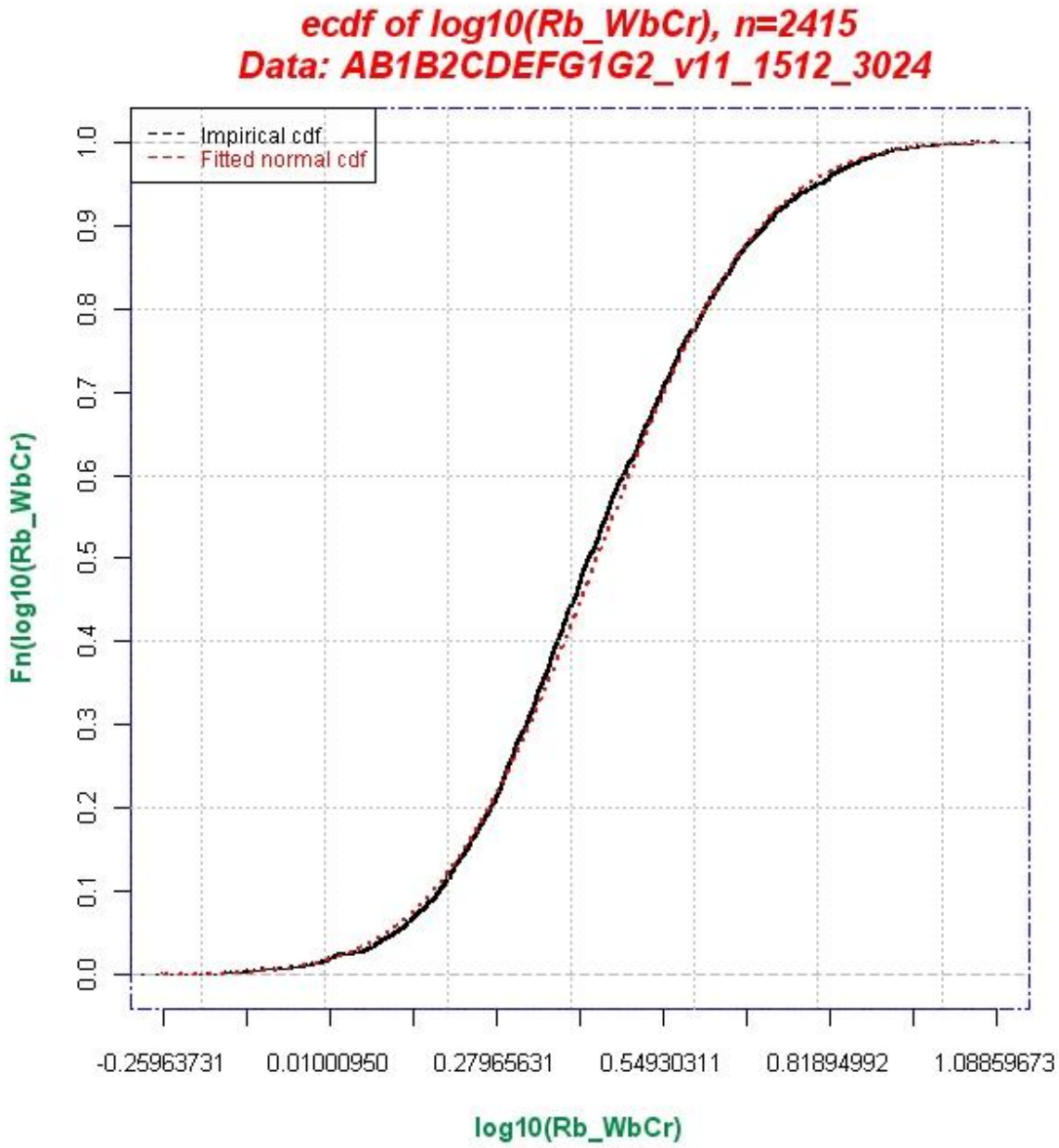

Figure 5.11: Empirical probability and the fitted normal probability distributions for the logarithmically transformed variable - ratio of outer bank radius of curvature to river channel width at the crossing (Rb/WbCr).

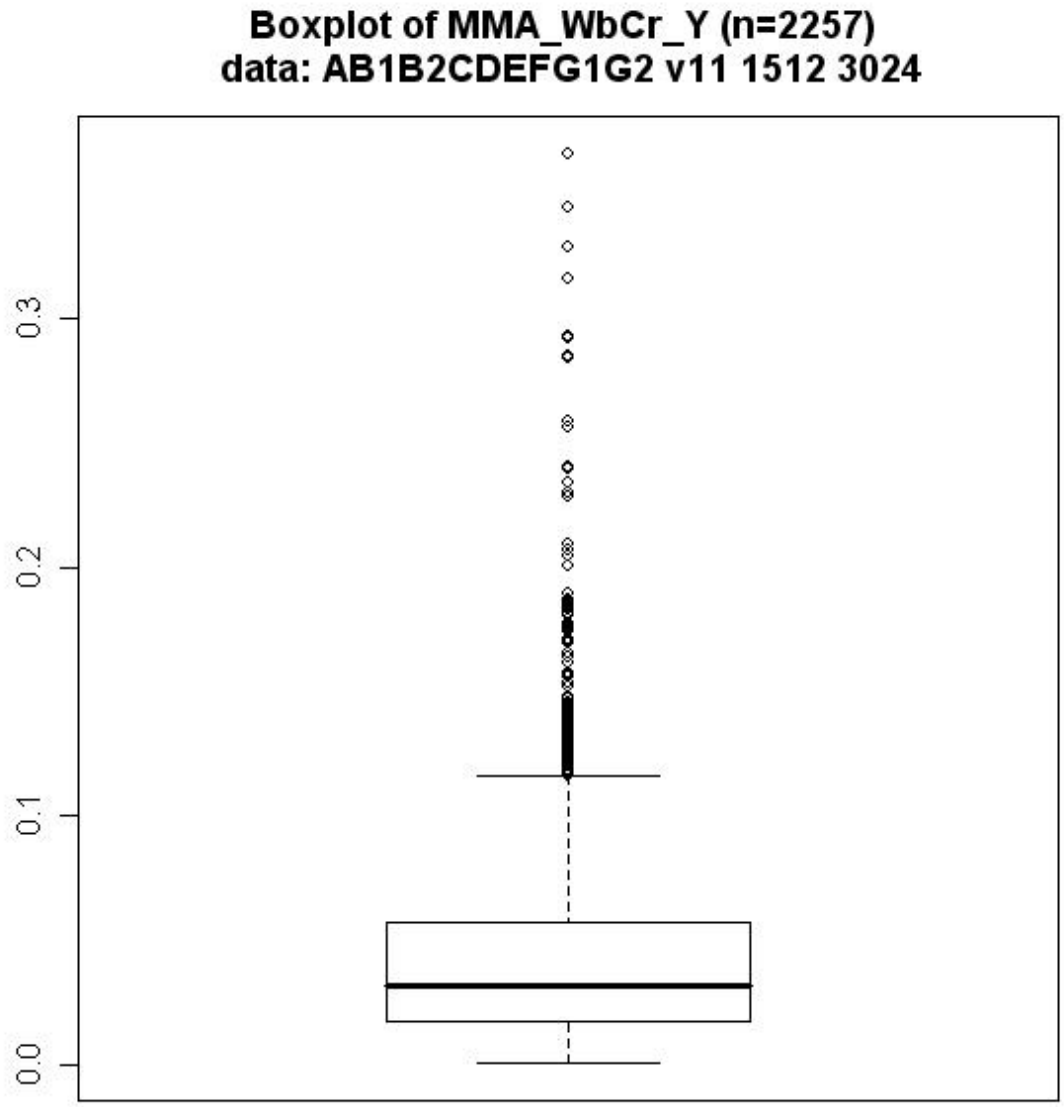

Figure 5.12: Box and whisker plot of the variable– dimensionless average annual migration at the bend apex (MMA/WbCr/Y).

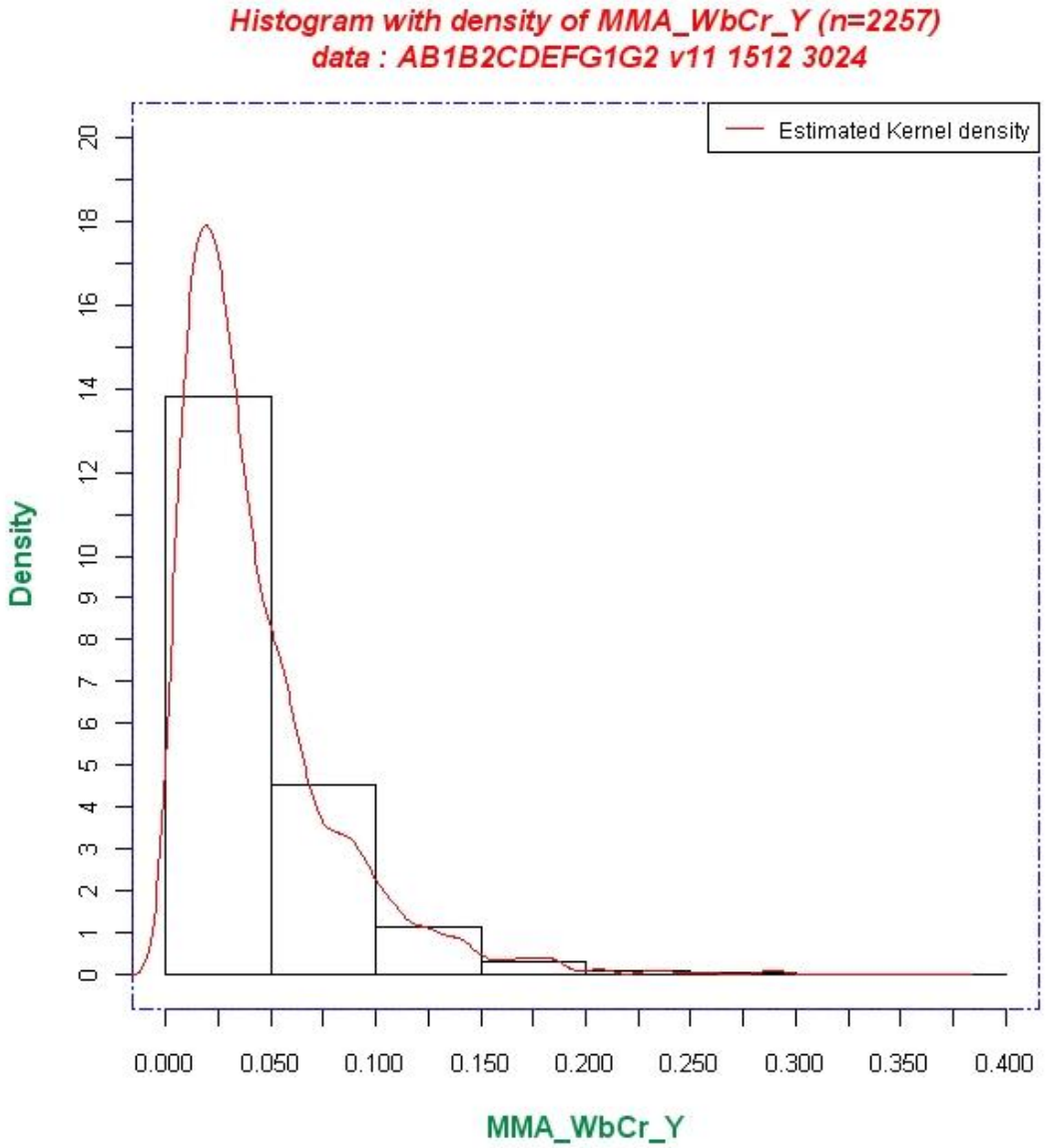

Figure 5.13: Histogram and estimated density of the variable – dimensionless average annual migration at the bend apex (MMA/WbCr/Y).

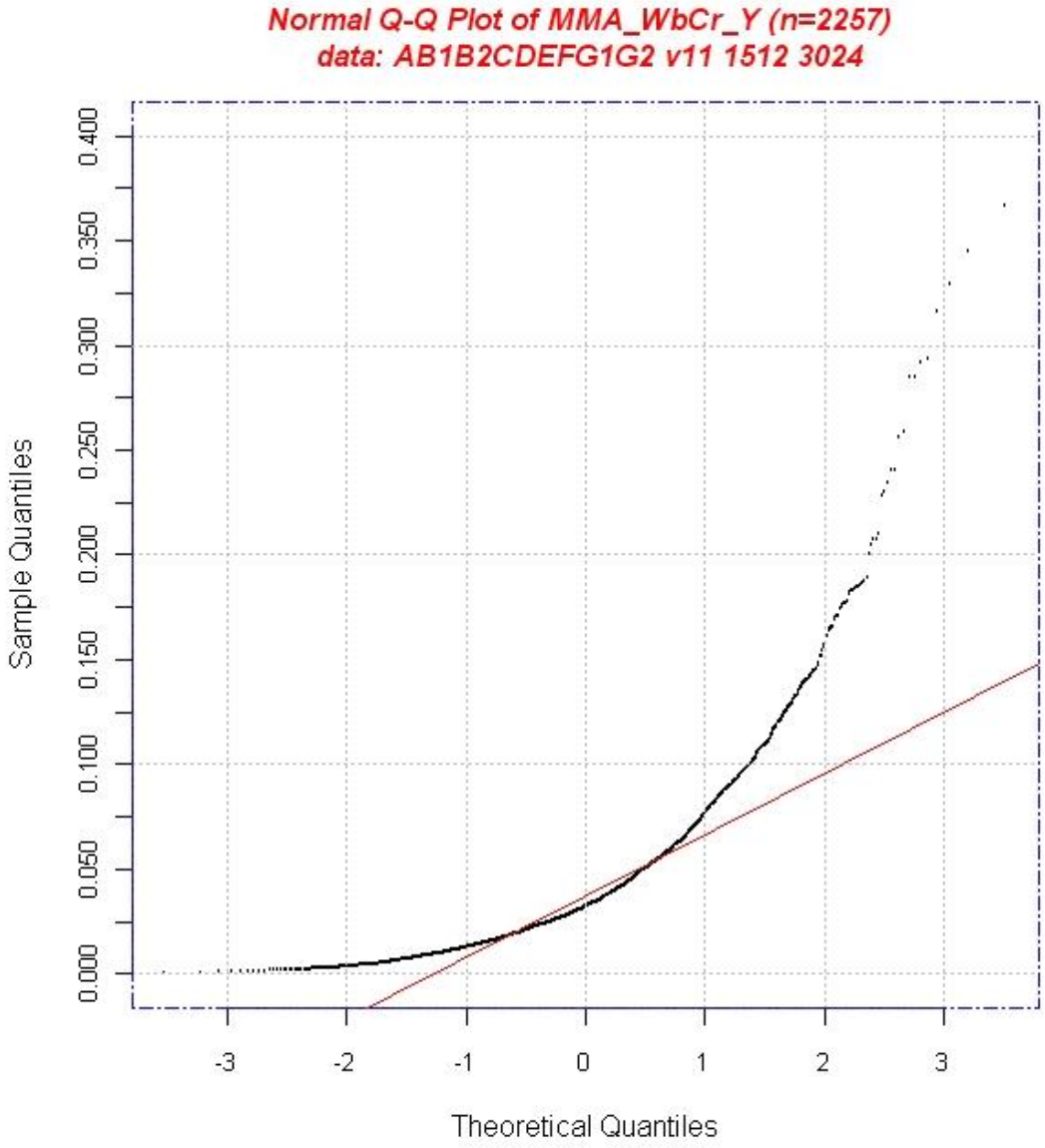

Figure 5.14: Normal probability plot for the variable – dimensionless average annual migration at the bend apex (MMA/WbCr/Y).

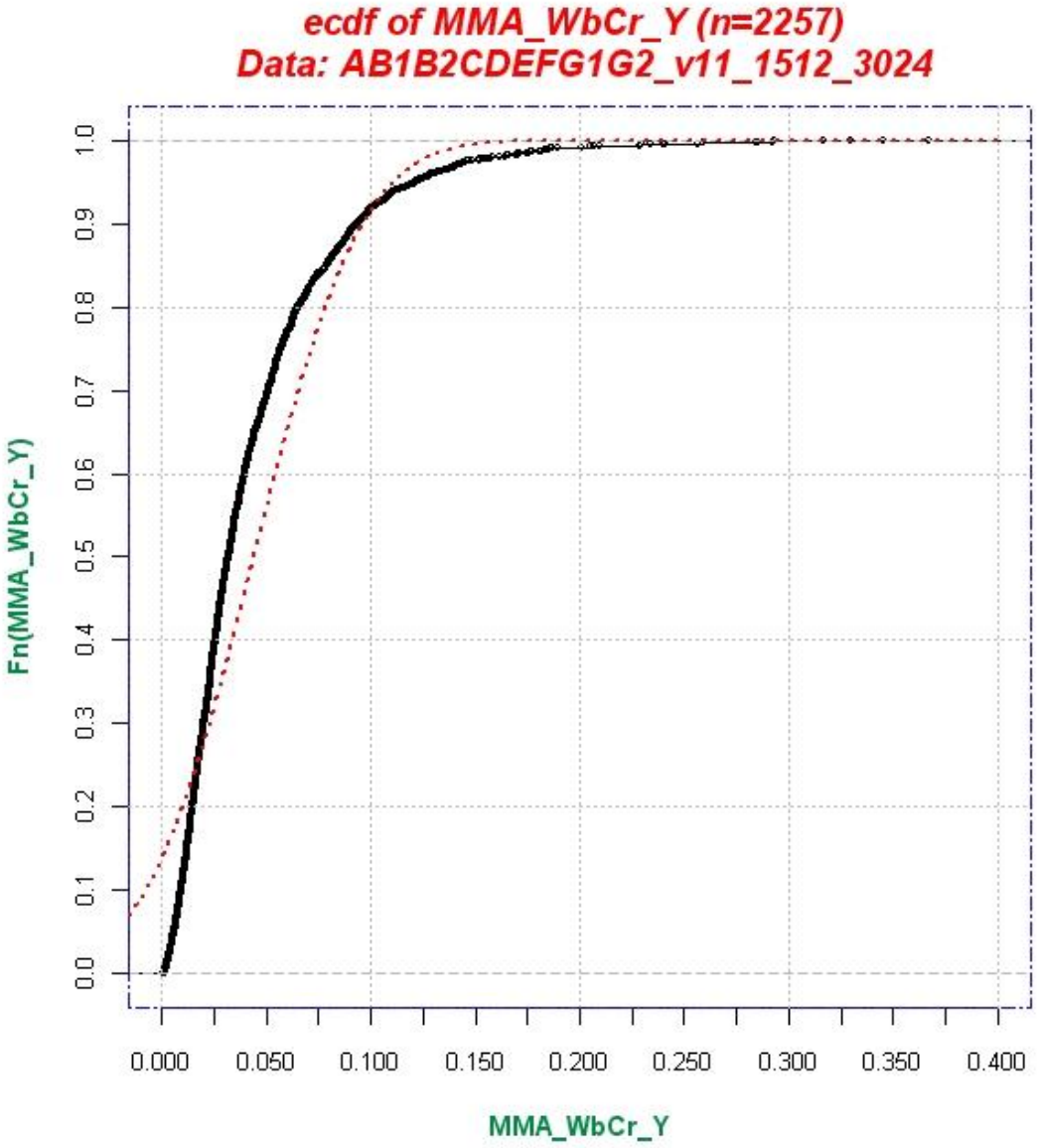

Figure 5.15: Empirical probability and fitted normal probability distributions for the variable – dimensionless average annual migration at the bend apex (MMA/WbCr/Y).

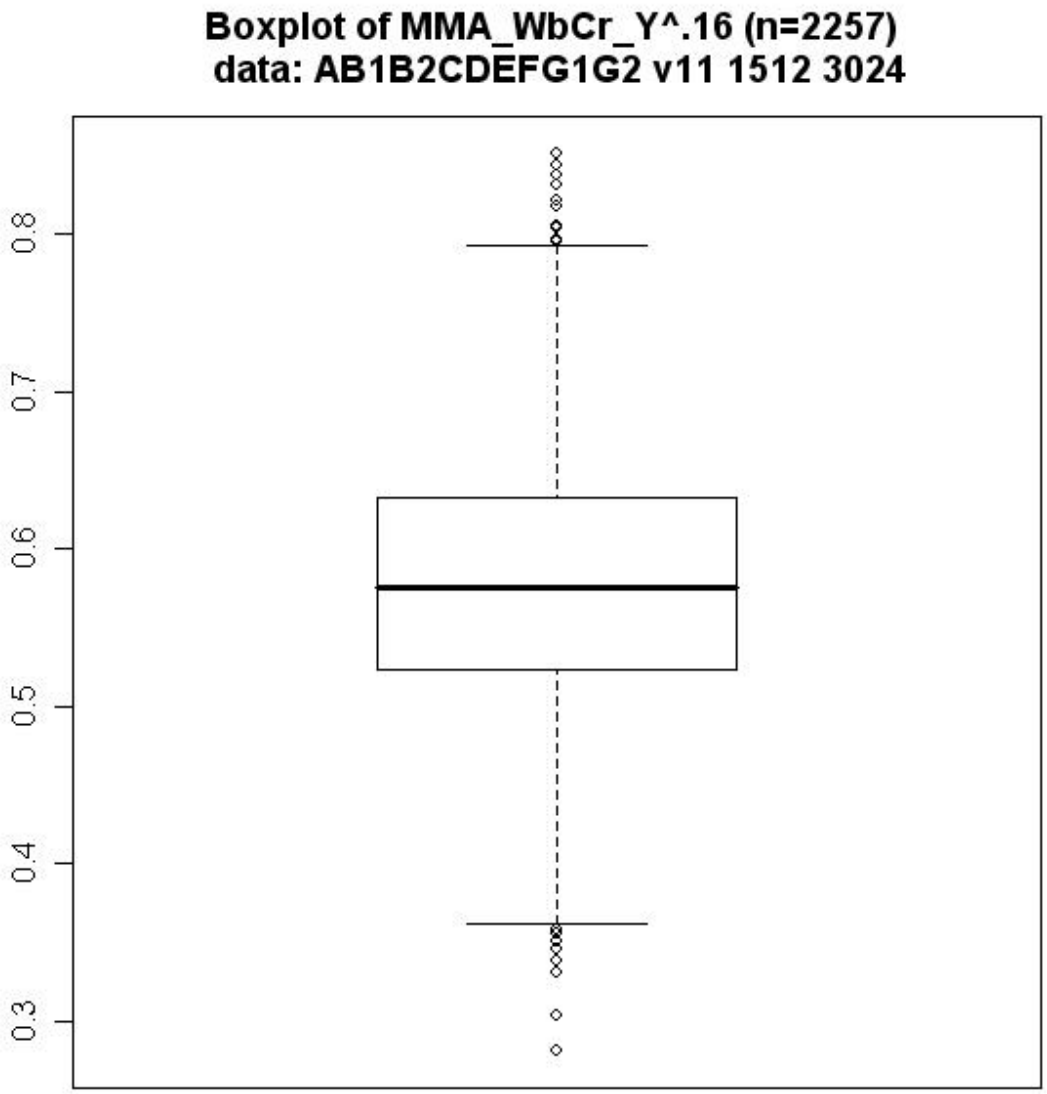

Figure 5.16: Box plot of the power transformed variable - dimensionless average annual migration at the bend apex $((MMA/WbCr/Y)^{0.16})$.

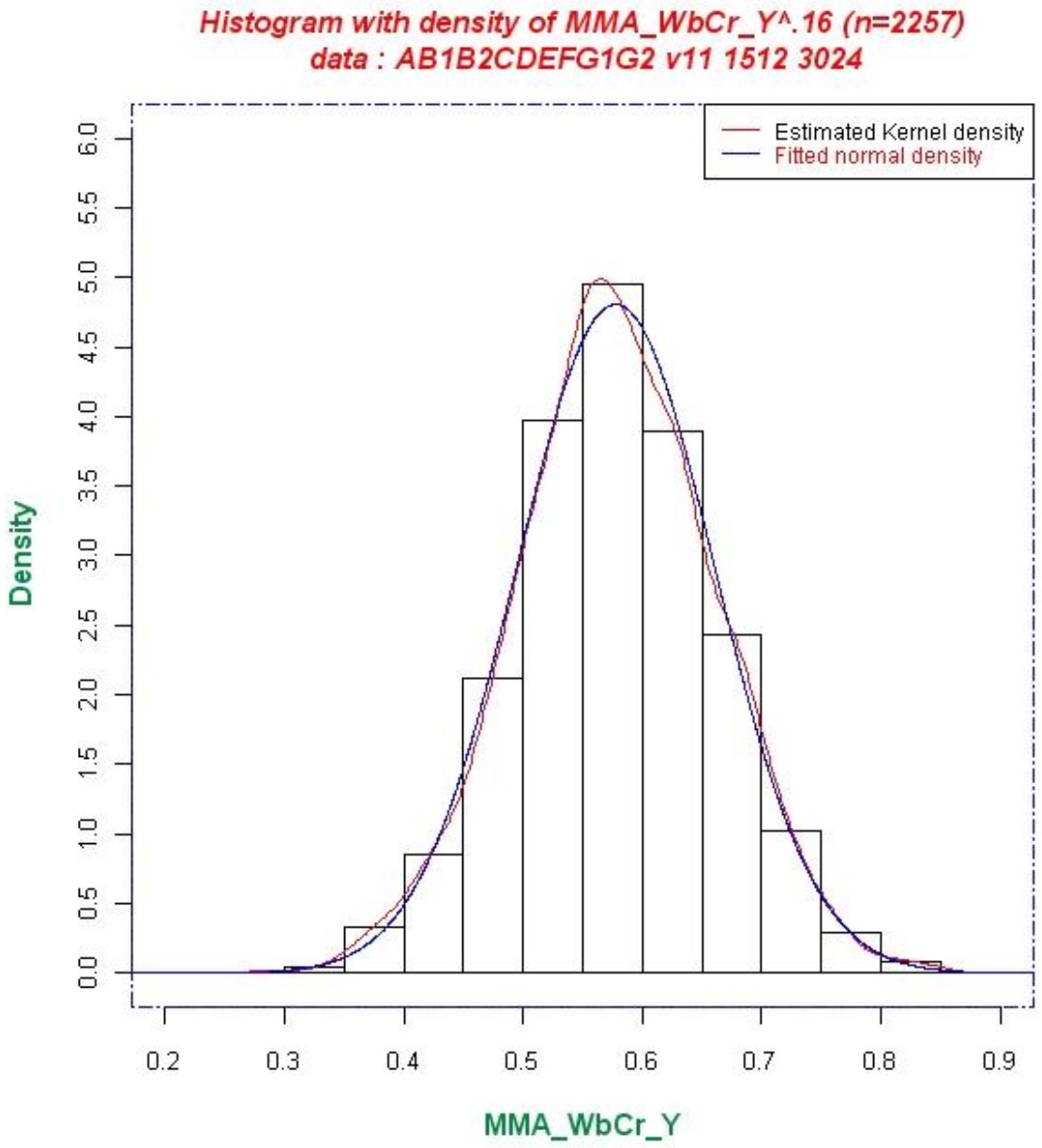

Figure 5.17: Histogram, estimated density and fitted normal density distributions for the power transformed variable - dimensionless average annual migration at the bend apex $((MMA/WbCr/Y)^{0.16})$.

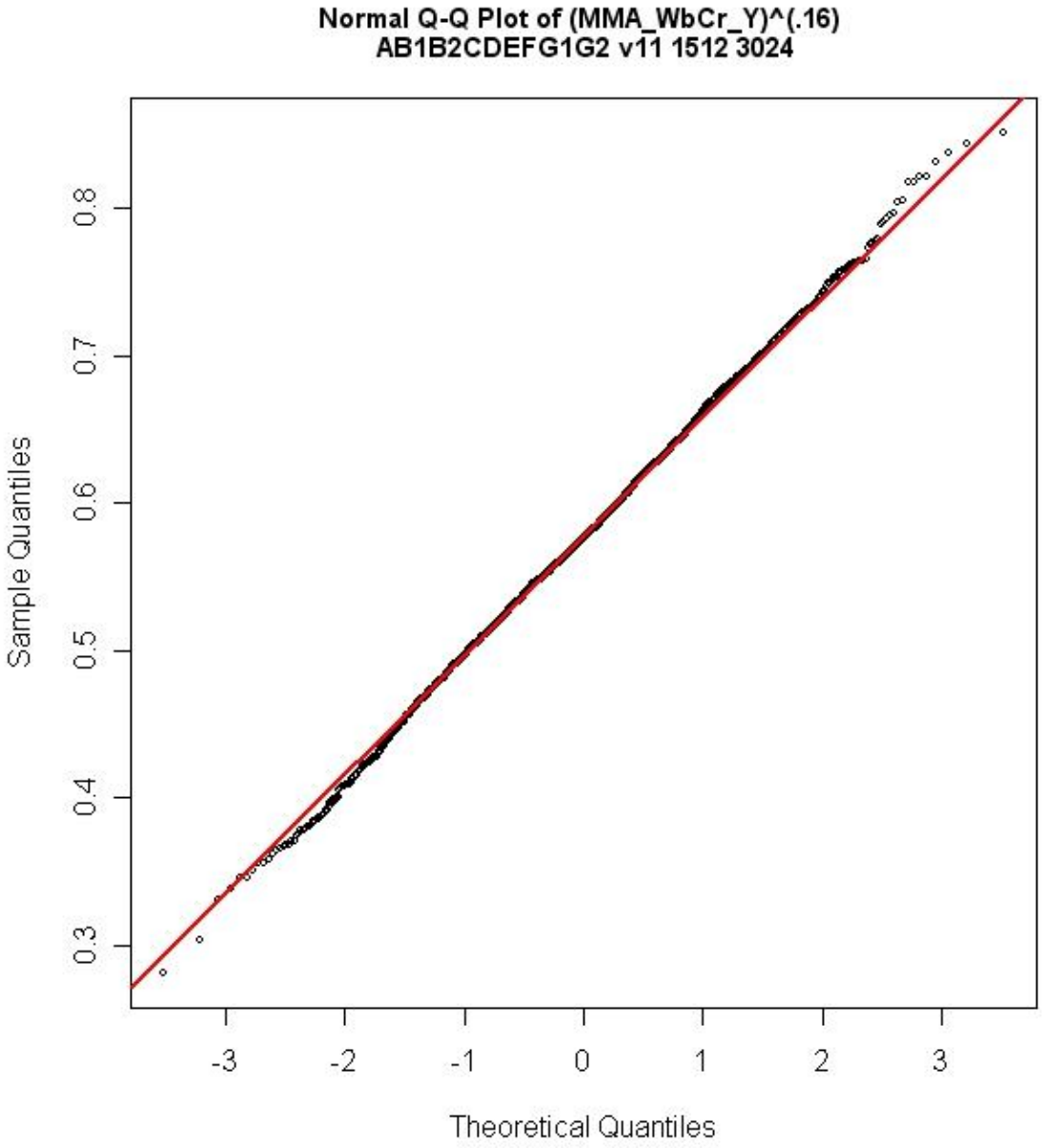

Figure 5.18: Normal probability plot for the power transformed variable – dimensionless average annual migration at the bend apex $((MMA/WbCr/Y)^{0.16})$.

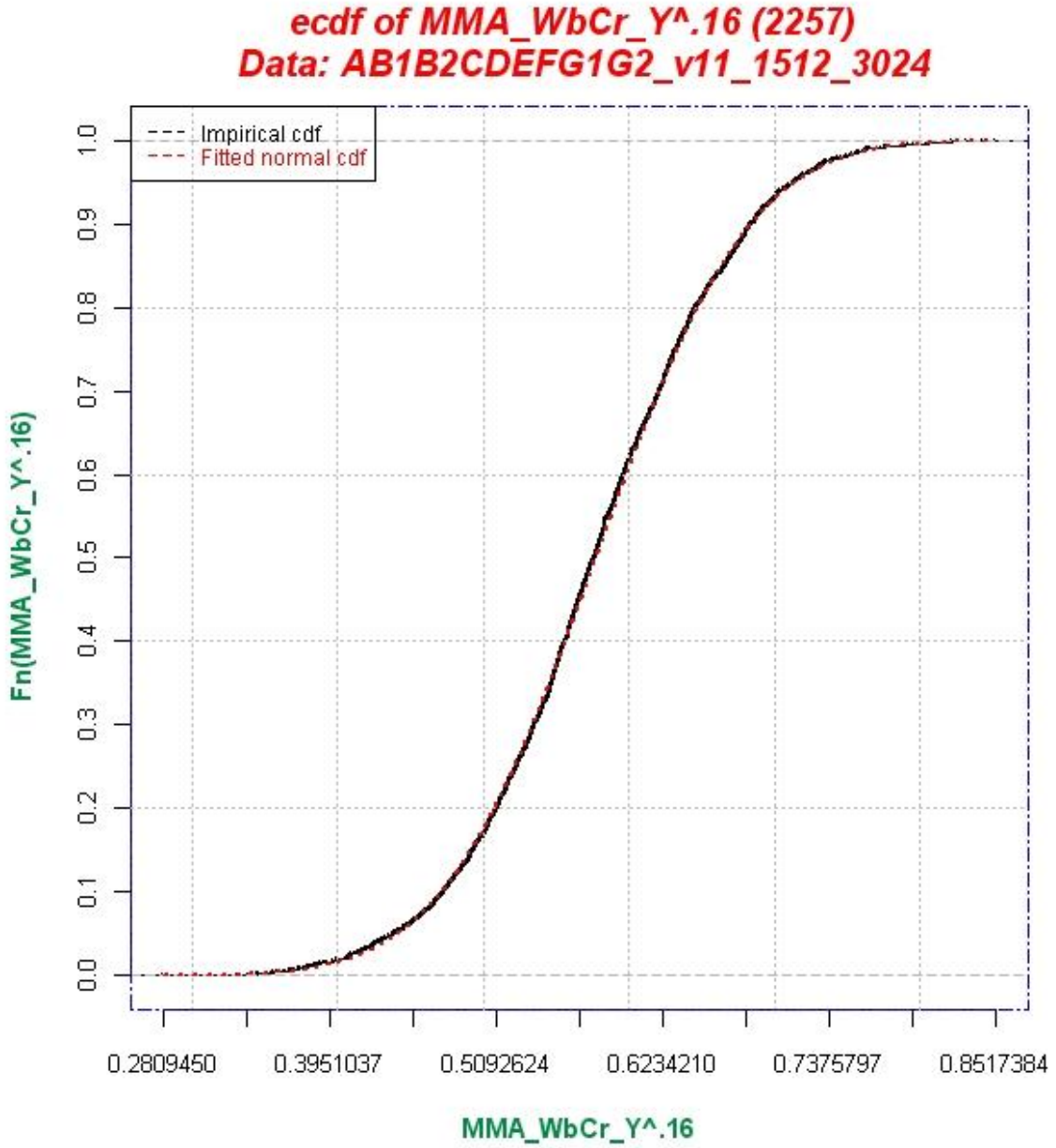

Figure 5.19: Empirical probability and fitted normal probability distributions for the power transformed variable – dimensionless average annual migration at the bend apex $((MMA/WbCr/Y)^{0.16})$.

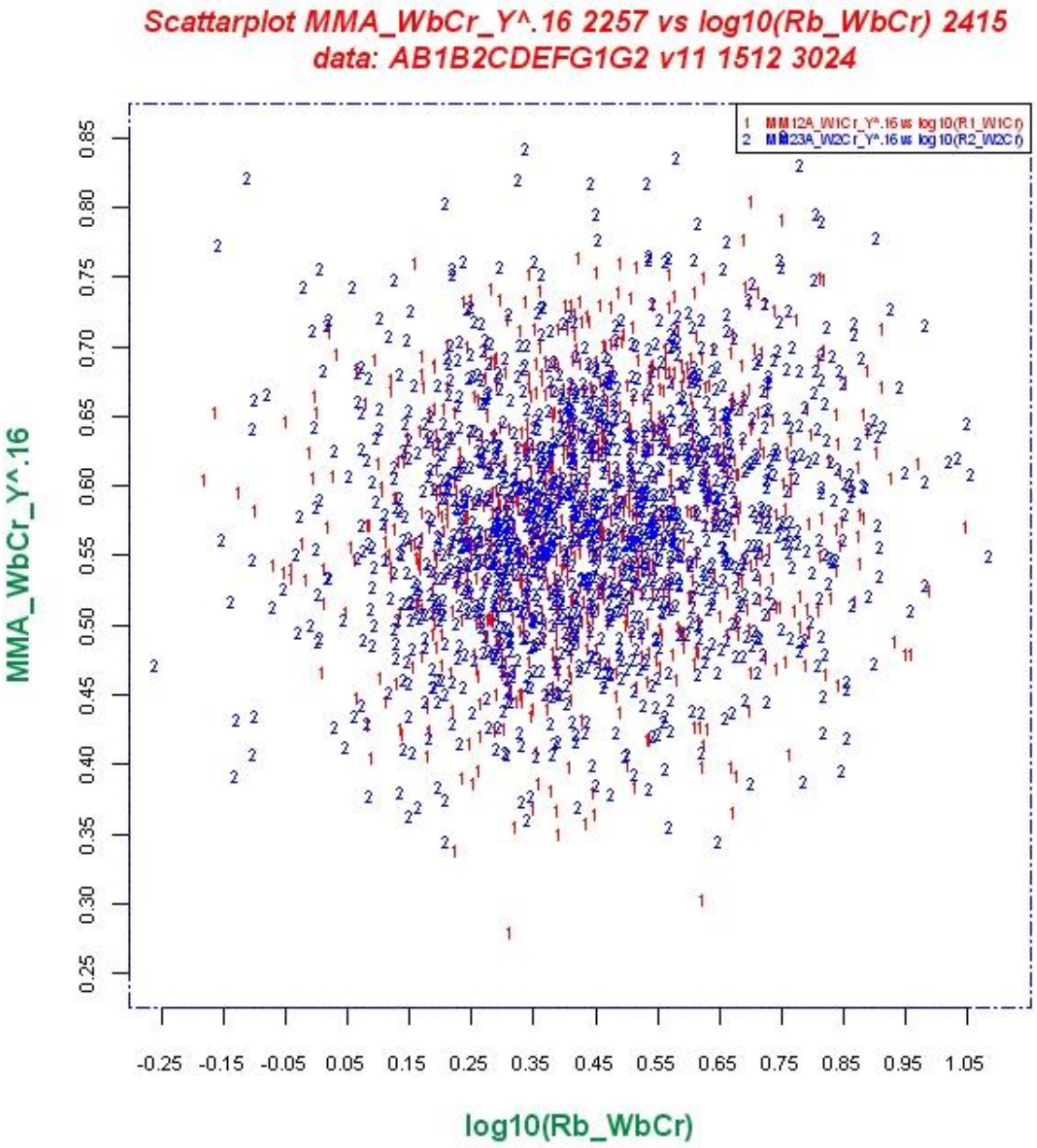

Figure 5.20: Scatter plot of the power transformed variable average annual dimensionless migration rate at bend apex $((MMA/WbCr/Y)^{0.16})$ versus the logarithmically transformed variable dimensionless outer bank radius of curvature ($\log_{10}(Rb/WbCr)$).

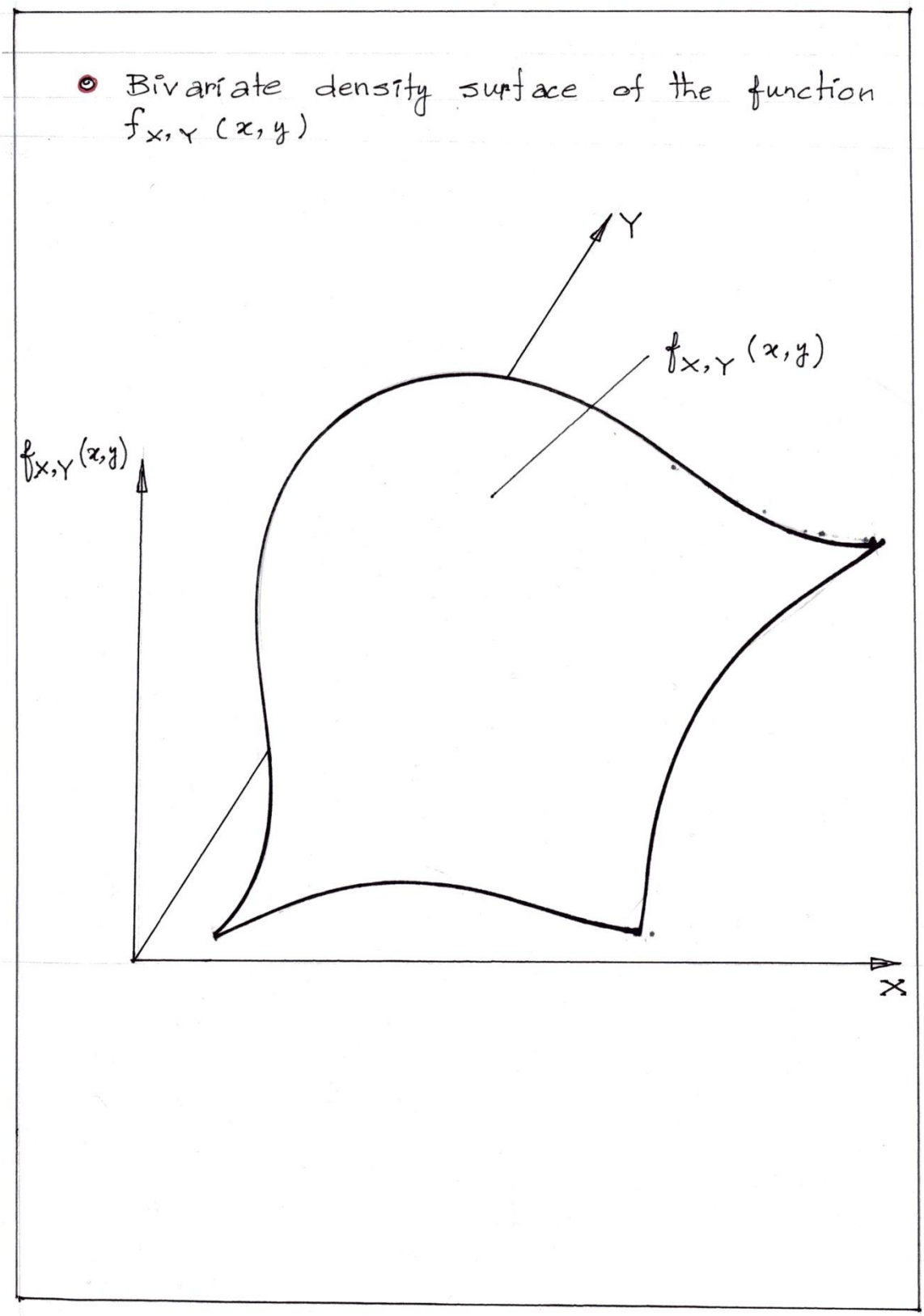

Figure 5.21: Graph of the bivariate density function $f_{X,Y}(x,y)$ indicating the bivariate density surface of the function.

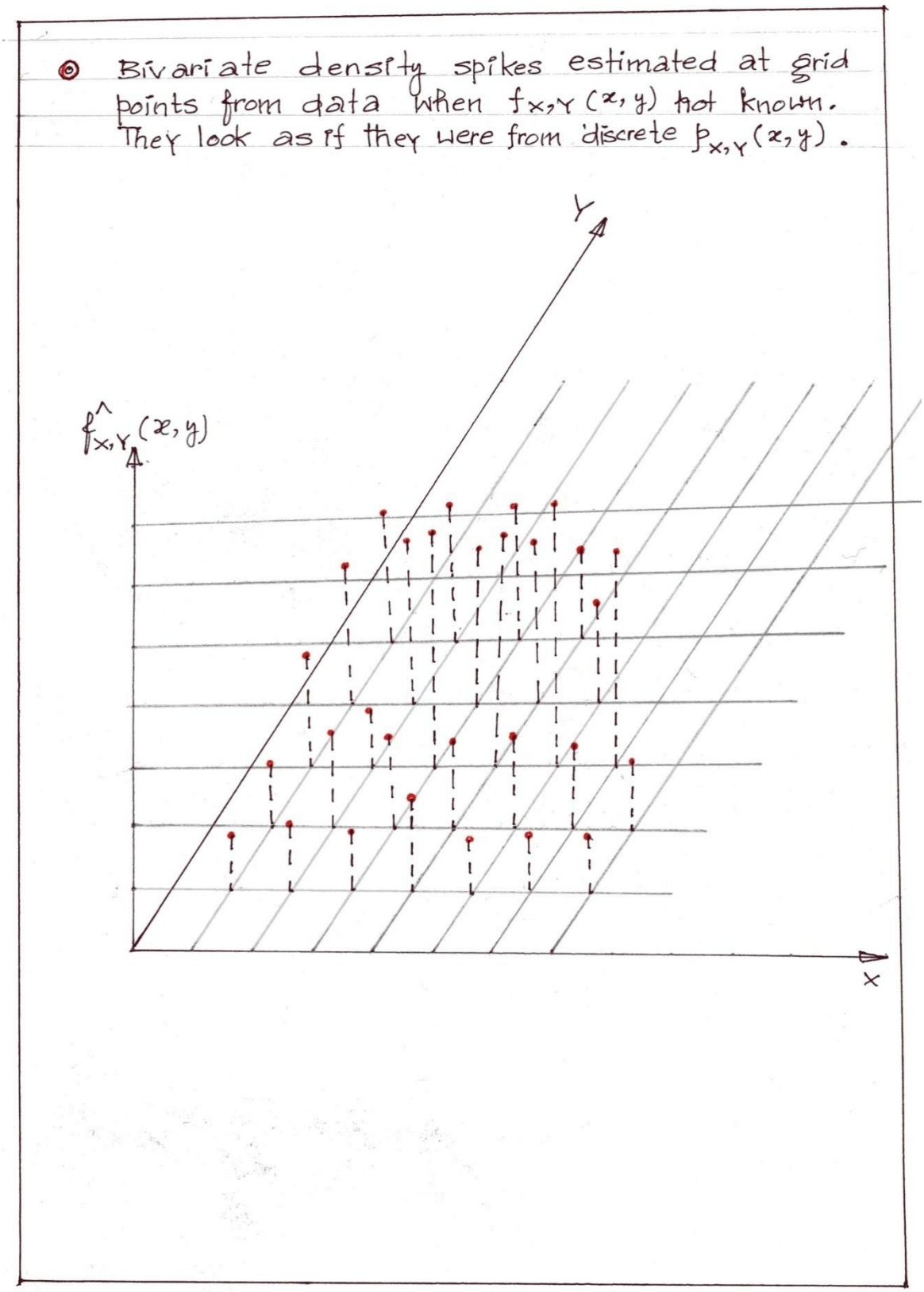

Figure 5.22: Estimated densities for the density function $f_{X,Y}(x,y)$ developed empirically from data at grid points when the theoretical density function is unknown. Resulting densities appear as if they were derived from joint analysis of discrete, random variables.

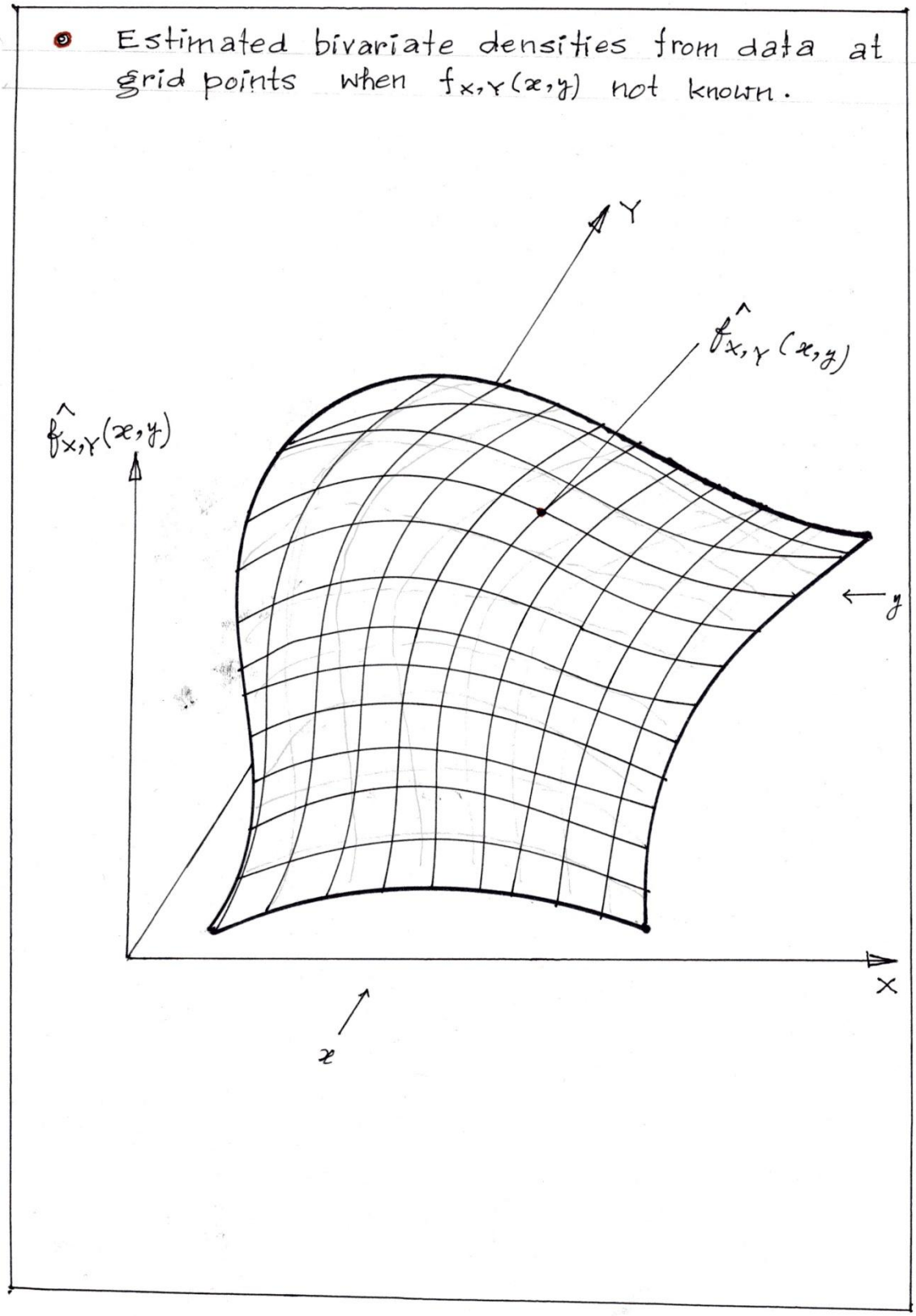

Figure 5.23: Graph of the gridded surface fitted to the estimated densities of the function $f_{X,Y}(x,y)$ illustrated in Figure 5.22.

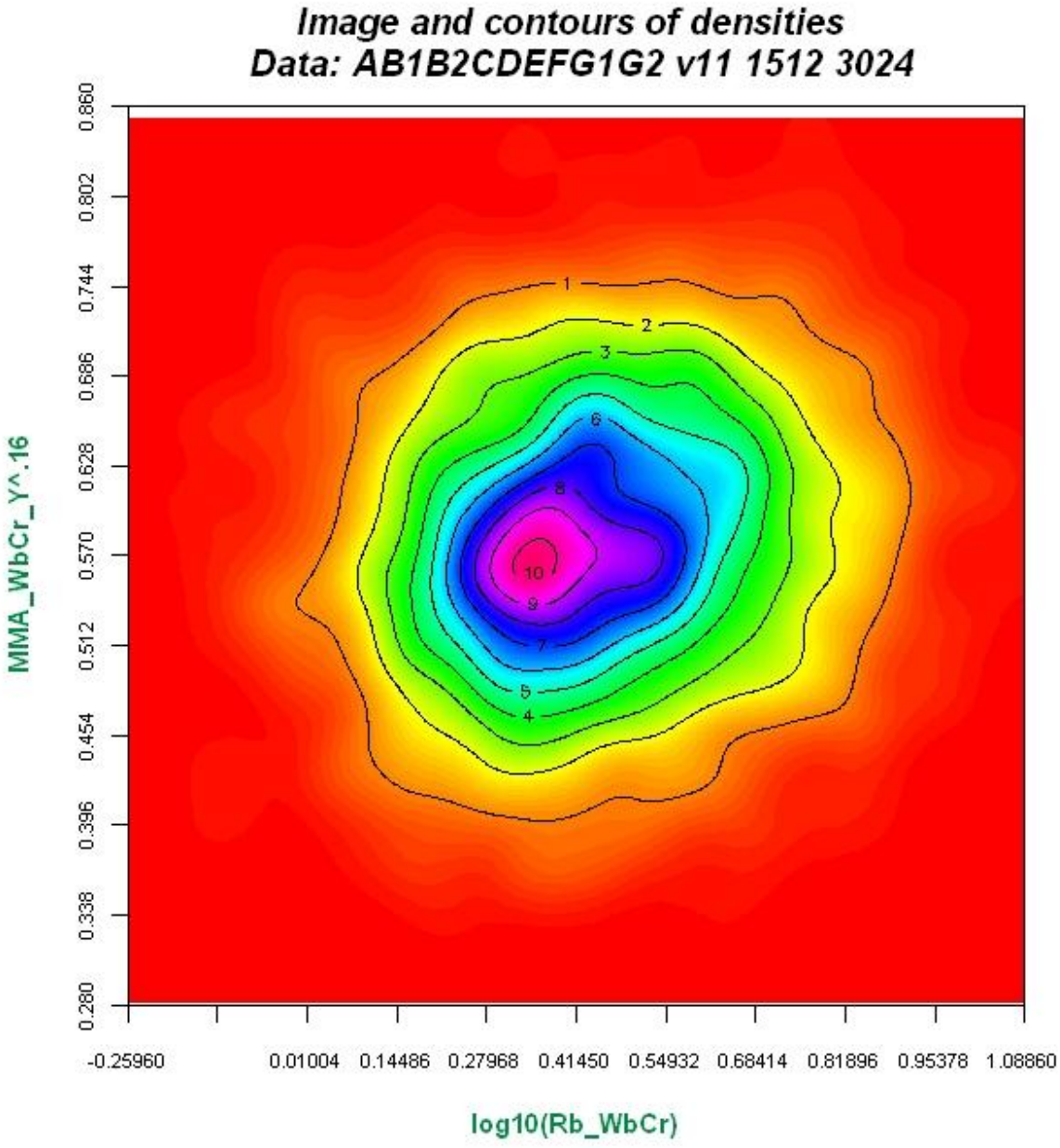

Figure 5.24: Concentration and contours of densities of the power transformed variable -average annual migration rate at the bend apex ($(MMA/WbCr/Y)^{0.16}$) plotted as a function of the logarithmically transformed variable - ratio of outer bank radius of curvature to river channel width at the crossing ($\log_{10}(Rb/WbCr)$).

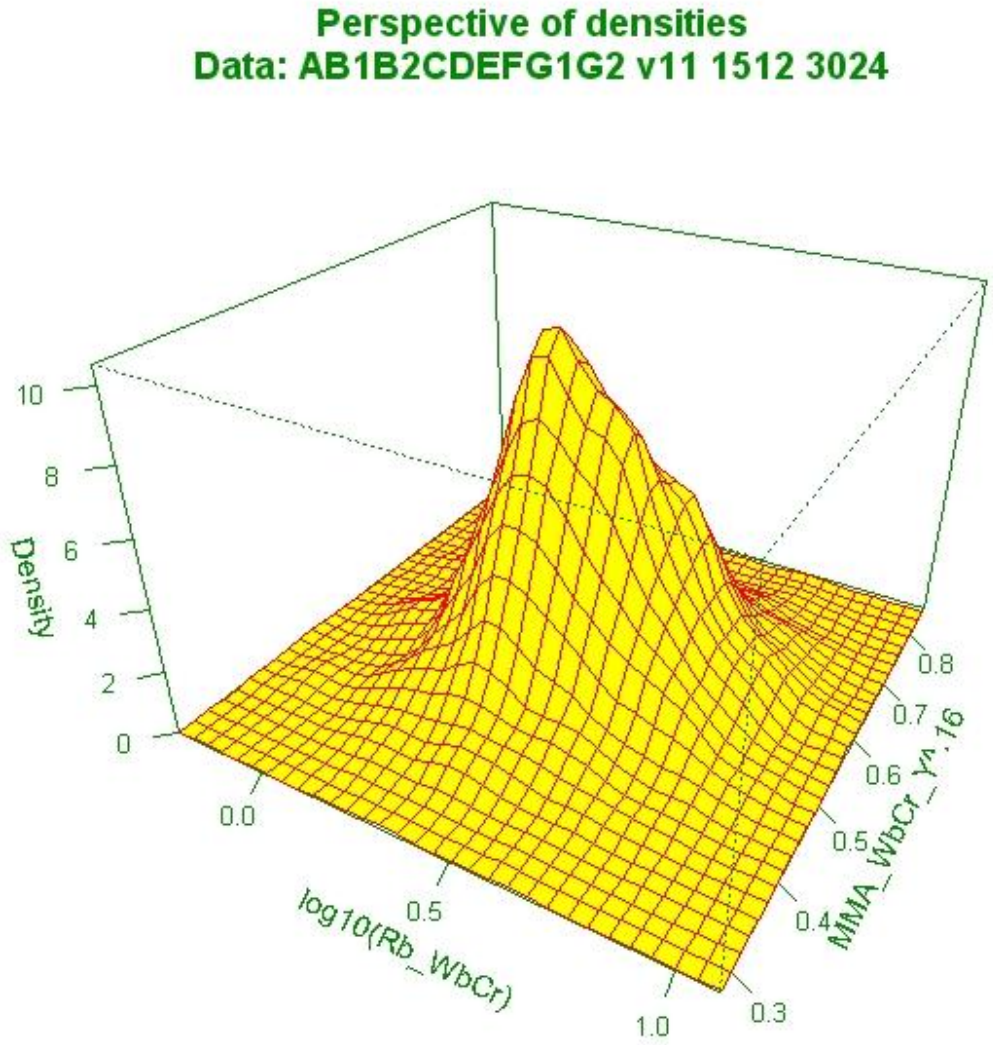

Figure 5.25: Perspective view of the joint probability density distribution for average annual migration rate at the bend apex $(MMA/WbCr/Y)^{0.16}$) as a function of the ratio of outer bank radius of curvature to river channel width at the crossing ($\log_{10}(Rb/WbCr)$).

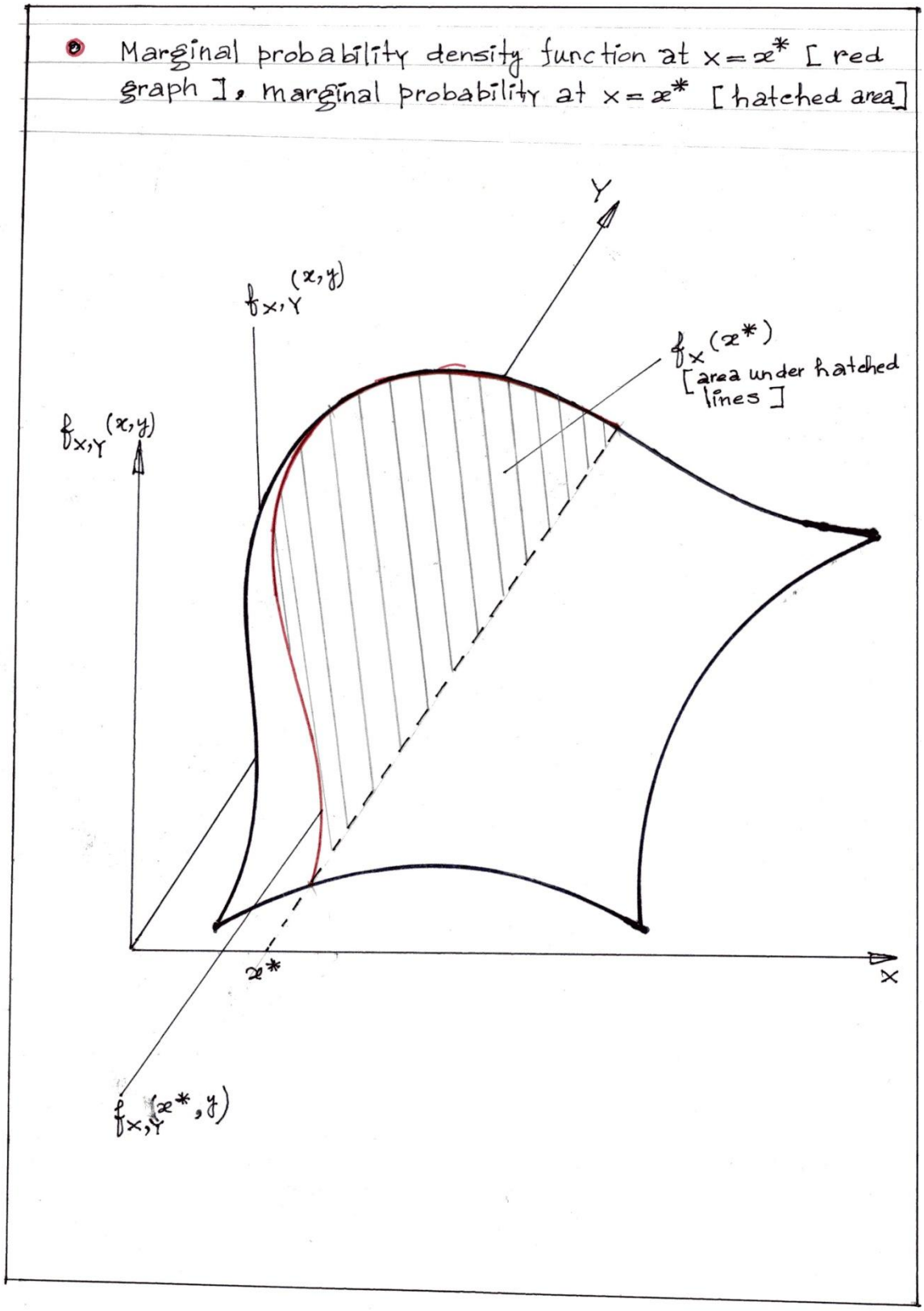

Figure 5.26: Graph showing the joint probability density function $f_{X,Y}(x^*,y)$ at X=x, and the marginal probability density function $f_X(x^*)$ at X=x*.

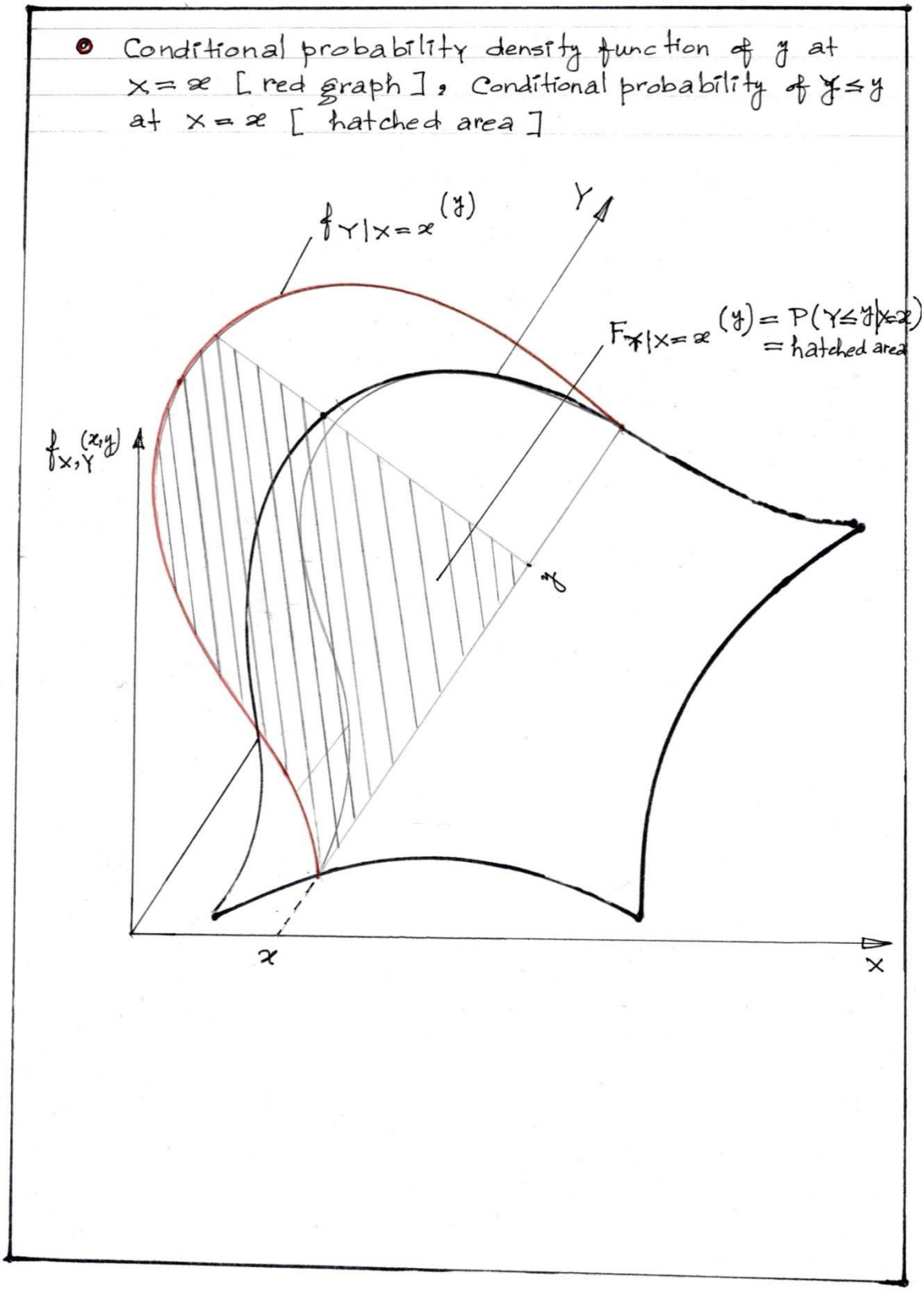

Figure 5.27: Graph showing the conditional probability density function $f_{Y|X=x}$ (y) given that X=x, and the conditional cumulative probability of Y<=y at X=x, P(Y<=y|X=x).

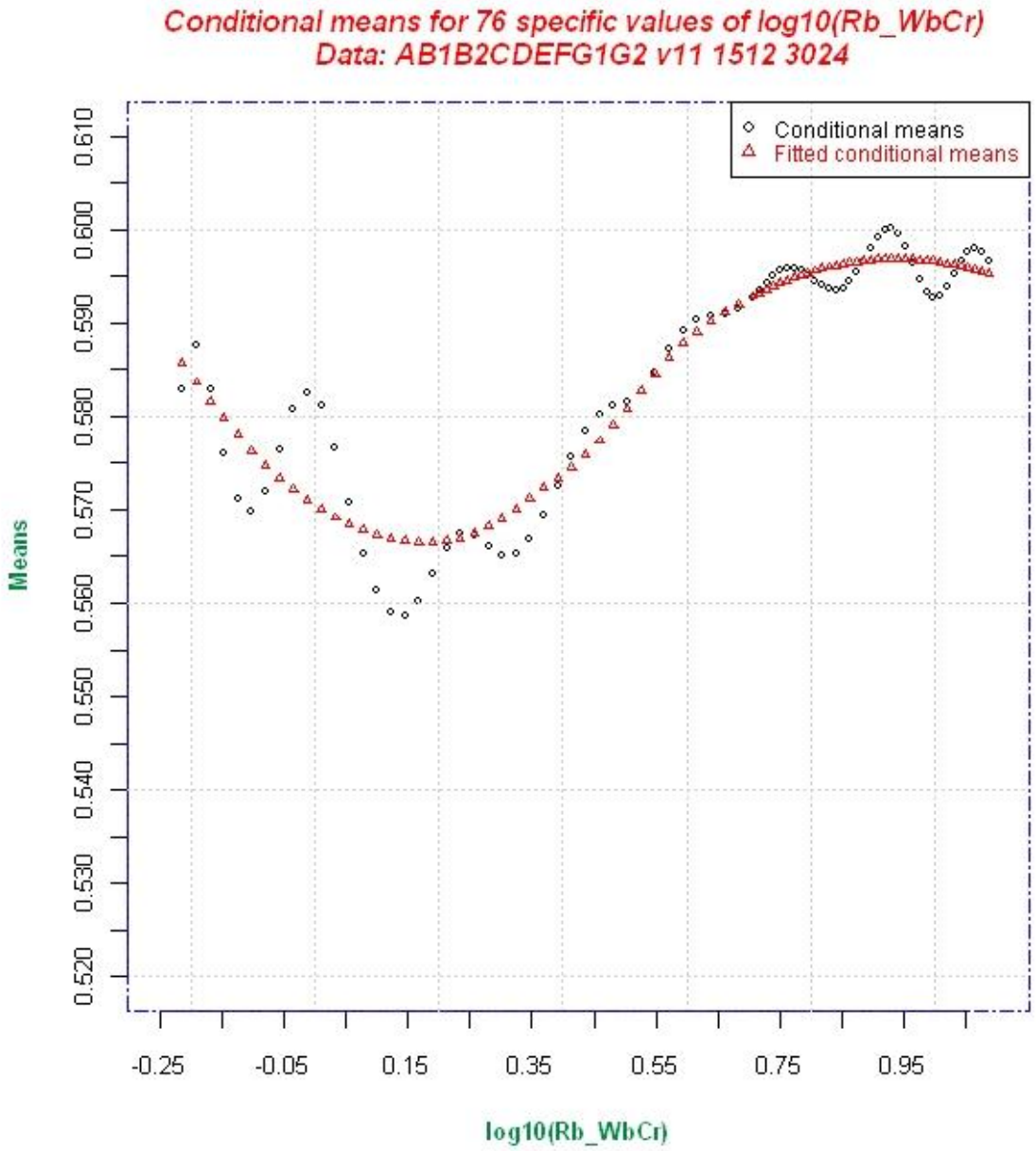

Figure 5.28: Conditional means at specified values of $\log_{10}$(Rb/WbCr).

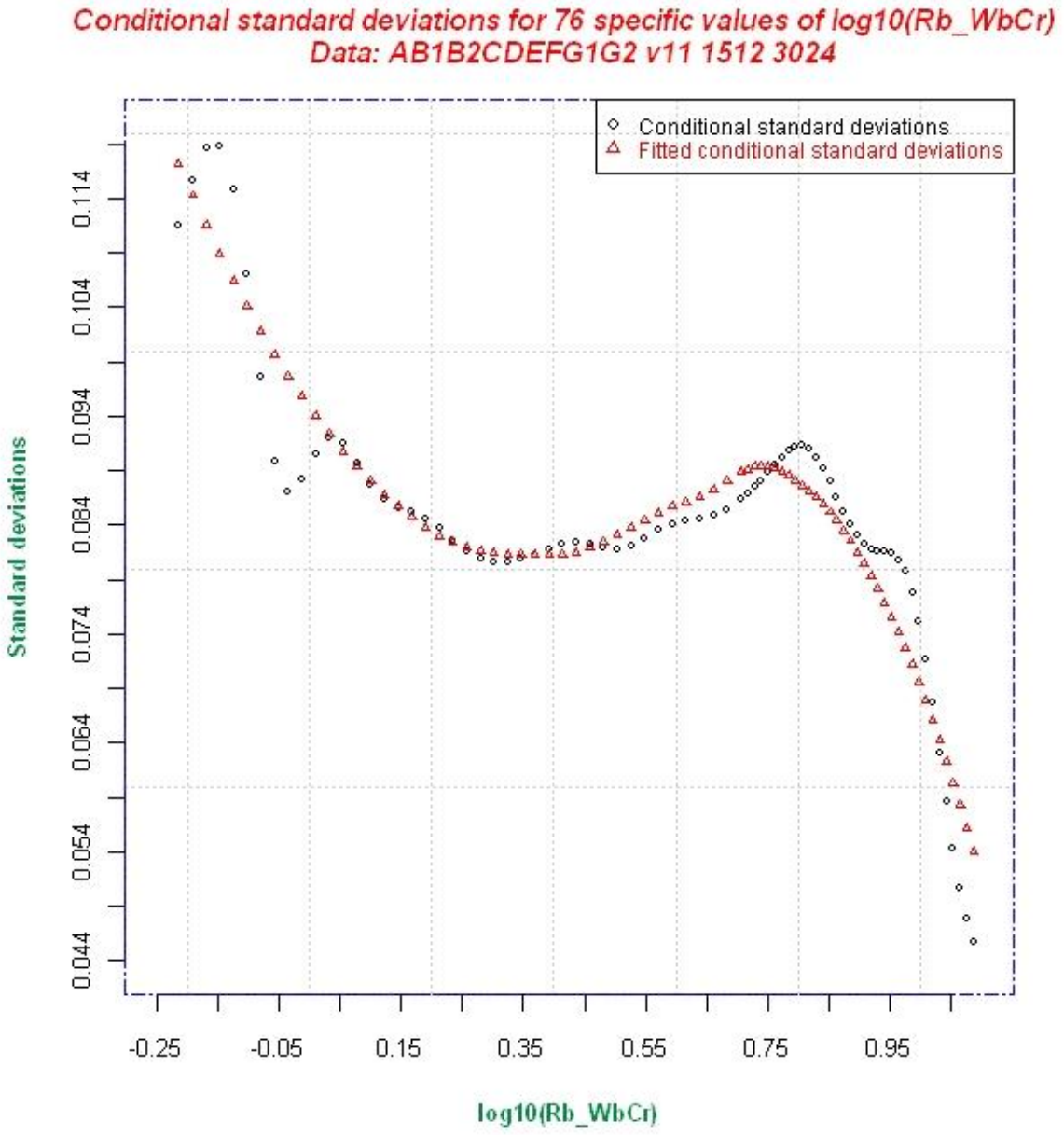

Figure 5.29: Conditional standard deviations at specified values of $\log_{10}$(Rb/WbCr).

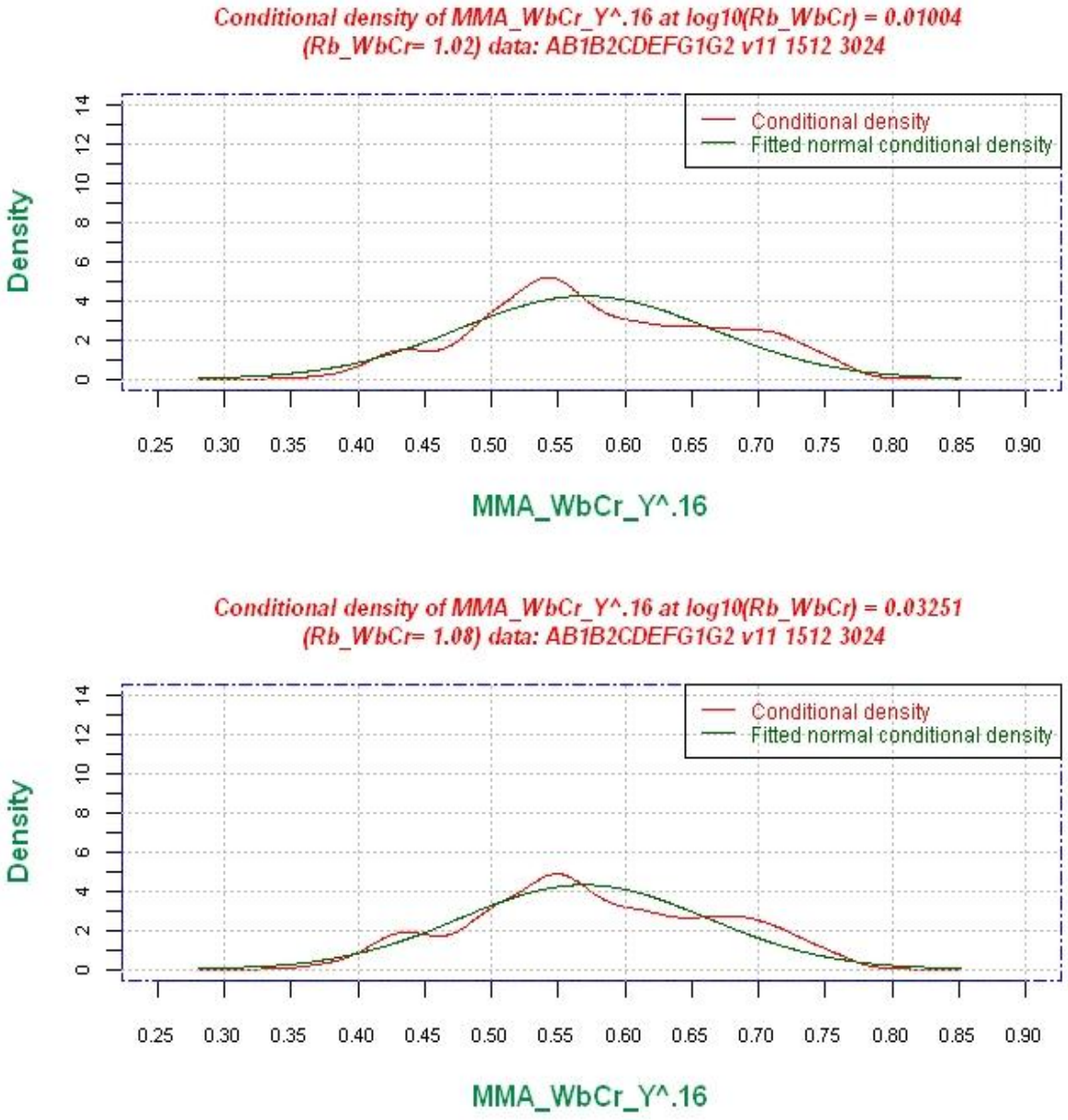

Figure 5.30: Upper graph. Conditional density of (MMA/WbCr/Y)^0.16 for $\log_{10}$(Rb/WbCr) = 0.01004 [i.e. Rb/WbCr = 1.02]. Lower graph. Conditional density of (MMA/WbCr/Y)^0.16 for $\log_{10}$(Rb/WbCr) = 0.03251 [i.e. Rb/WbCr = 1.08].

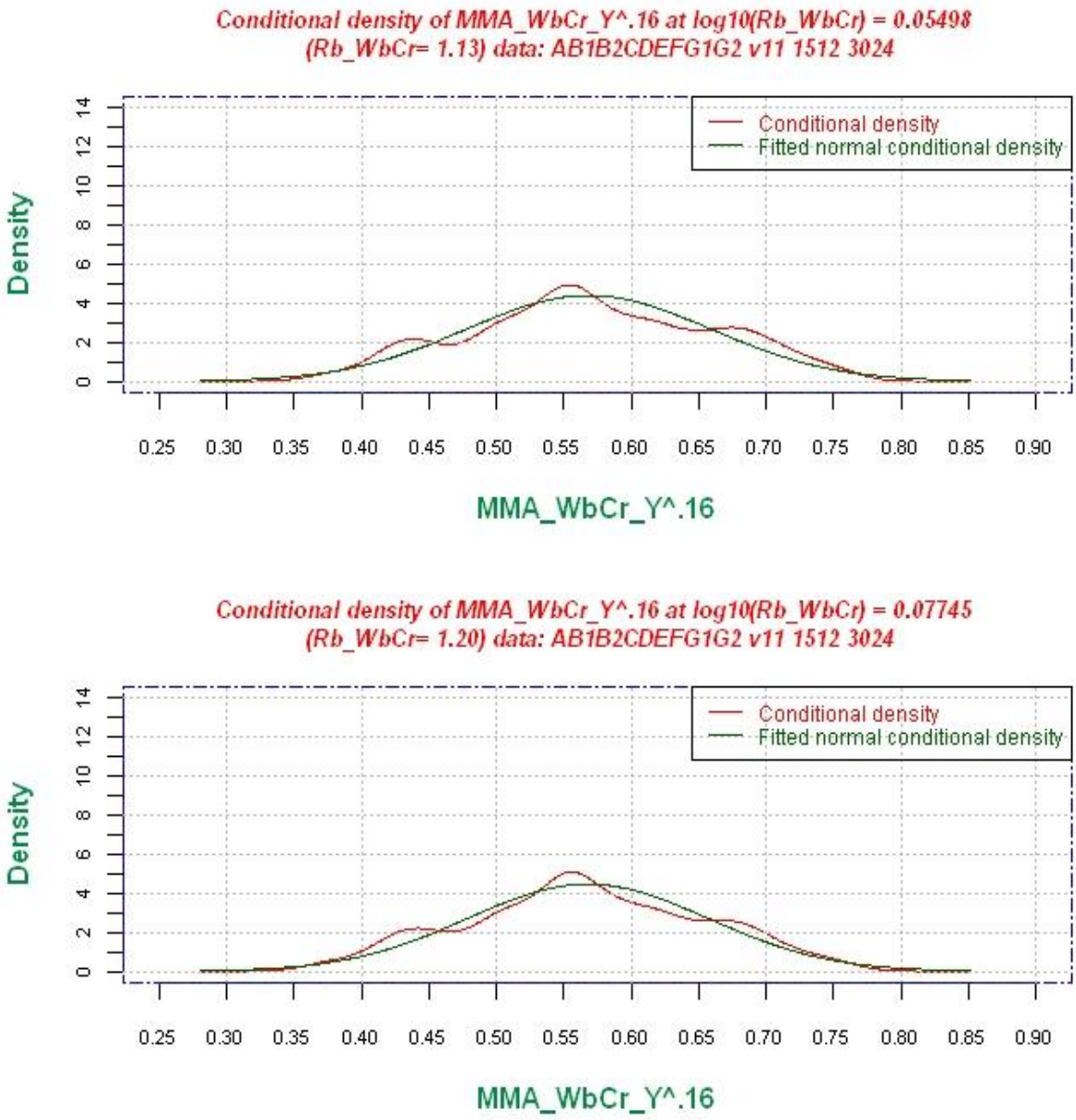

Figure 5.31: Upper graph. Conditional of (MMA/WbCr/Y)^0.16 for $\log_{10}$(Rb/WbCr) = 0.05498 [i.e. Rb/WbCr = 1.13]. Lower graph. Conditional density of (MMA/WbCr/Y)^0.16 for $\log_{10}$(Rb_WbCr) = 0.07745 [i.e. Rb/WbCr = 1.20].

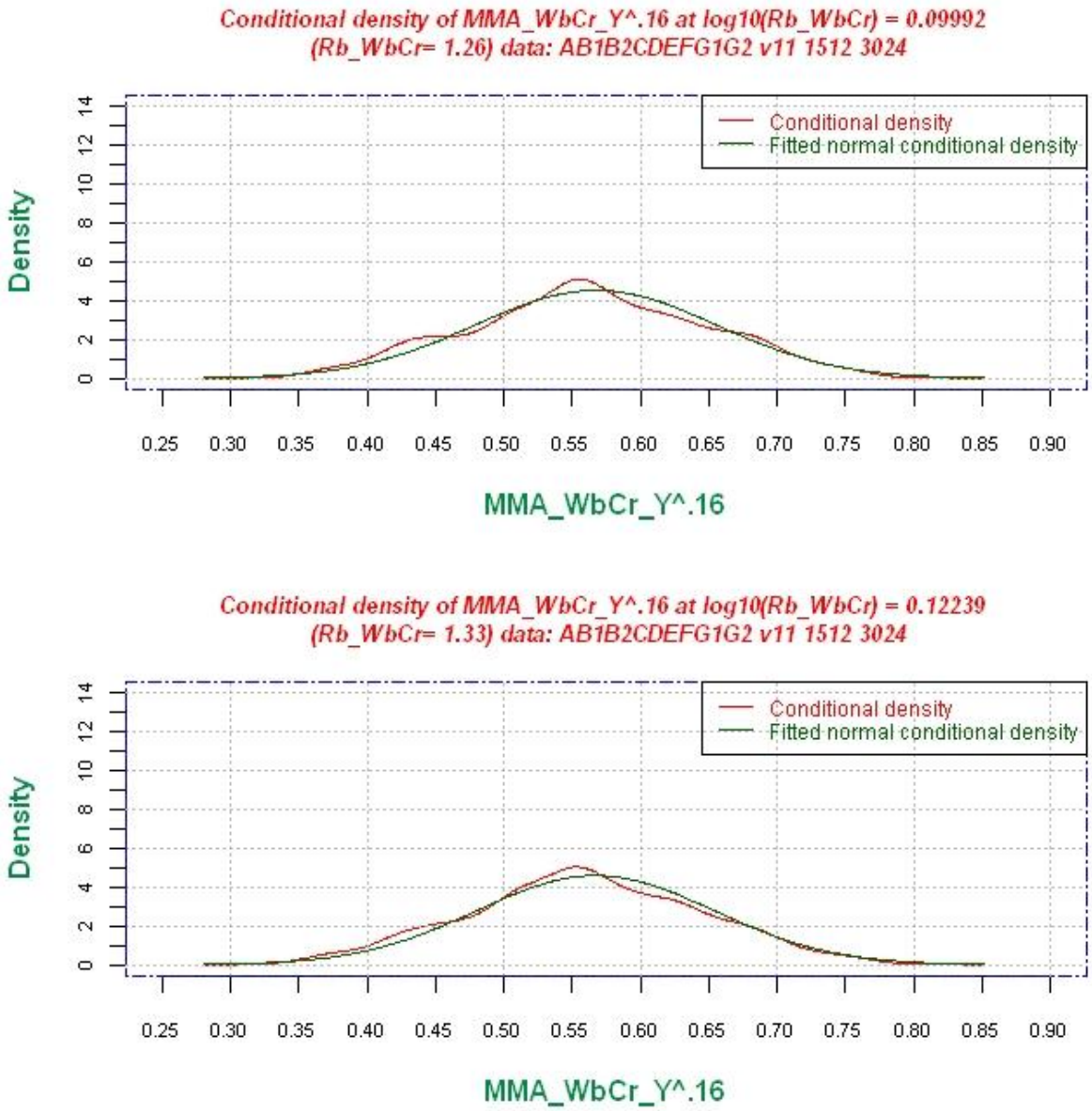

Figure 5.32: Upper graph. Conditional density of (MMA/WbCr/Y)^0.16 for $\log_{10}$(Rb/WbCr) = 0.09992 [i.e. Rb/WbCr = 1.26]. Lower graph. Conditional density of (MMA/WbCr/Y)^0.16 for $\log_{10}$(Rb/WbCr) = 0.12239 [i.e. Rb/WbCr = 1.33].

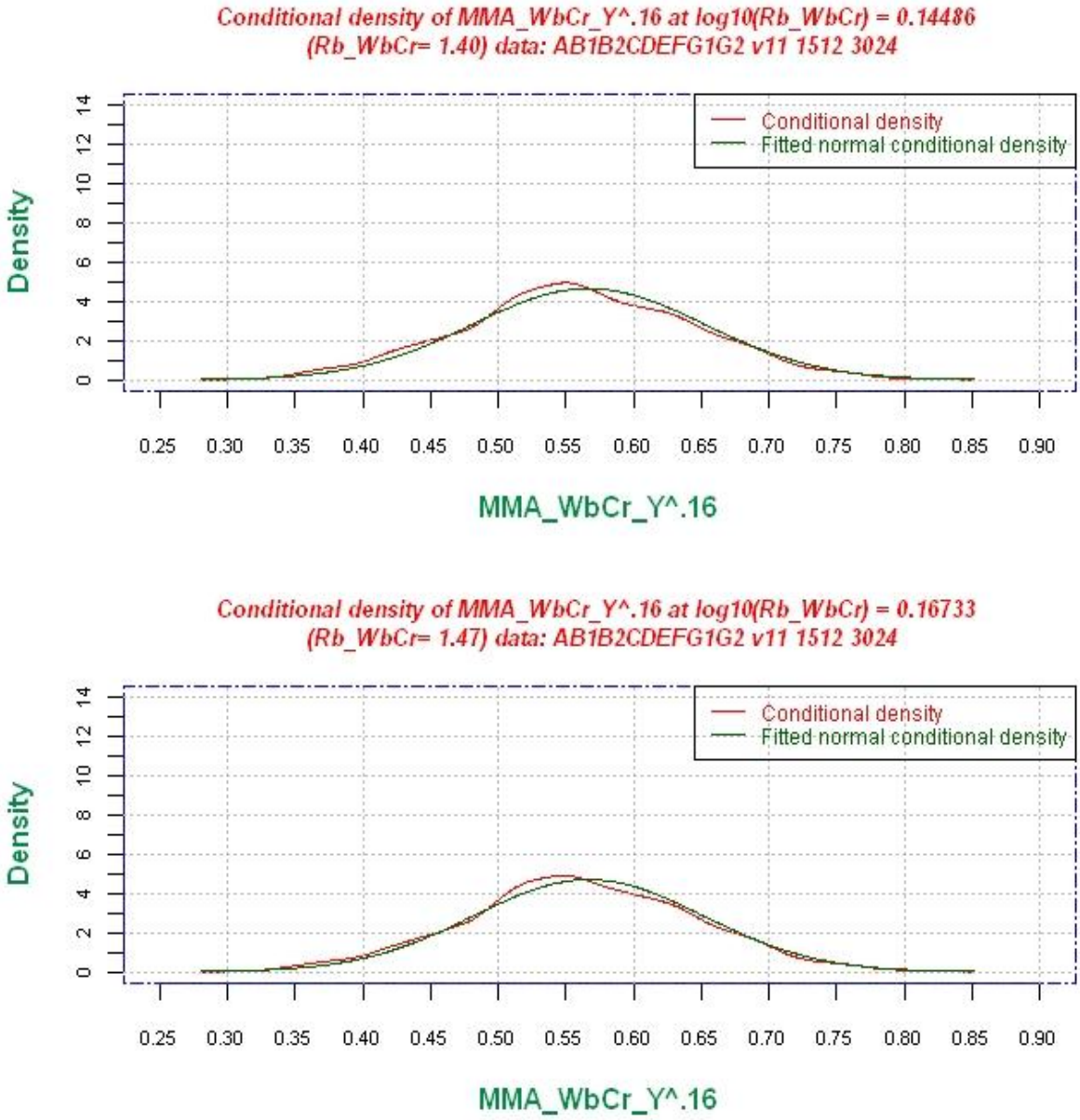

Figure 5.33: Upper graph. Conditional density of (MMA/WbCr/Y)^0.16 for $\log_{10}$(Rb/WbCr) = 0.14486 [i.e. Rb/WbCr = 1.40]. Lower graph. Conditional density of (MMA/WbCr/Y)^0.16 for $\log_{10}$(Rb/WbCr) = 0.16733 [i.e. Rb/WbCr = 1.47].

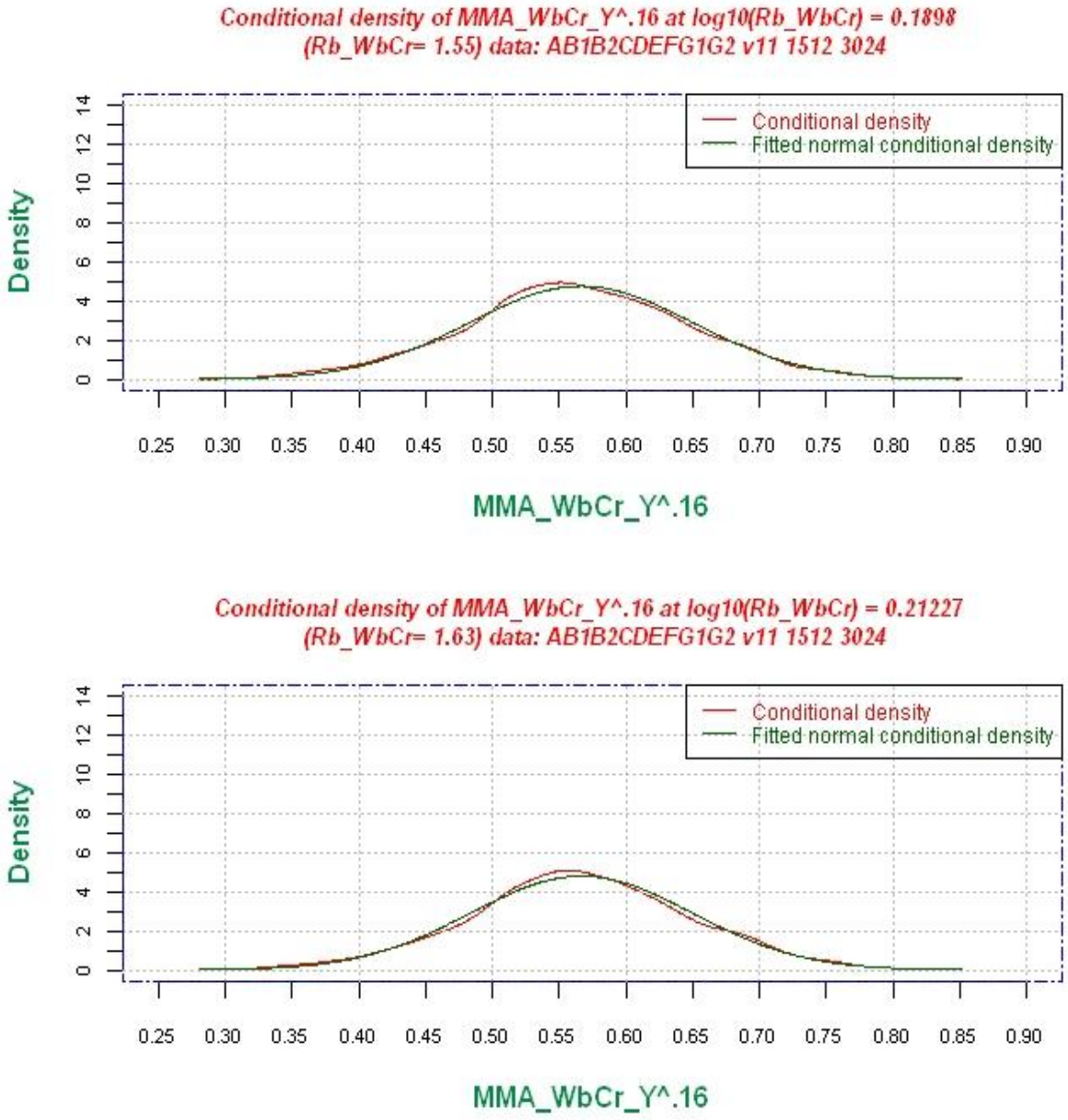

Figure 5.34: Upper graph. Conditional density of (MMA/WbCr/Y)^0.16 for $\log_{10}$(Rb/WbCr) = 0.1898 [i.e. Rb/WbCr = 1.55]. Lower graph. Conditional density of (MMA/WbCr/Y)^0.16 for $\log_{10}$(Rb/WbCr) = 21227 [i.e. Rb/WbCr = 1.63].

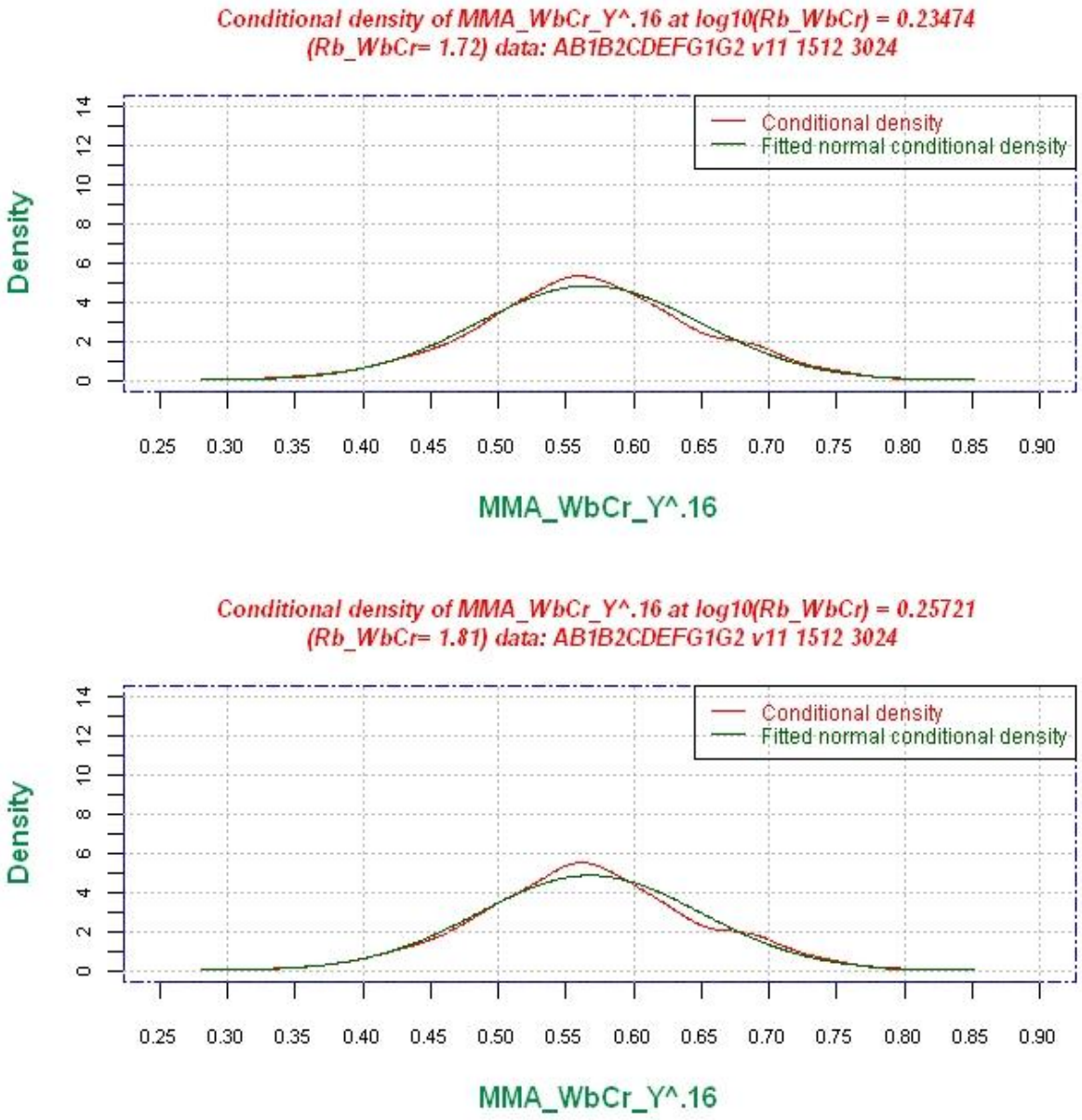

Figure 5.35: Upper graph. Conditional density of (MMA/WbCr/Y)^0.16 $\log_{10}$(Rb/WbCr) = 0.23474 [i.e. Rb/WbCr = 1.72]. Lower graph. Conditional density of (MMA/WbCr/Y)^0.16 for $\log_{10}$(Rb/WbCr) = 0.25721 [i.e. Rb/WbCr = 1.81].

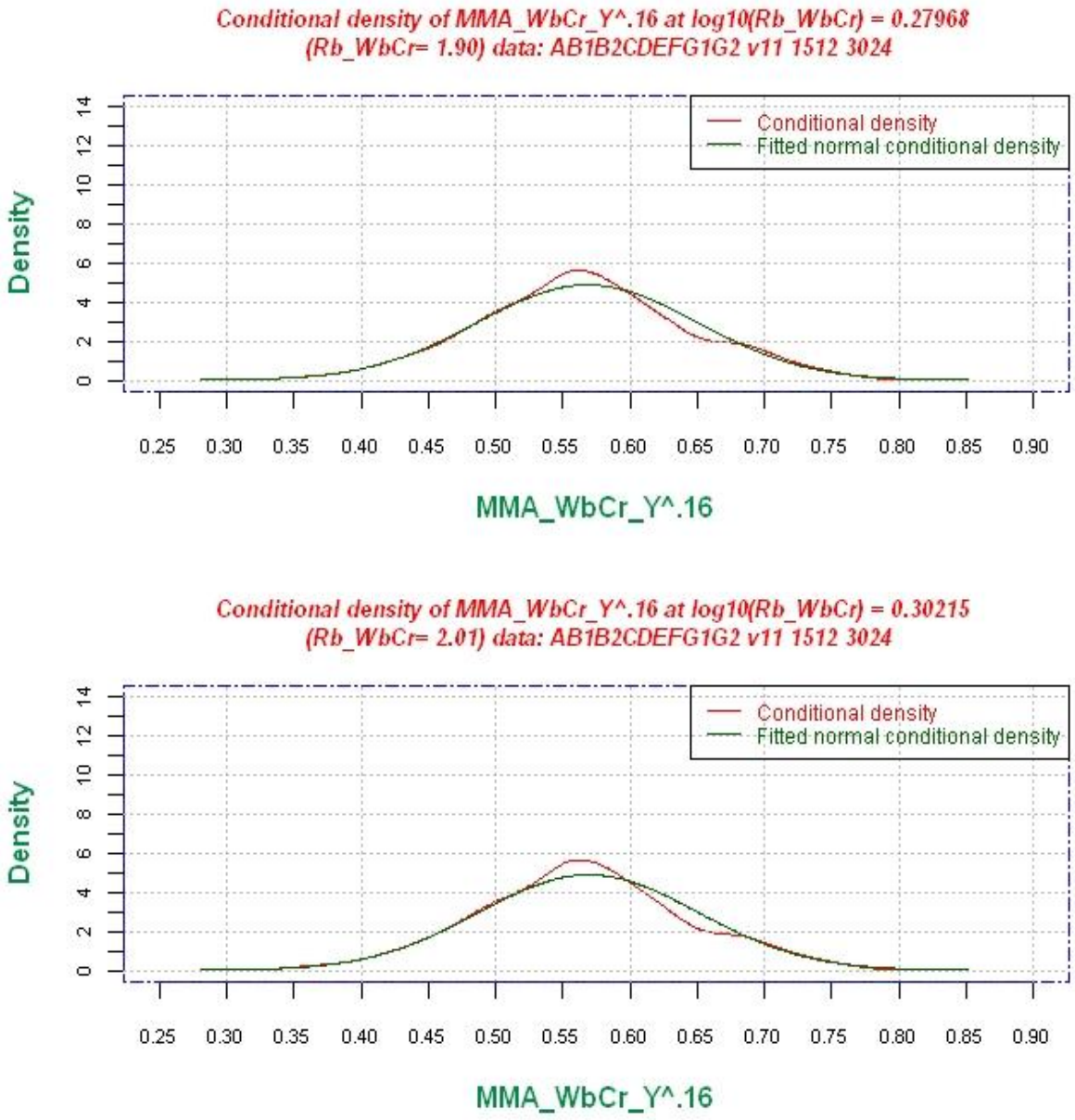

Figure 5.36: Upper graph. Conditional density of $(MMA/WbCr/Y)^{0.16}$ for $\log_{10}(Rb/WbCr)$ = 0.27968 [i.e. Rb/WbCr = 1.90]. Lower graph. Conditional density of $(MMA/WbCr/Y)^{0.16}$ $\log_{10}(Rb/WbCr)$ = 0.30215 [i.e. Rb/WbCr = 2.01].

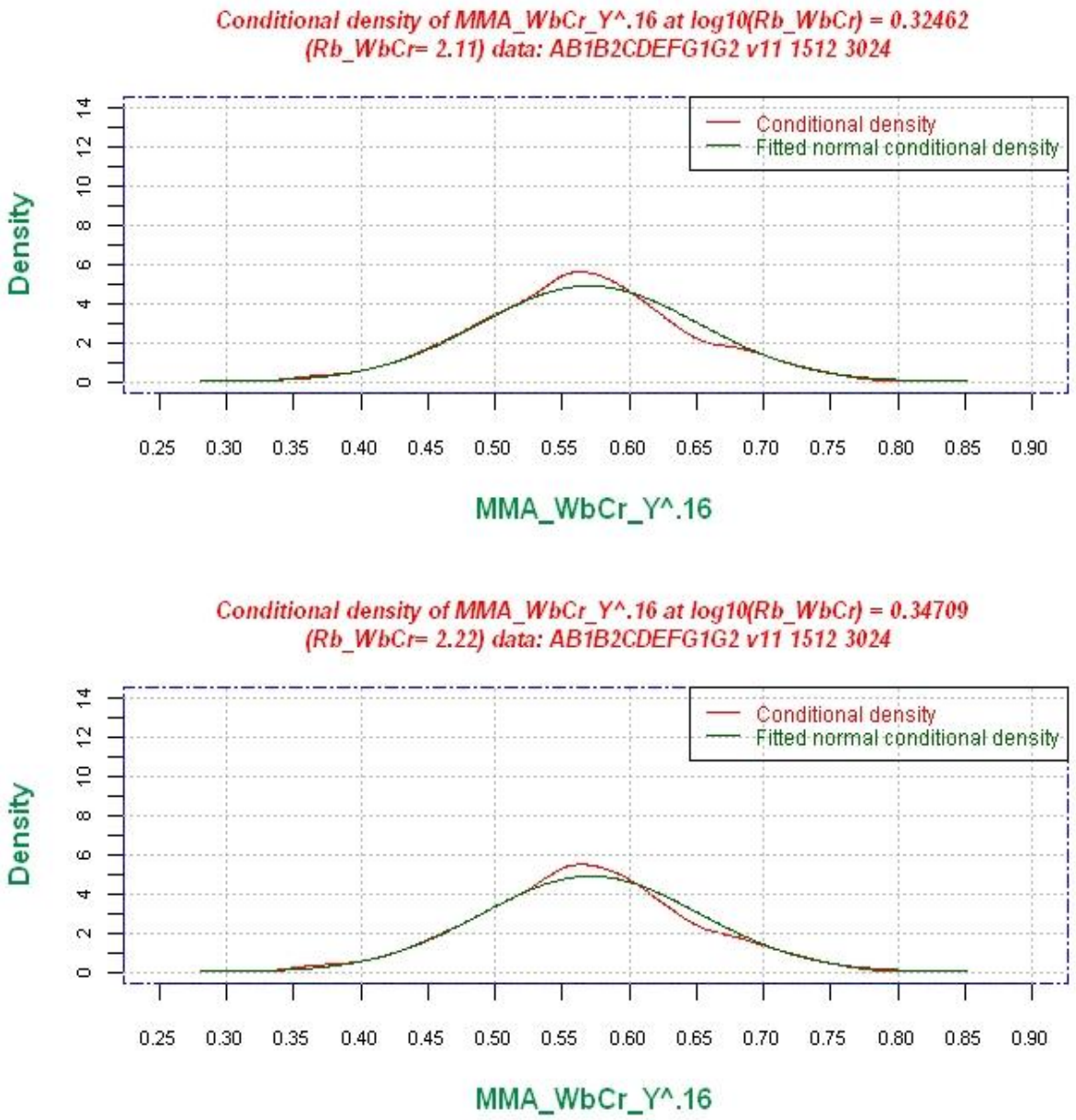

Figure 5.37: Upper graph. Conditional density of $(MMA/WbCr/Y)^{0.16}$ for $\log_{10}(Rb/WbCr) = 0.32462$ [i.e. Rb/WbCr = 2.11]. Lower graph. Conditional density of $(MMA/WbCr/Y)^{0.16}$ for $\log_{10}(Rb/WbCr) = 0.34709$ [i.e. Rb/WbCr = 2.22].

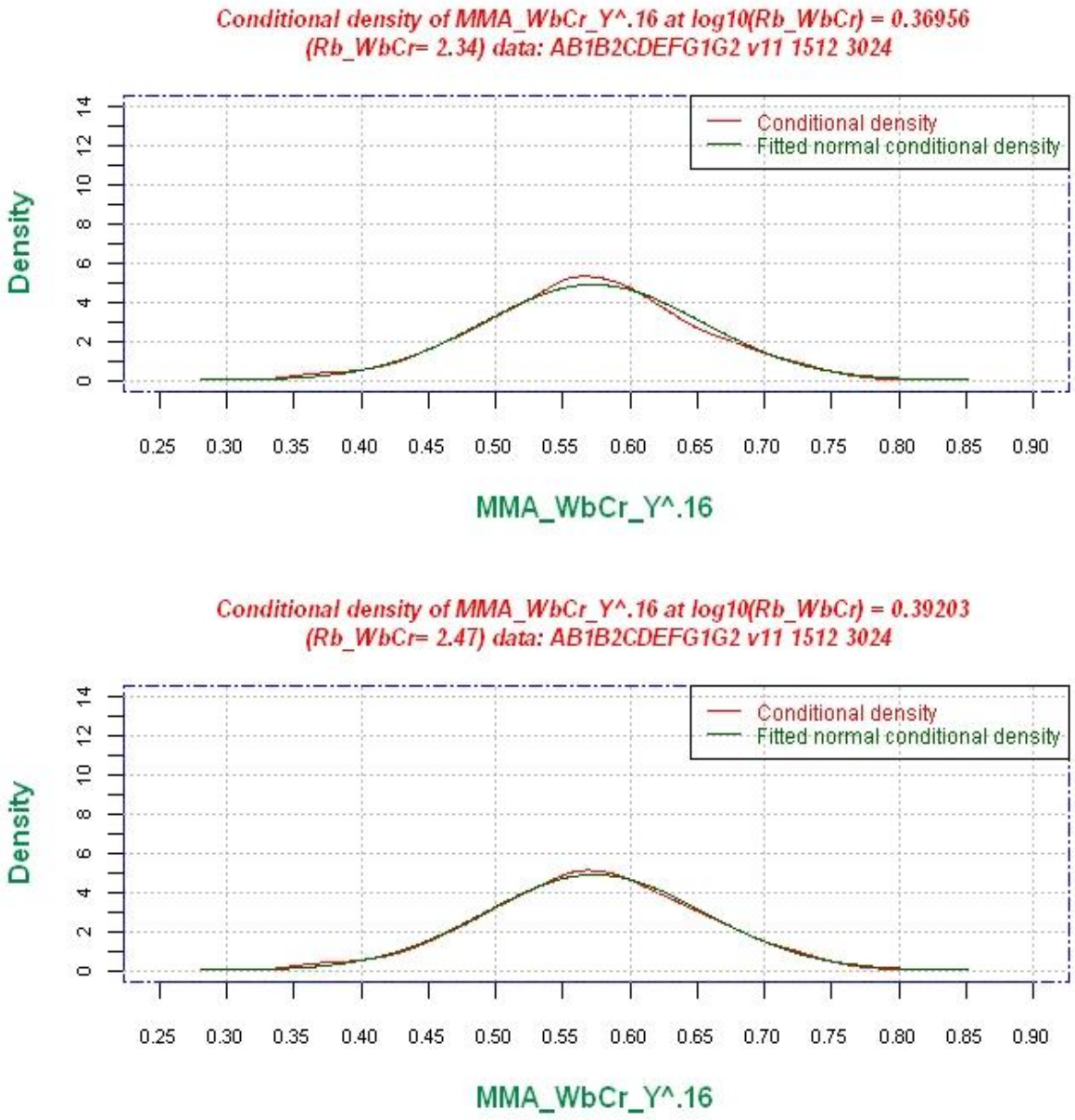

Figure 5.38: Upper graph. Conditional density of $(MMA/WbCr/Y)^{0.16}$ for $\log_{10}(Rb/WbCr)$ = 0.36956 [i.e. Rb/WbCr = 2.34]. Lower graph. Conditional density of $(MMA/WbCr/Y)^{0.16}$ $\log_{10}(Rb/WbCr)$ = 0.39203 [i.e. Rb/WbCr = 2.47].

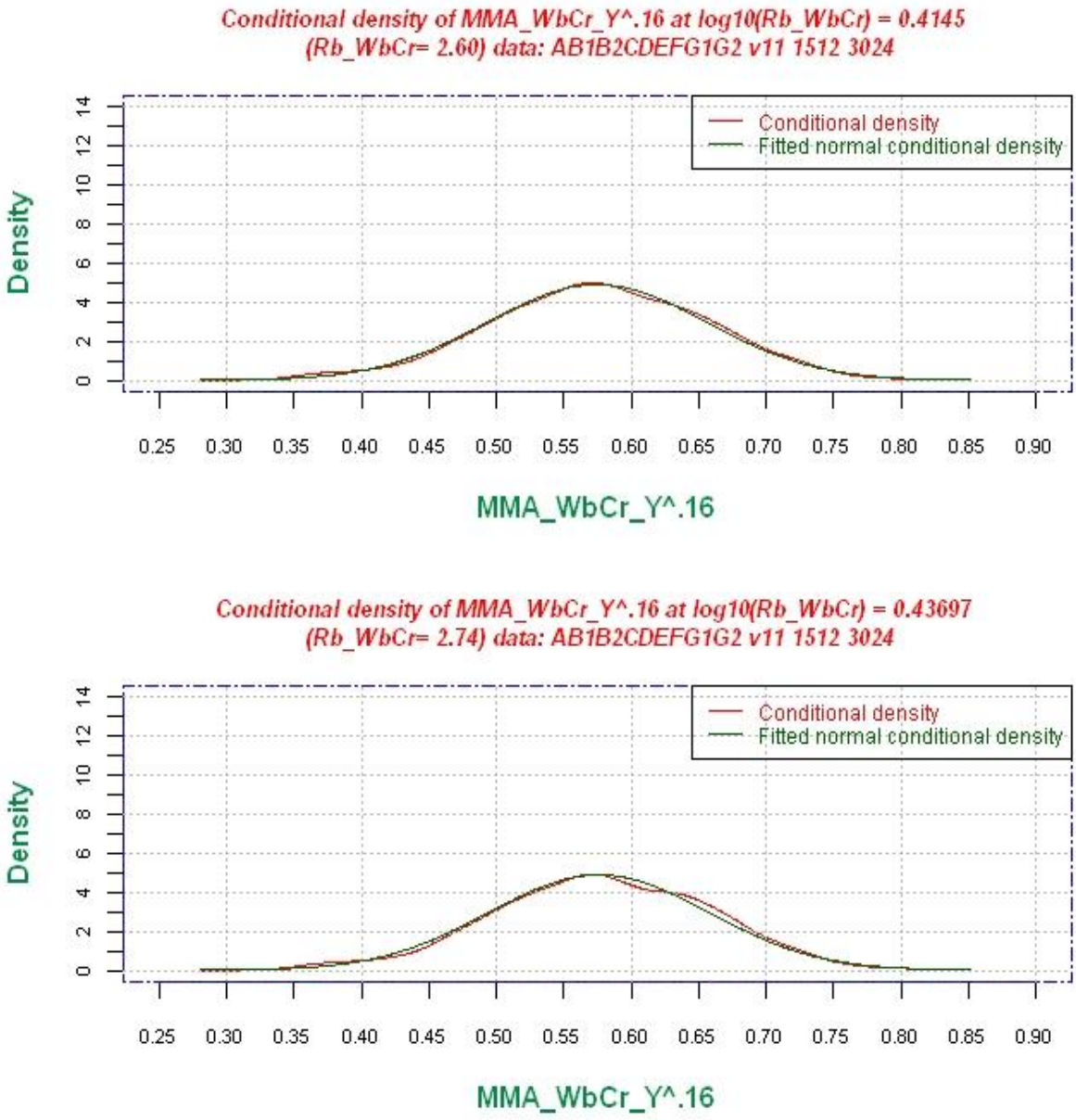

Figure 5.39: Upper graph. Conditional density of $(MMA/WbCr/Y)^{0.16}$ for $\log_{10}(Rb/WbCr)$ = 0.4145 [i.e. Rb/WbCr = 2.60]. Lower graph. Conditional density of $(MMA/WbCr/Y)^{0.16}$ for $\log_{10}(Rb/WbCr)$ = 0.43697 [i.e. Rb/WbCr = 2.74].

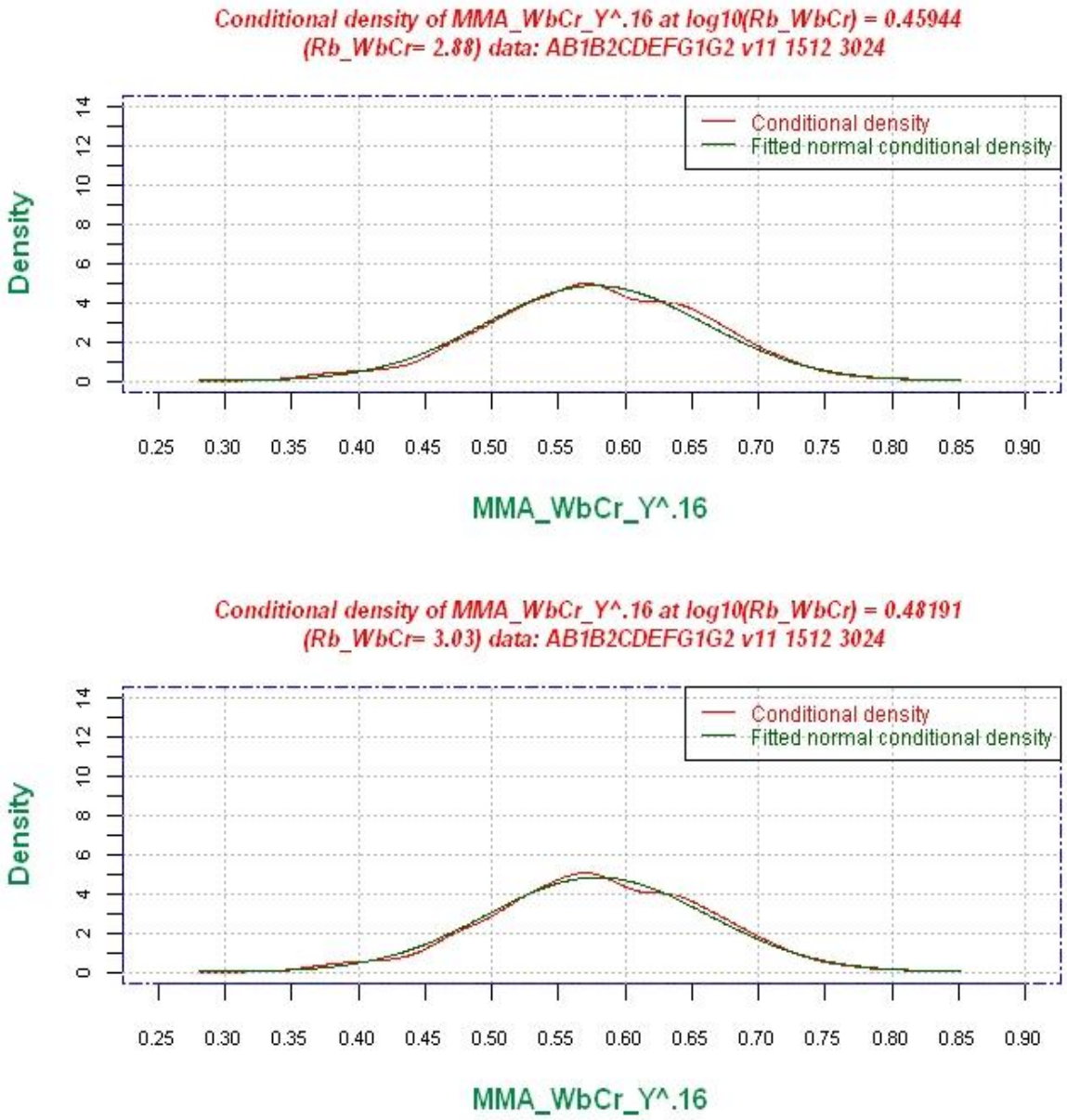

Figure 5.40: Upper graph. Conditional density of $(MMA/WbCr/Y)^{0.16}$ for $\log_{10}(Rb/WbCr)$ = 0.45944 [i.e. Rb/WbCr = 2.88]. Lower graph. Conditional density of $(MMA/WbCr/Y)^{0.16}$ for $\log_{10}(Rb/WbCr)$ = 0.48191 [i.e. Rb/WbCr = 3.03].

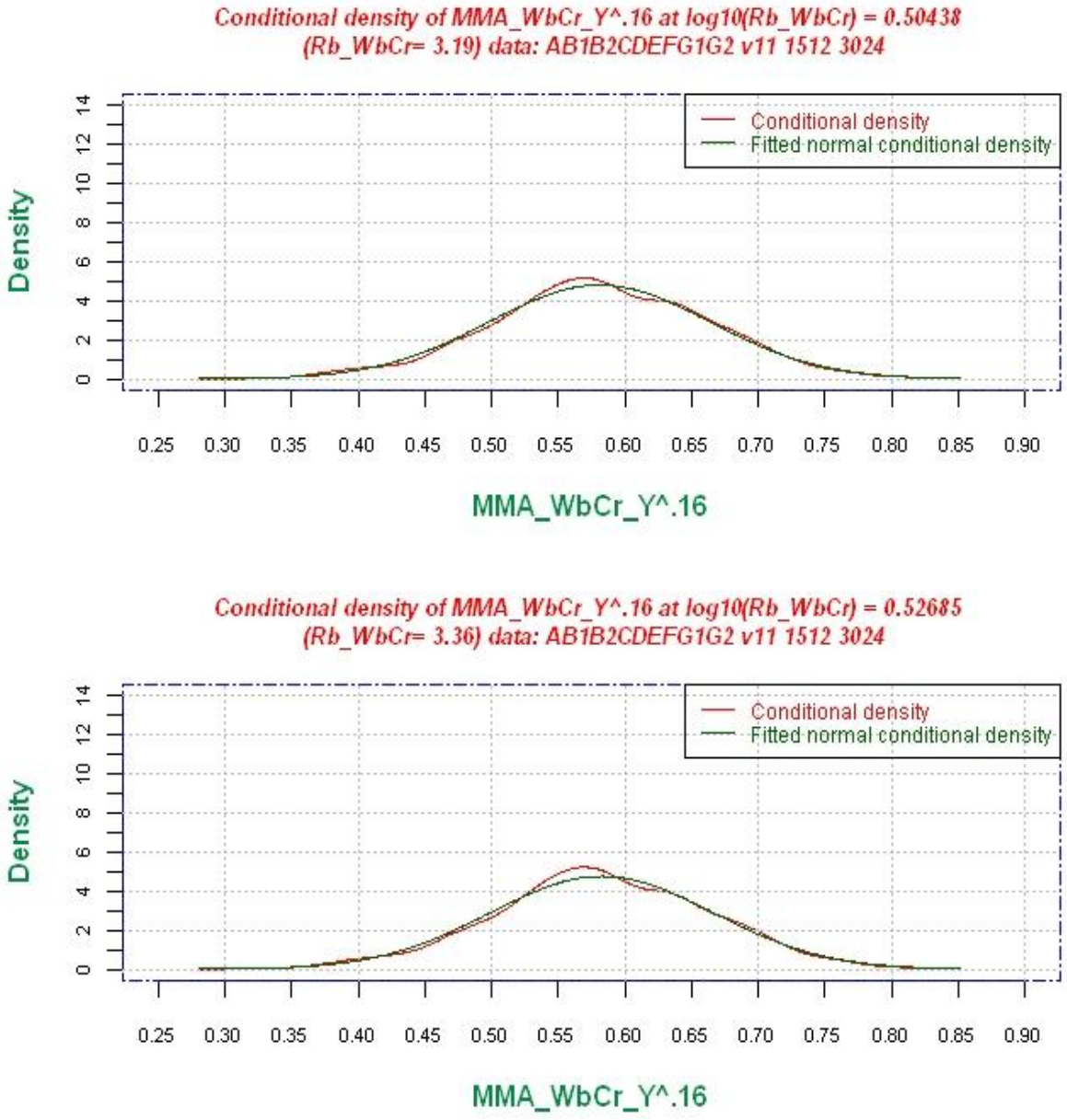

Figure 5.41: Upper graph. Conditional density of $(MMA/WbCr/Y)^{0.16}$ for $\log_{10}(Rb/WbCr)$ = 0.50438 [i.e. Rb/WbCr = 3.19]. Lower graph. Conditional density of $(MMA/WbCr/Y)^{0.16}$ for $\log_{10}(Rb/WbCr)$ = 0.52685 [i.e. Rb/WbCr = 3.36].

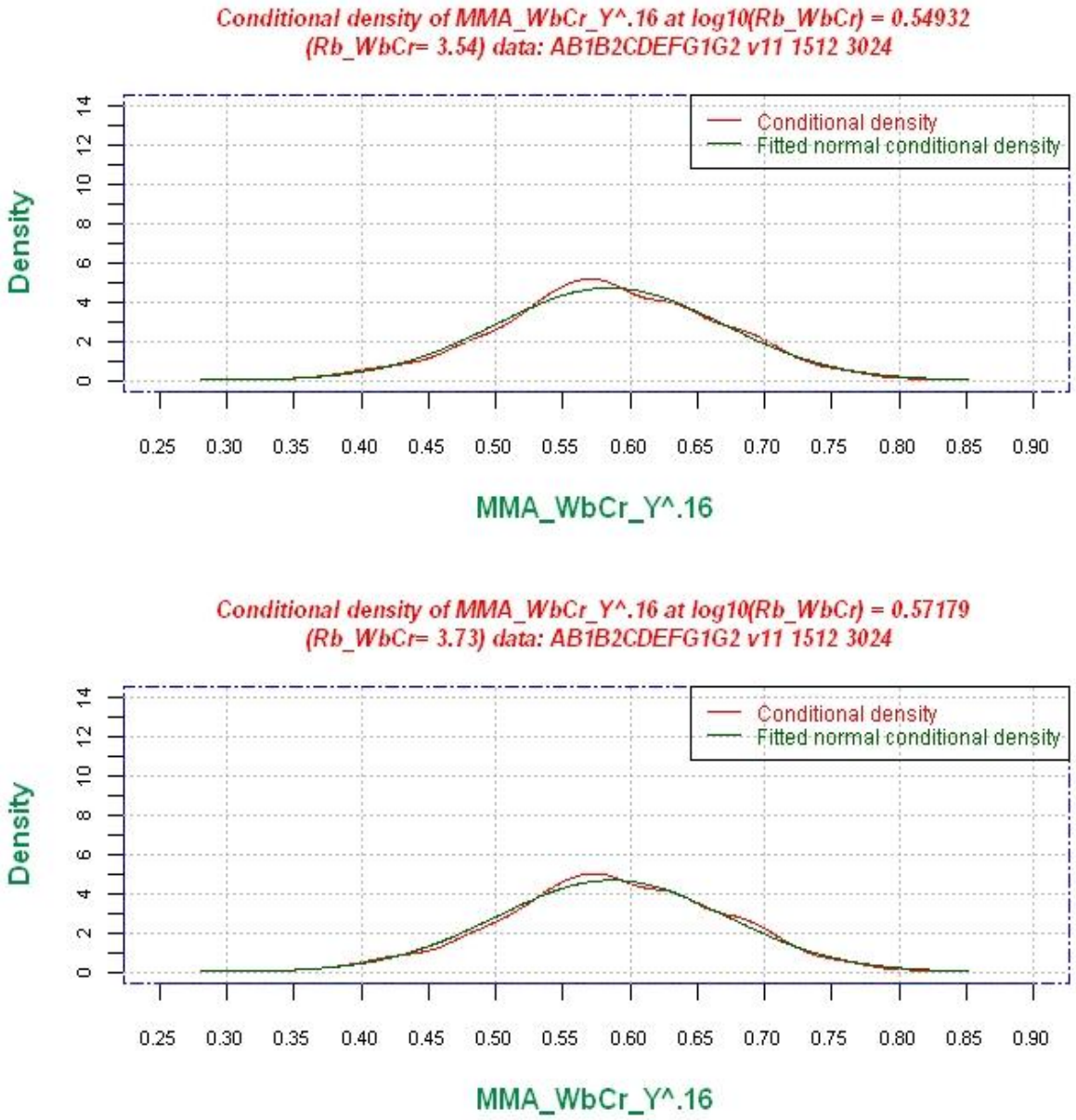

Figure 5.42: Upper graph. Conditional density of $(MMA/WbCr/Y)^{0.16}$ for $\log_{10}(Rb/WbCr) = 0.54932$ [i.e. Rb/WbCr = 3.54]. Lower graph. Conditional density of $(MMA/WbCr/Y)^{0.16}$ for $\log_{10}(Rb/WbCr) = 0.57179$ [i.e. Rb/WbCr = 3.73].

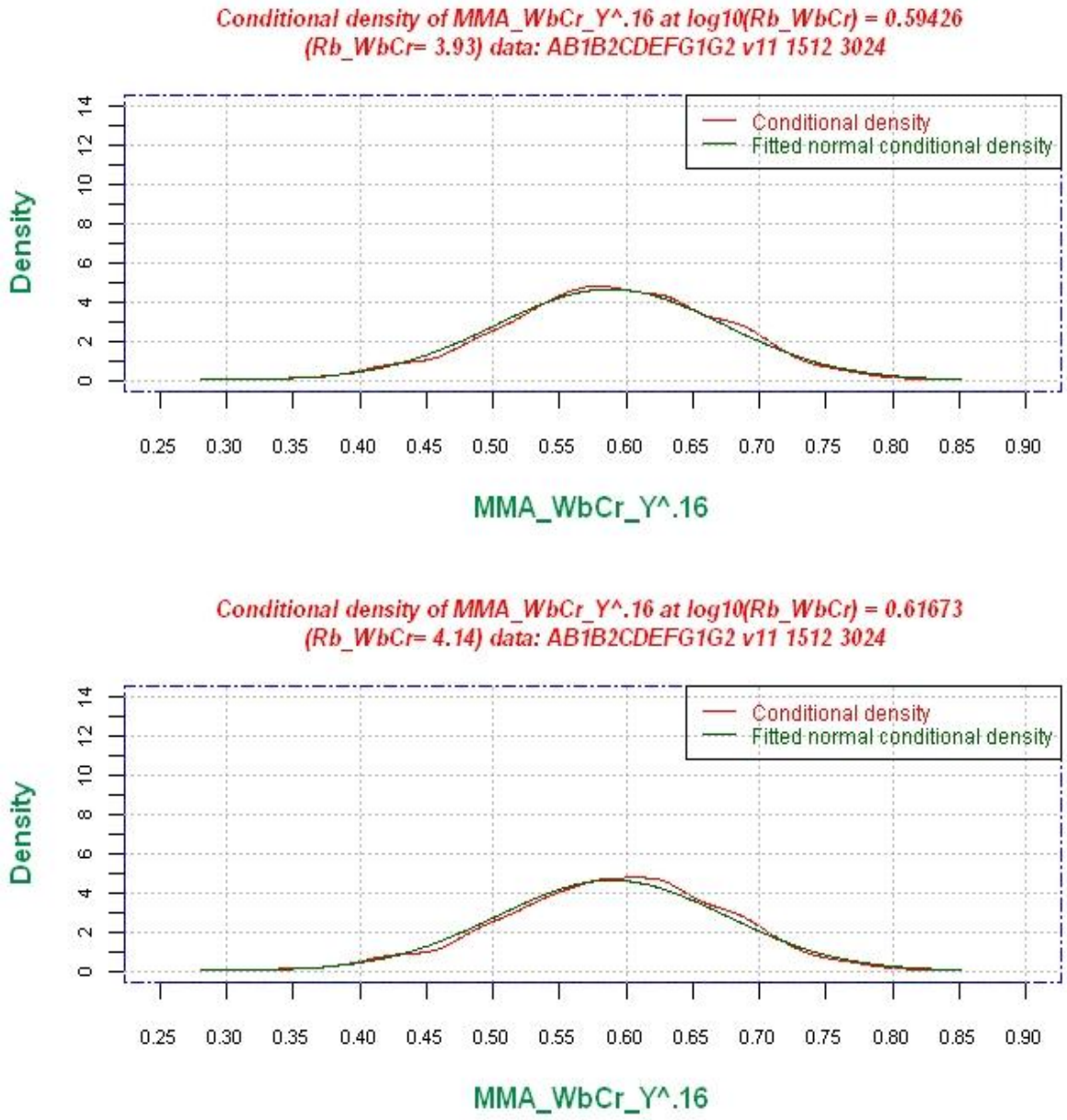

Figure 5.43: Upper graph. Conditional density of $(MMA/WbCr/Y)^{0.16}$ for $\log_{10}(Rb/WbCr)$ = 0.59426 [i.e. Rb/WbCr = 3.93]. Lower graph. Conditional density of $(MMA/WbCr/Y)^{0.16}$ for $\log_{10}(Rb/WbCr)$ = 0.61673 [i.e. Rb/WbCr = 4.14].

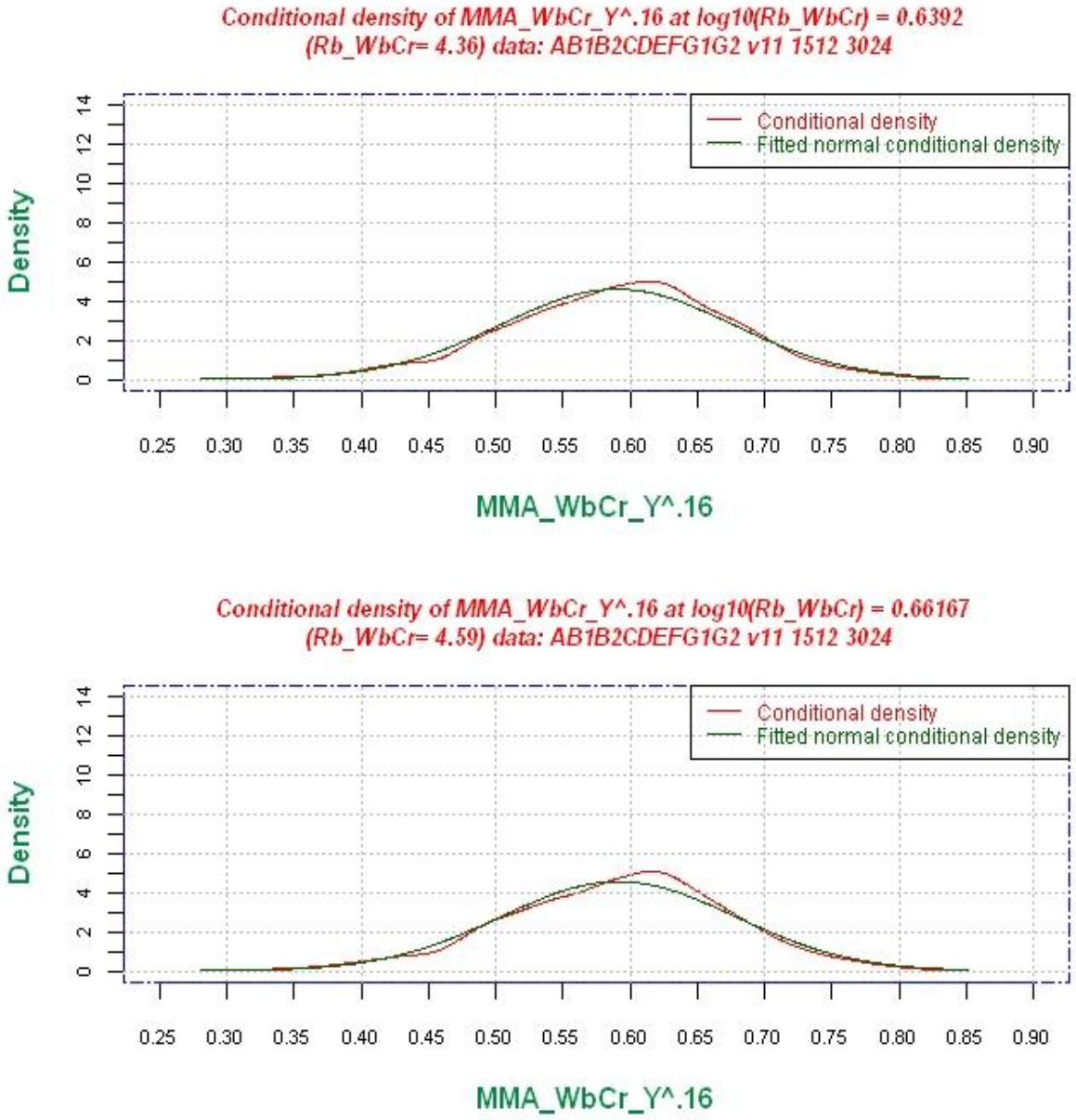

Figure 5.44: Upper graph. Conditional density of $(MMA/WbCr/Y)^{0.16}$ for $\log_{10}(Rb/WbCr)$ = 0.6392 [i.e. Rb/WbCr = 4.36]. Lower graph. Conditional density of $(MMA/WbCr/Y)^{0.16}$ for $\log_{10}(Rb/WbCr)$ = 0.66167 [i.e. Rb/WbCr = 4.59].

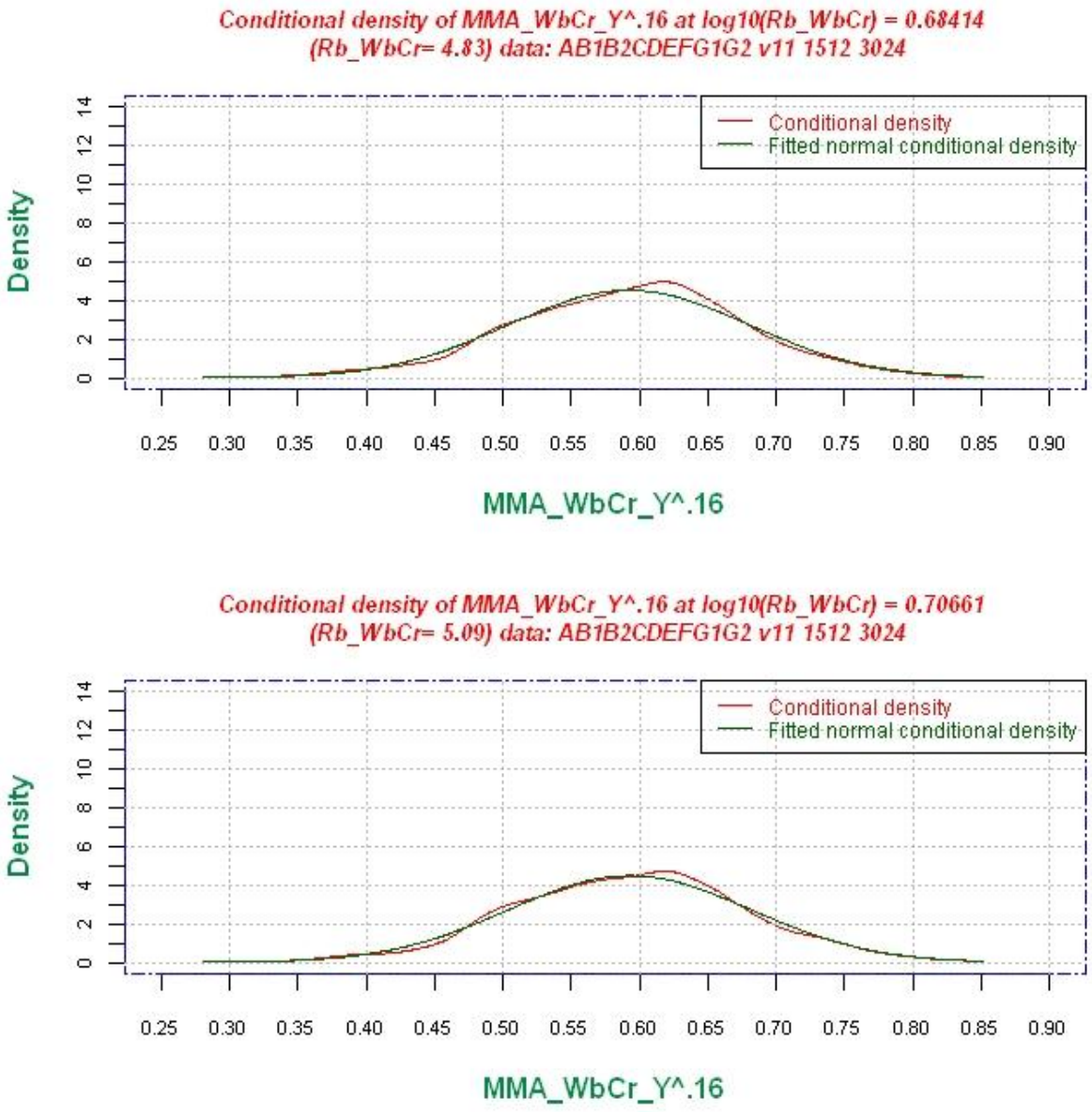

Figure 5.45: Upper graph. Conditional density of $(MMA/WbCr/Y)^{0.16}$ for $\log_{10}(Rb/WbCr)$ = 0.68414 [i.e. Rb/WbCr = 4.83]. Lower graph. Conditional density of $(MMA/WbCr/Y)^{0.16}$ for $\log_{10}(Rb/WbCr)$ = 0.70661 [i.e. Rb/WbCr = 5.09].

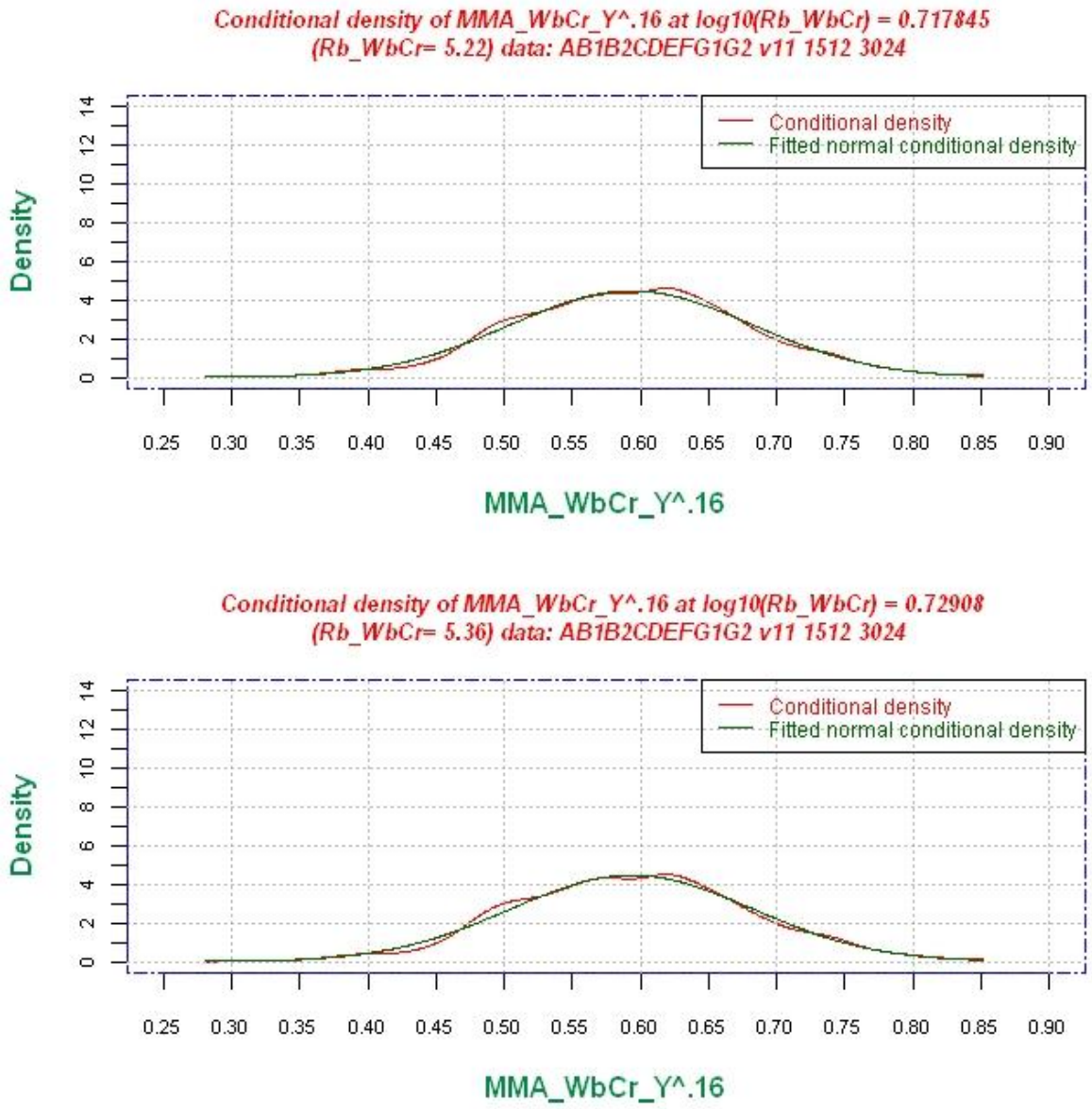

Figure 5.46: Upper graph. Conditional density of $(MMA/WbCr/Y)^{0.16}$ for $\log_{10}(Rb/WbCr)$ = 0.717845 [i.e. Rb/WbCr = 5.22]. Lower graph. Conditional density of $(MMA/WbCr/Y)^{0.16}$ for $\log_{10}(Rb/WbCr)$ = 0.72908 [i.e. Rb/WbCr = 5.36].

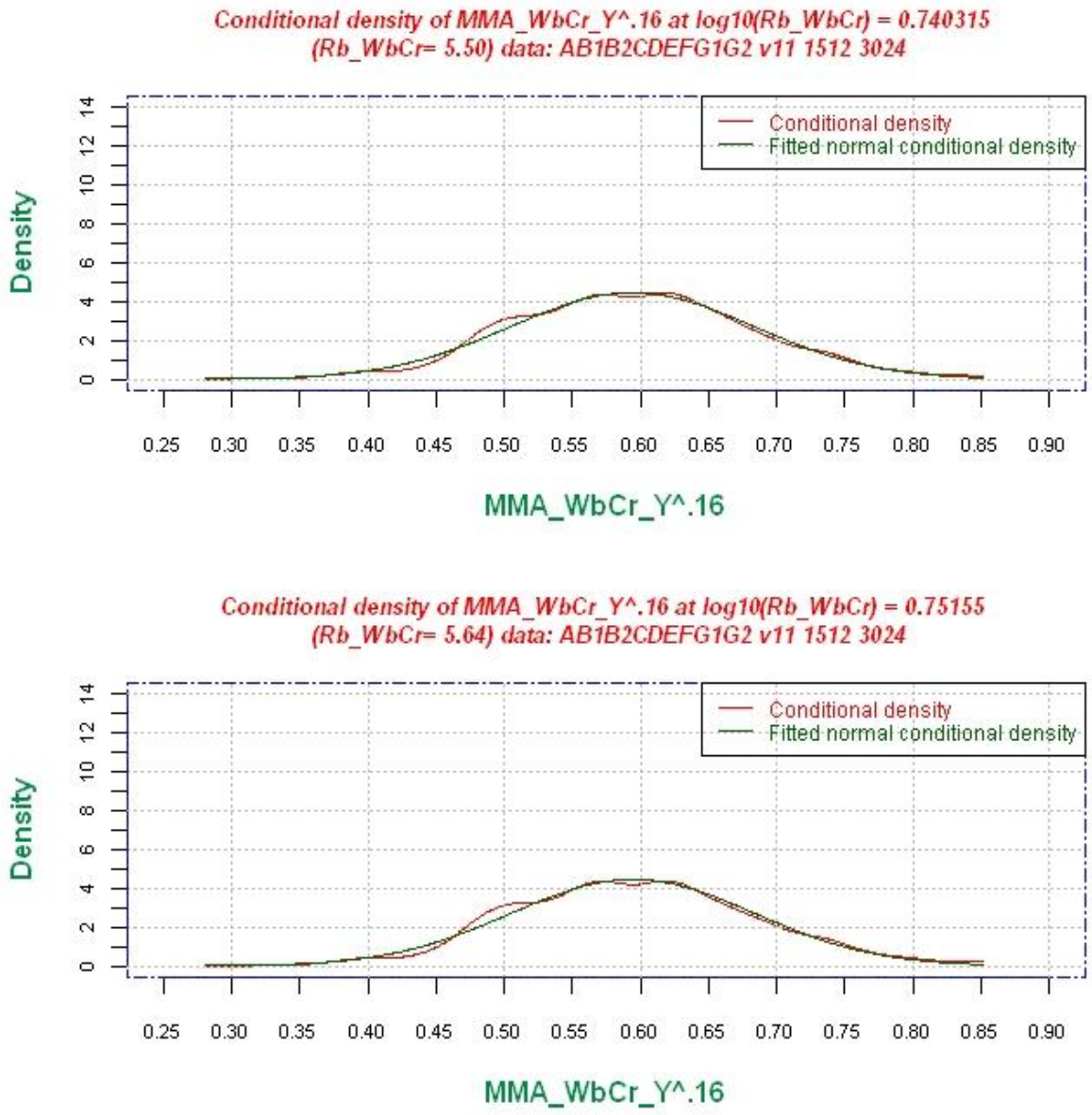

Figure 5.47: Upper graph. Conditional density of $(MMA/WbCr/Y)^{0.16}$ for $\log_{10}(Rb/WbCr)$ = 0.740315 [i.e. Rb/WbCr = 5.50]. Lower graph. Conditional density of $(MMA/WbCr/Y)^{0.16}$ for $\log_{10}(Rb/WbCr)$ = 0.75155 [i.e. Rb/WbCr = 5.64].

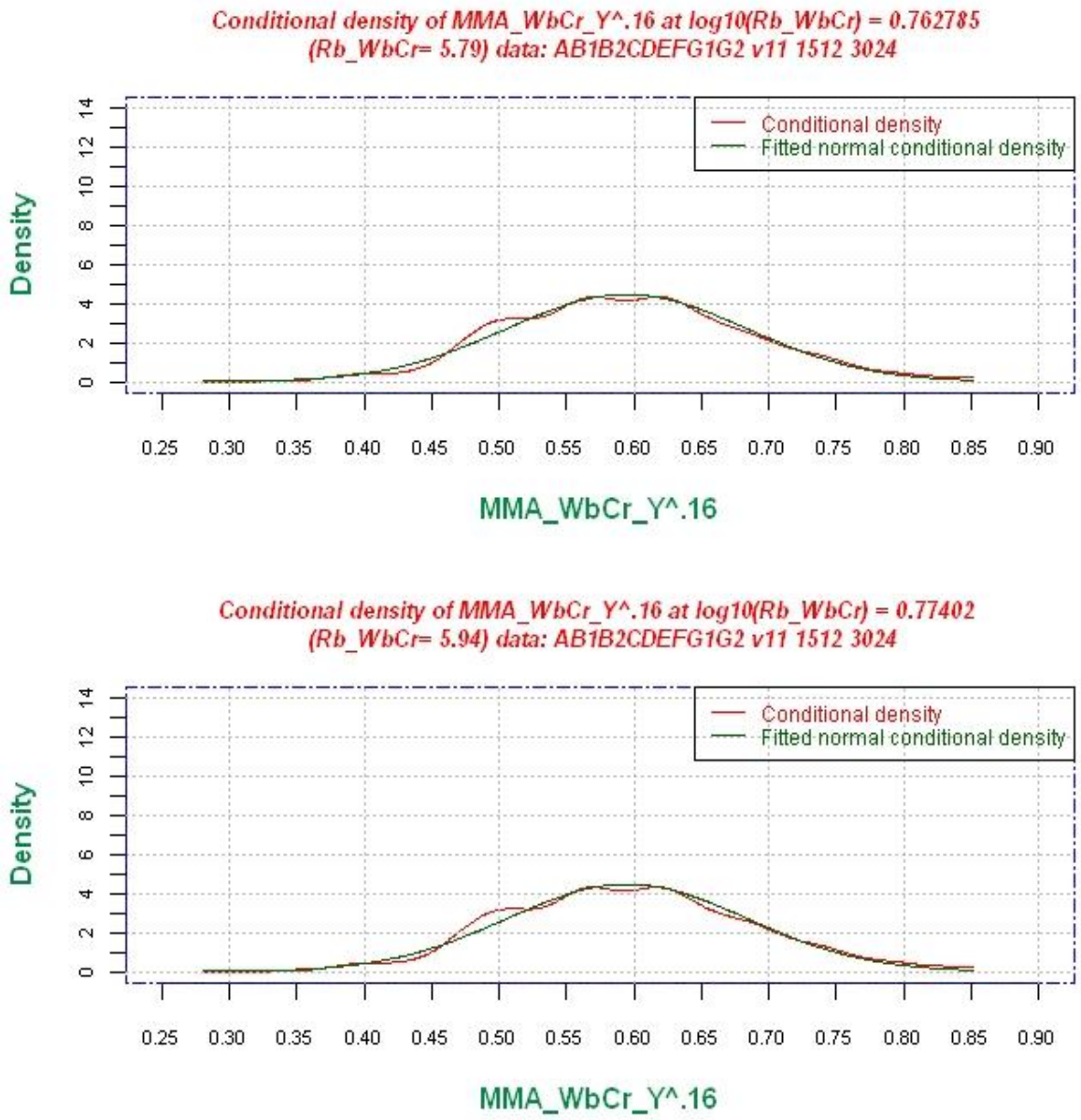

Figure 5.48: Upper graph. Conditional density of $(MMA/WbCr/Y)^{0.16}$ for $\log_{10}(Rb/WbCr) = 0.762785$ [i.e. Rb_WbCr = 5.79]. Lower graph. Conditional density of $(MMA/WbCr/Y)^{0.16}$ for $\log_{10}(Rb/WbCr) = 0.77402$ [i.e. Rb/WbCr = 5.94].

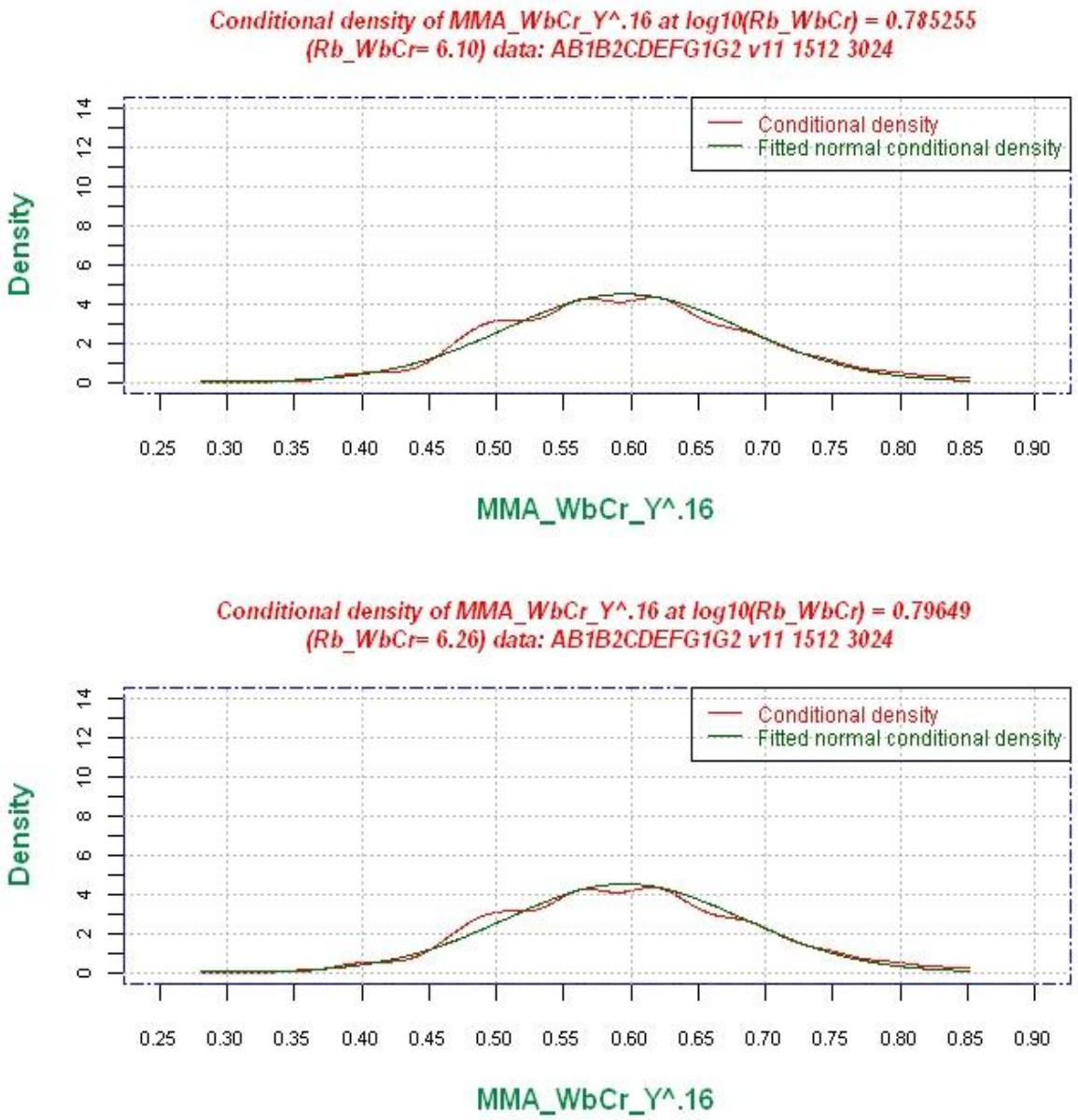

Figure 5.49: Upper graph. Conditional density of $(MMA/WbCr/Y)^{0.16}$ for $\log_{10}(Rb/WbCr) = 0.785255$ [i.e. Rb/WbCr = 6.10]. Lower graph. Conditional density of $(MMA/WbCr/Y)^{0.16}$ for $\log_{10}(Rb/WbCr) = 0.79649$ [i.e. Rb/WbCr = 6.26].

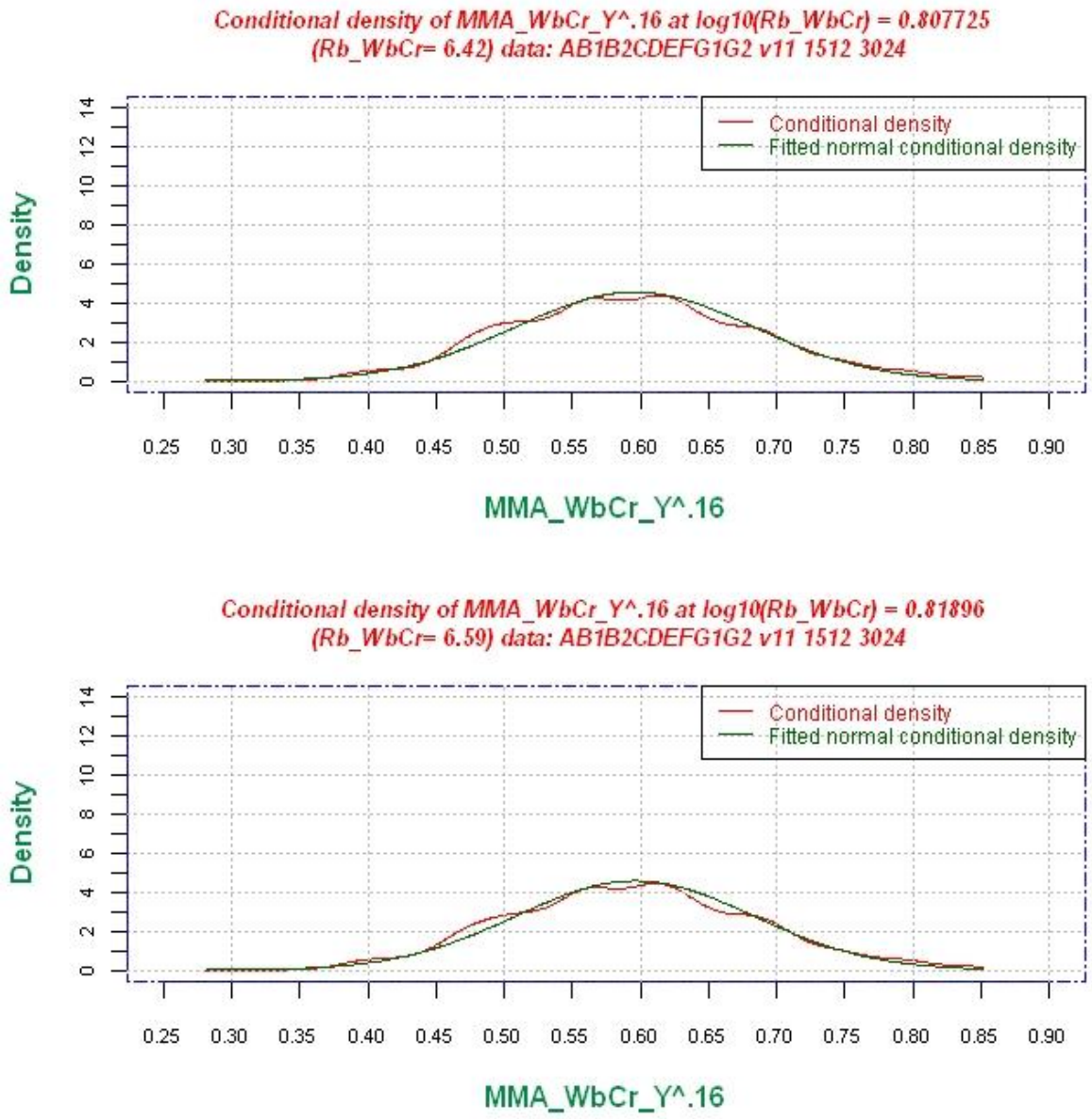

Figure 5.50: Upper graph. Conditional density of $(MMA/WbCr/Y)^{0.16}$ for $\log_{10}(Rb/WbCr) = 0.807725$ [i.e. Rb/WbCr = 6.42]. Lower graph. Conditional density of $(MMA/WbCr/Y)^{0.16}$ for $\log_{10}(Rb/WbCr) = 0.81896$ [i.e. Rb/WbCr = 6.59].

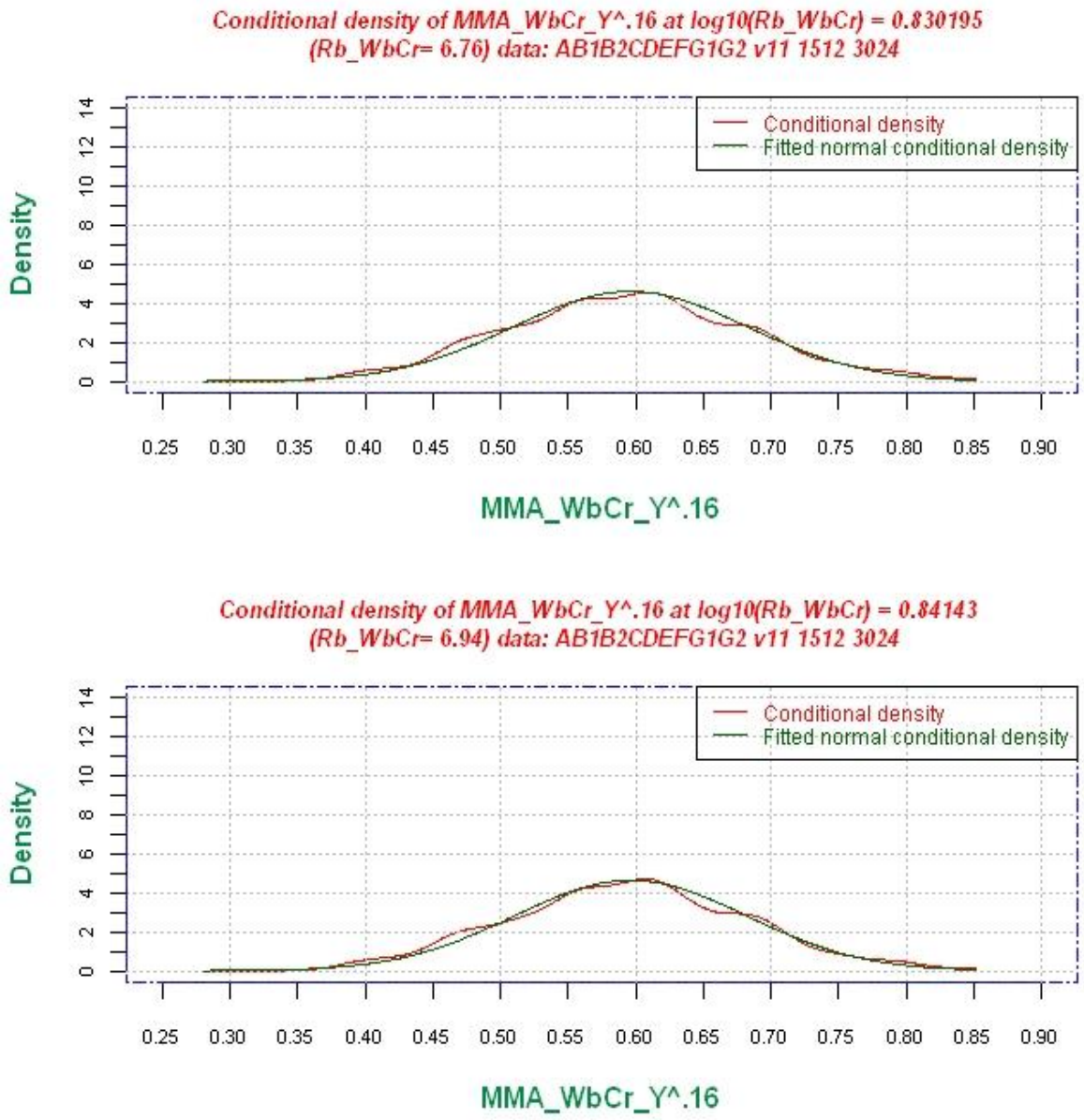

Figure 5.51: Upper graph. Conditional density of $(MMA/WbCr/Y)^{0.16}$ for $\log_{10}(Rb/WbCr)$ = 0.830195 [i.e. Rb/WbCr = 6.76]. Lower graph. Conditional density of $(MMA/WbCr/Y)^{0.16}$ for $\log_{10}(Rb/WbCr)$ = 0.84143 [i.e. Rb/WbCr = 6.94].

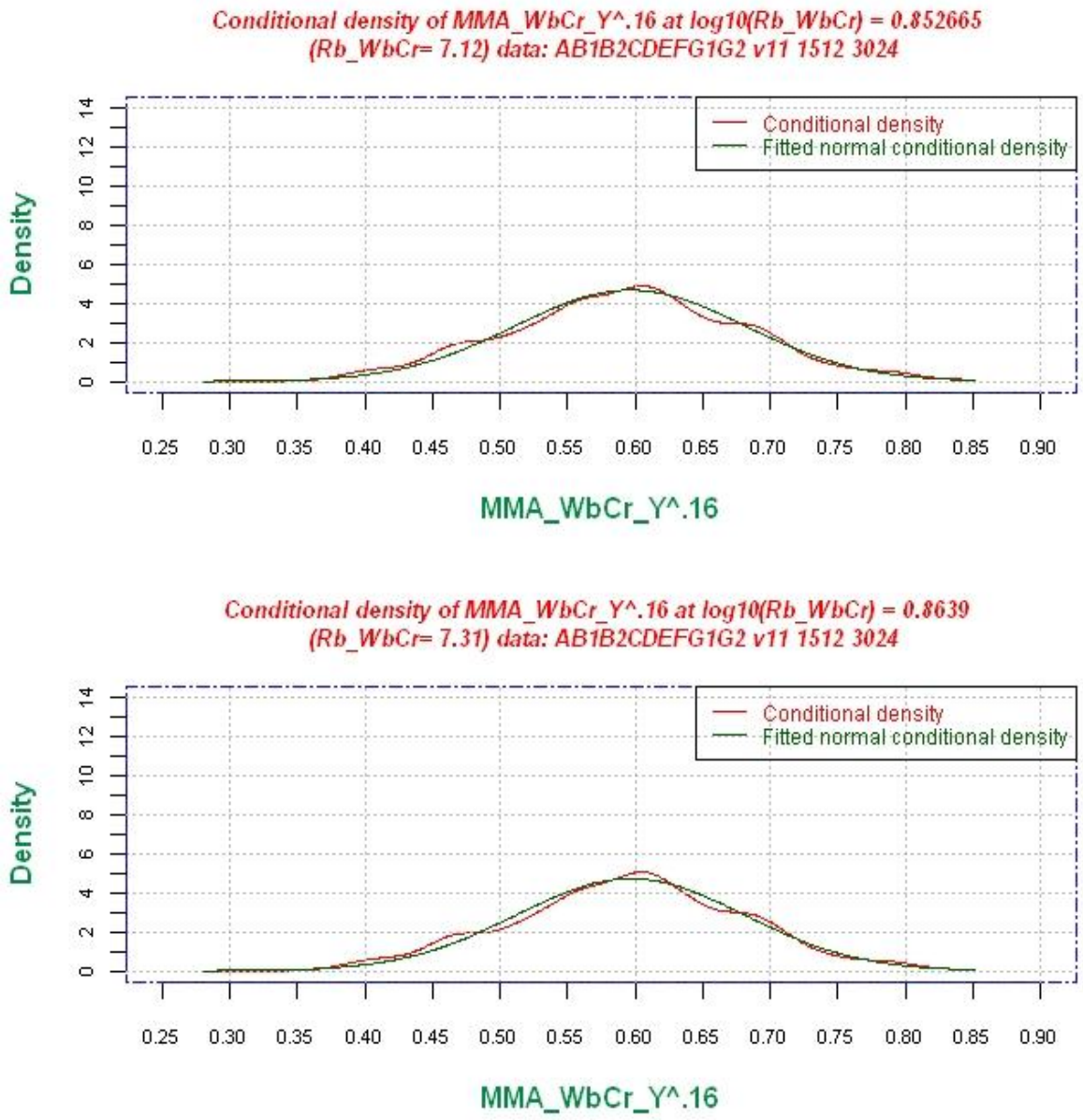

Figure 5.52: Upper graph. Conditional density of $(MMA/WbCr/Y)^{0.16}$ for $\log_{10}(Rb/WbCr) = 0.852665$ [i.e. Rb/WbCr = 7.12]. Lower graph. Conditional density of $(MMA/WbCr/Y)^{0.16}$ for $\log_{10}(Rb/WbCr) = 0.8639$ [i.e. Rb/WbCr = 7.31].

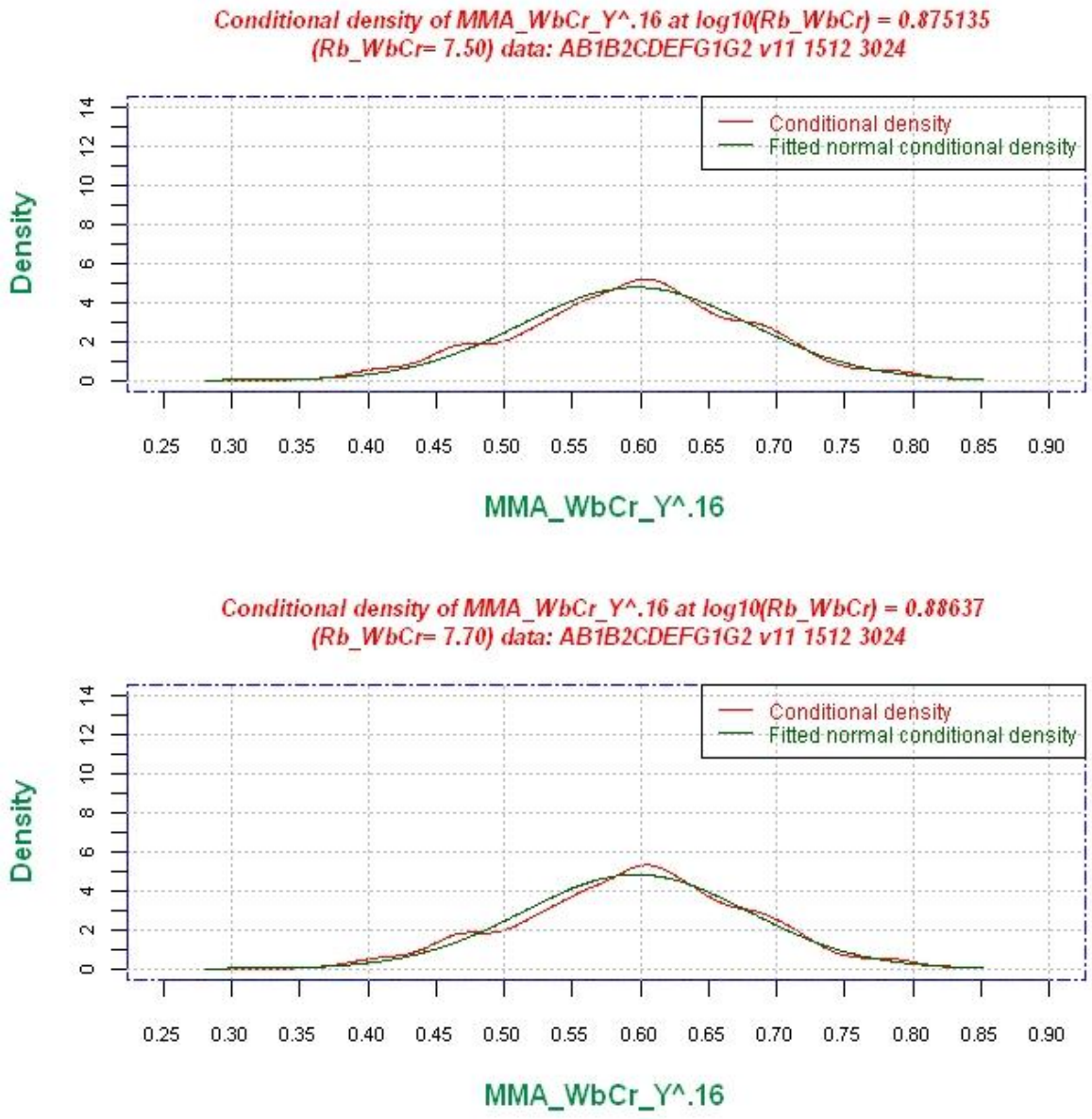

Figure 5.53: Upper graph. Conditional density of $(MMA/WbCr/Y)^{0.16}$ for $\log_{10}(Rb/WbCr) = 0.875135$ [i.e. Rb/WbCr = 7.50]. Lower graph. Conditional density of $(MMA/WbCr/Y)^{0.16}$ for $\log_{10}(Rb/WbCr) = 0.88637$ [i.e. Rb/WbCr = 7.70].

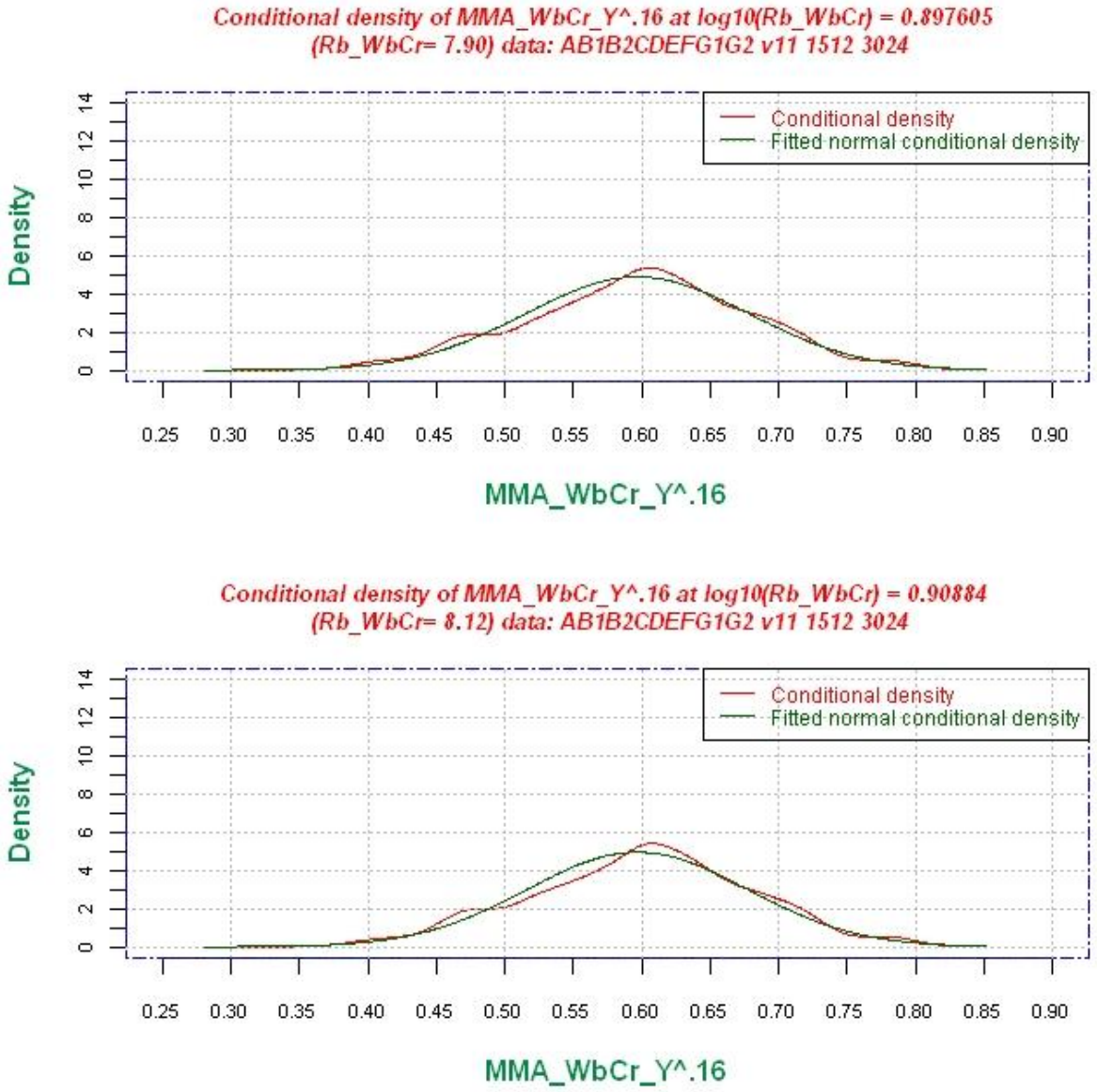

Figure 5.54: Upper graph. Conditional density of $(MMA/WbCr/Y)^{0.16}$ for $\log_{10}(Rb/WbCr)$ = 0.897605 [i.e. Rb/WbCr = 7.90]. Lower graph. Conditional density of $(MMA/WbCr/Y)^{0.16}$ for $\log_{10}(Rb/WbCr)$ = 0.90884 [i.e. Rb/WbCr = 8.12].

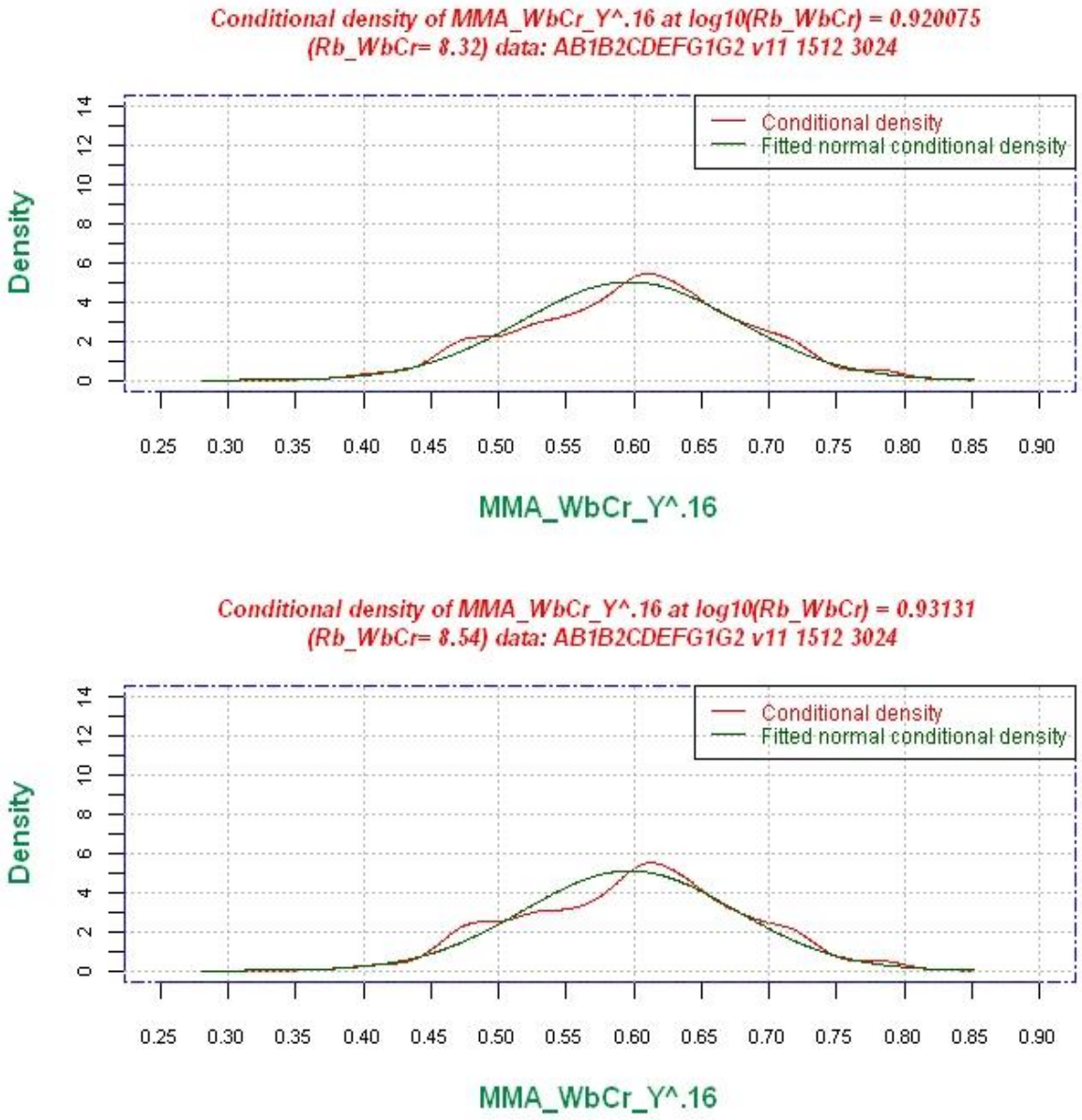

Figure 5.55: Upper graph. Conditional density of $(MMA/WbCr/Y)^{0.16}$ for $\log_{10}(Rb/WbCr)$ = 0.920075 [i.e. Rb/WbCr = 8.32]. Lower graph. Conditional density of $(MMA/WbCr/Y)^{0.16}$ for $\log_{10}(Rb/WbCr)$ = 0.93131 [i.e. Rb/WbCr = 8.54].

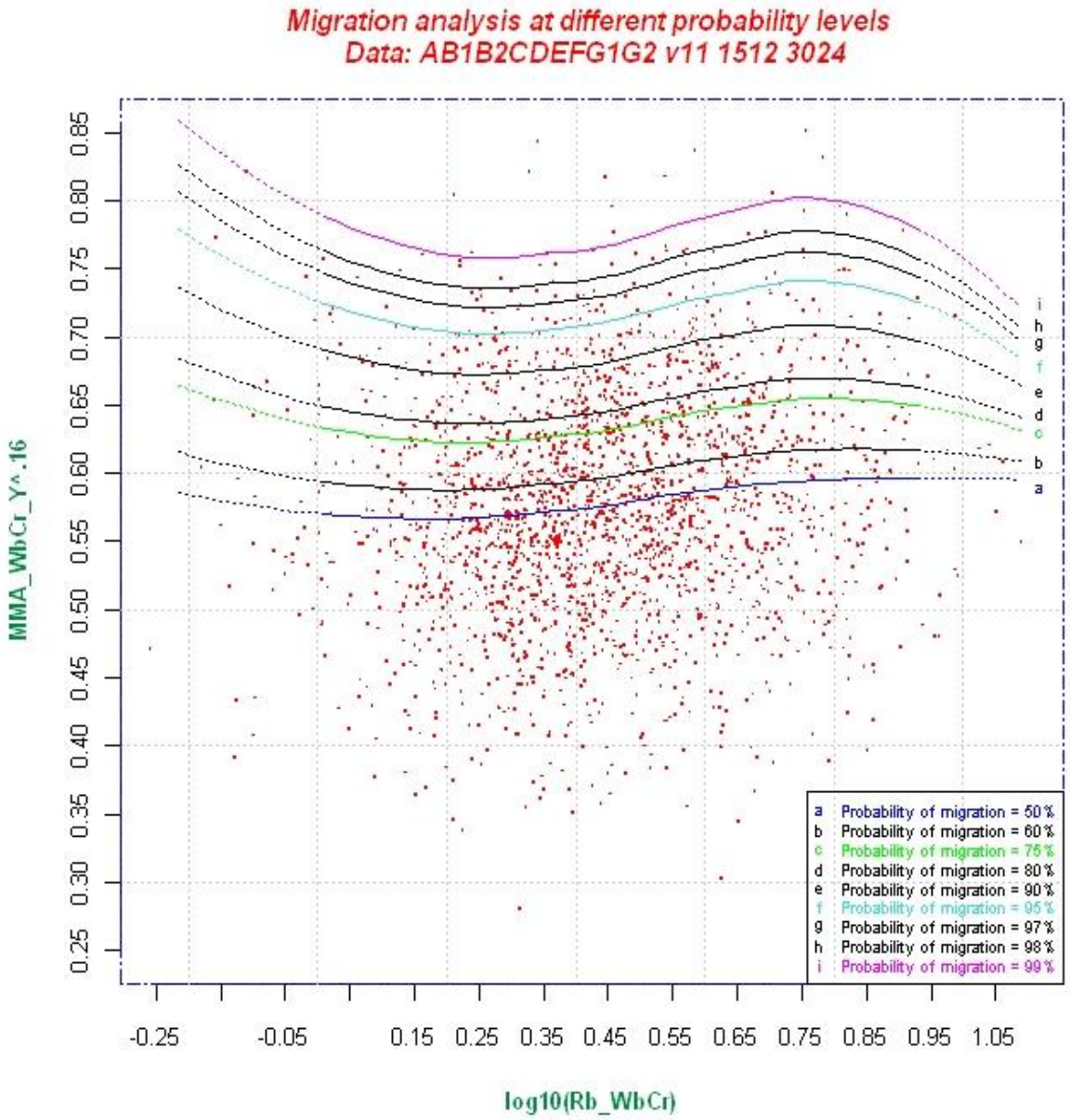

Figure 5.56: Probability curves for average annual meander migration rate at the bend apex not being exceeded, displayed different in terms of the transformed variables $(MMA/WbCr/Y)^{0.16}$ and $\log_{10}(Rb/WbCr)$).

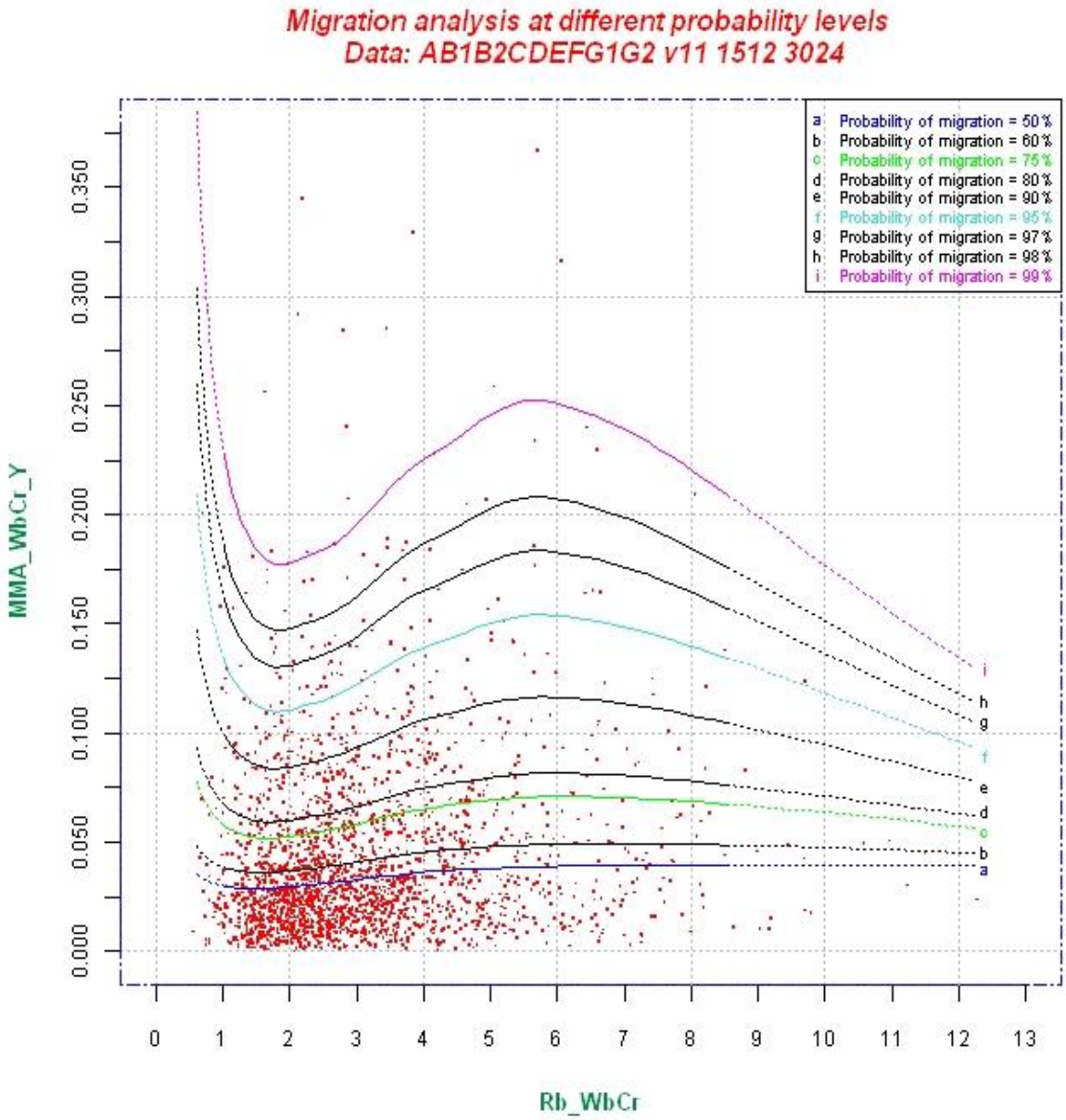

Figure 5.57: Probability curves for average annual meander migration rate at the bend apex not being exceeded, displayed different in terms of the untransformed variables (MMA/WbCr/Y) and (Rb/WbCr)).

Equations are just boring parts of mathematics. I attempt to see things in terms of geometr
--- Stephen Hawking

Chapter 6

Exploration and Testing of the Probabilistic Analysis of Bend Migration Using Period-wise Data and Data Derived from Random Division of Pooled Data

6.1 Introduction

In Chapter 5, a probabilistic method for predicting the migration rate for meander bends with specified geometries (R/W) at different probabilities of not being exceeded was developed. This Chapter presents and discusses the results of exploratory statistical investgations performed to test whether the method is robust. These tests involved examining the decision to pool the data from the two periods of observation in the UoN/HRW data set and determining the sensitivity of the probabilistic curves to sampling variability in the underpinning data.

6.2 Combining Data for the Two Time Periods into a Single Set

The dimensions and geometry of a meander bend change semi-continuously, in response to each of the formative flow events that it experiences. As the magnitude, duration, timing and sequencing of formative events differ for every bend, the outcome is a series of channel changes unique to each particular bend. These changes are cumulative and, in essence, each event sets up the antecedent conditions for the next one. However, consectutive floods may drive radically different styles and trends of bend growth and migration and consequently, while bend evolution in general can be represented using a sequence of normative stages (Hickin, 1978), the morphological 'memory' of each individual bend is relatively short, because it responds and adjusts quickly to ambient conditions and contemporary flows.

In the context of this study, it follows from these observations that, while an individual bend may retain its identity and be recognisable as being the same entity in aerial photographs taken decades apart, it would be expected that its late-stage morphology and evolutionary behaviour should be practically independent of its geometry during early-stage development. The corollary to this is that in the database, values of dimensionless bend radii (R/W) measured at T2 should no more than weakly correlate with those measured at T1. Similarly, values of dimensionless migration observed during the second period of observation (TP2) should not be significantly correlated with those measured during the first period (TP1).

To test whether this is true for the dimensionless radius (R/W), a scatter plot was produced with R2/W2Cr plotted as a function of R1/W1Cr (Figure 6.1). The null hypothesis is that there is no significant correlation between these variables beyond that expected due to randon chance. The alternative hypothesis is that the correlation between them is too strong to be the product of random chance. The geographical hypothesis is that the dimensionless radius at T2 is a function of that observed at T1 due to long-term memory of the bend's previous morphological condition. To investigate this, a simple linear regression was fitted to the data, with the intercept on the y-axis set to zero as, physically, it would be meaningless for the function to have any value other than zero for R2/W2Cr when R1/W1Cr = 0. The correlation coefficient is moderate (0.64), yielding a coefficient of determination of 0.41. Despite this, due to the very large size of the sample (n = 874), this correlation coefficient is indicated as being statistically significant at a 1% level of confidence. However, it would be invalid to conclude that this indicates a causal link between the data for the two time periods. Analysis of residuals reveals both non-constant variance (Figure 6.2) and non-normality of the residuals (Figure 6.3), which violate the underlying assumptions required for fitting a linear model to the data.

A similar scatter graph was plotted for the variable dimensionless migration (MMA/WCr/Y). (Figure 6.4). The correlation coefficient and coefficient of determination are both weak (0.33 and 0.11, respectively). Due to the large sample size (874) this correlation coefficient is also indicated as being significant at a 1% level of confidence. However, the results of residual analysis again

reveal non-constant variance (Figure 6.5) and non-normality (Figure 6.6) that invalidate linear regression of the data, as was the case for the dimensionless radius.

The conclusion to be drawn from these arguments is that there is a degree of correlation and probably pseudoreplication between the datasets for T1 and T2. This is unsurprising as 874 of the bends in the two sets are the same. However, the correlation coefficients are moderate to weak and the benefits of increasing the sample size by pooling the data were judged on balance to outweigh these costs. This finding justifies pooling the data sets for the two time periods to create a much larger data set when conducting the probabilistic analysis to express dimensionless meander migration rate as a function of dimensionless bend radius. In point of fact, these findings are unsurprising when further consideration is given to the make up of the data sets in T1 and T2. Due to rigorous screening and removal of suspect data points when the NCHRP database was converted to the UoN/HRW database, only about 800 of 1,512 bends originally included Time Period 1, were actually available used. Conversely, in Time Period 2, quality control removed far fewer bends and nearly 1,500 data points were available. It follows that between 600 and 700 data points (approximately doubling the sample size) were added in T2, representing bends that were removed in T1.

6.3 Time-wise Investigation of Erosion Rate Probability Distributions Based on Data for Time Periods 1 and 2

6.3.1 Justification

The probabilistic analyses of bend migration reported in Sections 5.3 to 5.6 were performed using a pooled data set that combines observations from Time Period 1 (TP1) and Time Period 2 (TP2). The purpose of pooling the data was to produce a larger, more comprehensive data set, as described in Section 5.2.3. However, it may be questioned whether period-wise data analysis (that is analysing data from TP1 and that from TP2 separately) might produce significantly different, probabilistic results and, if the analysis were to reveal a significant difference, what the causal explanation for that difference might be. This section addresses these questions.

6.3.2 Probability Analyses for TP1 and TP2

The time-wise (TP1 and TP2) distribution (scatter) of data is shown in Figure 5.3. In this exploratory analysis, period-specific analyses were conducted for these data, in exactly the same way as reported in Sections 5.3 to 5.6 for the pooled dataset.

The first point to note in comparing the distributions is that both the number of data points and the ranges of the x and y-variables differ between TP1 and TP2. For TP1, n = 874, while for TP2 n = 1,382 entries. These totals sum to the 2,256 data points in the pooled data set analysed previously. The lower number of entries for TP1 may be partially responsible for the narrower range of values for the dimensionless radius of curvature (R/WCr), which varies between 0.66 and 11.23 compared to a range of 0.55 to 12.26 for TP2. The range of values of the dimensionless migration rate (MMA12/W1Cr/Y) for TP1 (0.000358 to 0.26) is also smaller than that for TP2 (MMA23/W2Cr/Y) which is 0.001301 to 0.37. Since these data provide the basis for the empirical probability density estimation, differences in the ranges and extreme values (especially of dimensionless migration rate) would be expected to result in some differences, especially at the fringes of the data sets. The ranges of both the x and y data for TP2 also define the ranges of the pooled dataset. It would be expected, therefore, that the probability curves for TP2 and the pooled data set should differ less markedly.

The distributions of the x-variable for TP1 and TP2 were successfully normalised using common logarithmic transformations (Figures 6.7 to 6.10), as was the case for the pooled data (see Figures 5.4 to 5.11). The y-variables (migration per river channel width per year,) for TP1 and TP2 were successfully normalised using a power transformation. For TP1, the exponent in the power transformation was set to a value of 0.2 (Figures 6.11 to 6.14), while it was set to 0.14 for TP2. For comparison, the exponent for the pooled data was 0.16 (see Figures 5.12 to 5.19).

Probability curves ranging from a 1% to a 99% of not being exceeded were computed for the probability density functions derived for TP1 and TP2 (Figures 6.15, 6.16 and 6.17).

6.3.3 Comparison of Migration Rate Prediction Curves for TP1 and TP2

Similarities and differences between the outcomes of analyses performed for TP1 and TP2 may be identified by considering the curves for 1%, 5%, 10%, 25%, 50%, 75%, 90%, 95% and 99% probability of a given dimensionless rate of migration not being exceeded (Figures 6.18 to 6.26).

The curves with probabilities of not being exceeded of less than 50% are very similar. Even that for 75% does not change substantially between time periods, except for values of the dimensionless bend radius less than around 1.75 and greater than about 7.5. However, the curves with probabilities of 90% and higher differ more markedly in four respects:

1. peaks in the curves for TP2 are higher than those for TP1;
2. peaks occur at a slightly higher values of dimensionless bend radius for TP2 than TP1;
3. curves for TP2 rise steeply for values of R/WCr < ~1.75, while those for TP1 remain low;
4. curves for TP2 are noticeably higher for values of R/WCr > ~7.5, with the difference growing as the probability of not being exceeded increases from 90 to 99%.

6.3.4 Discussion

As discussed in Section 6.3.2, these differences may, at least in part, be attributed to the larger number of entries and wider range of values in the data for TP2 compared to TP1. However, consideration of the geomorphology of meander bends in general and the understanding of bend evolution that has emerged from long-term monitoring of bend behaviour (see Chapter 1, Sections 1.3 and 1.6), suggests that these findings are not only consistent with but also lend quantitative support to, the descriptive accounts of bend evolution reported by previous researchers, including Hickin and Nanson, Hooke and others (Hickin, 1974; Hickin and Nanson, 1975), and generalised accounts of the morphodynamics of bends in meandering rivers that may be found in any text book of fluvial geomorphology (Richards, 1982; Knighton, 1998).

The literature review reported previously established that meander bends that are free to evolve follow a somewhat similar and predictable life cycle that can be divided into periods of:

1. genesis and slow initial development,
2. rapid growth and/or migration,
3. stalling and termination.

This is highly relevant to the time-wise analysis of bends conducted in this section because segregating the data entries into sets representing TP1 and TP2 produces a *de facto* separation of the bends by age. This stems from the nature and origin of the database.

The bends in the data base were identified and selected by Dr. James Brice of the US Geological Survey as part of his original studies, which were performed in the 1960s. Brice had investigated bend migration based on comparison of aerial photographs with dates in the 1920s or 1930s and the 1960s. These dates and changes define the data and probability distributions for TP1 in the present study.

Ayres Associates built on Brice's work by adding another set of aerial photographs, taken in the 1990s. Differences between the morphologies and positions of the bends first identified by Brice (using aerial photographs taken in the 1920s and 1930s) in the 1960s and 1990s were used by Ayres to generate further data on bend geometry and migration. These dates and changes define the data and probability distributions for TP2 in the present study.

It follows that all the bends in the TP2 dataset were 30 to 40 years older at the beginning of that period of observation than they were at the beginning of TP1. Consequently, it must be the case that:

1. while some, perhaps many, of the entries in TP1 reflect the behaviour of bends during their period of initial slow development, none of the entries in TP2 reflect bends that are initially developing slowly because they were all more than 30 to 40 years old at the start of TP2.

2. while some entries in TP1 represent the behaviour of bends during their period of rapid growth and/or migration it is probable, given their older ages, that a much greater proportion of bends in TP2 are in that middle stage of the bend evolution life cycle;

3. bends with dimensionless radii <1.75 in the 1920s or 1930s (i.e. at the beginning of TP1), would have to persist in their termination stage for seven or eight decades in order to still exist at the end of TP2 in the 1990s (and so be included in the UoN-HRW database. This is only likely for bends on rivers with very slow rates of bend evolution. Conversely, bends with dimensionless radii <1.75 in the 1960s only have to persist for twenty to thirty years to still exist in the 1990s. This is possible for bends on much more active rivers.

Taking all of these observations concerning the range of data and the age of the bends together, it is possible to propose numerical and physical explanations for the differences between the curves for high probability levels in TP1 and TP2. Inspection of the data scatter in Figure 5.3 confirms that none of the data points for TP1 has a dimensionless migration rate higher than 0.26, while a number of points for TP2 exceed 0.26, with the highest recorded rate being significantly higher, at 0.37. This numerical fact accounts for the peaks in the curves for TP2 being higher than those for TP1.

The physical explanation for this outcome rests on consideration of the way that the data in the UoN-HRW database were collected. The fact that no new bends were added in TP2 means that *all* the bends are 30 to 40 years older in TP2 than they were in TP1, but the fact that *only* bends that persisted from the 1920s and 1930s to the 1990s are included would tend to exclude bends which were already mature at the beginning of TP1. All this makes it much more likely that bends would be in their middle period of evolution, which is characterised by rapid growth or migration, during TP2 compared to TP1 - explaining the higher peak values for migration rate in TP2.

The numerical explanation for the curves peaking at larger values of dimensionless bend radius in TP2 compared to TP1 is that long radius bends (with R/W values greater than about 7.5) have higher migration rates than those with similarly high R/W values in TP1. The physical explanation for this is that it would be expected because while many long radius bends in TP1 are

highly likely to have recently been initiated (and therefore be in their slow, initial growth stage), this is simply impossible during TP2 as all the bends were already at least 30 or 40 years old at the start of that period. These bends are likely to be in their period of rapid growth or migration despite their relatively long radius to width ratios, and it would be expected that they should display higher rates of migration. The effect of these higher rates on the shape of the probability curve is to drag the peak towards longer radius bends, explaining why the peaks of curves for TP2 are located to the right of those for TP1. Finally, numerical and physical explanations are needed for why the curves rise sharply for values of R/W less than about 1.75 in TP2, while they stay low for the equivalent values of the x-variable in the graph for TP1.

The numerical explanation for this is that data are sparse in this area of the graphs, making the shape of the curves for extremely high probabilities sensitive to the presence of a few very high values of dimensionless migration rate. The physical explanation for why some very high values are present in TP2 but not in TP1 stems from the fact only on quite stable rivers could have bends with very low R/W values in the the 1920s and 1930s that persisted until the 1990s. On more laterally active rivers, such bends would almost certainly be destroyed by a bend migrating from upstream – erasing them from the dateset. Conversely, bends on mobile rivers that have evolved to have R/W values less about 1.75 only have to persist for a further 30 to 40 years in order to be included in the dataset for TP2. It is known that very tight bends display erratic migrational behaviour that may include bursts of rapid shifting, and this explains why the curves for high probabilities of not being exceeded curve up steeply during TP2.

6.4 Probabilistic Analysis of Randomly Divided Data to Test the Impact of Sampling Variability

6.4.1 Justification for Randomly Dividing the BTP Dataset

In Section 6.3 of this chapter, the probabilistic analyses of bend migration were performed using pooled data set from Time Period 1 (TP1) and Time Period 2 (TP2) separately and it was demonstrated that pooling the data not only increased sample size but also made the dataset more comprehensive by widening the ranges of bend ages, types and evolutionary stages included

within it. These effects must increase the degree of confidence that can be placed in the results, as described in Section 6.3. However, in any empirical analysis changes related to random variability between samples of the same population are bound to lead to some variation in the results. However, if the between-sample variation is significant, this reduces confidence in the results because it reveals that they are sensitive to sampling errors.

It was, therefore, decided to test how sensitive the analysis and predictive method are to sampling variability, based on drawing pairs of random samples, each of 50% of the pooled data for both time periods (BTP) to examine whether differences in the probabilistic results were sufficiently large as to indicate that the method was not robust.

The relevant functions in the statistical software package, R were used to divide the pooled dataset (BTP) in half, with x-y pairs being randomly assigned to one half of the population or the other. Two experiments were performed. In the first experiment (Attempt 1), the resulting samples each have 1,128 values and are referred to as RD1 and RD2, respectively. Obviously, adding together RD1 and RD2 would reconstitute the pooled data set. In the second experiment (Attempt 2) the procedure was repeated, giving two more randomly determined sub-sets.

6.4.2 Probabilistic Analysis of the Two Pairs of Randomly Divided Data Sets (RD1 and RD2) and (R1 and R2)

The data distributions for the first pair of samples (RD1 and RD2) are shown in Figures 6.27 and 6.28. The data distributions for the second pair of samples (R1 and R2) are shown in Figures 6.29 and 6.30. The full statistical analysis (as performed in processing the data from pooled (BTP) – see Sections 5.3 to 5.6) and periodwise data sets (see Section 6.3**)** reported earlier) was applied to these samples to normalise the variables and generate probability curves.

In pre-processing the data in each sample, the x-variable (Rb/WbCr) was normalised using a common logarithmic transformation (for example, see Figures 6.31 to 6.34, for sample RD1), as was used for the BTP (see Figures 5.4 to 5.11). For the y-variable (MMA/WbCr/Y), normalisation was achieved using a power function with an exponent of 0.16 (for example, see Figures 6.35 to 6.38, for sample RD1), which was also similar to the transformation used for the BTP dataset.

Proability curves for the dimensionleass average annual migration rate (MMA12/W1Cr/Y) were produced for probabilities ranging from 1% to 99% to allow examination of the similarities and differences between their shapes for RD1 and RD2, R1 and R2, and BTP (Figures 6.39 to 6.43).

To facilitate comparison between the samples and the population, the curves for RD1 and RD2, R1 and R2 and BTP are plotted for selected probabilities of 5%, 25%, 50%, 75%, 90%, 95% and 99% in Figures 6.44 to 6.50.

6.4.3 Discussion

The first point to note is that there are marked differences in the ranges of the data between the random samples. For example, for RD1, values of the x-variable (dimensionless bend radius) range from 0.55 to 12.26 with the associated y-values (dimensionless bend migration rate) varying between 0.0012 and 0.37. The wide spread of data in RD1 contrasts with the relative narrow ranges for RD2, of 0.66 to 11.34 and 0.0004 to 0.33 for the x and y-variables, respectively.

Since the probability curves for each sample are derived from the data in that sample (through empirical density estimation), it follows that the range of the data and the distribution of the few points at the lower and upper bounds of the data ranges may impart considerable variation to the probability curves, especially for extreme values.

Reflecting this, while the five curves representing a 25% probability of the indicated dimensionless migration rate (Figure 6.45) are almost indistinguishable for mid-range values of the x-variable, they can be differentiated for very low (Rb/WbCr < 1) and very high ((Rb/WbCr > 8) values of dimensionless bend curvature. This is most probably explained by sparcity of data for bends with dimensionless curvatures less than 1 and greater than 8. However, between these boundaries, where the data are denser, the degree of inter-sample variability is clearly negligible.

In fact, these curves are almost horizontal, indicating that bend curvature has very little influence over migration rate for this low probability of exceedence. It may, therefore, be concluded from this graph and the exploratory analyses that underpin it, that:

1. there is only a 25% chance that the bankline at the outer bank in any bend in an alluvial river will shift at a rate slower than 2% of the channel width per annum, regardless of its planform geometry, and
2. this finding is insensitive to both sample size and sampling variability.

Similar conclusions can be drawn from the curves representing the median (50%) rate of bend migration (Figure 6.46), although median migration rates rate for longer bends (about 3% of the channel width per annum) are more noticeably higher than those for tighter bends (about 2.5% per annum).

In Figure 6.47, the shape of the curves for a 75% probability of not being exceeded are markedly different to those for 25 and 50% probabilities in that the rate of dimensionless bend migration is now more clearly a function of the dimensionless bend curvature.

For very tight bends, between-sample variation is now considerable, with strong divergence between the samples in each pair (that is: RD1 versus RD2, and R1 versus R2). The pattern is the same in each case, with the curves for RD1 and R1 both turning down, while those for RD2 and R2 rise steeply for values of Rb/WbCr less than about 1.5. However, the spread of the curves is greater for the R samples than it is for the RD pair. This indicates serious inter-sample variability that results firstly from the fact that there are very few points for very tight bends with Rb/WbCr < 1.5 and, secondly, because the bends that do fall into this range display widely varying rates of dimensionless migration.

The 75% curves for long radius bends (Rb/WbCr > 8) also diverge, but the grouping of the samples is different. At this end of the distribution the curves for RD1 and R2 plot higher, while it is those for RD2 and R1 are lower. This suggests that inter-sample variability is not systematic because the sense and relation of inter-sample differences and similarities varies between the upper and lower extremes of the distributions, rather than particular samples being ‘high’, ‘low’ or similar to one another across the range of dimension radii in some consistent fashion. The band of inter-sample variability is widest for Rb/WbCr > 10.

For dimensionless radii in the range 1.5 < Rb/WbCr < 8, the sample curves are very similar to one another and closely follow the shape of the probability curve for the BTP. It may be concluded that the method is robust in predicting that values of dimensionless bend migration rate with a 75% probability of not being exceeded that peak at about 7% of the channel width per annum for values of Rb/WbCr between around 5 and 7.

The shapes and relative positions of the curves for a 90% probability appear broadly similar to those for 75% (Figure 6.48), though differences between the curves due to inter-sample variability are more extreme. For example, for Rb/WbCr < 1.5, the curves for RD1 and R2 indicate that the dimensionless migration rate increases rapidly as bend radius shortens, while the curves for RD2 and R1 suggest the opposite. This casts doubt on the reliability of the analysis for very tight, short radius bends. That said, a notable advantage of the larger, BTP dataset (on which the predictive method developed in Chapter 5 depends) is that it plots close to the upper bound curves for RD1 and R2. This makes the rates of migration predicted using it conservative, in that the uncertainty introduced by sample variability is on the safe side. That is, compared to smaller, sub-samples its predictions are more likely to over-estimate migration rate more than under-estimate it.

For 1.5 < Rb/WbCr < 8, the curves in Figure 6.48 are similar in shape and position on the graph. Consequently, even at Rb/WbCr = 8, variability between the dimensionless migration rate predicted based on the BTP dataset (about 10.5% of the channel width per annum) and those indicated by the RD1 and RD2 pair of random samples is only +/- 1% of the channel width – which is probably acceptable as an error margin given the natural variability inherent to the morphologies and positions of alluvial streams.

However, the curves diverge markedly as dimension bend radius increases for longer radius bends (RB/WbCr > 8), due to the sparcity of data in this range and this leads to the conclusion that, at a 90% probability of not being exceeded, the predictive method becomes unreliable once the dimensionless bend radius exceeds about 10.

The curves for 95% probability are shown in Figure 6.49. Once again, the reliable range for prediction of the dimensionless migration rate extends between Rb/WbCr values of around 1.5 and 8. The peak annual migration rate is approximately 15% of the channel width and, as before, this is associated with values of the dimensionless radius between 5 and 7.

At this extremely high level of probability, the sensitivity of the analysis to sample variability is so high that the curves diverge widely for both low and high values of Rb/WbCr. This might effectively preclude using the method to make relaiable predictions of bend migration for both very tight and very long radius bends.

The same is also true for the 99% probability graph (Figure 6.50), the curves for which are similar to those for 90 and 95%, but for which between sample differences are even more marked. The peak migration rate within the safe operating range for the method is around 25% of the channel width per annum, which is a very rapid rate indeed. At Rb/WbCr = 8, the spread of the curves is 20 to 25%, while at Rb/WbCr = 1, it is 17.5 to 22.5%. These band widths are at the limit of what might be acceptable in terms of error bands on an extreme (99%) migration rate prediction.

The general conclusions that can be drawn from this exploratory analysis of sampling variability are that:

1. dimensionless bend migration rates with probabilities of 50% or less are practically independent of the dimensionless bend radius;
2. between values of the dimensionless bend radius between 1.5 and 8, the forms and positions of the curves appear to be insensitive to sampling variability, at least up to probabilities of 90 or 95%;
3. divergence of the curves for values of dimensionless curvature less than about 1.5 or greater than about 8 means that the predictive method is potentially unreliable in these ranges.

4. The curves for the BTP data set fall within the error band defined by sampling variability though for the short radius bends (Rb/WbCr < 1.5) they tend to lie at the upper bound of the spread. From this it may be concluded that, even allowing for the slight weakening effects of some pseudoreplication, pooling the data has improved the reliability of the predictive method by putting most of the sampling error on the safe side.

5. The BTP curves clearly illustrate that the predictive approach developed in Chapter 5 is as robust as possible given that natural variability in the behaviour of alluvial, meandering rivers and the paucity of bends with very long and very short dimensionless curvatures.

6. On the basis of bullet points from 1 to 5 above, the overall conclusion is that the probabilistic approach developed in this thesis probably represents an improvement over deterministic methods of prediction that do not and cannot account for uncertainty, sampling error and natural variability in the fluvial system.

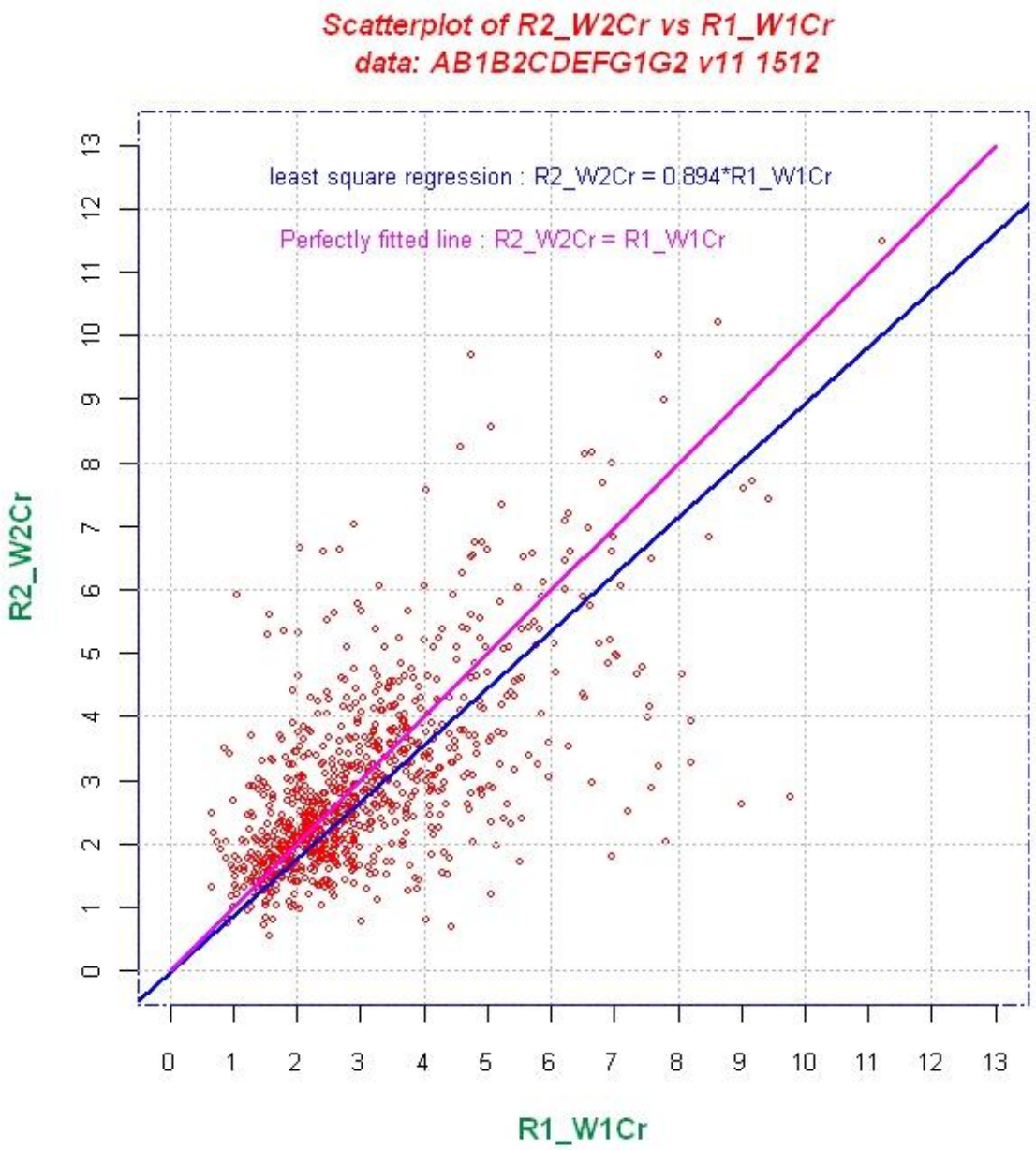

Figure 6.1: Scatter plot of R2/W2Cr versus R1/W1Cr with line of perfect agreement and least squares regression line (with intercept set to zero).

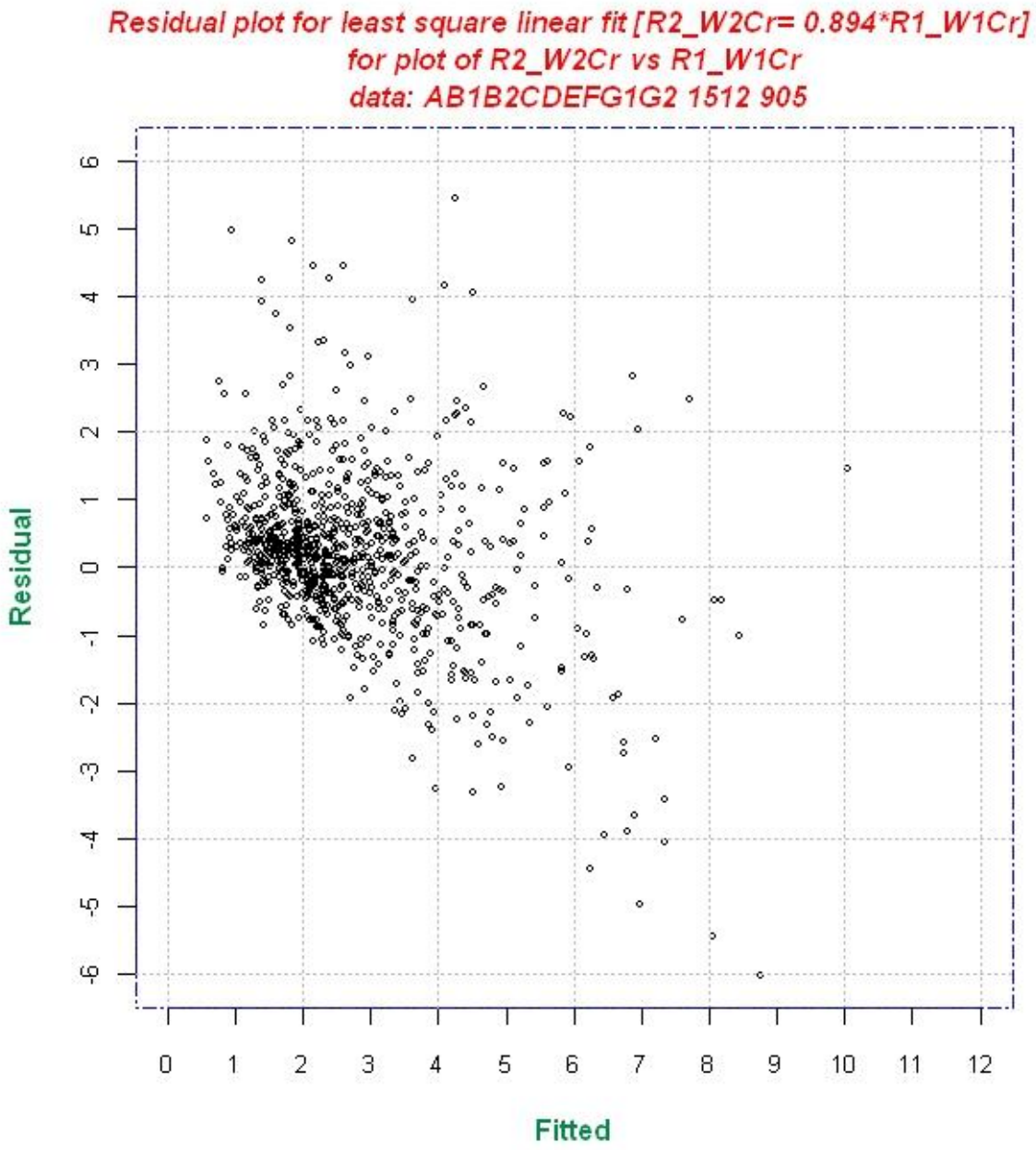

Figure 6.2: Analysis of residuals for the least squares linear regression line plotted in Figure 6.1 (R2/W2Cr = 0.894*R1/W1Cr). Residuals are plotted as a function of fitted values. Distribution illustrates that variance is not constant.

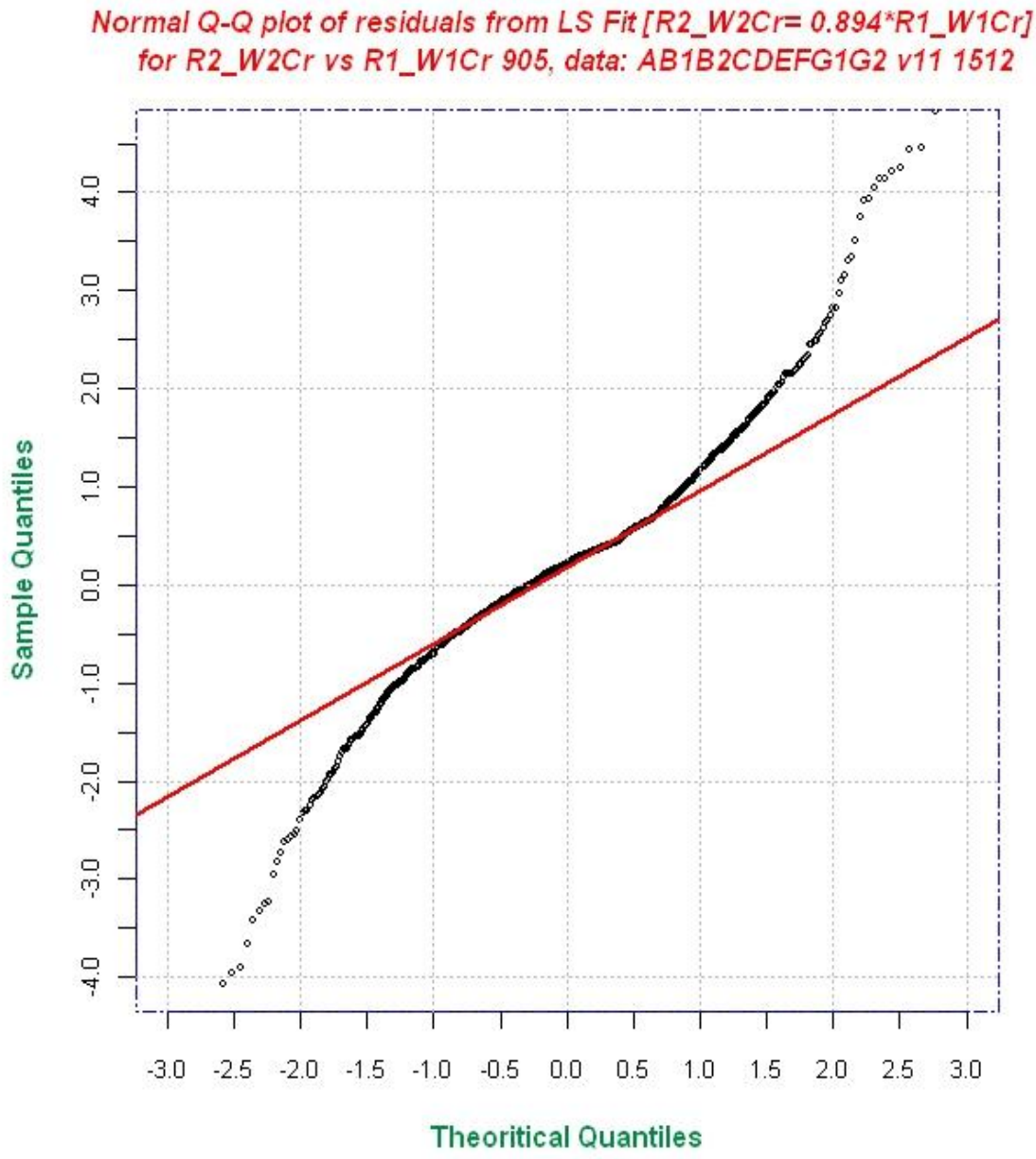

Figure 6.3: Normal QQ plot of residuals for the least squares linear regression line plotted in Figure 6.1 (R2/W2Cr = 0.894*R1/W1Cr). Distribution shows that residuals are not normally distributed.

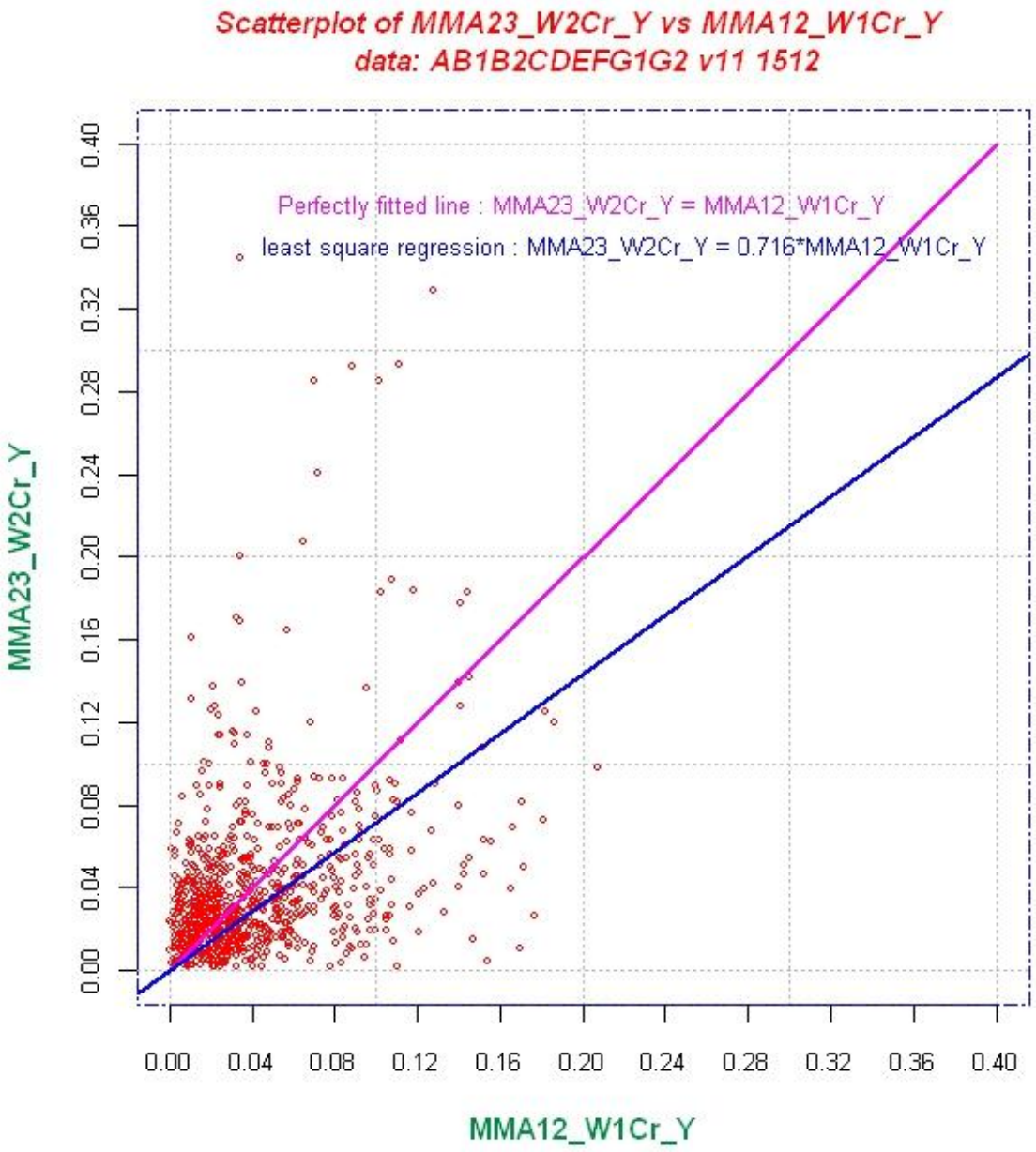

Figure 6.4: Scatter plot of MMA23/W2Cr/Y versus MMA12/W1Cr/Y with line of perfect agreement and least squares regression line (with intercept set to zero).

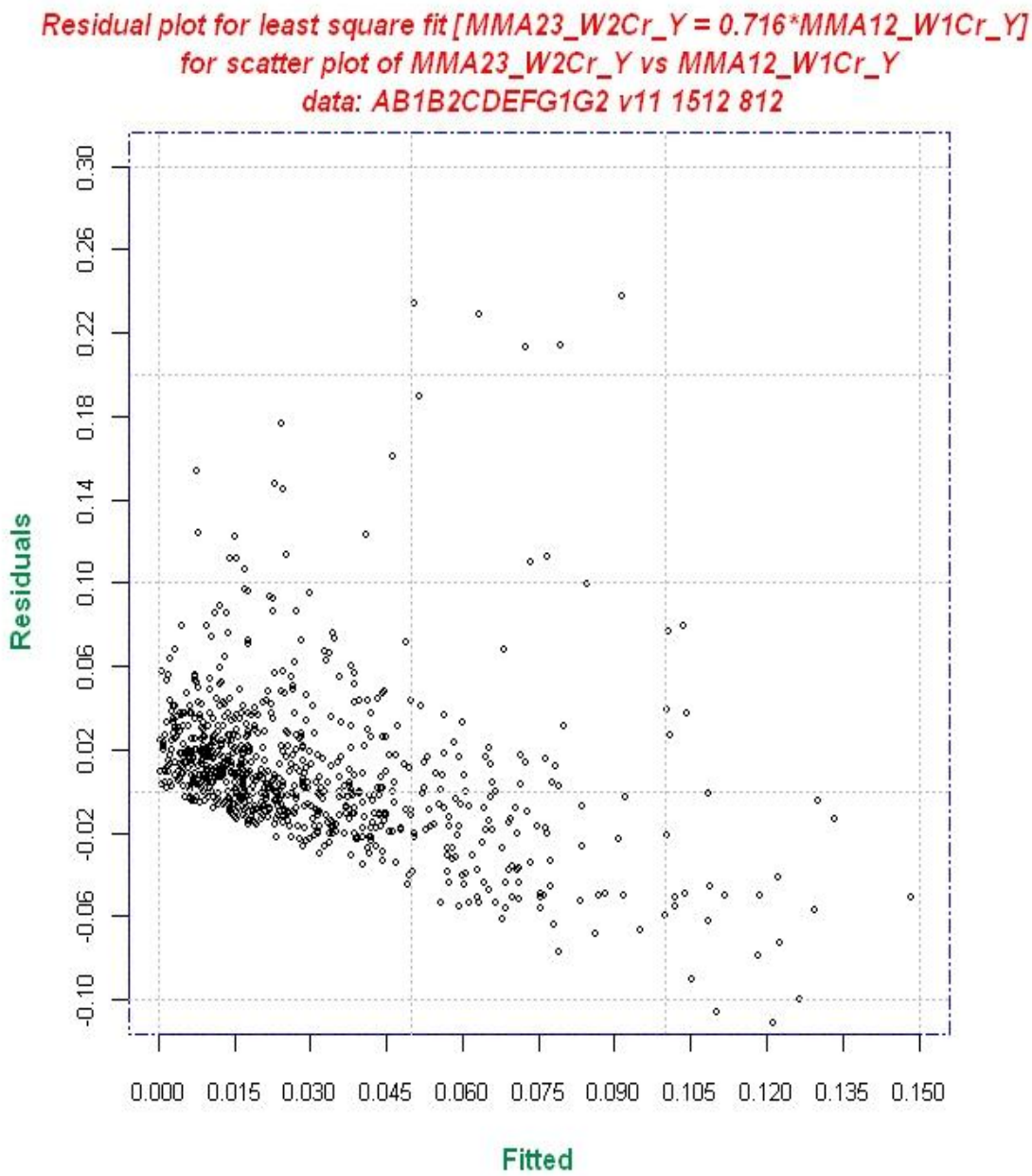

Figure 6.5: Analysis of residuals for the least squares linear regression line plotted in Figure 6.4: MMA23/W2Cr/Y = 0.716*RMMA12/W1Cr/Y). Residuals are plotted as a function of fitted values. Distribution shows that variance is not constant.

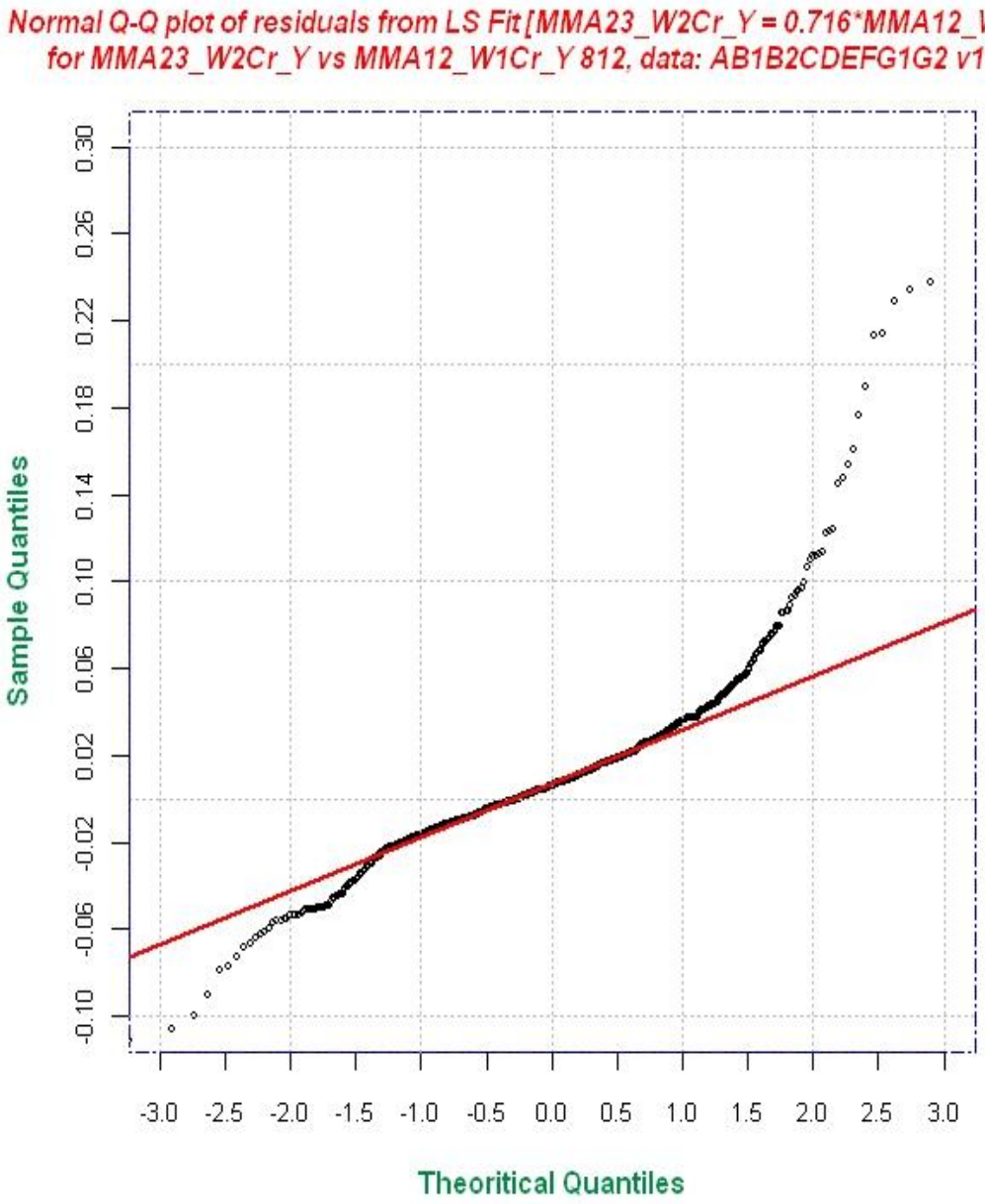

Figure 6.6: Normal QQ plot of residuals for the least squares linear regression line plotted in Figure 6.4: MMA23/W2Cr/Y = 0.716*RMMA12/W1Cr/Y). Results show that residuals are not normally distributed.

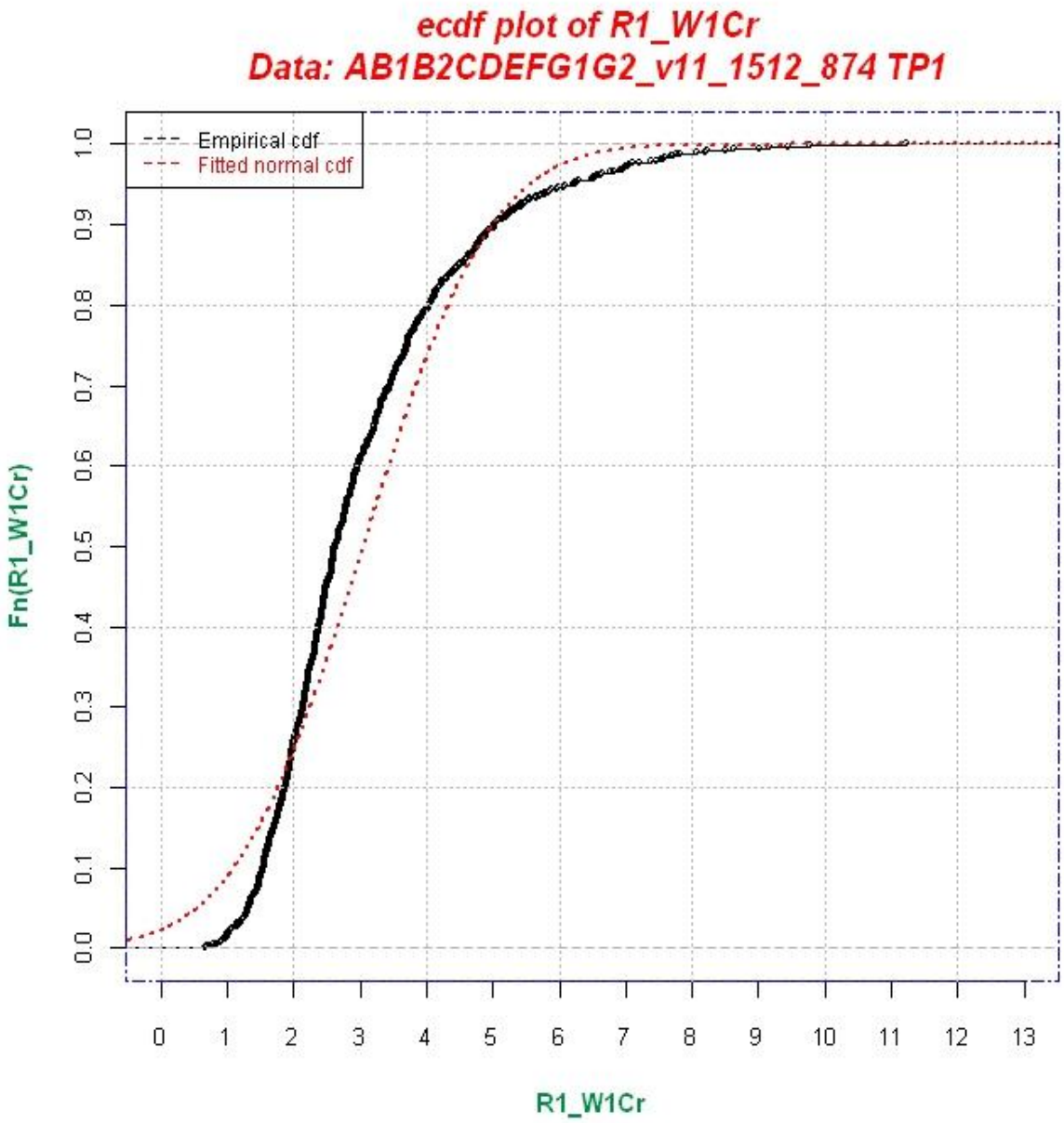

Figure 6.7: Empirical cumulative probability and fitted normal distributions for R1/W1Cr (ratio of outer bank radius of curvature to river channel width at the crossing at Time 1).

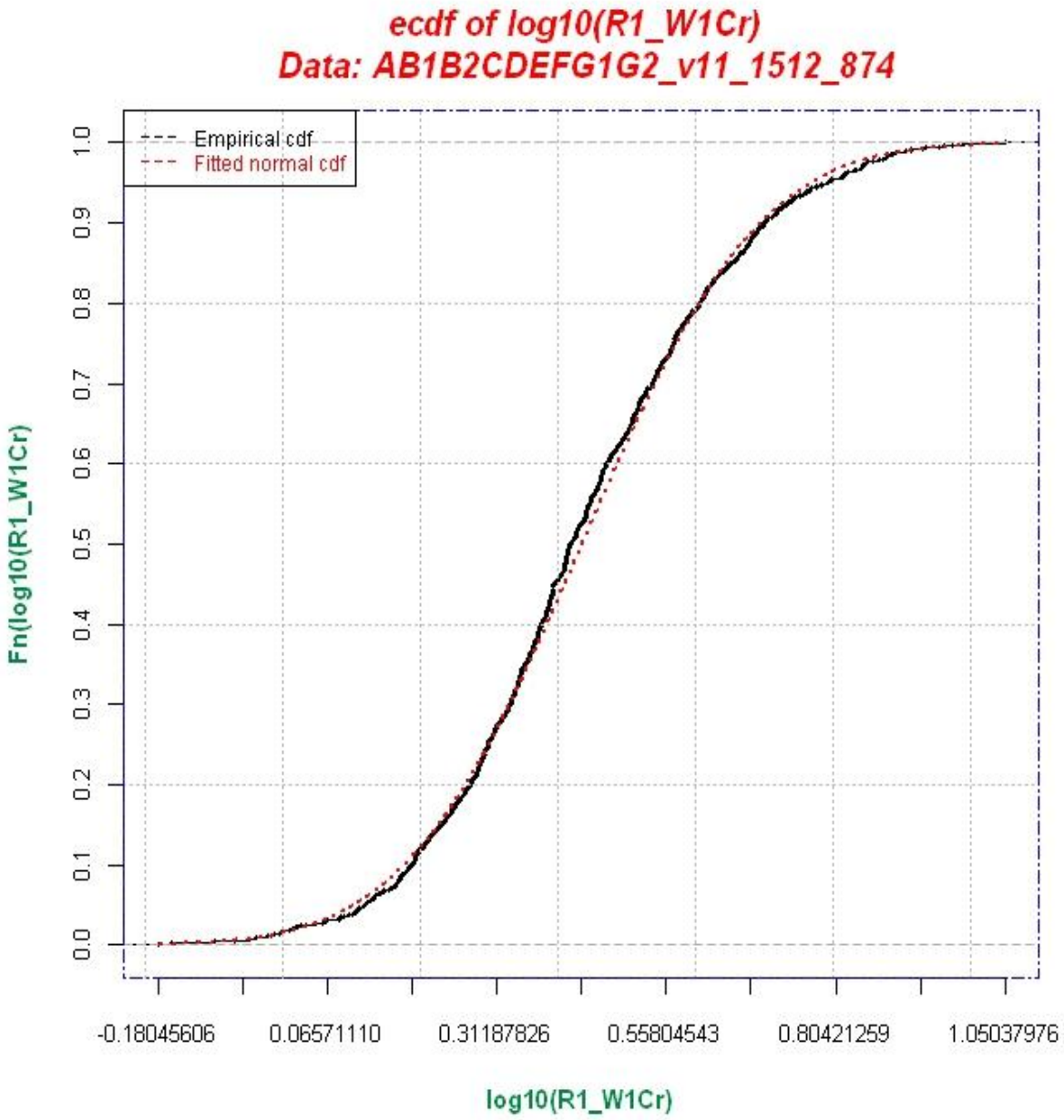

Figure 6.8: Empirical cumulative probability and fitted normal distributions for a logarithmic transformation of R1/W1Cr.

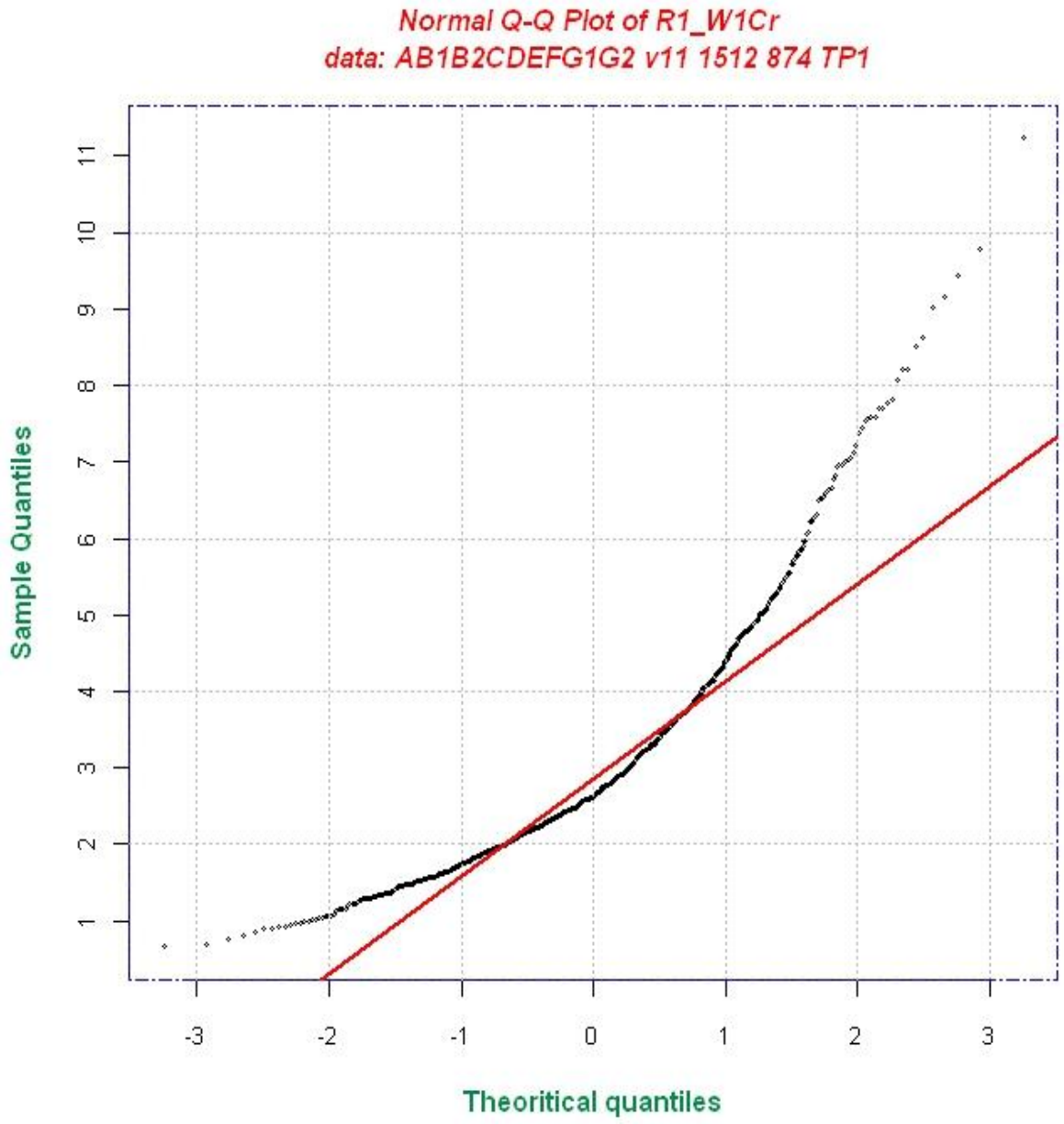

Figure 6.9: Normal probability plot for R1/W1Cr.

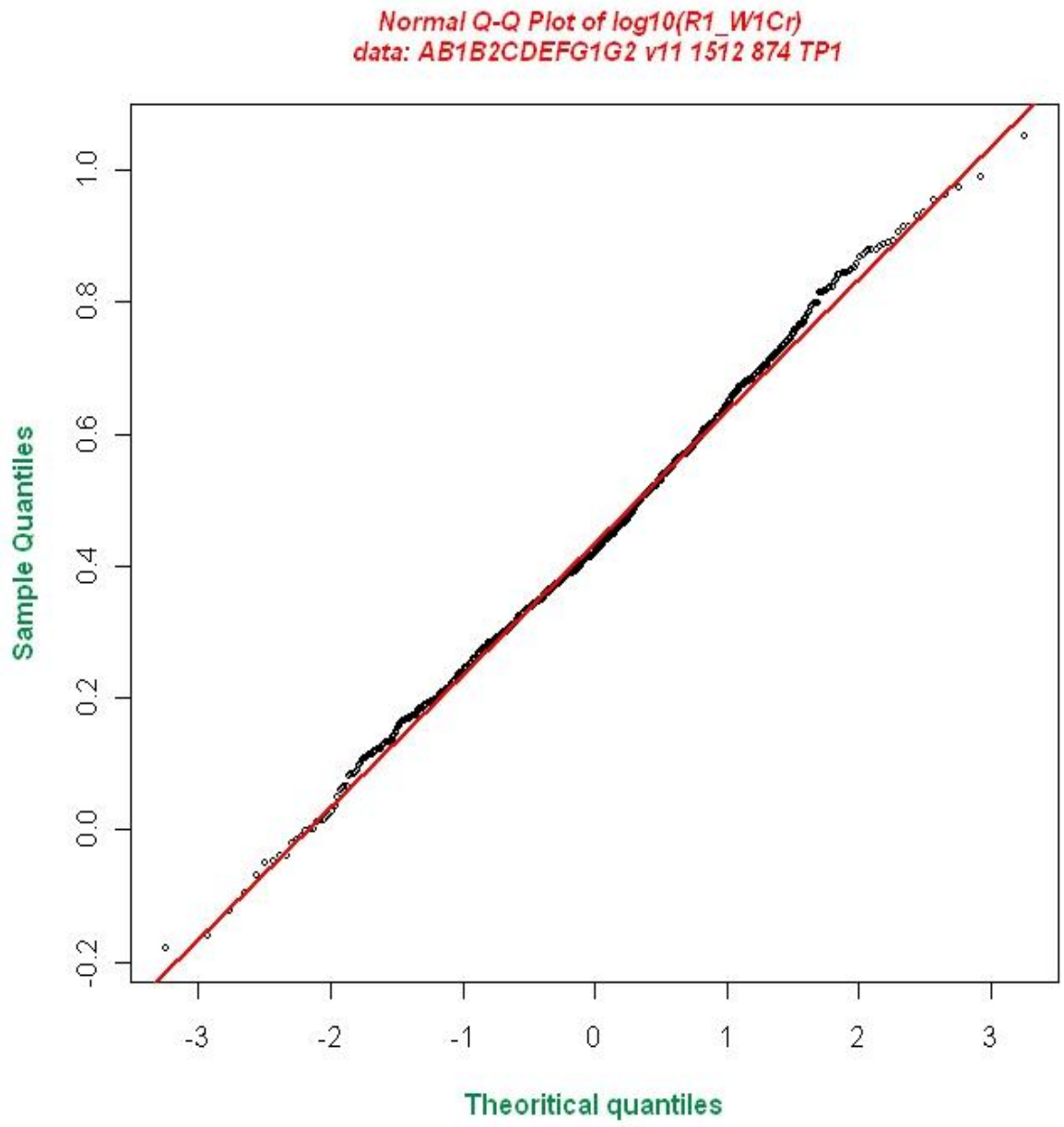

Figure 6.10: Normal probability plot for a logarithmic transform of R1/W1Cr.

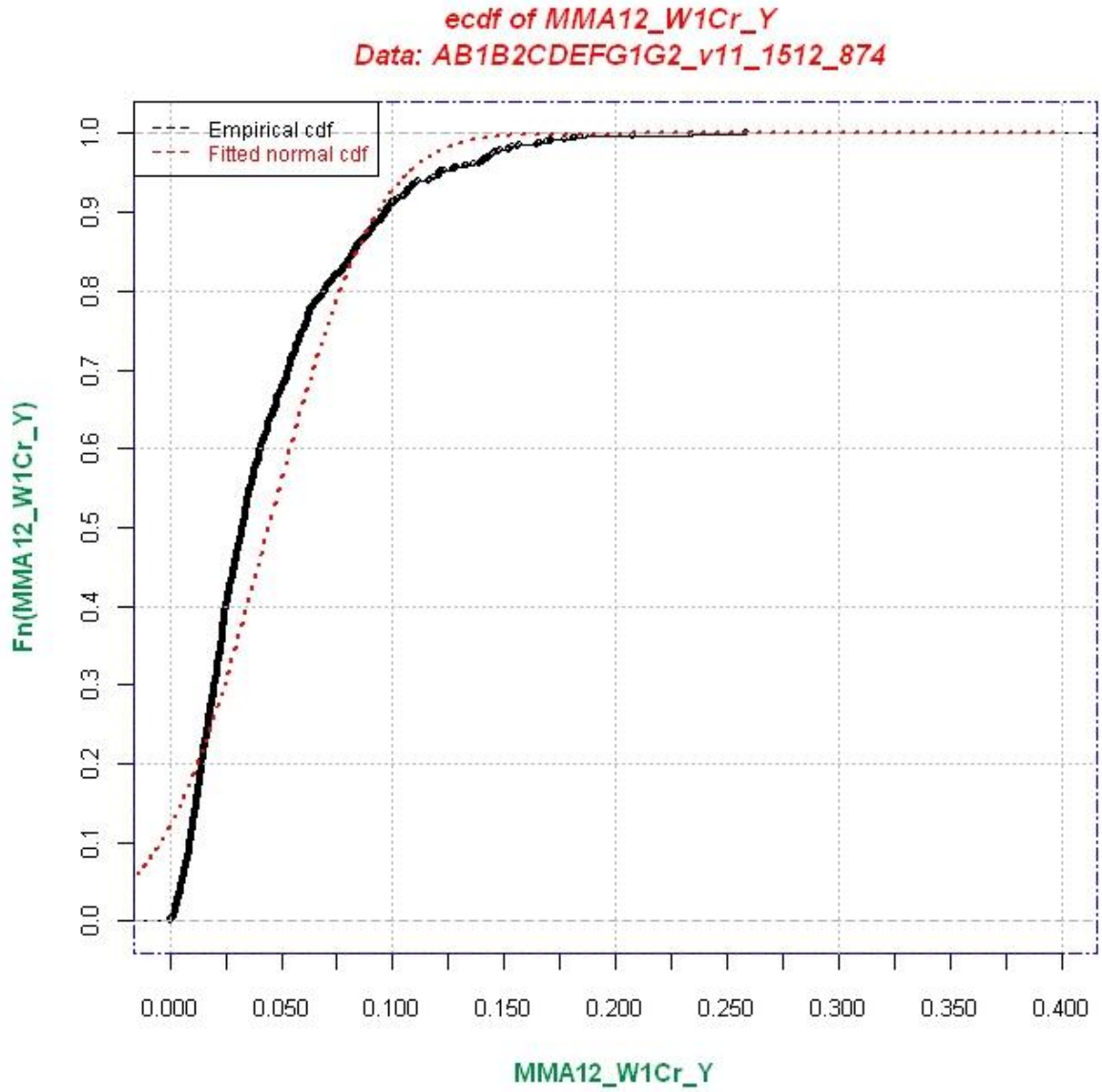

Figure 6.11: Empirical cumulative probability and fitted normal probability distributions for MMA12/W1Cr/Y (dimensionless average annual migration at the bend apex during Time Period 1).

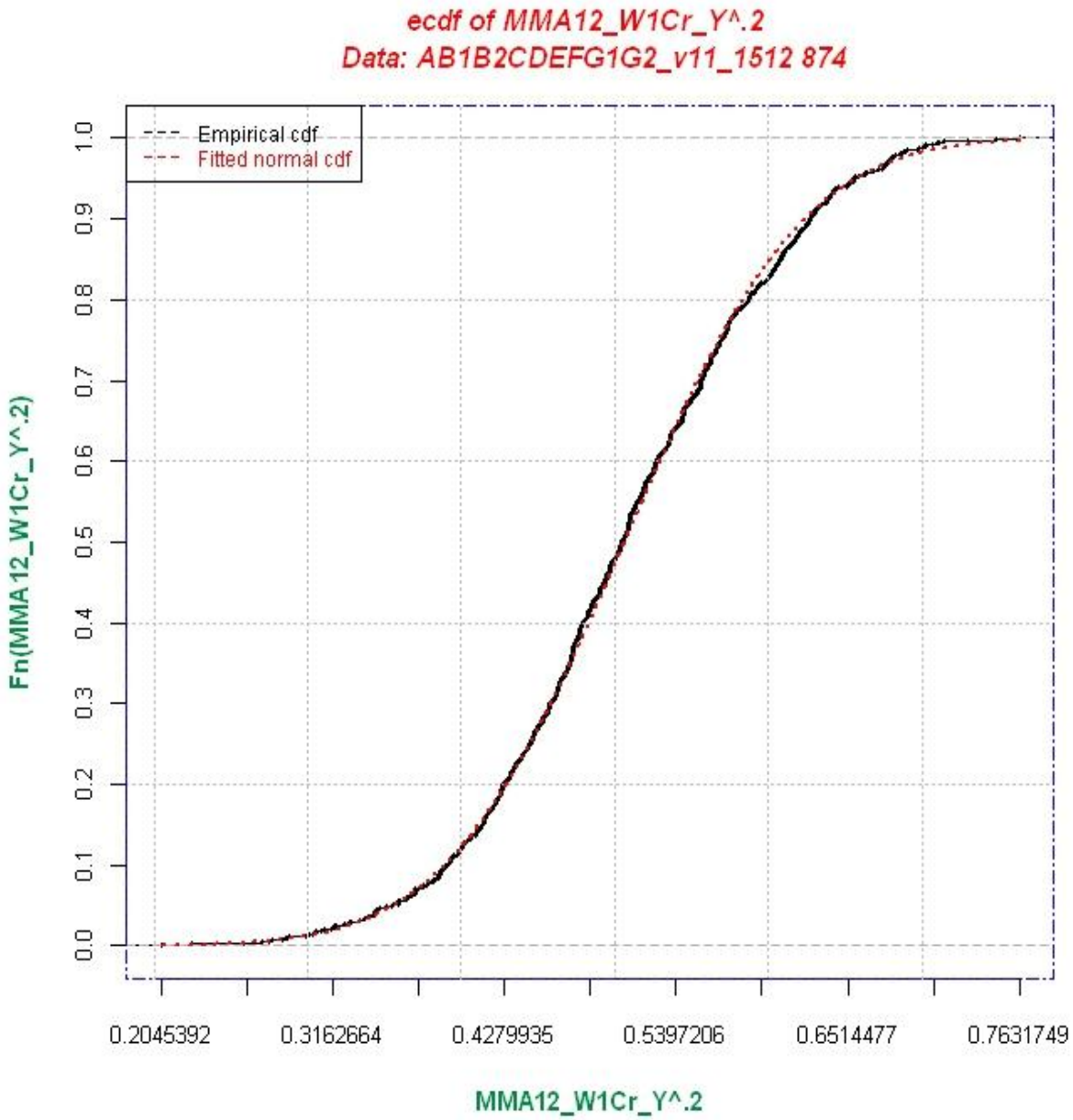

Figure 6.12: Empirical cumulative probability and fitted normal probability distributions for a power transformation of the dimensionless average annual migration at the bend apex during Time Period 1 ((MMA12/W1Cr/Y)^0.2).

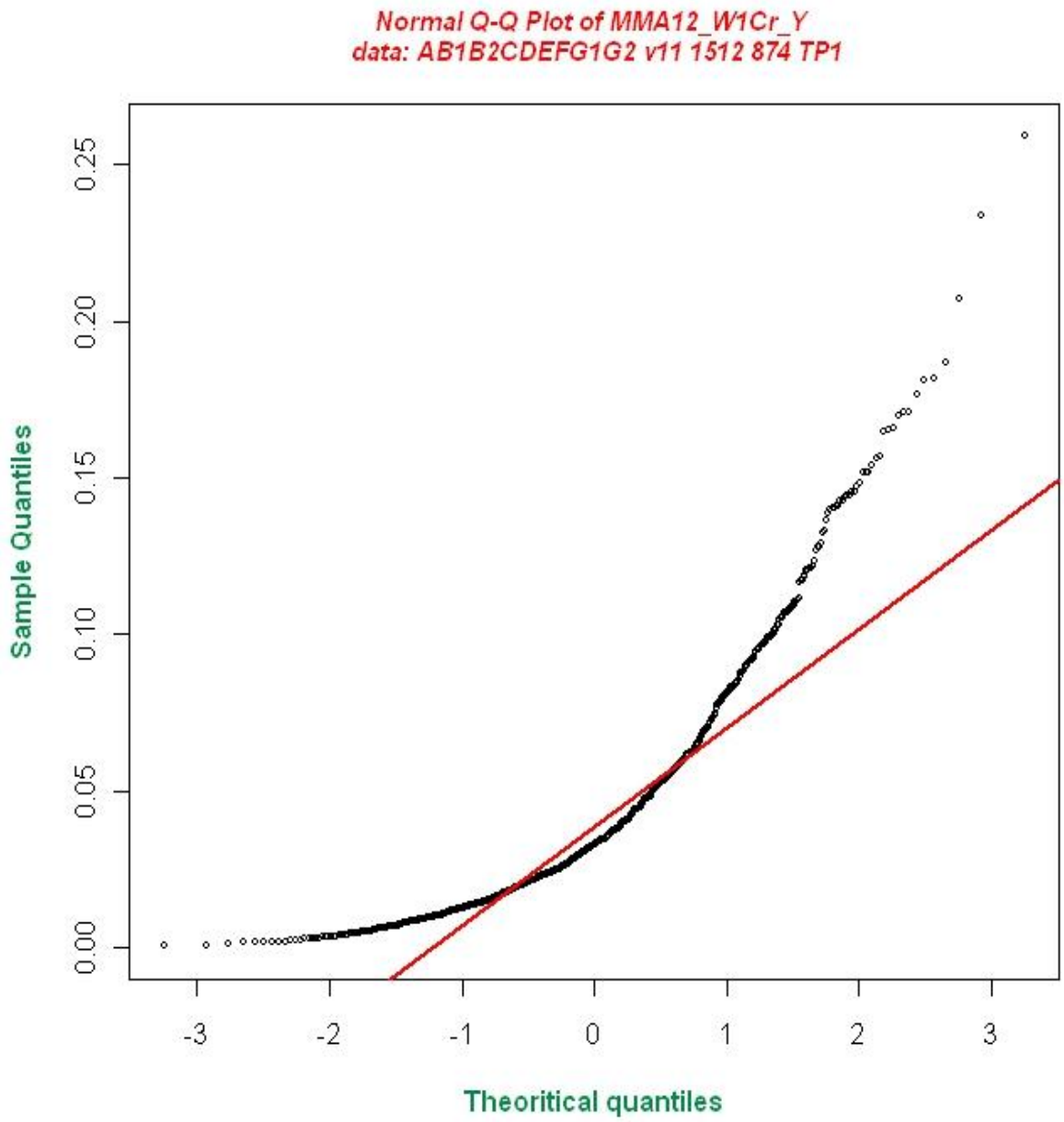

Figure 6.13: Normal probability plot for MMA12/W1Cr/Y.

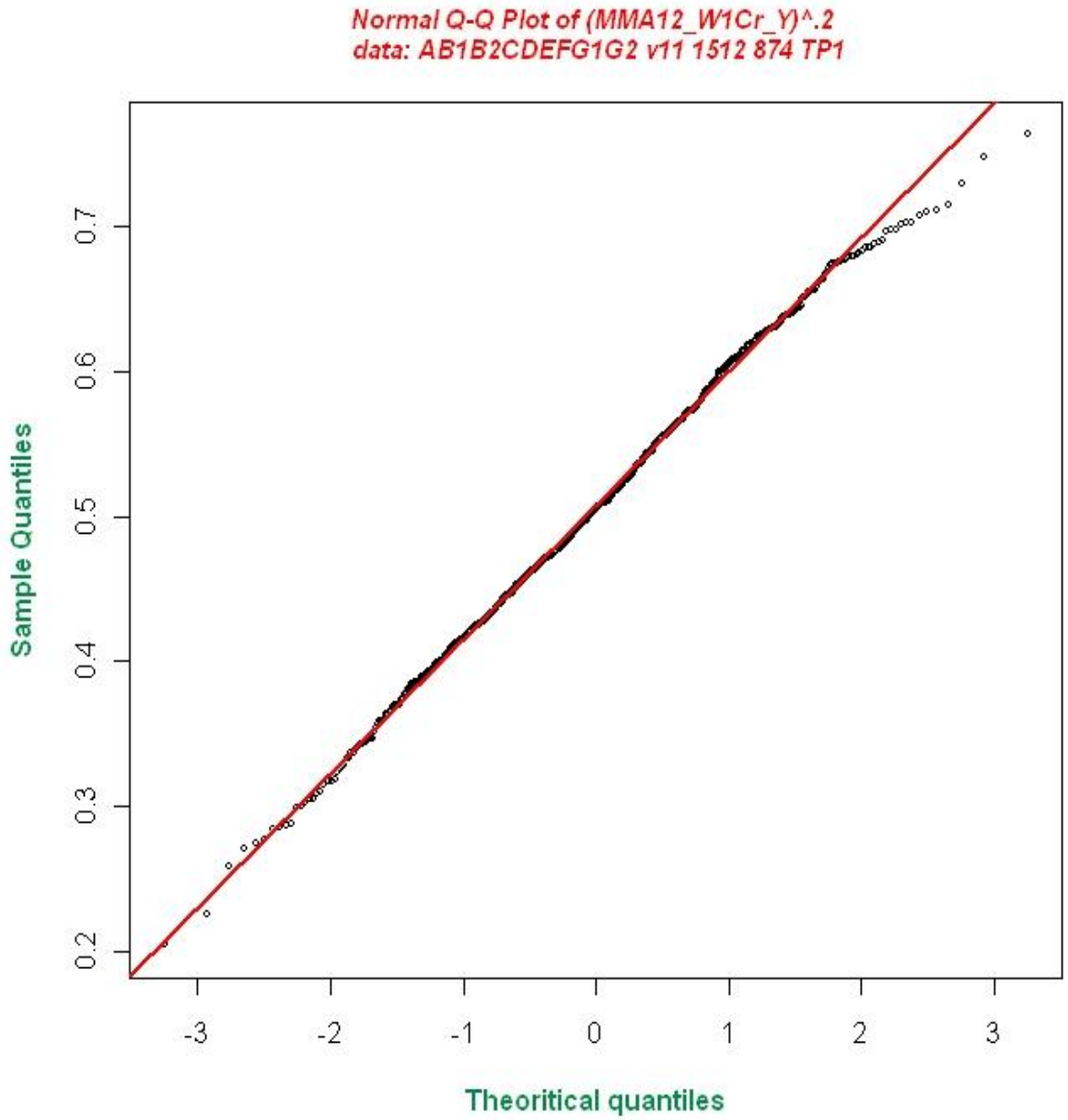

Figure 6.14: Normal probability plot for the power transformed dimensionless average annual migration at the bend apex during Time Period 1 ((MMA12/W1Cr/Y)^0.2).

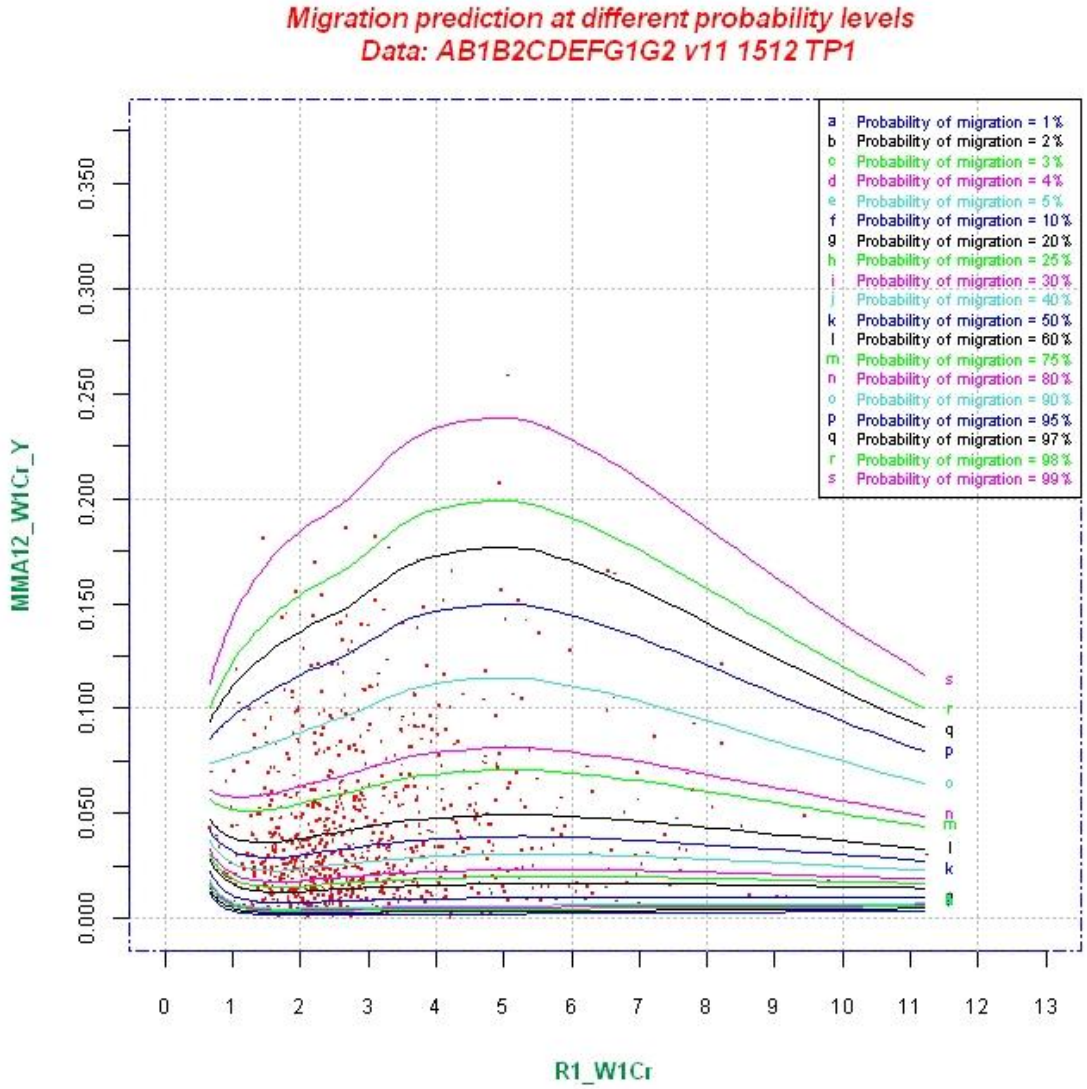

Figure 6.15: Probability curves for average annual migration rate during Time Period 1.

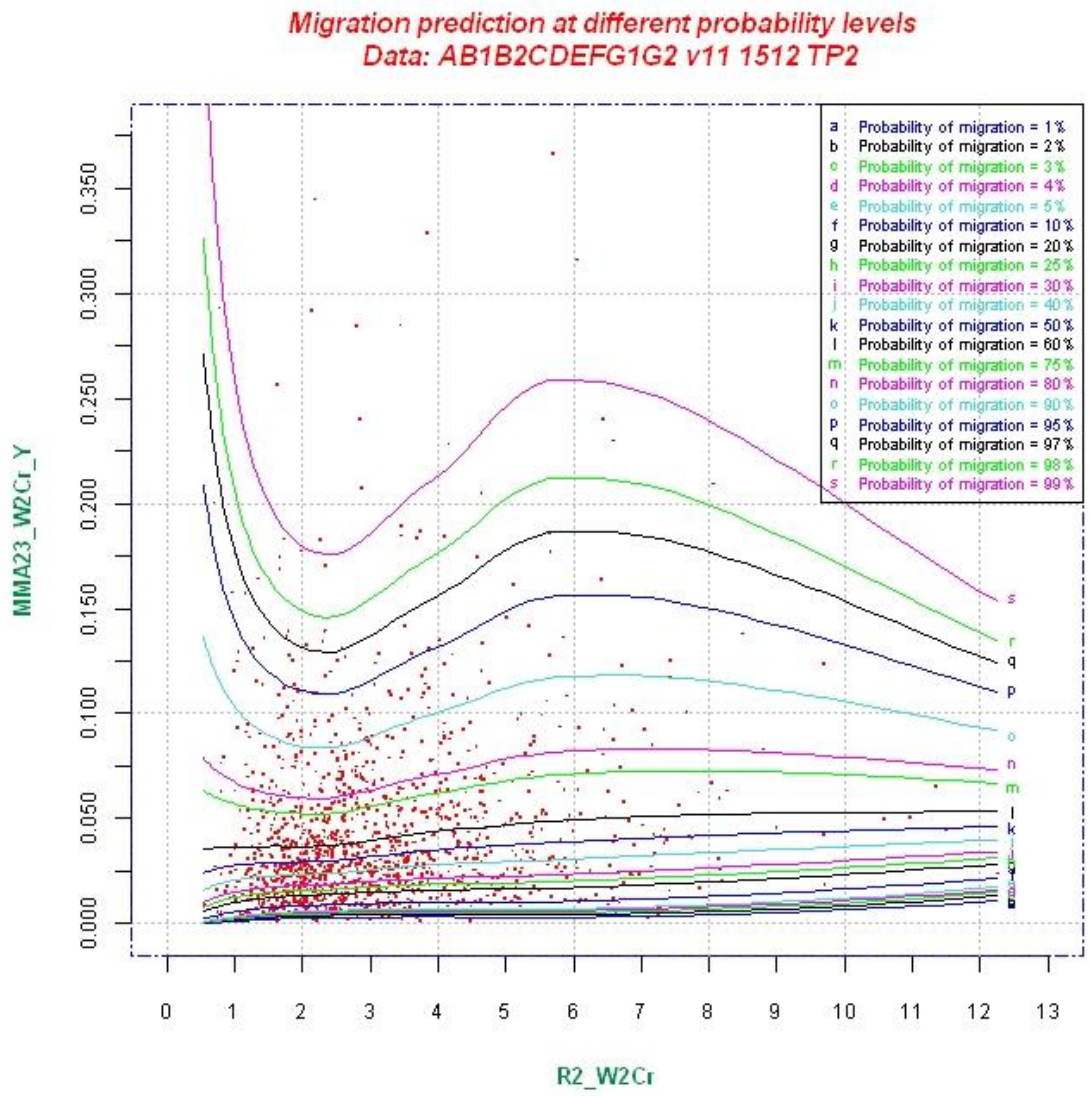

Figure 6.16: Probability curves for average annual migration rate during Time Period 2.

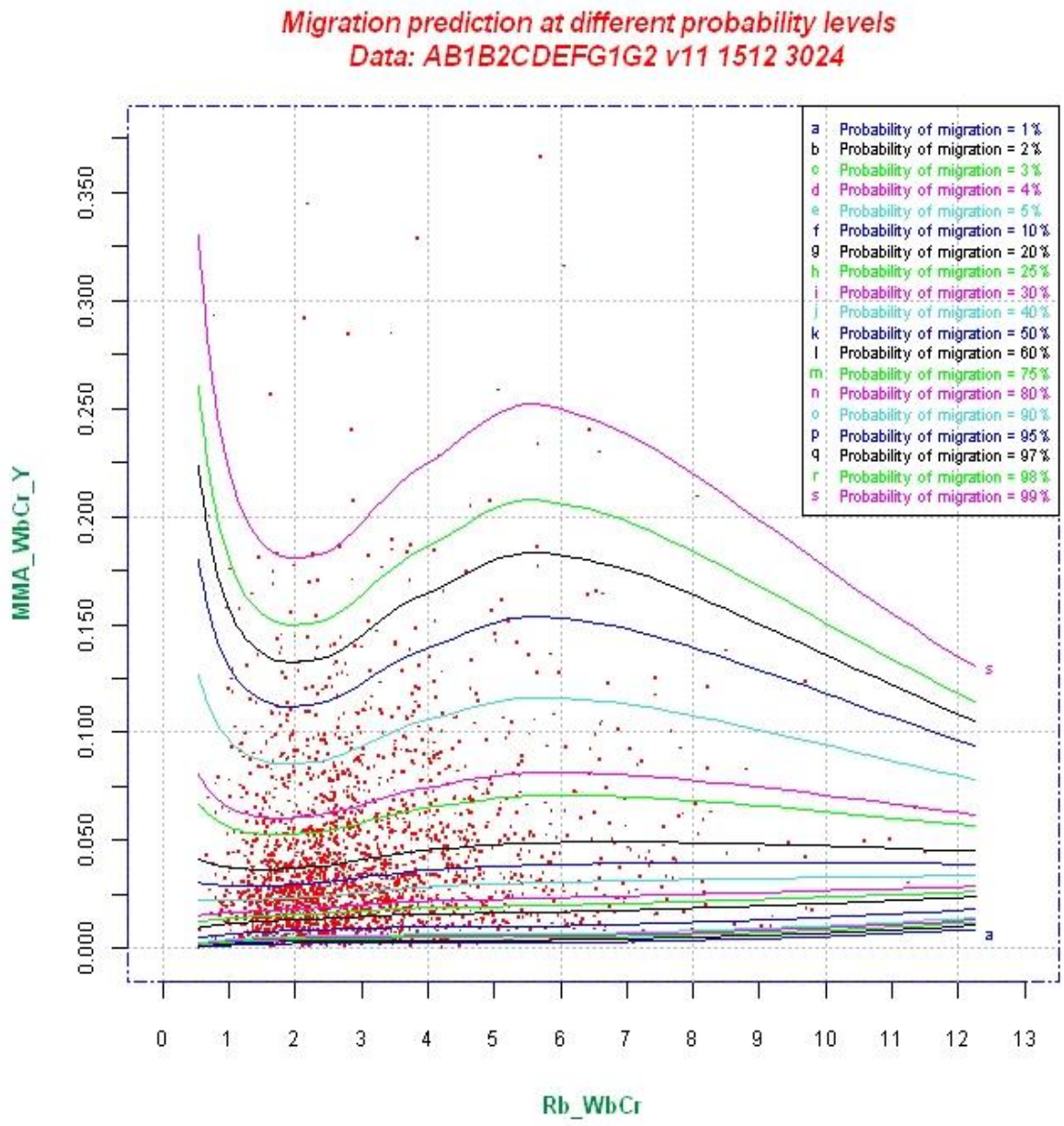

Figure 6.17: Probability curves for average annual migration rate based on pooling data from both time periods.

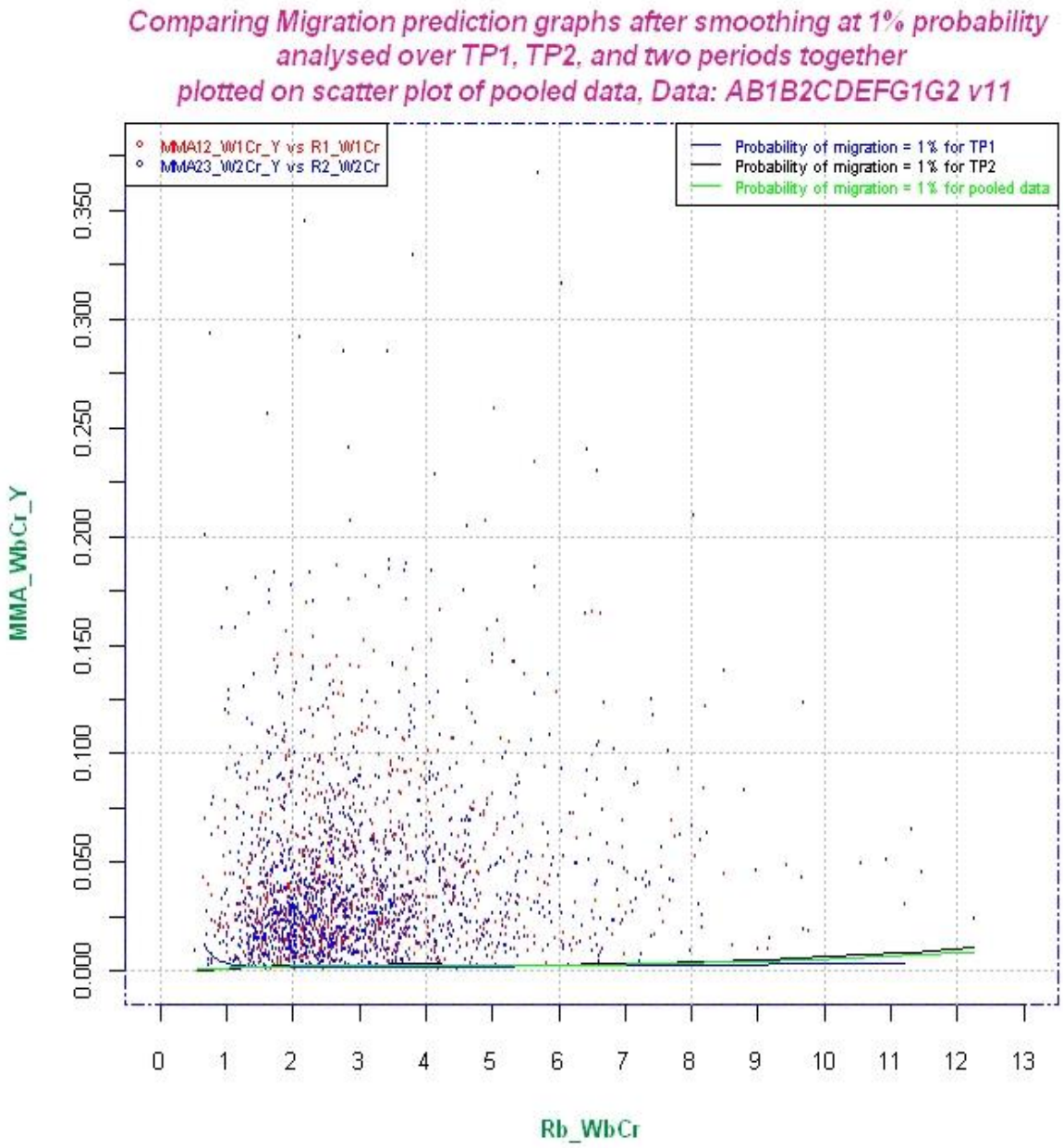

Figure 6.18: Comparison of smoothed probability curves at the 1% probability level obtained from analysis of data for Time Period 1, Time Period 2 and Pooled Data for both time periods.

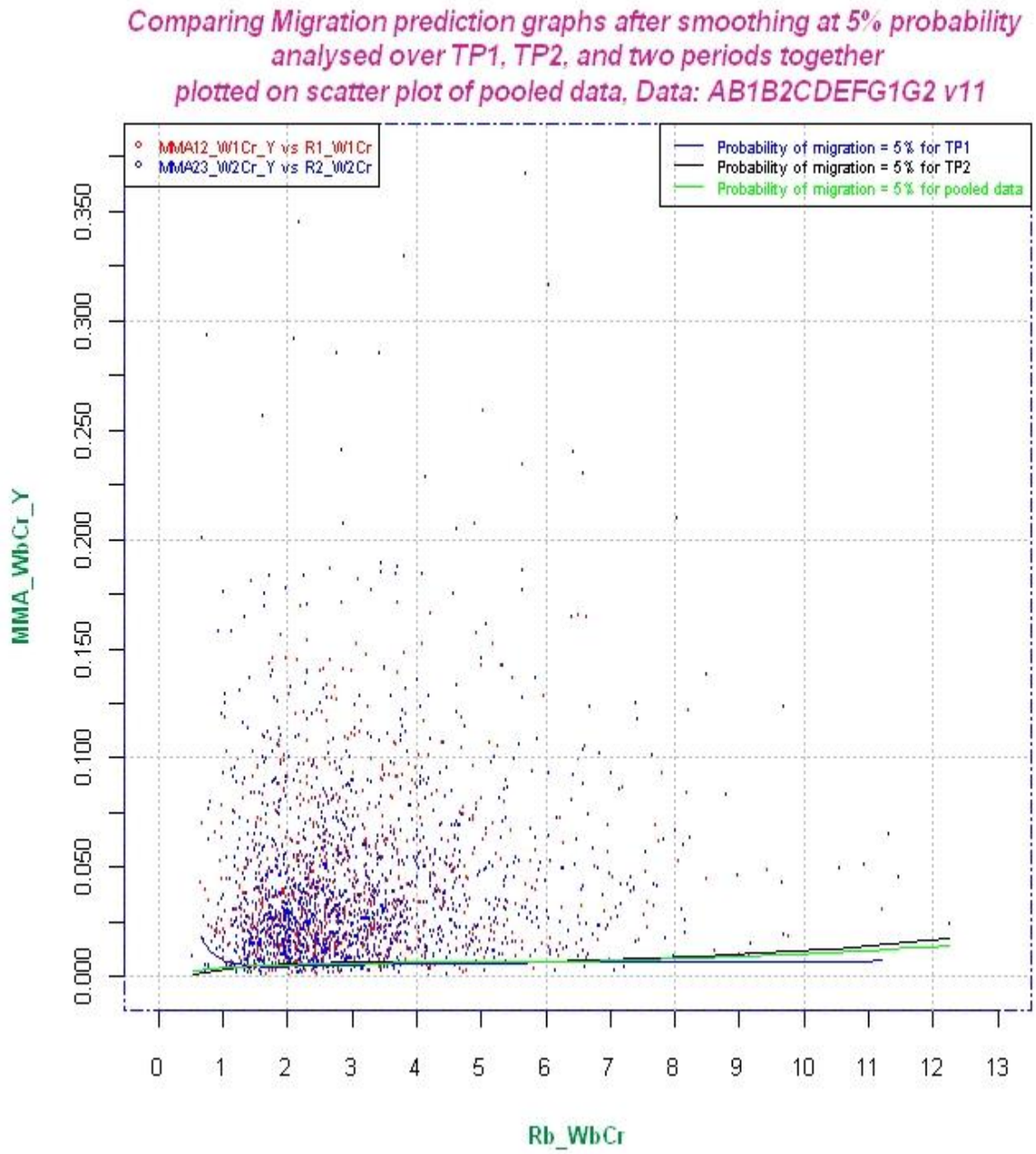

Figure 6.19: Comparison of smoothed probability curves at the 5% probability level obtained from analysis of data for time period 1, time period 2 and pooled data for both time periods.

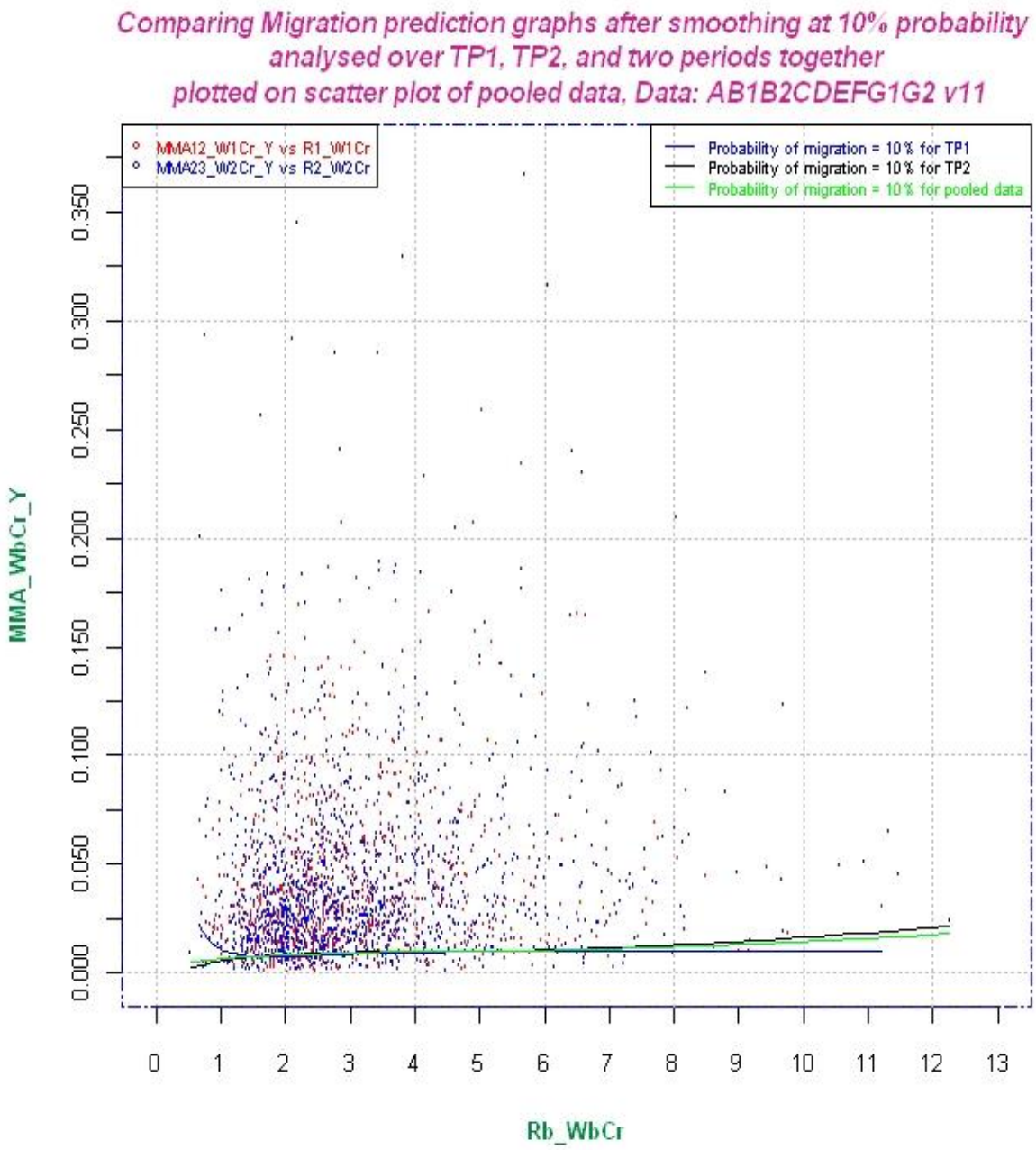

Figure 6.20: Comparison of smoothed probability curves at the 10% probability level obtained from analysis of data for time period 1, time period 2 and pooled data for both time periods.

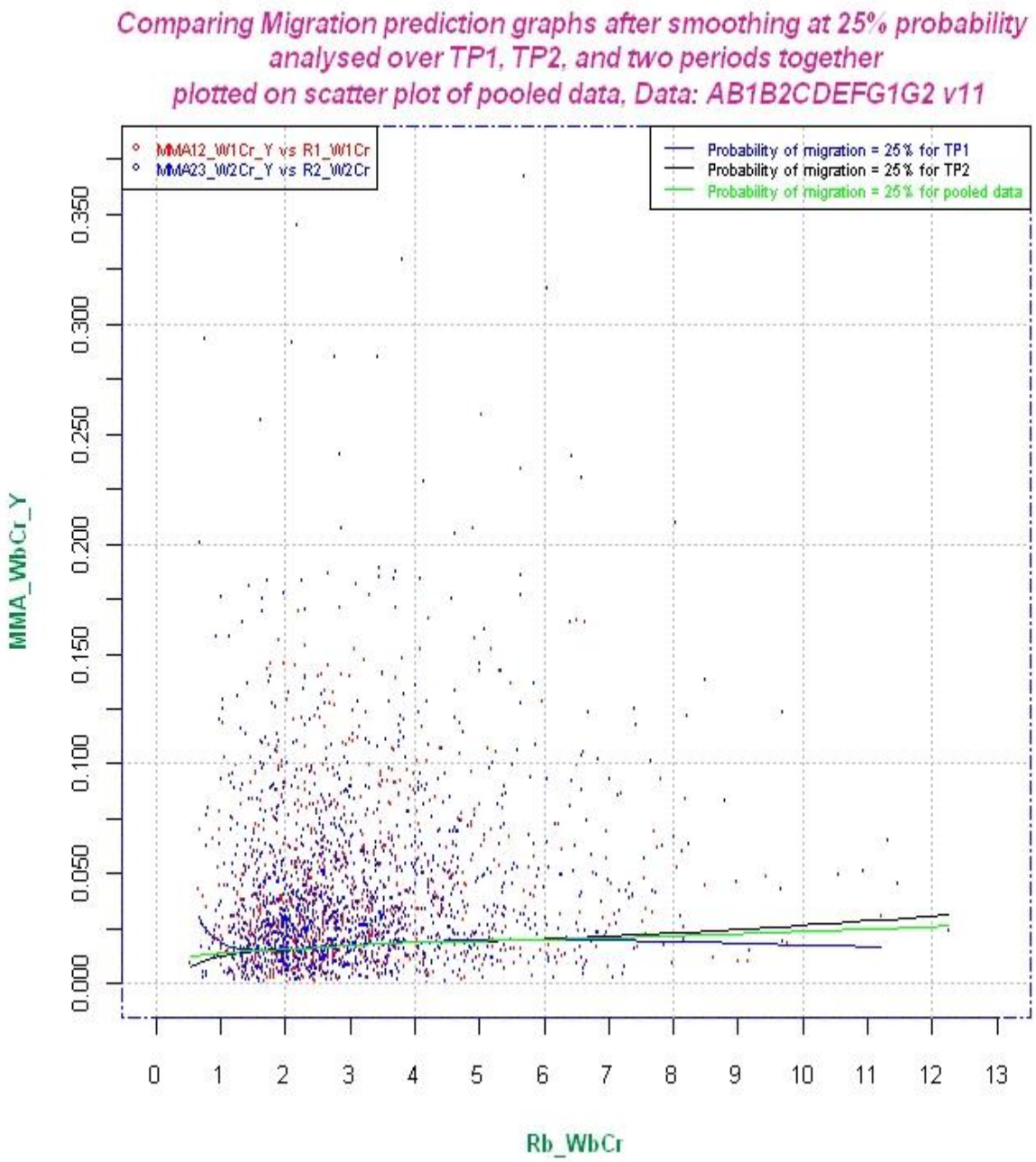

Figure 6.21: Comparison of smoothed probability curves at the 25% probability level obtained from analysis of data for time period 1, time period 2 and pooled data for both time periods.

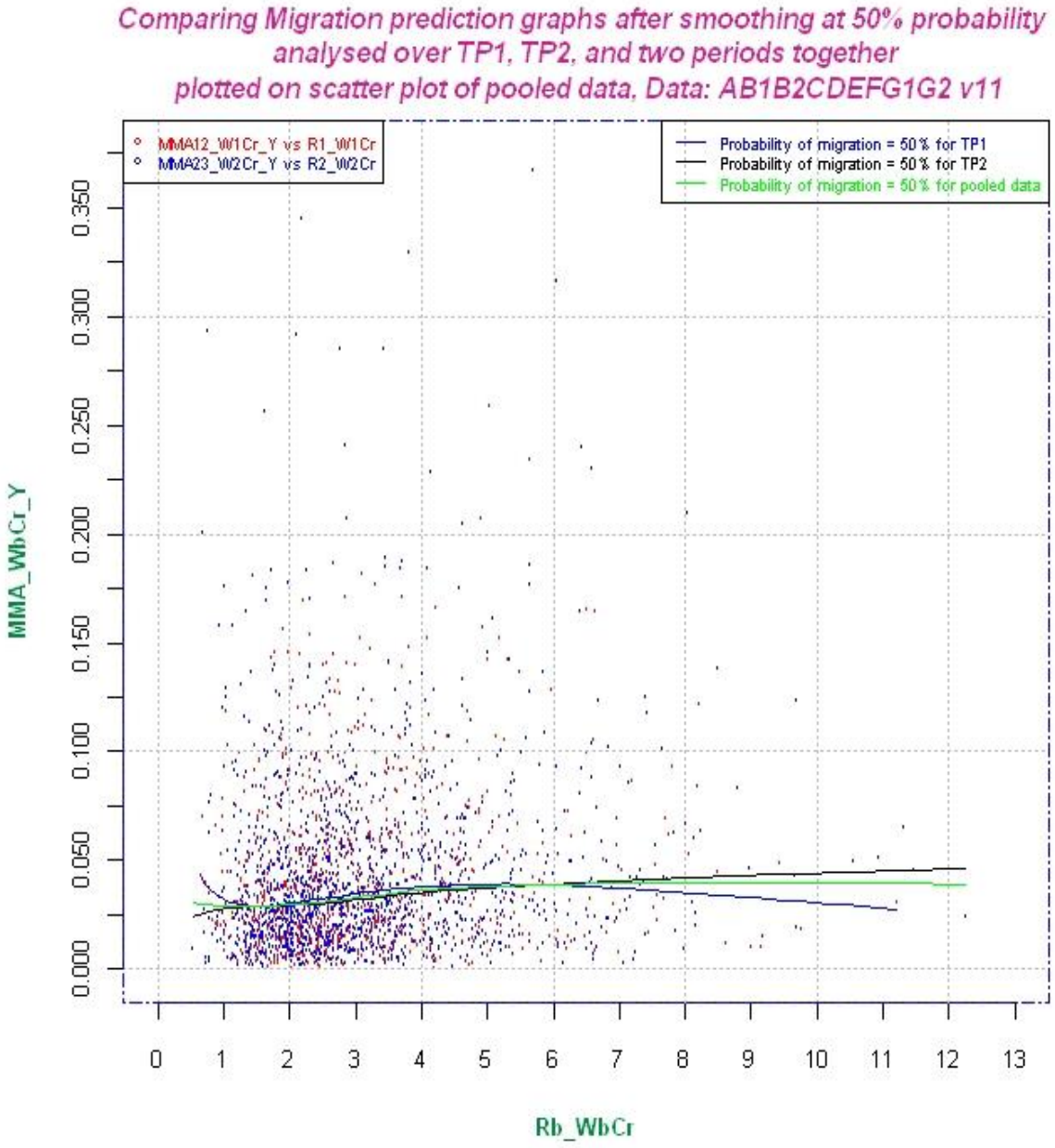

Figure 6.22: Comparison of smoothed probability curves at the 50% probability level obtained from analysis of data for time period 1, time period 2 and pooled data for both time periods.

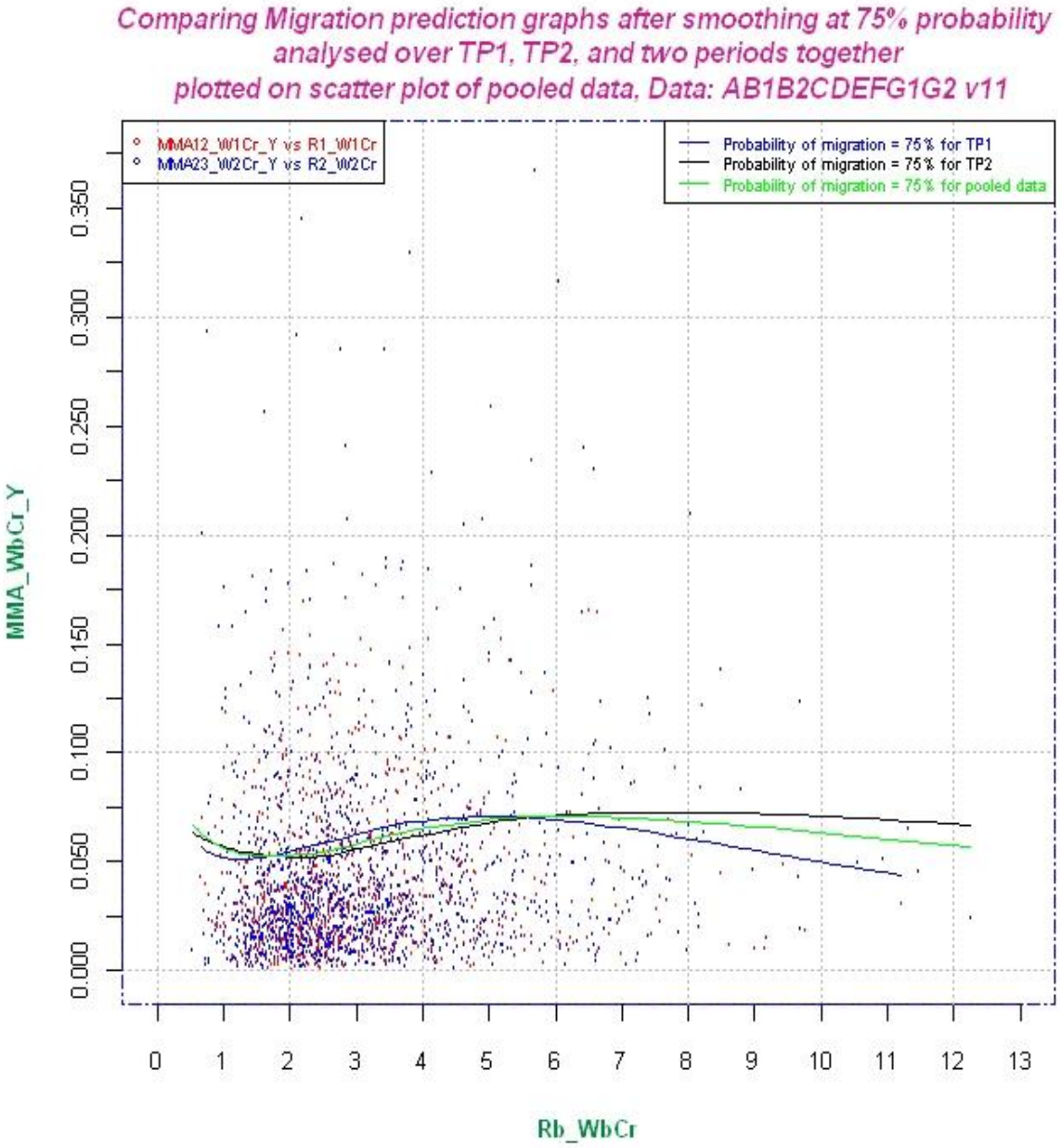

Figure 6.23: Comparison of smoothed probability curves at the 75% probability level obtained from analysis of data for time period 1, time period 2 and pooled data for both time periods.

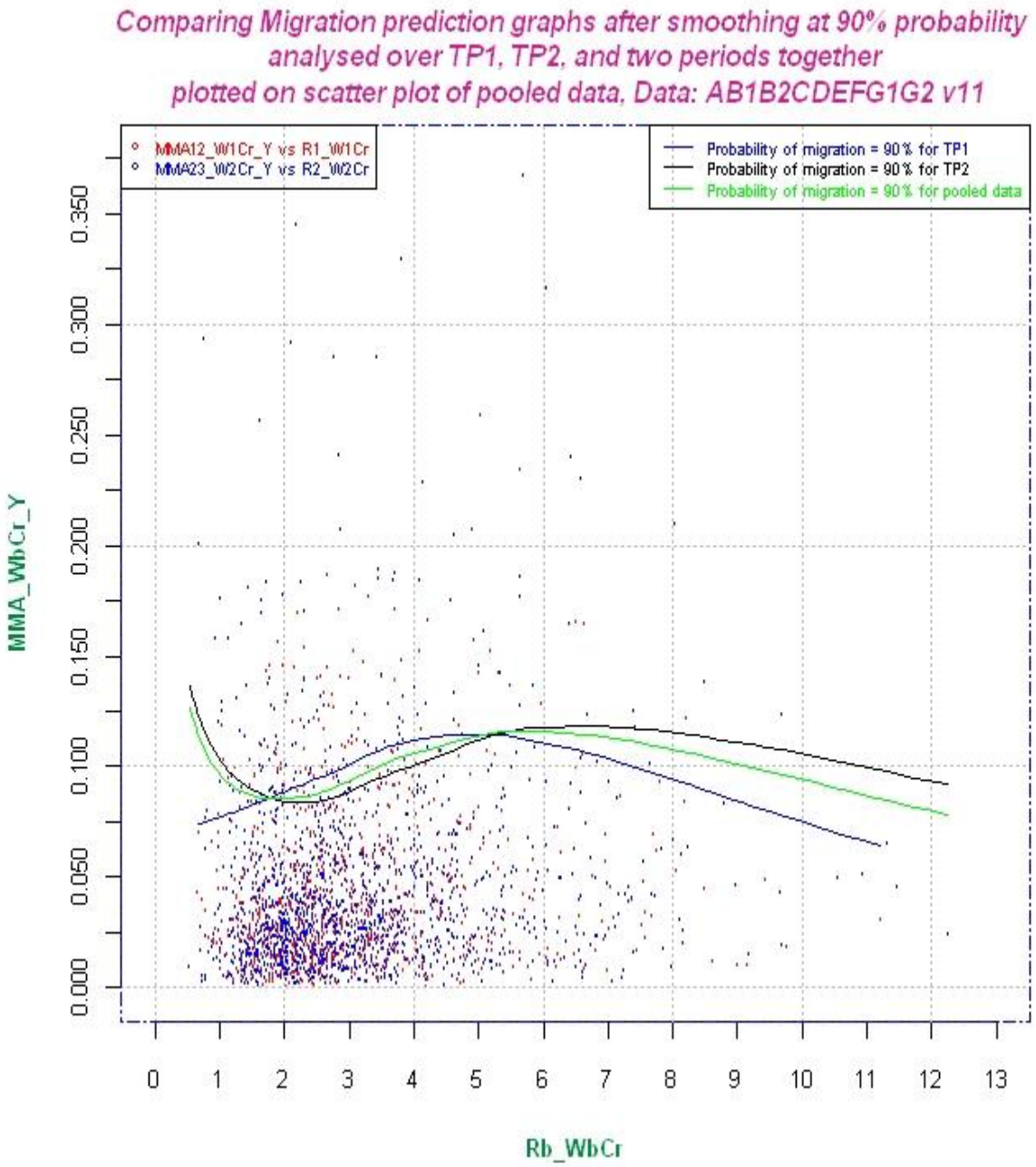

Figure 6.24: Comparison of smoothed probability curves at the 90% probability level obtained from analysis of data for time period 1, time period 2 and pooled data for both time periods.

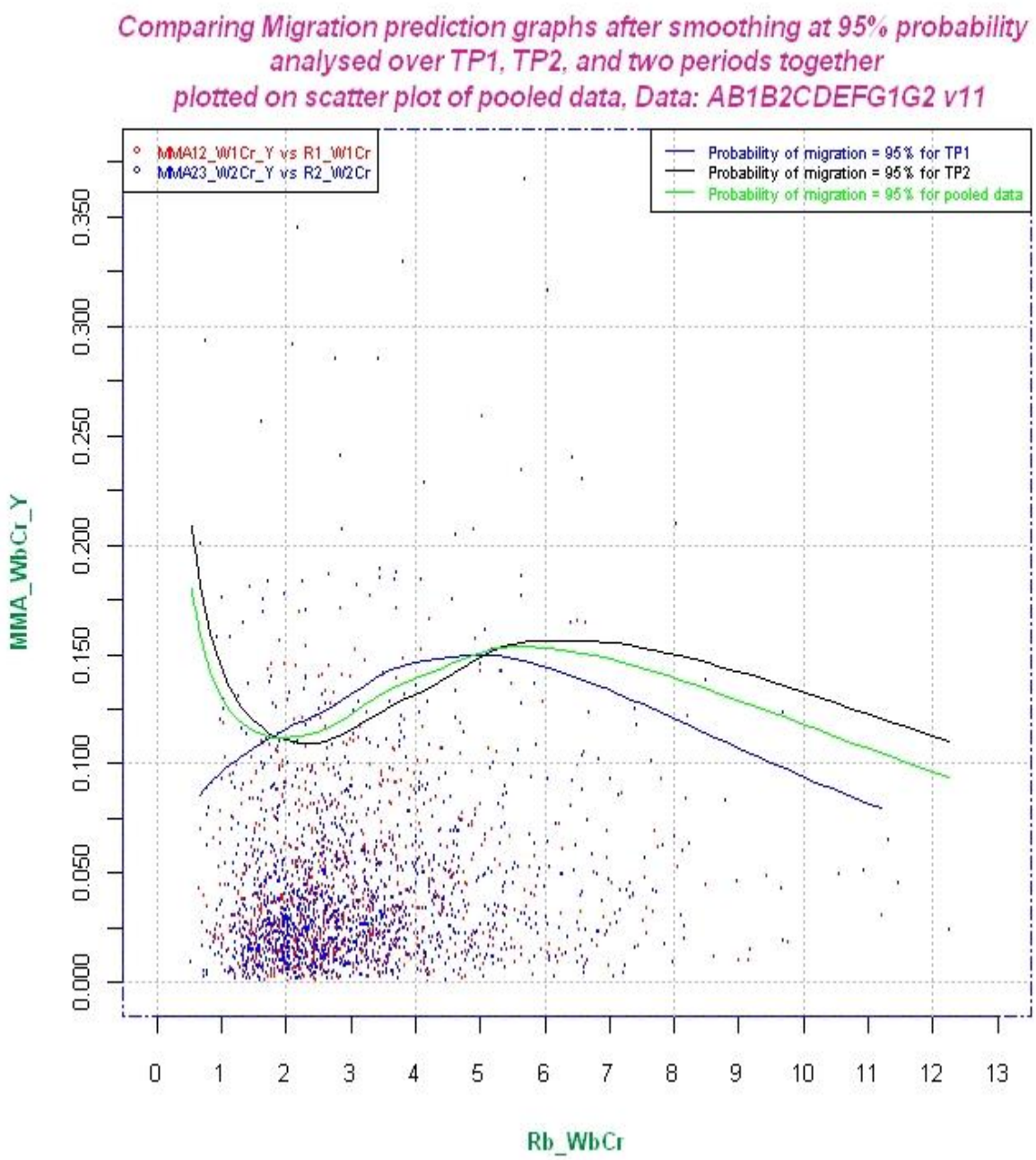

Figure 6.25: Comparison of smoothed probability curves at the 95% probability level obtained from analysis of data for time period 1, time period 2 and pooled data for both time periods.

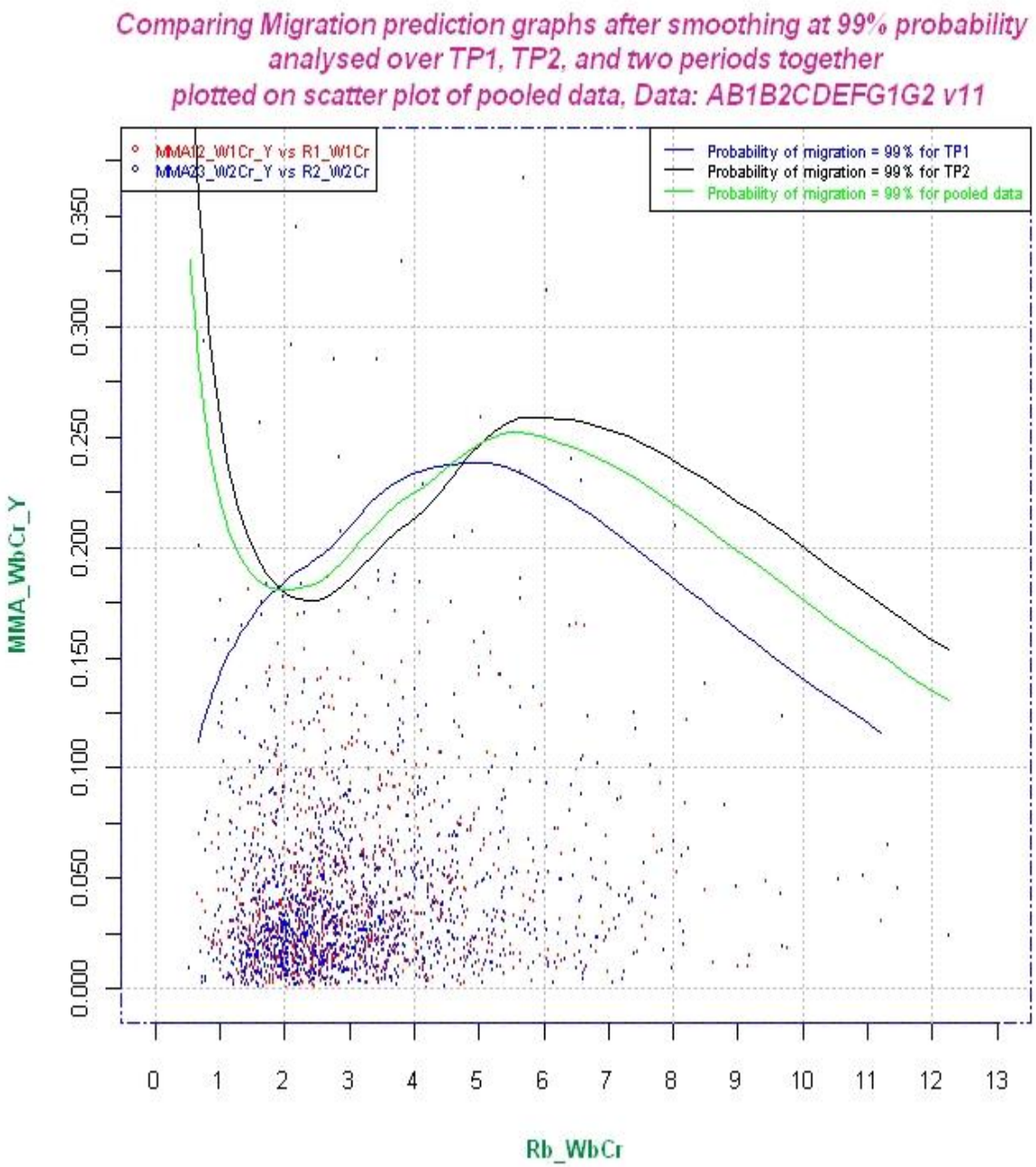

Figure 6.26: Comparison of 99% probability curves obtained from separate analyses for TP1, TP2 and BTP datasets.

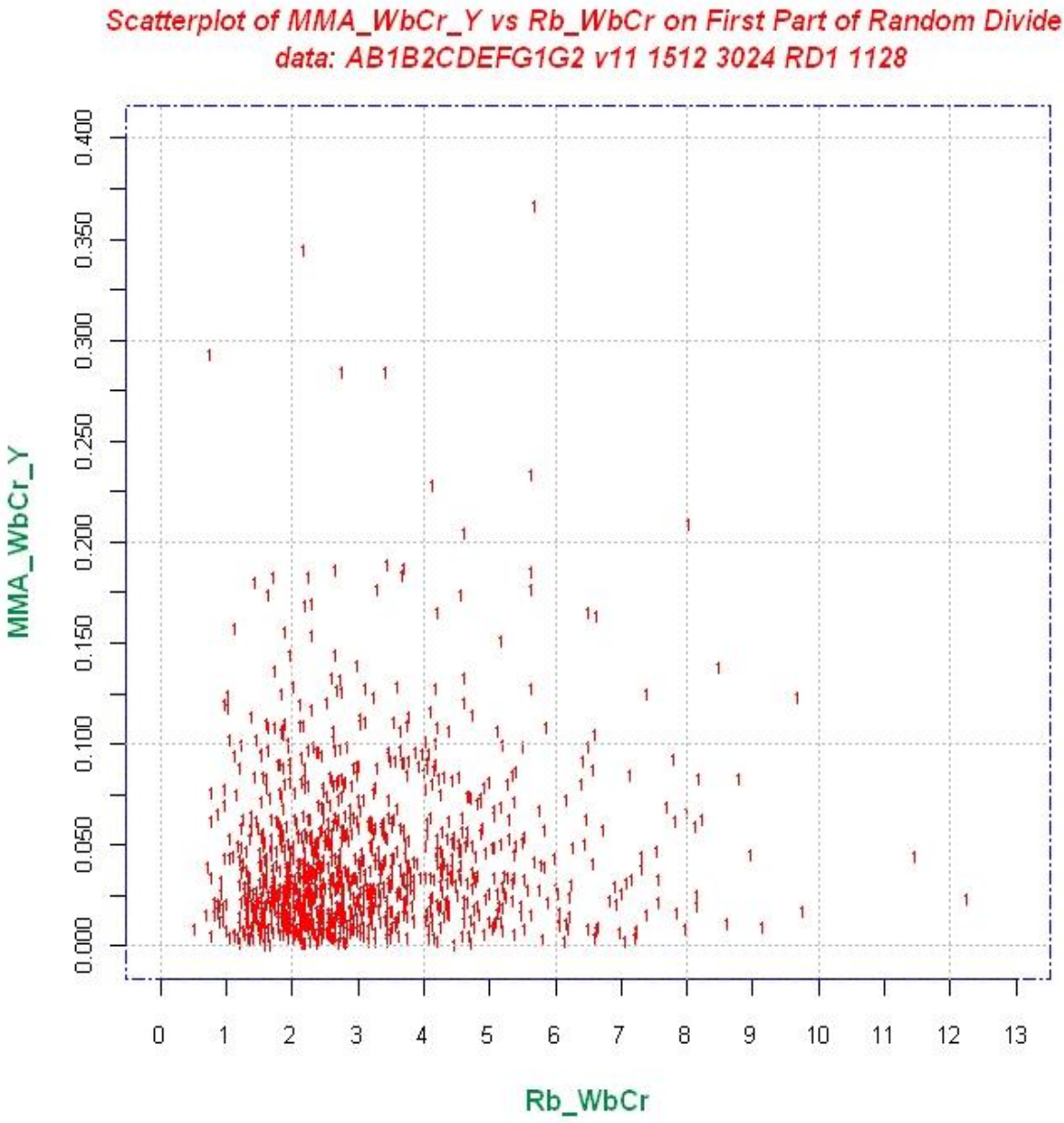

Figure 6.27: Scatter plot of dimensionless average annual migration rate measured at the bend apex (MMA/WbCr/Y) as a function of the ratio of outer bank radius of curvature to river channel width at the crossing (Rb/WbCr) for RD1 (Part 1 of randomly divided data, Attempt 1).

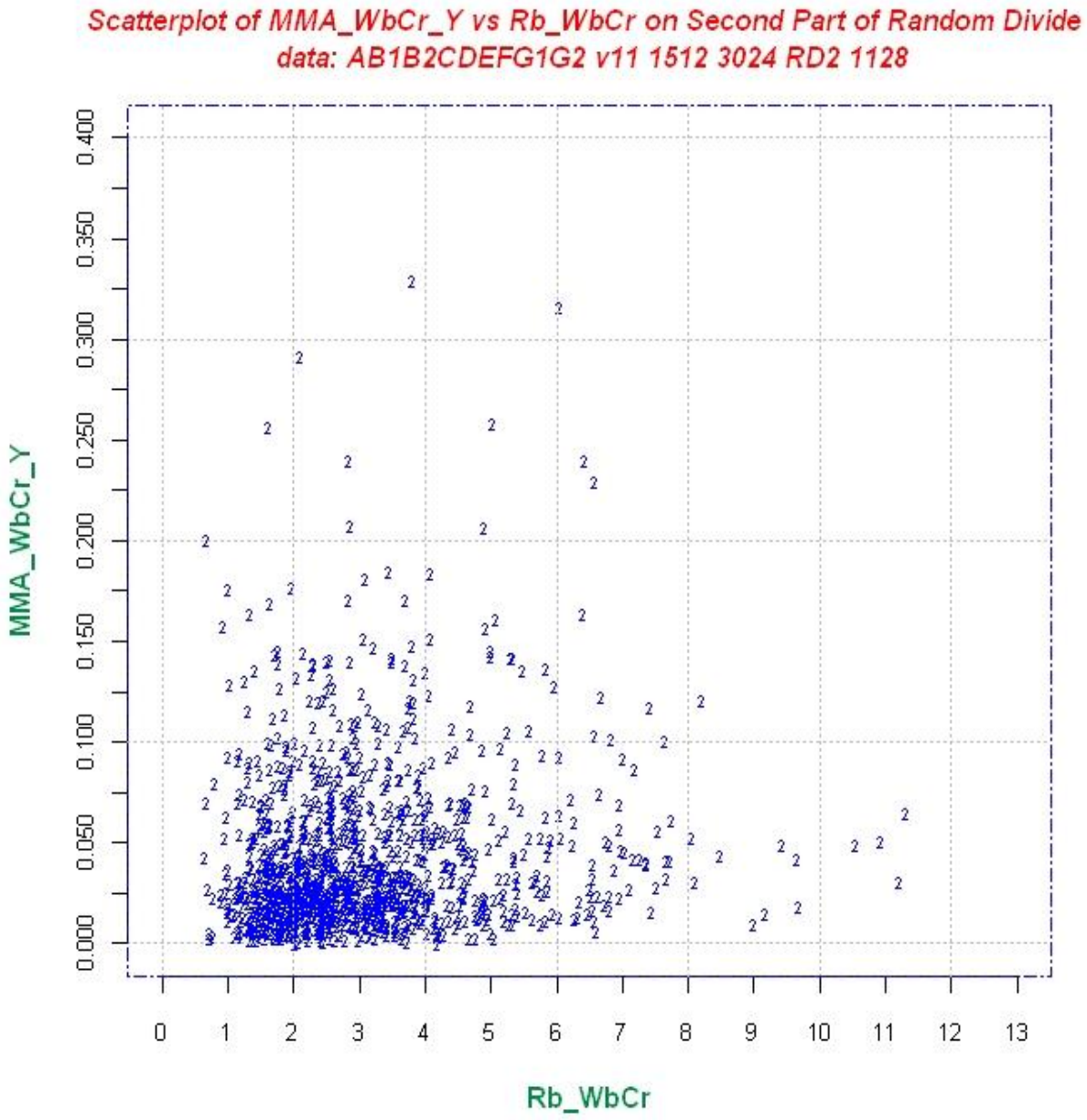

Figure 6.28: Scatter plot of dimensionless average annual migration rate measured at the bend apex (MMA/WbCr/Y) as a function of the ratio of outer bank radius of curvature to river channel width at the crossing (Rb/WbCr) for RD2 (Part 2 of randomly divided data, Attempt 1).

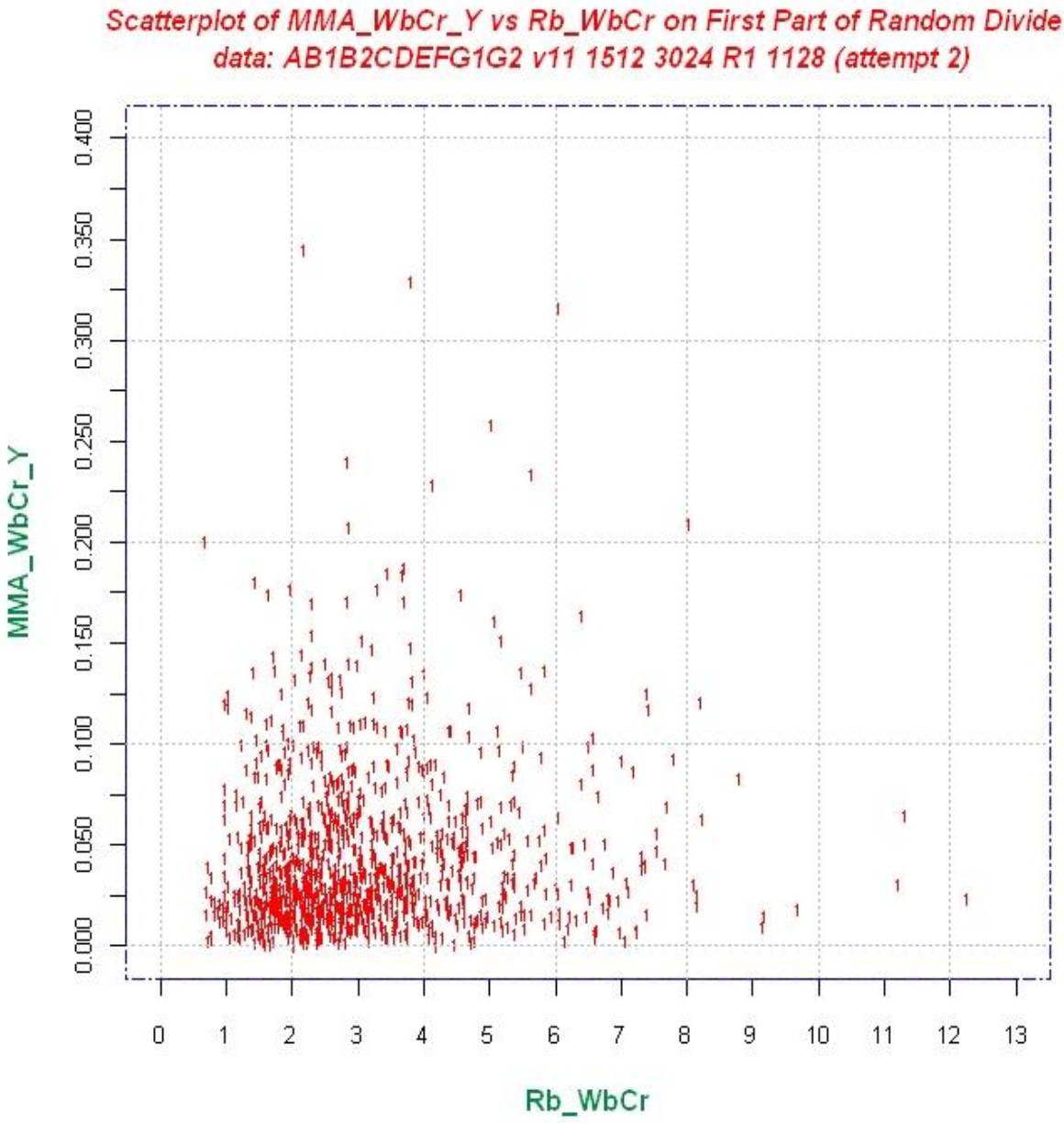

Figure 6.29: Scatter plot of dimensionless average annual migration rate measured at the bend apex (MMA/WbCr/Y) as a function of the ratio of outer bank radius of curvature to river channel width at the crossing (Rb/WbCr) for R1 (Part 1 of randomly divided data, Attempt 2).

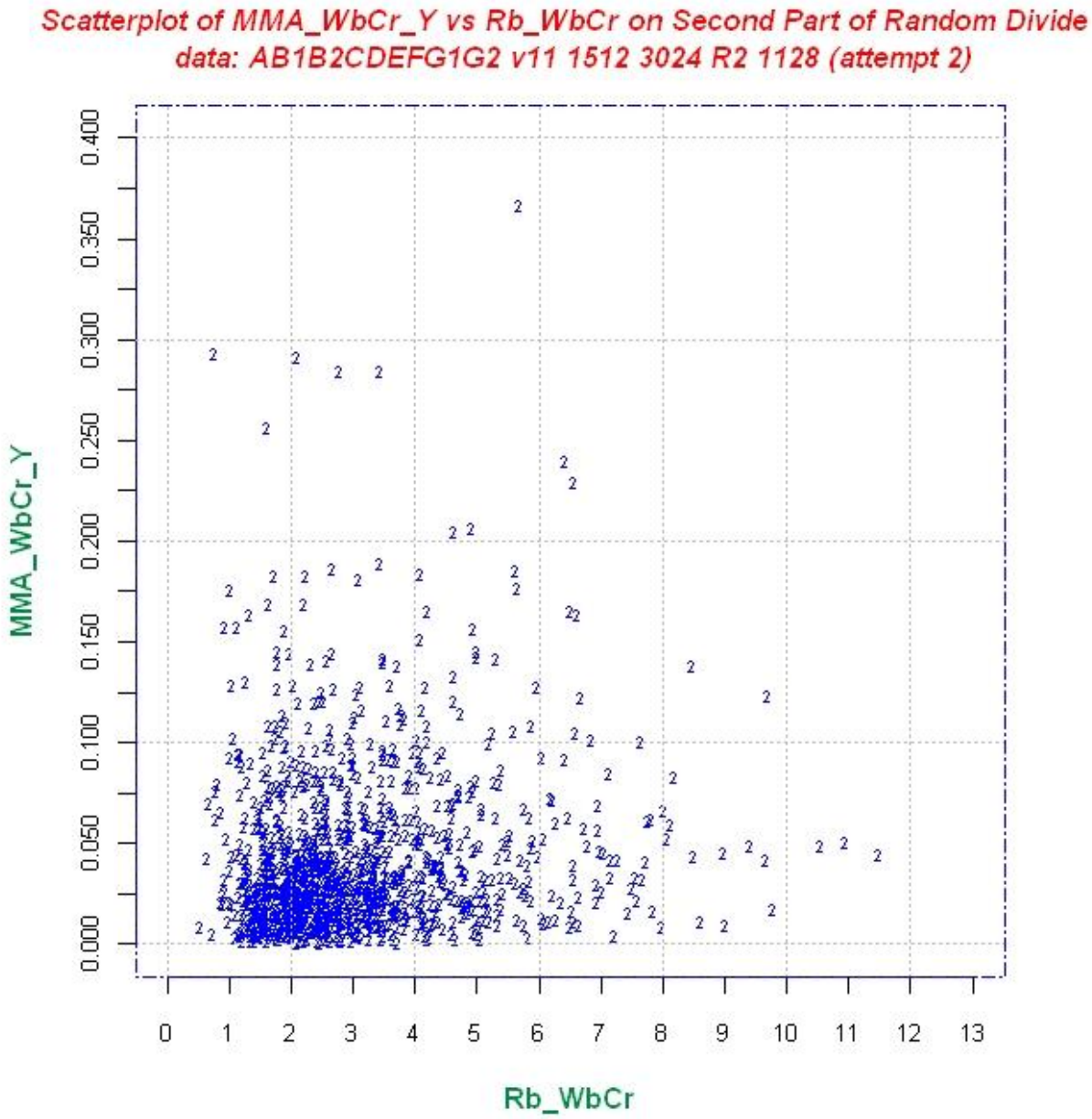

Figure 6.30: Scatter plot of dimensionless average annual migration rate measured at the bend apex (MMA/WbCr/Y) as a function of the ratio of outer bank radius of curvature to river channel width at the crossing (Rb/WbCr) for R2 (Part 2 of randomly divided data, Attempt 2).

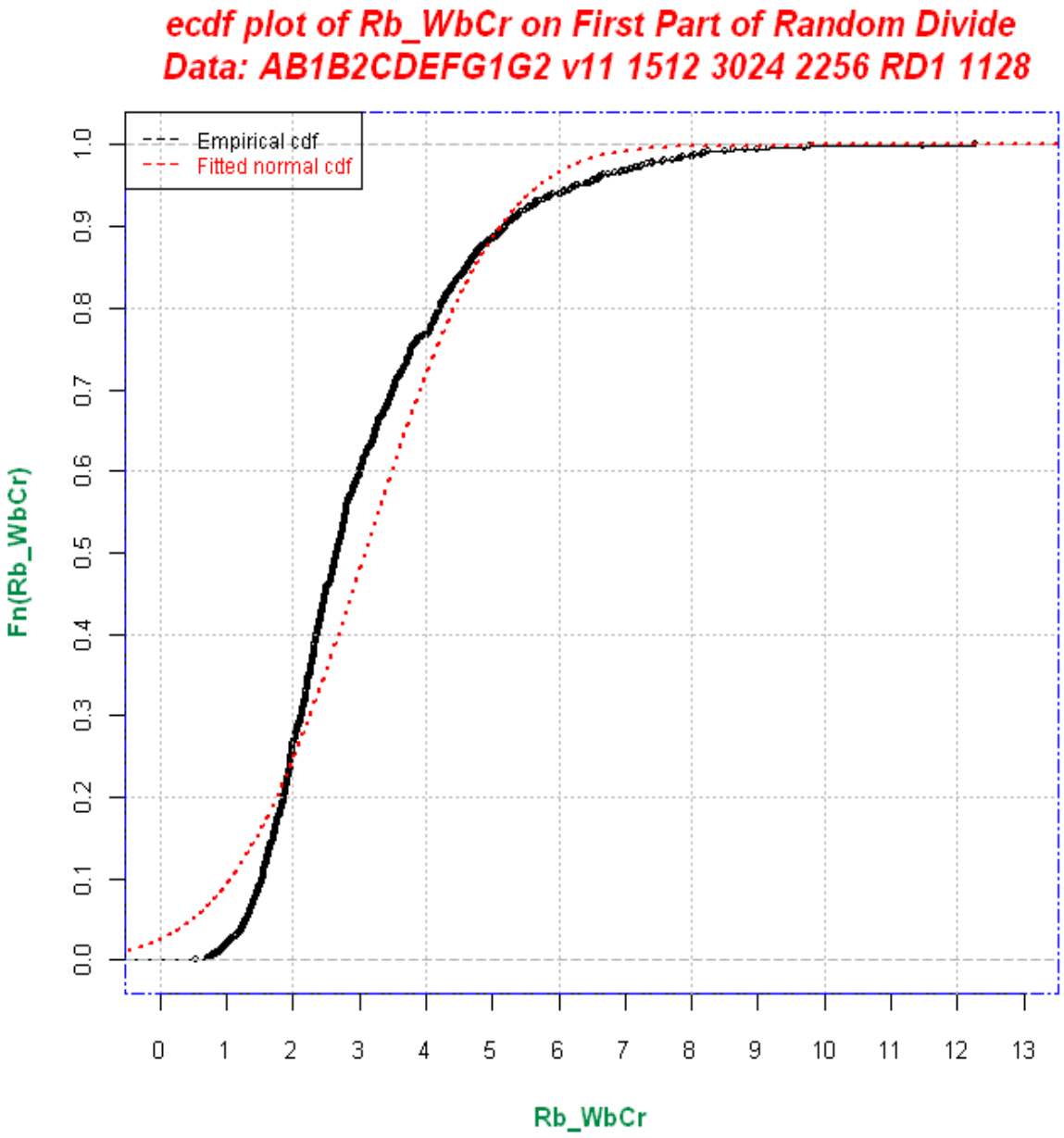

Figure 6.31: Empirical cumulative probability and fitted normal distributions for Rb/WbCr based on analysis of the RD1 data set (Part 1 of random division, Attempt 1).

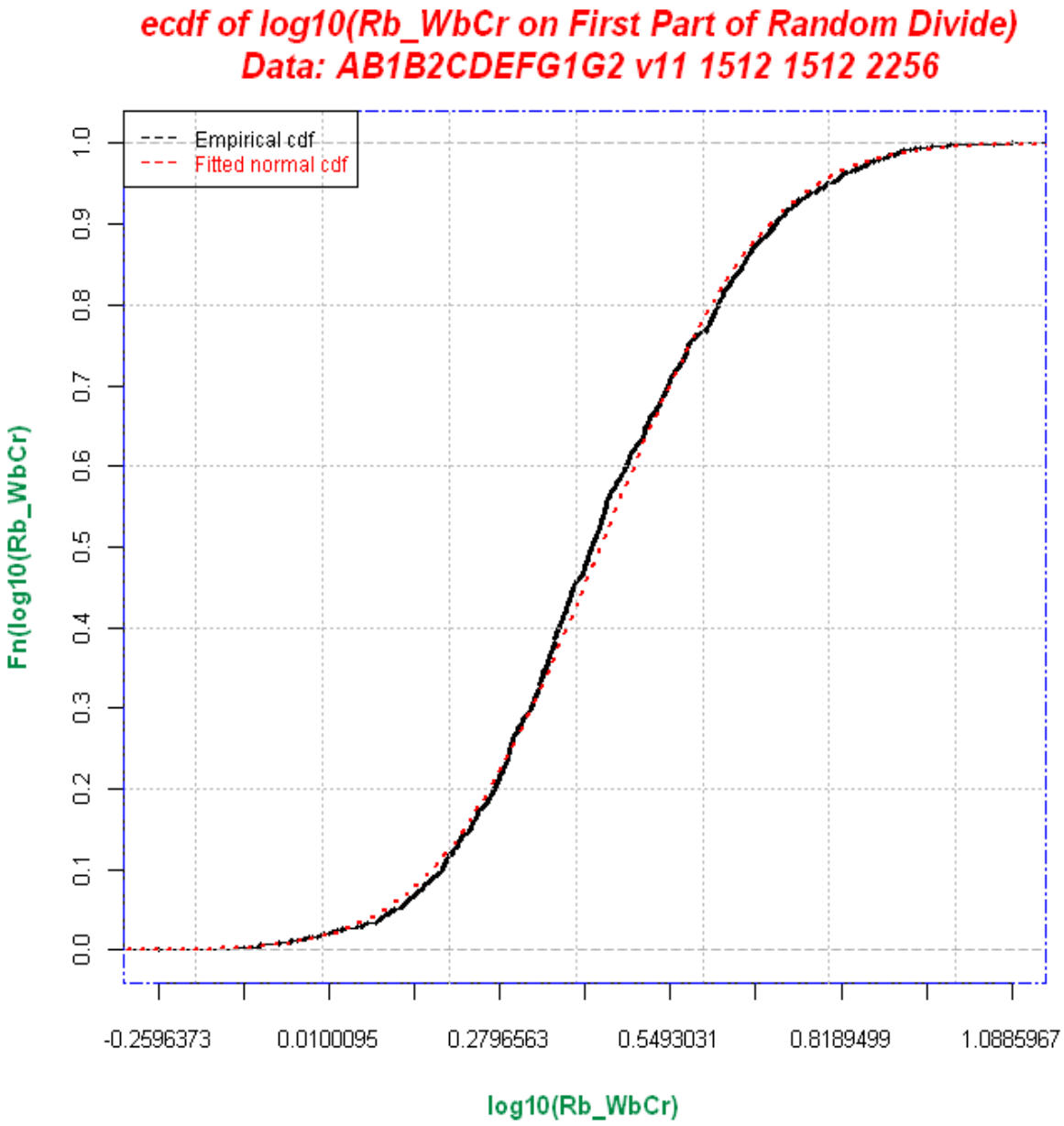

Figure 6.32: Empirical cumulative probability and fitted normal distributions for a logarithmic transformation of Rb/WbCr based on the RD1 data set (Part 1 of random division, Attempt 1).

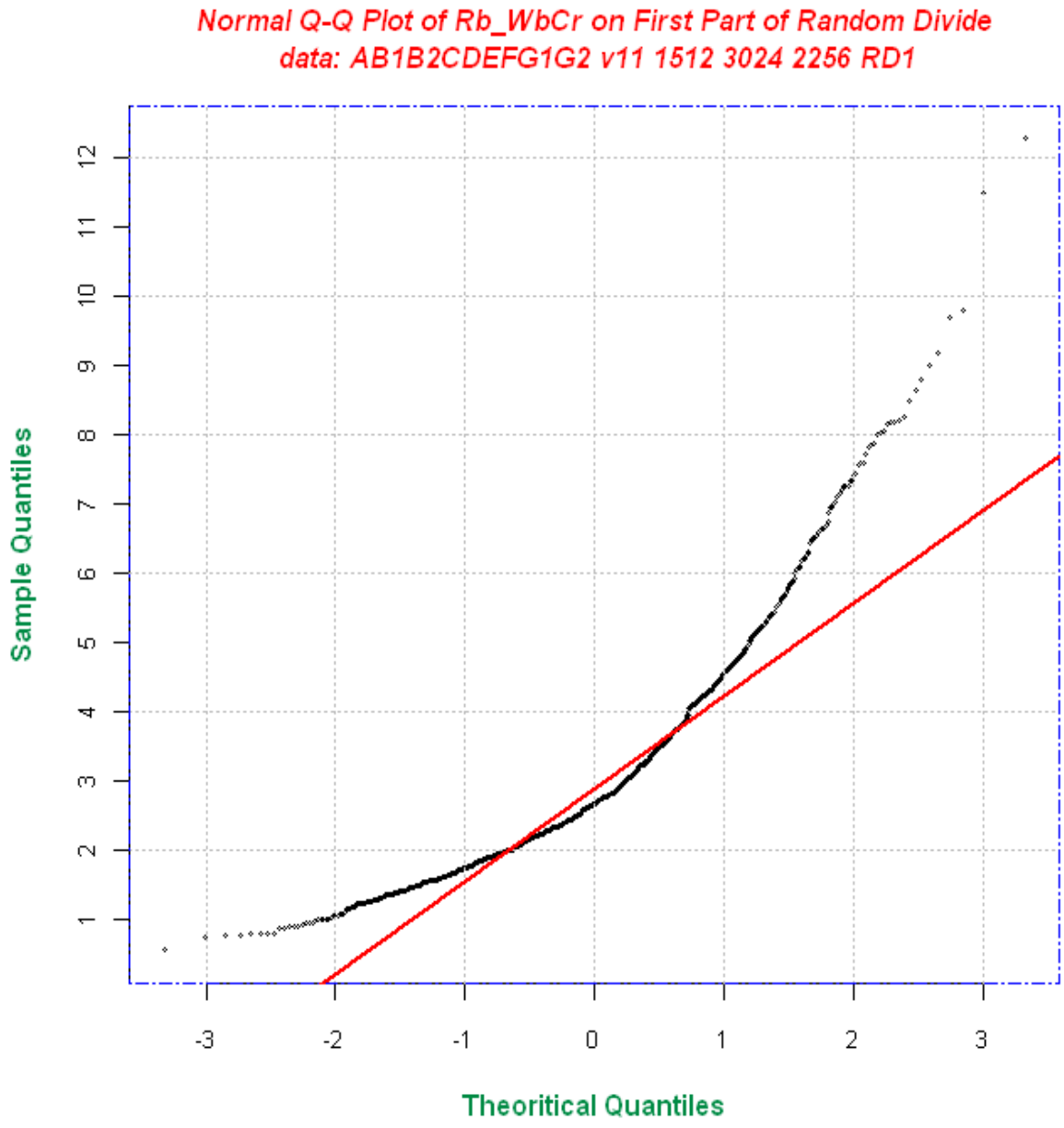

Figure 6.33: Normal probability plot for empirical cumulative probability and fitted normal distributions for Rb/WbCr based on the RD1 data set (Part 1 of random division, Attempt 1).

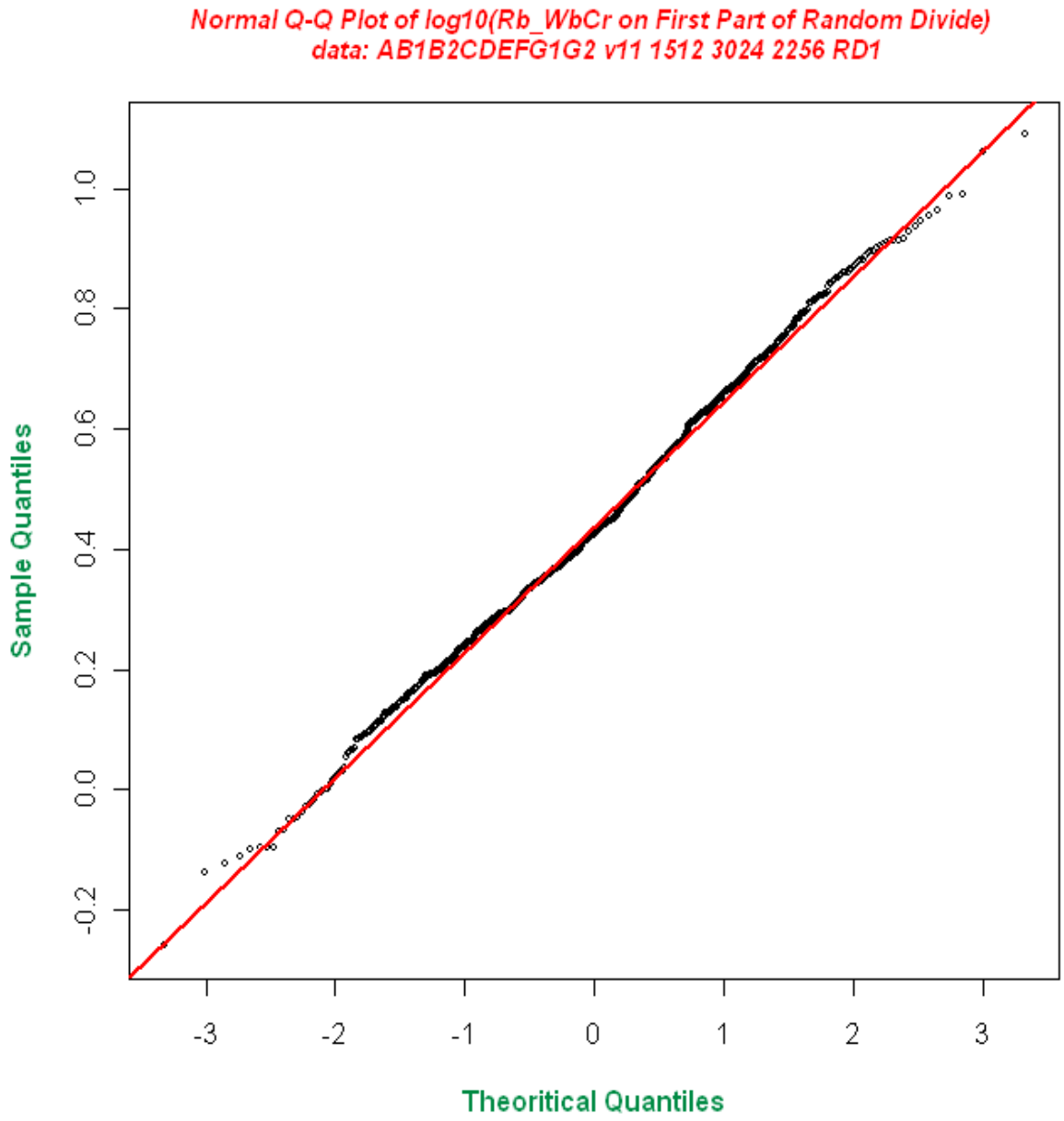

Figure 6.34: Normal probability plot for a logarithmic transformation of Rb/WbCr based on the RD1 data set (Part 1 of random division, Attempt 1).

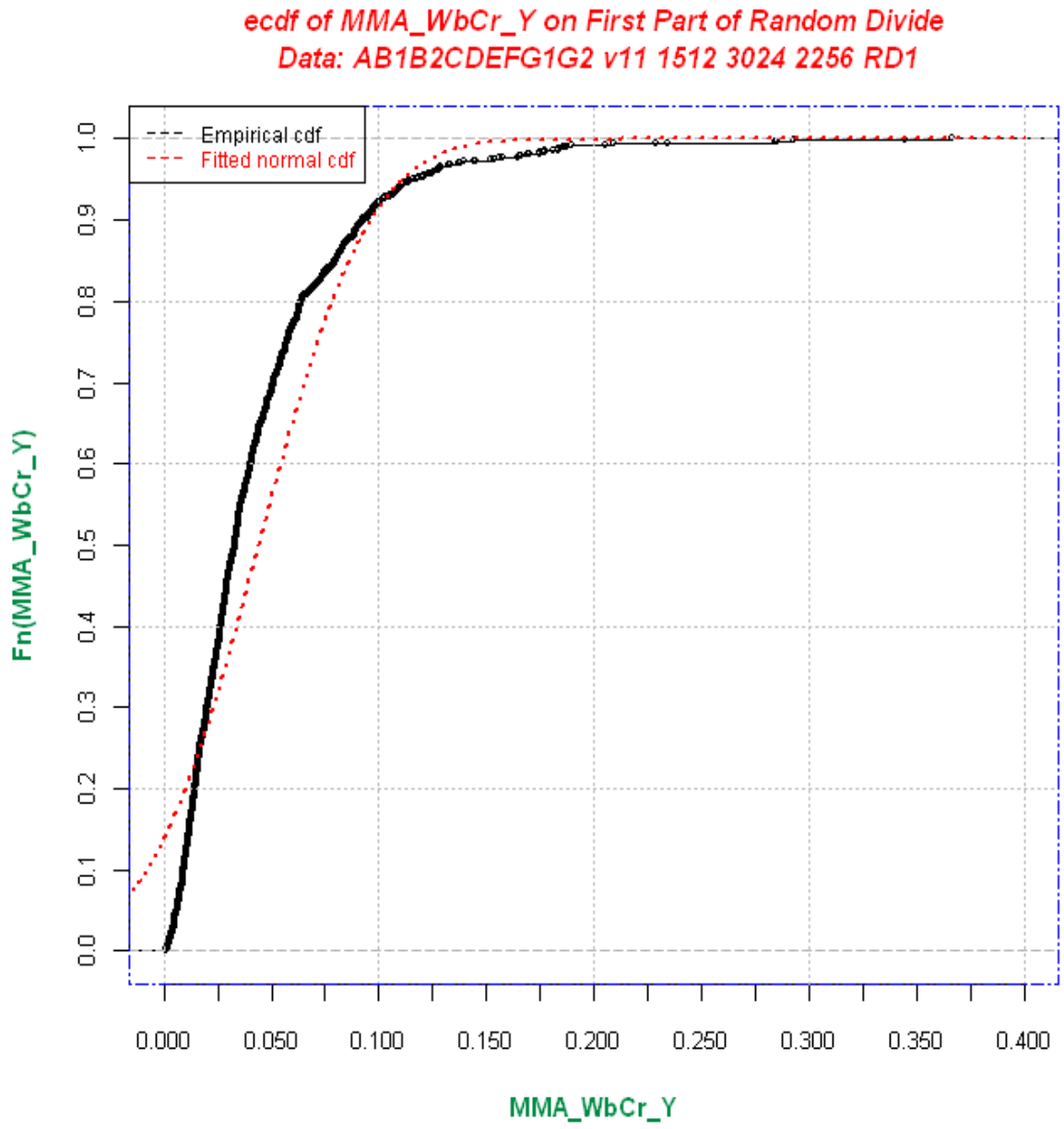

Figure 6.35: Empirical cumulative probability and fitted normal distributions for MMA/WbCr/Y based on the RD1 data set (Part 1 of random division, Attempt 1).

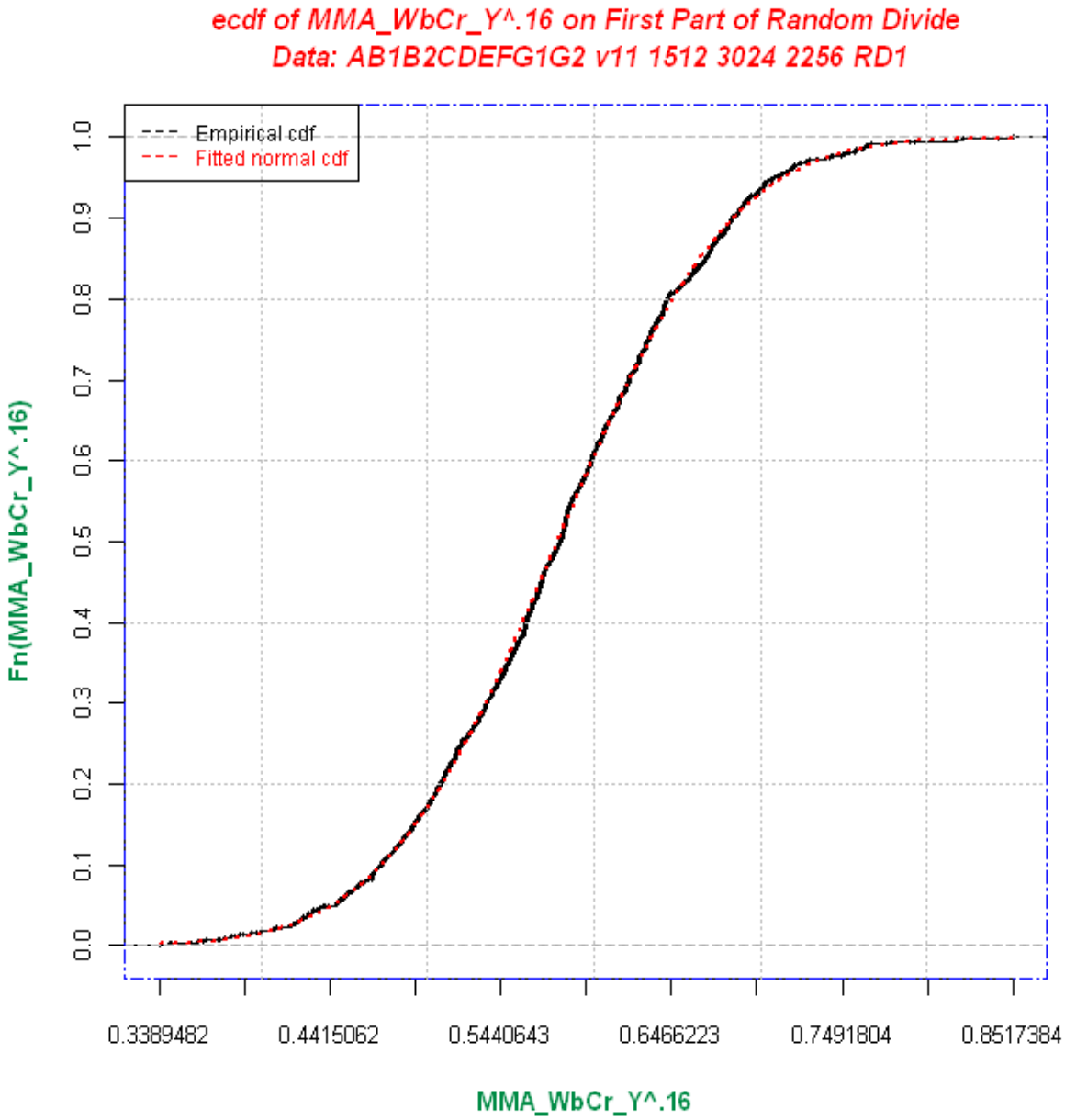

Figure 6.36: Empirical cumulative probability and fitted normal distributions for $(MMA/WbCr/Y)^{0.16}$ based on the RD1 data set (Part 1 of random division, Attempt 1).

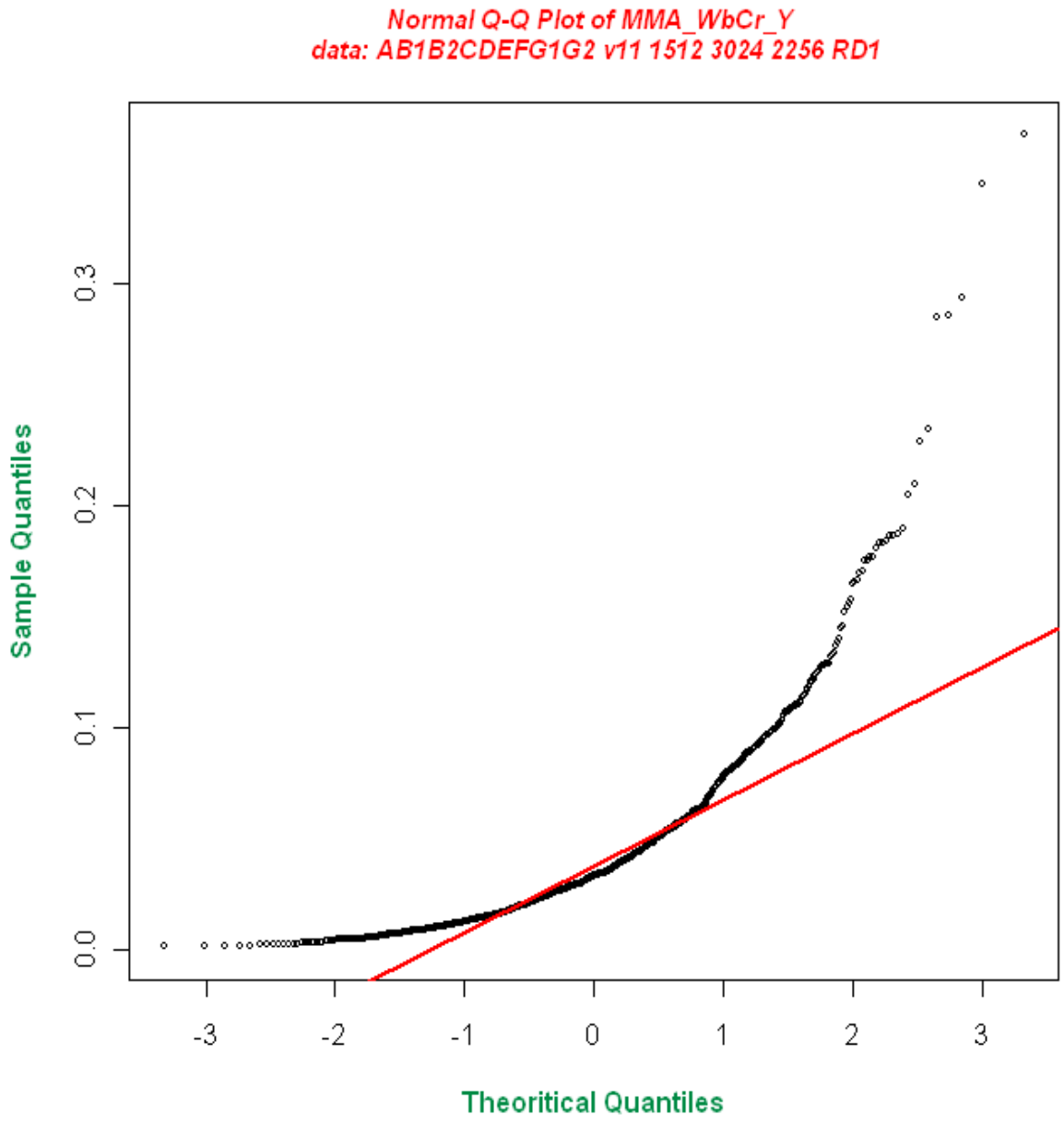

Figure 6.37: Normal probability plot for MMA/WbCr/Y based on the RD1 data set (Part 1 of random division, Attempt 1).

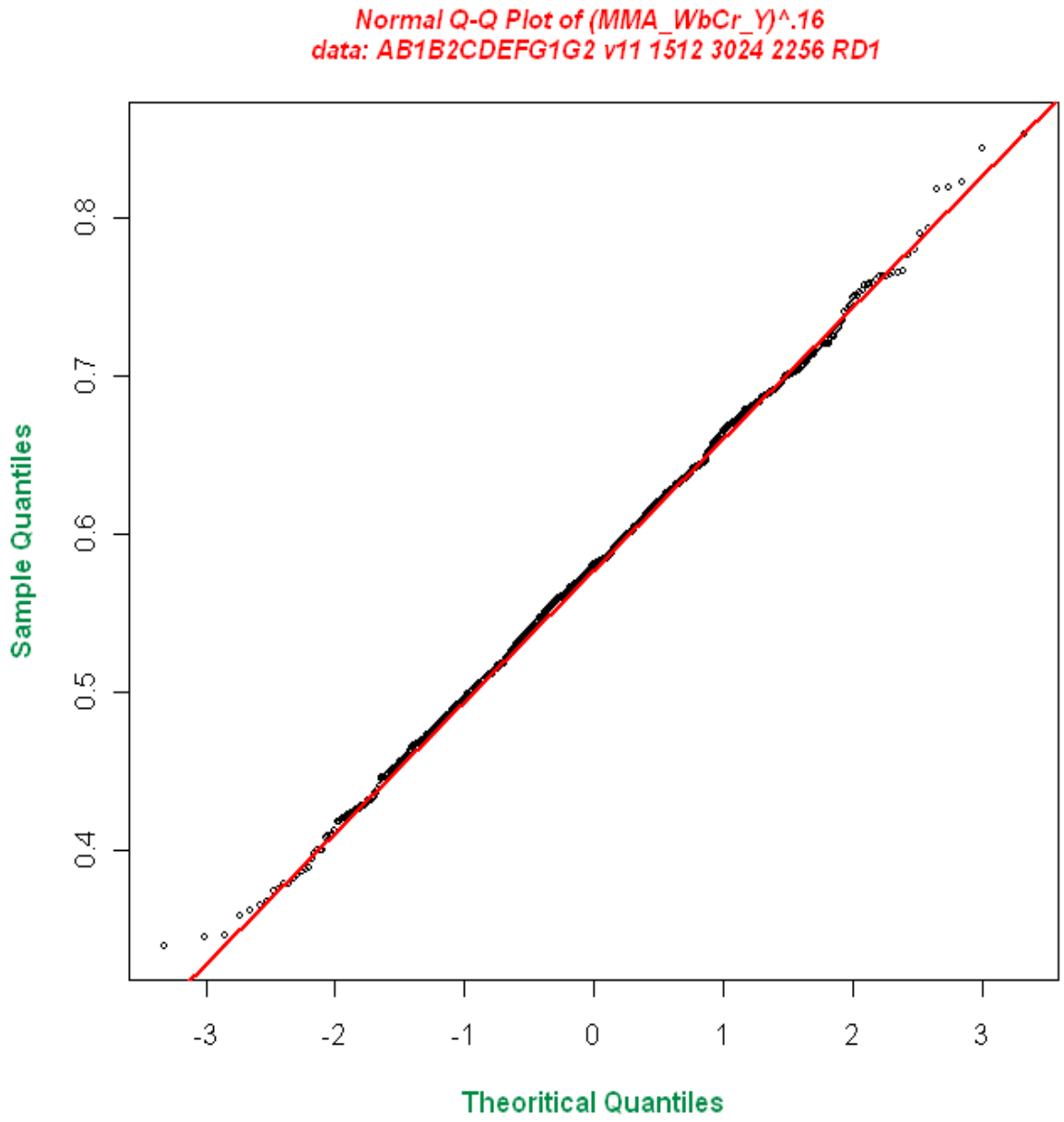

Figure 6.38: Normal probability plot for $(MMA/WbCr/Y)^{0.16}$ based on the RD1 data set (Part 1 of random division, Attempt 1).

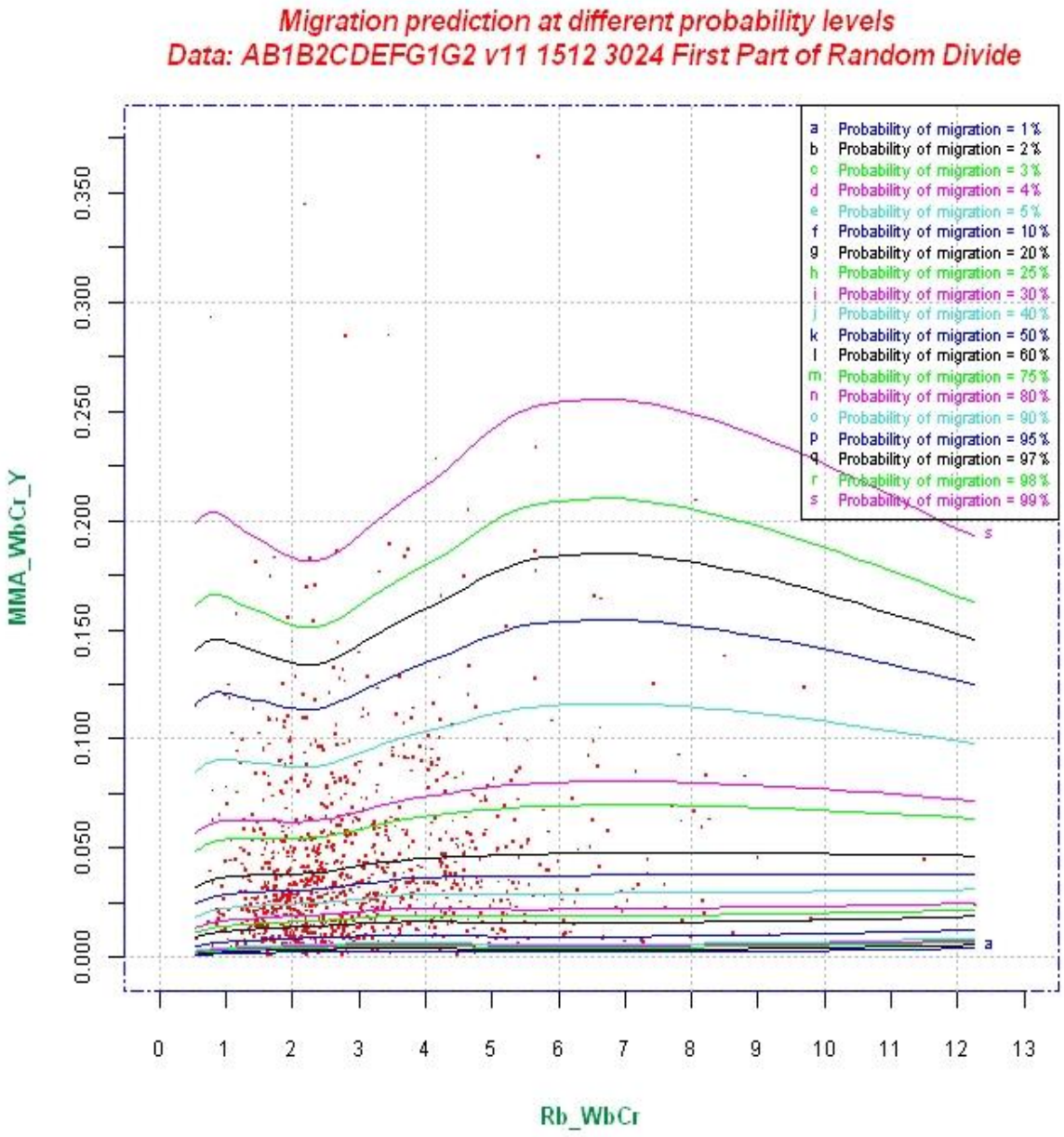

Figure 6.39: Probability curves for average annual migration rate for the first Random Sample in Attempt 1 - RD1.

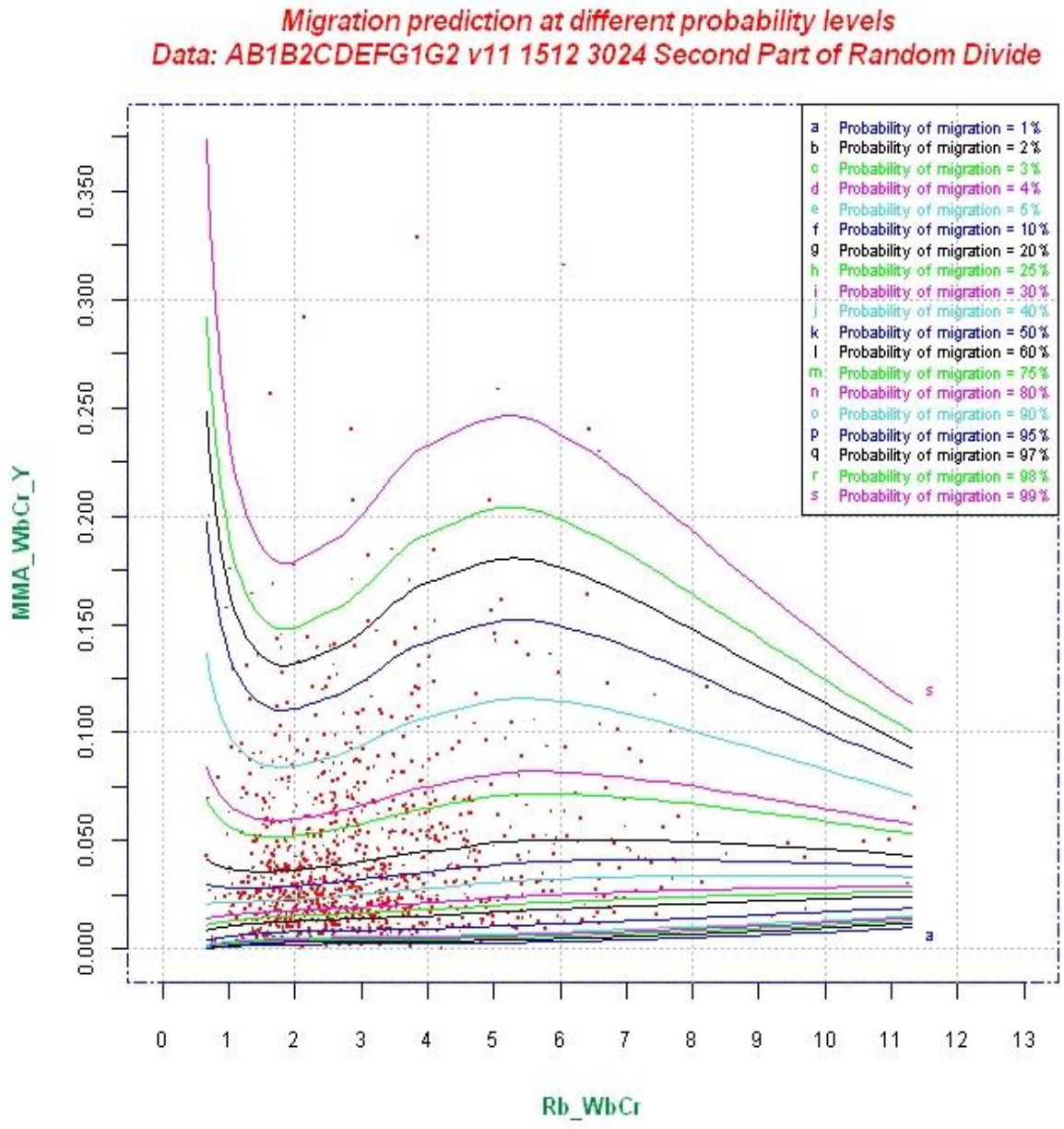

Figure 6.40: Probability curves for average annual migration rate for the second 50% Random Sample, in Attempt 1 - RD2.

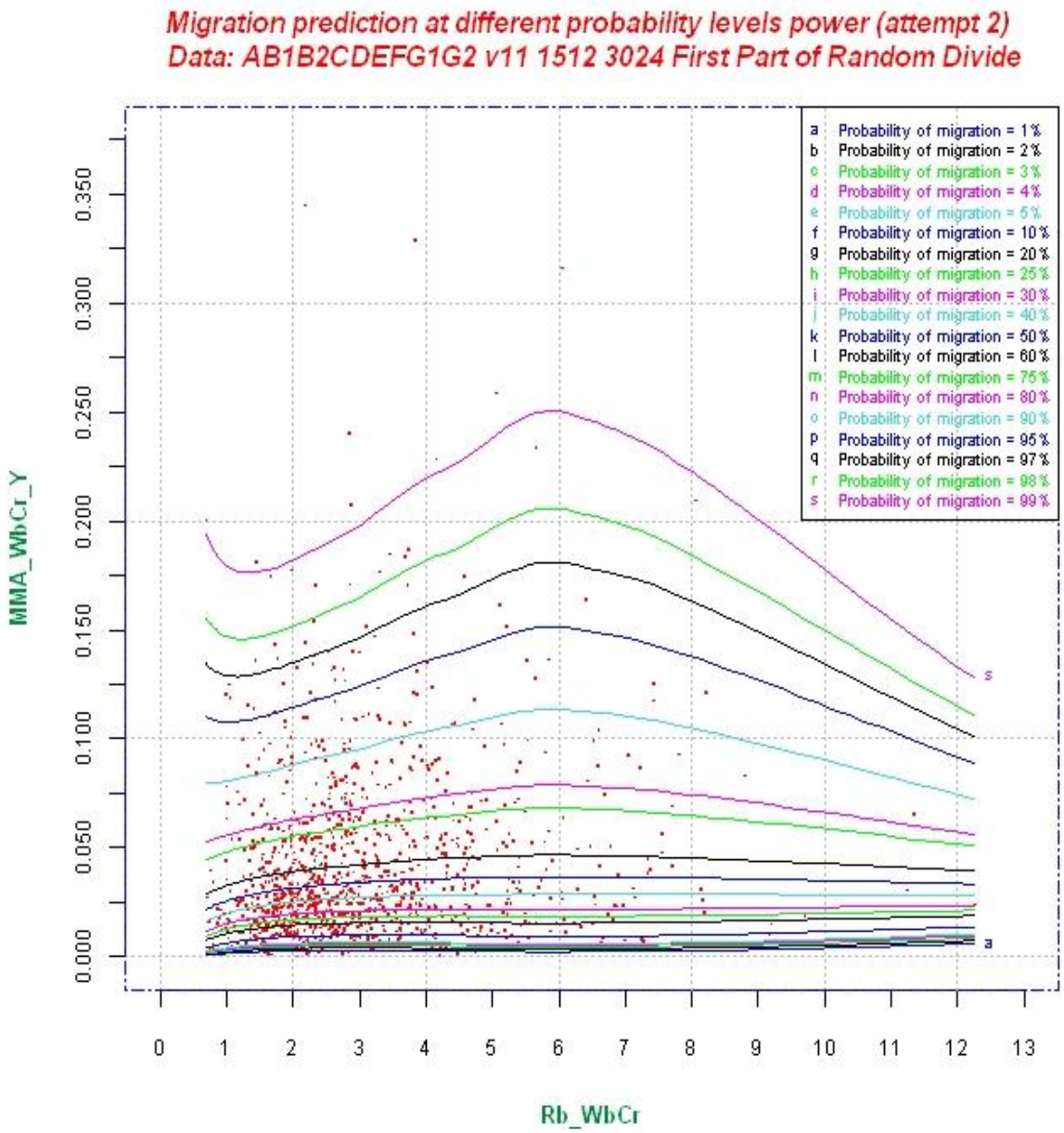

Figure 6.41: Probability curves for average annual migration rate for the first 50% Random Sample in Attempt 2 - R1.

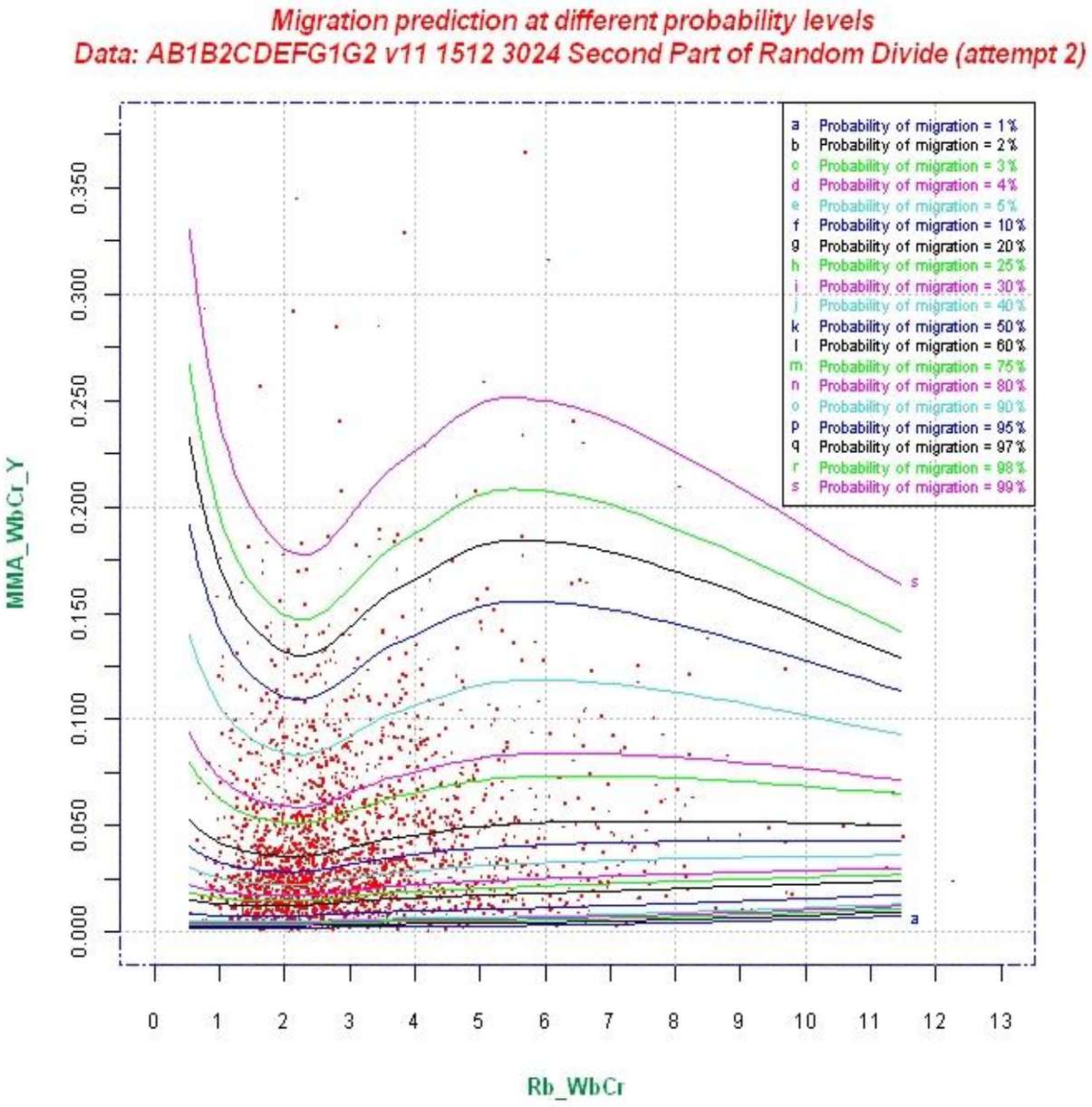

Figure 6.42: Probability curves for average annual migration rate for the second 50% Random Sample in Attempt 2 - R2.

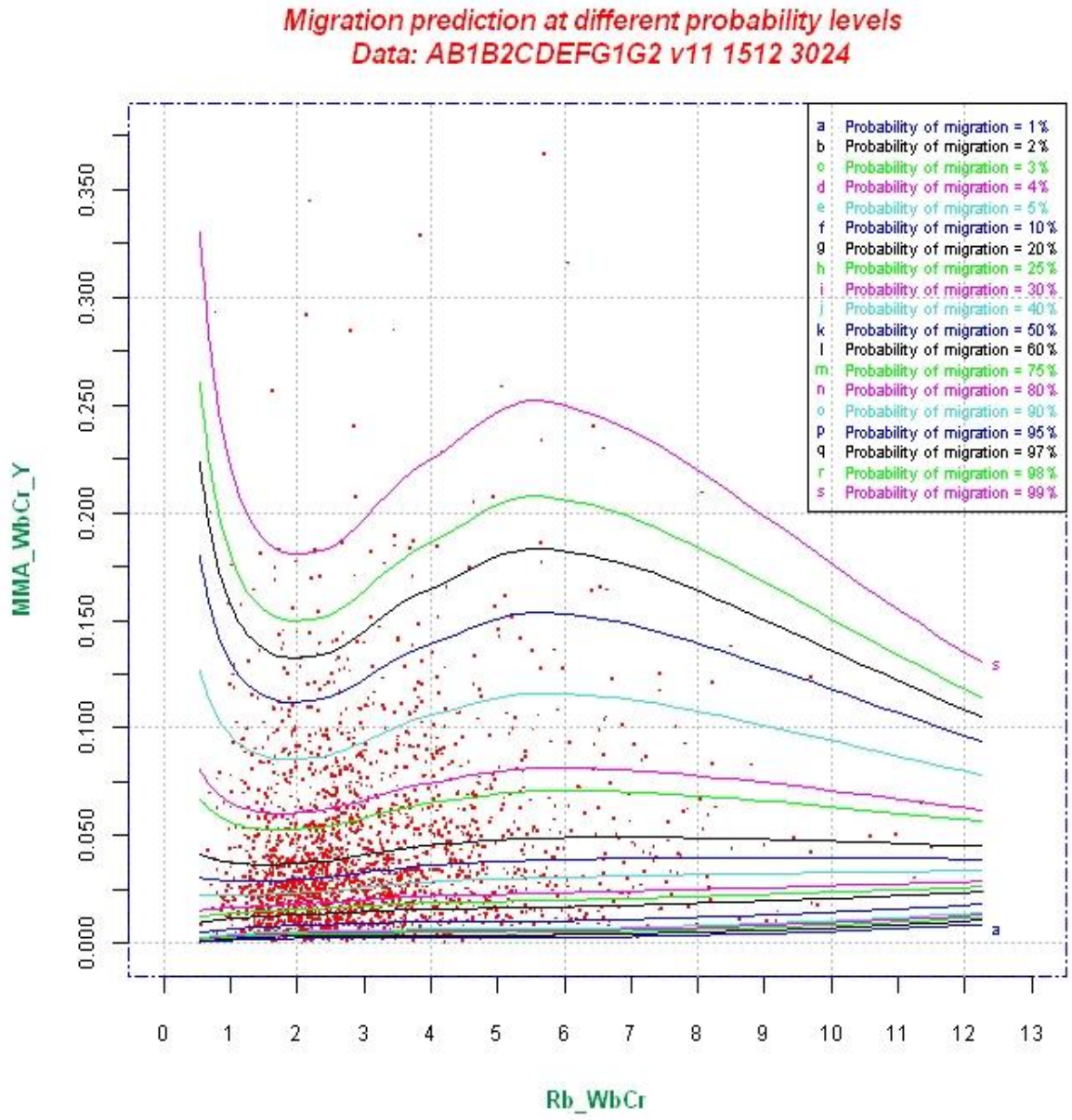

Figure 6.43: Probability curves for average annual migration rate for data pooled from both time periods - BTP.

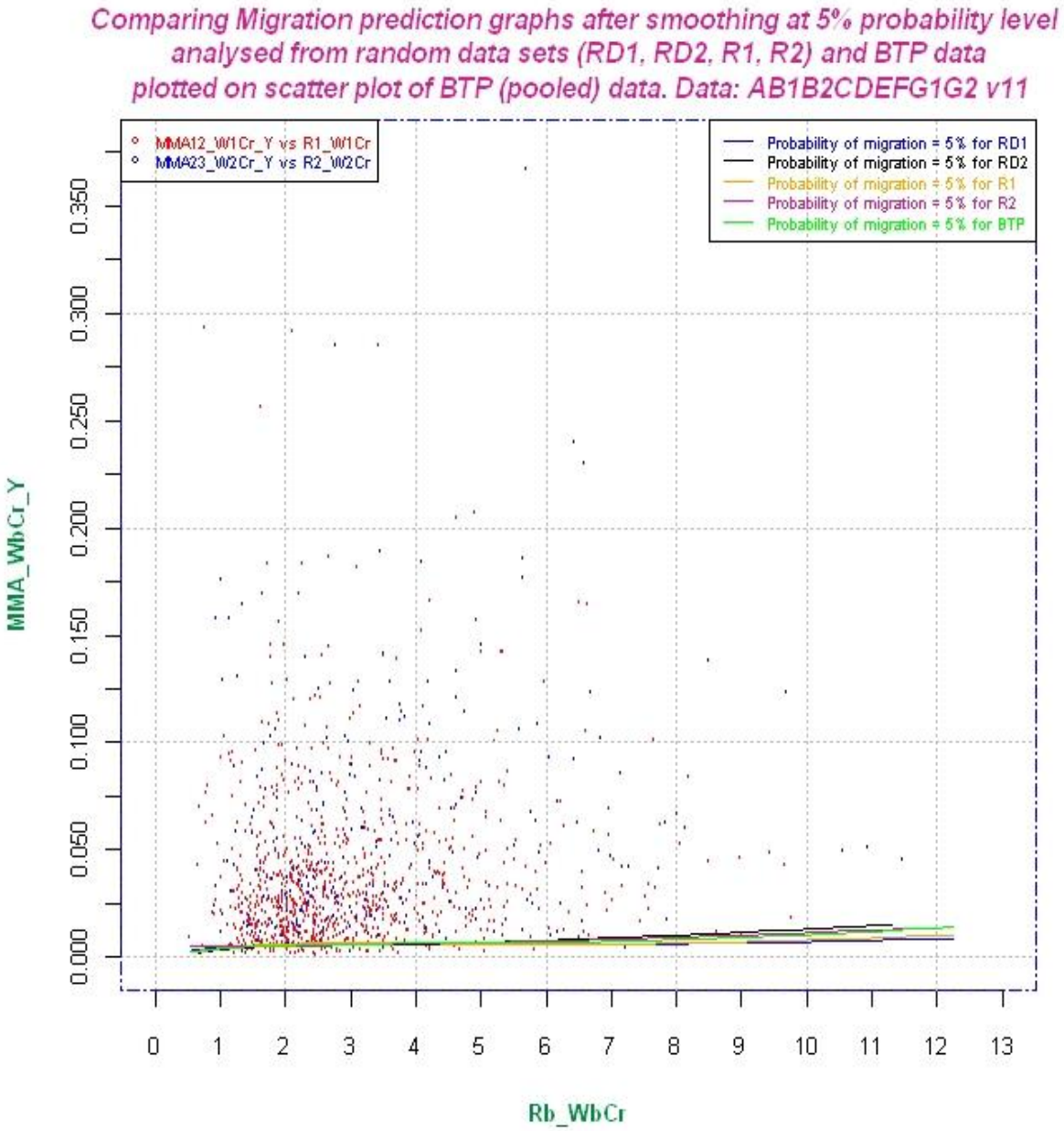

Figure 6.44: Comparison of smoothed 5% probability curves for RD1, RD2, R1, R2, and BTP.

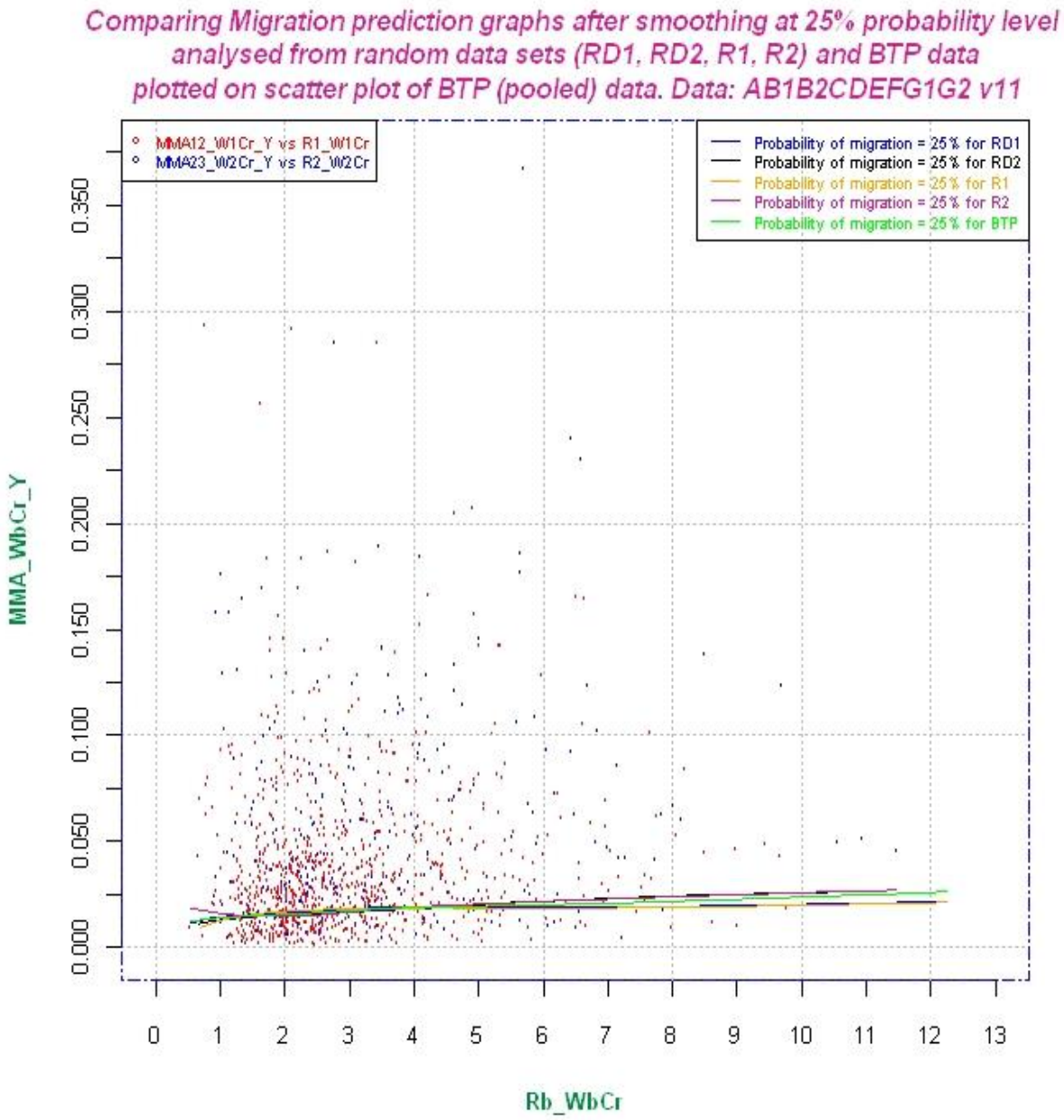

Figure 6.45: Comparison of smoothed 25% probability curves for RD1, RD2, R1, R2, and BTP.

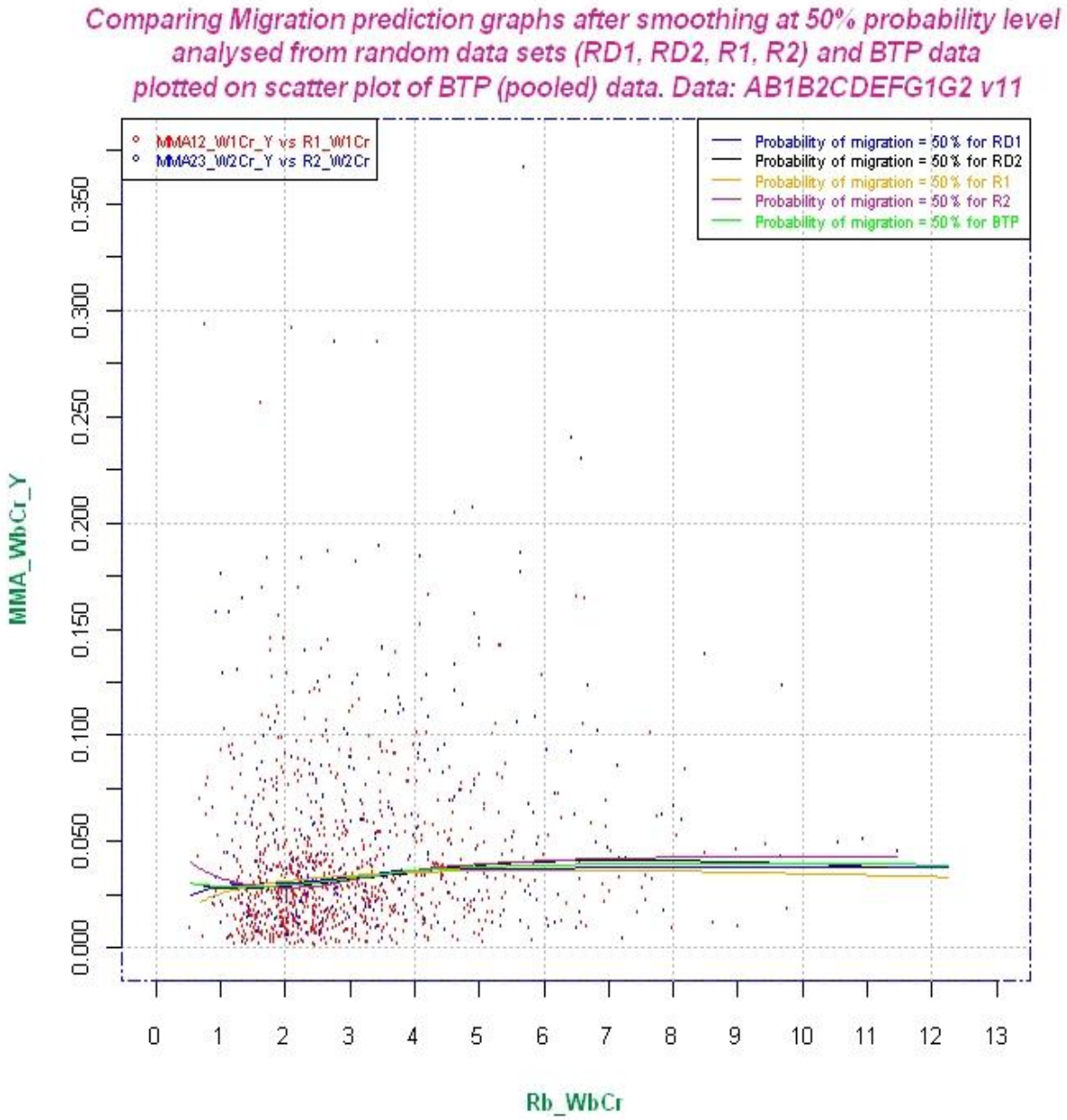

Figure 6.46: Comparison of smoothed 50% probability curves for RD1, RD2, R1, R2, and BTP.

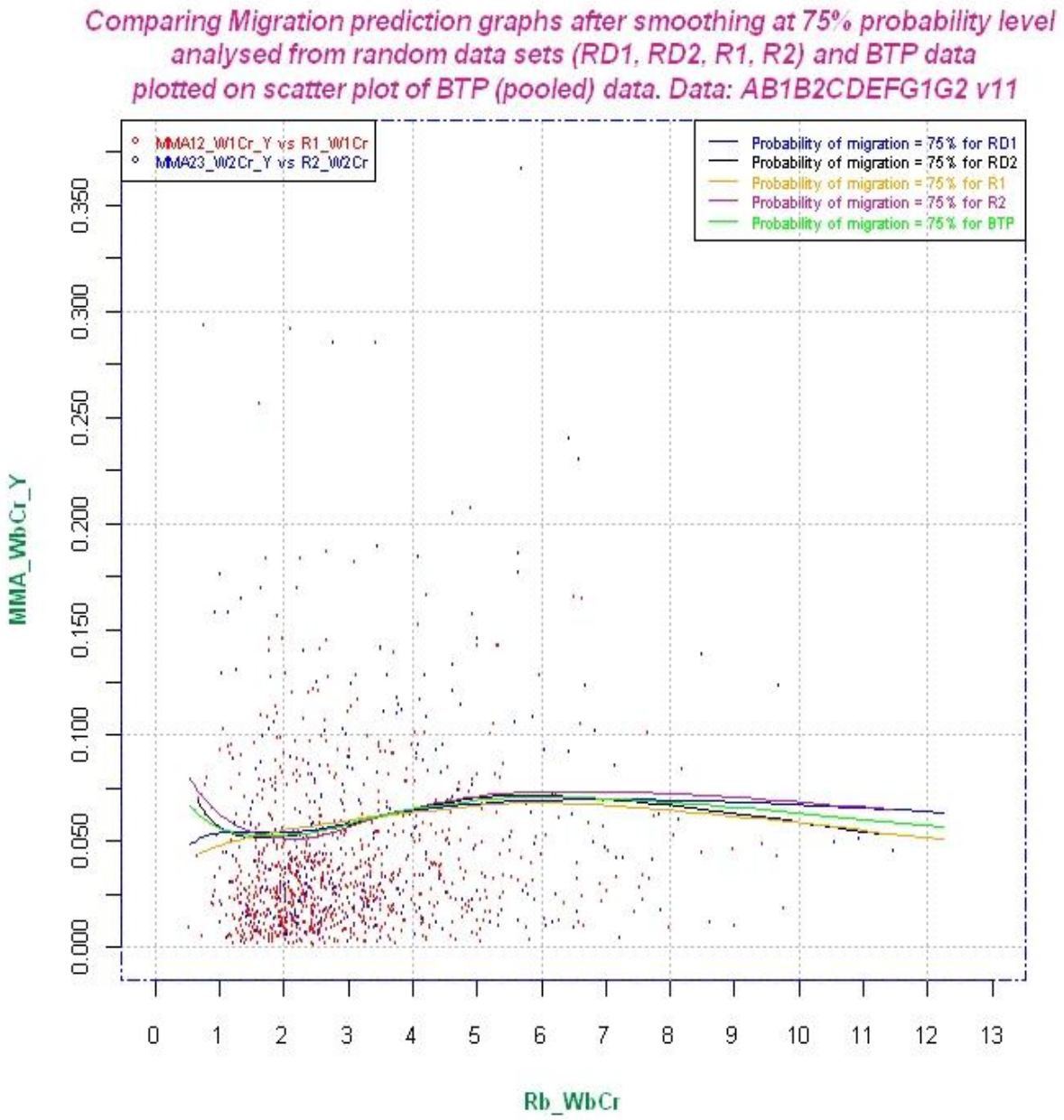

Figure 6.47: Comparison of smoothed 75% probability curves for RD1, RD2, R1, R2, and BTP.

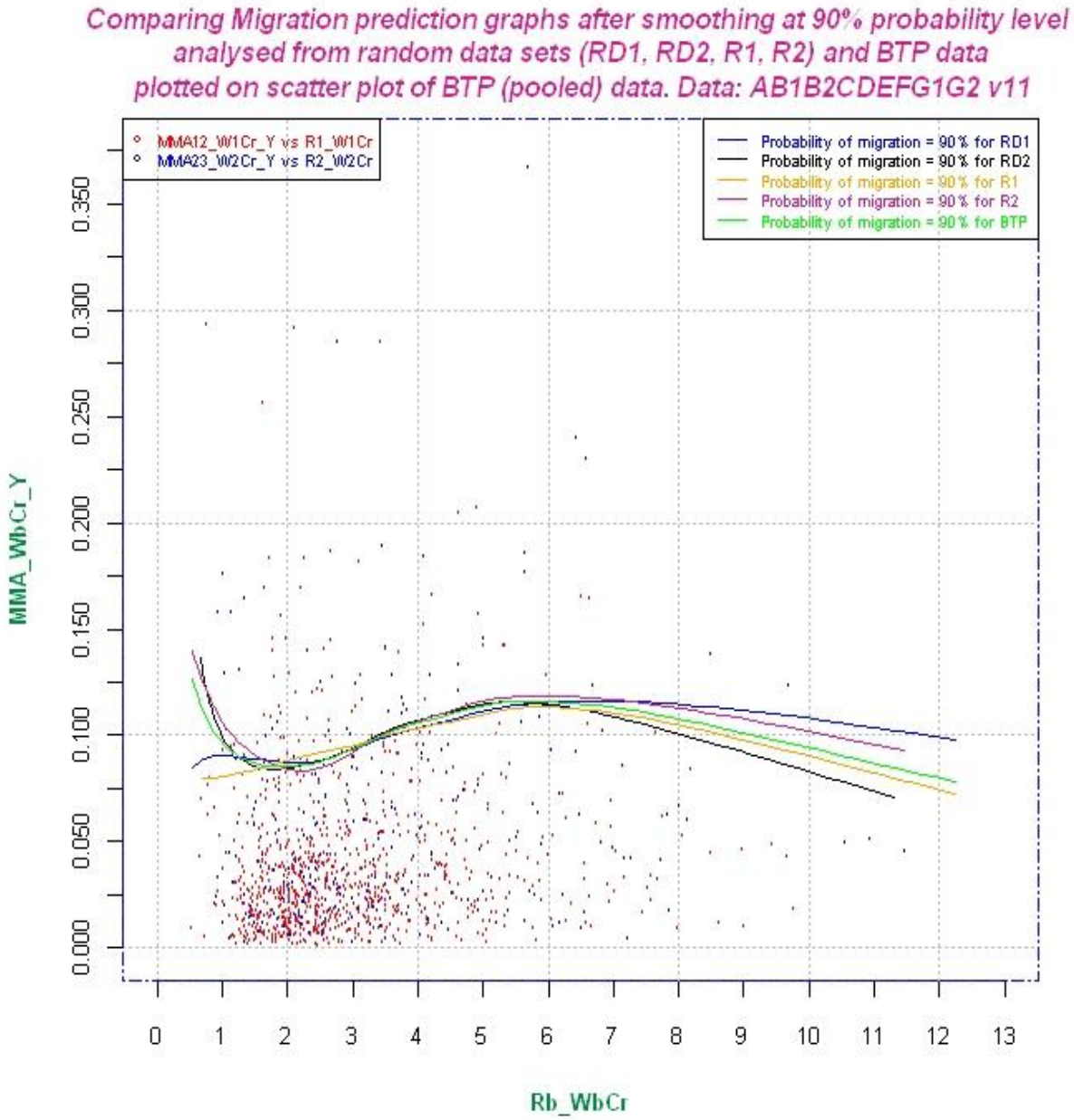

Figure 6.48: Comparison of smoothed 90% probability curves for RD1, RD2, R1, R2, and BTP.

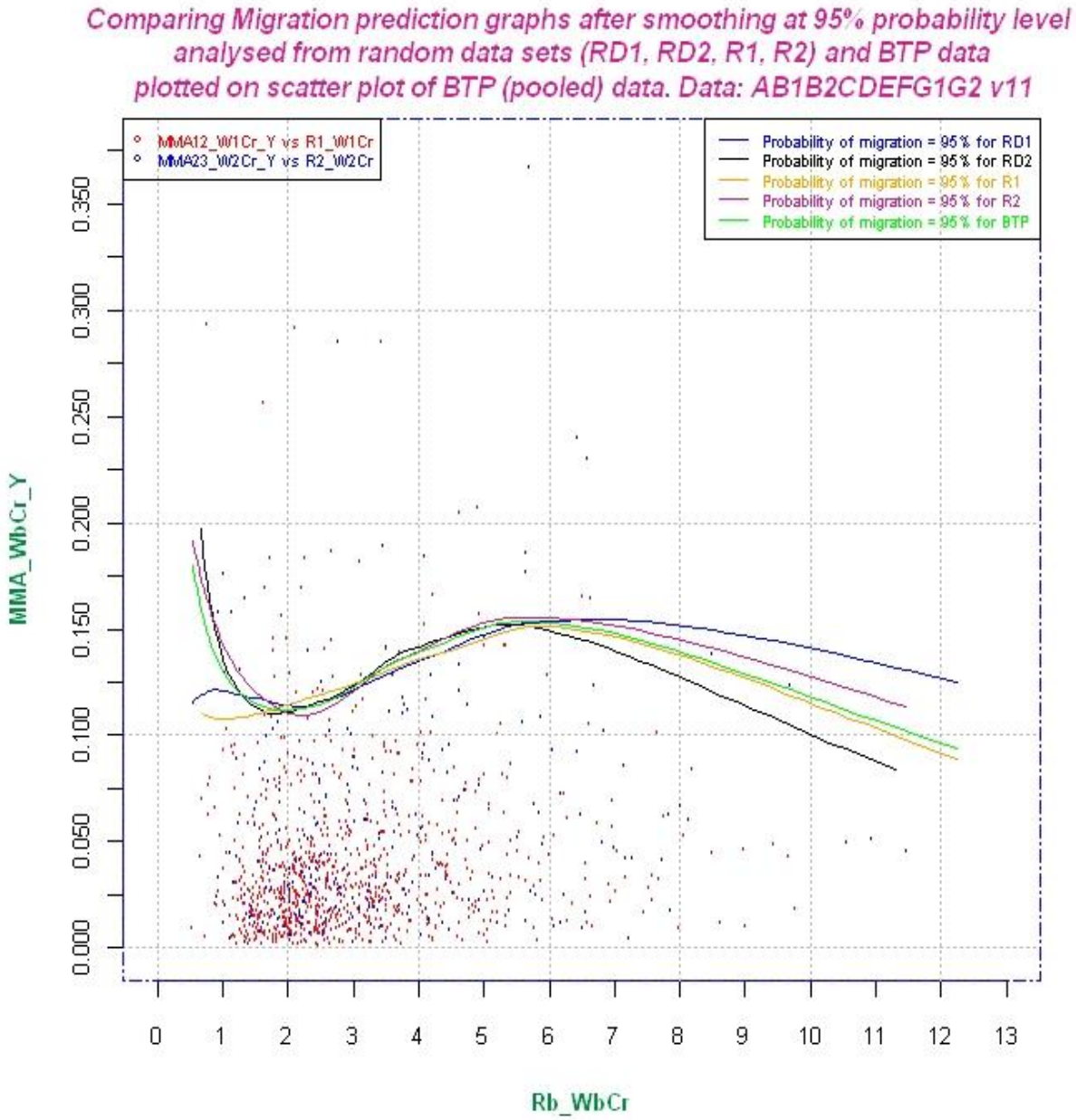

Figure 6.49: Comparison of smoothed 95% probability curves for RD1, RD2, R1, R2, and BTP.

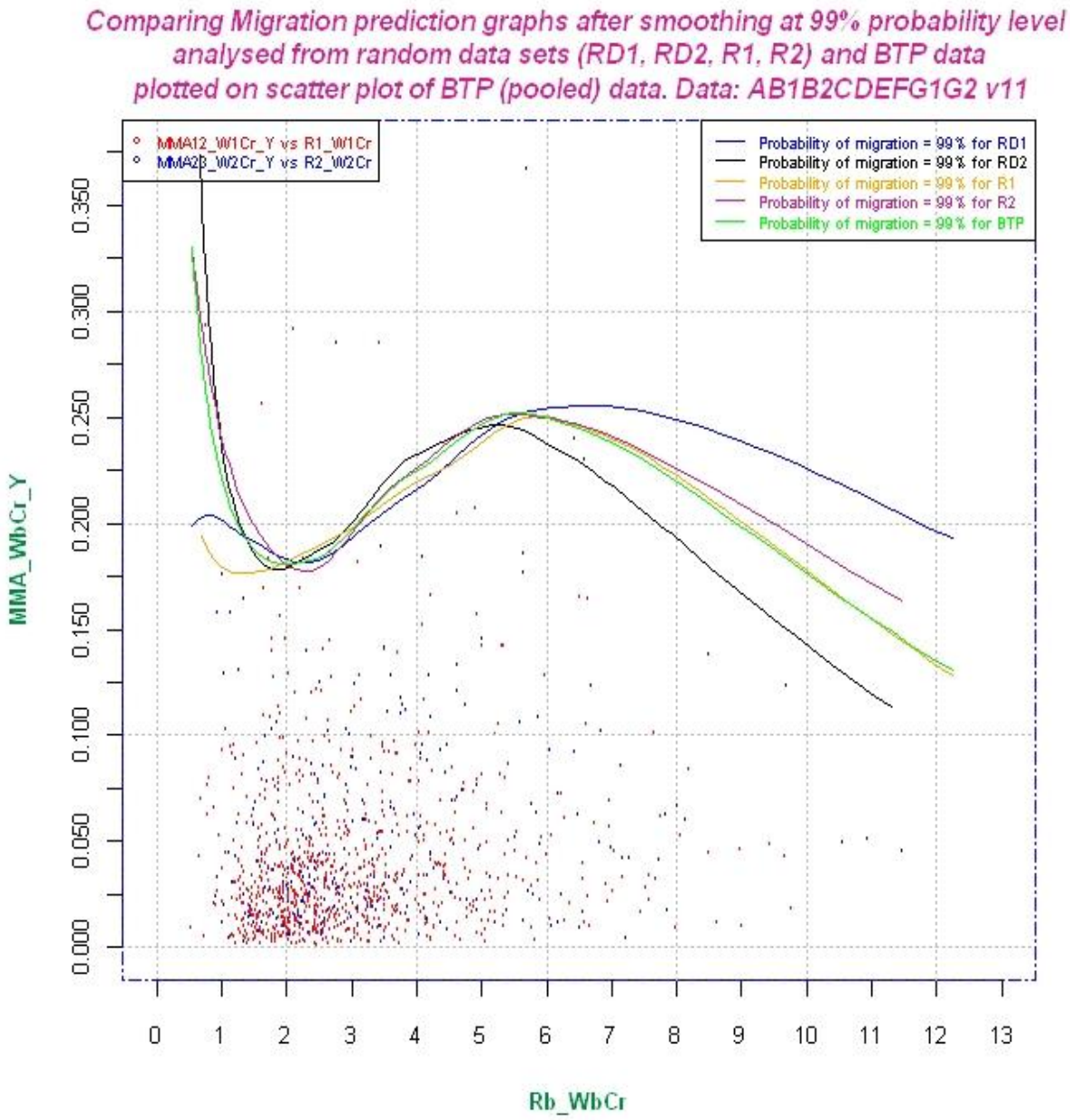

Figure 6.50: Comparison of smoothed 99% probability curves for RD1, RD2, R1, R2, and BTP.

The only certainty is that nothing is certain.

--- Pliny the Elder

Chapter 7
Migration Analysis and Risk Assessment

7.1 Overview

This chapter examines how the risks posed by a problematic bend in a meandering, alluvial stream can be assessed using the analyses and tools developed in the previous chapters. In principle, risk assessment is the basis for risk management and it is within that wider context that this chapter addresses the elements and challenges of risk management that a river engineer, scientist or manager using the tools must deal with when meander evolution causes the channel to move across a floodplain that is not in its natural state, but has been occupied and developed by people.

The data used to support risk assessment have already been described (see Chapter 4), as have the analyses (Chapter 5) and the outcomes of exploratory testing of the method to demonstrate its robustness and reliability (Chapter 6). However, these elements alone are insufficient to deliver a sound assessment of risk. Hence, this chapter considers the issues and deals with the problems to be overcome in practical application of the tools to risk assessment, starting with how to identify a 'bend' in the first place and concluding with a step-by-step account of how to calculate the risk that it poses to people, resources, assets or infrastructure on the floodplain.

7.2 Defining and Identifying the 'Bend' to be Assessed

7.2.1 The Ideal Meandering Planform

Before the risk associated with a particular bend in a meandering river (which has many bends) can be computed, it is of course necessary to identify and accurately characterise the bend to be

assessed. This requires the user to apply a consistent definition of what constitutes a 'bend' in a meandering stream, which, in practice, is seldom as intuitively obvious as it might appear. Reference to the 'text book' representation of a meandering channel, for example, as illustrated by the Central Board of Irrigation in India in Figure 7.1, suggests that identifying the bends should be straightforward.

According to this idealised representation, each meander comprises two, alternating bends separated by a relatively straight crossing reach. Hence, and taking into account the bend characteristic morphology of a meandering stream, a meander is a reach that extends over three inflection points with crossing bars or riffles and contains two complete bends, each with its own apex, scour pool, inner bank point bar, and outer bank river cliff (i.e. points A to H in Figure 7.1). It follows that the meander has the form of a wave, the length of which can be defined by starting at any point along either bank of the river and then following the curved path downstream to the equivalent point in the waveform. Customarily, however, the wavelength is measured between consecutive bend apices on the same bank (i.e. points B to I in Figure 7.1). In essence though, the meander form and its wavelength could just as well be specified as extending from points C to J in Figure 7.1.

In contrast, it is not possible to delineate a bend as starting and finishing at any arbitrary points along the sinuous planform. While, by definition, each meander includes two bends, in identifying a bend it would not be appropriate to start at the apex of a meander waveform (e.g. point B in Figure 7.1) and then follow along the curved path through points C, D to finish halfway through the wave length at point F, because the reach between B and F clearly does not constitute a 'bend' even though it occupies half the length of a meander. This is the case because *in the context of analysing the current and past geometries of a bend with a view to predicting the probability of different rates of future migration* a bend has particular planform, fluvial and morphological characteristics that drive and condition its evolutionary behaviour. In this light, the problem is that the channel between points B and F incorporates part of an upstream bend (Bend 1), an entire crossing reach and some portion of a second, downstream bend (Bend 2). The result is that, even

though the reach BF covers half a meander waveform, from a hydromorphological, mechanistic point of view it cannot be regarded as a 'bend' and most importantly it would not provide the basis for the analysis of past bend migration and the prediction of future risks. This argument may seem obvious when considered in terms of the 'textbook' meandering channel represented in Figure 7.1 but it is important to make this point very clearly, by reference to an idealised case, before addressing the more difficult problem of correctly identifying and delineating the study bend in a real meandering river.

Based on the planform of an ideal, meandering channel and bearing in mind this discussion, it may be concluded that, notwithstanding the existence of other definitions in the literature, the *starting point* for defining a 'bend' for the purposes of migration risk assessment may be taken as being:

A bend starts at the inflection point in the upstream crossing reach and ends at the inflection point in the next crossing reach downstream, encompassing the curved portion of the meander in between and extending over a distance equal to half the meander wavelength.

The importance of this initial debate and the generation of an idealised definition of a meander and a bend is that it provides the base for what follows. The point is that when considering a textbook, meandering stream there is no need to add qualifiers to the terms meander and bend such as 'simple' or 'compound'; the terms are themselves sufficient to define the feature and support its recognition by inspection - be that in the field or via an aerial photograph, satellite image or map. The literature reviewed in Chapter 1 tells a different story, of course. In nature, the pair of bends that constitute a meander are rarely symmetrical and neither are they a mirror image of each other. In fact, it is almost unknown for consecutive bends to be precisely equal in shape or size. Even so, experienced river scientists and engineers would agree that it is possible to identify a curve in the pattern of a sinuous stream as being a single entity – that is, a 'meander bend', because bends are an obvious, geometric component of the meandering planform. It follows that the challenge in identifying and delineating a 'bend' for the purpose of applying the

migration prediction tool developed herein lies in doing so in a rigorous, objective and, above all, repeatable manner that supports sound analysis and which produces reliable predictions of the probability that the calculated amount of migration will not be exceeded during the specified period of time.

7.2.2 Mathematical Bend Definition Based on Planform Concavity and Inflection

Based on the existence of ideal or textbook meandering and the definition of a bend that stems from consideration of idealised meandering, there is reason to believe that a 'bend' could simply be defined and hence recognised mathematically, based on two prominent, geometrical attributes of the planform of a sinuous channel:

(1) the presence of concavity at the outer margins of bends, and

(2) the necessity for a point of inflection to occur within the crossing reach between consecutive bends.

This supposition deserves exploration to determine whether it could be used by practitioners as a completely objective way of recognising a bend for migration risk assessment purposes. In this context, it is the *outer bankline* that is crucial because the analysis and tool are framed in terms of bend geometry expressed by the attributes of that feature.

Visually, the bankline is concave downwards if a portion of the curve it describes falls below a tangent to that curve and is concave up if the curve rises above the tangent. For example, Figure 7.2 illustrates downward concavity in a curve with the equation $y = - x^2$. Mathematically, it is possible to test for concavity by calculating and interpreting the values of the first and second derivatives of the equation defining the curve of the bankline, expressed in x-y coordinates.

The first derivative test for concavity: Over an interval of a differentiable function, the graph is concave up when the first derivative is increasing, and concave down when it is decreasing. This test is set out in Box 7.1.

Box 7.1

If y = f(x) is a differentiable function
I = interval over which the function is differentiated
y` = first derivative of the function

andy´ is increasing over I, ⟶ curvature for y = f(x) is concave up
or y´ is decreasing over I, ⟶ curvature for y = f(x) is concave down

The second derivative test for concavity: If a function is differentiated twice over an interval then the curve is concave upwards if the value of the second derivative is positive and concave down if it is negative. The second derivative test for concavity is set out in Box 7.2.

Box 7.2

If y = f(x) is a differentiable function
I = the interval over which the function is differentiated
y´´ = the second derivative of the function

andy´´ > 0 over I, ⟶ curvature for y = f(x) is concave up
or if y´´ < 0 over I, ⟶ curvature for y = f(x) is concave down

Visually, an inflection point in the bankline must occur in the curve between consecutive lengths of it with opposite senses of concavity. For example, Figure 7.3 illustrates the inflection point in a curve with the equation $y = x^3$

Mathematically, the point of inflection is where the graph of a function has a tangent line and where the concavity changes (Thomas and Finney, 1996). Hence, the second derivative has a value of zero at an inflection point. However, it should be noted that the second derivative may be undefined at the point of inflection.

In light of the mathematical definition of an inflection point, an objective definition of the extent of a 'bend' might be:

A bend extends between two, consecutive inflection points in a meandering river defined, for the purpose of migration risk assessment, by the curve of the outer bankline of that bend.

However, having defined the existence and extent a bend objectively it is now necessary to explore whether mathematical definitions can, *in practice*, provide a suitable approach for users needing to recognise and characterise a bend for migration analysis and risk assessment.

In theory, a user could use these mathematical definitions to identify the presence and extent of a problematic bend. However, there are fundamental problems with this approach that become apparent as soon as an attempt is made to apply it to a real reach of a meandering river. These problems stem from the fact that the planforms of real meanders do not display the regular, geometric patterns of ideal meanders, with the result that there may often be more than one candidate bend between each pair of consecutive inflection points. For example, Figure 7.4 shows a hypothetical river reach extending between two inflection points, labelled A and E. The reach A-E includes two bends separated by relatively straight reach. Visual inspection suggests that Bend 1 extends from A to C, with the bend apex being at B. Bend 2 extends from C to E, with the bend apex at D. It may be concluded that this is a double-headed meander loop and, for such features, the principle that a single bend will be found between consecutive inflection points is inapplicable. Attempting to recognise and characterise a bend using this rule when applying the bend migration analyses and prediction tool developed in Chapter 5 and tested in Chapter 6 would certainly lead to unreliable results. Figure 7.4 shows a hypothetical case, but it is easy to find such situations in nature, as demonstrated between points G and H on the meandering Souris River near Voltaire, North Dakota, USA (Figure 7.5), and the loop containing Bends 4 and 5 in the aerial photograph shown in Figure 7.6.

In fact, it is even possible to find three bends between consecutive inflection points (Figure 7.7). In this hypothetical example, it is easy to identify two bends (corresponding to Bends 1 and 2 in Figure 7.4) but closer inspection of the reach CDE suggests the presence of a third bend of lower curvature. Depending on the precise location of the asset at risk on the floodplain, any of these three bends could pose a significant threat and could, therefore, merit individual analysis. Despite its low curvature, the third bend might pose the highest risk if the asset lies in close proximity to its outer bank. Figure 7.7 is hypothetical, but a real example of this situation may be found between points I to J in Figure 7.5.

This finding indicates that while the sense of curvature cannot change between successive inflection points, it is distinctly possible for there to be two or more individual bends in a reach so defined. On this basis, the reach does not constitute a ‘bend’ but might more accurately be defined as a *monocave*, where:

A monocave is a reach between consecutive inflection points in a serpentine river (that is: highly sinuous) that displays a single sense of concavity, but which includes more than one bend.

Inspection of rivers with mature, tortuous meandering planforms reveals even more complex situations, where a feature that can be identified as single large-scale, loop (loop in a general sense, not a loop as defined by Brice (1983)) contains not only more than one bend, but more than *monocave*, and hence, more than one contemporary meander. This type of two-phase meandering is demonstrated not only in Figure 7.8, which shows a hypothetical example, but also in the reach between points X and Y of the Souris River in Figure 7.5. Such a complex loop broadly has the appearance of a shepherd's crook where:

A crook is a large-scale, complex loop in a mature, tortuously meandering river that contains more than one bend, more than a monocave and, hence, more than one contemporary meander.

In summary, exploration of the potential for mathematical analysis of bankline concavity and inflection demonstrates that this can only provide a simple, objective method of recognising and characterising a bend for the purpose of migration risk assessment in the case of idealised, textbook meandering channels. Consideration of hypothetical examples that mimic features observed in the planforms of real meandering rivers shows that single bends do not always extend from one inflection point to the next and reveals that it is possible to identify not only bends and intervening straight reaches, but also multiple bends within monocaves or crooks that contain multiple bends, straights, and meanders within a single, much larger planform feature.

It must, therefore, be concluded that, at present, planform complexity in naturally meandering rivers rules out development of a totally objective, theoretically-based method of recognising and characterising a 'bend' for the purpose of migration analysis and risk assessment. The only feasible alternative is for users familiar with river mechanics and fluvial geomorphology to systematically break the reach in question down into crooks, monocaves and bends, identify bends with the potential to pose a hazard to a floodplain asset or assets, and perform risk assessments for all such bends that may pose a hazard to people, resources, assets or infrastructure located in the morphologically active portion of the floodplain.

7.3 Performing Bend Migration Analysis

7.3.1 Overview

Having identified a problematic bend, to embark on migration risk assessment it first necessary to measure the geometric parameters required for migration analysis and prediction. Clearly, the measurements must be made in accordance with the ways in which the data used in developing the analysis were collected and in ways appropriate to application of the migration prediction tool.

In a general sense, the independent variable used in analysis and prediction of the average annual migration rate involves measuring the radius of curvature of the bend and the channel width. However, as discussed in Chapter 1 and in the preceding sections of this chapter, the bends of real meandering streams do not follow regular, mathematical curves and, in detail, no two bends are the same. Therefore, for all the reasons explained previously in this thesis, it is inevitable that the actual planform attributes of a bend must be approximated by those of a circular arc that best fits the curve of the outer bankline over the extent of the bend that is actively migrating.

If migration analysis and prediction are to be performed reliably, fitting the circular arc to the curve of the outer bank requires that the user makes significant decisions concerning selection of:

(i) to which part of the bend, and

(ii) over what extent of bankline,

the circular arc is fitted.

Indeed, the success of a bend migration analysis and prediction depends on satisfactory selection of the fitted arc. This issue will be explored and demonstrated later in the chapter, using examples from natural streams.

In this research, future *bend migration* is the focus and, hence, the first attribute of the bend to be considered is the migration zone in the bend: that is, the extent of the outer bankline that is likely to be involved in future migration. In analysing and predicting migration, this is related to the

bend's *radius of curvature,* which is represented by the radius of a circle fitted to the outer bankline. Bend migration is represented in the analysis by shifting of the *bend apex*. Hence, it is vital to accurately identify the apex of the problematic bend. It is also relevant to consider *Bend orientation* as this affects the direction of migration. Hence, it is necessary to measure the orientation of the bend by drawing a line that joins the centre of the arc fitted to the bend to its apex. These bend attributes are illustrated in Figure 7.9.

7.3.2 Characterising the Bend

This is, perhaps, the most important task in migration analysis. Having identified the problem bend, the user should take the following steps to characterise it, prior to measuring the attributes necessary to support migration analysis and prediction:

1. Delineate the active migration zone;
2. Identify the bend apex;
3. Fit a circular arc to the bankline in the active migration zone in such a way that as much bankline as possible coincides with the fitted circular arc;
4. Measure the bend (i.e outer bankline) radius.

In delineating the active migration zone, where historical information is available, the extent of the bend that is involved in migration may be based on the past behaviour of the bankline around the problem bend. Field reconnaissance can add valuable additional information on the extent of the currently active migration zone through establishing upstream and downstream limits to the steep river cliff that often indicates the actively retreating portion of the outer bankline.

In identifying the bend apex, it must be remembered that this may not necessarily be located in the middle of the active migration zone. For example, if the bend is asymmetrical, its apex will be skewed up or downstream. The apex represents a very important feature of the bend and one that must be located before any attempt is made to fit a circular arc to the curve of the outer bank in the active migration zone. Usually, when fitting the circular arc every attempt should be made to ensure that it passes through the bend apex. However, there may be circumstances where the apex

protrudes into the floodplain from the surrounding bankline. Under these circumstances, forcing the circular arc through the apex may result in a poor overall fit. Where this is the case, a compromise must be made, with the junction of a line defining the bend axis and the fitted arc taken as the bend apex for migration analysis and prediction purposes. The distance between the centre of the best fitted circle and bend apex (or selected point on the fitted circular arc) then indicates the bend radius.

7.3.3 Practical Issues

Migration analysis involves four geometric elements: bend apex, bend orientation line, radius of curvature and crossing width. The analysis takes *apex migration* as being representative of bend migration (see Section 4.2 in Chapter 4). In the steps set out above, it is stressed that fitting the circular arc representing the curvature of the outer bank starts by reference to the bend apex, so identifying this feature is crucial. This can be illustrated by reference to Figure 7.10, which shows a reach famous for its tortuous meander bends in the Mississippi River near Greenville, Mississippi.

Inspection reveals that two separate bends (ABC and CDE) can be recognised within the longer *monocave* reach: ABCDE. The apices of both these bends may easily be identified and circular arcs fit the curves of the outer banklines conformably. Considering the likely active migration zones of the bends, the subtended angle for the fitted circular arc at ABC is 93°, while that at bend CDE is slightly smaller, at 85°. The good fit of the circular arcs and the fact that they fit substantial portions of the banklines at the bends suggests that the calculated radii of these arcs should be adequate to support reliable migration analysis and prediction.

Having identified the problem bend, the next step is to make the relevant measurements. This may be approached in one of two ways:

1. The user can take prototype measurements on site. This can be difficult if the site is inaccessible or the bend is too large, which may make it impossible to measure its radius in the field. However, if it is possible to visit the bend, this will certainly help in identifying the extent of the current migration zone and recognising the bend apex.
2. The user can use aerial photographs, satellite images or maps in making the measurements.

7.3.4 Example

Application of the principles and considerations of the issues raised above can be demonstrated based on a stretch of a natural river. This demonstration is given below in Box 7.3

Box 7.3

Purpose: Demonstration of how to identify, characterise and measure a problem bend in practice

Source: Reach map of bends in the Mississippi River near Greenville, Mississippi, USA (Figure 7.10) that were commented on by Lane (1957). Map scale: 1 cm = 1,462.7 m. The bends used in this demonstration come from the sub-reach that extends between points X and Y.

Careful inspection of the monocave reach ABCDE leads to recognition of two bends with active migration zones. The first (ABC) has its apex B while the second (CDE) has its apex at D, where island I appears to be promoting outer bank retreat. Circular arcs may be fitted conformably to the outer banklines in both these bends, increasing confidence that they have been accurately identified. However, it is possible that a user might decide to treat the entire monocave (ABCDE) as a single bend with its apex at point C and the outcome of this selection is also considered in the worked example presented here.

Measurements made for the single, large bend (ABCDE), with its apex at C, would yield:

Extent of active migration zone = BD
Outer bank radius of curvature = 1,741 m
Width at upstream crossing (at point A) = 878 m
Width at downstream crossing (at point E) = 951 m
Average width at crossings = 914 m
R/W = 1.9

Conversely, if it is recognised that the monocave loop contains two bends, measurements yield:

For bend ABC:

Extent of active migration zone ABC
Bend apex location = B
Outer bank radius of curvatute = 388 m
Width at upstream crossing (at point A) = 878 m
Width at downstream crossing (at point C) = 439 m
Average width at crossing = 658 m
R/W = 0.56 (nb. as this is less than 1, the probability analysis should NOT be applied)

And for the bend CDE:

Extent of active migration zone from midway between B & D to midway between D & E
Bend apex location = D
Outer bank radius of curvature = 190 m
Width at upstream crossing (at point C) = 439 m
Width at downstream crossing (at point E) = 951 m
Average width at crossing = 695 m
R/W = 0.27 (nb. as this is less than 1, the probability analysis should NOT be applied)

The worked example in Box 7.3 clearly illustrates the profound importance of correctly identifying and characterising the problem bend in that a decision to treat the entire monocave ABCDE as one bend produces a completely different set of bend measurements to those produced when the presence of two bends is recognised. Indeed, when two bends are (correctly) identified, it emerges that the probability analysis should not be applied at all. It follows that failure to correctly identify the problem bend will definitely lead to inaccurate and unreliable migration analysis and, ultimately, a weak assessment of future migration risk. Therefore, it is of the uttermost importance to correctly identify and characterise the problem bend(s)**.** This highlights the need for users to draw on all available evidence when identifying bends and this should include consideration of scale effects and *self-similarity* in the bends. The conclusion is that the entire planform pattern of a complex, meandering river must be included in the inspection, so that active and relic bends can properly be differentiated and measured. Otherwise, misleading outcomes are inevitable. This topic is discussed further in Section 8.9 of Chapter 8.

7.4 Risk Assessment

7.4.1 Bend Migration as a Hazard

A hazard is a phenomenon the occurrence of which causes a threat to life, health, property or the environment. Hence, for example, a flood event may not be regarded as a hazard unless it has the potential to cause harm: that is unless it poses a *threat*.

A hazard may be dormant or active. An example of a dormant hazard would be a volcano that has not erupted for several centuries, but which would threaten a village if it were to do so. With respect to its latency as a hazard, a bend in a meandering river would usually be regarded as being active, since a river is a dynamic geomorphic agent capable of eroding its banks and consuming part of the floodplain at any time, in response to the cumulative action of repeated, channel formative flows or the impact of one or more flood events.

From the causation point of view, hazards fall into two categories - natural and anthropogenic. An earthquake is an example of a natural hazard as its occurrence is unaffected by the actions of

people. Conversely, a construction site is an anthropogenic hazard as it is artificially created and can cause harm to people visiting the site or even passing by close by to it. However, a blend of the two categories can exist in that a natural event that would not normally pose a threat may do so due to being manipulated by humans. For example, mis-management of water storage in a flood control reservoir might lead to the emergency spillway passing a flow of unnatural magnitude or timing that results in sudden, severe flooding downstream: which may pose a threat to property, or even life.

The threats posed by different hazards are quite different. For example, an earthquake is a sudden event that is difficult to observe and not currently predictable. Its duration is short, but its impacts may be catastrophic. Conversely, stream bank erosion is an almost continuous process that can be observed and predicted; the effects of which are cumulative and chronic, rather than sudden and acute. Even so, the cause of an earthquake (energy building up in the underlying rock strata) is almost continuous when considered on a geological timescale and, hence, in that sense the process is, like bank erosion, incremental. The threat is greater only because of the magnitude and sudden occurrence of the hazard, coupled with the lack of fore warning.

The threat posed by a bank erosion hazard is also different because bank retreat is an observable phenomenon that can be detected easily if anybody troubles to look for it. Also, most bank erosion can be prevented (albeit at cost to the riparian and river environments), while preventive measures are impossible for an earthquake. Hence, the possibility exists for either predicting and mitigating or preventing an erosion hazard in a way that is not feasible for many other natural hazards.

However, how an erosion hazard is studied and regarded is an important consideration. Conceptually, this introduces a broad range of considerations with regard to the spatial and temporal dimensions of the hazard and whether the threat it poses is perceived and assessed objectively or subjectively. In the spatial dimension, the hazard posed by bank erosion is not uniformly distributed across the floodplain. The probability of erosion attacking a point at a given distance back from the bankline of a meandering stream is much lower at the crossing than it is adjacent to the concave bank of a bend and this must be recognised when the threat posed by the erosion hazard is considered.

With respect to the temporal dimension, the design life of a structure built in the floodplain becomes an issue when the threat posed to it by the bank erosion hazard is being considered. For example, the designer of a piece of long-term infrastructure such as a railway must look ahead decades or centuries when deciding on the alignment of the permanent way and setting the minimum set back distance from the river, lest his or her descendents be faced with a hazardous situation. Conversely, the designer of prefabricated changing rooms at a sports facility need look no further ahead than a generation, as the useful lifespan of the building is no more than twenty years.

People living and working in the floodplain must themselves gauge the threat posed by hazards associated with the river, including erosion. In this respect issues of subjectivity and perception come to the fore and many individuals and organisations will struggle to make sensible judgements regarding how a current erosion hazard should be taken into account in planning, designing and maintaining dwellings, assets and infrastructure. The problem is even more difficult with respect to future situations and hazards that may take years or decades to emerge.

Taking these considerations together demonstrates the necessity and importance of recognising the presence, nature and severity of an erosion hazard as a precursor to performing any type of risk assessment. It also highlights the need for the assessor to have the knowledge, experience and expertise necessary to support sound judgement in applying a risk assessment tool to any erosion-related hazard, including bend migration.

7.4.2 Bend Migration as a Risk

The word ‘risk’ is frequently used in multiple ways by people in all walks of life, but in a formal ‘risk assessment’ it conveys a particular meaning that differs from that in everyday usage. Of particular importance is the need to differentiate between risk and uncertainty.

Frank (1921) stated that, “Uncertainty must be taken in a sense radically distinct from the familiar notion of risk, from which it has never been properly separated.” He then went on to show that risk always involves measureable uncertainty. More recently, Douglas (2007, 2009) proposed useful and well organised definitions of uncertainty and risk:

Uncertainty: The lack of complete certainty, that is, the existence of more than one possibility. The "true" outcome/state/result/value is not known.

Measurement of uncertainty: A set of probabilities assigned to a set of possibilities. For example, if we say, "There is a 30% chance that there will be a rainfall tomorrow".

Risk: A state of uncertainty where some of the possibilities involve a loss, catastrophe, or another undesirable outcome.

Measurement of risk: A set of possibilities each with quantified probabilities and quantified losses. For example, "There is a 30% probability that the bank will run into debt of $3 million due to the impact of recession".

By this definition, measuring risk involves gauging the loss caused by an event (in terms of assets or money) and the associated probabilities. With respect to the definition of risk associated with the hazard posed by a migrating bend, it follows that:

Migration risk = The consequences of the hazard x The probability of that hazard occurring (7.1)

7.5 Bend Migration Risk Assessment

Clearly, assessment of the risk associated with bend migration is concerned not only with the probability of erosion, but also with its consequences. These consequences relate primarily to the economic importance of the assets (resources, buildings or infrastructure) that might be affected by future bend migration. The importance of avoiding damage may also relate to the political situation and the investment strategy of the local authority or owner of the asset(s) at risk. Possibly, even the personal perceptions and influence of the land or asset owner may be a consideration.

Therefore, in selecting the probability level to be applied in predicting the future erosion rate, care must be exercised in considering the *consequences* should the predicted rate be exceeded. These consequences should be determined by recognising the importance of the assets from all relevant points of view (potentially including financial, social, political, environmental and even military dimensions, as well as potential economic losses). In practice, the level of risk that is acceptable

should be determined by suitably qualified personnel, acting as consultants to the agency or asset owner concerned.

Developing a practical risk assessment tool would not be an appropriate aim for doctoral research in Geography and is therefore beyond the scope of this thesis. Notwithstanding this, it is certainly appropriate to consider how the probabilistic analysis developed here can and will be developed for practical applications in river engineering and management. Hence, general guidance on assessing migration risk is presented in Box 7.4, taking Bend 6 in Figure 7.6 as a hypothetical example of a problematic bend that presents a threat to a pumping station to be constructed on the floodplain.

Herein, it is possible only to set out general guidance to be applied in assessing migration risk, taking Bend 6 in Figure 7.6 as a hypothetical example of a problematic bend and presenting this as a worked example in Box 7.4, below.

In this practical example, migration analysis is used to predict the average annual migration rate for the problem bend (that is, the erosion hazard) at a selected probability level, by applying the prediction tool developed in Section 5.7. The risk associated with the predicted hazard is then assessed using Equation 7.1.

Box 7.4

Assets located in the floodplain adjacent to the outer margin of a migrating bend in an actively meandering, alluvial river may be damaged or destroyed if the bank retreats sufficiently for the river to attack them.

As a case example, consider the case of an irrigation pumping station to be located in the floodplain of a meandering, alluvial river in Bangladesh. The closer the station is to the river, the less the sponsors must spend on pump capacity. But the sponsors wish to protect their investment and ask, "How far back from the bank edge should the pumping station be positioned to avoid it being attacked by the river within the next 10 years?" Because the station is a valuable asset that is difficult to relocate, the sponsors specify a 90% probability that it will not be attacked within 10 years.

I. Predicting the Magnitude of Migration based on the Bend Apex (P.MMA)

Considerations:
p = probability of hazard occurring = 90%
P.TP = time period over which risk assessment will be made = 10 years

Measurements of bend geometry at beginning of the prediction period:
The probabilistic analysis begins by taking the necessary measurements of bend geometry for **Bend 6** in **Figure 7.6** and generating the input parameters as follows:

R_b = radius of curvature of the best-fit, circular arc at outer bank = 215.1 m
W_{bcr} (u/s) = channel width at crossing upstream of the bend = 68.5 m
W_{bcr}(d/s) = channel width at crossing downstream of the bend = 73.5 m

In this case the channel width at the crossings up and downstream of the bend is different and so the average is used to provide a more stable and representative measure, rather than the width at the upstream crossing alone.

Computations:
W_{bcr} = average crossing width at the beginning of the prediction period = 71 m
R_b/W_{bcr} = dimensionless bend radius at the beginning of the prediction period = 3

The graphical form of the bend migration prediction tool (Figure 5.57) may be used to predict the average annual migration rate with a 90% probability of not being equalled or exceeded. To do this:

Locate the value 3 on the x-axis, move up vertically to the 90% curve, then read the corresponding point of y-axis. This yields:

Average annual dimensionless bend migration rate = 0.095

Alternatively, the tabular form of the prediction tool (Table 5.8) may be used to estimate the annual dimensionless rate of bank retreat with a 90% probability of not being equalled or exceeded:

Selecting the row corresponding to R_b/W_{bCr} = 3
Finding the column for probability level = 90%
Reading the value in the cell where the selected row and column meet, which yields 0.094

The predicted extent of bank retreat due to bend migration during the specified period at a 90% probability can then be computed from:
$P.MMA = (MMA/W_{bcr}/Y) \times W_{cr} \times P.TP = 0.095 \times 71 \times 10 =$ **68m**

Based on this calculation, it is possible to recommend that siting the pumping station 68 m away from the river would reduce the probability of it being damaged or destroyed by bank erosion due to meander migration during the next decade to less than 10%

II. Migration Risk Assessment

Suppose siting the station that far back from the river requires equipping it with high power pumps imported from abroad. These pumps would be expensive to purchase and difficult to maintain in Bangladesh compared to less powerful, domestic pumps, making the scheme no longer feasible. The Sponsor then asks, "What would be the risk if the station were positioned 40 m back from the bank, which is the maximum distance feasible for domestic pumps?"

The probability that more than 40 m of bank retreat (that is the migration hazard) will occur during the next 10 years may also be predicted using Table 5.8.

For 40 m of bank migration in 10 years, the annual rate is 4 m per year. Hence, the dimensionless annual retreat rate for this river is:

MMA = 4/71 = 0.056

In Table 5.8, in the row corresponding to $R_b/W_{bCr} = 3$ is:

Rb/WbCr	50%	60%	75%	80%	90%	95%	97%	98%	99%
3.03	0.033	0.041	0.058	0.067	0.094	0.123	0.145	0.163	0.197

Hence, the probability of MMA not being equal to or greater than 0.056 is approximately 75%. It follows that the probability of a pumping station 40 m back from the bank being attacked by the river due to bend migration is close to 25%.

The consequences were this erosion to occur may be expressed in terms of the value of the pumping station equipped with domestic pumps (£100,000). The risk is that consequence multiplied by the probability that its destruction due to bank erosion will actually occur (Equation 7.1). Hence:

Erosion risk = Consequences of the hazard * probability of occurrence of that hazard
= 100,000 x 0.25
= £25,000

Armed with this risk estimate, the sponsor can decide whether to accept this risk or invest some additional money in bank protection works to prevent any bank retreat and so protect the asset from attack. This decision would be guided by the cost/benefit ratio between the capital and maintenance costs of bank protection versus the benefit of eliminating the risk that the pumping station might be destroyed within a decade of its installation.

It might well be the case that installing the type of heavy protection necessary to effectively stabilise the bank on its present alignment for 10 years could not be done for £25,000. However, the tool could then be used to evaluate other options too – for example using soft measures to reduce the retreat rate to an acceptable (but non-zero) rate. In either case, a risk-based cost-benefit decision could be made.

Box 7.4 illustrates how the probabilistic analysis might be used to make a risk-based decision on how far back from the river bank to position a piece of key infrastructure. It also shows how the analysis can be used to support a Quantitative Risk Assessment (QRA) for a fixed asset located at a known distance from the edge of the outer bank of a problematic bend. These are but two examples of the practical utility of the analysis. Another common application would be to use the probabilistic analysis to estimate the risk to a diffuse floodplain asset such as an arable field adjacent to the outer margin of an active meander bend. However, a different type of risk calculation is required in such applications.

In the case of a point asset, the consequences (damages) of bend migration are zero up until the point where the retreating bank undermines the asset. At that point the asset is damaged or destroyed, depending on the type of infrastructure, In the case of an arable field, damage begins

as soon as the bank retreats at all. Damage then accrues with increasing migration distance, as the area consumed by the river grows.

In this type of application, consequences increase progressively as the bend migrates and the risk (probability x consequence) is represented by the area under a curve defining the relationship between the probability of the bank retreating a given distance (x-variable) and the damage should it do so (y-variable). The risk is represented by the area under the curve, which may be calculated by integrating the probability-damage curve between zero and an upper bound probability limit (e.g. 50%, 90%, 99%) specified by the user.

The probability-damage curve is different for every case, being a function of both the bend characteristics and the area and value of the land at risk, necessitating a site-specific risk analysis.

Engineers and river scientists performing river analyses to support management or restoration could improve the quality and reliability of the information supplied to decision makers using QRA and they constitute the potential 'end users' for practical tools based on the probabilistic analysis developed in this thesis. However, they will require both clear guidance on how to apply the analysis and some understanding of the statistics that underpins it. Production of a Guidance Manual and a published paper will, therefore, be the subject of my work with the aim of issuing the Guidance Manual and submitting the paper within 12 months of the award of the doctorate.

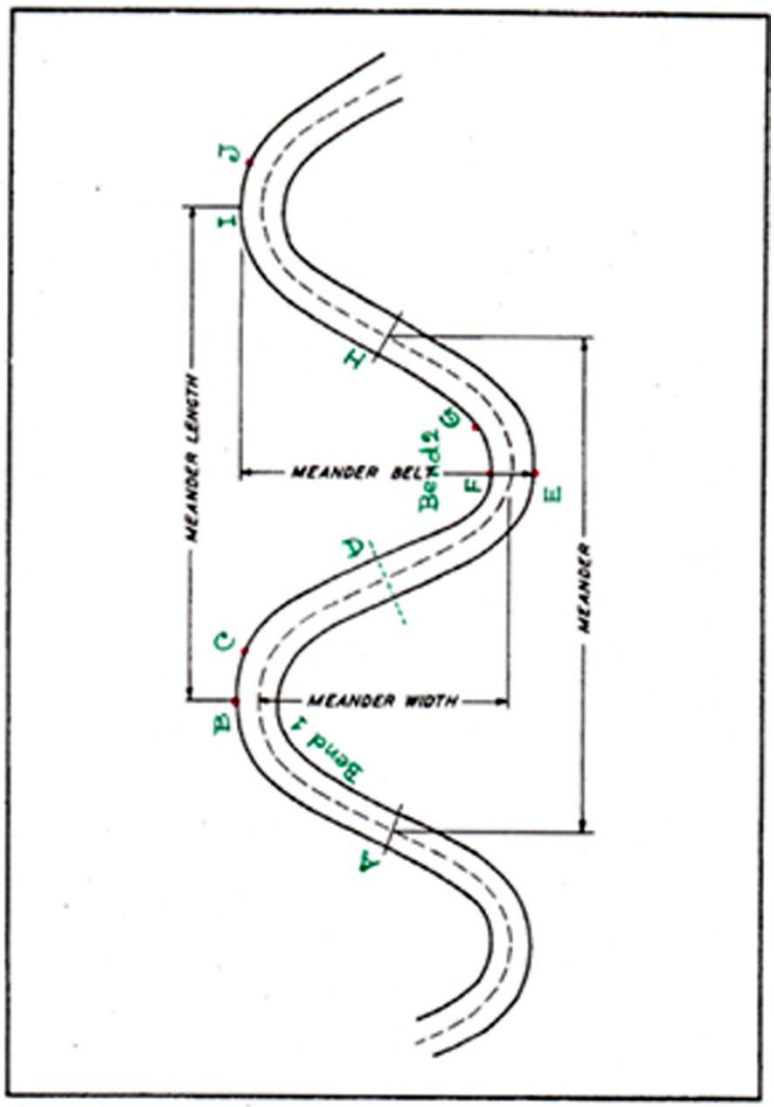

Figure 7.1: Definition sketch of a meandering channel as recommended by the Central Board of Irrigation of India (adapted from Lane, 1957).

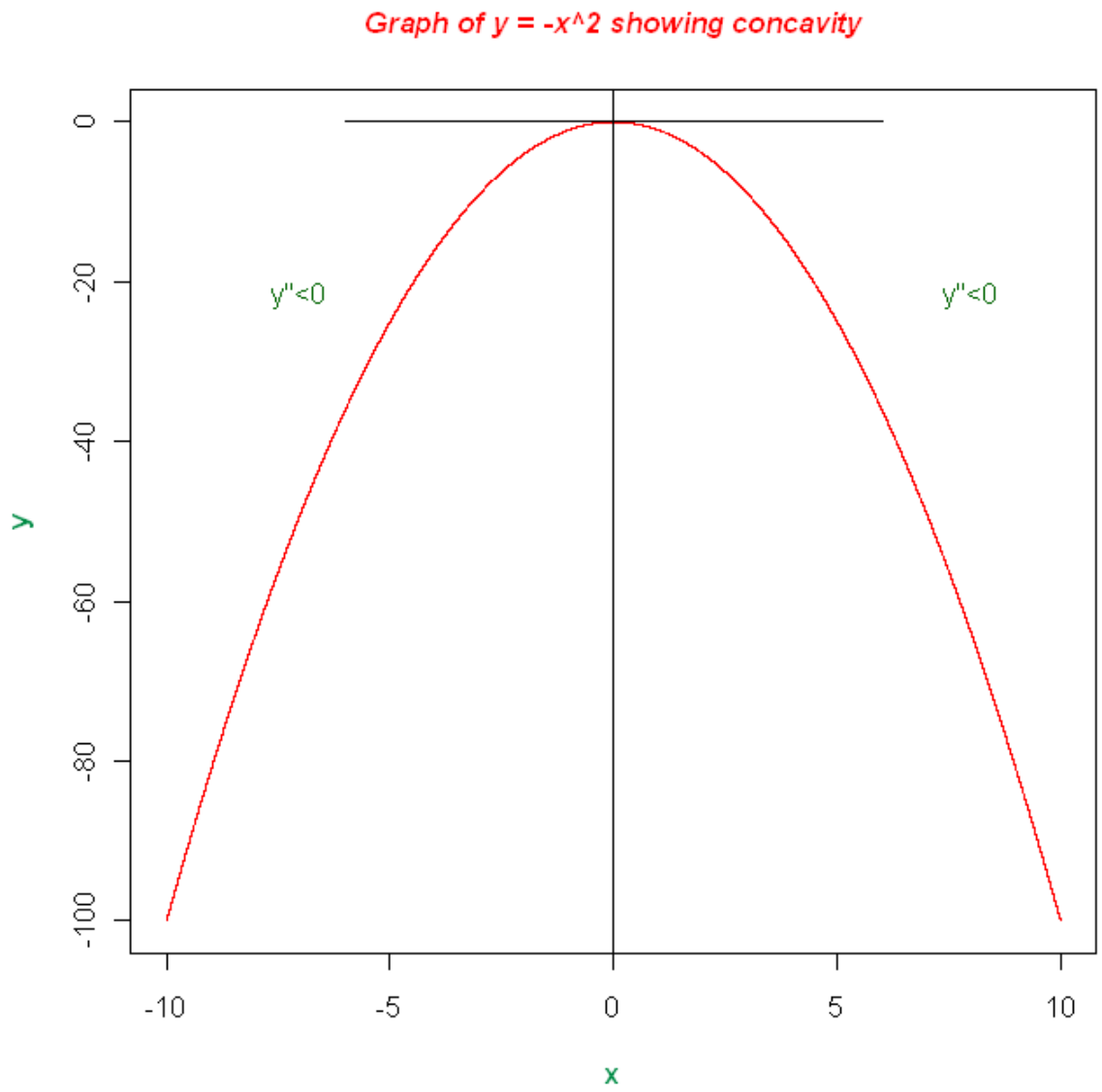

Figure 7.2: Graph to illustrate downward concavity in the curve for, $y = -x^2$.

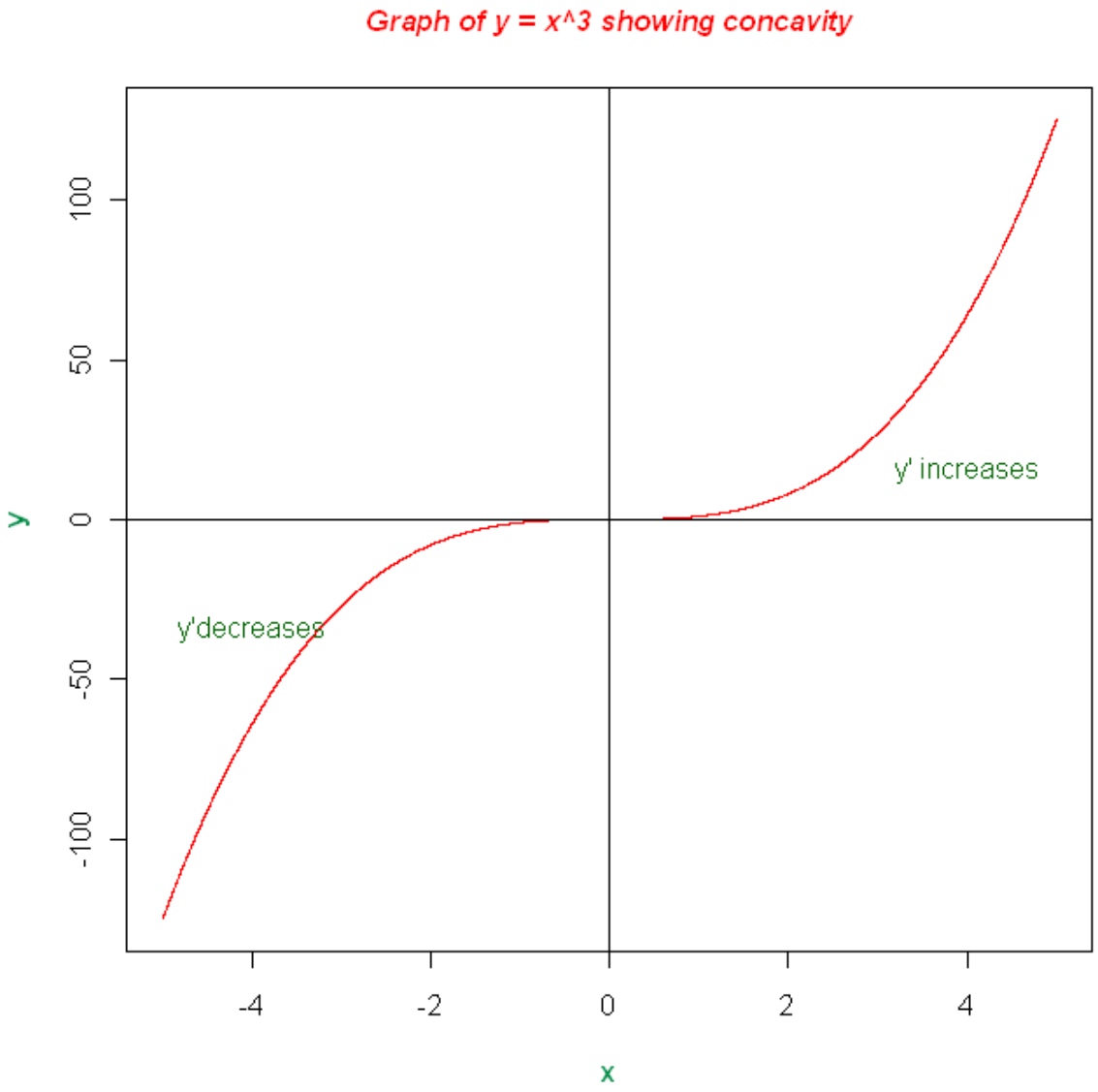

Figure 7.3: Graph to illustrate concavity in the curve for, $y = x^3$.

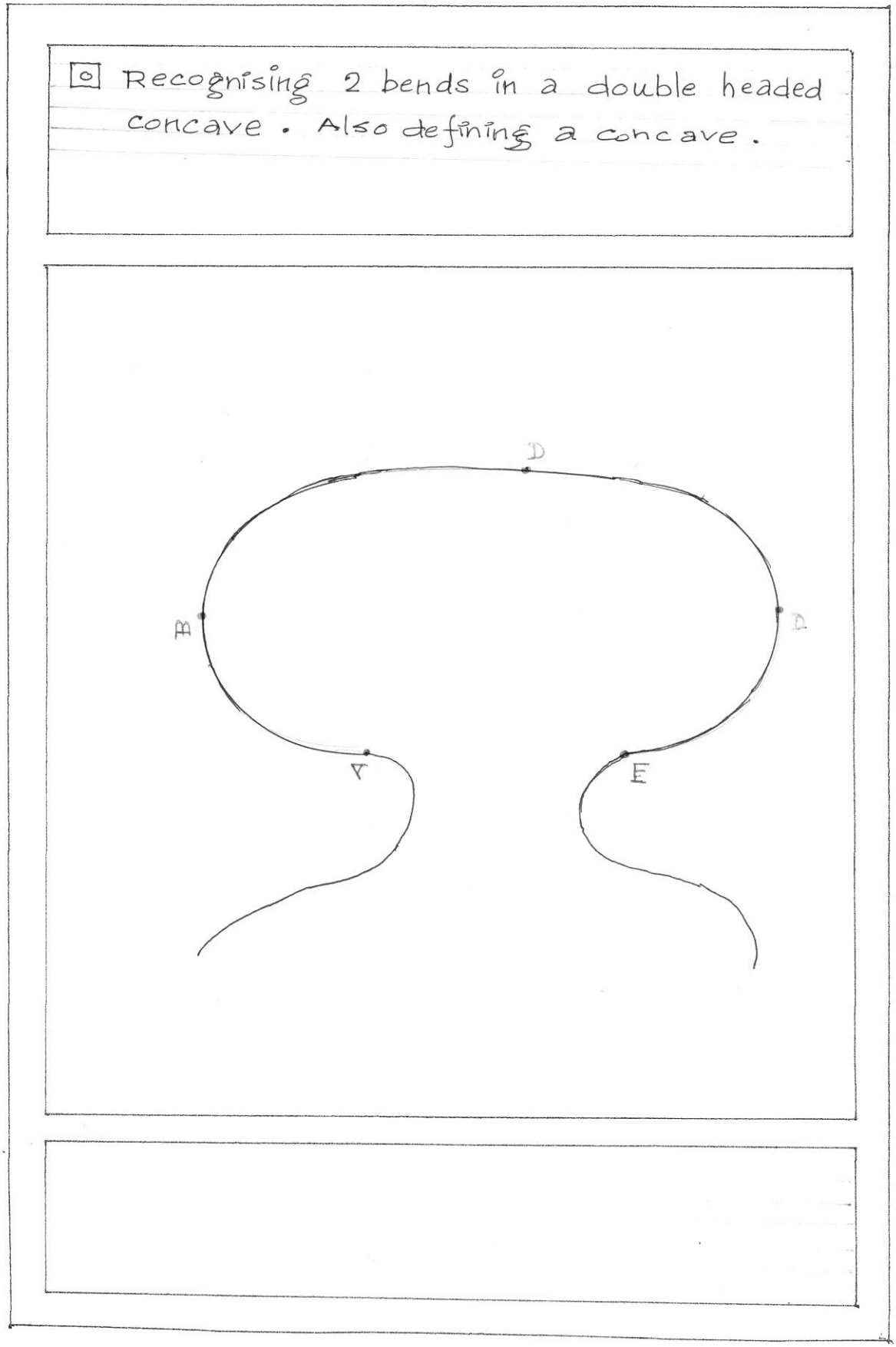

Figure 7.4: Sketch to illustrate the possibility that two bends may be found between consecutive inflection points in a double-headed meander loop.

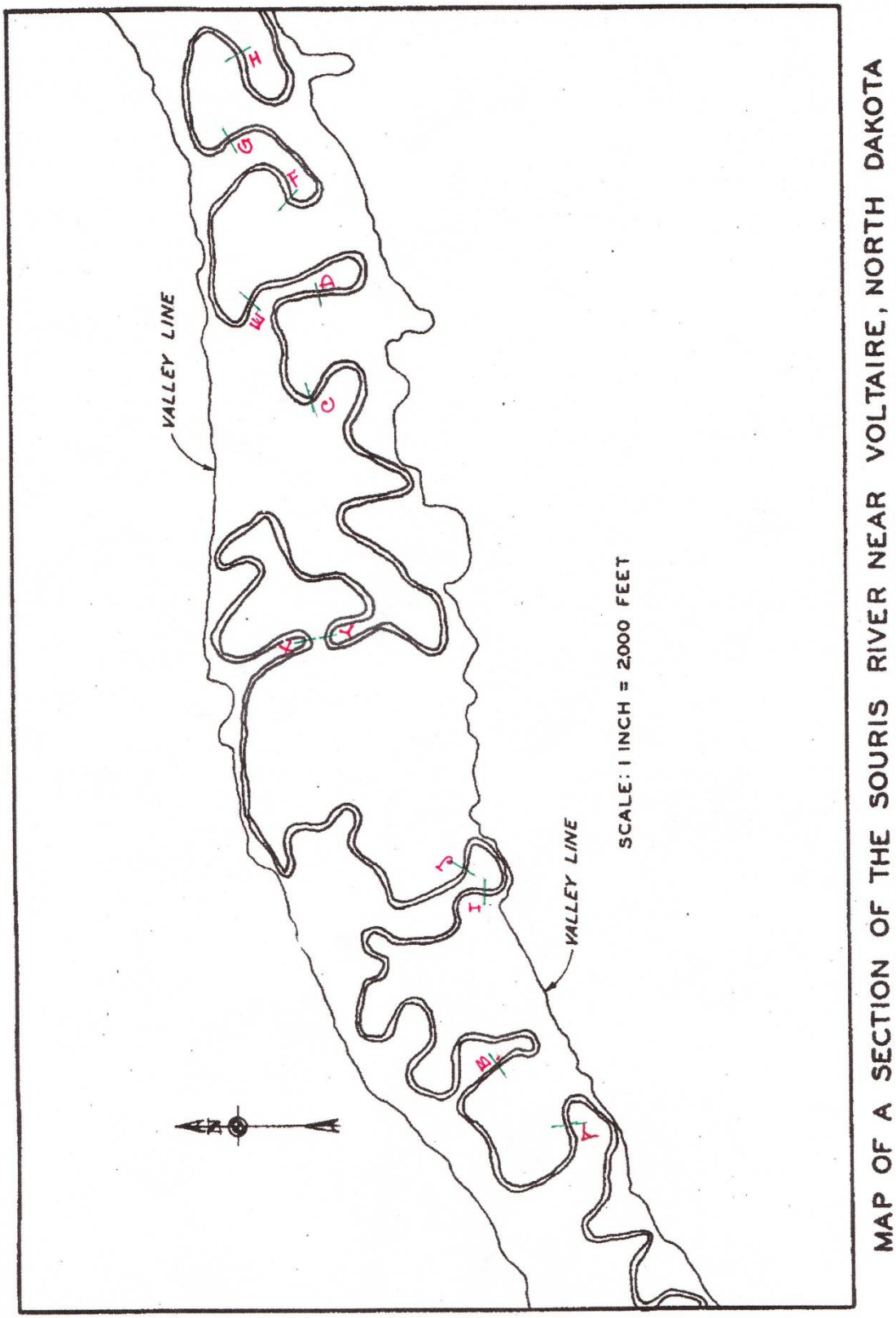

Figure 7.5: Map showing a reach of the meandering Souris River near Voltaire, North Dakota, USA (adapted from Lane, 1957).

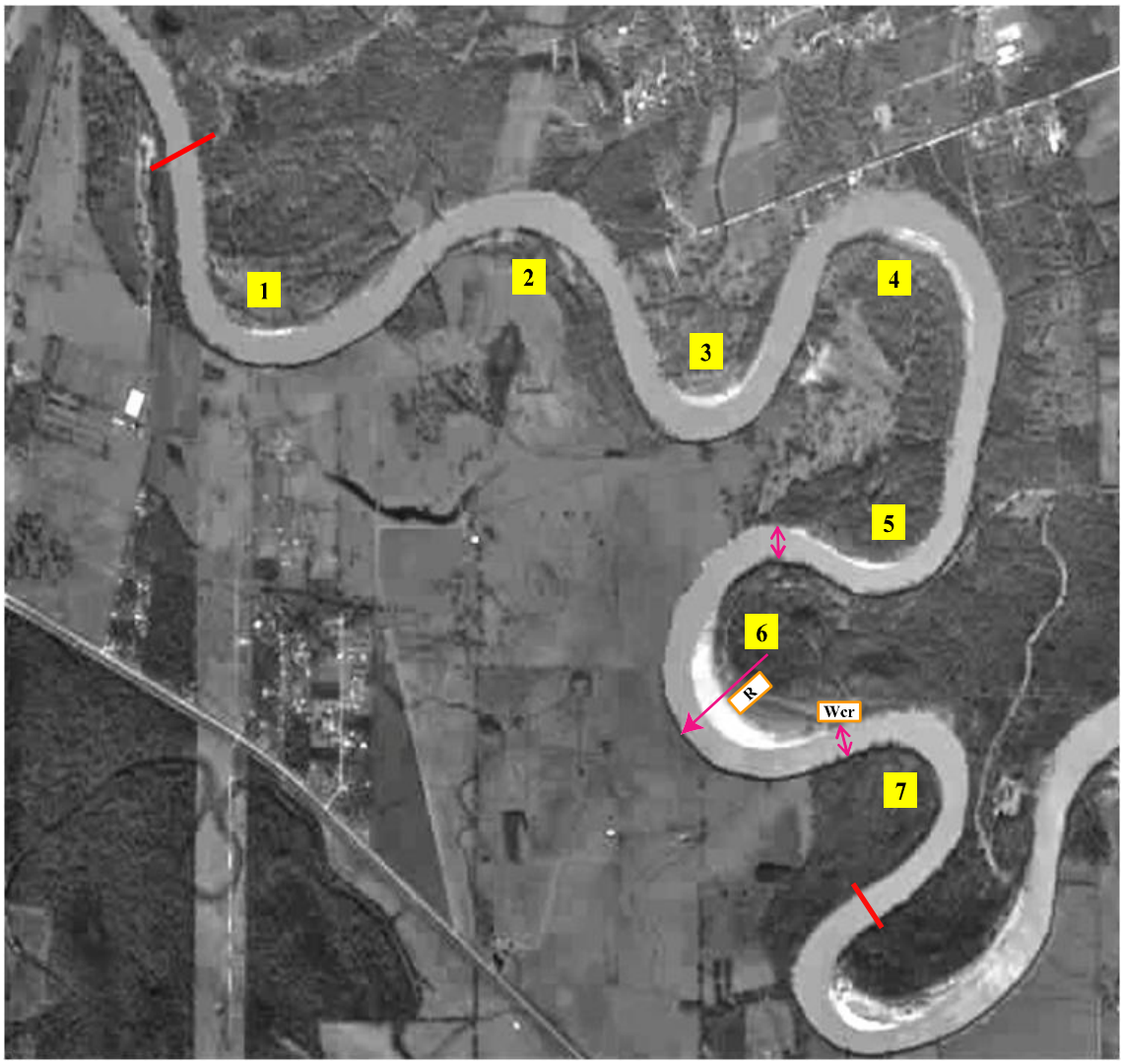

Figure 7.6: Example of the occurrence of two bends (4 and 5) between consecutive inflection points in a meandering river with a double-headed meander loop. This reach also supports the sample risk assessment based on analysis of bend geometry and prediction of the probability of future migration causing an erosion hazard at Bend 6.

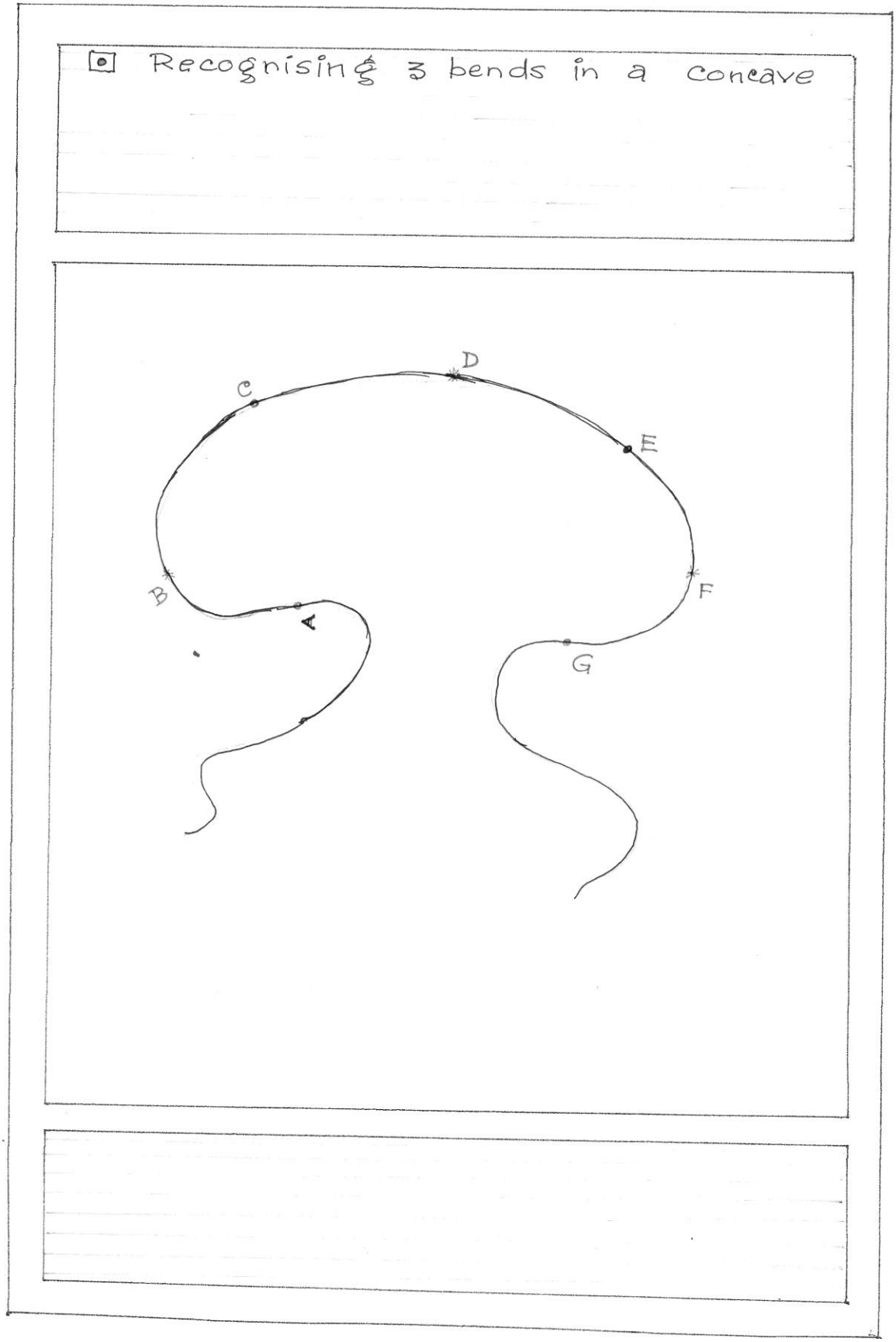

Figure 7.7: Sketch to illustrate the possibility that three bends may be found between consecutive inflection points in a loop that has a single bankline concavity (termed here a *monocave*).

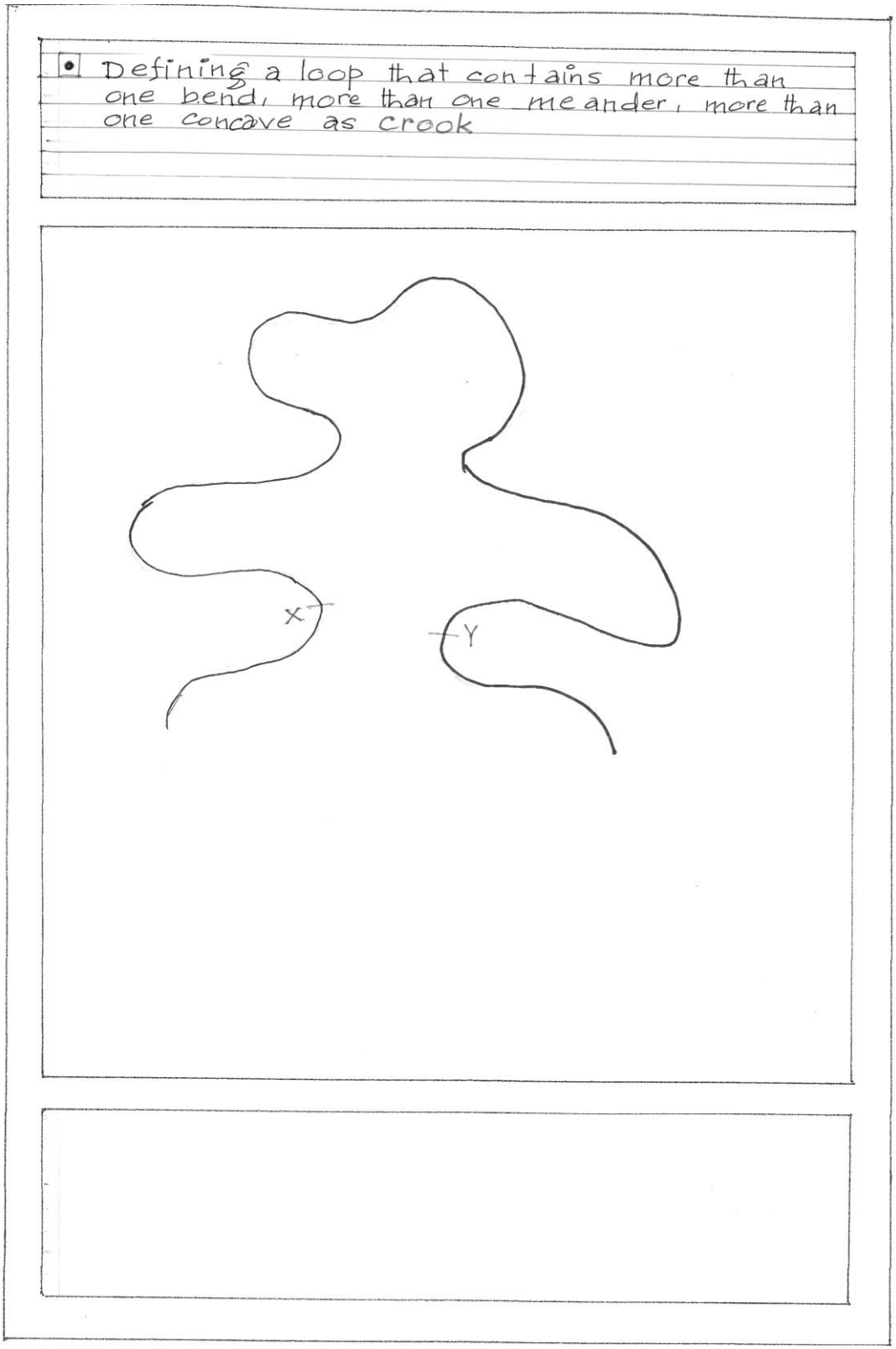

Figure 7.8: Sketch to illustrate the possibility that a complex loop may contain not only more than one bend, but also multiple concave bankline segments (*monocaves*) and contemporary meanders. This large-scale, planform feature is termed here a *crook.*

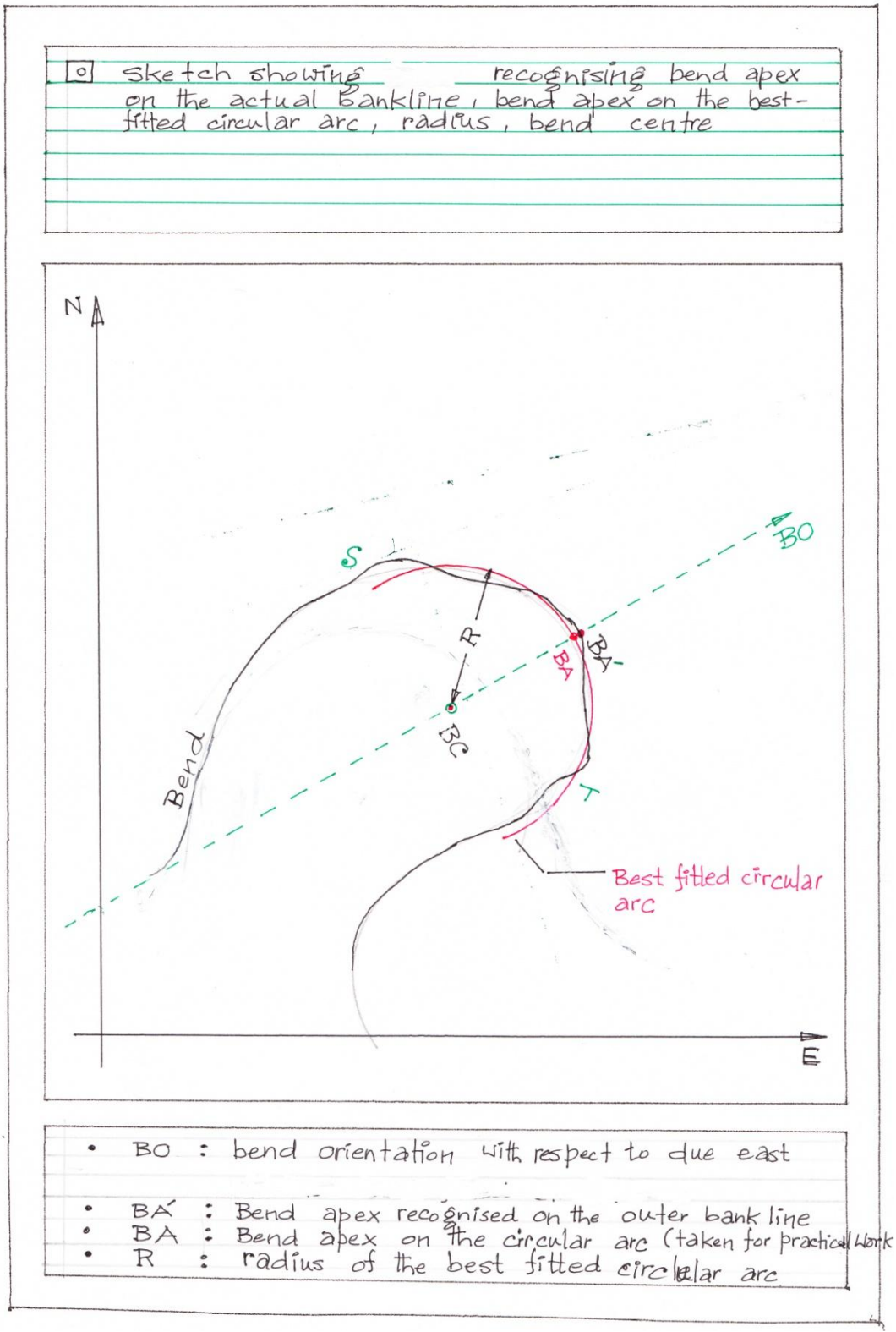

Figure 7.9: Sketch illustrating how the extent, axis, apex and radius of a bend are defined and measured.

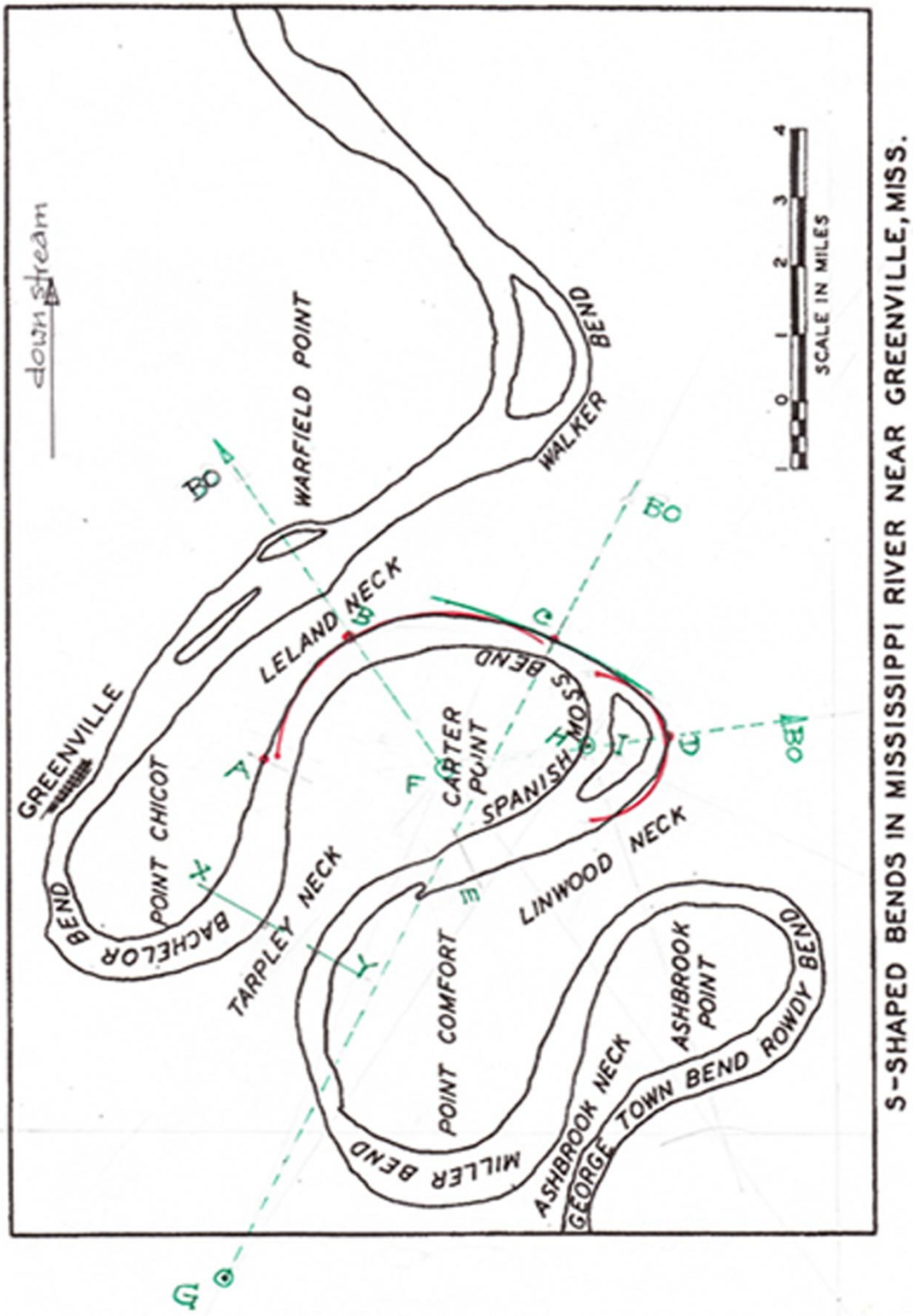

Figure 7.10: Example of recognising bends and fitting circular arcs to the outer banklines for migration risk assessment based on a tortuous reach of the Mississippi River near Greenville, Mississippi, USA (adapted from Lane, 1957).

As far as the propositions of mathematics refer to reality, they are not certain; and as far as they are certain, they do not refer to reality

.---Albert Einstein

Chapter 8
Discussion

8.1 Overview

While discussion has featured at relevant points in the preceding chapters, issues that over-arch the analysis and prediction of bend migration and those that can only properly be considered on the basis of having read about the analyses and tools developed and demonstrated herein has been reserved for this current chapter. In addressing these issues, this chapter not only examines them in light of what has gone before, it also supplements and complements the coverage already provided in the respective chapters.

At the outset of the research project described in this thesis, the vision was that it would produce a probabilistic tool that used a sound, analytical approach in producing objective estimates of the future average annual rates and directions of bend migration, while also being easy to apply and accessible to users not necessarily expert in river mechanics or fluvial geomorphology. In the course of investigating bend migration, performing the analysis and developing the tool it has emerged that the need for *some* expertise in river science or engineering is unavoidable in using the prediction tool because the decisions must be made concerning *when* to apply the tool and *how* to define and characterise the bend to which it is applied demand both insight and sound judgement on the part of the user. In this context, this chapter mixes discussion of the issues surrounding application of the tool with practical advice on using it appropriately and cautionary statements for users concerning its limitations.

8.2 Stable, Active and Passive Meandering

8.2.1 Introduction

The bend migration prediction tool developed here is based on analysis of reaches of rivers in the USA that were selected by James Brice and other fluvial geomorphologists on the basis that they represented a large sample of alluvial streams with meandering planforms that could be considered to be in dynamic equilibrium over timescales of years to decades. The channels of such streams are characterised as being *self-formed* and *free to adjust* in time and space. Under these circumstances, the parameters defining the channel cross-section, slope and planform are dependent variables controlled by the flow and sediment regimes, and the characteristics of the valley floor (floodplain) and the boundary materials (including vegetation). Provided that the controlling variables do not change through time, the morphology of the channel adjusts to them so that they become (at the reach-averaged scale) time invariant and a condition of dynamic stability is achieved.

It follows that the predictive tool must not be applied arbitrarily to the bends of just any river with a sinuous planform. It must first be established that the river in the study reach meets the criteria necessary for it to be considered to be meandering, self-formed, and free to migrate across its floodplain. The implication is that candidate streams must be investigated prior to application of the predictive tool with the aim of identifying and screening out streams that do not meet the necessary criteria to be suitable for assessment using the bend migration prediction tool.

8.2.2 Stable Meandering

The primary characteristic of an alluvial stream is that it is 'self-formed' – that is the channel is the product of the sequence of flows and associated sediment loads experienced at the site in question and the channel forming materials are the result of deposition and reworking of sediments supplied by the river itself in the past. It follows that rivers formed in materials

different to those making up the contemporary sediment load may be 'non-alluvial'. For example, a river may be bounded by stiff, consolidated clays, perhaps laid down long ago when the valley floor was inundated to form a lake, that are far less erodible than the sand and silt making up the sediment load of the modern river. Under these circumstances the planform may be sinuous, but the channel is immobile due to the high erosion resistance of its banks relative to the erosivity of the current flow regime. In this case, the condition is one of static rather than dynamic equilibrium.

Rivers that are stable in this static sense may have a distinctly sinuous planform that represent a relict form of meandering. Such rivers display well developed bends of moderate to high curvature but, unlike the bends in an alluvial stream, these bends do not migrate, instead remaining stationary for years or decades with no perceptible change in bankline position. The Ouchita River between Jonesville, Louisiana and Camden, Arkansas, USA is a good example of a statically stable, meandering river.The planform in this reach was shown by Biedenharn et al. (1984) to have been stable for over 160 years, with bankline movement being restricted to just six, isolated locations. It follows that early consideration of the channel's stability status is important in assessing the suitability of the bend migration prediction tools in assessing future erosion risks in a reach as, without this, misleading predictions could result.

8.2.3 Active Meandering versus Passive Meandering

Even when a sinuous river is flowing through alluvium, it may not necessarily be migrating across its floodplain. In this context, Thorne (1997) stressed the importance of recognising the existence of *passive* as well as *active* meandering and differentiate between them when classifying the river morphologically.

Actively meandering streams can be identified on the basis that their bends characteristically shift through erosion at the outer, cut-bank (which has the form of a steep, river cliff) and deposition on the point bar at the inside of the bend (which is a broad, shelving bar with or without a chute channel). Also, actively meandering channels display a particular relationship between planform

position and bed morphology, which features a single, continuous, scour pool close to the outer bank in each bend and a distinctive, riffle or transverse bar in each crossing reach. Additionally, they follow the generalised rules for meander geometry established many years ago by Leopold et al. (1964) and modified by numerous subsequent researchers according to which the wavelength of the meanders should be of the order of 10 to 14 times the width of the stream.

It follows that, according to Thorne (1997) sinuous river channels that do not possess these morphological features, associations and geometric attributes are probably not actively meandering and are more likely to be meandering *passively*.

Passive meandering occurs in rivers that are to a degree 'underfit': that is the stream that currently occupies the channel is not the one that formed it. Due to diminution of discharge, the flow strength is now insufficient to drive bankline shifting and so the flow is the slave of the morphology, even at bankfull discharge. The stream follows a sinuous course not because it has and is developing it, but because it is following a path inherited from a previous, more powerful forebear that it cannot alter to match its own hydraulics and sediment dynamics. A good example of a passively meandering stream is the Afon Elan in Wales (Richards, 1982). This watercourse meets Thorne's criteria for passive meandering in that it has multiple riffles with intervening pools in the crossing reaches, more than one pool in each bend, and a meander wavelength that is much greater than 14 times the channel width. Planform evolution in passively meandering streams is slow and tends to produce 'two-phase' meandering (Brice Types F or G), as new meanders scaled on the current width develop within or are superimposed on much longer, relict bends inherited from the older, more powerful stream. If the smaller, 'active' bends in a passively meandering river do pose a hazard to floodplain property or infrastructure, it is vital that their extents and geometries are correctly identified prior to risk assessment using the probabilistic tool. Further commentary on active versus passive meandering can be found in Thorne (1997, Box 7.2).

In summary, it is recommended that a basic study of channel morphology and stability be performed, using an appropriate form of geomorphological reconnaissance or investigation (see Thorne et al. (2010) for examples), to screen out stable, non-alluvial and passively meandering reaches prior to applying the risk prediction tool.

8.3 'Freely' Migrating Meanders

8.3.1 Impediments to Bend Migration

The research performed in this project has focused solely on the behaviour of the freely migrating bends of actively meandering rivers with alluvial channels. However, even though bends formed in alluvium are characterised as 'freely moving' the degree to which they are truly 'free' to evolve is not the same at all times or at all points along the course of an alluvial stream. In fact, the properties of alluvium are anything but uniform and unchanging. This may be the result of natural phenomena or it may be the outcome of past or future human interventions in the fluvial system. It therefore becomes relevant to consider the possibility that natural and anthropogenic 'controls' will affect future meander morphology and bend migration rate when attempting to predict the risks posed to floodplain property or infrastructure.

It is perhaps only in laboratory model experiments, where the floodplain is formed in homogeneous sand, that meanders are truly 'free' to grow and migrate and it is perhaps significant that it is only laboratory channels that are customarily regular in their geometry and behaviour (for examples, see the flume studies of Tiffany and Nelson 1939, Friedkin 1945, Ackers and Charlton 1970). Commenting on the contrasting behaviour of flume and river bends, Hickin (1983) noted that a preoccupation with 'equilibrium' forms and flume studies had led to the dismissal of facets of natural meander behaviour such as cut-offs as, 'transient disturbances in fluvial systems'. However, having observed rivers in nature he went on to conclude that, "many river reaches may be in a transient state - permanently!"

The fact is that in nature rivers flow through non-homogeneous alluvium and, additionally, migrating bends may encounter other controls ranging from local outcrops of erosion resistant deposits to rock revetments that are geological or artificial in origin, respectively. Also, the banks, riparian corridors and floodplains of natural rivers are vegetated to different extents. It is now well established that the type and density of vegetation strongly influence rates and distributions of bend shifting and planform

evolution in alluvial streams and that interactions between channel morphology, channel shifting and vegetation are dynamic and, hence, complex (Perucca et al., 2007).

As long ago as the 1980s, Hickin (1984) noted that bank and riparian vegetation could slow bank retreat by increasing resistance to flow and bank material strength, while in-channel vegetation promoted bar formation and concave bank bench deposition, especially through the formation and breaching of woody debris jams. It follows that the growth, death or clearance of vegetation on and behind the outer bank, and/or the accumulation or removal of woody debris from the channel can significantly affect the rate of bend migration.

The term ‘alluvium’ itself covers a wide range of different sedimentary materials which may have contrasting geotechnical properties. Consequently, the erodibility and mass stability of a retreating bank may vary markedly within a single bend even though it is formed in materials that are mapped as being uniform. This can help explain why the shape of real bends seldom mimics that of classical or textbook, meandering rivers. For example, when migration takes a bend to the edge of the currently active meander belt, it may encounter older, stronger backswamp deposits that have accumulated in natural flood basins and sloughs in the floodplain. The result is that the migration rate of the bend slows, although not to zero as backswamp deposits are erosion resistant rather than being unerodible.

Even within the alluvium of the meander belt, a bend may encounter an outcrop of erosion resistant clay that is short in streamwise extent in comparison to the length of the bend. The classic example of this is the ‘clay plug’, which then constitutes a ‘hard point’ in the outer bank of a bend (Thorne, 1997). This can slow or even halt migration locally, while allowing the surrounding bank to continue to retreat. The pattern of deformation of the bend that results depends on the location and extent of the clay plug. For example, Fisk (1944) described how, on the Mississippi River, a bend that encounters a clay plug at its apex usually grows by erosion on each side of the hard point to become ‘double headed’. In contrast, if a clay plug is encountered by the downstream limb of a migrating bend, movement of that limb slows while that of the upstream limb continues unabated, leading to compression of the bend and, eventually, a cut-off.

It must be concluded that when erosion resistant material or a band or patch of particularly dense vegetation is encountered by the retreating, outer bank of a bend, there are morphological responses both locally and throughout the bend that generate changes in both migration rate and direction. It follows that irregularities in the banklines and deformities in the bend geometries of an actively meandering stream are indications of non-homogeneity in the floodplain materials. The presence of irregular banklines and deformed bends can easily be detected by field reconnaissance and/or inspection of available maps, aerial photographs and other remotely sensed images and the necessary work should be performed prior to analysing and predicting migration of a bend in order to assess the likelihood that evolution of the bend may progress in a manner radically different from that expected in a 'free bend' and at a rate significantly faster or slower than that predicted using the probabilistic tool developed here.

The message from this discussion is that when dealing with alluvial rivers, users of the migration rate prediction tool should expect 'freely migrating meanders' to be the exception rather than the norm. The possibility that a problematic bend will encounter an impediment that affects its migration during the period of prediction is very real and this must be taken into consideration when the probability level for the migration prediction is selected. Where the consequences of the bend attacking the asset at risk are severe, the precautionary principle dictates that the user put uncertainty concerning the magnitude and direction of migration on the safe side by calculating the risk assuming a 'worst case' scenario with respect to the possible impacts of non-uniformity in the floodplain materials or variability in vegetation density on future bend movement.

8.3.2 Cut-offs

Recent studies of planform evolution in actively meandering channels have demonstrated limitations to the applicability of the concept of dynamic equilibrium in meandering rivers. The results of sustained monitoring indicate that relatively long periods of progressive and incremental channel lengthening through bend growth are interrupted by short periods of intense shortening through a cascade of bend cut-offs (Hooke, 2004). Consequently, the behaviour of meander bends

is highly non-linear and, is, therefore unpredictable using simplified, mechanistic approaches, which further validates the suitability of the empirical, probabilistic treatment adopted here (Hooke, 2007).

Observational work on the River Bollin in the UK has shown that, in the short-term, bend growth and other local adjustments are responsive to flood events, but that longer term bend migration is related to meander evolution and the occurrence of cut-offs in ways that are almost independent of the occurrence of individual events (Hooke, 2008). This supports the prediction tool developed here with respect to incremental meander migration, but highlights the fact that the possibility that a problem bend may be subject to cut-off before the end of the period of prediction is not evaluated. Further, even if the problem bend itself is not cut-off, the occurrence of cut-offs in the bends up or downstream can also profoundly affect its migration. Specifically, a cut-off upstream of the problem bend steepens the approach reach (increasing the sediment supply and so promoting aggradation) and alters the alignment along which flow enters the problem bend, which can increase the rate of bend migration. Conversely, a cut-off downstream may trigger degradation that regresses upstream to entrench the problem bend, perhaps increasing near-bank scour depth, destabilising the outer bank and accelerating its rate of retreat.

The likelihood that a particular bend will be cut-off in the near future can be assessed using a 'cut-off ratio' based on the ratio of the bend amplitude to its chord length (Klaassen and Van Zanten, 1989), while the imminent occurrence of a cluster of cut-offs is somewhat predictable based on the theory that meandering represents a form of self-organised behaviour (Stolum 1996, 1998). According to this theory, above a threshold value of sinuosity (3.14 for unconfined meanders, but lower where the valley floor width is less than the meander belt width) a cluster of cut-offs is highly likely to occur.

In practice, the problem bend being cut-off during the period of prediction would produce uncertainty on the safe side in that it would most likely reduce the risk to an asset in the floodplain adjacent to the outer bank. However, cutting-off of either of the adjacent bends has the potential

to accelerate migration in the problem bend and so the potential for either single or multiple cut-offs should always be checked as part of morphological assessment of the study reach.

8.4 Tectonic Activity

A clear relationship exists between tectonic activity in a region and high catchment sediment yields (Macklin and Lewin, 1997). Good examples of this relationship may be found in the coastal basins of California and Alaska. Tectonic activity may be manifest in a number of geological phenomena that affect rivers and bend migration either directly or indirectly.

Earthquakes – the occurrence of an earthquake can lead directly to severe river bank retreat through processes of collapse or even liquefaction. This accelerates bend migration locally and also introduces a slug of sediment into the river system, which can drive major changes in morphology in the fluvial system downstream, perhaps leading to river pattern metamorphosis (Sarker, 2009).

Faults – a fault crossing a river valley can impart changes to the terrain and geotechnical properties of the valley floor. A clear example of this is the 'Eocene Hinge Line' that crosses the Jamuna River in the vicinity of Sirajganj, Bangladesh (Alam et al., 1990; Khan, 1991; Thorne et al., 1993). Historically, the river shows clearly contrasting planform characteristics, morphological behaviours and rates of bend migration on either side of the fault line, even though the flow and sediment regimes are unchanged.

Uplift or Subsidence – uplift or subsidence due to slow, epeirogenic seismic activity beneath the valley floor can disrupt the long profile of a river and drainage networks, leading to changes in channel pattern and migration rate (Macklin and Lewin, 1997). In uplift situations, reaches on either side of the axis of uplift will exhibit different morphological behaviours. Generally, the river on the upstream side of the uplifting dome will tend to increase its sinuosity, with bends becoming more active than those on the downstream side. Subsidence creates the opposite

patterns of morphological change on the downstream side of the axis of subsidence. An example of these fluvial responses to uplift occurs in the Mississippi River around the Monroe Dome in the Lower Mississippi Valley (Burnett and Schumm, 1983).

The evidence provided by these and many other well documented cases of the morphology and migratory behaviour of rivers being affected by tectonic activity indicates that at the very least a cursory investigation should be made in order to assess whether a problem bend is or may be subjected to earthquake, faulting or neotectonic activity that could influence bend migration in ways that lie outside the predictive capacity of the probabilistic tool developed here. When the possibility for one or more seismic influences is identified, it will be necessary to assess their potential impacts and, if the consequences of the migration hazard are severe, ensure that uncertainty concerning the impacts of tectonics on migration rate are put on the safe side by assuming 'worst case' scenario for the effects of tectonics on future bend migration.

8.5 Potential Climate and Catchment Changes

The two most important factors influencing channel morphology and morphological changes over periods of decades to centuries are the flow (water discharge) and sediment (catchment sediment supply) regimes. Over graded timescales, these act as independent variables, interacting with the valley terrain and the properties of the floodplain alluvium and vegetation to drive channel adjustment and evolution. In this regard, assumptions intrinsic to application of the prediction tool are that the river is dynamically adjusted to the current flow and sediment regimes, and that these regimes will not change radically during the period over which migration is to be predicted. This is the case because even relatively subtle changes in the flow and or sediment regimes may trigger disproportionate morphological responses, potentially including planform metamorphosis. For example, prior to 1914, the Cimarron River in southwest Kansas flowed through a narrow, sinuous, incised channel. However, in response to a series of floods, it had by 1931 metamorphosed into a wide, shallow, braided channel with an almost straight alignment (Schumm, 1977).

In the case of the Cimarron River, the change in discharge resulted from a climatic fluctuation that generated a prolonged wet period with more frequent floods, but the flow regime may also be altered by changes in the catchment area upstream. Catchment changes that are known to have the capacity to impact the flow regime significantly include urbanisation and other forms of land-use change such as deforestation or careless aforestation, mineral or gravel mining, water abstraction or river regulation involving dam construction, and inter-basin transfers. Similarly, the supply of sediment to the river, and hence the sediment regime, may also be affected by changes to the sources of sediment and/or their connectivity to the drainage network associated with any of the above changes to the catchment. Typical morphological responses to changes in the flow and sediment regimes established by Schumm (1977) are listed in Table 8.1.

Table 8.1: Morphological responses to changes in dominant discharge and the associated sediment load in a fluvial system (from, Schumm, 1977).

Change	Change in river morphology
Q_s^+, $Q_w^=$	aggradation, channel instability, wider and shallower channel
Q_s^-, $Q_w^=$	incision, channel instability, narrower and deeper channel
Q_w^+, $Q_s^=$	incision, channel instability, wider and deeper channel
Q_w^-, $Q_s^=$	aggradation, channel instability, narrower and wider channel
Q_s^+, Q_w^-	aggradation, channel instability
Q_s^+, Q_w^+	fluvial processes increased in intensity
Q_s^-, Q_w^-	fluvial processes decreased in intensity
Q_s^-, Q_w^+	incision, channel instability, deeper, wider(?) channel

Key: Q_s = sediment discharge, Q_w = water discharge, $^+$ = increase, $^-$ = decrease, $^=$ = unchanged, ? = uncertain response.

This table (and similar, subsequent versions), indicates general trends of morphological response to changes in dominant discharge and sediment load, but provides no specific information on the impacts of particular combinations of change in accelerating or decelerating rates of bend migration in a meandering river. It is, however, obvious that the fluvial processes responsible for driving bend migration (as described in Chapter 1) will respond to changes in dominant (channel forming) discharge and associated sediment load, and this will directly impact rates and distributions of bend migration.

In detail, the scale and extent of changes to bend behaviour are likely to be site and situation specific, so that no generalised way exists to predict them *a priori*. Rather, it is necessary for the user to consider how sensitive the channel in the study reach is to destabilisation or metamorphosis (perhaps through classifying the stream using, for example, the Montgomery and Buffington (1997) typology) and then factor this into selection of the appropriate probability level for the risk calculation, bearing in mind the potential for climate, land use and river regulatory changes in the catchment upstream and the consequences of under-predicting the risk associated with bend migration.

8.6 Bend Evolution Stage

In Chapter 1 it was explained how the initiation, development and eventual termination of a bend could be divided into different stages, characterised by contrasting rates and directions of migration. Generally, bends grow slowly during the initiation stage and then migrate more quickly as they mature and their curvature increases (Hickin, 1978). Migration becomes erratic as the ratio of R/W decreases close to or less than one and the bend terminates.

This account could be taken to imply that if the curvature of a bend is low (that is R/W is high) it must be in the initiation stage of development and its migration rate will be slow. However, inspection of the data in the UoN/HRW database (see Figure 5.3) demonstrates that this cannot be taken as a general rule and it should not necessarily be assumed when a migration risk assessment is being performed. For example, although this is unlikely, bends with R/W values between 6 and 8 *may* migrate at rates in excess of 20% of the channel width per annum.

The cautionary note that emerges is that a high radius of curvature to width ratio does not necessarily mean that a bend is in the initiation phase and will, therefore, grow slowly. It is quite possible for two bends with similarly high radius of curvature to width ratios to migrate at entirely different rates and this is reflected in the range of migration rates represented by different probability levels in the prediction tool. It is therefore dangerous for users to make assumptions

concerning the evolutionary stage of a bend based on its curvature alone and further evidence drawn from historical aerial photographs and the setting of the bend (especially if this is within a monocave or crooked loop) must also be considered before any judgement is made.

8.7 Bend Radius and Channel Width

In exploring the functional relationship between bend migration rate and the ratio of radius of curvature to channel width (R/W), previous researchers have used different measures of bend geometry to define the dimensionless curvature. For example, Bagnold (1960) used centre line radius of curvature, while Hickin (1975) used the mean radius of curvature of scroll bars in the floodplain. Nanson and Hickin (1983**)** used an average radius of the inner bank with two separate radii being calculated: one around the apex and the other away from apex. Lagasse et al. (2003) measured radius of curvature at the outer bankline, but more recently Nicoll and Hickin (2009) rejected use of the outer bankline because vegetation may obscure it in aerial photographs. They instead used the radius of a circle fitted to the curve of the centre line of the bankfull width. However, they still used the vegetation lines along the banks to define that width! In this study, the radius of a circular arc fitted to the outer bankline around the bend apex has been used to represent bend curvature for reasons explained earlier in the thesis.

The point of this discussion is to make it clear that there is variation in the way that curvature is represented and that there is no consensus on which way is the best. This is not a trivial point as differences between the calculated curvature of a bend based on different ways of measuring its radius are not negligible. Also, it is important to remember this variability when comparing the distribution of migration rate as a function of R/W produced in this study with similar plots published elsewhere. Finally, if secondary data are used to perform a risk assessment using the predictive tool developed here, it is vital that the user ascertain precisely how the bend radius that is to be used as an input value was measured and to what component of channel geometry it applies. In the same way, care has to be taken when using a channel width to non-dimensionalise the bend radius. The meesage is that failure to perform simple quality control checks on the input data could result in an unreliable estimation of risk.

8.8 Consideration of the Spread of Data in the Migration–Radius of Curvature Scatter Plot

Several authors have produced scatter plots similar to Figure 5.3 and it is prudent to compare these plots to that produced here in order to judge its credibility. For example, Hooke (1991) prepared such a plot using data from the Beaton River and other rivers in Canada, Rivers Bollin and Dane in the UK and the Red River in the USA (Figure 8.1). In this plot the highest dimensionless migration rate is around 0.18 widths/year. This is quite consistent with the scatter plot developed in this research (Figure 5.3) on which only 19 out of 2,257 bends, representing less than 1%, of the data points, plot above a value of 0.18 widths/year on the y-axis.

However, the UoN/HRW data set contains some dimensionless average annual migration rates inexcess of 0.3 widths/year. These extreme values, though very small in number, certainly influence the probability density functions fitted to the data (see Chapter 5) which, in turn, influence the mirgration rate prediction curves. The occurrence of extreme points should not be unexpected given that the data set is far larger than that available to Hooke and, while the probability of such rapid migration is very small, it is not zero. The point here is that the great size and careful quality control applied to the UoN/HRW data set can give users confidence that erosion rates predicted using the curves for very high probabilities that the predicted rate will not be exceeded are indeed unlikely to be equalled or exceeded. This is vital when the consequences of the erosion hazard actually occurring are basically unacceptable and must be avoided through a conservative prediction of the possible bend migration rate.

8.9 Scale Effects and Self-Similarity

Application of the predictive tool requires that the problem bend is represented as a geographical object. However, the shape and properties of any geographical object vary as a function of the scale at which it is measured. For example, if the object to be represented in some analysis was the long profile of a reach (see Figure 1.5 for three examples), it is clear that the outcome would

be quite different depending on the length of the reach selected for analysis and the spacing of measurement points used to represent the bed in that reach. It is clear from even cursory inspection of Figure 1.5 that a large number of closely spaced measurement points would reveal far greater variability in bed elevations than would a sparse set of widely spaced points. Hence, the *spatial density* of measured data affects the representation of the object. This issue becomes even more significant when there is a repetitive pattern in the feature – for example if the interval between widely spaced measurement points were to coincide with the spacing of pools in the bend profile, the recorded data would underestimate the true elevation of the bed.

Also, the length and location of the reach selected to represent the bed in Figure 1.5 would clearly influence the characteristic of the resulting object, especially because the bed profiles possess a degree of self-similarity: that is they display features with similar geometries that nest within one another and are repeated at a variety of scales. The classic example of how the selection of scale is important in measuring length of a geographic object was recounted by Longley et al. (2001). In 1967, Benoit Mendelbrot asked the question, 'How long is the coastline of Maine?' If a divider is set to a measurement scale of 100 km, the recorded length of the coastline is 340 km. However, if a scale of 50 km is selected, the length of the coastline becomes 355 km. Chosen measurements spaced at 25 km intervals increase this length to 415 km. This illustrates why scale-effects must be considered when measuring and interpreting any geographical feature such as a coast or, indeed the channel of a river.

The morphology of a meandering river includes repetitive features and a high degree of self-similarity. Hence, selection of the appropriate measurement density and scale is crucial to properly representing the geometry of the problem bend. In practice, the density of measurements that can be used to, for example, delineate the outer bankline in a problem bend is likely to be dictated by the resolution of the available maps, aerial photographs or satellite images. However, it is imperative that, in spite of any practical difficulties in preparation, measurements are made in such a way that the object created by them is a suitable model of the prototype.

The necessity and importance of properly recognising actively migrating bends within a meandering river stems from the fact that bends with multiple scales of curvature (bend,

monocave, or crook) may be present in the planform. This was discussed in Sections 7.2 and 7.3 and that discussion is not repeated here. However, the point to be stressed again is that scale effects may obscure actively migrating bends and so hinder proper recognition of the extent and geometry of a problem bend. Users must, therefore, be diligent in finding a suitable map, satellite image or aerial photograph and they must exercise due care when identifying the problem bend, fitting the circular arc to it and taking accurate measurements of key bend and channel parameters.

8.10 Migration Hazard, Probability and Risk

In Chapter 7, bend migration was identified as a hazard to assets on the floodplain. The threat posed by this hazard during a specified period of time depends on the magnitude and direction of bend migration, in relation to the location of an asset on the floodplain. The magnitude of shifting during a specified time interval is the scalar variable predicted using the tool developed here. The direction of shifting is a vector and this makes it inherently more difficult to predict. It is on the basis of evaluating this threat quantitatively that the probability level in the prediction tool should be selected. In practice then, the tool is applied to establish the probability that the average annual rate of migration at the bend apex necessary for the hazard to be realised within a specified period will be equalled or exceeded – resulting in the asset being attacked, damaged or destroyed by bank erosion or, more probably, resulting in the need for counter measures to prevent this disaster. It follows that the threat posed by a bend depends not only on its migration rate, but also on the proximity of the asset and its position relative to the bend.

The predictive tool proposed in this thesis provides a rational and scientifically sound approach to assessing the threat posed by bend migration in an alluvial, meandering river based on the probability that a problem bend will attack an asset within the prescribed period of time. However, in the 21st century, decision making with respect to environmental hazards and their management is no longer based on assessing the *probability* of the hazard being realised (in this case erosion attacking the asset) and taking steps to prevent this occurrence; decisions are now based on the management of the associated *risk,* where risk is broadly defined as the probability of the event occurring, multiplied by the consequences should it do so.

These consequences are usually expressed monetarily: that is, in terms of economic or financial costs. Of particular concern are the financial losses suffered by the owners of the asset at risk, who might be a farmer who owns valuable milking barn or grain silo, a business person who owns a factory on the floodplain, or a river authority responsible for the provision of flood defence assets such as embankments or pumping stations close by the river. Direct losses may include lost crops and the cost of buying replacement land or rebuilding the asset. Consequential damages may also be important and can include loss of business or market share and flood damage to properties and other assets formerly protected by a breached flood embankment. In addition, if the asset is of wider significance there may be economic losses. For example, if a railway line has to be closed due to an erosion hazard, this may disrupt regional or even national transport and communications, resulting in damage to the wider economy that is irrecoverable.

However, modern risk assessments also recognise that not all risks are financial and economic costs that can be expressed in monetary terms. For example, the loss of a well may be of little consequence financially or economically but could represent a catastrophe for a small community dependent upon the well for a convenient supply of safe drinking water. Hence, the social costs may be significant. Similarly, the destruction of valuable and rare floodplain habitats may have disproportionate environmental consequences to endangered or key species and ecosystems that cannot easily be expressed in monetary units.

The migration prediction tool supplies just one of the parameters necessary to perform a bend migration risk assessment. It is important to remember that in selecting the appropriate level of probability in that assessment the aim is to inform decision making with respect to how the *risk* is to be managed and that depends also on the value placed on the asset and the financial, economic, social and environmental consequences should the erosion hazard be realised. Only when the consequences of the bankline reaching the asset have been evaluated can the risk be assessed, with the results used to inform management of that risk through, for example, relocating the asset to a safer place, taking steps to mitigate or reduce its vulnerability to damage, or undertaking counter measures to reduce the probability of it being attacked by the river within the prescribed period. Clearly, these matters require inputs from socio-economic and environmental experts,

rather than being solely the responsibility of the river engineer or fluvial geomorphologist. Nevertheless, the step by step account of risk assessment set out in Box 7.4 provides a template for calculating the average annual migration rate that will lead to the bend apex reaching a given location in the floodplain within a specified period of time, and this is the first requirement for a scientifically-based assessment of the risk to an asset at that location.

8.11 The Case for Development of Type-Specific Prediction Tools

The UoN/HRW database contains data for nine different categories of meandering river, classified according to the modified Brice Typology (explained in Section 4.1 and illustrated in Figure 5.1). The data available for each modified Brice Type are listed here in Table 8.2. In the research reported thus far, data for all types of meandering river have been pooled to produce a single, large dataset. That dataset has been analysed probabilistically to develop a prediction tool that is equally applicable to a problem bend on any type of meandering stream. However, the option exists to analyse data for each modified Brice Type separately, with the purpose of producing an individual, Type-specific prediction tool for each type of river. To explore the merits of doing so, a range of graphical statistical techniques and numerical descriptors are employed here to compare the distributions of data in the files created for the different Brice Types and consider whether the use of Type-specific prediction tools is justified.

Table 8.2: Bend radius and migration rate data available for each Modified Brice Type

Brice Type	Sites	Bends	Time Period 1			Time Period 2			Both Periods		
			n total	n miss	n avail	n total	n miss	n avail	n total	n miss	n avail
A	7	61	61	45	16	61	3	58	122	48	74
B1	19	199	199	94	105	199	21	178	398	115	283
B2	37	365	365	100	265	365	5	360	730	105	625
C	41	423	423	91	332	423	41	382	846	132	714
D	6	46	46	13	33	46	18	28	92	31	61
E	18	217	217	121	96	217	40	177	434	161	273
F	5	34	34	27	7	34	0	34	68	27	41
G1	6	125	125	105	20	125	2	123	250	107	143
G2	2	42	42	42	0	42	0	42	84	42	42
All	**141**	**1512**	**1512**	**638**	**874**	**1512**	**130**	**1382**	**3024**	**768**	**2256**

* All zero migrations removed. n = number values for both variables that are available or missing.

Of the various meandering river types represented in the database, Type C rivers (characterised by single phase meandering and bends that are (i) wider than crossings and (ii) feature point bars) represent the largest single group, with 714 data records (Table 8.2). Also, rivers with these attributes conform most closely to 'classic' or textbook meandering. Hence, in considering the other types of river, data distributions for Type C are taken as a point of reference. Also, scatter plots for each type of river will, in turn, be superimposed on that for Type C meanders, to support visual interpretation of similarities and differences.

Variation in the values of dimensionless bend radius and dimensionless average annual migration rate between the different Brice Types was investigated statistically and the results are listed in Tables 8.3 and 8.4, respectively.

Table 8.3 reveals that the sample sizes for A, D, F and G2 are all less than 100. This must be borne in mind when considering the distributions of these variables. Variations between representative statistics for the different Brice Types are small. For these distributions, the median is a better measure of central tendency than the mean because the data are strongly skewed to the right and the mean value is heavily influenced by a few extreme values. With the exception of Type G1, median values clustered around the median for all bend types (2.67) and lie in a narrow range between 2.6 and 3. In terms of dispersion, the coefficients of variation are also quite similar, clustering around the same value for all bends (0.51) and ranging only from 0.45 to 0.55 with average of 0.50.

Table 8.3: Tukey's five number summary and other descriptors for R_b/W_{bCr}

Modified Brice Type	N	Min	Q1	Median	Q3	Max	Range	IQR	Mean	sd	SE	cv
A	74	0.94	2.26	3.1	5.09	9.19	8.25	2.83	3.63	1.81	0.21	0.50
B1	283	0.75	1.99	2.76	3.76	9.7	8.95	1.77	3.14	1.59	0.09	0.51
B2	625	0.55	1.96	2.59	3.57	11.23	10.68	1.61	2.93	1.36	0.05	0.46
C	714	0.69	1.94	2.58	3.51	9.02	8.33	1.57	2.87	1.37	0.05	0.48
D	61	0.66	2.26	3.1	4.01	7.81	7.15	1.75	3.24	1.45	0.19	0.45
E	273	0.73	2.05	2.68	3.81	9.79	9.06	1.76	3.14	1.61	0.10	0.51
F	41	0.93	1.76	2.94	4.45	8.26	7.33	2.69	3.37	1.84	0.29	0.55
G1	143	0.74	2.33	3.93	5.45	12.26	11.52	3.12	4.22	2.34	0.20	0.55
G2	42	1.72	2.27	2.94	4.1	10.96	9.24	1.83	3.47	1.85	0.29	0.53
Averages		0.85	2.08	2.94	4.18	9.72	8.87	2.09	3.31	1.67	0.16	0.50
Parameters calculated for all bend Types	2256	0.55	1.99	2.67	3.78	12.26	11.71	1.79	3.09	1.58	0.21	0.51

With respect to the dimensionless migration rate (Table 8.4), differences between bend types are apparent in the calculated statistics. This is consistent with what would be expected based on the geomorphological attributes of rivers with channels of these types. For example, Type A channels are incised and would be expected to migrate relatively slowly. Type B1 channels are of uniform width and the lack point bars. Brice termed such channels as 'canaliform' and Schumm (1977) identified them as being dominated by suspended load and relatively stable. Type B2 channels are similar to B1 but are wider at bends, indicating some retreat of the outer bank even though no point bar has formed. The bends of Type C meandering rivers are 'classic' in form being wider than the crossings and having prominent point bars. As expected, the median migration rate for Type C bends is nearly double that for Types A and B. According to Schumm (1977), Type D channels (wider at bends, with wide point bars and chute channels) should be more mobile still and this is reflected in the median migration rates and standard errors in Table 8.4.

Table 8.4: Tukey's five number summary and other descriptors for MMA/W_{bCr}/Y

Modified Brice Type	n	Min	Q1	Median	Q3	Max	range	IQR	Mean	sd	SE	cv
A	74	0.0023	0.0101	0.0249	0.0336	0.0867	0.0844	0.0235	0.0253	0.0179	0.0021	0.71
B1	283	0.0016	0.0122	0.0212	0.0337	0.1097	0.1081	0.0215	0.0267	0.0208	0.0012	0.78
B2	625	0.0006	0.0146	0.0245	0.0407	0.2565	0.2559	0.0262	0.0322	0.0274	0.0011	0.85
C	714	0.0004	0.0274	0.0460	0.0766	0.3450	0.3446	0.0493	0.0584	0.0470	0.0018	0.80
D	61	0.0063	0.0333	0.0619	0.0930	0.2073	0.2010	0.0597	0.0714	0.0490	0.0063	0.69
E	273	0.0013	0.0157	0.0307	0.0524	0.1759	0.1746	0.0367	0.0386	0.0324	0.0020	0.84
F	41	0.0012	0.0115	0.0215	0.0402	0.1309	0.1297	0.0288	0.0306	0.0284	0.0044	0.93
G1	143	0.0026	0.0247	0.0461	0.0874	0.3668	0.3642	0.0627	0.0635	0.0567	0.0047	0.89
G2	42	0.0059	0.0329	0.0623	0.1027	0.2401	0.2342	0.0699	0.0734	0.0507	0.0078	0.69
Average		0.0025	0.0213	0.0394	0.0655	0.2393	0.2369	0.0442	0.0493	0.0396	0.0035	0.81
Parameters calculated for all bend types	2256	0.0004	0.0175	0.0320	0.0572	0.3668	0.3664	0.0397	0.0441	0.0406	0.0040	0.92

The spatial organisation of width in Type E channels is irregular and so it is not surprising that their bends migrate at only half rate of Type D channels – which feature a concentration of width and erosive activity at bends. Type F channels are 'underfit' and so it is unsurprising that their bends migration statistics are similar to those for relatively stable Types A and B. Type G channels represent an important category of channels with two phase meandering: that is, active, short wavelength bends are superimposed on the longer wavelength curves, monocaves and crooks. The active bends of Type G1 meandering channels lack point bars and yet their median

migration rate matches that of Type C, single phase bends. Type G2 channels, with bends that are wider than the crossings and feature point bars, have the highest median migration rate of all (it slightly exceeds that for Type D channels). These results indicate that the active bends in Type G meandering rivers have, on average, the greatest potential for rapid migration.

While the measures of central tendency for bend migration rate differ substantially, the coefficients of variation are remarkably similar, only ranging from 0.7 to 0.93.

Figures 8.2 to 8.9 present scatter plots for each Brice Type compared to the scatter of data for Type C channels. Considering the most extreme rates of bend migration, there are just 19 data points rates that exceed 0.2 wy^{-1} (Figure 5.3). Of these: 2 represent Type B2 (Figure 8.4), 11 Type C (Figure 8.5), 1 Type D (Figure 8.5), 4 Type G1 (Figure 8.8) and 1 Type G2 (Figure 8.9). This indicates that extreme rates of bend migration have been documented for all but bends in Types A, B1, E and F channels. Given the geomorphological characteristics of channel of these types discussed above (Schumm 1977) it would be surprising if they were capable of displaying extreme behaviour. Conversely, consideration of the Brice Types of bends with very high migration rates demonstrates that extreme values cannot be ruled out for Types B2, C, D and G channels.

Examination of the scatter plots for Brice Types A, B1 and F shows that migration rates for the bends monitored on rivers with these types meandering were markedly lower than those on Type C meandering rivers. In fact, the maximum migrations rates Brice Types A, B1 and F were only 0.09, 0.11 and 0.13 wy^{-1}, respectively (Table 8.4). Given their morphological characteristics (Figure 5.1) this finding is as expected.

However, in examining the extent and pattern of points in Figures 8.2 to 8.9, also makes it apparent that the low number of data points may be masking the true scatter of the migration rates for some types of rivers. This is particularly likely for Types A, D, F and G which, combined make up less than 10% of the database. The limited number of data points for individual types of meandering severely curtails the potential for their individual analysis.

Having reviewed the similarities and differences in the descriptive statistics and scatter graphs for the different modified Brice Types, and bearing in mind the limited quantity of data available for some of them, it can now be considered whether it would be justified to develop a migration prediction tool for each one or whether the single, generalised prediction tool developed earlier in this thesis is more appropriate.

Based on the statistical and visual investigation recounted here, it should be concluded that there is a strong case for developing tools specific to particular types of meandering, although it is doubtful that this should go as far as having one per modified Brice Type. For example, it would seem sensible to combine modified Brice Types A, B1 and F, all of which displayed low rates of migration that were consistent with their known behaviour and relatively high degree of morphological stability. Conversely, tools specific to the modified Brice Type appear justified for Types B2, C, D, E, G1 and G2.

Unfortunately, such analysis, although desirable had to be ruled out in this research project due to the limited number of observations available in the UoN/HRW database. While the 2,256 pairs of data available in the pooled data set are certainly sufficient to support a probability analysis that produces a robust outcome, the same cannot be said even for the largest sub-set of data pairs (714), representing Type C channels. If further data could be assembled, then analyses for individual types of meandering would be justified, both morphologically and statistically.

Despite the statistical case for Type-specific migration analyses and tools, the utility of developing such approaches may be questioned on practical grounds. The problem with such tools would be that, in order to apply them accurately and so produce reliable assessments of migration risk, the user must first *correctly* classify the type of meandering displayed by the study river in the problem reach. This is not a trivial task. For example, in an aerial photograph taken at low flow the channel may appear to be of Type F when at an intermediate stage it looks a lot more like a Type C. Similarly, a slightly higher stage still, that inundates sloughs behind the point bars, may lead the user to classify the same stream as Type D. The migration rates predicted by Type-

specific tools for meanders classed as Types F, C and D would be substantially different, introducing uncertainty and, potentially serious errors due to mis-classification. While stage-dependent pattern changes could be accommodated for by an experienced river engineer or fluvial geomorphologist, a degree of subjective interpretation of planform features would still remain and there would, inevitably, be disagreements between experts even on the same team concerning the correct classification of a particular reach.

This point can be amply illustrated by comparing the distribution of bends by modified Brice Type in the NCHRP and UoN/HRW databases (Table 8.5 and Figure 8.10), remembering that the databases actually represent the same bends, but that the classification of each and every bend in the NCHRP database was checked as part of this study by the writer with assistance from his supervisor.

The results indicate notable differences in the numbers of bends classified as being Types B2, C, E and F (Column 4 in Table 8.5). These differences are particularly important given that bends of these types constitute the bulk of the bends in the database (Columns 5 and 6 in Table 8.5).

Each of the classifications was performed a team comprising experienced engineers and geomorphologists. However, in a chi-squared test performed to establish whether the distributions of bends by type were significantly different, the p-value of the resulting chi-squared statistic was almost zero, indicating that the two distributions *are* significantly different.

Consequently, if a Type-specific migration prediction were to be developed and applied, it is highly likely that errors would result due to mis-classification of some problem bends. Clearly, it would not be enough to depend on inspection, which has been shown to be difficult even for experienced engineers and geomorphologists.

Until an objective basis for typing bends is developed and proven, the probability of mis-classification will remain high and this could be dangerous. For example, if a Type D bend were to be misclassified as being Type B1, this could lead to a serious under-prediction of the

probability of migration because the error would be on the hazard side, not on the safe side. It could, therefore, be argued that publication of a Type-specific prediction method at this time might not only be premature, but also imprudent.

Table 8.5: A comparative account on bend numbers on River Types and associated statistics

Modified Brice Type	No. of bends in NCHRP database	No. of bends in UoN/HRW database	Differences (%)	Total No. of bends in pooled dataset	No. bends selected for analysis	% Bends selected for analysis
A	61	61	0	122	74	61
B1	232	199	-17	398	283	71
B2	207	365	43	730	625	86
C	634	423	-50	846	714	84
D	48	46	-4	92	61	66
E	137	217	37	434	273	63
F	19	34	44	68	41	60
G1	125	125	0	250	143	57
G2	42	42	0	84	42	50

Summing up, the distinctions between different types of meandering are not, in practice, as clear cut as they appear in the sketches in Figure 5.1, sample sizes for individual types are relatively small and the differences in the scatter plots are not so sharp that development of a categorical tool appears to be *essential*. In the light of these findings, the general tool developed and reported in this thesis turns out to be a robust and appropriate outcome given the unalterable attributes of meandering streams and the strengths and limitations of the UoN/HRW database. Further, the ease of use of the generalised tool should make it attractive to end users wishing to make quantitative risk assessments in practical situations, particularly where resources of data, time and specialist expertise are limited. The point is that the range of possible migration rates represented in the generalised scatter plot, and the tables related to it, cover the entire spread of those observed for bends of all Brice Types. Consequently, users who are sufficiently confident in their ability to identify different types of meandering can compensate for the lack of type-specific prediction tools by selecting a level of probability appropriate to the morphological properties and modified Brice Type of the reach in question.

8.12 Closure

The tool proposed here to predict the rate of bend migration is simple to apply in the sense that a user assessing a problematic bend has only to measure the radius of the outer bank and the average width at the crossings up and downstream. Having calculated the ratio of these two parameters, he or she can quickly determine the predicted average annual migration for the bend apex for a selected level of probability using the tables and graphs in Section 5.7. Clearly, application of the tool does not require a considerable investment of time and resources.

However, the apparent simplicity and ease of application of the tool should not mask the challenges inherent to a migration risk assessment that stem from the need to accurately recognise and delineate the extent of the problem bend, avoid the problems associated with scale and self-similarity, account for possible variability in the erosion resistance of the bank due to nonuniformities in the floodplain alluvium or vegetation, detect the presence of geological or artificial constraints to migration, and anticipate whether either the problem bend or those adjacent to it are likely to be cut off within the prediction period. These are important issues that manifestly influence the risk to assets on the floodplain and they need to be considered and factored in to the risk assessment by adjusting the selected probability level accordingly. The inevitable conclusion is that it would be pointless and potentially misleading to perform a risk assessment unthinkingly and solely on the basis of a hastily measured pair of radius and width measurements.

Successful application of the prediction tool also depends on correctly gauging the value of the asset or assets at risk, including not only financial and economic losses should the predicted rate of bend migration be exceeded, but also considering the potential social, environmental and consequential impacts. Careful and comprehensive consideration of the consequences of the erosion hazard being realised is also essential to selecting the appropriate probability level when applying the prediction tool to make a risk assessment.

Therefore, though application of this tool need not consume substantial amounts of time and resources it does require the user to pay close attention to the planform morphology of the study reach, to consider carefully the importance and value of the asset at risk and to exercise a degree of sound judgement in interpreting the outcomes of the risk assessment.

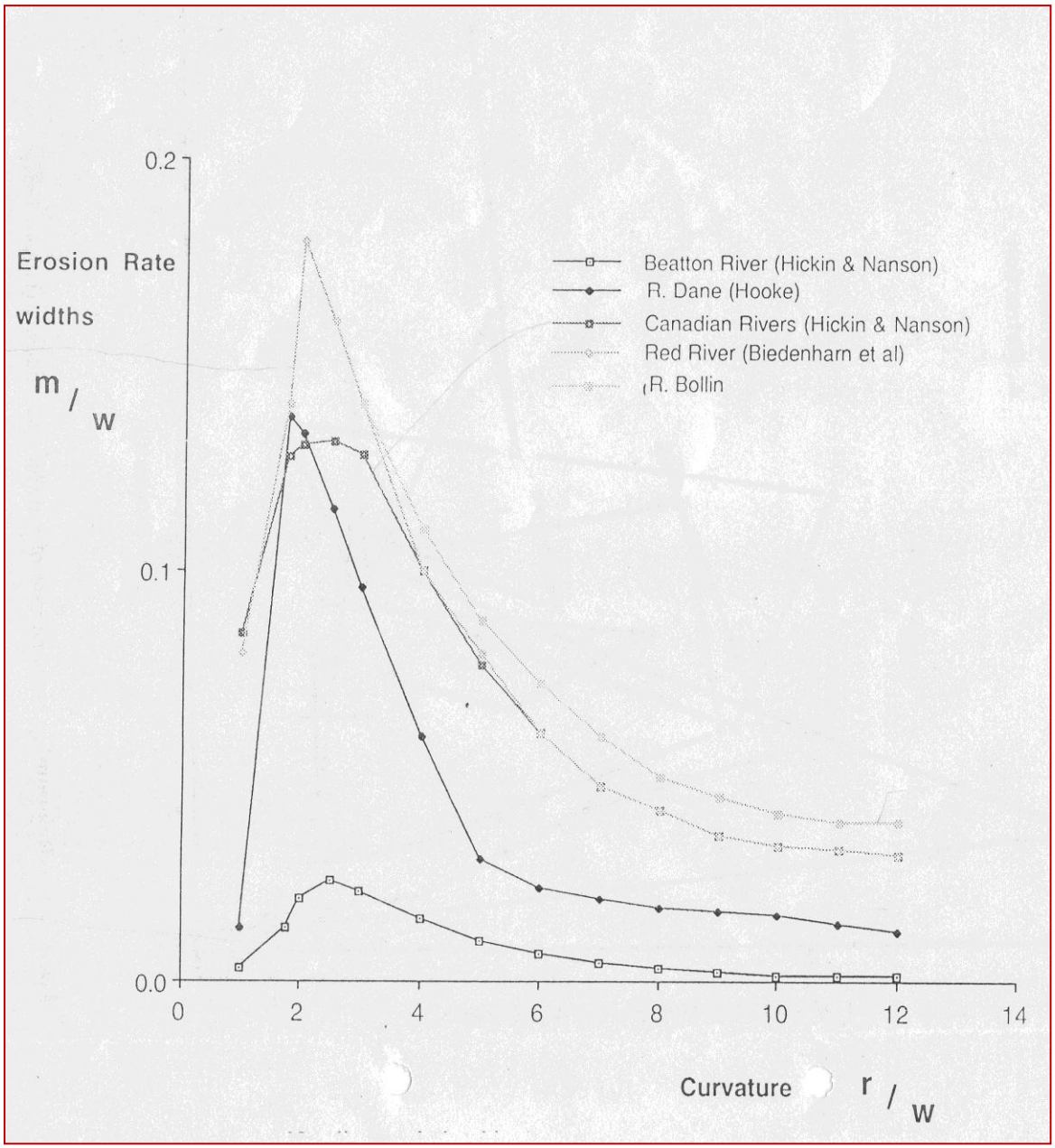

Figure 8.1: Envelope curves for the annual, dimensionless rate of erosion as a function of dimensionless radius of curvature (from Hooke, 1991).

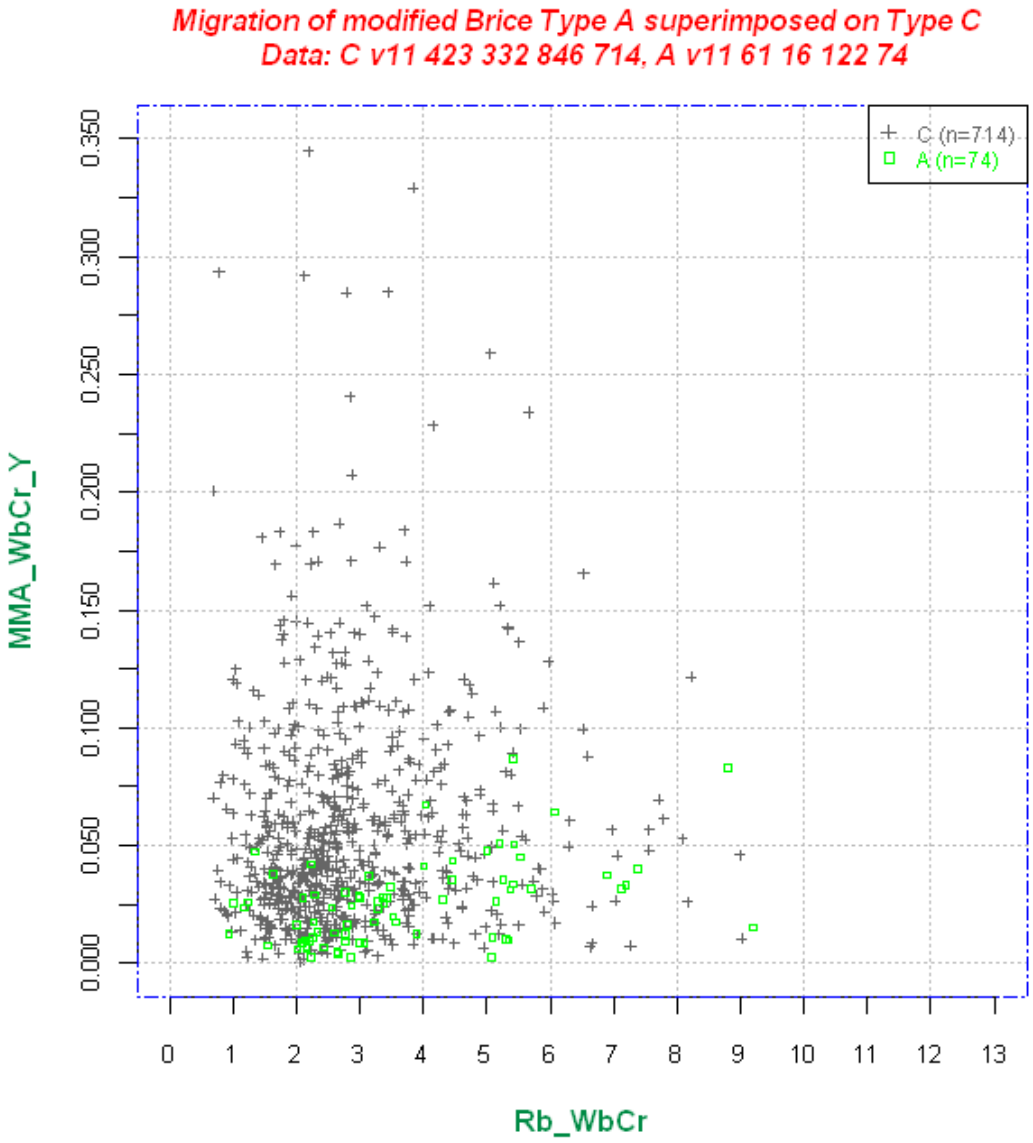

Figure 8.2: Comparison of scatter graphs for modified Brice Type A and Type C rivers.

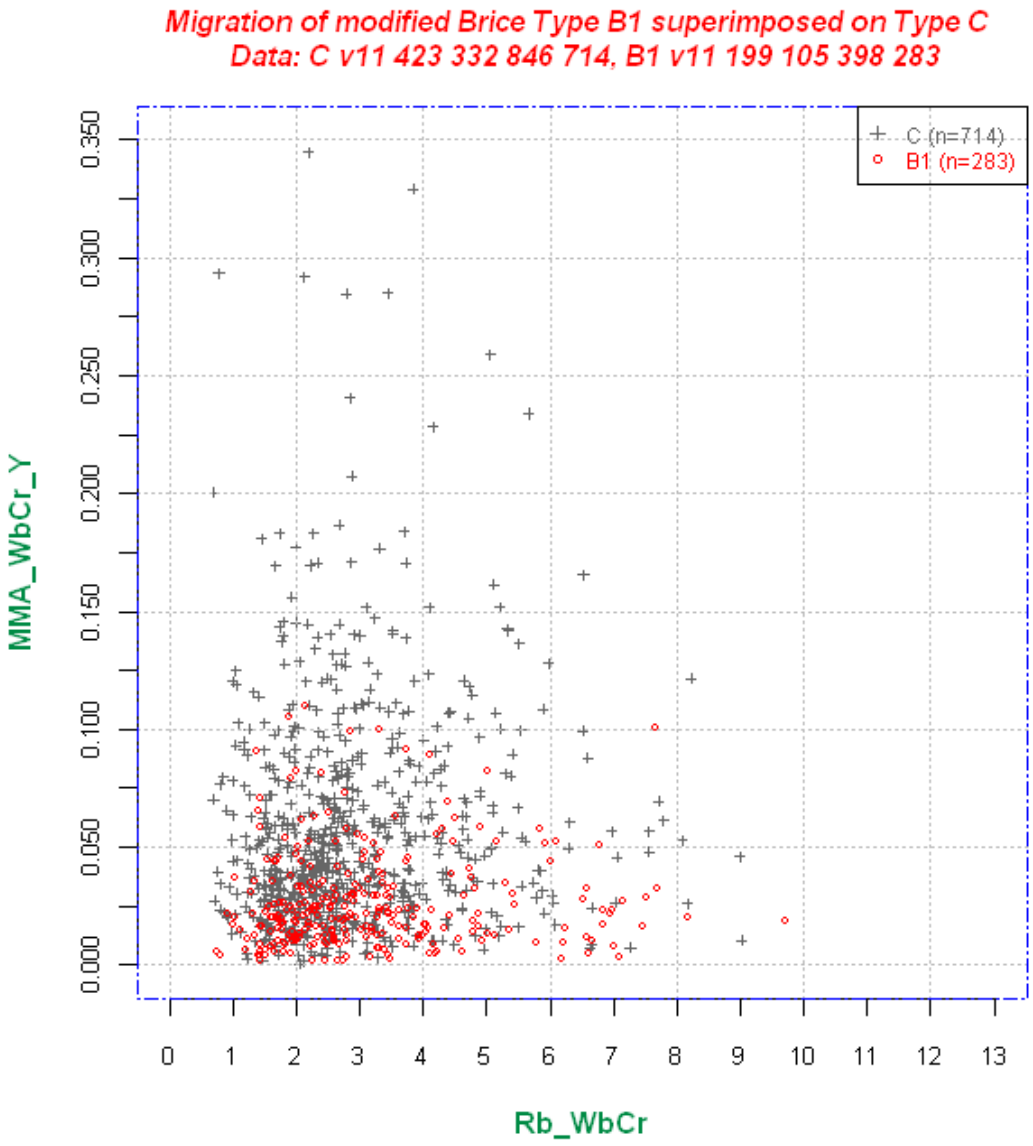

Figure 8.3: Comparison of scatter graphs for modified Brice Type B1 and Type C rivers.

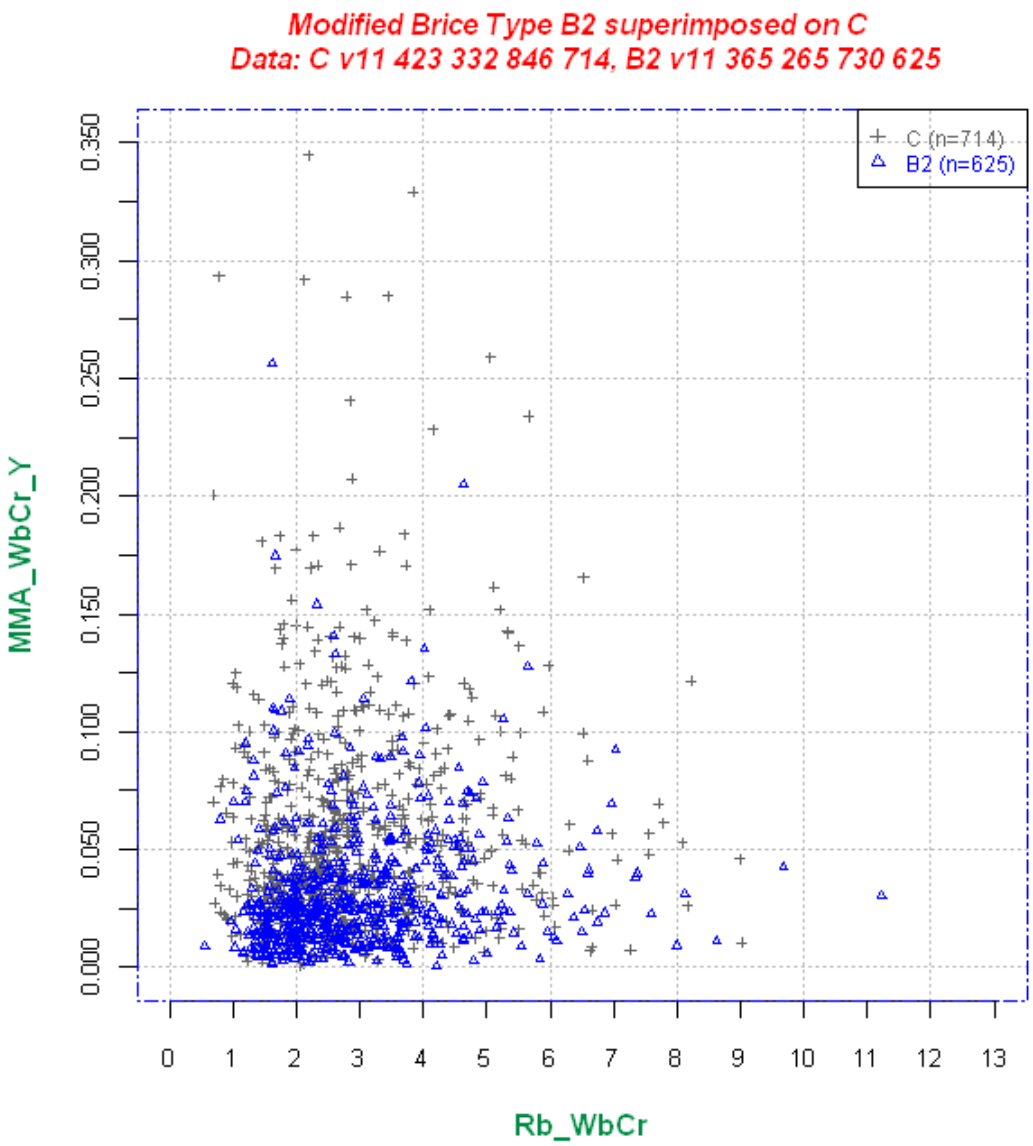

Figure 8.4: Comparison of scatter graphs for modified Brice Type B2 and Type C rivers.

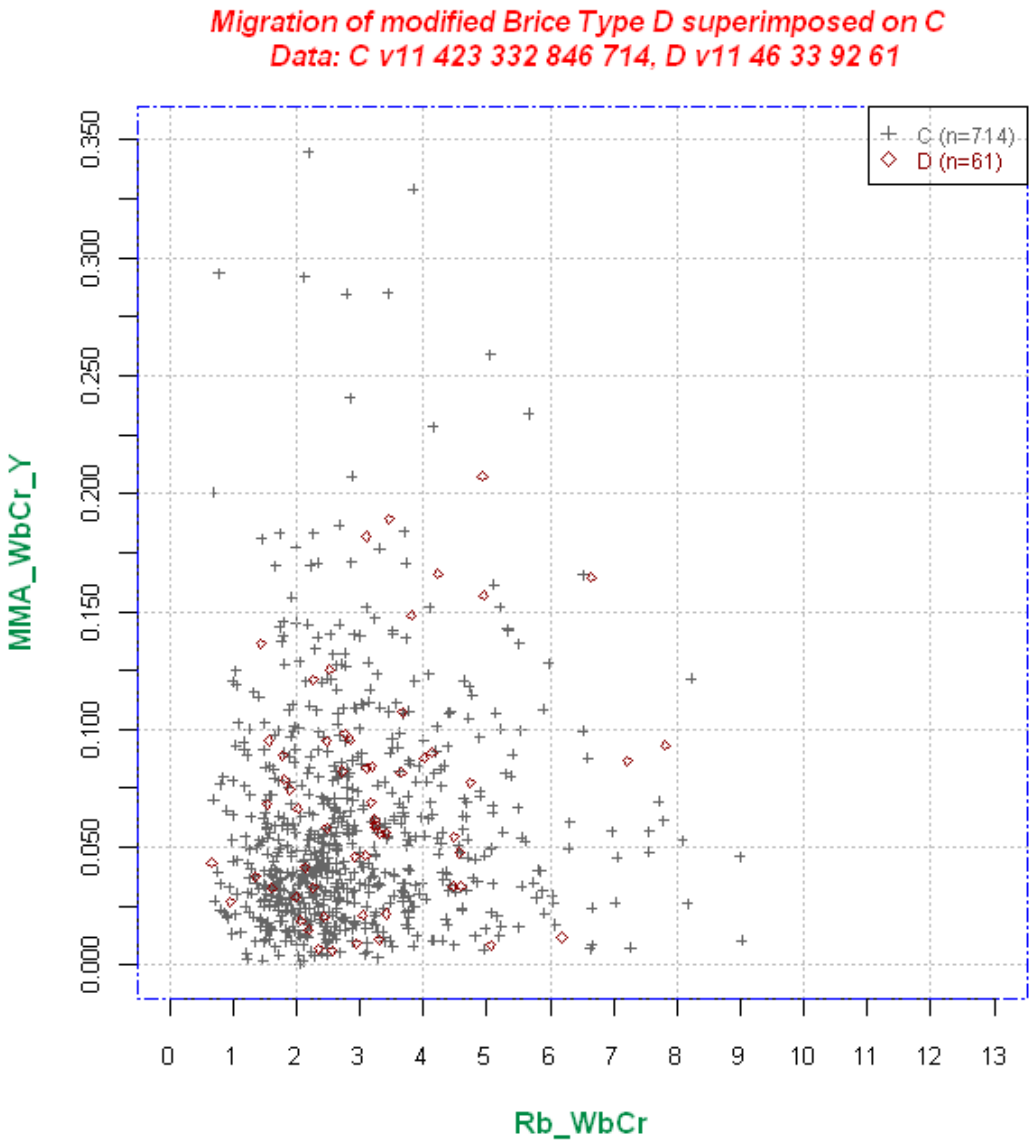

Figure 8.5: Comparison of scatter graphs for modified Brice Type D and Type C rivers.

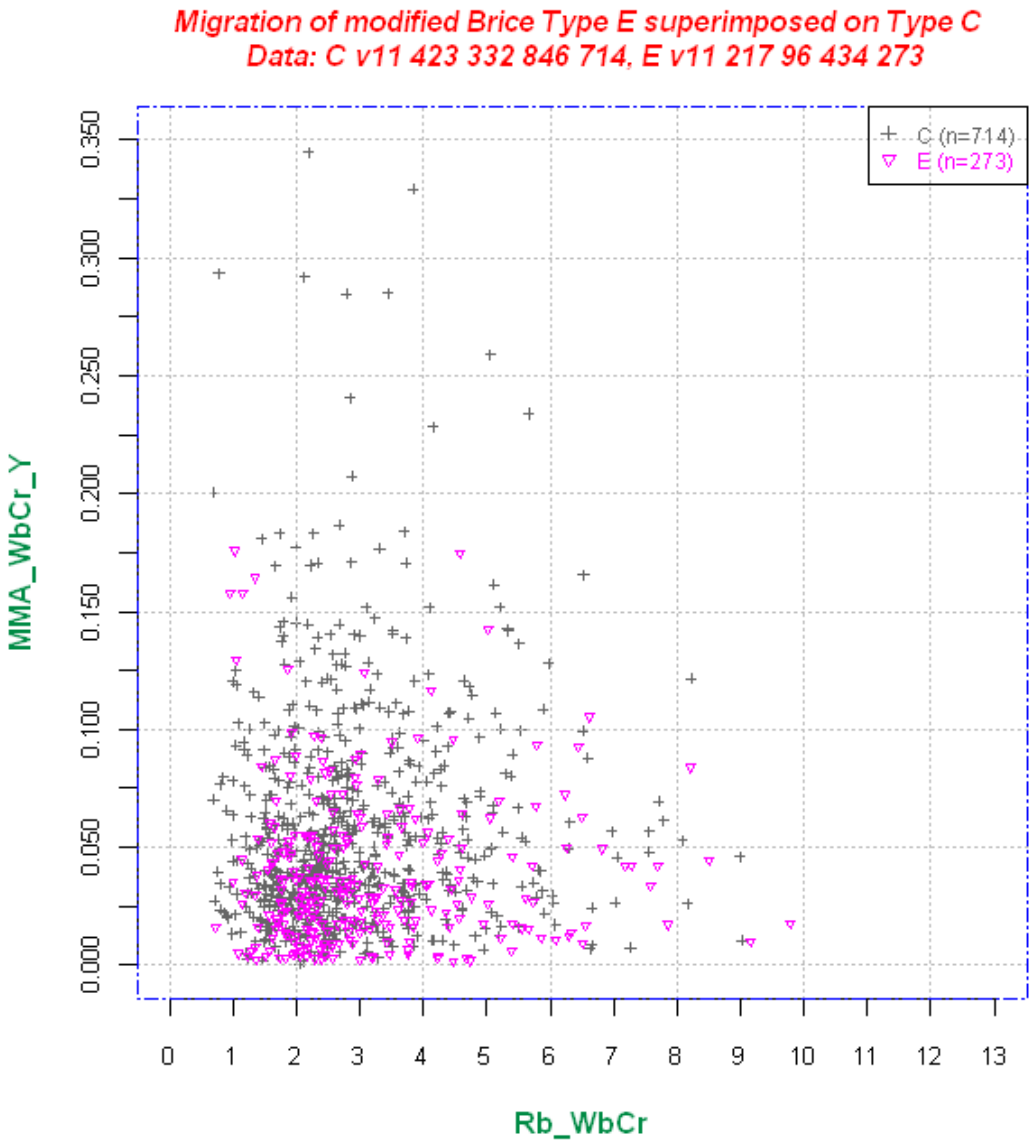

Figure 8.6: Comparison of scatter graphs for modified Brice Type E and Type C rivers.

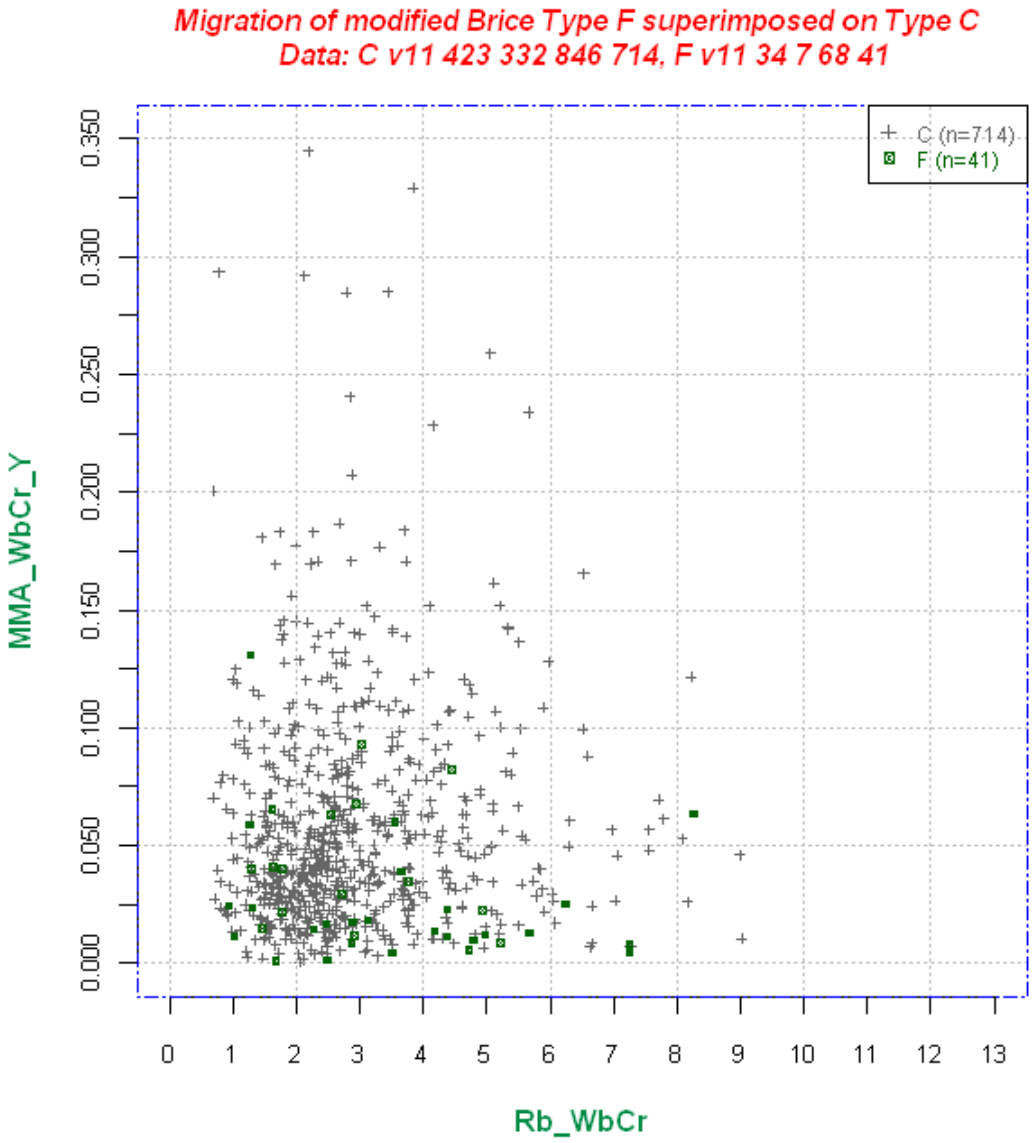

Figure 8.7: Comparison of scatter graphs for modified Brice Type F and Type C rivers.

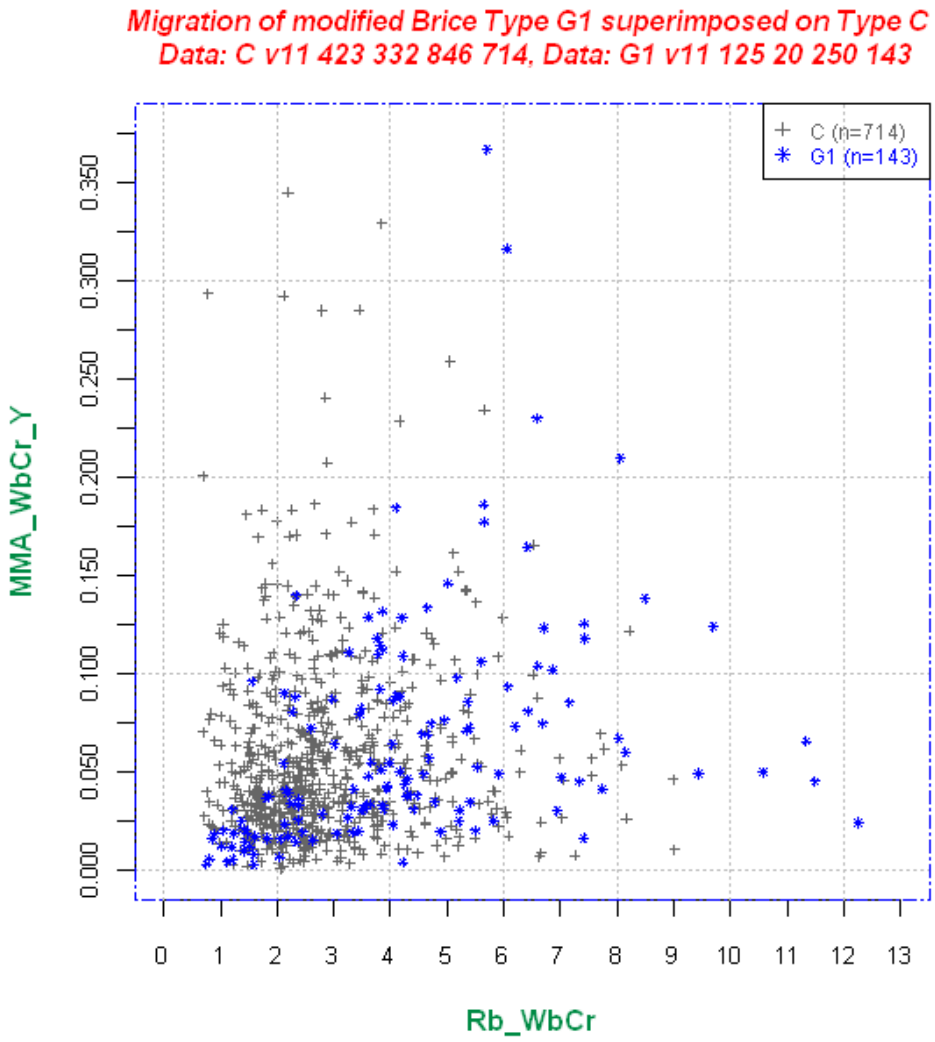

Figure 8.8: Comparison of scatter graphs for modified Brice Type G1 and Type C rivers.

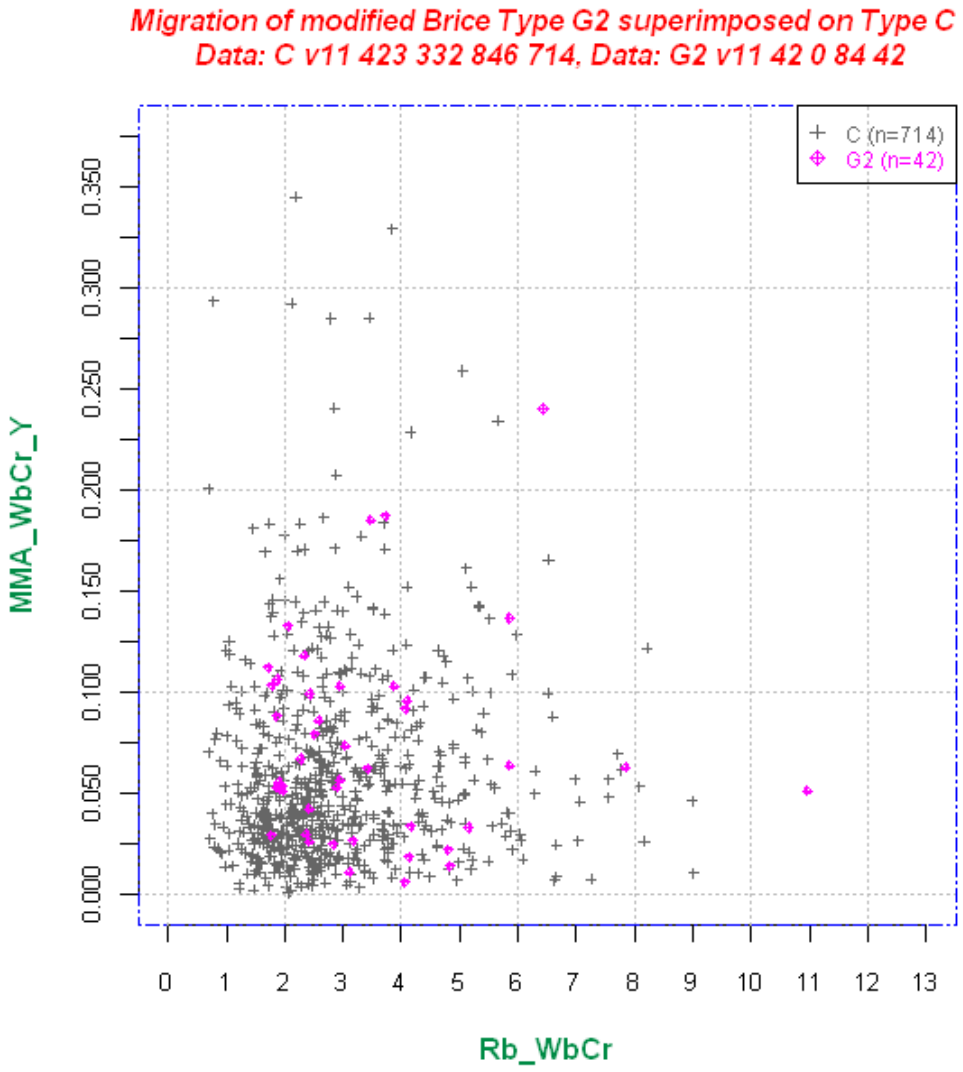

Figure 8.9: Comparison of scatter graphs for modified Brice Type G2 and Type C rivers.

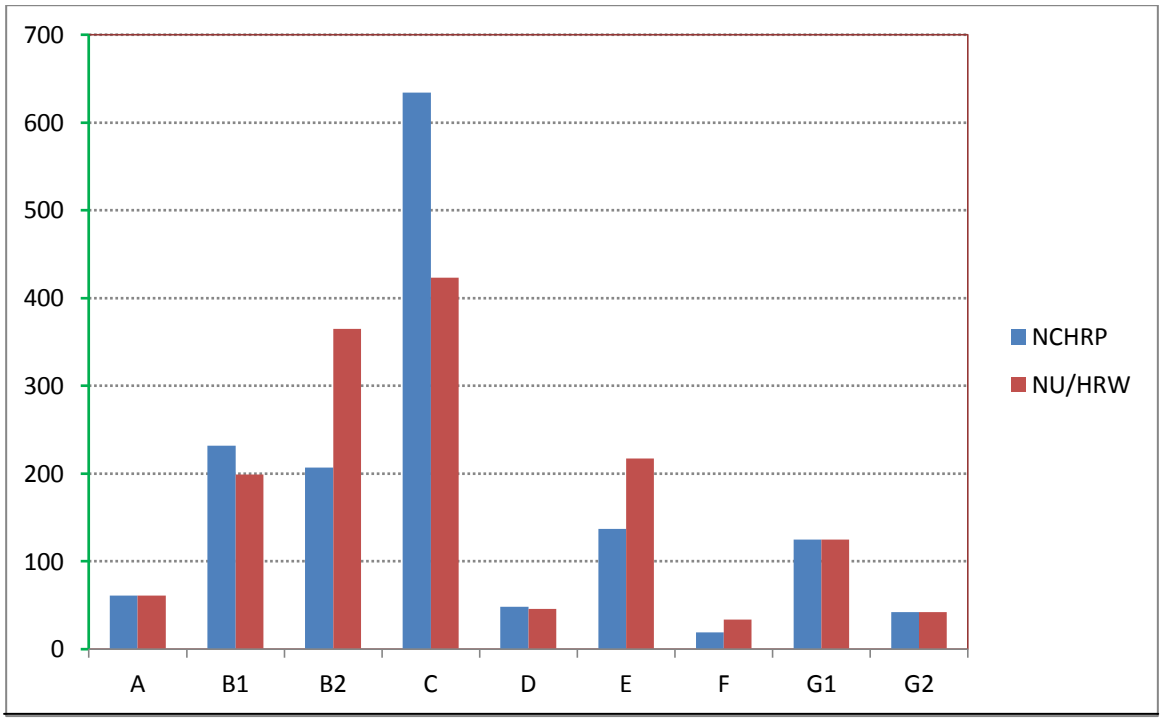

Figure 8.10: Comparison of bend frequencies by Brice Type in the NCHRP and UoN/HRW databases. Differences reflect the outcomes of re-classification performed during this study.

False facts are highly injurious to the progress of science, for they often endure long; but false views, if supported by some evidence, do little harm, for every one takes salutary pleasure in proving their falseness.

--- Charles Darwin

Chapter 9
Conclusions, Limitations and Research Recommendations

9.1 Conclusions

9.1.1 Research Context and Aim

In Chapter 1, it was stated that:

*The **aim** of this research is to develop an original, scientifically-based, and practical approach to the risk-based prediction of the hazard associated with bend migration that accounts for the uncertainty inherent to the morphological behaviour of rivers.*

Rivers are perhaps the most dynamic geomorphological systems agent on the earth. This dynamism stems from their energetic hydrodynamics, capacity to erode sediment, transport it over long distances, sorting it in the process, and using it to build sedimentary features of huge scale and importance. The fluvial system is naturally governed by, and responds to changes in, multiple controlling factors ranging in scale from regional climate and geology, to basin and local terrain, soils and vegetation. For early civilisations, the propensity of rivers to flood surrounding land and change their courses at will discouraged permanent settlement along valley bottoms and those communities that did occupy the floodplain adapted to the risks there by raising their homes on mounds and, when bank erosion approached, retreating to other, safer locations.

However, through artifice, people acquired the capability to 'tame' at least the smaller, less unruly watercourses and, gradually, social development and economic growth led to more and more

settlements and structures being built along or near river channels. In parallel, increasingly stringent efforts were made to protect people and property from flooding, leading to the construction of hundreds of thousands of kilometres of embankments along the courses of the world's rivers. At the same time, inland communication routes have become focused on river valleys and so the number of road and rail bridges has mushroomed. For example, the USA alone has around half a million bridges that cross watercourses. In terms of risk, it is sobering to read that every bridge in the Swat Valley, Pakistan was destroyed by the 2010 flood on the River Indus.

The truth is that, in the modern era, it is very seldom feasible to 'retreat' in the face of bank erosion because settlements, private property and public infrastructure represent valuable, fixed assets. Under these circumstances, society needs to be able to make sensible decisions concerning the management of risks associated with bank erosion and channel migration – processes that are concentrated at the outer margins of bends in meandering rivers.

It is in this context that the need arises to make quantitative predictions of possible future rates and likely future directions of meander bend migration. This is a challenging task and it would be beyond the capability of this or any other doctoral thesis to meet that need entirely. Having said that, the dire need for predictive capacity that is practical and accessible to end users needing to address and solve problems in LEDCs as well as MEDCs justifies the approach taken in the research reported in this thesis.

The research reported here represents an early but scientifically sound step towards delivering bend migration prediction tools that account for uncertainty and take a risk-based approach, while also being comprehensive and easily to apply in practice. The outcome of the work should, therefore, be not only of academic interest but should also contribute to progress towards delivery of a practical methodology and a useful tool for use by practicing river scientists, engineers and managers. On this basis, it may be concluded that the overall aim of the research has been achieved.

Chapter 1 also set out a series of specific objectives, each of which represents a significant, subsidiary aim in itself. Each of these objectives is revisited in the following section.

9.1.2 Research Objectives

Objective 1: To study and define modes of bend migration in a meandering streams with different types of morphology

Since the focus of this research was on bend migration, due emphasis was given to studying the various modes of bend movement. Reviewing the literature revealed that bend movement and development may be *simple* or *complex*. Simple development takes place through the operation of a single mode of movement. Complex development results from the simultaneous operation of multiple modes of movement. The literature reports that there are four modes of movement: *extension*, *translation, expansion* and *rotation.*

Extension and translation are customarily defined with reference to bend orientation, with extension described as being in the direction of the axis of the bend and translation being described as being normal to the bend axis. Expansion is a radial movement with respect to the centre of the bend in previous time point and is, hence, independent of extension or translation. Rotation is a change in the orientation of the bend (defined by the heading of an axis drawn from the centre of curvature to the bend apex) that does not involve migration of the bend centre in any direction. Any form of complex development can be resolved into a combination of these four simple modes. This review identified the modes of movement responsible for bend migration and highlighted the importance of roles played by bend orientation and the location of the apex.

Further, original, investigation of the planimetric outcomes of different modes and combinations of bend movement performed as part of the research reported here established that both simple and complex bend development can be resolved into normal (cross-stream) and tangential (long-stream) components. In this any movement of the bend apex can be expressed in terms of *normal and tangential migration*. It is suggested that these two components of migration may usefully be employed in explaining migration measured at the bend apex.

Objective 2: To select an analysis approach suited to development of a practical tool for predicting the rate of future bend migration

The literature confirmed that no process-based, numerical model capable of simulating bend migration in real rivers of periods of years to decades currently exists. As a general rule, "The only complete model of a river is the river itself". In this sense, historical records of river behaviour convey the integrated effects of all past fluvial events and morphological responses. While the past behaviour of the river may not, in detail, be repeated in the future, it does provide the basis for envisaging possible future behaviours, for which the probability of occurrence can be quantified when an adequate quantity and quality of historical data are available to support the analysis.

Based on consideration of the limitations of existing, theoretically-based models, the uncertainties involved in characterising bend geometries and floodplain properties, and the unknowable status of the sequence of future hydrological events it was concluded that deterministic predictions of bankline retreat due to bend migration cannot be made reliably. It was, therefore, decided that an empirically based, probabilistic approach to prediction provides the only practical means of making the predictions needed to inform risk assessment and decision making regarding risk management.

It has long been recognised that the dimensionless rate of bend migration (M/W) is related to the stage of bend evolution (initiation, growth, translation, termination) and that this can be represented by the ratio of the bend radius of curvature to the channel width (R/W), as per the functional relationship given in Equation 1.1. It was decided to analyse bend migration based on these parameters and use the dimensionless form of the bend radius as the independent variable in the probabilistic analysis. As the aim was to make predictions of future bend migration, the values of bend radius and channel width used in the analysis were those at the beginning of a period of migration. Bend migration was expressed as a dimensionless annual rate (M/W) averaged over the period of record.

The direction in which a bend has migrated can also be ascertained through analysis of its historical positions and orientations. However, initial analysis and exploration of available records of bend migration revealed inherent difficulties in attempting to use documented changes in the past orientation of a bend together with changes in the orientation of its migration to predict its future direction. In the event, the uncertainties and complexities of trying to characterise and predict the migration vector restricted development of the probabilistic migration analysis to delivery of a practical tool to predict migration rate.

Objective 3: To determine how best to represent bend curvature for the purpose of predicting migration rate in practice

Researchers investigating the relationship between bend migration and radius of curvature have used various ways of defining bend curvature. Most use the radius of the channel centre which lies midway between the banklines identified on an aerial photograph, a map, or less often through a field survey. However, defining and delineating the centre line of an actively meandering channel having well developed bars and featuring banks with successive vegetation growth can be difficult both in principle and in practice. Also, the erosion hazard that this research is primarily interested in occurs at the outer bank rather than at the channel centre line. Finally, the top of outer bank is usually easier to define both in principle and in practice as it is a relatively sharp edge. For all these reasons it was decided to use the curve of the outer bank to represent the curvature of the bend. Since the outer bank of a bend in a meandering river does not follow a regular geometric shape, it is the radius of the *best-fitted circular arc* to the outer bankline in the zone of active migration that is used in this research.

It is also necessary to non-dimensionalise the radius to eliminate scale effects. As noted earlier, this is customarily achieved by dividing it by the channel width. For this purpose the average of the widths measured at the crossings immediately up and downstream of the study bend has been used since these widths have advantages over the width at bend apex morphologically and statistically (see Chapter 5). With regard to morphological considerations, at a crossing the channel width is more stable and, compared to the inner bank at the bend, the banklines are higher

and are formed in older more consolidated materials - making them easier to identify. Also, from a hydraulic/fluvial point of view, at the bend apex only some portion of a channel width near the outer bank carries downstream flow. Finally, statistically, data for width measured at the apex are more dispersed than those for the crossings, indicating that they are less suitable for supplying measures of central tendency.

Objective 4: To select a bend feature suitable for characterising bend migration rate and the hazard posed by this migration

In the literature some investigators compute mean migration by dividing the area eroded by the migrating bend by the length eroded along the previous bankline. This is, effectively, the average width of the eroded area. This value may be useful in characterising the mean, linear distance by which the outer bank of the bend has eaten into the floodplain, but it would not be relevant with respect to whether a fixed asset located on the floodplain was or was not likely to have been attacked, since this depends more on the maximum rather than the average amount of migration at outer bank.

There is also a general belief in the literature that outer bank migration can adequately be represented by movement recorded at the bend centre (that is: the centre of curvature of a circular arc fitted to the bend). This was investigated in depth (see Chapter 3) and it was concluded that this is, in fact a misconception.

In the literature, bend migration is often evaluated by consideration of the shifting of the centre line of the channel at the bend between two successive points in time. However, the aim of this research is to analyse and predict the hazard to assets on the floodplain associated with bend migration and, from a mechanistic point of view, it is erosion of the outer bank threatens those assets. Hence, the emphasis in this analysis must be on outer bank migration when representing and evaluating bend migration. Further, it is at the bend apex that the axis of the bend meets the curve of the outer bank. The location of the apex relative to the centre of curvature also defines the minimum radius of curvature of the bend, which is important in influencing the rate of migration. Based on these theoretical and practical considerations, it was decided to select the

bend apex as the feature to represent the bend in terms of defining bend coordinates (Easting and Northing) at the start and end of the study period, and calculating the rate and direction of migration. Further, it in terms of movement of the bend apex that the refined database, probabilistic analysis and prediction tool developed herein are defined (see Chapter 4).

Objective 5: To obtain, quality check and analyse a suitable database of historical bend geometries and movements

The National Cooperative Highway Research Program (NCHRP) of the USA, under the direction of the Transportation Research Board (TRB), undertook a project with the objective of developing a practical methodology to predict the rate and extent of channel migration in proximity to road bridges. The results were published by Lagasse et al. (2003). The NCHRP database includes data for 1,505 bends taken from 125 locations on 89 rivers spread across 24 American States. The rivers were classified into nine categories of meandering (based on a modified Brice Typology). Bend geometry data in the database were measured from aerial photographs and maps representing the bends in the 1930/40s, 1950/60s and 1990s.

This research obtained the NCHRP database for use as its main source of bend geometry and migration data. As this research uses an empirical, probabilistic approach, the quality and quantity of data are of paramount importance. Therefore, before using the data for this research it was necessary to perform a thorough quality check (QC), correct errors where possible, remove erroneous records where it was not possible to make corrections, and review the Brice typing of all study reaches.

The QC task proved to be extremely important as rigorous inspection revealed numerous errors and inconsistencies. QC involved careful checking and cross-checking of all records, application of exploratory statistical techniques, logical and intuitive reasoning, close inspection of the original aerial photographs and maps, and numerous telephone calls and e-mail exchanges with the originators of the database. It was also necessary to use the records of bend location on the dates of the relevant aerial photographs or maps to compute the migration rate and direction for

the bend apex as these parameters were not included in the NCHRP database. After a concerted and time consuming effort, a new database was compiled and checked. This refined database is called the *University of Nottingham/HR Wallingford Database*, or more briefly the UoN/HRW Database. A complete history of data correction and summary data for each record prior to and following correction can be found in the Appendix to Chapter 4.

Prior to bivariate, probabilistic analysis, variables were subjected to univariate analysis in order to investigate their distributions. The distributions of both dimensionless radius and migration rate were found to be heavily right-skewed. A normal distribution has many advantages statistically and the x-variable (R_b/W_bCr) was normalised by a logarithmic transformation and the y-variable ($MMA/W_bCr/Y$) was normalised by a power transformation.

The purpose of the probabilistic analysis was to support prediction of the rate of meander migration, expressed using the transformed variable $(MMA/W_bCr/Y)^{0.16}$ for a known value of the ratio of bend radius to width, expressed using the transformed variable $\log_{10}(R_b/W_bCr)$. Hence, empirical, bivariate densities were computed using the two dimensional kernel *density estimation* method. This method computes densities at square grid points formed by lines on an (x,y) plane parallel to x-axis and y-axis. Hence, the conditional density function of $(MMA/W_bCr/Y)^{0.16}$ was computed from the bivariate density function for a large number of selected values of $\log_{10}(R_b/W_bCr)$ extending across the entire range of values for $\log_{10}(R_b/W_bCr)$. Finally, a fitted normal conditional density function for $(MMA/W_bCr/Y)^{0.16}$ was computed for each selected value of $\log_{10}(R_b/WbCr)$. Details of the data analysis may be found in Chapter 5 and the Appendix to Chapter 5.

Objective 6: To develop a probabilistic, predictive tool for bend migration rate

Using the fitted normal conditional density function described above, rates of meander migration were estimated corresponding to: 50%, 60%, 75%, 80%, 90%, 95%, 97%, 98%, and 99% probability of not being exceeded. The resulting curves are presented in Figure 5.57.

Three zones can be identified in probabilistic migration prediction curves. The left zone, where the curves are shown as dotted lines, covers values dimensionless bend radius (R_b/W_bCr) less than 1. This zone corresponds to late stage meander behaviour (the termination stage in Hickin and Nanson's evolutionary classification). The middle zone, where the curves are shown as solid lines, covers the range $1 < R_b/W_bCr < 8.5$. This zone includes the meander growth and migration stages of Hickin and Nanson. The right zone, where the curves are again represented by dotted lines, covers values of $R_b/W_bCr > 8.5$. This corresponds to the meander initiation stage of Hickin and Nanson. The probabilities expressed on the graph are that the migration rate (the y-variable) will be equal to or less than the value predicted for the specified bend curvature (x-variable). Mathematically, this is expressed in Equation 5.5.

To use the graph, a user calculates the ratio of bend radius to channel width (R/W) for the problem bend and locates this value on the x-axis in Figure 5.57. The user then selects the level of probability based on a judgment of the acceptable risk that the asset in question will be attacked by bank erosion within the prediction period. The migration rate is then read from y-axis for the specified bend curvature and probability level. Hence, in practice, the tool is simple to use. Details of the probabilistic analysis and prediction tool may be found in Chapter 5, while the robustness of the analysis and its sensitivity to sampling variability are explored and tested in Chapter 6.

Objective 7: To demonstrate how the risk to an asset on the floodplain posed by a problem bend can be assessed by reviewing and discussing the prediction tool on a step by step basis

The risk associated with a hazard depends on the probability that it will occur multiplied by the consequences should it do so and this is considered in Chapter 7. In Chapter 7 it is demonstrated that bend migration risk can be quantified using Equation 7.1. It follows that assessment of migration risk requires not only calculation of the probability that migration will result in the asset at risk being subjected to bank erosion, but also estimation of the consequences of this happening. The consequences relate primarily to the economic importance of the asset(s) (natural resources, buildings or infrastructure) at risk. However, other impacts

(social, political, military, environmental) may also be significant and these too should be accounted for in the risk assessment.

In selecting the acceptable level of probability that the predicted rate of migration will not be exceeded (leading to unacceptable damage or destruction of the asset at risk), care should be exercised by the user in considering all the possible consequences should this occur. These should be determined by recognising the importance of the asset(s) from the points of view of all relevant stakeholders. Establishing a multi-criteria method for evaluating the consequences of bend migration is an important research need that should be addressed urgently, but it is well beyond the scope of this thesis.

Developing a practical risk assessment tool would not be an appropriate aim for doctoral research in Geography. However, achieving Objective 7 called for demonstration of how the risk to an asset on the floodplain posed by a problem bend could be assessed using a prediction tool based on the probabilistic analysis developed herein and to this end Box 7.4 illustrates how the probabilistic analysis might be used to make a risk-based decision on how far back from the river bank to position a piece of key infrastructure. Another common application would be to use the probabilistic analysis to estimate the risk to a diffuse floodplain asset such as an arable field adjacent to the outer margin of an active meander bend, a situation in which damage occurs as soon as the bank begins to retreat and then accrues as migration distance increases. In Chapter 7, the basis for assessing this type of risk based on the area under a probability-damage curve was identified and it was established that, as probability-damage curve is different for every case, a tool suitable for site-specific risk analysis would be required.

It is concluded that engineers and river scientists performing river analyses to support management or restoration constitute the potential 'end users' for practical QRA tools based on the probabilistic analysis developed in this thesis. It is further recognised that these end users will require guidance on how to apply the analysis backed up by some understanding of the statistics that underpins it.

In this thesis, only general guidelines are supplied and, given the serious threats to infrastructure and risks to human and natural resources associated with river shifting worldwide, a high priority will be placed on production of such a Guidance Manual and a published paper to support it within 12 months of the award of the doctorate.

9.2 Limitations

9.2.1 Overview

Although the research reported in this thesis has achieved its objectives, the work is not without its limitations and these should be acknowledged. Also, it is prudent to caution potential users of the tools derived here concerning these limitations.

9.2.2 Limitations Stemming from the Distributions of the Data

The first limitation to be recognised is that the conditional densities for the x-variable in Figure 5.57. Migration rates associated with bends of very tight (R/W < 1) and very long (R/W > 8.5) curvature are not well described by the fitted normal conditional densities (see Chapter 5 for details). This is due to the relatively low number of data points for bends that plot on the fringes of the sample space. The sparse data in these areas is not a sampling problem; it reflects the rarity of such bends in nature, which has been widely commented on in the literature (as discussed in Chapter 1). Nevertheless, the fact remains that the UoN/HRW database lacks sufficient entries for short and long radius bends to support confident analysis of bend migration rates across the full spectrum of bend curvatures likely to be encountered in practice.

Hence, in applying the migration rate prediction tool when assessing future migration risks, users should exercise greater caution when dealing with bends that have R/W values less than one or greater than 8.5. This is why the probability curves are dotted in the zones on the left and right of Figure 5.57. In highly sensitive cases, where the consequences of under-estimating the average

annual migration rate are particularly serious, it would be prudent to gather further information from, for example, historical records chronicling the past behaviour of very short or long radius bends in the reach around the problem bend, to supplement a probabilistic prediction using the tool developed here.

Limitations should similarly be noted with respect to the y-variable in Figure 5.57. A wide range of possible migration rates is possible for any particular value of the x-variable. The scatter includes some very high average annual migration rates (in excess of 20% of the width per annum: see Figure 5.3) and these strongly influence predicted migration values for high probabilities of the predicted rate not being exceeded. Yet the absolute number of data points upon which possibility and probability of these extreme rates is predicated is very small: in fact just 19 points plot above 0.2 on the y-axis. It follows that confidence in the validity of the curves for the highest probabilities must be tempered by the knowledge that they are based on less than twenty observations of such extreme migration in nature.

In this context, users should be aware that, when compared to envelope curves for bend average annual migration rate published in the literature, predictions based on curves for the highest probabilities of not being exceeded appear conservative. This suggests that uncertainty introduced by the low number of observations of extreme behaviour in the dataset is on the safe side and suggests that very high probability levels should be reserved for situations where the consequences of damage or destruction of the asset at risk are so serious that under-predicting the bend migration rate is simply unacceptable.

9.2.3 Limitations Stemming from the Nature of the Data

Further limitations stem from the fact that the empirical research reported here is based on ‘snap shot’ observations that were made 20 to 30 years apart on what were believed by the original researcher to be freely migrating bends in actively meandering, alluvial river reaches. It follows that the analyses and findings are valid only with respect to actively meandering, alluvial rivers in

which bends are free to migrate across a floodplain that is wider than the meander belt. This is a limited subset of meandering rivers, which are themselves a sub-set of alluvial rivers in general that also includes streams with straight, braided and anastomosing planforms. Consequently, application of the predictive tools derived from the analyses is likewise limited to freely migrating bends in alluvial, actively meandering reaches.

The records used to support the analysis represent bend migration as being a discrete variable. That is the position of bends on two or three occasions is represented with no information concerning what happened *between* those observations. The distance moved by the apex of the bend between observations is then divided by the length of time between them (usually 20 to 30 years) to generate the average annual rate of migration. In fact, migration is a semi-continuous process driven by the occurrence of hydrological and geotechnical events that cause the bank to retreat. Consequently, the rate of migration for a single year may range from near zero to values much higher than that recorded in the database. The limitation is then that, because the migration rates used in the analysis are multi-decadal averages, the results represent behaviour of the study bends at a decadal scale.

It follows that great care should be exercised by users performing short-term risk assessments for assets that are close enough to the outer bank line that they may be attacked within a few years. In such situations, the risk assessor needs additional information concerning the potential for the problem bend to experience short-duration bursts of high magnitude migration.

9.2.4 Limitations Stemming from the Implicit Assumption of Dynamic Stability

The analysis and tools reported here are based on data gathered from river reaches selected by the original researchers specifically because they were shown to have been in a state of dynamic stability during the 40 to 60 year period over which bend migration was measured. Strictly, this limits the validity of the results to rivers where the morphology of the channel is in meta-stable, dynamic equilibrium: that is it is adjusted to flow and sediment regimes that are on average, time

invariant. The corollary to this is that the probabilities attached to different rates of bend migration do not represent morphological responses to externally imposed step changes or perturbations of sufficient magnitude to disturb the meta-stable equilibrium condition.

In fact, a wide range of environmental and human phenomena operating from the basin to the bend scale may trigger complex morphological responses that alter the future migratory behaviour of a problem bend from that expected based on its stage of evolution and curvature. In Chapter 8, the various climatic, catchment and management changes that would most likely affect bend migration were discussed. Bearing them in mind, it could be argued that, in a future characterised by climate change and accelerating pressures on catchments associated with population growth and the intensified exploitation of natural resources, multi-decadal periods of dynamic equilibrium in rivers are likely to become the exception rather than the norm and that this should be taken on board when assessing migration risks.

In sensitive cases, it is recommended that the analytical method presented here should be used as a screening tool. That is to say that, given the very serious consequences of failure of major infrastructure – including loss of life – it would be prudent to at first ascertain whether the potential for bend migration to compromise the structure using this tool, but then follow up that assessment with a more sophisticated treatment in cases where the screening tool has identified that a significant potential risk exists.

9.3 Recommended Further Research

As described in Section 1.3, the relationship between bend migration and curvature established by Hickin and Nanson, and supported by many subsequent researchers, is based on the principle that, following inception, bend growth accelerates as the ratio of radius of curvature to channel width decreases. As the bend evolves further, the decreasing R/W value reaches a critical value somewhere between 4 and 2, at which bend growth is replaced by downstream translation and the rate of migration is maximised. The migration rate then slows and the bend enters the termination stage due to continued decrease in R/W to a value of about 1 or less. This pattern of bend

behaviour is taken by most river scientists and fluvial geomorphologists as explaining the characteristically right-skewed, uni-modal peak in the upper envelope curve between R/W values of 2 and 4 in plots of M/W against R/W.

This pattern of bend behaviour is clearly present in Hickin and Nanson's (1975) results for the Beaton River where data for 10 study bends were derived from meander scroll bars (see Figure 2.1). When, in 1983, Nanson and Hickin added six more data points, the overall shape of the scatter was maintained though variation in the range of migration rates associated with a particular value of R/W increased. In 1986, Nanson and Hickin brought the number of data points up to 118 by adding data from 18 other rivers, and they added upper and lower envelope curves. While the upper envelope showed the expected asymmetrical 'hump', no such feature was found in the lower envelope. This pattern has been confirmed by subsequent researchers including, for example, Biedenharn et al. (1989) based on data from the Red River, USA. This is also the case for the data compiled in the research reported here (see Figure 5.3). While the peak in the upper envelope for the data is a prominent feature of these scatter plots, it is important to note that the majority of bends experience low migration rates; even those with R/W values between 2 and 4.

There may seem to be nothing new in this account of bend evolution and the 'classic' scatter plots that account is widely accepted as explaining and that would be correct if, in fact, the scatter plot was derived by compiling the life histories of evolving bends. However, that is not actually the case. If an individual bend was monitored annually over its life span of, say, 40 years, then 40, sequential data points could be plotted on the scatter graph. If many bends were so monitored, the data set obtained would indeed represent the evolutionary behaviours of bends and trends of typical behaviour could be discerned based on the amalgamated, time based records.

But that is not how the data in the scatter plots published in the research literature were compiled. In fact, the plotted migration data come from a large number of bends that have been observed at a *single point in time, or at best two or three points in time*. Consequently, the data do not

represent the evolutionary traces of bends from inception to termination. There is an untested, implicit assumption that R/W is a proxy variable representing evolutionary stage.

It is, therefore, recommended that further research be performed to investigate whether Hickin and Nanson's account of bend evolution *is* actually a valid description of the behaviour displayed by freely migrating bends in actively meandering rivers with alluvial channels. This should be possible given the recent, massive increase in the availability of aerial photographs stretching back to the 1920s and satellite images from the late-1960s onwards. It is predicted here that important new insight, understanding and explanation of bend behaviour will be gained from monitoring how the rate and direction of bend migration respond to changes in bend curvature on a bend by bend basis, over prolonged periods that approach or exceed the lifespan of individual bends.

Understanding how bend curvature interacts with evolutionary stage to control migration rate and direction as the bend progresses through its life stages would allow the critical values of R/W to be better defined and would greatly enhance our ability to explain and, therefore, predict bend migration for both scientific and practical purposes.

References

Ackers, P and Charlton, F. G., 1970. *Geometry of small meandering streams.* Proceedings of the Institution of Civil Engineers, Supplement volume 1970. London: The Institution of Civil Engineers.

Alam, M.K., Hasan, A.K.M.S., Khan, M.R. and Whitney, J.W., 1990. *Geological Map of Bangladesh*. Geological Survey of Bangladesh, Dhaka, Bangladesh

Ashworth P., Bennett, S., Best, J. L., and McLelland, S., 1996. *Coherent Flow Structures in Open Channel*. Chichester : John Wiley and Sons, , UK.

Alabyan, A.M. and Chalor, R.S., 1998. *Types of River Channel Patterns and Their Natural Controls*. Earth Surface Processes and Landforms. 23, pp. 467-474.

Bagnold, R.A., 1960. *Some Aspects of the Shape of River Meanders*. Professional Paper of the United State Geological Survey, 181E, pp. 135-144.

Bathurst, J.C., Thorne, C.R., and Hey, R.D., 1977. *Direct Measurements of Secondary Currents*. In: River Bends, Nature, 269, 5628, pp. 504-506.

Bathurst, J.C., Thorne, C.R., and Hey, R.D., 1979. *Secondary Flow and Shear Stress at River Bends*. Journal of the Hydraulics Division, ASCE, 10, Proc. Paper 14906, pp. 1277-1295, and discussion. 106, No. HY10, pp. 1710-1713 and Closure, 107, HY5, pp. 644-647.

Begin, Ze'ev B., 1986. *Curvature Ratio and Rate of River Bend Migration Update.* Journal of Hydraulic Engineering, 112, 10, pp. 904-908.

Biedenharn D S, Raphelt N K and Montague C A, 1984. *Long Term Stability of the Ouchita River*. In: River Meandering: Proceedings of the Conference 'Rivers '83', New Orleans, Louisiana, 24-26 October 1983. New York: American Society of Civil Engineers, pp. 126-137.

Biedenharn, D.S., Combs, P., Hill, G.J., Pinkard, C., and Fred, Jr., Pinkston, C.B., 1989. *Relationship Betwen Channel Migration and Radius of Curvature on the Red River*. In: S. S. Wang edited, Sediment Transport Modelling, Proceedings of the International Symposium on Sediment Transport Modelling, New Orleans, August 1989, ASCE, pp. 536-541.

Brice, J.C., 1973. *Meandering pattern of the White River in Indiana: an analysis*. In: Morisawa, M., ed., Fluvial Geomorphology. Binghampton: Binghamtom State University of New York, pp. 178-200.**Brice, J.C., 1974.** *Evolution of meander loops. Bulletin of Geological Society of America*. 85, pp. 581-586.

Brice, J.C., 1975. *Air Photo Interpretation of the Form and Behavior of Alluvial Rivers*. Final Report to the U.S. Army Research Office, Washington, D.C.

Brice, J.C., 1977. *Lateral Migration of the Middle Sacramento River. California.* USGS Water Resources Investigation 77-43, 51 p.

Brice, J C, 1982. *Stream channel stability assessment*. Federal Highway Administration Report : RHWA/RD-82/021, 41p.

Brice, J.C., 1983., *Factors in Stability of Relocated Channels*. Journal of Hydraulic Engineering, ASCE, 109, 10, pp. 1298-1313.

Brice, J C, 1984. *Planform properties of meandering rivers*. In: River Meandering, Proceedings of the Conference 'Rivers '83', New Orleans, Louisiana, 24-26 October 1983. New York: American Society of Civil Engineers.

Burnett A. W. and Schumm S A, 1983. *Active Tectonics and River Response in Louisiana and Mississippi*. Science, 222, pp. 49-50.

Carson, M.A. and Lapointe, M.F., 1983. *The Inherent Asymmetry of River Meander Planform*. Journal of Geology, 91, pp. 41-55.

Carson, M.A., 1986. *Characteristics of High-energy Meandering Rivers*. The Canterbury Plains, New Zealand, *Geological Society of America Bulletin*, 97, pp. 886-895.

Chang, H.H., 1984. *Analysis of River Meanders*. Journal of Hydraulic Engineering, ASCE, 110, 1, pp. 37-50.

Chang, H.H., 1984. *Modeling of River Channel Changes*. Journal of Hydraulic Engineering, ASCE, 110, 2, pp. 157-172.

Cherry, D. S., Wilcock, P R and Wolman, M G, 1996. *Evaluation of methods for forecasting planform change and bankline migration in flood-control channels*. Department of Geography and Environmental Engineering, The Johns Hopkins University. The report prepared for the US Army Core of Engineers Waterways Experiment Station, Vicksburg, Mississippi, USA.

Chitale S. V., 1970. *River Channel Patterns*. Proceedings of American Society of Civil Engineers, Journal of the Hydraulics Division, 96, pp. 201-220.

Chitale, S.V., 1973. *Theories and Relationships of River Channel Patterns.* Journal of Hydrology, 19, pp. 285-308.

Cunge, J.A., 1984. *Feasibility of Mathematical Modeling of Meanders*. In: Elliott, C.M. (ed.), River Meandering, *Proceedings of the conference 'Rivers '83'*, ASCE, New Orleans, LA, pp. 794-809.

Daniel, J.F, 1971. *Channel movement of meandering Indiana Streams*. Professional Paper of United States Geological Survey, 732-A.

Darby, S.E. and Thorne, C.R., 1993. *Approaches to Modeling Width Adjustment in Curved Alluvial Channels*. Working Paper 20, Department of Geography, University of Nottingham, 90p.

Darby, S.E., Thorne, C.R., and Simon, A., 1996. *Numerical Simulation of Widening and Bed Deformation of Straight Sand-bed Rivers II: Model Evaluation*. Journal of Hydraulic Engineering, 122, 4, pp. 194-202.

Davis, D.H., 1908. *A Study of River Meanders on the Middle Rouge (Michigan)*. Journal of Geology, pp. 755-764.

Dietrich, W. E., Smith, J. D. and Dunne, T., 1983. *Boundary Shear Stress, Sediment Transport and Bed Morphology in a Sand-Bedded River Meander During High and Low Flow.* In: C. M Elliott (ed.) River Meandering, Proceedings of the Conference 'Rivers '83', New Orleans, Louisiana, 24-26 October 1983. New York: American Society of Civil Engineers, New York, pp. 622-639.

Einstein, H.A. and Shen, H.W., 1964. *A Study of Meandering in Straight Alluvial Channels*. Journal of Geophysical Research, 69, pp. 5329-5347.

Elgammal, A., Duraiswami, R., Harwood, D. and Davis, L.S., 2002. Background and Foreground Modelling Using Nonparametric Kernel Density Estination for Visual Surveillance. Proceedings of the IEEE, 90, 7, pp. 1151-1163.

Ferguson, R.I., 1973. *Regular Meander Path Models.* Water Resources Research, 9, pp. 1079-1086.

Ferguson, R.I., 1975. *Meander irregularity and wavelength estimation*. Journal of Hydrology, 26, pp. 315-333.**Ferguson, R.I., 1984**. *The Threshold Betwen Meandering and Braiding*. In: Channels and Channel Controls Structures, Proceedings of the First International Conference on Hydraulic Design in Water Resources Engineering. Berlin: Springer Verlag, pp. 6-15–6-29.

Fisk, H.N., 1944. *Fine-grained Alluvial Deposits and their Effects on Mississippi River Activity*. U.S. Army Core of Engineers, Engineer Research and Development Centre, The Waterways Experiment Station, 2, Vicksburg, Mississippi.

Friedkin, J.F., 1945. *A Laboratory Study of the Meandering Alluvial Rivers*. US Army Core of Engineers, Engineer Research and Development Centre, The Waterways Experiment Station, Vicksburg, Mississippi.

Garcia, M.H., Bittner, L., and Nino, Y., 1994. *Mathematical Modeling of Meandering Streams in Illinois: A Tool for Stream Management and Engineering*. Department of Civil Engineering, University of Illinois at Urbana-Champaign, Urbana, IL.

Harvey, M.D., 1989. *Meanderbelt Dynamics of the Sacramento River.* Proceedings, California Riparian Systems Conference, USDA Forest Service General Technical Report PSW-110, pp. 54-61.

Henderson, F.M., 1966. *Open Channel Flow.* New York: MacMillan, 522 p.

Hickin, E.J., 1974. *The Development of Meanders in Natural River-Channels*. American Journal of Science, 274, pp. 414-442.

Hickin, E.J. and Nanson, G.C., 1975. *The Character of Channel Migration on the Beaton River, Northeast British Columbia, Canada.* Geological Society of America Bulletin, 86, pp. 487-494.

Hickin, E.J, 1977. *The analysis of river planform responses to changes in discharge*. In: River Channel Changes, K. J. Gregory editor. Chichester: John Wiley and Sons, pp. 249-264.

Hickin, E.J., 1978. *Hydraulic Factors Controlling Channel Migration*. In: R. Davidson-Arnott and W. Nickling (eds.), Research in Fluvial Geomorphology, Proceedings of the 5th Guelph Symposium on Geomorphology, pp. 59-66.

Hickin, E.J., 1983. *River Channel Changes: Retrospect and Prospect*. In: J.D. Collinson and , J. Lewin (eds.), Modern and Ancient Fluvial Systems, Basil Blackwell, Oxford, pp. 61-83.

Hickin E J, 1984. *Vegetation and River Channel Dynamics*. The Canadian Geograhpher, 28, 2, pp.111-126.

Hickin, E.J. and Nanson, G.C., 1984. Lateral *Migration Rates of River Bends*. Journal of Hydraulic Engineering, ASCE, 110, 11, pp. 1557-1567.

Hooke, J.M., 1977. *The distribution and Nature of Changes in river channel pattern*. In: K.J. Gregory, editor, River Channel Changes. Chichester: John Wiley, pp. 265-280.

Hooke, J.M., and Harvey, A.M., 1983. Meander *Changes in relation to bend morphology and secondary flows. In: J.D. Collinson and J.M. Lewin editors, Modern and Ancient Fluvial Systems. Oxford: Basisl Blacwell, pp. 121-132.*

Hooke, J.M., 1984. *Changes in river meander : a review of techniques and results of analyses*. Progress in Physical Geography, 8, 4, pp. 473-508.

Hooke, J.M., 1991. *Non-linearity in River Meander Development: Chaos Theory and Is Implications*, Department of Geography, University of Portsmouth, Working Paper 19, 13 p.

Hooke, J.M. and Redmond, C.E., 1992. *Causes and Nature of River Planform Changes*. In: P. Billi, R.D. Hey, , C.R. Thorne and P. Tacconi (eds.), Dynamics of Gravel-bed Rivers. Chichester: John Wiley and Sons, pp. 557-571.

Hooke, J.M., 2004. *Cutoffs galore!: occurrence and causes of multiple cutoffs on a meandering river*. Geomorphology, 61, pp. 225–238.

Hooke, J.M., 2007. *Spatial instability, mechanisms and propagation of change in an active meandering river*. Geomorphology, 84, pp. 277–296.

Hooke, J.M., 2008. *Temporal variations in fluvial processes on an active meandering river over a 20-year period*. Geomorphology, 100, pp. 3–13.

Hubbard, D., 2007. *How to Measure Anything: Finding the Value of Intangibles in Business.* John Wiley & Sons, 46 p.

Hubbard, D., 2009. *The Failure of Risk Management: Why It's Broken and How to Fix It*. John Wiley & Sons.

Ikeda, S., Parker, G. and Sawai, K., 1981. *Bend Theory of River Meanders, Part1: Linear Development*. Journal of Fluid Mechanics, 112, pp. 363-377.

Khan, F.H., 1991. *Geology of Bangladesh*. University Press Ltd., Dhaka, Bangladesh.

Klaassen, G.J. and Zanten, B.H.J.V., 1989. *On cutoff ratios of curved channels*. In: Proceedings of the 23rd Congress of the IAHR, Ottawa, Canada. IAHR.

Knight, F.H., 1921. *Risk, Uncertainty and Profit.* Boston: Houghton Mifflin Company, The Riverside Press.

Knighton, D., 1998, *Fluvial Forms and Processes*. London: Arnold, 335 p.

Lagasse, P.F. et al, 2003. *Methodology for Predicting Channel Migration.* Final Report, Prepared for National Cooperative Highway Research Program, Transportation Research Board, National Research Council, USA. Prepared by Ayres Associates Inc, Fort Collins, Colorado, USA.

Lagasse, P.F. et al, 2004. Handbook *for Predicting Stream Meander Migration. NCHRP Report 533,* Prepared for National Cooperative Highway Research Program, Transportation Research Board, Washington D.C., USA. Prepared by Ayres Associates Inc, Fort Collins, Colorado, USA.

Lane, EW, 1957. *A study of shape of channels formed by natural streams flowing in erodible materials*. Corps of Engineers Sediment Studies Program, US Army Corps of Engineer Division, Missouri River; Omaha, Nebraska. M. R. D Sediment Series No. 9.

Lapointe, M.F. and Carson, M.A., 1986. *Migration Patterns of an Asymmetric Meandering River: The Rouge River, Quebec*. Water Resources Research, 22, 5, pp. 731-743.

Lawler, D.M., Thorne, C.R and Hooke, J.M, 1997. *Bank Erosion and Instability*. In: Applied Fluvial Geomorphology for River Engineering and Management, Colin R Thorne et al editors. Chichester: John Wiley and Sons

Leeder, M.R., 1973. *Fluviatile fining upwards cycles and the magnitudes of paleochannels.* Geology Magazine, 110, pp. 265-276.

Leopold, L.B. and Wolman, M.G., 1957. *River Channel Patterns: Braided, Meandering and Straight*. U.S. Geological Survey Professional Paper, 182B, 85 p.

Leopold, L. B. and Wolman, M. G., 1960. *River Meanders. Bulletin of the Geological Society of America*, 71, pp. 769-794.

Leopold, L.B, Wolman, M.G., and Miller, J.P., 1964. *Fluvial Processes in Geomorphology*. San Francisco: Freeman Press, 522 p.

Leopold, L.B. and Langbein, W.B., 1966. *River Meanders.* Scientific American, 214, 6, pp. 60-69.

Lewis, G.W. and Lewin, J., 1983. *Alluvial Cutoffs in Wales and the Borderlands*. IAS Special Publication No. 6, J.D. Collinson and J. Lewin (eds.), pp. 145-154.

Longley, P. A. et al, 2001. *Geographic Information Systems and Science*. Chichester: John Wiley and Sons.

Mackin, J.H, 1956. *Cause of braiding by a graded river (Abstract)*. Bulletin of the Geological Society of America, 67, pp. 1717-1718.

Macklin, M.G. and Lewin, J., 1997. *Channel, Floodplain and Drainage Basin Response to Environmental Change*. In: Applied Fluvial Geomorphology for River Engineering and Management, Colin R Thorne et al editors. Chichester: John Wiley and Sons

Martinson, H.A. and Meade, R.H., 1983. *Channel Changes of Powder River 1938-1978, Powder River Country, Montana*. U.S. Geological Survey, Hydrologic Invest. Atlas, HA-0661.

Montgomery, D.R. and Buffington, J.M., 1997. *Channel-reach Morphology in Mountain Drainage Basins*. Geological Society of America Bulletin, 109, pp. 596-611.

Moody-Stuart, M., 1966. *High and Low Sinuosity Stream deposits, with Examples from the Devonian of Spitsbergen*. Journal of Sediment and Petroleum, 36, pp. 1102-1117.

Mosselman, E., 1995. *A Review of Mathematical Models of River Planform Changes*. In: C.R. Thorne, and A. Thompson (eds.), Geomorphology at Work, Earth Surface Processes and Landforms, 20, 7, pp. 661-670.

Nagabhushanaiah, H.S., 1967. *Meandering of Rivers*. Bulletin of the International Association of Scientific Hydrology, 12, 1, pp. 28-43.

Nanson, G.C., 1980. *A Regional Trend to Meander Migration*. Journal Geology, 88, pp. 100-108.

Nanson, G.C. and Hickin, E.J., 1983. *Channel Migration and Incision on the Beatton River*. Journal of Hydraulic Engineering, ASCE, 109.

Nanson, G.C. and Hickin, E.J., 1986. *A Statistical Analysis of Bank Erosion and Channel Migration in Western Canada*. Geological Society of America Bulletin, 97, pp, 497-504.

Nicoll, T. J. and Hickin, E. J, 2009. *Planform Geometry and Channel Migration of Confined Meandering Rivers on the Canadian Prairies*. Geomorphology (2009), doi: 10.1016/j.geomorph.2009.10.005

Odgaard, A.J., 1989. *River-Meander Model I: Development.* Journal of Hydraulic Engineering, ASCE, 115, 11, pp. 1433-1450.

Odgaard, A.J., 1989. *River-Meander Model II: Application*. Journal of Hydraulic Engineering, ASCE, 115, 11, pp. 1451-1464.

Perucca, E., Camporeale, C. and Ridolfi, L., 2007. *Significance of the Riparian Vegetation Dynamics on Meandering River Morphodynamics*. Water Resources Research, 43, pp. 1-10.

Peterson, M. S., 1986. *River Engineering*. New Jersey: Printice-Hall

Petts, G.E., Moller, H., and Roux, A.L. (eds.), 1989. *Historical Change of Large Alluvial Rivers, Western Europe.* , Chichester: John Wiley and Sons, 355 p.

Richards, K., 1982. *Rivers: Form and Process in Alluvial Channels*. , London: Methuen, 358 p.

Rust B.R., 1978. *A classification of alluvial channel systems*. In: Fluvial Sedimentology, Andrew D. Miall editor, Memoir 5. Calgary: Canadian Society of Petrolium Geologists, 1978.

Sarker, M.H., 2009. *Morphological Response of the Brahmaputra-Padma-Lower Meghna River System to the Assam Earthquake of 1950*. Unpublished PhD thesis, University of Nottingham, 345 p.

Schumm, S.A., 1963. *Sinuosity of Alluvial Rivers of the Great Plains.* Bulletin of the Geological Society of America, 74, pp. 1089-1100.

Schumm, S. A., 1977. *The Fluvial Systems*. New York: Wiley.

Schumm, S.A., Erskine, W.D. and Tilleard, J.W., 1996. *Morphology, Hydrology, and Evolution of the Anastomosing Ovens and King Rivers. Victoria, Australia*. Geological Society of America Bulletin, 108, 10, pp. 1212-1224.

Sikder, M.A.S, 1997. *Hydraulic Studies at Bifurcations in Alluvial Rivers with Complex Morphology*. Unpublished M.Sc in Water Resources Engineering thesis, Free University Brussels and Catholic University Louvain, Belgium, 92p. text.

Smith, D.G., 1976. *Effect of Vegetation on Lateral Migration of Anastomosed Channels of a Glacier Meltwater River*. Bulletin of the Geological Society of America, 87, pp. 857-860.

Smith, S.A. and McLean, 1984. *A Model for Meandering Rivers.* Water Resources Research, 20, pp. 1310-1315.

Sidorchuk, A. and Matveev, B., 1997. *Channel Processes and Erosion Rates in the Rivers of the Yamal Peninsula in Western Siberia*. In: L.J. Olive, R. J. Loughran and, J.A. Kesby (eds.), Variability in Stream Erosion and Sediment Transport, IAHS-AISH Publication 224, pp. 197-202.

Simon, A. and Darby, S.E., 1997. *Process-form Interactions in Unstable Sand-bed River Channels: A Numerical Modeling Approach*. Geomorphology, 21, pp.85-106.

Stolum, H.H., 1996. *River Meandering as a Self-organisation Process*. Science. 271, 5256, pp. 1710– 1713.

Stolum, H.H., 1998. *Planform Geometry and Dynamics of Meandering Rivers*. Geological Society of America Bulletin, 110, pp. 1485– 1498.

Sun, T., Meakin, P., Jossang, T., and Schwarz, K., 1996. *A Simulation Model for Meandering Rivers*. Water Resources Research, 32, 9, pp.2937-2954.

Thomas, G.B. and Finney, R.L., 1996. *Calculus and Analytic Geometry*. Delhi: Pearson Education Asia, Fith Indian Reprint.

Thorne, C.R. and Lewin, J., 1979. *Bank Processes, Bed Material Movement and Planform Development in a Meandering River*. In: D.D. Rhodes and G.P. Williams (eds), Adjustments of the Fluvial System, Kendall/Hunt Publishing Co, Dubaque, IA, USA, pp. 117-137.

Thorne, C.R., 1982. *Processes and Mechanisms of River Bank Erosion*. In: R.D. Hey, J.C. Bathurst and C.R. Thorne (eds.), Gravel-bed Rivers, John Wiley and Sons, New York, pp. 227-71.

Thorne, C.R., Zevenbergen, L.W., Pitlick, J.C., Rains, B., Bradley, J.B., and Julien, P.Y., 1985. *Direct Measurements of Secondary Currents in a Meandering Sand-bed River*. Nature, 316, 6022, pp. 746-747.

Thorne, C.R. and Osman, A.M., 1988a. *The Influence of Bank Stability on Regime Geometry of Natural Channels*. In: , W.R. White (ed.), International Conference on River Regime, Hydraulics Research Limited. , Chichester: John Wiley and Sons, p. 135-147.

Thorne, C.R. and Osman, A.M., 1988b. *Riverbank Stability Analysis II: Applications*. Journal Hydraulic Engineering, ASCE, 114, p. 151-172.

Thorne, C.R., 1991. *Bank Erosion and Meander Migration of the Red and Mississippi Rivers, USA*. In: F.H.m. Van de Ven, , D. Gutnecht, , D.P., Loucks and K.A. Satewicz (eds.), Hydrology for the Water Management of Large Rivers, IAHS-AISH Publication 201, p. 301-313.

Thorne, C.R., 1992. *Bend Scour and Bank Erosion on the Meandering Red River, Louisiana*. In: P.A. Carling and G.E. Petts (eds.), Lowland Floodplain Rivers: Geomorphological Perspectives. Chichester: John Wiley and Sons Ltd., p95-115.

Thorne, C.R, Russell, A.P.G. and Alam, M.K., 1993. *Planform Pattern and Channel Evolution of the Brahmaputra River, Bangladesh*. In: J.L. Best and C.S. Bristow (editors), Braided Rivers, Special Publication of the Geological Society, No.75. London: The Geological Society, p257-276.

Thorne, C.R, 1997. *Channel Types and Morphological Classification*. In: Colin R Thorne et al editors, Applied Fluvial Geomorphology for River Engineering and Management, Chichester: John Wiley and Sons.

Thorne, C R, Soar, P J, Skinner, K S and Sear, D. A., 2010. *Investigating, Characterising and Managing River Sediment Dynamics*. In: , D.A Sear, , M.D. Newson and , C. R. Thorne (eds) Guidebook of Applied Fluvial Geomorphology, London: Thomas Telford, pp. 120-195.

Tiffany, J.B. and Nelson, G. A., 1939. *Studies of Meandering of Model-streams*. Transactions of the American Geophysical Union, 20, pp. 644-649.

Tukey, J.W., 1977. *Exploratory Data Analysis.* Reading, Massachusetts: Addison-Wesley.

Weihaupt, J.G., 1989. *Disparities in the Forms of River Meanders and Oxbow Lakes*. Water Resources Publications, Littleton, CO, 184 p.

Whittlow, J., 1984. *Dictionary of Physical Geography.* , London: Penguin, 591 p.

Wilkinson, R.D., 2011. Lecture handout on G14CST: Computational Statistics. School of Mathematical Sciences, Univerity of Nottingham.

Williams, G.P., 1986. *River Meanders and Channel Size.* Journal of Hydrology, 88, 1-2, pp.147-164.

Appendix to Chapter 3

A3.1 Investigations Based on Scaled Drawing

Three features of bend geometry are considered:– bend centre (BC), bend radius (R), and bend orientation (BO) in describing any movement of a bend. Changes through time in any or all of these elements could produce 7 scenarios of meander movement:

Case 1 : BC unchanged, R changed, BO changed
Case 2 : BC changed, R unchanged, BO changed
Case 3 : BC changed, R changed, BO unchanged
Case 4 : BC unchanged, R unchanged, BO changed
Case 5 : BC unchanged, R changed, BO unchanged
Case 6 : BC changed, R unchanged, BO unchanged
Case 7 : BC changed, R changed, BO changed

These cases were investigated using scaled drawing to see whether the bend centre can adequately represent bend migration, and whether migration based on taking the bend apex to represent the bend yields the same amount of movement as computing it based on the bend centre and adding bend expansion to the movement of the bend centre. In examining these cases, the symbols and notation used are defined at the beginning of the thesis in the section on 'Symbols and Notations'.

Case 1: BC unchanged, R changed (increased), BO changed

Bend 1 is the initial position of a bend at a time T1 in Figure A3.1. PQ is the arc of the circle that best fits the bend with its centre at BC1, radius R1 (R1 = 3 cm), and orientation BO1 (90^{o}). BA1 is the bend apex - that is, the mid-point of the arc PQ. To define the bend orientation due east is the reference direction and orientation angles are measured with counter clockwise as the positive sense. It is important to mention that it is not an absolute necessity to measure the orientation with respective to due east in order to describe the movement of a single bend, but the NCHRP Study

measured bend orientation with respect to due east. For easy comprehension, therefore, due east is retained as the reference direction for this investigation.

Over a period TP12 the bend evolved to its new position, Bend 2, at T2. JK is the arc of the circle that best fits the bend, with its centre at BC2, a radius R2 (R2 = 4 cm), and bend orientation BO2 (70^o). BA2 is the bend apex (that is the mid-point of the arc JK). In this scenario, the bend apex BA1 moved in the downstream direction to a new position BA2. Figure A3.1 shows that, even though BC did not change its position at all, but the apex moved a considerable distance. Movement of the centre is defined as MMC12 (i.e. meander migration of the bend centre from T1 to T2) and bend apex movement is MMA12 (i.e. meander migration of the bend apex from T1 to T2). The change in radius is ΔR12 (i.e. the change in radius of curvature from T1 to T2). The bend has assumed its new position by expanding in radius and also changing its orientation.

In this case, apex movement involves two components: extension and translation. The location of the bend centre has remained unchanged, though the bend apex has moved considerably. Movement of the bend centre, therefore, cannot be considered to be representative in describing the migration of the bend. Figure A3.1 shows that MMC12 = 0 cm, ΔR12 = 1 cm and MMA12 = 1.6 cm. The amount of migration taking the bend centre movement and the radius change together is 1 cm (MMC12 + ΔR12 = 0 cm + 1 cm = 1 cm). *Hence, in this case, bend apex migration cannot be described by bend centre migration and change in radius added together.*

Case 2: BC changed, R unchanged, BO changed

This case is illustrated in Figure A3.2. As this case is similar to that for Case 1, the details are not repeated. In this scenario, the bend apex (BA) moves in the downstream direction. Although BC moves to a new position it should be noted that the apex movement is not the same as that of the bend centre. In Figure A3.2, MMC12 = 1.1 cm, ΔR12 = 0 cm and MMA12 = 1.7 cm. The amount of migration taking bend centre movement and change in radius together is 1.1 cm (MMC12 + ΔR12 = 1.1 cm + 0 cm = 1.1 cm). *Hence, in this case, bend apex migration cannot, therefore, be described by the bend centre migration and change in radius taken together.*

Case 3: BC changed, BR changed (increased), BO unchanged

This case is illustrated in Figure A3.3. In this case, the bend apex moves in the downstream direction from BA1 to BA2. In the Figure A3.3 it can be seen that though BC moves to a new position from BC1 to BC2, the amount of apex movement is not the same as that of the bend centre. As can be seen in Figure A3.3, MMC12 = 1.05 cm, ΔR12 = 2 cm, and MMA12 = 2.9 cm. The amount of migration taking bend centre movement and radius change taken together is 3.05 cm (MMC12 + ΔR12 = 1.05 cm + 2 cm = 3.05 cm). *In this case the bend apex migration cannot, therefore, be described by the bend centre migration and change in radius taken together.*

Case 4: BC unchanged, BR unchanged, BO changed

This case is illustrated in Figure A3.4. In this case, the bend apex (BA) moves in the downstream direction. It may seem that if the bend centre and bend radius remain unchanged, bend cannot move. However, it must be noted that the bend is not considered to be a whole circle. Only the migrating portion of the bend, which is only an arc of a circle, is measured and compared. PQ is the arc of the best-fit circle for the older bend. The new bend is represented by the arc of the best-fit circle JK. It should be noted that two possible models are examined here: a combination of various scenarios which arise by changing the elements – bend centre, radius and apex – pertaining to the bend in question in order to see whether a bend centre can represent bend migration and whether migration based on bend apex movement could yield the same amount of migration as taking bend centre movement and adding expansion to it.

In this case, whereas the location of the bend centre remained unchanged, the bend apex moved. Bend centre migration cannot, therefore, be describe migration of the bend. As can be seen in Figure A3.4, MMC12 = 0 cm, ΔR12 = 0 cm and MMA12 = 3.05 cm. The amount of migration taking the bend centre movement and radius change together is 0 cm (MMC12 + ΔR12 = 0 cm + 0 cm = 0 cm). *In this case, bend apex migration cannot, therefore, be described by the bend centre migration and change in radius taken together.*

Case 5: BC unchanged, BR changed (increased), BO unchanged

This case is illustrated in Figure A3.5. In this case, the bend apex (BA) moves in the direction of the previous bend orientation. The bend moves through radial expansion and extension. Although BC does not move at all, the bend apex moves from BA1 to BA2. In this case bend centre migration can, therefore, describe migration of the bend. The amount of the apex movement is equal to the expansion of bend radius. Figure A3.5 shows that MMC12 = 0 cm, ΔR12 = 1 cm and MMA12 = 1 cm. The amount of migration taking bend centre movement and radius change taken together is 1 cm (MMC12 + ΔR12 = 0 cm + 1 cm = 1 cm). *Therefore, in this case bend apex migration can be represented by bend centre migration and change in radius taken together*.

Case 6: BC changed, BR unchanged, BO unchanged

This case is illustrated in Figure A3.6. BO1 = 90^{o} = BO2 and the bend apex (BA) moves through extension from BA1 to BA2. Since BO remains unchanged, BC moves from BC1 to BC2. In Figure A3.6, MMC12 = 0.9 cm, ΔR12 = 0 cm and MMA12 = 0.9 cm. The amount of migration taking bend centre movement and radius change together is 0.9 cm (MMC12 + ΔR12 = 0.9 cm + 0 cm = 0.9 cm). *In this case, the bend apex migration can, therefore, be described by the bend centre migration and the change in radius taken together*.

Case 7: BC changed, BR changed, BO changed

This case is illustrated in Figure A3.7. The bend apex (BA) moves through both extension and translation. BC and BA both move, but with different magnitudes and directions. In Figure A3.7, MMC12 = 1.5 cm, ΔR12 = 1 cm and MMA12 = 3.45 cm. The amount of migration taking bend centre movement and radius change together is 2.5 cm (MMC12 + ΔR12 = 1.5 cm + 1 cm = 2.5 cm). *In this case bend apex migration cannot, therefore, be described by bend centre migration and change in radius taken together*.

In the cases where bend radius changed, in all cases it was assumed that this occurred through expansion. However, similar outcomes would be obtained if contraction of the bend radius was considered. The results of the cases described above are summarised in Table A3.1.

Table A3.1: Bend migration generated by changes in bend centre location, radius and orientation

Cases	Whether BC migrates	Whether BA migrates	Comments
1	No	Yes	BC cannot represent migration. BA movement is not equal to BC movement and radius expansion taken together.
2	Yes	Yes	BA movement is not equal to BC movement and radius expansion taken together.
3	Yes	Yes	BA movement is not equal to BC movement and radius expansion taken together.
4	No	Yes	BC cannot represent migration. BA movement is not equal to BC movement and radius expansion taken together.
5	Yes	Yes	BC cannot represent migration. BA movement is equal to BC movement and radius expansion taken together.
6	Yes	Yes	BA movement is equal to BC movement and radius expansion taken together.
7	Yes	Yes	BA movement is not equal to BC movement and radius expansion taken together.

To summarise, if all the cases described above are taken together it can be concluded that bend centre movement cannot fully represent the migration of a bend. Similarly, bend apex movement cannot be computed through computing the migration of the bend centre and adding to it the change in bend radius .

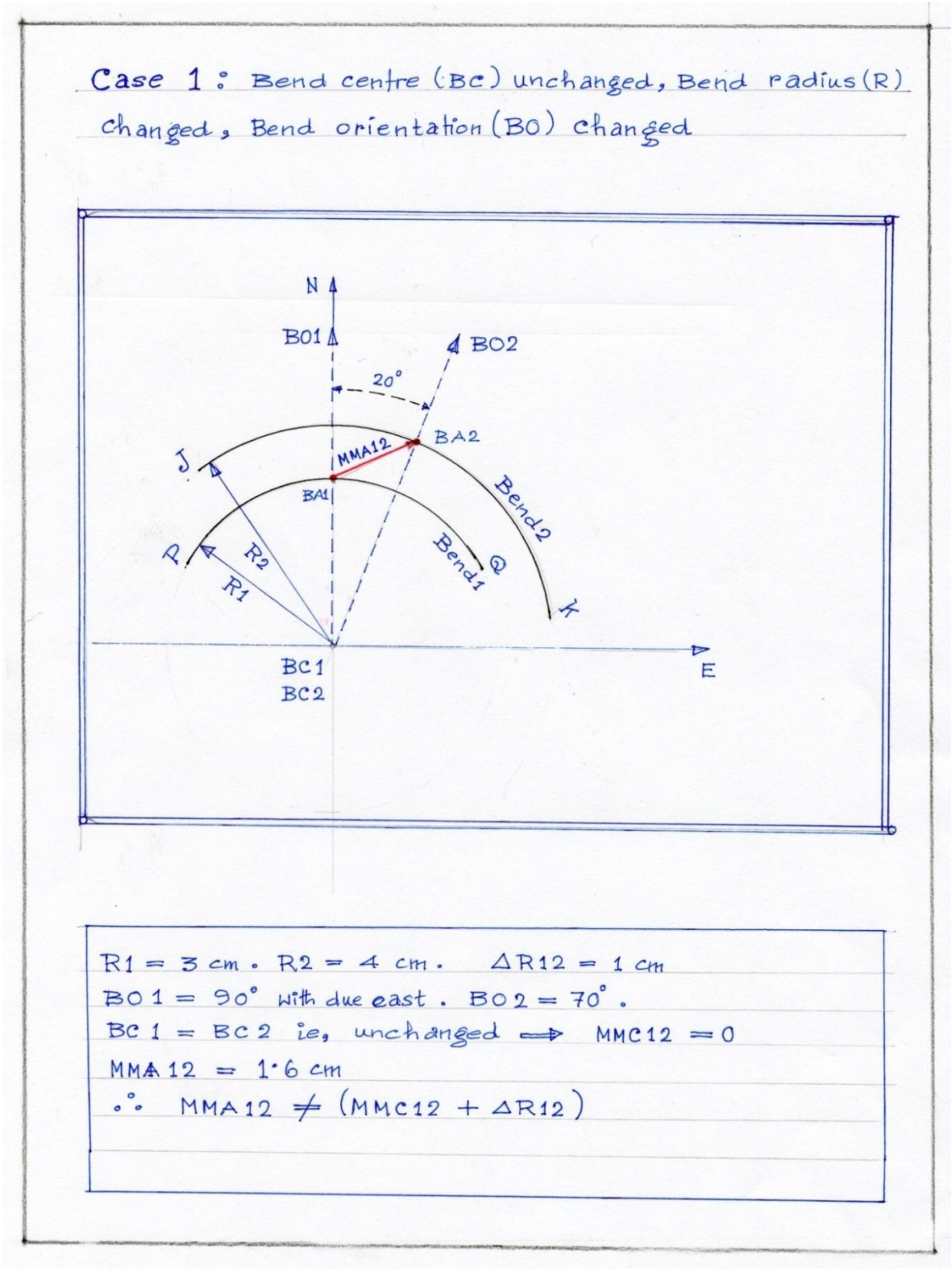

Figure A3.1: Checking the representation of bend movement while bend centre remains unchanged, radius changes, orientation changes, and also whether bend apex movement is the same as the bend centre movement plus change in radius over a time period.

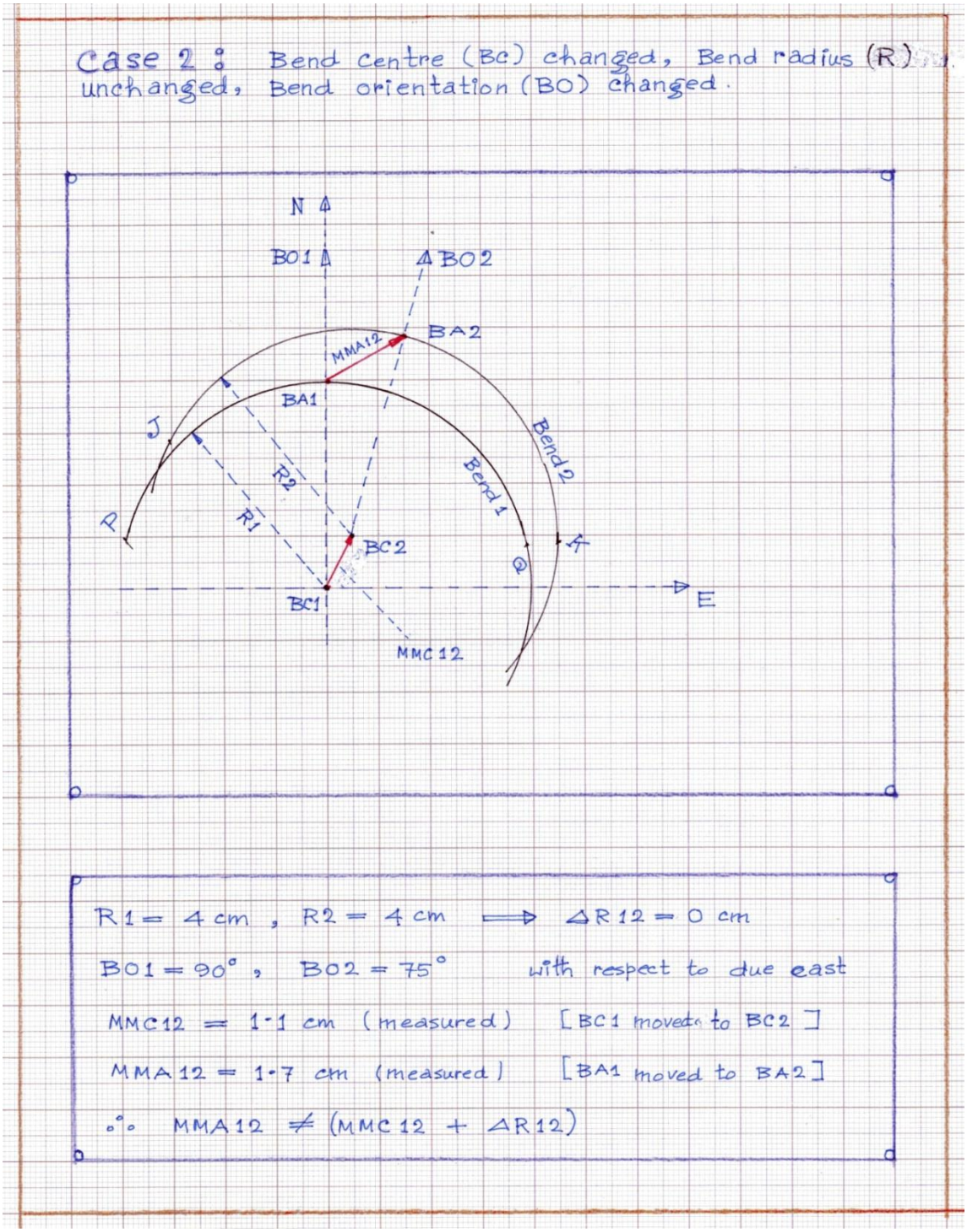

Figure A3.2: Checking the representation of bend movement while bend centre changes, radius remains unchanged, orientation changes, and also whether bend apex movement is the same as the bend centre movement plus change in radius over a time period.

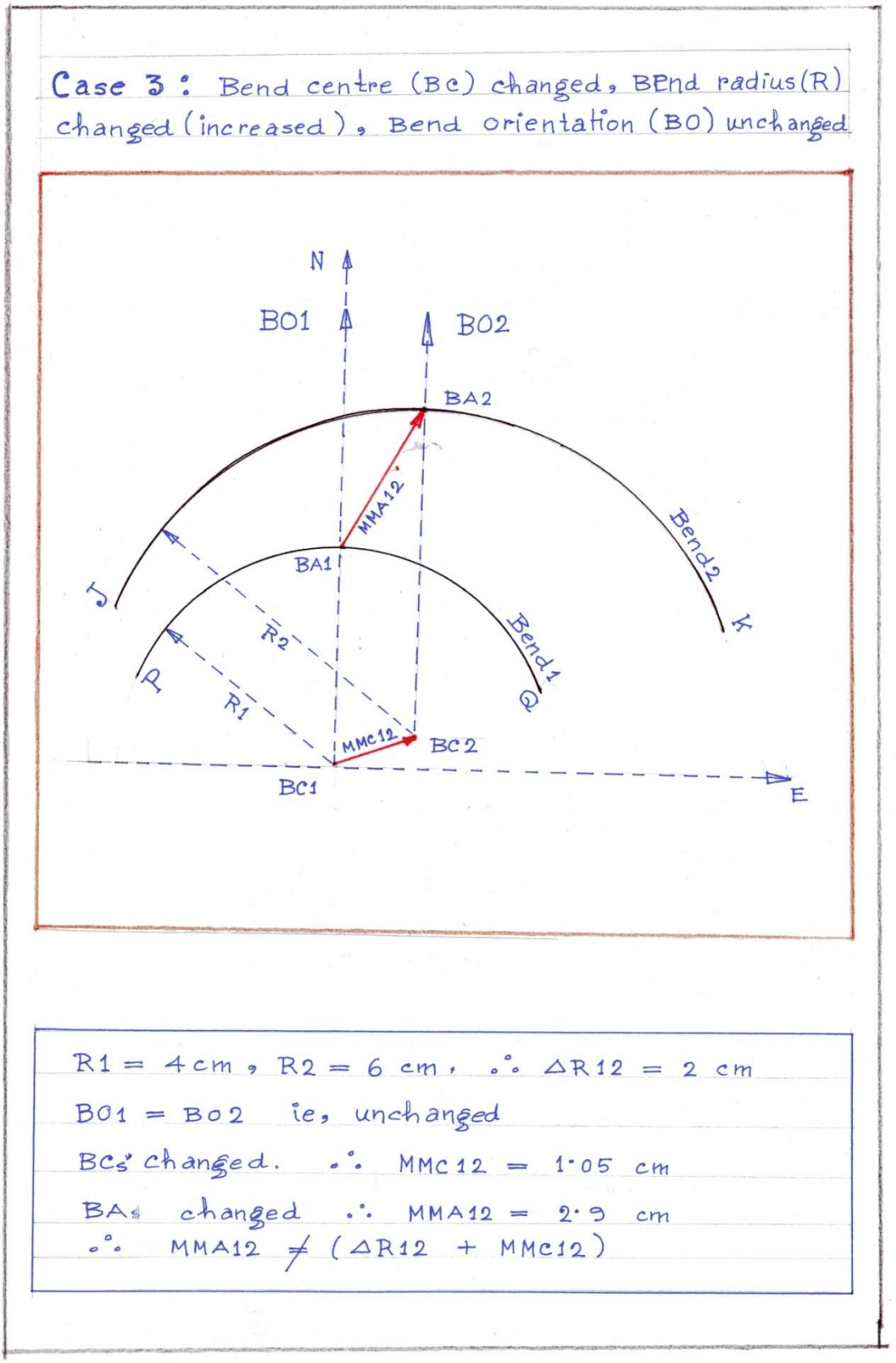

Figure A3.3: Checking the representation of bend movement while bend centre changes, radius changes, orientation remains unchanged, and also whether bend apex movement is the same as the bend centre movement plus change in radius over a time period.

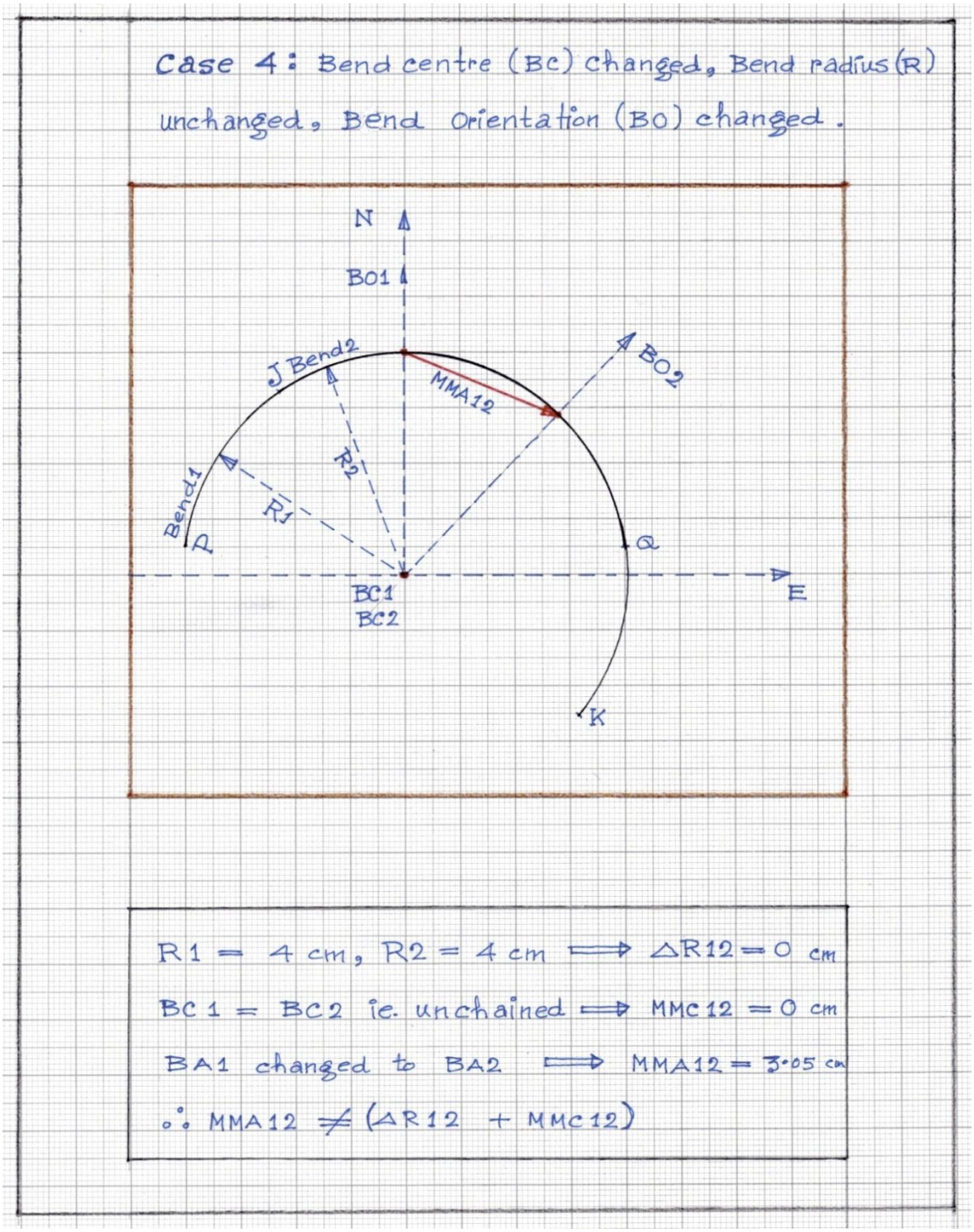

Figure A3.4: Checking the representation of bend movement while bend centre changes, radius remains unchanged, orientation changes, and also whether bend apex movement is the same as the bend centre movement plus change in radius over a time period.

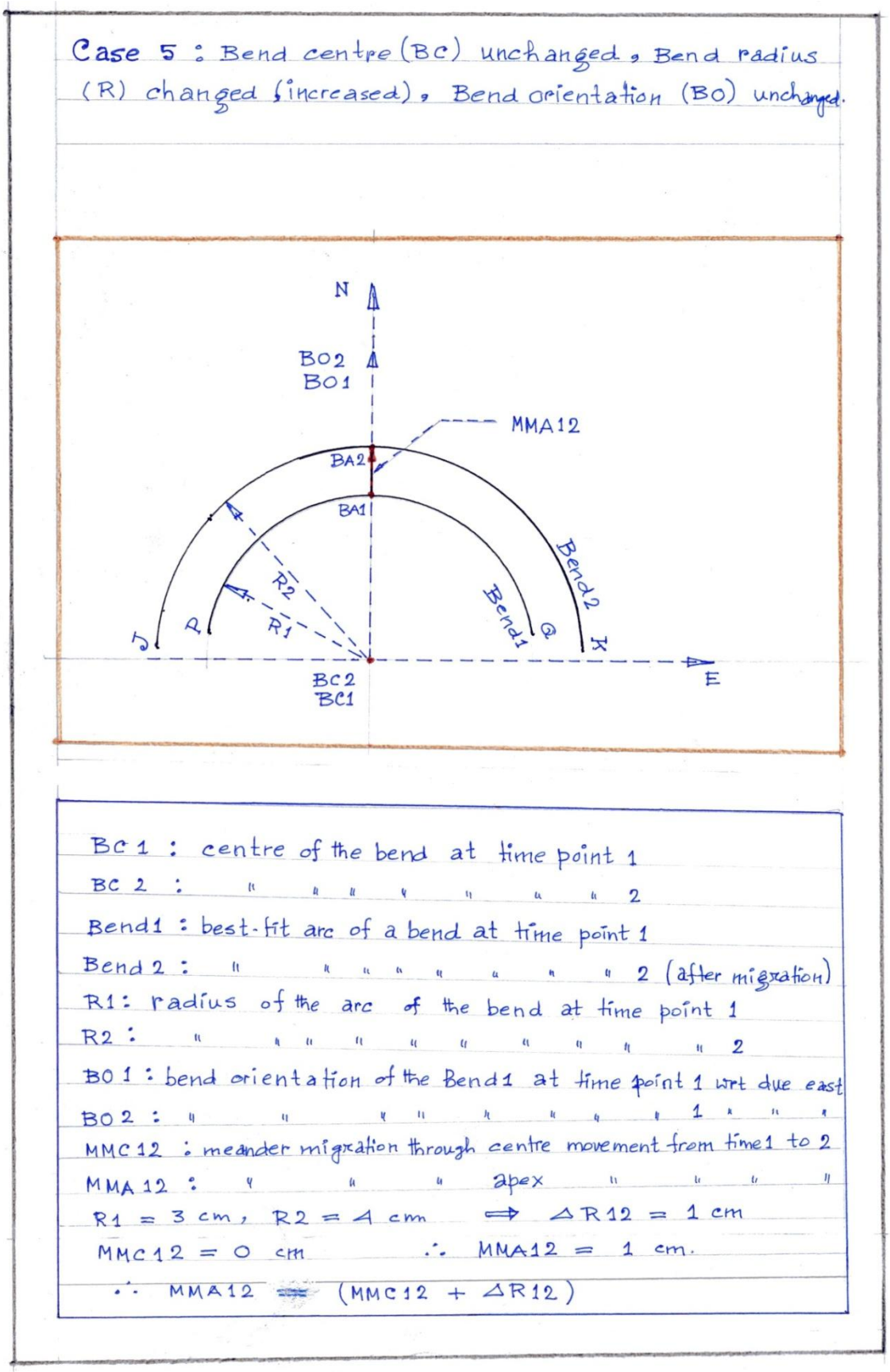

Figure A3.5: Checking the representation of bend movement while bend centre remains unchanged, radius changes, orientation remains unchanged, and also whether bend apex movement is the same as the bend centre movement plus change in radius over a time period.

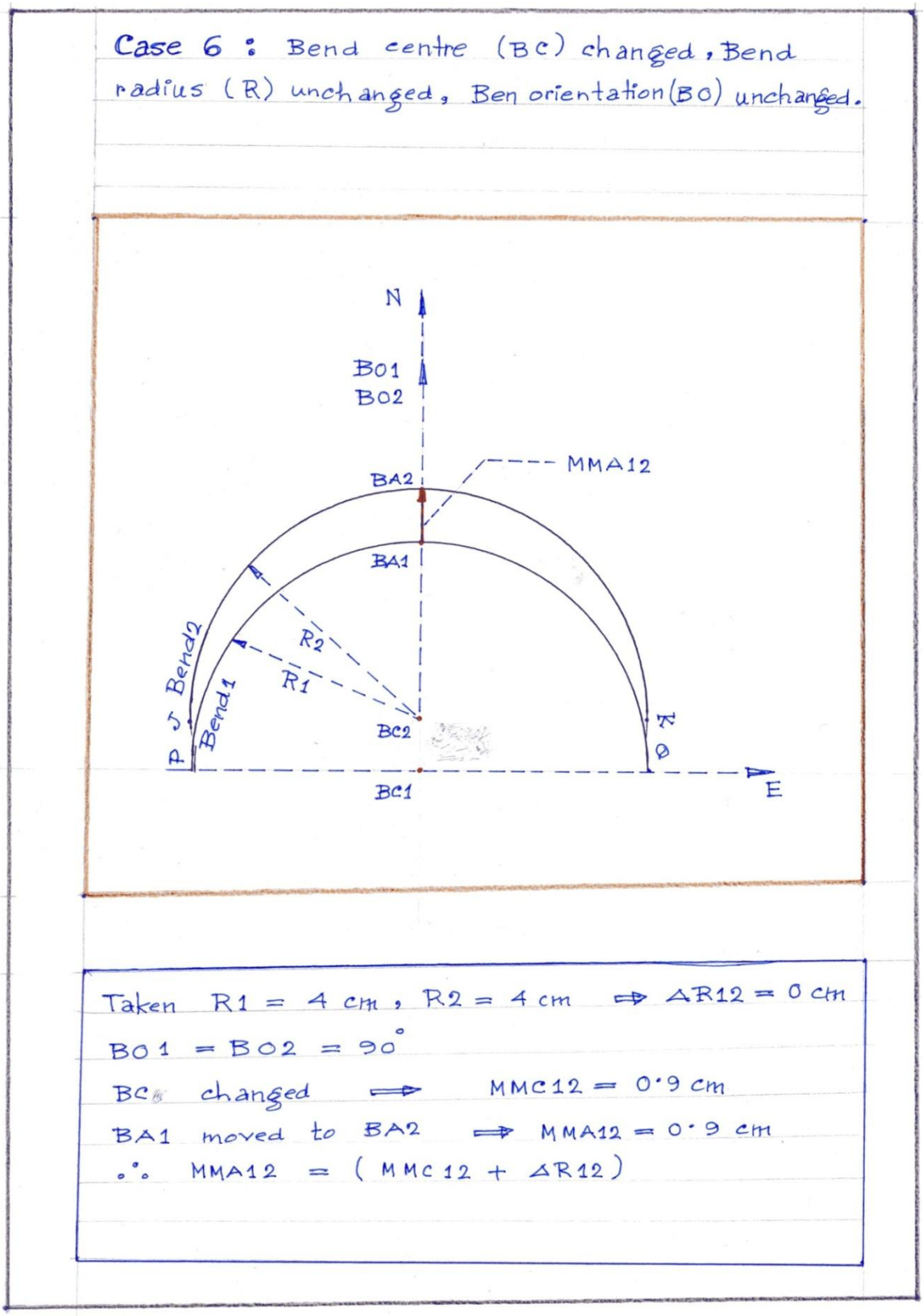

Figure A3.6: Checking the representation of bend movement while bend centre changes, radius remains unchanged, orientation remains unchanged, and also whether bend apex movement is the same as the bend centre movement plus change in radius over a time period.

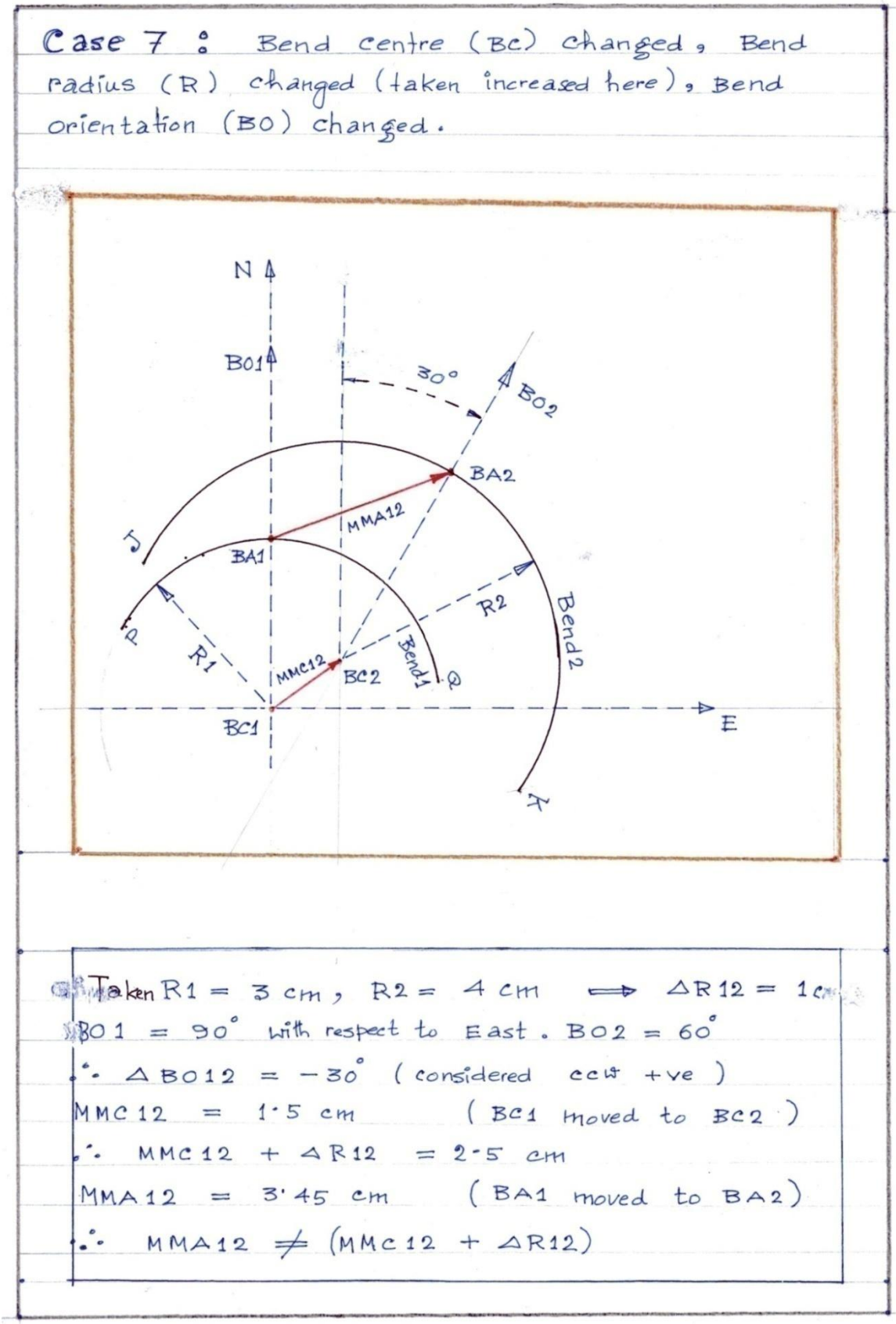

Figure A3.7: Checking the representation of bend movement while bend centre changes, radius changes, orientation changes, and also whether bend apex movement is the same as the bend centre movement plus change in radius over a time period.

Appendix to Chapter 4

A4.1 History of Data Correction on NCHRP Data at Initial Stage

With a view to building a new, error-free, refined database, compilation of data from NCHRP data-disks resulted in the bend summary in Table 3.1. Here are further examples of errors corrected at this stage.

Site 19: Yellow Creek, near Rothville, MO, B1, 15 bends

Bend 5 At time 1 (1936) Easting value is seen 0 (while Northing is 4380497) which appears to be impractical. Values for the measurements are seen as 0 at T2 (1970). Perhaps no measurements were taken, since cutoff occurred at this time. However, values must not be 0.

Decision: Bend 5 excluded.

Site 15. Des Moines River, Location 1, near Tracy, IA, C, 6 bend

This site has 6 bends in NCHRP database. Except Bend 1, there is no Northing data at all (in the row for northing coordinate information is given on whether the bend is left-handed or right-handed). Without northing data the other information for Bends 2-6 can not be useful.

Decision: Bends 2-6 excluded.

Site 55. Tallahalla Creek, near Runnelstown, MS, C, 12 bends

This site has 12 bends in NCHRP database. No data available at all three time points in case of Bend 12. Only 0 is seen as data value that appears to be impractical. For instance, easting and northing coordinate must not be zero.

Decision: Bend 12 excluded.

Site 60. Washita River, Location 1, Anadarko, OK, C, 7 bends

This site has 7 bends in NCHRP database. In case of Bend 5 data values at TP1 (1955) and TP2 (1974) are seen as 0 against all necessary variables (say, coordinates of bend centre, bend orientation etc). Data available at TP3 can not be useful for this research.

Decision: Bend 5 excluded

Eight bends have thus so far been excluded from the NCHRP database. We intended to keep proper records of any changes to the database by giving version number.The resulting database with 1497 bends is now refined to Version 2. This version is tidied up by numbering of sites, locations, and rivers. The version with these changes is called Version 3. Then following corrections were made on this version:

Site 4: Sacramento River, Compton Landing, CA, D, 4 bends

Northing values were quantified by 8-digit number, which should not be true. Because throughout the entire NCHRP database northing coordinates are written in 7-digit number.

Decision: All 4 bends excluded.

Now the resulting database assumes version 4 with 1493 bends. Afterwards we started exploratory statistical analysis through using a number of statistical techniques in order to gain understanding about the correctness of the data, its distribution etc. At first we started with Type C, since this type has around 43% of the data fall under this category. Then we did in the same way on other types of data. In this endeavour we went through different versions of the database. Based on this statistical exploration and examination of the available maps and aerial photographs supplied in the NCHRP data-disks it was felt necessary to check and where necessary re-classify the Brice-types allocated to the bends. Hence, further efforts were made to correct the database until it was believed to be as close as possible to being error free. The result was achieved in Version 9 of the database. The history of the corrections is given in Section A4.2 below.

A4.2 History of Data Correction on NCHRP Data from Database Version 9 Containing 1493 Bends

River Type A: Single phase, equiwidth, incised or deep channel

Site 1: Canooche River, near Claxton, GA, A, 13 bends

From the scatter plot it is surprisingly seen that for all bends the bend migration over Time Period 1 is zero. Here T1 (time point 1) is 1940, T2 (time point 2) is 1968 and T3 (time point 3) is 1993. Why is the zero migration for all bends? From the NCHRP data base it is found that all basic measurements related to a bend for all bends at T1 and T2 are exactly the same. These basic measurements are Easting at bend centre, Northing at bend centre, outer bank radius of curvature, channel width at crossing, channel width at bend apex, valley orientation, bend orientation. Among these measurements only valley orientation could be the same for all bends over a time period. As a result a stationary situation was considered over 28 years. Therefore, computed migration at bend apex resulted in zero which is impractical where as over second time period (25 years) there is considerable migration for those same bends.

Decision: Omit all basic measurements related to T1 for all bends.

Site 2: Licking River, near Romey, KY, A, 7 bends

Except Bend 4 for all other bends all basic measurements (E's, N's, R's, WCr's, WA's, VO's, BO's) at T1 and T2 are exactly the same.

Decision: Omit all basic measurements related to T1 for all bends, except Bend 4.

Site 3: Mud River, near Beechland, KY, A, 7 bends

For all bends all basic measurements (E's, N's, R's, WCr's, WA's, VO's, BO's) at T1 and T2 are exactly the same.

Decision: Omit all basic measurements related to T1 for all bends.

Site 4: Patoka River, near Patoka, IN, A, 10 bends

For all bends all basic measurements (E's, N's, R's, WCr's, WA's, VO's, BO's) at T1 and T2 are exactly the same, except Bend 3 and Bend 10.

Decision: Omit all basic measurements related to T1 for the Bends 1, 4-9.

Site 5: Red River, near Stanton, KY, A, 7 bends

Site 6: Rolling Fork River, near Boston, KY, A, 11 bends

For all bends all basic measurements (E's, N's, R's, WCr's, WA's, VO's, BO's) at T1 and T2 are exactly the same.

Decision: Omit all basic measurements related to T1 for all bends.

Site 7: Rough River, near Dundee, KY, A, 6 bends

River Type B1: Single phase, equiwidth channel

Site 1: Big Fork River, near Lindford, MN, B1, 16 bends

The problem of this river site resulted from the fact that each and every bend of this site has the same Northing value at T1 and this constant value is 5364786.85 m! The same problem occurs even at T2 and the constant Northing is 5364772.91 m! These measurements appear to be impractical. Here T1 at 1940, T2 at 1962 and T3 is 1995.

Decision: Omit all Northing values for all bends at T1 and T2.

Site 2: Buffalo Creek, near Glencoe, MN, B1, 20 bends

May be a C, as there are point bars in 1967, but these are not visible in 1950 or 1994. Width is variable though. Therefore, the situation suggests type E.

Decision: Reclassify as E.

Site 3: Buttahachie River, Location 1, Caledonia, MS, B1, 15 bends

Site 4: Buttahachie River, Location 2, near Sulligent, MS, B1, 20 bends

All basic measurements (E's, N's, R's, WCr's, WA's, VO's, BO's) at T1 and T2 are exactly the same for the bends 2-7, 9-14, 16, 19-20.

Decision: Omit all basic measurements related to T1 for the Bends 2-7, 9-14, 16, 19-20.

Site 5: Fishing Creek, near Endfield, NC, B1, 22 bends

All basic measurements (E's, N's, R's, WCr's, WA's, VO's, BO's) at T1 and T2 are exactly the same for all bends except Bend 3.

Decision: Omit all basic measurements related to T1 for all bends except Bend 3.

Site 6: Hatchie River, near Sunny Hill, TN, B1, 10 bends

Site 7: Hawk Creek, near Minnesota Falls, MN, B1, 16 bends

Bend 6, TP1 This bend is affected by channelisation of a tributary just upstream and a bend cutoff in the bend upstream. It has a large point bar too. Therefore, it is not a B1 bend and is not acting naturally.

Decision: Omit all basic measurements at T1.

Bend 12, TP1 This bend has not moved so much, certainly not three times the channel width in 17 years.

Decision: Omit all basic measurements at T1.

Site 8: Little River, near Idabel, OK, B1, 6 bends

Decision: Reclassify as B2.

Site 9: Neuse River, Kingstone, NC, B1, 10 bends

All basic measurements (E's, N's, R's, WCr's, WA's, VO's, BO's) at T1 and T2 are exactly the same for all bends.

Decision: Omit all basic measurements related to T1 for all bends.

Site 10: Ouchita River, Arkadelphia, Site 2, AR, B1, 5 bends

Decision: Reclassify as B2.

Site 11: Pea River, Ariton, AL, B1, 15 bends

Bend 5: Only aerial photographs available at T3 = 1992. From this photograph between Bend 4 and Bend 6, the shape of Bend 5 is not truly distinct. This means that downstream end of Bend 4 (up to its downstream inflection point) nearly covers the bend 5, Probably due to this, the bend shows a very high, unusual value of ratio of radius of curvature to river channel width at crossing. If we look at the scatter plot (not given in this report) with whole set of data from this

B1 type (data: B1 v8 231 462), we will see a big gap between Rb/WbCr = 10 and Rb/WbCr = 15. The two data points for two time periods from this bend lie nearly at 15. Therefore, they appear to be very doubtful.

Decision: Bend 5 should be discarded.

All basic measurements (E's, N's, R's, WCr's, WA's, VO's, BO's) at T1 and T2 are exactly the same for the Bends 4-5, 7-10, 12, 14-15.

Decision: Omit all basic measurements related to T1 for the Bends 4-5, 7-10, 12, 14-15.

Site 12: Pee Dee River, Pee Dee, SC, B1, 9 bends

Site 13: St. Josheph River, near Newville, IN, B1, 13 bends

Site 14: Sugar Creek, near Bengal, IN, B1, 7 bends

Bend 2: A channel avulsion occurred around Bend 1 and thus Bend 2 was affected by this avulsion. Therefore, bend should not be considered as a freely moving bend.

Decision: Omit Bend 2.

Site 15: Wabash River, Location 3, near Lodi, IN, B1, 4 bends

Site 16: Wabash River, Location 4, near Darwin, IN, B1, 2 bends

Site 17: Wabash River, Location 5, St. Francisville, Site 1, IN, B1, 4 bends

Site 18: Wabash River, Location 5, St. Francisville, Site 2, IN, B1, 3 bends

Site 19: Yellow Creek, near Rothville, MO, B1, 14 bends

Bend 2: This bend was affected by bridge construction during second time period since 1970. Therefore, it suggests omission of data point over TP2. However, all bends here show zero meander migration. Evidently, both data points should be omitted.

Decision: Omit Bend 2.

Bend 5: At time 1 (1936) Easting value is 0 (while Northing is 4380497) which appears to be impractical. Values for the measurements are seen as 0 at T2 (1970). Perhaps no measurements were taken as a cutoff occurred at this time. However, values cannot be 0.

Decision: Bend 5 excluded.

All basic measurements (E's, N's, R's, WCr's, WA's, VO's, BO's) at T1 and T2 are exactly the same for all bends.

Decision: Omit all basic measurements related to T1 for all bends.

Site 20: Yellow Medicine River, near Hanley Falls, MN, B1, 20 bends

Bend 4, TP1: Movement of this bend is very hard to perceive in photo's and appears to be part of channel shifting within an entrenched reach. Therefore, situation suggests omission of the bend from being considered at T1.

Decision: Omit all basic measurements related to T1.

Type E river has variable width in both space and time. Also for Type E it is difficult for the operator to define width. Hence, uncertainty is greater and this is reflected in the graphs (scatter plot of this site, data: B1 v8 231 462).

Decision: Reclassify as Type E.

River Class B2: Single phase, wider at bends, no bars

Site 1.Alabama River, Between Confluence and Clairborne L & D, AL, B2, 17 bends

Site 2. Apalachicola River, Location 1, Bristol, FL, B2, 5 bends

Site 3. Apalachicola River, Location 2, Orange, FL, B2, 7 bends

Site 4. Big Racoon Creek, Coxville, IN, B2, 10 bends

This is a B2 river. However, in NCHRP database it was put under Type C. After checking with Ayres this site was correctly placed under Type B2.

Bend 6: Nearly all basic measurements (E's, N's, R's, WCr's, WA's, VO's) at T1 and T2 are exactly the same for this bend.

Decision: Omit all basic measurements related to T1 for this bend.

Site 5. Black Warrior River, Tuscaloosa, AL, B2, 10 bends

Bend 9, TP2: Bend 9 has a large point bar and an embayment in the outer bank. It is not behaving as a B2-type bend and is completely atypical for this river reach.

Decision: Omit data related to T3.

Site 6. Choctawhatchee River, Caryville, Site 2, FL, B2, 14 bends

Site 7. Congaree River, Gadsden, SC, B2, 13 bends

Site 8. De Moines River, Location 5, Eldon, IA, B2, 6 bends

Site 9. Edisto River, Givhans, SC, B2, 11 bends

Site 10: Iowa River, Location 3, Iowa City, Site 1, IA, B2, 9 bends

Bend 6, TP1: In first period for this bend increases in width from 51 to 77 m! Also, bend radius increases from 134 to 217m! Therefore, it appears that bend migration is not the main cause of the high bank shifting value. Situation suggests omitting this bend.

Decision: Leave data.

Site 11: Leaf River, Location 2, near Hattiesburg, Site 2, MS, B2, 7 bends

Site 12: Lumber River, Fair Bluff, NC, B2, 22 bends

All basic measurements (E's, N's, R's, WCr's, WA's, VO's, BO's) at T1 and T2 are exactly the same for all bends.

Decision: Omit all basic measurements related to T1 for all bends.

Site 13: Neches River, Evadale, TX, B2, 11 bends

Site 14: Nowood River, South of Ten Sleep, WY, B2. 17 bends

Bend 17: This bend shows a very high migration for TP1. No data available in TP1. Bend 17 has a very short radius and narrow width in 1967. The bend used in 1994 is actually not the same bend as revealed from the aerial photographs. Therefore, this bend should be omitted.

Decision: Omit the bend

Site 15: Ouchita River, Arkadelphia, Site 1, AR, B2, 5 bends

Site 16: Sacramento River, Location 1, near Nights Landing, CA, B2, 4 bends

Site 17: Satilla River, near Waycross, GA, B2, 11 bends

Site 18: Savanah River, Agusta, GA, B2, 14 bends

Site 19: Wateree River, Camden, SC, B2, 6 bends

Site 20: White River, Orville, Site 1, IN, B2, 8 bends

River Type C: Single phase, wider at bends with point bars

Site 1. Altamaha River, Doctortown, GA, C, 12

Decision: Reclassify as B2.

Site 2. Amite River, Felixville, LA, C, 8 bends

Bend 6, TP2: Rapid shift of this very tight bend is due to a chute-cutoff in Bend 5 immediately upstream (scatterplot of overall data of C for TP2, data: C v9 627, not provided). This type of behaviour is unusual but characteristic of very tortuous, C- type rivers.

Decision: ok.

Site 3. Big Black River, Location 1, near Big Black, MS, C, 15 bends

Site 4. Big Black River, Location 2, Bovina, MS, C, 9 bends

Site 5. Big Black River, Location 3, Durrant, MS, C, 13 bends

Site 6. Big Black River, Location 4, Pickens, MS, C, 15 bends

Site 7. Brazos River, Thomsons, TX, C, 7 bends

Site 8. Brouillets Creek, near Universal, IN, C, 22 bends

Bend 5, TP1 This bend has identical Northings at T1 (1949) and T2 (1972). This is probably a punching error, but we do not know which Northing is correct. So it is suggestive to omit Northings at T1 and T2.

Decision: Omit Northings related to T1 and T2.

Bend 16 Bend radius in 1949 (T1) is 237.5 m that is much too long. This represents change in river direction, not meander bend radius. Bend radius should be about 80 m. Therefore, other data involving this bend should not be correct. This suggest the omitting the bend.

Decision: Omit the bend

Site 9. Cahaba River, Sprott, AL, C, 7 bends

Site 10. Cedar River, near Conesville, IA, C, 4 bends

Site 11. Chickasway River, Kittrell, Site 1, MS, C, 7 bends

Bend 5, TP1 This bend over TP1 showed zero migration. It resulted from the fact that identical Eastings, Northings, Radii, Valley Orientations, Bend Orientations are the same at T1 and T2.

Decision : Omit all Eastings, Northings, Radii, Valley Orientations, Bend Orientations at T1 and T2.

Site 12. Chickasway River, Kittrell, Site 2, MS, C, 7 bends

Site 13. Choctawhatchee River, Caryville, Site 1, FL, C, 13 bends

Decision: Reclassify as B2

Site 14. Conecuh River, Brewton, AL, C, 8 bends

Site 15. Des Moines River, Location 1, near Tracey, IA, C, 1 bend

Site 16. Des Moines River, Location 2, near Eddyville, IA, C, 6 bends

Decision: Reclassify as B2

Site 17. De Moines River, Location 4, Ottumwa, IA, C, 2 bends

Decision: Reclassify as B2

Site 18. Des Moines River, Location 6, below St. Francisville, IA, C, 9 bends

Site 19. East Nishnibotna River, Red Oak, IA, C, 7 bends

Site 20. English River, Kalona, IA, C, 13 bends

Site 21. Genesse River, Near Genesseo, NY, C, 10 bends

Site 22. Iowa River, Location 1, near Belle Plaine, IA, C, 12 bends

Site 23. Iowa River, Location 2, Marshaltown, IA, C, 11 bends

Site 24. Iowa River, Location 3, Iowa City, Site 2, IA, C, 11 bends

Site 25. Kanaranzi Creek, near Ellsworth, MN, C, 20 bends

Bend 7, TP1 (the position of the data point on scatter plot C v9 627 over TP1). Rapid shift is due to a chute cut-off which is a characteristic of such short radius bends and is what makes them dangerous. Therefore, one can expect this migration and thus point is ok.

Decision: ok

Site 26. Kansas River, Location 1, Ogden, KS, C, 10 bends

The river reach containing Bends 2 – 4 is simple of Type C. But longer reaches including Bends 1 and 5 – 7 have a channel within the channel which indicates Type F. In overall consideration it would be better to reclassify as Type F.

Decision: Reclassify as Type F

Site 27. Kansas River, Location 2, Topeka, KS, C, 7 bends

Underfit stream with wandering channels, especially bends that are less constrained, say Bend 7.

Decision: Reclassify as F

Site 28. Leaf River, Location 1, near Bethel, MS, C, 11 bends

Site 29. Leaf River, Location 2, near Hattiesburg, Site 1, MS, C, 8 bends

Bend 6, TP2 (the amount of high migration and the position of data point in scatter plot) The position and amount of migration may indicate doubt of its validity. But bend is eroding into highly erodible sand deposits. Therefore, the data point appears to be ok.

Decision: ok

Site 30. Line Creek, near Waugh, Site 2, AL, C, 5 bends

Decision: Reclassify as B1.

Site 31. Middle Fork Powder River, near Kaycee, WY, C, 16 bends

Decision: Reclassify as E

Site 32. Mississippi River, Jacobson, Site 1, MN, C, 11 bends

Point bars only in some bends and very poorly developed. Other bends are wider but do not have point bars.

Decision: Reclassify as B2

Site 33. Mississippi River, Jacobson, Site 2, MN, C, 14 bends

Decision: Reclassify as B2

Site 34. Nodaway River, near Burlington Junction, MO, C, 4 bends

Site 35. Ochlocknee River, Havana, FL, C, 10 bends

Decision: Reclassify as B2

Site 36. Pearl River, Location 1, near Bogalusa, LA, C, 18 bends

Decision: Reclassify as B2

Site 37. Pearl River, Location 2, near Columbia, MS, C, 10 bends

Bend 2, TP1 Here for this site T1 is 1952, T2 is 1977 and T3 is 1997. Could not have been in the location specified for 1952 when considered in relation to Bend 1 and the pattern the meander scars in the flood plain. This suggests the data related to T1 appear to be in error and all data should be omitted.

Decission: Omit all data for this bend related to time point 1 at 1952.

Bend 10, TP1 All basic measurements (E's, N's, R's, WCr's, WA's, VO's, BO's) at T1 and T2 are exactly the same for this bend.

Decision: Omit all basic measurements related to T1.

Site 38. Powder River, near Broadus, Site 1, MT, C, 9 bends

Point bars are quite well vegetated. No point bar which is required for the site to be as Type C. Therefore, the situation suggests reclassification of this site as B2.

Decision: Reclassify as Type B2

Site 39. Powder River, near Broadus, Site 2, MT, C, 11 bends

The Northing data value of the bend centre for all bends in T1 (1939) is exactly the same and it is 5007600.21 m. Clearly there is an error either in measurements or data entry. It is impossible to recover the correct data values without access to the grid co-ordinates for bends in 1939. Therefore, it is necessary to omit the data related to time point 1 at 1939.

Decision: Omit data for all bends related to time point 1 at 1939.

Site 40. Powder River, near Broadus, Site 3, MT, C, 15 bends

Site 41. Powder River, near Broadus, Site 4, MT, C, 4 bends

Site 42. Powder River, near Broadus, Site 5, MT, C, 10 bends

Bend 3, TP1 In the aerial photographs it is seen that the bend is right bank concave, but migrates westwards in first period (from 1939 to 1967). This was a chute cut-off, not really a bend migration by outer bank erosion.

Decision: Omit data related to T1.

Site 43. Powder River, near Broadus, Site 6, MT, C, 8 bends

Site 44. Republican River, Location 1, Benkleman, NE, C, 10 bends

The river channel width is poorly defined and highly variable. Therefore, this site should better be reclassified as Type E.

Decision: Reclassify as Type E.

Site 45. Republican River, Location 2, McCook, NE, C, 5 bends

The river channel width is poorly defined and highly varable. Therefore, this site should better be reclassified as Type E.

Decision: Reclassify as Type E

Site 46. Republican River, Location 3, Orleans, NE, C, 11 bends

Bend 1-11 The Northing of the bend centre for all bends in T3 (1993) is the same and it is 4447225.99 m. This is obviously a data entry error.

Decision: Omit basic measurements related to T3.

The river channel width is poorly defined and highly variable. Therefore, this site should better be reclassified as Type E.

Decision: Reclassify as E

Site 47. Republican River, Location 4, Concordia, KS, C, 9 bends

The river channel width is poorly defined and highly variable. Therefore, this site should better be reclassified as Type E.

Decision: Reclassify as Type E

Site 48. Root River, near Houston, MN, C, 10 bends

For this site aerial photographs are available at T1 (1947), T2 (1968) and T3 (1994). A valley wall is seen around bend 9 and 10 on the photograph taken in 1994. There is a sign of less sedimentary features/point bars in TP2 than in TP1. Possibly river regulation/flood control structures reduced the sediment load and thus point bar formation between 1960s and 1990s. Moreover, on the scatter plot (data : C v8 607) of meander migration for this site it is seen that in general the magnitude of migration is higher over TP2 than that over TP1. Therefore, in overall consideration the site can be left as Type C for TP1. But for TP2 it can be reclassified as Type B2.

Decision: Leave the site related to data at T1 and T2 as Type C. But reclassify the site related to data at T2 and T3 as Type B2. 1 site of type B2 is thus evolved.

Site 49. Sabine River, near Merryville, LA, C, 7 bends

Site 50. Sacramento River, Location 2, Colusa, CA, C, 5 bends

Throughout the reach there is a sign of engineering interventions. Bends are impacted by the presence of revetments and bypass flood control structures. Here time points of measurements of data are 1935, 1964 and 1998. Only one photograph is available in NCHRP database in 1998. On this photograph the riveted bends are Bend 1, Bend 4 and Bend 5. Again the rest two bends - Bend 2 and Bend 3 are located either side of Colusa Weir and Bypass. Therefore, there might been influence on the bends. Between these two bends, Bend 3 has been more affected since it is downstream of weir and bypass. It was not mentioned when the structures were implemented. However, for other sites (Location 6, Hamilton City; Location 7, Tehama) the time of implementation of revetment is found as 1980s. So, one can reasonably believe that the revetments for this site were built at the same time.

Bend 2 It is less affected by engineering interventions as mentioned above but still implicated.

Bend 3 It is located right next to a major irrigation and flood control channel offtake. It can not be considered “normal” or representative of bends in alluvial channels.

Bend 4 It has a revetment along part of the outer bank, which distorting its evolution and shifting.

Decision: Omit Bend 2 and Bend 3. Omit data related to T3 for Bend1, Bend 4 and Bend5.

Site 51. Sacramento River, Location 6, Hamilton City, CA, C, 3 bends

Here time points of measurements are 1935, 1964 and 1998. On photograph in 1998 the river at Bend 1 is a fan like (several branched channel). Around 1970 cutoff around Bend 1.The reach is modified by engineering interventions. Bend 2 and Bend 3 were riveted in 1980s and thus affected in free evolution.

Decision: Omit data related to T3 for all 3 bends.

Site 52. Sacramento River, Location 7, near Tehama, CA, C, 2 bends

Plan form is a bit complex. There are split flows.

Decision: Reclassify as Type D.

Site 53. Smoky Hill River, Location 1, near Chapman, Site 1, KS, C, 22 bends

Site 54. Smoky Hill River, Location 2, near Junction City, KS, C, 18 bends

Site 55. Tallahalla Creek, near Runnelstown, MS, C, 11 bends

Site 56. Tombigbee River, near Amory, MS, C, 9 bends

Bends 7,8, TP2 Aerial photograph is available in T3 (1996). On this photographs they are really one bend, no inflection point in between. Therefore, we should not consider these bends for the analysis.

Decision: Omit data related to T3 for these two bends.

Decision on reclassification: Reclassify as Type B2

Site 57 Tongue River, South of Miles City, MT, C, 9 bends

Decision on reclassification: Reclassify as Type B1.

Site 58 Trinity River, Romayor, TX, C, 7 bends

Decision on reclassification: Reclassify as Type B2

Site 59. Wapsipinicon River, De Witt, IA, C, 10 bends

Site 60. Washita River, Location 1, Anadarko, OK, C, 6 bends

Site 61. White River, Orville, Site 2, IN, C, 6 bends

Decision on reclassification: Reclassify as Type B2.

Site 62. Wild Rice River, Twin Valley, MN, C, 18 bends

Here T1 is 1948, T2 is 1965 and T3 is 1997. Diversion structure appears on the photographs in 1997 but not in earlier time point ie, in 1966. (Here is a inconsistency that about second time point in the database workbook of NCHRP for numerical measurement date is mentioned as 1965, but the date on the aerial photograph is seen as 1966). In the scatter plot of migration generally higher migration is seen for all bends over TP1 than that over TP2. Therefore, we could conclude that the construction of river regulation structure changed Brice Type from C to B2 over first (may be partly) and second time period.

Decision Reclassify the site related to data at T1 and T2 as Type C. However, reclassify the site related to data at T2 and T3 as Type B2. Hence, 1 site of type B2 is thus evolved.

Site 63. Zumbro River, Kellog, MN, C, 20 bends

River Type D : Single phase, wider at bends, point bars, chutes common

Site 1. Carson River, near Weeks, NV, D, 6 bends

Site 2. Kansas River, Location 3, Manhattan, KS, D, 13 bends

Site 3. Rock River, near Rock Valley, IA, D, 17 bends

In the scatter plot (data: D v8 44 88) a cluster of data points at TP1 of Bends 8, 9, 12 lie much further away from the usual position of the rest of the points. Then a question may arise onto mind whether the migration for those bends are ok. In effect, this is a dangerous river, prone to large chute cut-offs and rapid shifting under some poorly defined circumstances.

Decision: Probably the best to leave these bends in the data set.

Site 4. Sacramento River, Location 4, Bute City, CA, D, 4 bends

In the scatter plot (data: D v8 44 88) some data points (Bend 1, 2, 4) lie/cluster much further away from the usual position of the rest of the points. Then a question may arise onto mind whether the migration for those bends are ok. Not only this site, looking at the other sites under other Types, it can be said that Sacramento River is very active in

changing its channel. It is also heavily modified by past and present interventions by engineers fro irrigation, drainage, flood control and channel stabilization. It is a difficult river –but probably reflects the risks associated with rivers of Type D.

Decision: Probably the best to leave these bends in the data set.

Site 5. Sacramento River, Location 5, near Ordbend, CA, D, 4 bends

In the scatter plot (data: D v8 44 88) few data points (Bend 1, 4 for TP1) lie much further away from the usual position of the rest of the points. Then a question may arise onto mind whether the migration for those bends are ok. Those are very unstable bends affected by structures, dangerous for shifting and changes in R and W.

Decision: Probably the best to leave these bends in the data set.

River Type E: Single phase, irregular width variation

Site 1. Apalachicola River, Location 3, Rock Bluff, FL, E, 3 bends

Decision: Reclassify as B2

Site 2. Black River, Poplar Bluff, MO, E, 8 bends

Decision: Reclassify as B1

Site 3. Cottonwood River, Leavonworth, MN, E, 14 bends

Bend 12, TP1 This data point showed a very high migration. Measuring shift of bend on air photos indicated around 2 river width bend shift between 1950 (T1) and 1967 (T2). Therefore, the measured data in the database must be an error as it indicates shifting of greater than 7 widths. Probably the problem was in the referencing of photos at time T1.

Decision: Omit basic measurements related to T1.

Bend 7, TP1 Same cause of error happened at this bend

Decision: Omit basic measurements related to T1.

Site 4. Des Moines River, Location 3, above Chillicothe, IA, E, 6 bends

Site 5. Fawn River, near Scott, IN, E, 21 bends

Site 6. Line Creek, Waugh, Site 1, AL, E, 14 bends

Site 7. Little Pea Dee River, Galivants Ferry, SC, E, 10 bends

Site 8. Minnesota River, Location 1, Judson, MN, E, 13 bends

All 13 bends over TP1 showed very high unusual migration, even there is a point which showed as high as more than 200% migration of the river channel width at crossing per year! Inspection revealed that there is problem with coordinate for Northing at T1 (1950). The same Northing value (4896933 m) for all bends. Then it appears that Northing of all bends pivoted along a fixed line passing through this value. But the aerial photograph at 1950 does not support this. Therefore, it is error which causes unusual migration.

Decision: Omit Northing coordinate for all bends at T1.

Site 9. Minnesota River, Location 2, Belle Plaine, MN, E, 7 bends

The scatter plot for migration for this site, no data point is plotted on it. No measurement had been taken at T2. As a result, no migration was found over TP1 and TP2.

Site 10. Rice Creek, Fridley, MN, E, 20 bends

Unusual migration over TP2. Here T1 is 1970, T2 is 1989 and T3 is 1994. Thus period 2 is only 5 years which is realy too short compared to all other site among all Types of rivers ie, across the global database. Probably the problem is associated with T2, a time point like 1989 should not be there. Because across the database T1 in 1930s/1940s, T2 is 1955s/60s, and T3 is 1990s. Therefore, as a time period 1989 – 94 is doubtful for inclusion anyway! Moreover, even one can cast a doubt on T1 as 1970. Logically, T2 should be 1970 and T3 should be 1994. However, if data related to T2 are omitted, that will meet the correction purpose.

Decision: Omit basic measurements related to T2 for all bends.

Site 11. Wabash River, Location 1, Clinton, IN, E, 4 bends

Site 12. Wabash River, Location 2, near Fairbanks, IN, E, 3 bends

Site 13. Wolf River, Rossville, TN, E, 14 bends

River Type F: Two phase, underfit, low water sinuosity, wandering

Site 1. Cimmaron River, Location 1, near Fairview, OK, F, 4 bends

Bend 1, TP1 The bend show an unusual migration than other bends of this site. Here migration occurs where a bend in the low flow channel is $\pi/2$ out of phase with a bend in the high flow channel. Hence, migration is complex. But this is a characteristic of 2-phase meandering in Type F channels. Hence, the best is to leave the point in the data set.

Decision: Leave the data point in the data set.

Site 2. Cimmaron River, Location 2, near Waynoka, OK, F, 5 bends

Site 3. Kansas River, Location 4, Wamego, KS, F, 8 bends

Site 4. Washita River, Location 2, Jollyville, OK, F, 2 bends

Not truly a type F as the low flow and channel meander wavelengths are the same.

At this site the river width increases by a factor between 2.4 and 5 over the 55 year period of record. This is a non-stationary condition indicating progressive change in morphology with time. This bank retreat associated with this process can not be predicted based on R/W.

Decision: Remove this site from consideration.

River Type G1: Two phase, bimodal bankful sinuosity, equi-width channel

Site 1. Little Missouri River, near Alzada, MT, G1, 20 bends

Site 2. Rum River, near West Point, MN, G1, 20 bends

Site 3. Saline River, Tescott, KS, G1, 24 bends

Bend 16, TP2 Width at crossing is only 16.5 m! This can not be correct.

Decision: Omit width at the crossing at T2 (1992)

Site 4. Smoky Hill River, Location 4, Mentor, KS, G1, 17 bends

Bend 15, 17 TP2 These bends are very mobile but data appear to be valid. Here some of bank migration is due to widening at bend.

Decision: Leave the bend in the data set

Bend 14 TP2 This is not an active meander bend. This is an old loop in the larger phase of meandering: Now Relict. Bend should be omitted.

Decision: Omit all basic measurements related to T2

Site 5. Solomon River, Location 1, Benington, KS, G1, 20 bends

Site 6. Solomon River, Location 2, Solomon, KS, G1, 24 bends

River Type G2: Two phase, bimodal bankfull sinuosity, wider at bends with point bars

Site 1. Smoky Hill River, Location 1, near Chapman, Site 2, KS, G2, 20 bends

Site 2. Smoky Hill River, Location 3, near Solomon, KS, G2, 22 bends

Table A4.1: Retainment/Movement of sites from one Brice Type to another through data correction by reclassification (from Version 10 to Version 11)

Before (in NCHRP database)		**Retained in / Movement to**		**After (in UoN/HRW database)**		**Remarks**
Types	No. of sites	Types	No. of sites	Type	No. of sites	
A	7	A	7	A	7	No site reclassed
B1	20	B2	2	B1	19	
		E	2			
B2	20			B2	37	No site reclassed
C	63	B1	2	C	41	2 evolved as B2
		B2	14			
		D	1			
		E	5			
		F	2			
D	5			D	6	No site reclassed
E	13	B1	1	E	18	
		B2	1			
F	4			F	5	1 site omitted
G1	6			G1	6	No site reclassed
G2	2			G2	2	No site reclassed
	140				**141**	

Here are the accounts on how the table works, meaning a tally is given in the following:

For Type A

All 7 sites remained as Type A in the UoN/HRW database.

For Type B1

There were originally 20 sites in NCHRP database. From among them, 2 sites moved out to B2, and 2 sites moved out to E. Again, 2 sites moved in from C, and 1 site from E. Hence, finally 19 sites are in UoN/HRW database.

For Type B2

There were originally 20 sites in NCHRP database. From among them, 14 moved out to C, 1 to E. Again, 2 sites moved in from B1. Hence, finally 37 sites are in UoN/HRW database.

For Type C

There were originally 63 sites in NCHRP database. From among them, 2 sites moved out to B1, 14 sites to B2, 1 site to D, 5 sites to E, and 2 sites to F. Again, 2 sites evolved as B2 (see Site 48 and 62 above under the description of Type C). Hence, finally 41 sites are in UoN/HRW database.

For Type D

There were originally 5 sites in NCHRP database. 1 site moved out in from Type C. Hence, finally 6 sites are in UoN/HRW database.

For Type E

There were originally 13 sites in NCHRP database. From among them, 1 site moved out to B1, 1 to B2. Again, 2 sites moved in from B1, and 5 sites from C. Hence, finally 18 sites are in UoN/HRW database.

For Type F

There were originally 4 sites in NCHRP database. 1 site removed (Site 4, see above). 2 sites moved in from C. Hence, finally 5 sites are in UoN/HRW database.

For Type G1

All 6 sites remained as Type G1 in the UoN/HRW database.

For Type G2

All 2 sites remained as Type G2 in the UoN/HRW database.

A4.3 List of River Sites after Data Correction and Reclassification (sites on Version 11 containing 1512 bends)

River Type A: Single phase, equiwidth, incised or deep channel

Site 1: Canooche River, near Claxton, GA, A, 13 bends

Site 2: Licking River, near Romey, KY, A, 7 bends

Site 3: Mud River, near Beechland, KY, A, 7 bends

Site 4: Patoka River, near Patoka, IN, A, 10 bends

Site 5: Red River, near Stanton, KY, A, 7 bends

Site 6: Rolling Fork River, near Boston, KY, A, 11 bends

Site 7: Rough River, near Dundee, KY, A, 6 bends

River Type B1: Single phase, equiwidth channel

Site 1: Big Fork River, near Lindford, MN, B1, 16 bends

Site 2. Black River, Poplar Bluff, MO, B1, 8 bends

Site 3: Buttachie River, Location 1, Caledonia, MS, B1, 15 bends

Site 4: Buttachie River, Location 2, near Sulligent, MS, B1, 20 bends

Site 5: Fishing Creek, near Endfield, NC, B1, 22 bends

Site 6: Hatchie River, near Sunny Hill, TN, B1, 10 bends

Site 7: Hawk Creek, near Minnesota Falls, MN, B1, 16 bends

Site 8: Line Creek, Waugh, Site 2, AL, B1, 5 bends

Site 9: Neuse River, Kingstone, NC, B1, 10 bends

Site 10: Pea River, Ariton, AL, B1, 14 bends

Site 11: Pee Dee River, Pee Dee, SC, B1, 9 bends

Site 12: St. Josheph River, near Newville, IN, B1, 13 bends

Site 13: Sugar Creek, near Bengal, IN, B1, 6 bends

Site 14: Tongue River, South of Miles City, MT, C, 9 bends

Site 15: Wabash River, Location 3, near Lodi, IN, B1, 4 bends

Site 16: Wabash River, Location 4, near Darwin, IN, B1, 2 bends

Site 17: Wabash River, Location 5, St. Francisville, Site 1, IN, B1, 4 bends

Site 18: Wabash River, Location 5, St. Francisville, Site 2, IN, B1, 3 bends

Site 19: Yellow Creek, near Rothville, MO, B1, 13 bends

River Class B2: Single phase, wider at bends, no bars

Site 1.Alabama River, Between Confluence and Clairborne L & D, AL, B2, 17 bends

Site 2. Altamaha River, Doctortown, GA, B2, 12

Site 3. Apalachicola River, Location 1, Bristol, FL, B2, 5 bends

Site 4. Apalachicola River, Location 2, Orange, FL, B2, 7 bends

Site 5. Apalachicola River, Location 3, Rock Bluff, FL, B2, 3 bends

Site 6. Big Racoon Creek, Coxville, IN, B2, 10 bends

Site 7. Black Warrior River, Tuscaloosa, AL, B2, 10 bends

Site 8. Choctawhatchee River, Caryville, Site 1, FL, B2, 13 bends

Site 9. Choctawhatchee River, Caryville, Site 2, FL, B2, 14 bends

Site 10. Congaree River, Gadsden, SC, B2, 13 bends

Site 11. De Moines River, Location 2, near Eddyville, IA, B2, 6 bends

Site 12. De Moines River, Location 4, Ottumwa, IA, B2, 2 bends

Site 13. De Moines River, Location 5, Eldon, IA, B2, 6 bends

Site 14. Edisto River, Givhans, SC, B2, 11 bends

Site 15. Iowa River, Location 3, Iowa City, Site 1, IA, B2, 9 bends

Site 16. Leaf River, Location 2, Hattiesburg, Site 2, MS, B2, 7 bends

Site 17. Little River, near Idabel, OK, B2, 6 bends

Site 18.: Lumber River, Fair Bluff, NC, B2, 22 bends

Site 19. Mississippi River, Jacobson, Site 1, MN, B2, 11 bends

Site 20. Mississippi River, Jacobson, Site 2, MN, B2, 14 bends

Site 21. Neches River, Evadale, TX, B2, 11 bends

Site 22. Nowood River, South of Ten Sleep, WY, B2, 16 bends

Site 23. Ochlocknee River, Havana, FL, B2, 10 bends

Site 24. Ouchita River, Arkadelphia, Site 1, AR, B2, 5 bends

Site 25. Ouchita River, Arkadelphia, Site 2, AR, B2, 5 bends

Site 26. Pearl River, Location 1, Bogalusa, LA, B2, 18 bends

Site 27. Powder River, near Broadus, Site 1, MT, B2, 9 bends

Site 28. Root River, Houston, MN, B2, 10 bends

Site 29. Sacramento River, Location 1, near Nights Landing, CA, B2, 4 bends

Site 30. Satilla River, near Waycross, GA, B2, 11 bends

Site 31. Savanah River, Agusta, GA, B2, 14 bends

Site 32. Tombigbee River, near Amory, MS, B2, 9 bends

Site 33. Trinity River, Romayor, TX, B2, 7 bends

Site 34. Wateree River, Camden, SC, B2, 6 bends

Site 35. White River, Orville, Site 1, IN, B2, 8 bends

Site 36. White River, Orville, Site 2, IN, B2, 6 bends

Site 37. Wild Rice River, Twin Valley, MN, B2, 18 bends

River Type C: Single phase, wider at bends with point bars

Site 1. Amite River, Felixville, LA, C, 8 bends

Site 2. Big Black River, Location 1, near Big Black, MS, C, 15 bends

Site 3. Big Black River, Location 2, Bovina, MS, C, 9 bends

Site 4. Big Black River, Location 3, Durant, MS, C, 13 bends

Site 5. Big Black River, Location 4, Pickens, MS, C, 15 bends

Site 6. Brazos River, Thomsons, TX, C, 7 bends

Site 7. Brouillets Creek, Universal, IN, C, 21 bends

Site 8. Cahaba River, Sprott, AL, C, 7 bends

Site 9. Cedar River, Conesville, IA, C, 4 bends

Site 10. Chickasway River, Kittrell, Site 1, MS, C, 7 bends

Site 11. Chickasway River, Kittrell, Site 2, MS, C, 7 bends

Site 12. Conecuh River, Brewton, AL, C, 8 bends

Site 13. De Moines River, Location 1, near Tracey, IA, C, 1 bend

Site 14. De Moines River, Location 6, below St. Francisville, IA, C, 8 bends

Site 15. East Nishnibotna River, Red Oak, IA, C, 7 bends

Site 16. English River, Kalona, IA, C, 13 bends

Site 17. Genesse River, Near Genesseo, NY, C, 10 bends

Site 18. Iowa River, Location 1, near Belle Plaine, IA, C, 12 bends

Site 19. Iowa River, Location 2, Marshaltown, IA, C, 11 bends

Site 20. Iowa River, Location 3, Iowa City, Site 2, IA, C, 11 bends

Site 21. Kanaranzi Creek, near Ellsworth, MN, C, 20 bends

Site 22. Leaf River, Location 1, near Bethel, MS, C, 11 bends

Site 23. Leaf River, Location 2, near Hattiesburg, Site 1, MS, C, 8 bends

Site 24. Nodaway River, Burlington Junction, MO, C, 4 bends

Site 25. Pearl River, Location 2, Columbia, MS, C, 10 bends

Site 26. Powder River, near Broadus, Site 2, MT, C, 11 bends

Site 27. Powder River, near Broadus, Site 3, MT, C, 15 bends

Site 28. Powder River, near Broadus, Site 4, MT, C, 4 bends

Site 29. Powder River, near Broadus, Site 5, MT, C, 10 bends

Site 30. Powder River, near Broadus, Site 6, MT, C, 8 bends

Site 31. Root River, Houston, MN, C, 10 bends

Site 32. Sabine River, Merryville, LA, C, 7 bends

Site 33. Sacramento River, Location 2, Colusa, CA, C, 3 bends

Site 34. Sacramento River, Location 6, Hamilton City, CA, C, 3 bends

Site 35. Smoky Hill River, Location 1, near Chapman, Site 1, KS, C, 22 bends

Site 36. Smoky Hill River, Location 2, near Junction City, KS, C, 18 bends

Site 37. Tallahalla Creek, Runnelstown, MS, C, 11 bends

Site 38. Wapsipinicon River, De Witt, IA, C, 10 bend

Site 39. Washita River, Location 1, Anadarko, OK, C, 6 bends

Site 40. Wild Rice River, Twin Valley, MN, C, 18 bends

Site 41. Zumbro River, Kellog, MN, C, 20 bends

River Type D: Single phase, wider at bends, point bars, chutes common

Site 1. Carson River, near Weeks, NV, D, 6 bends

Site 2. Kansas River, Location 3, Manhattan, KS, D, 13 bends

Site 3. Rock River, near Rock Valley, IA, D, 17 bends

Site 4. Sacramento River, Location 4, Bute City, CA, D, 4 bends

Site 5. Sacramento River, Location 5, near Ordbend, CA, D, 4 bends

Site 6. Sacramento River, Location 7, Tehama, CA, C, 2 bends

River Type E: Single phase, irregular width variation

Site 1 : Buffalo Creek, near Glencoe, MN, B1, 20 bends

Site 2. Cottonwood River, Leavonworth, MN, E, 14 bends

Site 3. Des Moines River, Location 3, above Chillicothe, IA, E, 6 bends

Site 4. Fawn River, near Scott, IN, E, 21 bends

Site 5. Line Creek, Waugh, Site 1, AL, E, 14 bends

Site 6. Little Pea Dee River, Galivants Ferry, SC, E, 10 bends

Site 7. Middle Fork Powder River, Kaycee, WY, C, 16 bends

Site 8. Minnesota River, Location 1, Judson, MN, E, 13 bends

Site 9. Minnesota River, Location 2, Belle Plaine, MN, E, 7 bends

Site 10. Republican River, Location 1, Benkleman, NE, C, 10 bends

Site 11. Republican River, Location 2, McCook, NE, C, 5 bends

Site 12. Republican River, Location 3, Orleans, NE, C, 11 bends

Site 13. Republican River, Location 4, Concordia, KS, C, 9 bends

Site 14. Rice Creek, Fridley, MN, E, 20 bends

Site 15. Wabash River, Location 1, Clinton, IN, E, 4 bends

Site 16. Wabash River, Location 2, near Fairbanks, IN, E, 3 bends

Site 17. Wolf River, Rossville, TN, E, 14 bends

Site 18 : Yellow Medicine River, near Hanley Falls, MN, B1, 20 bends

River Type F: Two phase, underfit, low water sinuosity, wandering

Site 1. Cimmaron River, Location 1, near Fairview, OK, F, 4 bends

Site 2. Cimmaron River, Location 2, near Waynoka, OK, F, 5 bends

Site 3. Kansas River, Location 1, Ogden, KS, C, 10 bends

Site 4. Kansas River, Location 2, Topeka, KS, C, 7 bends

Site 5. Kansas River, Location 4, Wamego, KS, F, 8 bends

River Type G1: Two phase, bimodal bankfull sinuosity, equi-width

Site 1. Little Missouri River, near Alzada, MT, G1, 20 bends

Site 2. Rum River, near West Point, MN, G1, 20 bends

Site 3. Saline River, Tescott, KS, G1, 24 bends

Site 4. Smoky Hill River, Location 4, Mentor, KS, G1, 17 bends

Site 5. Solomon River, Location 1, Benington, KS, G1, 20 bends

Site 6. Solomon River, Location 2, Solomon, KS, G1, 24 bends

River Type G2: Two phase, bimodal bankfull sinuosity, wider at bends with point bars

Site 1. Smoky Hill River, Location 1, near Chapman, Site 2, KS, G2, 20 bends

Site 2. Smoky Hill River, Location 3, near Solomon, KS, G2, 22 bends

A4.4 University of Nottingham / HR Wallingford Database

The database is held by the School of Geography at the University of Nottingham. A copy may be obtained by making a request to the School's web master (currently Ms Claire Chambers) who will arrange access to the School's ftp site, from which the database may be downloaded. Those wishing to download the database will be asked to register, though there will be no charge for the database, nor will restrictions be placed on its use for research and teaching. The School reserves the right to request an administrative fee and (if appropriate) a royalty if the database is to be used for commercial profit, however.

A state-wise account of names of the rivers in the UoN/HRW database are given in the following Table A4.2.

Table A4.2: State-wise list of names of the rivers in the UoN/HRW database

States	Rivers
Alabama	Buttahatchie River
	Line Creek
	Pea River
	Alabama River
	Black Warrior River
	Cahaba River
	Conecuh River
Arkansas	Ouachita River
California	Sacramento River
Florida	Ochlocknee River
	Apalachicola River
	Choctawhatchee River
Georgia	Altamaha River
	Canoochee River
	Satilla River
	Savanah River
Iowa	Des Moines River
	Iowa River
	Cedar River
	East Nishnibotna River
	English River
	Rock River
	Wabash River
	Wapsipinicon River
Illinois	Wabash River

States	Rivers
Indiana	Sugar Creek
	Wabash River
	Big Racoon Creek
	White River
	Brouillets Creek
	Fawn River
	Patoka River
	St. Joseph River
Kansas	Kansas River
	Republican River
	Smoky Hill River
	Saline River
	Red River
	Rolling Fork River
	Solomon River
Kentucky	Rough River
	Licking River
	Mud River
	Red River
	Rolling Fork River
Louisiana	Sabine River
	Pearl River
	Amite River
Mississippi	Chickasawhay River
	Leaf River
	Black River
	Leaf River
	Pearl River
	Tallahalla Creek
	Buttahatchie River
	Tombigbee River
	Big Black River
Missouri	Nodaway River
	Black River
	Yellow Creek
Minnesota	Wild Rice River
	Kanaranzi Creek
	Root River
	Zumbro River
	Buffalo Creek
	Cottonwood River
	Minnesota River
	Rice Creek
	Yellow Medicine River
	Rum River
	Big Fork River
	Hawk Creek
	Mississippi River

States	Rivers
Montana	Tongue River
	Powder River
	Little Missouri River
Nebraska	Republican River
Nevada	Carson River
North Carolina	Fishing Creek
	Neuse River
	Lumber River
New York	Genesse River
Oklahoma	Washita River
	Cimarron River
	Little River
South Carolina	Pee Dee River
	Congaree River
	Edisto River
	Little Pee Dee River
	Wateree River
Tennessee	Wolf River
	Hatchie RIver
Texas	Neches River
	Trinity River
	Brazos River
Wyoming	Nowood River
	Middle Fork Powder River

A4.5 Scenario-Based Computation of the Coordinates of the Bend Apex

Notations used here have been given in Section 4.2.1.

Step 1: Extracting the coordinates of the bend centre, the radius of curvature and the bend orientation

This section has been described in Section 4.2.1.

Step 2: Computing the eastern and northern components of the radius of curvature

The easterly and northerly components of the radius of curvature may be calculated by trigonometry based on the radius (R) and the angle (αBCBA) between the line connecting BC and BA, and due east. The general formula is:

The eastern component of the radius = Rcos (αBCBA) (A4.1)

The northern component of the radius = Rsin (αBCBA) (A4.2)

For example, in the sample case (Bend 1, Altamaha River, Doctortown, GA) in 1941 (Time 1), αBC1BA1= [360° - BO1] = 360° - 341° = 19°

This indicates that in 1941 (Time 1) the bend apex was located to the south-east of the bend centre. Therefore, the easting of the bend apex (BA1) was greater than that of the bend centre (BC1), but the northing of BA1 was less than that of BC1.

Step 3: Computing the coordinates of the bend apex

Depending on the position of a bend orientation in the quadrant in the Easting-Northing coordinate plane, there are four different scenarios for the location of the bend apex with respect to the position of the bend centre. We will have to use appropriate formula depending on the scenario to compute the coordinates of the bend apex. The four scenarios are illustrated in Figure 4.1 and set out below.

Scenario 1: 0° < BO < 90° (BO lies in the 1st quadrant)

This scenario suggests that bend apex is located somewhere **North-East** with respect to the location of the bend centre, meaning easting coordinate of the bend apex is greater than that of the bend centre and northing coordinate of the bend apex is also greater than that of the bend centre. Therefore, we can use the following formula to calculate the coordinate of the bend apex.

EBA > EBC $\Longrightarrow$ EBA = EBC + Rcos(αBCBA) (A4.3)

NBA > NBC $\Longrightarrow$ NBA = NBC + Rsin(αBCBA) (A4.4)

Scenario 2: 90° < BO < 180° (BO lies in the 2nd quadrant)

This scenario suggests that the bend apex is located somewhere **North-West** with respect to the location of the bend centre, meaning easting coordinate of the bend apex is less than that of the bend centre and northing coordinate of the bend apex is greater than that of the bend centre. Therefore, we can use the following formula to calculate the coordinate of the bend apex.

$$EBA < EBC \Longrightarrow EBA = EBC - R\cos(\alpha BCBA) \quad \text{(A4.5)}$$

$$NBA > NBC \Longrightarrow NBA = NBC + R\sin(\alpha BCBA) \quad \text{(A4.6)}$$

Scenario 3: 180° < BO < 270° (BO lies in the 3rd quadrant)

This scenario suggests that the bend apex is located somewhere **South-West** with respect to the location of the bend centre, meaning easting coordinate of the bend apex is les than that of the bend centre and northing coordinate of the bend apex is also less than that of the bend centre. Therefore, we can use the following formula to calculate the coordinate of the bend apex.

$$EBA < EBC \Longrightarrow EBA = EBC - R\cos(\alpha BCBA) \quad \text{(A4.7)}$$

$$NBA < NBC \Longrightarrow NBA = NBC - R\sin(\alpha BCBA) \quad \text{(A4.8)}$$

Scenario 4: 270° < BO < 360° (BO lies in the 4rh quadrant)

This scenario suggests that the bend apex is located somewhere **South-East** with respect to the location of the bend centre, meaning that easting coordinate of the bend apex is greater than that of the bend centre and northing coordinate of the bend apex is les than that of the bend centre. Therefore, we can use the following formula in order to calculate the coordinates of the bend apex.

$$EBA > EBC \Longrightarrow EBA = EBC + R\cos(\alpha BCBA) \quad \text{(A4.9)}$$

$$NBA < NBC \Longrightarrow NBA = NBC - R\sin(\alpha BCBA) \quad \text{(A4.10)}$$

This section has set out a method for computing the coordinates of the bend apex when the coordinates of the bend centre, radius of curvature and bend orientation are known. The relevant steps for the sample bend are set out below in Box A4.1.

Box A4.1: Sample calculation to find the coordinates of a bend apex

In this sample calculation, the data come from Bend 1 (BIN: 2B18), the Altamaha River, Doctortown, GA, (Brice Type B2) at Times 1 (1941) and 2 (1968).

Step 1: *Extract the coordinates of the bend centre, the radius of curvature and the bend orientation at Time 1:*

EBC1 = 425064 m, NBC1 = 3500642 m, R1 = 496.8, BO1 = 341°

Step 2: *Compute the easterly and northerly components of the radius of curvature :*
αBC1BA1 = 360° - 341° = 19°

Eastern component = Rcos(αBC1BA1)
= 496.8cos(19°)
= 469.7 m
Eastern component = Rsincos(αBC1BA1)
= 496.8sin(19°)
= 161.7 m

Step 3: *Compute the coordinates of the bend apex:*

Since the value of BO is 341°, Scenario 4 applies

The easting of the bend apex,
EBA1 = EBC1 + R1cos(αBC1BA1) (following Equation A4.9)
= 425064 + 469.73
= 425534 m

The northing coordinate of bend apex, (following Equation A4.10)
NBA1 = NBC1 – R1sin(αBC1BA1)
= 3500642 – 161.74
= 3500480 m

Appendix to Chapter 5

A5.1 Statistical Methods

Empirical Cumulative Distribution Function

In statistics an empirical cumulative probability distribution function, ecdf in short, is a cumulative probability distribution function obtained through accumulating of probability for sample data. It works on the concept of the relative frequency, so this cumulative probability is nothing but a cumulative relative frequency of the data sample, as its name implies. Therefore, be the data from a discrete random variable or from a continuous random variable, ecdf is a discrete step function. Since all data points constitute the total probability equals to 1, therefore at each data point the probability concentrates by the amount of 1/n (n is the number of data points). This means each step height is the same and equal to 1/n.

Let X_1, X_2, X_3, ..., X_n be iid random variables with cdf $F_X(x)$, then ecdf is defined as

$Fn(x_i)$ = ((number of data points in the sample) <= x_i) / total number of data points
= i/n

Hence, we can put the definition of ecdf in another way that follows : the ecdf $F_n(x)$ is defined as the proportion of X values less than or equal to x.

R computes ecdf with the definition as outlined above ie, with i/n. However, there may be conservative attempt in order to find it, where it is defined as $F_n(x_i) = i/(n + 1)$.

The use of ecdf : An ecdf plot can investigate whether a data set at hand follows a particular distribution by comparing with the plot of expected cdf under that particular model by being over laid on the same plot. Moreover, this function has good implication in statistical tests. One sample and two sample Kolmogorov-Smirnov test functions compute test statistics that are derived from this function.

Probability Plot

We often need to know the distribution of a data sample at hand. At first we need to assume/guess/suspect a possible theoretical probability distribution that the data set may follow. Then the theoretical cumulative distribution function for that suspected model is equated against an empirical cumulative distribution function in order to find the model scores. Then sample data are plotted against the model scores and is looked for a straight line to judge whether the data sample follows the probability distribution that was suspected earlier. In this way probability plotting is a graphical statistical technique that is used to assess whether a dataset follows a particular probability distribution.

Method of assessment

If we have a data set such as y1, y2, y3, ..., yi, ..., yn, then we can follow the procedure

1. Ranking the data set as y(1), y(2), y(3), ..., y(i), ..., y(n)
2. Finding xi from the following equation, F(xi) = i/(n+1). Where F(xi) is the cdf of the theoretical distribution model and Xi is the ith model score
3. Plotting y(i) against xi
4. Ideally, obtaining a straight line from the data points suggests that the data support the model

Selection of the axis for plotting may vary. The statistical package R plots sample quantiles along y-axis and theoretical quantiles along the x-axis. However, the statistical package MINITAB does not even plot the model scores. Rather it plots expected cdf under model along the y-axis and ordered sample data along the x-axis.

Considering an empirical cdf is not a constant one as given above. For example, the above one, i/(n+1) is taught in the course G1STA: Statistics, School of Mathematical Sciences, University of Nottingham. However, *NIST/SEMATECH e-Handbook of Statistical Methods*, http://www.itl.nist.gov/div898/handbook/, date: 17/02/10, uses the following formula :

$$x(i) = 1 - x(n) \quad \text{for } i = 1$$

$$x(i) = (i - 0.3175)/(n + 0.365) \quad \text{for } i = 2, 3, ..., n-1$$

$$x(i) = 0.5^{(1/n)} \quad \text{for } i = n$$

The probability plotting has also another advantage. If a straight line is fromed by the plotting points or an approximate straight line is achieved, the measure of the intercept with the y axis offers an estimate of the location parameter and the slope does an estimate of the scale parameter.

Normal Probability Plot

The normal probability plot is a special case of the probability plot, when normal cdf is used as a theoritical model. This plot answers the question wheter the data follows a normal distribution or not, if not then answer the nature of departures from normality. However, in this case instead of cdf of normal probability model rather standardised normal cdf is used. Usually the ordered data set are plotted along y-axis and standardised normal score is done along the x-axis. The statistical package R uses standardised normal score and plot them along the x-axis.

In principle formation of a straight line or approximately a straight line should be a good indication of suggesting the normal model that the data follow. However, R has capacity to add a straight line to the normal probability plot where the line is formed by the points of upper quartile and lower quartile of the data values. This line thus acts as a reference line for comparison to check how well the plotting points fall/match on the straight line.

Kolmogorov-Smirnov Test

In statistics Kolmogorov-Smirnov test has use for both one sample and two sample data sets with different purposes. This test applies to only continuous distribution. The test uses comparison of distribution functions.

One sample test

One sample KS test is used to ascertain whether the data in the sample follow a suspected particular distribution. Since many statistical procedures require normality assumptions, therefore the test is widely used to test whether the data were derived from the normal population. As a test procedure the KS test compares the empirical cumulative probability distribution function of the data with that of the assumed theoretical distribution. The test statistic is the maximum distance (called Kolmogorov distance) between the empirical and theoretical cdf. The test statistic then uses the Kolmogorov distribution for the acceptance or rejection of the null hypothesis. The test statistic is as given in Wikipedia

$$D_n = \sup_x |F_n(x) - F(x)|$$

where Fn(x) is the cdf of the data needs to be tested, F(x) is the cdf of the assumed reference/hypothesised distribution, Dn is the maximum distance between cdfs, n is the number of data points in the sample.

Two sample test

Two sample KS test is used to ascertain whether two data samples come from the same probability distribution. Therefore, obviously the test should be a useful test. As null hypothesis the test assumes that both data sets have been derived from the same distribution. In this case the test statistc is as given in Wikipedia

$$D_{n,n'} = \sup_x |F_n(x) - F_{n'}(x)|.$$

where Fn(x) is the ecdf of the first sample, $F_{n'}(x)$ is the ecdf of the second, $D_{n,n'}$ is the maximum distance between ecdfs, n is the number of data points in the first sample and n´ is the number of data points in the second sample. The order first and second does not matter.

Since maximum distances are distributed in the Kolmogorov distribution. Therefore, as implied the test statistic is evaluated in the right tail of the distribution in order to decide acceptance or rejection of null hypothesis.

Advantages

- One good advantage is that the distribution of test statistic does not depend on its underlying cdfs.

Disadvantages

- It works for only continuous distribution.
- A serious one is in case of one sample test the probability distribution function must be fully known meaning that estimated parameters from the sample can not be used in finding cdf.
- When ties found in the test statistic exact p-values can not be computed.

A5.2 Limits to Analysis

The graphs in this appendix (Figure A5.1 to A5.13) were used to set limits to the applicability of the analytical method, based on the goodness of fit between the actual and

theoretical distributions. The agreement between the actual and theoretical distributions for bends with the dimensionless curvatures indicated was insufficient to support the analysis. For this reason, the limits to the analysis were set between R/w = 1 and 8.5.

A5.3 An explanation of how 76 grids were selected for computing conditional densities

Densities were computed at 601 grids with transformed variables. For the purpose of probability calculations performed when developing the predictive tool (for both tabular and graphical results) conditional densities were computed for the x-variable ($\log_{10}$(R/W)) at slices spaced every 10 grids up to 431 grids, so that the x-values in the resulting prediction tools were sufficiently closely spaced to avoid having to interpolate between widely spaced values. However, due to the variable selected being logged, maintaining a 10-grid-gap would result in wide gaps in the untransformed R/W values for higher values of $\log_{10}$(R/W). To avoid this, it was decided to reduce the spacing above 431 grids to a 5-grid gap. As a result, the x-variable was divided into 78 slices for the purpose of computing the density functions. However, it should be recalled that, in developing the prediction tool, the lowest two slices (i.e. at the left hand border of the distribution) were ommitted due to there being too much variation in fitting the probability distribution for the predictions to be reliable.

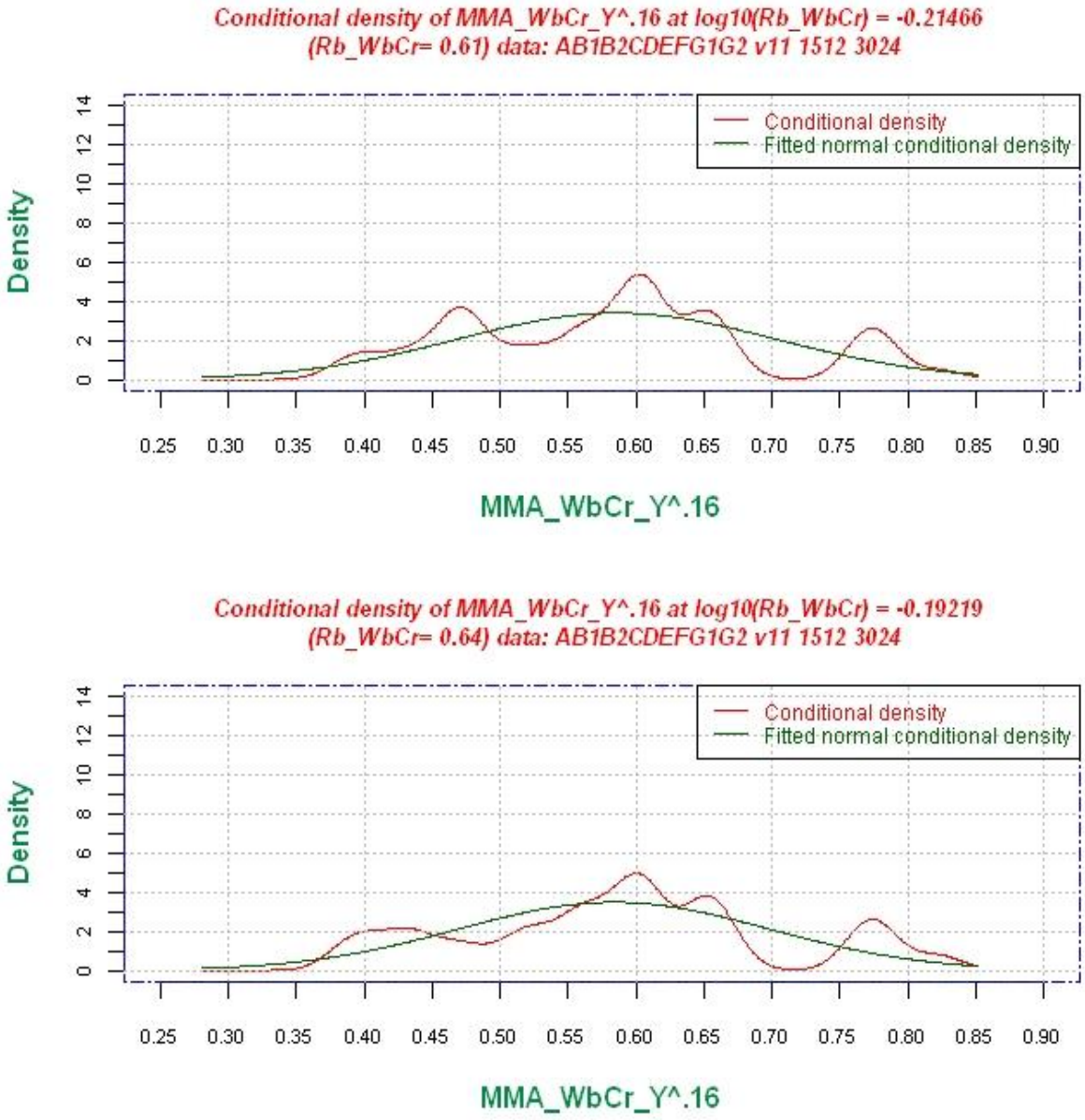

Figure A5.1: Upper graph. Conditional density of $(MMA/WbCr/Y)^{0.16}$ for $\log_{10}(Rb/WbCr) = -021466$ [i. e. Rb/WbCr = 0.61] Loer graph. Conditional density of $(MMA/WbCr/Y)^{0.16}$ for $\log_{10}(Rb/WbCr) = - 019219$ [i.e. Rb/WbCr = 0.64]

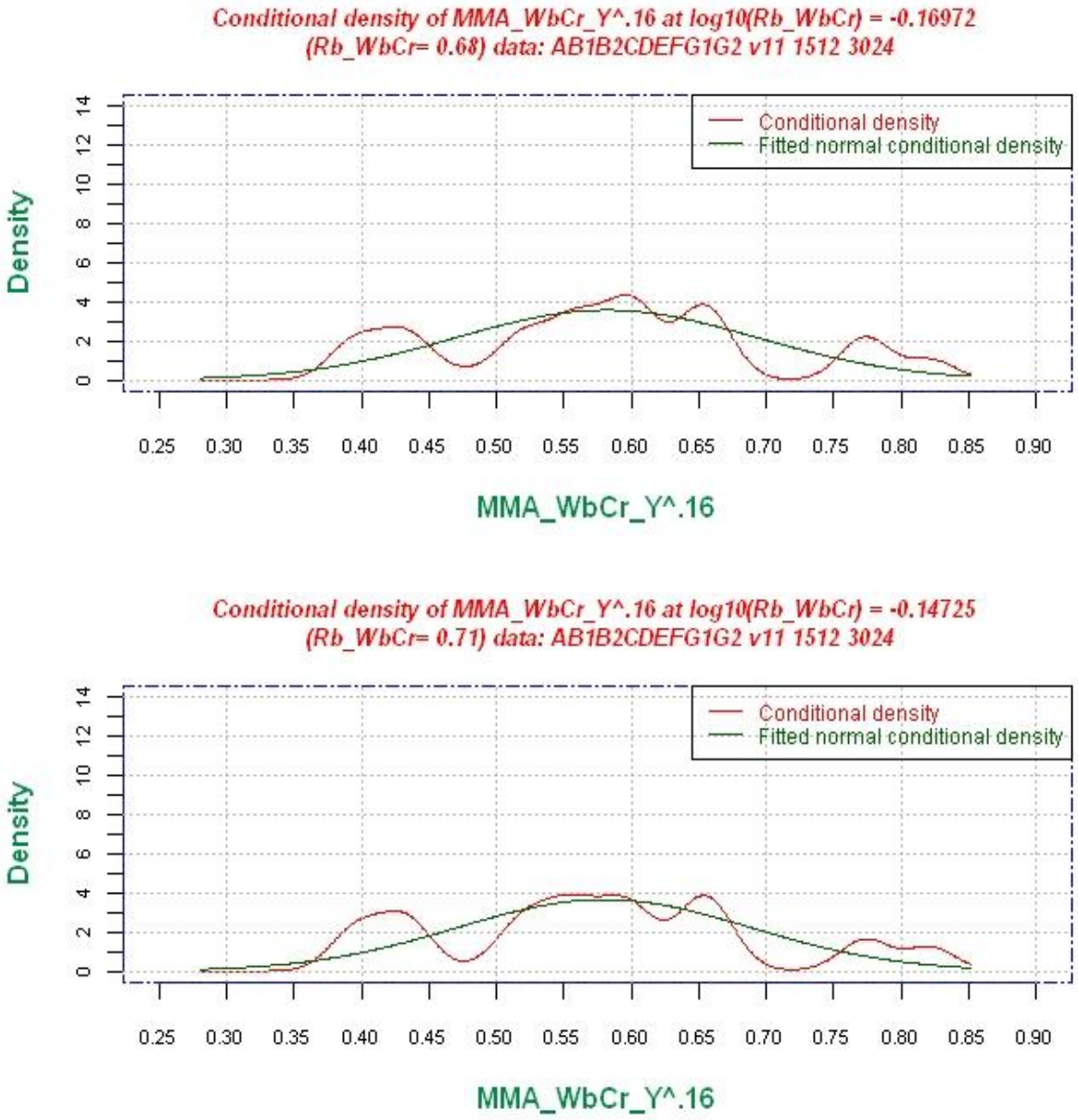

Figure A5.2: Upper graph. Conditional density of $(MMA/WbCr/Y)^{0.16}$ for $\log_{10}(Rb/WbCr) = -0.16972$ [i.e. Rb/WbCr = 0.68] Lower graph. Conditional density of $(MMA/WbCr/Y)^{0.16}$ for $\log_{10}(Rb/WbCr) = -0.14725$ [i.e. Rb/WbCr = 0.71]

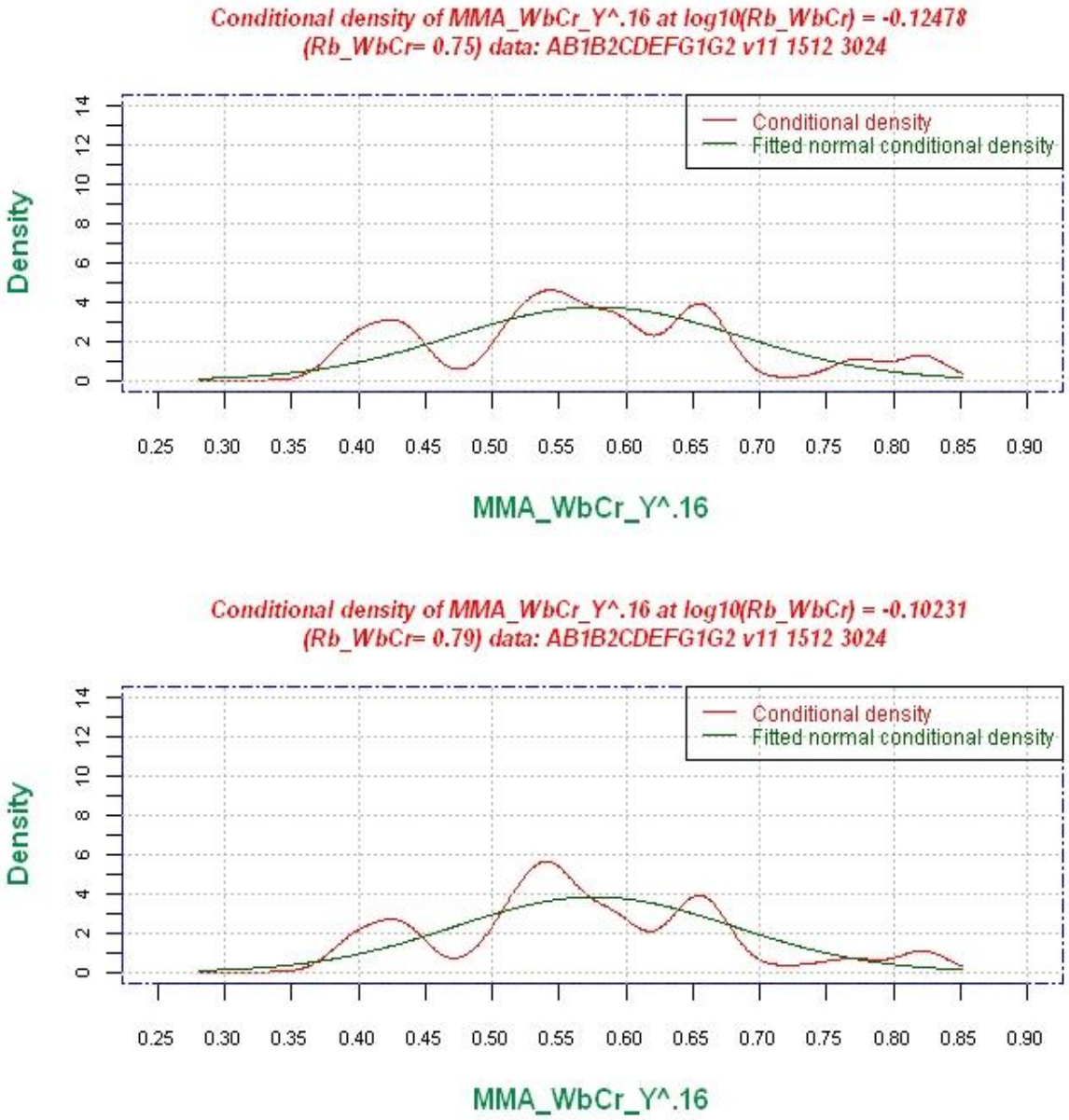

Figure A5.3: Upper graph. Conditional density of $(MMA/WbCr/Y)^{0.16}$for $\log_{10}(Rb/WbCr)$ = -0.12478 [i.e. Rb/WbCr = 0.75] Lower graph. Conditional density of $(MMA/WbCr/Y)^{0.16}$ for $\log_{10}(Rb/WbCr)$ = -0.10231 [i.e. Rb/WbCr = 0.79]

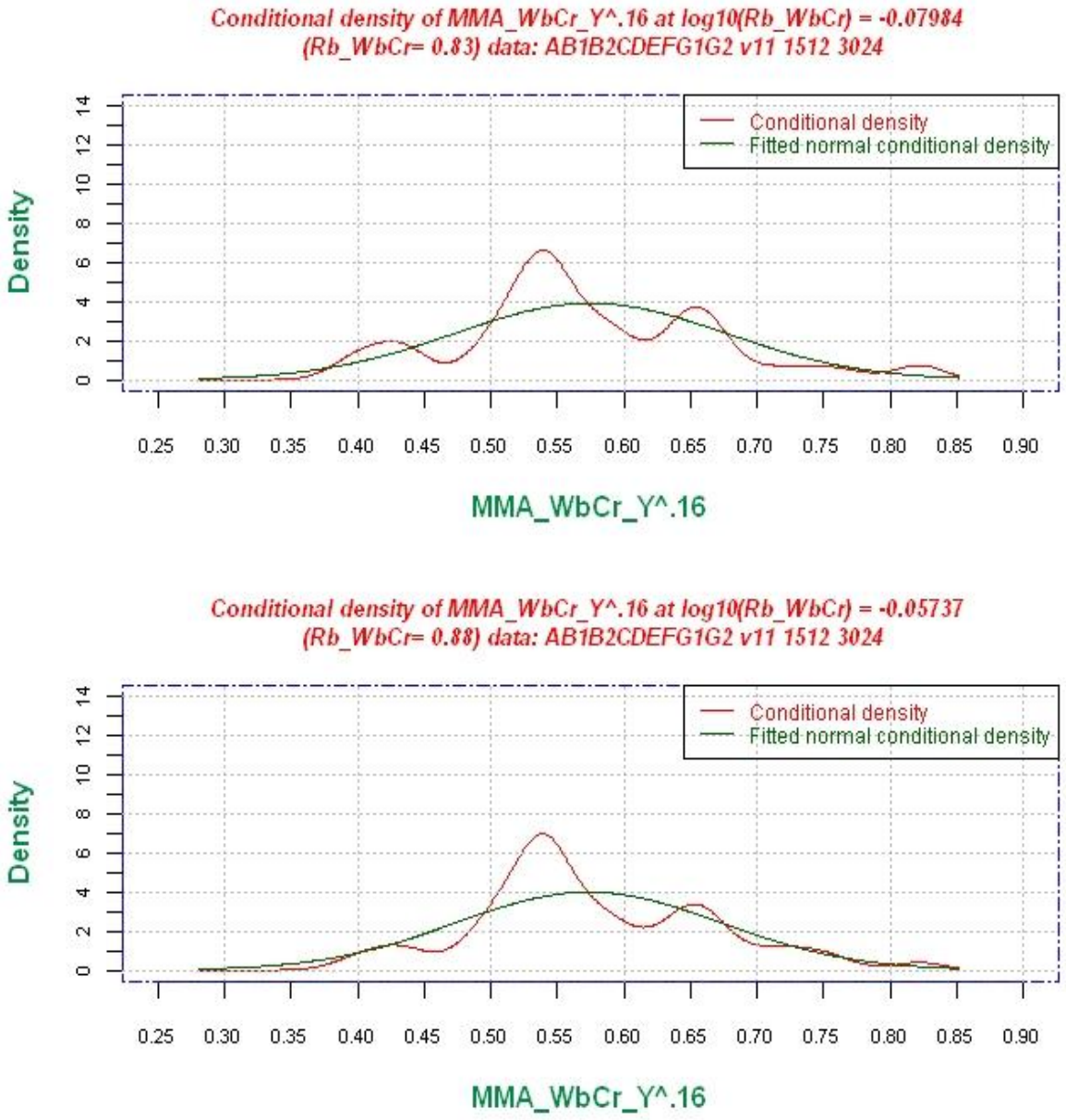

Figure A5.4: Upper graph. Conditional density of $(MMA/WbCr/Y)^{0.16}$ for $\log_{10}(Rb/WbCr) = -0.07984$ [i.e. Rb/WbCr = 0.83] Lower graph. Conditional density of $(MMA/WbCr/Y)^{0.16}$ for log10(Rb/WbCr) = - 0.05737 [i.e. Rb/WbCr = 0.88]

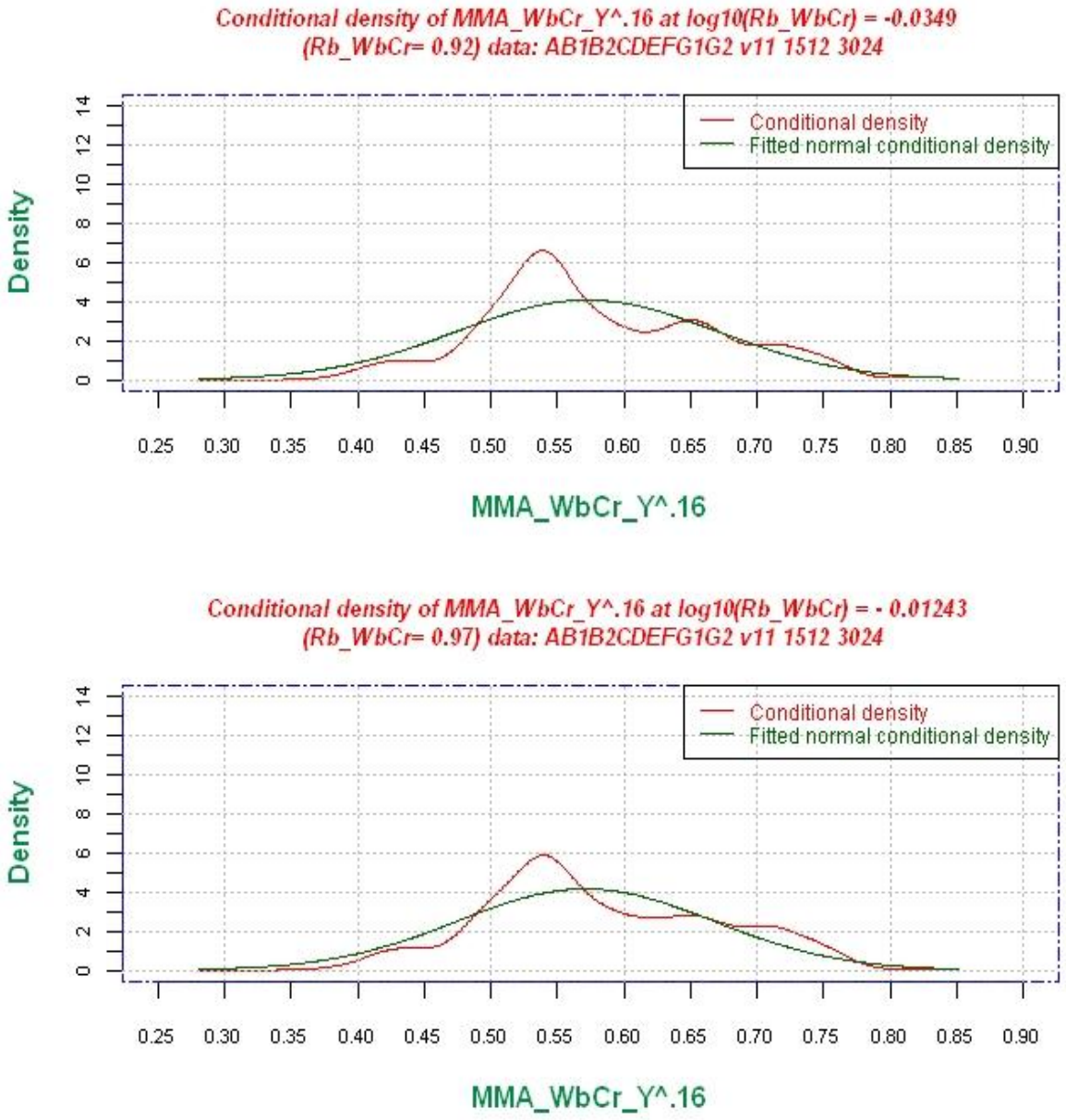

Figure A5.5: Upper graph. Conditional density of $(MMA/WbCr/Y)^{0.16}$ for $\log_{10}(Rb/WbCr) = -0.0349$ [i.e. Rb/WbCr = 0.92] Lower graph. Conditional density of $(MMA/WbCr/Y)^{0.16}$ for $\log_{10}(Rb/WbCr) = -0.01243$ [i.e. Rb/WbCr = 0.97]

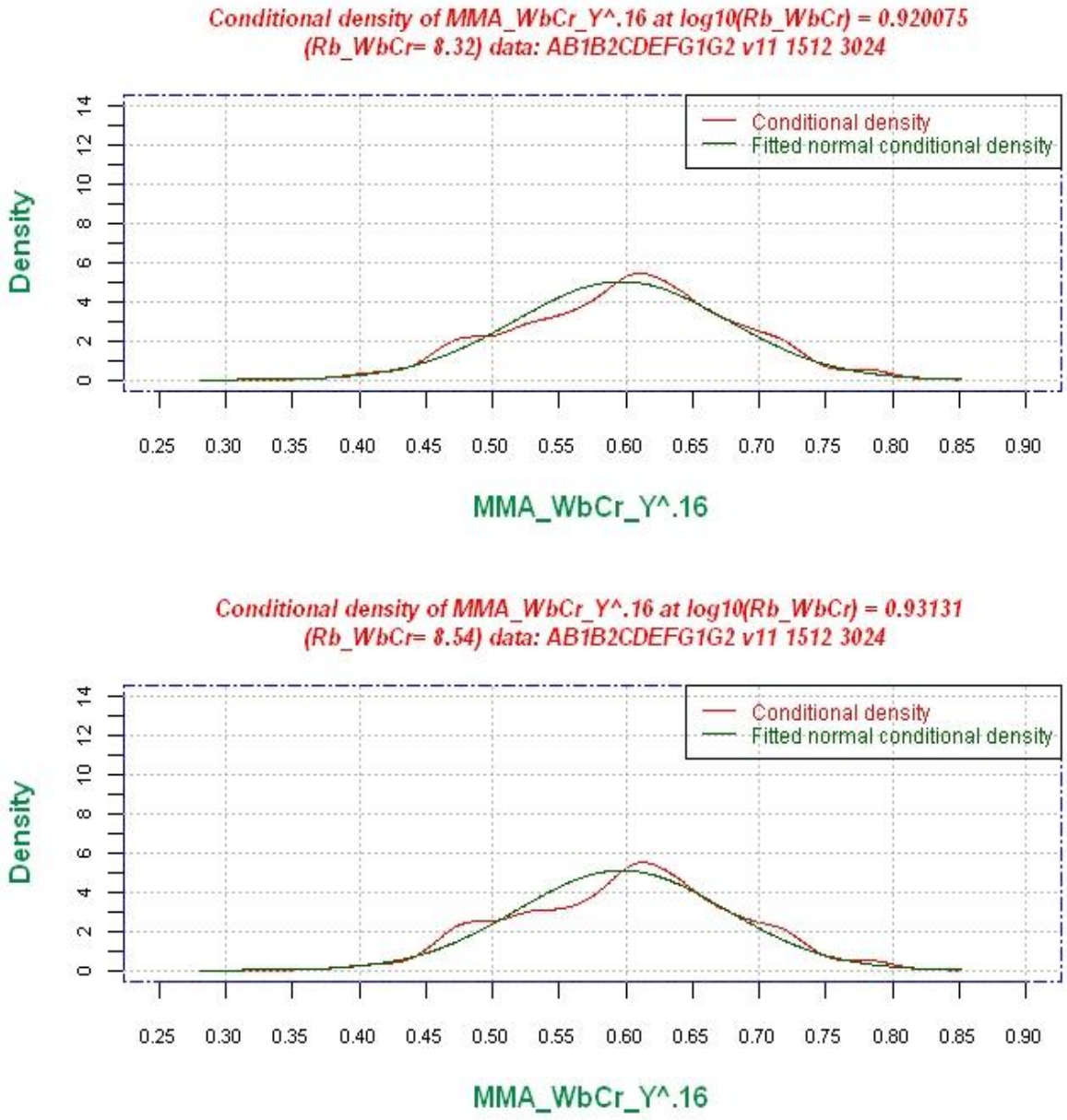

Figure A5.6: Upper graph. Conditional density of $(MMA/WbCr/Y)^{0.16}$ for $\log_{10}(Rb/WbCr)$ = 0.920075 [i.e. Rb/WbCr = 8.32]. Lower graph. Conditional density of $(MMA/WbCr/Y)^{0.16}$ for $\log_{10}(Rb/WbCr)$ = 0.93131 [i.e. Rb/WbCr = 8.54].

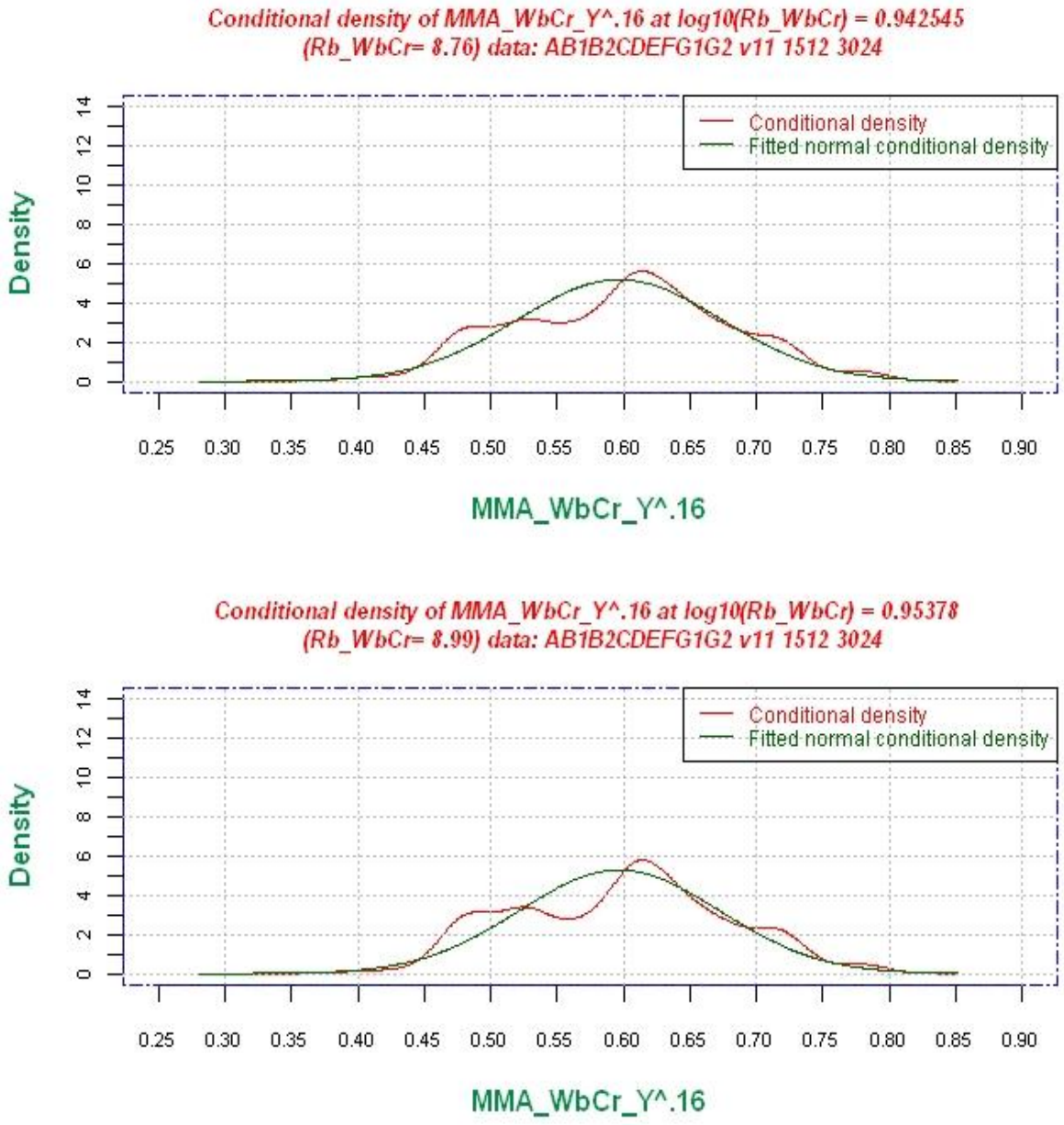

Figure A5.7: Upper graph. Conditional density of $(MMA/WbCr/Y)^{0.16}$ for $\log_{10}(Rb/WbCr)$ = 0.942545 [i.e. Rb/WbCr = 8.76]. Lower graph. Conditional density of $(MMA/WbCr/Y)^{0.16}$ for $\log_{10}(Rb/WbCr)$ = 0.95378 [i.e. Rb/WbCr = 8.99].

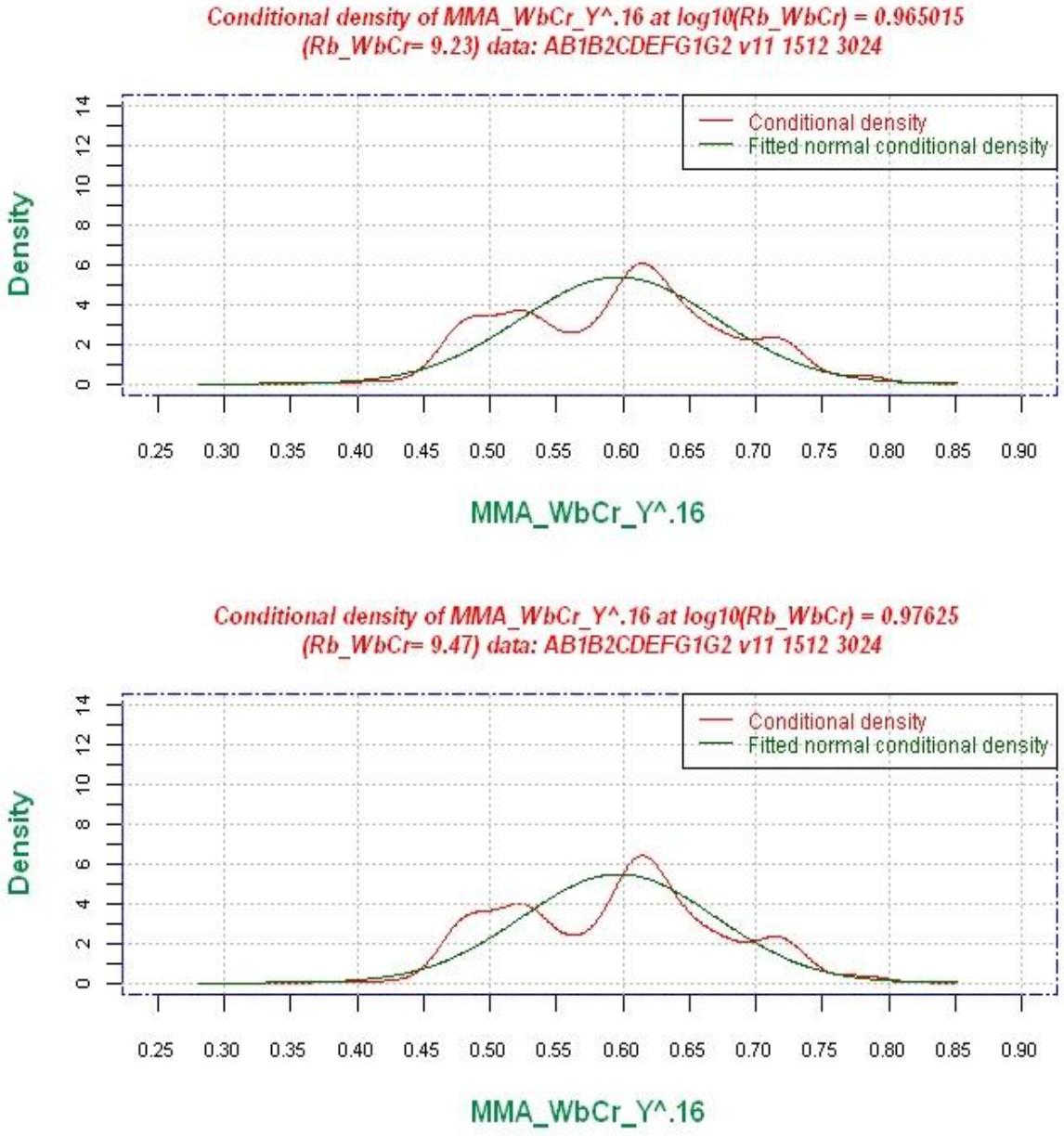

Figure A5.8: Upper graph. Conditional density of $(MMA/WbCr/Y)^{0.16}$ $\log_{10}(Rb/WbCr)$ = 0.965015 [i.e. Rb/WbCr = 9.23]. Lower graph. Conditional density of $(MMA/WbCr/Y)^{0.16}$ for $\log_{10}(Rb/WbCr)$ = 0.97625 [i.e. Rb/WbCr = 9.47].

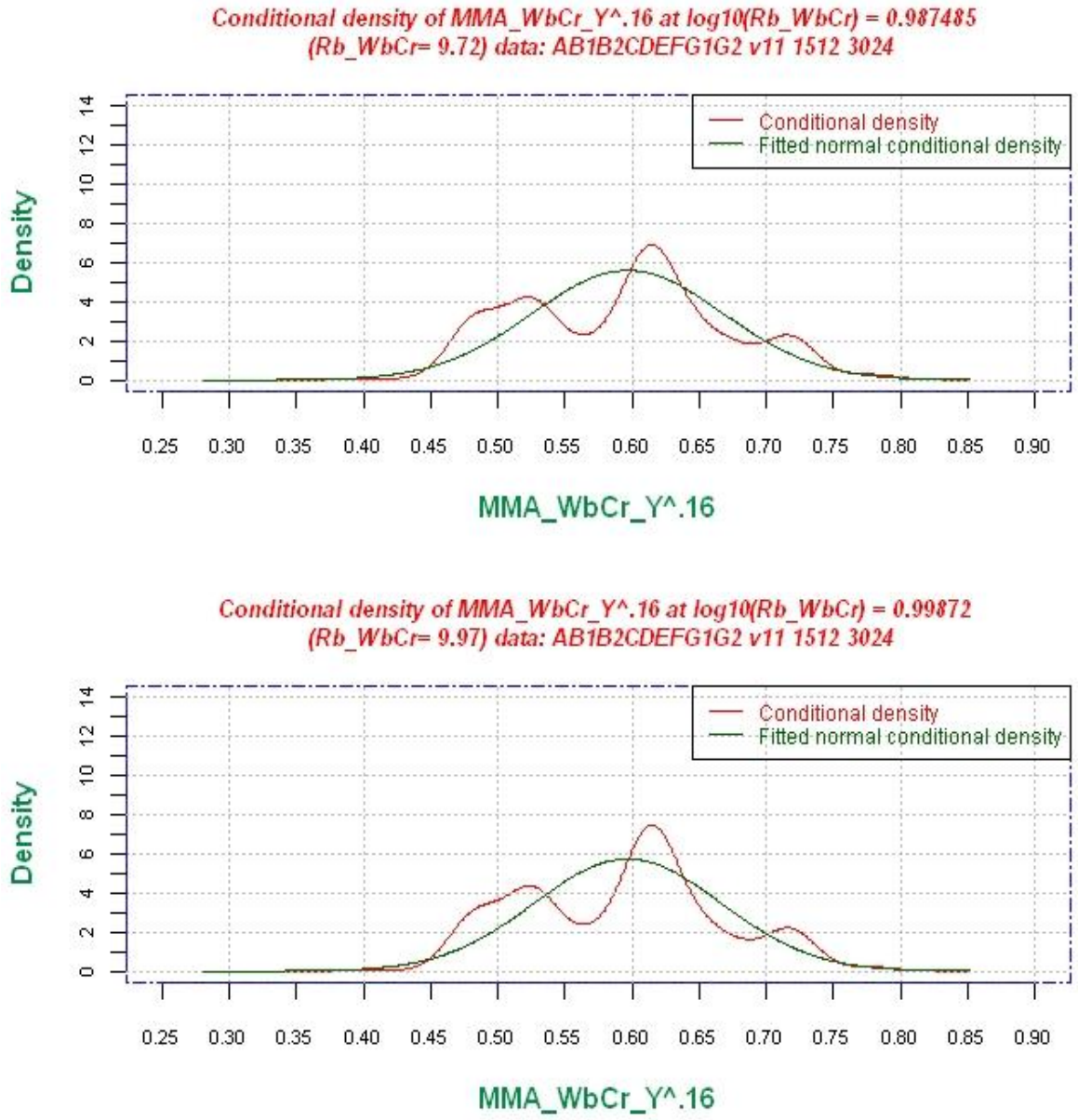

Figure A5.9: Upper graph. Conditional density of $(MMA/WbCr/Y)^{0.16}$ for $\log_{10}(Rb/WbCr)$ = 0.987485 [i.e. Rb/WbCr = 9.72]. Lower graph. Conditional density of $(MMA/WbCr/Y)^{0.16}$ for $\log_{10}(Rb/WbCr)$ = 0.99872 [i.e. Rb/WbCr = 9.97].

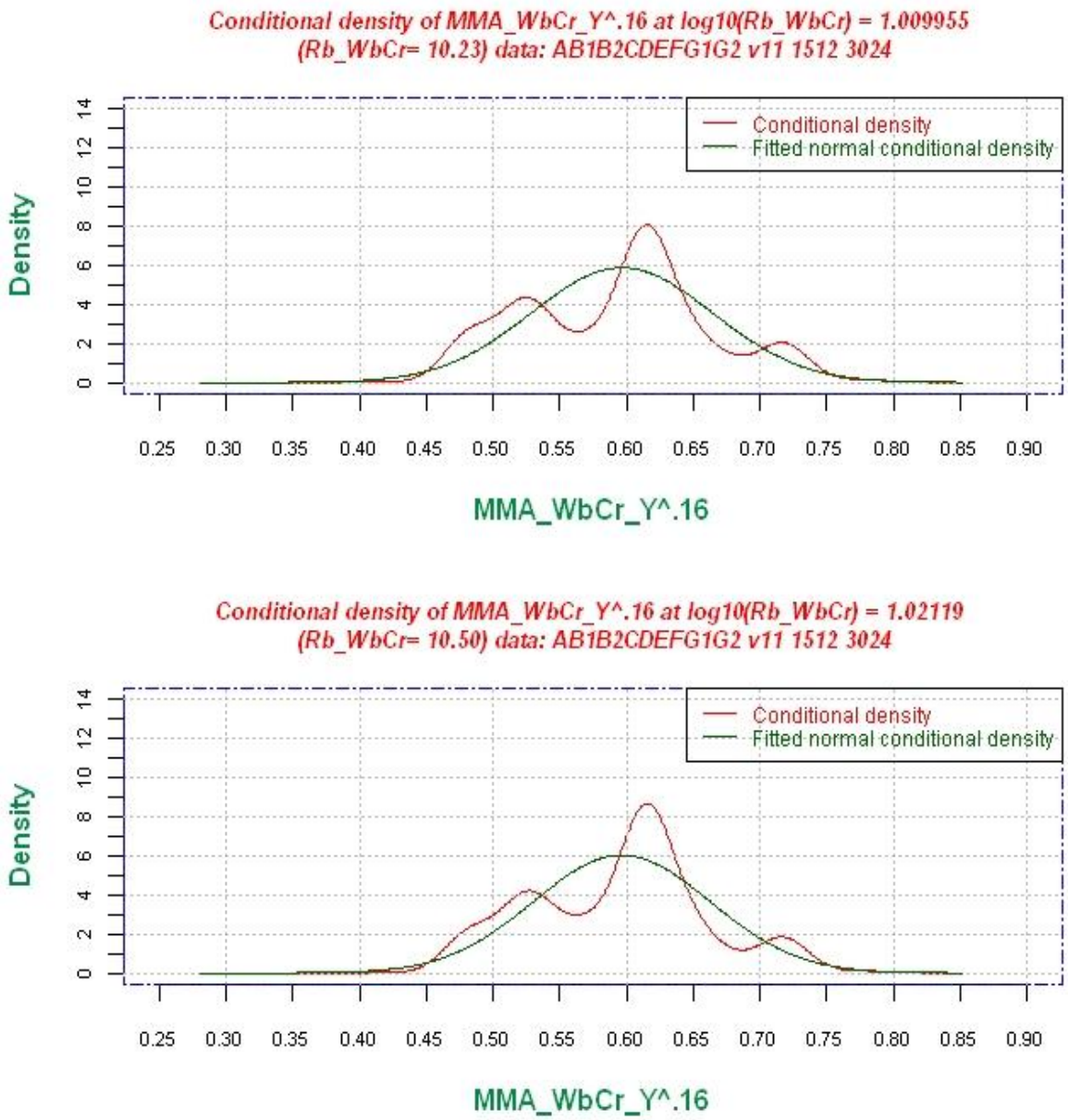

Figure A5.10: Upper graph. Conditional density of $(MMA/WbCr/Y)^{0.16}$ for $\log_{10}(Rb/WbCr)$ = 1.009955 [i.e. Rb/WbCr = 10.23]. Lower graph. Conditional density of $(MMA/WbCr/Y)^{0.16}$ for $\log_{10}(Rb/WbCr)$ = 1.02119 [i.e. Rb/WbCr = 10.50].

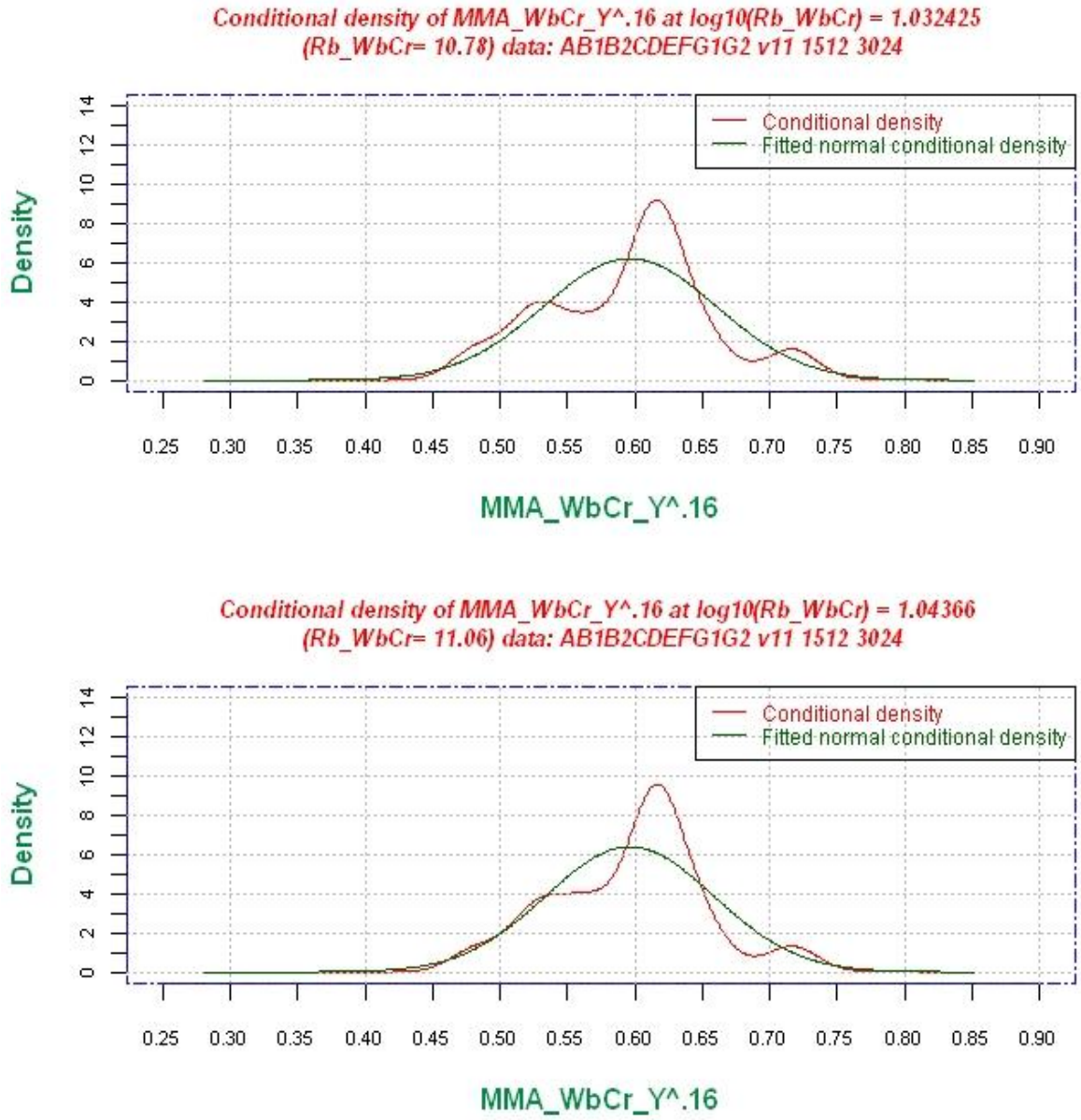

Figure A5.11: Upper graph. Conditional density of $(MMA/WbCr/Y)^{0.16}$ for log10(Rb_WbCr) = 1.032425 [i.e. Rb/WbCr = 10.78]. Lower graph. Conditional density of $(MMA/WbCr/Y)^{0.16}$ for $\log_{10}(Rb/WbCr) = 1.04366$ [i.e. Rb_WbCr = 11.06].

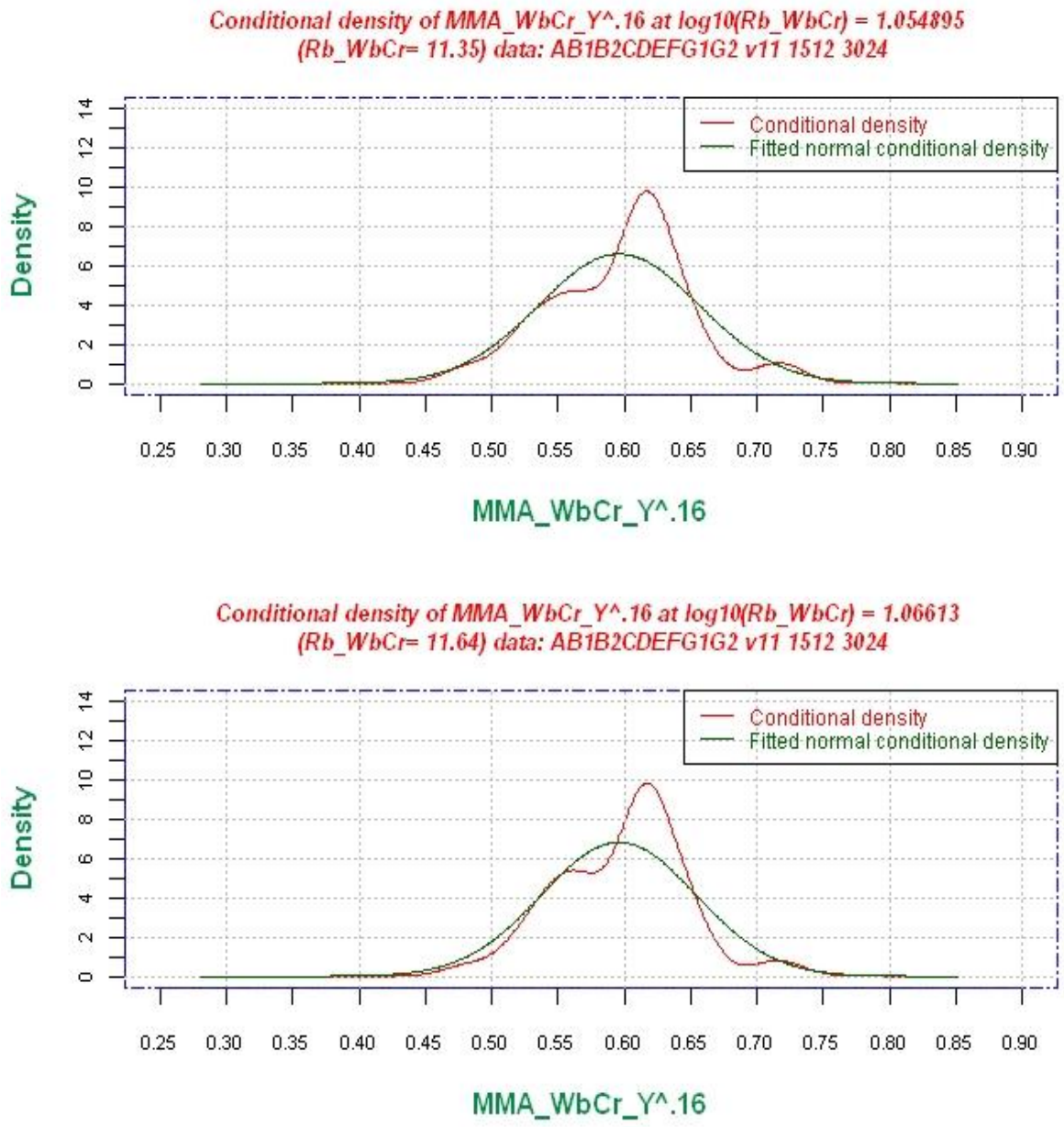

Figure A5.12: Upper graph. Conditional density of $(MMA/WbCr/Y)^{0.16}$ for $\log_{10}(Rb/WbCr)$ = 1.054895 [i.e. Rb/WbCr = 11.35]. Lower graph. Conditional density of $(MMA/WbCr/Y)^{0.16}$ for $\log_{10}(Rb/WbCr)$ = 1.06613 [i.e. Rb/WbCr = 11.64].

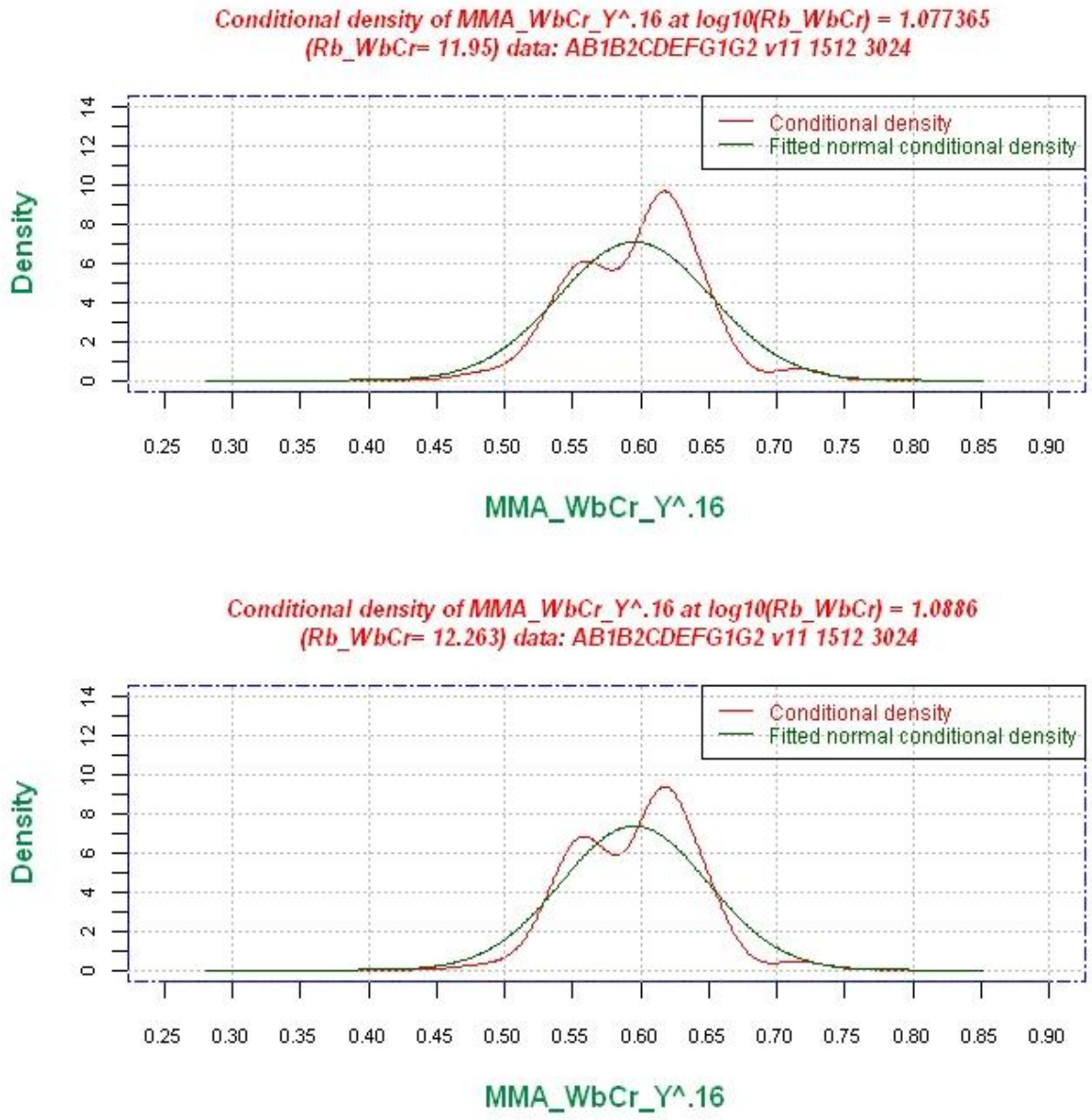

Figure A5.13: Upper graph. Conditional density of $(MMA/WbCr/Y)^{0.16}$ for $\log_{10}(Rb/WbCr)$ = 1.077365 [i.e. Rb/WbCr = 11.95]. Lower graph. Conditional density of $(MMA/WbCr/Y)^{0.16}$ for $\log_{10}(Rb/WbCr)$ = 1.0886 [i.e. Rb/WbCr = 12.263].